National Research Council Canada

Conseil national de recherches Canada

NRC · CNRC

Canadian Journal of Fisheries and Aquatic Sciences

Journal canadien des sciences halieutiques et aquatiques

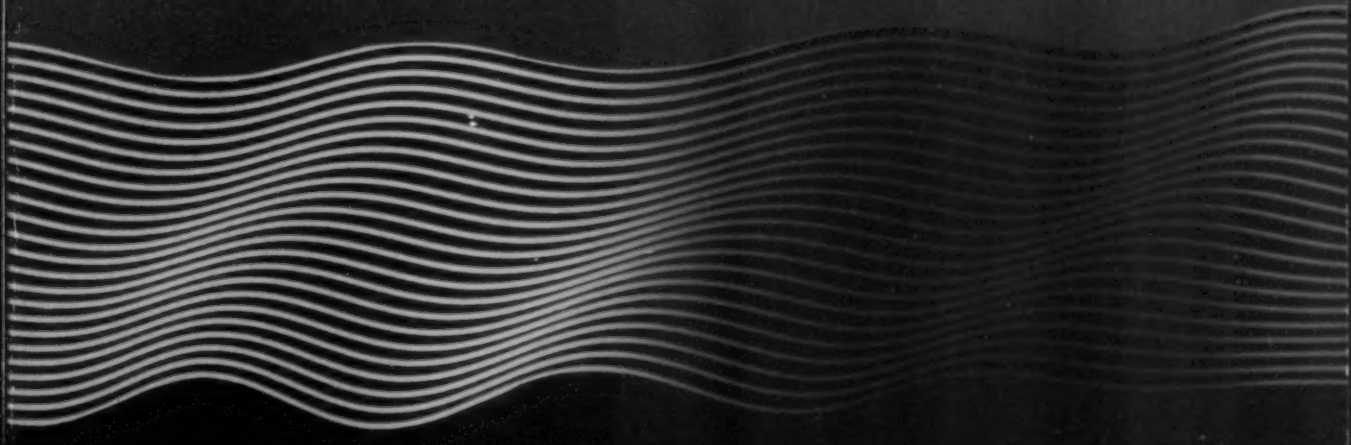

http://www.nrc.ca/cisti/journals

ISSN 0706-652X / CJFSDX 57(5) 875–1112 (2000)

The *Canadian Journal of Fisheries and Aquatic Sciences*, previously published as *Contributions to Canadian Biology* 1901–1925, *Contributions to Canadian Biology and Fisheries* 1926–1934, *Journal of the Biological Board of Canada* 1934–1937, and *Journal of the Fisheries Research Board of Canada* 1938–1979, is issued monthly to form annual volumes of 12 numbers plus supplements.

Editorial policy: The Journal publishes original research articles, perspectives (syntheses, critiques, re-evaluations), discussions (comment and reply), and rapid communications. Manuscripts may concern cells, organisms, populations, communities, ecosystems, or processes that affect aquatic systems. They may cover a range of disciplines including biology and ecology of marine and freshwater organisms, limnology, oceanography, physiology, toxicology, genetics, economics, disease, and management. Preference will be given to manuscripts that emphasize understanding of observed phenomena and interpretation of experimental results. The Journal encourages papers that lead from clearly stated purpose or rationale and from testable hypotheses, concepts, or questions to identifiable conclusions or syntheses. Such papers may amplify, modify, question, or redirect accumulated knowledge embodied in contemporary perceptions of a particular state of aquatic sciences. The Journal discourages papers that are essentially descriptive, except in emerging disciplines; have only site-specific or local applications (a certain year, place, taxon, chemical compound, etc.); only confirm previously established principles; or apply standard techniques without breaking new methodological ground.

Manuscripts for publication should be submitted to the Editors, Canadian Journal of Fisheries and Aquatic Sciences, Department of Zoology, University of Guelph, Guelph, ON N1G 2W1, Canada (519-824-4120 ext. 2646; fax: 519-767-9798; e-mail: cjfas@uoguelph.ca).

Submissions in either English or French are acceptable. The information must be original, that is, not copyrighted, published, or submitted elsewhere except in abstract form or unless by written consent of the Editor. NRC accepts no responsibility for statements or opinions expressed by a contributor. Acceptance of an advertisement, announcement, or other material does not imply endorsement by either the *Journal*'s Editors or NRC. The use of proprietary names does not imply endorsement of the product or company.

Correspondence concerning accepted manuscripts and corrected proofs should be sent to NRC Research Press, National Research Council of Canada, Ottawa, ON K1A 0R6, Canada.

Instructions to Authors are published once a year in the first issue of each volume. Copies are available from NRC Research Press or from our Web site. The **Publication Policy** of NRC Research Press is also available at our Web site:
http://www.nrc.ca/cisti/journals/rj.html

Microfilm: Issues from 1934 through the current volume can be purchased on 16- or 35-mm microfilm. Photocopies of individual articles or issues can be purchased from University Microfilms International, 330 North Zeeb Road, Ann Arbor, MI 48106, U.S.A.

U.S. periodical postage paid at Champlain, N.Y., and at additional mailing offices. Attention U.S. POSTMASTER: Send address changes to **Canadian Journal of Fisheries and Aquatic Sciences**, c/o USACAN Media Distribution Center, P.O. Box 2888, Plattsburg, NY 12901, U.S.A.

Publié sans interruption depuis 1901, le *Journal canadien des sciences halieutiques et aquatiques* a paru sous plusieurs titres : *Contributions to Canadian Biology* 1901–1925, *Contributions to Canadian Biology and Fisheries* 1926–1934, *Journal of the Biological Board of Canada* 1934–1937, et *Journal of the Fisheries Research Board of Canada* 1938–1979. Le *Journal* paraît tous les mois, formant ainsi un volume de 12 numéros, et offre en plus jusqu'à deux suppléments par année.

Politique éditoriale : On publie, dans le Journal, des articles rendant compte de recherche originale, des perspectives (synthèses, critiques et réévaluations), des discussions (commentaires et réponses) et des communications rapides. Les documents peuvent porter sur les cellules, organismes, populations, communautés, écosystèmes ou processus qui affectent les systèmes aquatiques. Ils peuvent relever de divers domaines y compris la biologie et l'écologie des organismes marins et d'eau douce, la limnologie, l'océanographie, la physiologie, la toxicologie, la génétique, l'économie, la pathologie et la gestion. On accorde la préséance aux articles qui contribuent à la compréhension de phénomènes observés et à l'interprétation de résultats expérimentaux. On invite les auteurs à soumettre des articles ayant des objectifs précis ou relevant d'hypothèses, de concepts ou de questions vérifiables et se terminant par de solides conclusions ou d'utiles synthèses. Ces articles enrichissent, changent, mettent en question ou réorientent les connaissances acquises sur divers aspects des sciences aquatiques. On décourage toutefois la soumission d'articles simplement descriptifs (à moins qu'il ne s'agisse de nouvelles disciplines), d'application très limitée (applicables à une seule année, une seule région ou un seul taxon, portant sur un unique composé chimique, etc.); d'articles qui ne font que reprendre les principes énoncés dans des articles précédents; et d'articles rendant compte de l'application de normes sans gain de méthodologie.

Les auteurs voudront adresser leurs **manuscrits** aux directeurs scientifiques, Journal canadien des sciences halieutiques et aquatiques, Department of Zoology, University of Guelph, Guelph, ON N1G 2W1, Canada (519-824-4120 poste 2646; télécopieur : 519-767-9798; adresse électronique : cjfas@uoguelph.ca).

Les contributions peuvent être en anglais ou en français. Elles doivent être originales, c.-à.-d. qu'elles ne doivent pas avoir fait l'objet d'un copyright, avoir été publiées ou soumises ailleurs, sauf sous forme abrégée ou avec le consentement du rédacteur. Le CNRC ne se tient en aucune façon responsable des opinions exprimées par un collaborateur ou des déclarations qui pourrait faire ce dernier. La publication d'annonces publicitaires, d'avis et autres n'implique pas l'endossement de leur contenu par les directeurs du *Journal* ou du CNRC. L'utilisation des noms de marques de commerce ne signifie aucunement une sanction du produit en question ou de la compagnie qui le fabrique.

La correspondance ayant trait aux manuscrits acceptés et les **épreuves corrigés** doivent être envoyées aux Presses scientifiques du CNRC, Conseil national de recherches du Canada, Ottawa, ON K1A 0R6, Canada.

Recommandations aux auteurs sont publiés une fois par année dans le premier numéro de chaque volume. Des copies, ainsi que la **Politique de publication**, sont disponibles auprès des Presses scientifiques du CNRC ou au site Web :
http://www.nrc.ca/cisti/journals/rj.html

Microfilms : On peut acheter sur microfilms de 16 ou 35 mm tous les numéros depuis 1934. Des photocopies d'articles ou de numéros individuels sont aussi en vente auprès de University Microfilms International, 330 North Zeeb Road, Ann Arbor, MI 48106, É.-U.

This journal is indexed or abstracted in / Ce journal est signalé ou résumé dans
ABSEARCH, Aquatic Sciences and Fisheries Abstracts, Biological Abstracts, Biological & Agricultural Index, CAB Abstracts, Chemical Abstracts, Current Contents, Elsevier BIOBASE, Environmental Abstracts, Environmental Periodicals Bibliography, GEOBASE, GeoRef, Life Sciences Collection, Meteorological and Geoastrophysical Abstracts, Oceanic Abstracts, PASCAL Database, and Science Citation Index.

Volume 57, Number 5, May 2000

Canadian Journal of Fisheries and Aquatic Sciences

Published by the National Research Council of Canada

Volume 57, numéro 5, mai 2000

Journal canadien des sciences halieutiques et aquatiques

Publié par le Conseil national de recherches du Canada

Editors / directeurs scientifiques John C. Roff and Moira M. Ferguson

Assistant to the Editors / adjointe aux directeurs scientifiques **Holly Foster**

Associate Editors / directeurs scientifique associés

D. Boisclair, *Université de Montréal*
U. Borgmann, *Environment Canada, Burlington*
S.E. Campana, *DFO/MPO, Dartmouth*
D.G. Dixon, *University of Waterloo*
A.E. Dizon, *National Marine Fisheries Service, La Jolla, Calif.*
J.J. Dodson, *Université Laval*
J.A. Downing, *Iowa State University*
K.T. Frank, *DFO/MPO, Dartmouth*
D.F. Houlihan, *University of Aberdeen, Aberdeen, Scotland*
F.A. Huntingford, *University of Glasgow*
J.A. Hutchings, *Dalhousie University*
G.S. Jamieson, *DFO/MPO, Nanaimo*
B. Jonsson, *Norwegian Institute for Nature Research, Oslo, Norway*
L. Legendre, *Université Laval*
D.M. Mason, *NOAA-Great Lakes Environmental Research Laboratory, Ann Arbor, Mich.*
A. Mazumder, *University of Victoria*
D.L. Parrish, *Vermont Cooperative Fish and Wildlife Research Unit (USGS/BRD), University of Vermont*
P. Pepin, *DFO/MPO, St. John's*
R.M. Peterman, *Simon Fraser University*
E.E. Prepas, *University of Alberta*
T.M. Powell, *University of California, Berkeley, Calif.*
T.J. Quinn II, *University of Alaska–Fairbanks, Juneau, Alaska*
T.P. Quinn, *University of Washington*
R.D. Robarts, *Environment Canada, Saskatoon*
B. Sainte-Marie, *DFO/MPO, Mont-Joli*
P.F. Sale, *University of Windsor*
D.W. Schindler, *University of Alberta*
S.J. Smith, *DFO/MPO, Dartmouth*
W.G. Sprules, *University of Toronto*
R.J. Thompson, *Memorial University of Newfoundland*
C.J. Walters, *University of British Columbia*
R.D. Ward, *CSIRO Division of Fisheries, Australia*
C.M. Wood, *McMaster University*
B. de Young, *Memorial University of Newfoundland*

NRC Research Press / Presses scientifiques du CNRC

Editor-in-chief / directeur général **Bruce P. Dancik**

Assistant Editor-in-chief / directeur général adjoint **Iain E.P. Taylor**

Journals Program / Programme des revues

(Fax / télécopieur : 613-952-7656; e-mail / adresse électronique : research.journals@nrc.ca;
URL: http://www.nrc.ca/cisti/journals/)

Director / directrice **Aldyth Holmes**

Business Manager / gestionnaire des affaires **Paul McClymont**

Managing Editor / rédactrice administrative **Cecily M. Pearson (613-993-9099)**

Publication Officer / agente de publication **Jennifer McColl**

Advertising / annonces publicitaires **Judy Heyman (613-993-0151)**

Reprints / tirés à part **Roxanne Landriault (613-990-2254)**

Subscriptions / abonnements **Helen Goulet (613-993-9084)**

© National Research Council of Canada 2000. World rights reserved.
No part of this publication may be reproduced, stored, or transmitted in any form or by any means, without the written permission of the publisher, except as stated below.

The National Research Council of Canada grants **permission*** to individuals to make single copies of articles for personal use. Any person may reproduce short excerpts from articles in the journal for any purpose that respects the moral rights of authors, provided that the source is fully acknowledged. As a courtesy, the consent of authors of such material should be obtained directly from the author.

Authorization to reproduce items for other than personal use, as stated above, is granted by the National Research Council of Canada provided that the copyright fee of $7.00 per copy is paid directly to CANCOPY, One Yonge Street, Suite 1900, Toronto, ON M5E 1E5, Canada.

*The above permission does not extend to other kinds of copying, such as copying for general distribution, for advertising, or promotional purposes, for creating new collective works, or for resale. For such copying, arrangements must be made with the publisher, National Research Council of Canada, Ottawa, ON K1A 0R6, Canada.

© Conseil national de recherches du Canada 2000. Tous droits réservés.
Il est interdit de reproduire, de sauvegarder ou de transmettre quelque partie de la présente publication dans quelque format ou de quelque façon sans le consentement écrit de l'éditeur, à l'exception des conditions suivantes.

Le Conseil national de recherches du Canada accorde aux particuliers le droit de faire des copies individuelles pour leur usage personnel. Toute personne peut reproduire de courts extraits des articles de la Revue pour autant que les droits moraux de l'auteur soient respectés et que la mention de provenance soit clairement indiquée. Il est de convenance de demander le consentement de l'auteur avant de faire mention de son travail.

On obtiendra l'autorisation de reproduire des articles à d'autres fins que l'usage personnel (tel qu'on l'a décrit ci-dessus) auprès du Conseil national de recherches du Canada pour autant que des redevances de droits d'auteurs de 7,00 $/copie soient versées au CANCOPY, 1, rue Yonge, bureau 1900, Toronto, ON M5E 1E5, Canada.

*La permission ci-dessus ne s'applique pas à la reproduction à grande échelle, telle que la reproduction aux fins de distribution générale, publicitaire ou promotionnelle, de compilation de nouveaux ouvrages collectifs ou de revente. Dans de tels cas, il faudra ratifier une entente particulière avec l'éditeur, le Conseil national de recherches du Canada, Ottawa, ON K1A 0R6, Canada.

Subscription information

The *Canadian Journal of Fisheries and Aquatic Sciences* (ISSN 0706-652X) is published monthly by the National Research Council of Canada. 2000 annual subscription rates (second class postage) for Canada are $630CAN institutional and $191CAN personal, for US & foreign $630US institutional and $191US personal. For air mail add $150US to foreign rate. Canadian customers please include 7% GST (business no. 12149 1807 RT 0275). Subscriptions are entered for the calendar year. Remittances should be made payable to the Receiver General for Canada credit NRC. Price for regular single issues: institutional, $80.00; personal, $25.00. Supplements will be priced separately. Special rates apply to members of Canadian scientific and engineering societies if they subscribe through their respective societies.

There are no refunds on cancelled subscriptions once delivery has begun. Claims for missing issues should be made within four months (N. America) or six months (outside N. America) following the date of publication. The publisher expects to supply missing issues only when losses have occurred in transit and when the reserve stock will permit. For change of address and subscription enquiries: Subscription Office, NRC Research Press, National Research Council of Canada, Ottawa, ON K1A 0R6, Canada; tel: 613-993-9084; fax: 613-952-7656; e-mail: research.journals@nrc.ca.

Microform backfiles are available from UMI, P.O. Box 1346, Ann Arbor, MI 48106-1346, U.S.A., and Micromedia Ltd., 20 Victoria St., Toronto, ON M5C 2N8, Canada.

All issues of the *Canadian Journal of Fisheries and Aquatic Sciences* since 1996 are available on the Web. Pricing information can be found at

http://www.nrc.ca/cisti/journals/

Renseignements sur l'abonnement

Journal canadien des sciences halieutiques et aquatiques (ISSN 0706-652X) est une publication mensuelle du Conseil national de recherches du Canada. Le prix de l'abonnement annuel au Canada (courrier de deuxième classe) est de 630 $CAN pour les organismes et de 191 $CAN pour les particuliers. À l'étranger (y compris les É.-U.), le prix de l'abonnement est de 630 $US pour les organismes et de 191 $US pour les particuliers. L'expédition par avion exige des frais de 150 $US en sus du prix d'abonnement à l'étranger. Les clients du Canada doivent ajouter la TPS de 7% (numéro d'entreprise 12149 1807 RT 0275). Les abonnements sont pour l'année civile. Tout paiement doit être adressé au Receveur général du Canada, crédit du CNRC. Le prix par numéro est de 80 $ pour les organismes et de 25 $ pour les particuliers. Le prix des hors-série varie. Les membres des sociétés canadiennes de sciences et de génie bénéficient de taux préférentiels en s'abonnant via leurs sociétés respectives.

Aucun remboursement ne sera accordé ni aucune annulation acceptée une fois que les livraisons auront commencé. Les réclamations de numéros manquants devront être soumises dans les quatre mois (Amérique du Nord) ou dans les six mois (à l'extérieur de l'Amérique du Nord) suivant la date de publication. L'éditeur ne fournira de numéros manquants que si le document a été perdu pendant l'expédition et que si le stock le permet. Adressez tout changement d'adresse ou toute question quant à l'abonnement au : Bureau des abonnements, Presses scientifiques du CNRC, Conseil national de recherches Canada, Ottawa, ON K1A 0R6, Canada; téléphone : 613-993-9084; télécopieur : 613-952-7656; adresse électronique : research.journals@nrc.ca.

On peut obtenir les fichiers rétrospectifs sur **microforme** auprès de UMI, P.O. Box 1346, Ann Arbor, MI 48106-1346, É.-U., et auprès de Micromedia Ltée, 20 rue Victoria, Toronto, ON M5C 2N8, Canada.

À partir de 1996, tous les numéros de *Journal canadien des sciences halieutiques et aquatiques* sont accessibles sur le Web. On trouvera des renseignements sur les tarifs à

http://www.nrc.ca/cisti/journals/rjfr.html

Seasonal photoreactivity of dissolved organic matter from lakes with contrasting humic content

Måns J. Lindell, H. Wilhelm Granéli, and Stefan Bertilsson

Abstract: We studied seasonal variability in photodegradation of dissolved organic carbon (DOC) resulting from artificial ultraviolet-A (UV-A) and UV-B irradiation. Water samples were taken approximately monthly from the surface layers of two oligotrophic lakes with contrasting humic content, situated in southern Sweden. Lake water was filter-sterilized (0.2 μm) and exposed to artificial UV radiation in quartz tubes. Potential DOC photodegradation, measured as a photoproduction of dissolved inorganic carbon (DIC) and oxalic, malonic, formic, and acetic acid in irradiated samples, was observed throughout the sampling period. In addition, exposure to UV radiation resulted in a decrease in DOC, absorbance, and humic substance fluorescence. The photoproduction of DIC and the low molecular weight (LMW) organic acids varied seasonally, being generally higher in winter and spring (December–May), while DOC appeared to become less photoreactive after the extensive exposure to solar radiation during summer. Production rates of both DIC and LMW organic acids were approximately eight times higher in the humic lake despite that the DOC concentration was only two times higher than in the clearwater lake. This is most probably due to the high input of allochthonous DOC and the resulting higher absorbance to DOC ratio in the humic system. Furthermore, the longer hydraulic residence time in the clearwater system could have resulted in an accumulation of residual DOC, recalcitrant to further photodegradation.

Résumé : Nous avons étudié la variabilité saisonnière de la photodégradation du carbone organique dissous (COD) causée par le rayonnement artificiel UV-A et UV-B. Des échantillons d'eau ont été prélevés à intervalle d'un mois environ dans les couches superficielles de deux lacs oligotrophes à teneur humique différente situés dans le sud de la Suède. L'eau des lacs a été stérilisée par filtration (0,2 μm) et exposée à un rayonnement UV artificiel dans des tubes à quartz. La photodégradation potentielle du COD, mesurée en termes de photoproduction de carbone inorganique dissous (CID) et d'acides oxalique, malonique, formique et acétique dans les échantillons irradiés, a été observée tout au long de la période d'échantillonnage. De plus, l'exposition au rayonnement UV a provoqué une baisse du COD, de l'absorbance et de la fluorescence des substances humiques. La photoproduction de CID et des acides organiques à faible poids moléculaire (FPM) variait selon la saison, et elle était généralement plus élevée en hiver et au printemps (déc. – mai), tandis que le COD semblait moins photoréactif après une longue exposition au rayonnement solaire pendant l'été. Les taux de production de CID et d'acides organiques (SPM) étaient environ 8 fois plus élevés dans le lac humique, malgré le fait que la concentration de COD y était seulement 2 fois plus élevée que dans le lac aux eaux claires; cela est très probablement dû à l'apport élevé de COD allochtone et aux rapports plus élevés de l'absorbance au COD qui en résultent dans le système humique. De plus, le temps de séjour hydraulique plus long dans le système aux eaux claires peut avoir provoqué une accumulation de COD résiduel, résistant à toute autre photodégradation.

[Traduit par la Rédaction]

Introduction

High molecular weight (HMW) organic molecules have previously been considered to have long turnover times in aquatic ecosystems compared with the rapidly utilized low molecular weight (LMW) organic pool (Fenchel and Blackburn 1979; Chrost and Faust 1983). This view has recently been revised, since some HMW organic compounds exhibit turnover times comparable with those of biolabile LMW molecules (Tranvik 1990; Amon and Benner 1996).

Sunlight, and especially ultraviolet (UV) radiation (wavelength <400 nm), may play a significant role in the turnover and dynamics of dissolved organic carbon (DOC) in lakes. Photochemical reactions could affect DOC, both through complete oxidation into dissolved inorganic carbon (DIC) (Salonen and Vähätalo 1994; Miller and Zepp 1995; Granéli et al. 1996) and by transformation of large molecules into LMW organic substances, directly available for bacterioplankton utilization (reviewed by Moran and Zepp 1997). Consequently, photochemical reactions could partly explain supersaturation of CO_2 in lakes and oceans (Cole et al. 1994) through either a direct abiotic oxidation of DOC into DIC or indirectly through increased respiration due to stimulated bacterial growth caused by the photochemical produc-

Received April 23, 1999. Accepted August 4, 1999.
J15114

M.J. Lindell and H.W. Granéli.[1] Department of Ecology/Limnology, Lund University, S-223 62 Lund, Sweden.
S. Bertilsson.[2] Department of Water and Environmental Studies, Linköping University, S-581 83 Linköping, Sweden.

[1]Author to whom all correspondence should be addressed. e-mail: wilhelm.graneli@limnol.lu.se
[2]Present address: Department of Civil and Environmental Engineering, The Ralph M. Parsons Laboratory, Massachusetts Institute of Technology, Cambridge, MA 02139, U.S.A.

© 2000 NRC Canada

tion of bacterial substrates (Lindell et al. 1995; Wetzel et al. 1995).

Many recent discussions on photooxidation are based on the assumption that DOC exhibits similar photosensitivity to solar radiation, independent of past light history (Valentine and Zepp 1993; Scully et al. 1996; Granéli et al. 1998). These studies demonstrate similarities in DOC photodegradability on a spatial scale but disregard the potential for changes on a temporal scale. The photodegradability of DOC by solar radiation may decrease with prolonged light exposure (Geller 1986; Kulovaara and Backlund 1993; Lindell et al. 1995), resulting in the accumulation of photorecalcitrant DOC (Thomas and Lara 1995; Naganuma et al. 1996). Geller (1986) observed a photochemical stimulation of bacterial growth potential on dissolved organic matter (DOM) from lake water sampled during winter but not for samples from the summer period. The decreased photoreactivity potential during summer noted by Geller (1986), as well as by other authors (Kulovaara and Backlund 1993; Lindell et al. 1995), may be explained by a limited capacity for photochemical production of biologically labile DOC from HMW organic matter. Still, DOC may continue to degrade upon further light exposure, forming less bioavailable end products and potentially causing an accumulation of nonlabile DOC (Keil and Kirchman 1994). Alternatively, there could be a complete photooxidation of DOC into inorganic forms (Granéli et al. 1996). In this case, depth and hydraulic residence time of the lake, as well as the input of DOC to the system, could be key factors regulating the DOC photosensitivity by affecting the mean exposure time of the DOC to solar radiation (Schindler et al. 1997).

We hypothesized that the potential for epilimnetic lake DOC to undergo photochemical reactions changes seasonally and depends on the previous exposure of the organic material to solar radiation. Two oligotrophic lakes of contrasting humic content were sampled monthly and the ability of artificial UV radiation to produce DIC and some LMW carboxylic acids was assessed. Two different irradiation treatments were used in order to evaluate the relative importance of short-wavelength UV radiation (UV-B, 280–320 nm) relative to long-wavelength UV radiation (UV-A, 320–400 nm) in this aspect. We hypothesized that the photooxidation potential would be high in winter and early spring, since DOC present in the lake at that time would have been largely protected from solar radiation during winter. In addition, photolabile DOC could have entered the lake from the drainage area and from the hypolimnion during lake turnover (Salonen and Vähätalo 1994). Consequently, potential photooxidation would be low in late summer and fall when the epilimnetic water has been extensively exposed to solar radiation during summer, while input of hypolimnetic water and water from the drainage area would have been prevented due to the stratification.

Methods

Photochemical reactivity of lake water DOC was studied in filter-sterilized samples incubated in UV-transparent quartz tubes under an artificial radiation source. These lamps emitted UV radiation with intensities close to that observed at noon on a clear summer day in southern Sweden (Fig. 1). To evaluate the relative importance of UV-B and UV-A radiation, respectively, we used a Mylar film to exclude wavelengths below 318 nm (Fig. 1). Two experiments were performed. In the first experiment, two lakes were sampled monthly. Changes in the production of DIC and four LMW carboxylic acids, as well as the decrease in fluorescence, absorbance, and DOC upon exposure to UV radiation, were followed in order to describe seasonal trends in potential DOC photoreactivity. The second experiment was a test of the methodology used in the first experiment, as well as being a detailed study of DIC production and O_2 consumption during prolonged exposure of water samples to UV radiation. DIC is here defined as the sum of dissolved CO_2, H_2CO_3, HCO_3^-, and CO_3^{2-} and does not include CO.

Two lakes of contrasting humic content were sampled in the seasonal study, Lake Fiolen (clear water) and Lake Skärshultsjön (humic) (Table 1). The lakes are situated in the region of the South Swedish highlands, close to the limnological field station at Aneboda (the Einar Naumann Laboratory, 57°07′N, 14°34′E), about 30 km north of the city of Växjö. Both lakes are oligotrophic and have a low acid-buffering capacity with a few minor creeks entering the lakes. Lake Fiolen has a comparatively long hydraulic recidence time (4 years), a high transparency (Secchi depth 5–6 m), clear water (10 mg Pt·L^{-1}), and a median DOC content of 5.5 mg·L^{-1}. In contrast with Lake Fiolen, Lake Skärshultsjön may be characterized as a humic lake with a short retention time (7 months), a Secchi depth of less than 2 m, brown water (80 mg Pt·L^{-1}), and a DOC content of approximately 12 mg·L^{-1} (Meili 1992). The lakes have previously been used in other studies of DOC photodegradation (cf. Lindell et al. 1995; Bertilsson and Tranvik 1998; Granéli et al. 1998). Sampling was performed approximately monthly (every 3–5 weeks) during more than a year (May 1995 to September 1996).

Meteorological data (solar radiation per month, mean air temperature, and total precipitation per month) were obtained from the Swedish Meteorological and Hydrological Institute at the nearby Växjö airport, 30 km southeast from the lakes (SMHI 1995, 1996).

Lake water was taken from the epilimnion at the deepest part of each lake using a 2-m-long, 50-mm inside diameter Plexiglas™ tube, which was emptied into a 10-L polyethylene container. The water was stored cold (+4°C) in the dark until measurements of photooxidation were performed (within 1–7 days). Water was pressure filtered stepwise through 142-mm Gelman A/E and 0.2-μm membrane filters (Supor-200™, Gelman Sci.) into 10-L Pyrex bottles. Finally, the water was filter-sterilized under low vacuum (<300 mbar (30 kPa)) directly into quartz or borosilicate tubes (inside diameter = 40 mm, length = 200 mm, volume = 190 mL) using 0.2-μm VacuCap™ filters (Gelman Sci.). Before use, tubes were first washed in dilute hydrochloric acid (1:10) and then thoroughly rinsed in deionized water and either autoclaved or heat-sterilized overnight at 140°C. Borosilicate tubes were wrapped in aluminium foil and were used as dark controls.

We discovered that the silicone stoppers used for sealing the tubes on the seven first sampling occasions (April–October 1995) released LMW carboxylic acids (acetic and formic acids) and also caused a production of DIC upon exposure to UV radiation. We made several tests to evaluate the degree of contamination. We incubated sterile filtered water from both lakes in quartz glass test tubes with stoppers made of both silicone and glass under the same intensity of UV-B and UV-A radiation as was used in the experiments, both in short- (1 day) and long-term (up to 5 days) exposures. Based on these tests, the results of the seven first sampling occasions for DIC and LMW carboxylic acids have been corrected for a silicone contamination approximately corresponding to 3 μg C·L^{-1}·h^{-1} as DIC and 2 μg C·L^{-1}·h^{-1} as LMW carboxylic acids in Lake Fiolen (constituting 30 and 50%, respectively, of photooxidation of DOC into DIC and LMW carboxylic acids in Lake Fiolen). We could not detect any release of organic molecules or DIC production from silicone stoppers in dark controls. For Lake

© 2000 NRC Canada

Fig. 1. Spectral characteristics of the artificial light source used (dashed line) in comparison with natural solar radiation (solid line) in Lund (southern Sweden) at noon close to summer solstice. The transmission spectrum of the Mylar foil used to screen out UV-B radiation is also shown (dashed–dotted line).

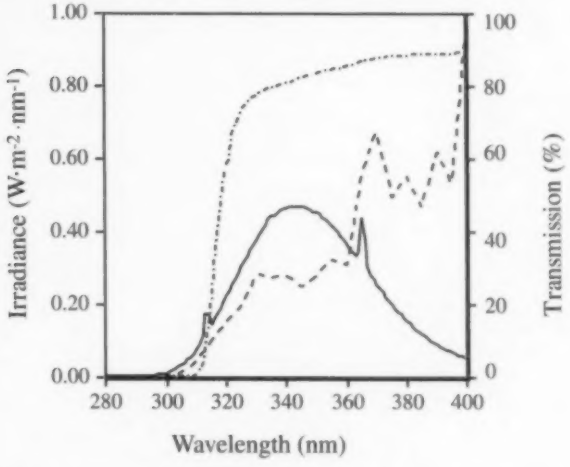

Skärshultsjön water, no significant photorelease from silicone stoppers to the water phase could be verified (probably due to the high photodegradation rates of DOC in water from Lake Skärshultsjön). Still, LMW carboxylic acids and DIC have been corrected as above. We changed to glass stoppers on the eighth sampling occasion (November 1995) and onward, and we strongly recommend that silicone not be used in any experimental setup exposed to light if, for example, organic molecules, DIC, or bacteria are to be studied.

The tubes with lake water were exposed horizontally at 19 ± 1°C, 30 cm beneath eight lamps (UV-A-340, Q-Panel Co.) emitting both UV-B and UV-A radiation. The UV-B radiation (1.91 $W \cdot m^{-2}$) was similar to the natural solar radiation at noon during clear summer conditions in southern Sweden (1.5–2.0 $W \cdot m^{-2}$), but the UV-A radiation (23 $W \cdot m^{-2}$) was slightly lower than natural solar radiation (35 $W \cdot m^{-2}$) due to low emission in the longer UV-A wavelength bands (Fig. 1). The tubes also emit radiation in the photosynthetically active radiation (PAR) wavelength band but at low intensities (<5 $W \cdot m^{-2}$). Incubations lasted for 22 ± 2 h. An exposure of 24 h is equal to UV-B radiation of 170 $kJ \cdot m^{-2}$ and UV-A radiation of 2000 $kJ \cdot m^{-2}$ (total UV radiation of 2170 $kJ \cdot m^{-2}$), approximately corresponding to 7 days of UV-B radiation and 4 days of UV-A radiation during summer in southern Sweden. It should also be noted that the PAR component of solar radiation is active in the photodegradation of DOC (Granéli et al. 1998). Spectral irradiance of the radiation source was measured with a spectroradiometer (model 752, Optronics Lab.) at the beginning of the study (Fig. 1). Any changes in radiation intensities due to ageing of light tubes were followed throughout the study by using a radiometer (IL-1400A, International Light Inc.) connected to broad-band UV-A and a UV-B sensors. Four light tubes were replaced during the period to maintain constant radiation emission from the lamps. One set of samples ($n = 5$) from each lake was exposed to full radiation, a second set was covered with Mylar foil (Du Pont de Nemours®; quality Mylar D™, cutoff at 318 nm) excluding UV-B radiation (Fig. 1), and a third set of tubes was covered with aluminium foil for use as dark controls.

After incubation, the tubes were first used for DIC analysis. At least three DIC measurements were made for each tube, resulting in a coefficient of variation of less than 2% (see Granéli et al. 1996). DIC was calibrated using standard solutions of carbonate in serum bottles.

Sterile filtered water (0.2 µm) for analysis of DOC was transferred into acid-rinsed, precombusted (+500°C overnight) glass vials with Teflon-lined screw caps, stored at 4°C, and analysed no more than 3 days after the irradiation. DOC was analysed by the Pt-catalysed high-temperature combustion method using a Shimadzu TOC-5000 total carbon analyser (Granéli et al. 1996).

The concentrations of some LMW carboxylic acids (acetic, formic, malonic, and oxalic acids) were measured in frozen subsamples using a previously described capillary ion electrophoresis based method (Bertilsson and Tranvik 1998). Duplicate subsamples were analysed on a Quanta 4000 capillary electrophoresis system (Millipore) equipped with a fused silica capillary (75 µm inner diameter). The mobile phase was a 1,2,4,-benzene tricarboxylic acid buffer (pH 7.9) with an electroosmotic flow modifier (0.5 mM). An electrokinetic preconcentration at 5 kV was used to inject samples, and a separation voltage of 15 kV was applied. These settings directed both the electroosmotic flow of the buffer and the flow of analytes towards the capillary outlet, where analytes were detected by universal indirect UV detection at 254 nm. Molybdate was added to all samples as an internal standard, and standard curves (linear regression, $r^2 > 0.99$, $n > 4$) were obtained by spiking selected samples with a concentrated mixed standard solution to obtain final concentrations exceeding maximum concentrations in experimental incubations.

Aliquots of water from the irradiated water and dark controls were used for measurements of absorbance at 250 nm using a Beckman DU®650 spectrophotometer equipped with a 1-cm quartz cuvette.

Humic substance fluorescence was measured using a Shimadzu RF-1501 spectrofluorometer equipped with a 10 × 10 mm quartz cuvette, with excitation at 355 nm and emission at 455 nm (bandwidths = 10 nm). For each series of measurements, fluorescence was calibrated against a 0.01 M quinine sulphate solution in sulphuric acid.

Mean production rates of DIC and the measured LMW carboxylic acids for each treatment were calculated. Observed differences between light and dark treatments were interpreted as photochemical DIC or LMW carboxylic acid production from DOC. The difference between full radiation and Mylar-covered treatments was considered to reflect the effect from UV-B radiation.

The second experiment was performed on sterile filtered water from the two lakes sampled in August 1996. The water was continuously exposed to the same UV radiation source as above (Fig. 1) for up to 11 days (261 h) in order to follow an extended photodegradation of DOC. The radiation dose for this period was UV-B at 1800 $kJ \cdot m^{-2}$ and UV-A at 18 900 $kJ \cdot m^{-2}$. The total exposure period corresponded to approximately 30 days of summertime UV-B and 40 days of corresponding UV-A irradiation under natural sunlight in southern Sweden. Duplicate samples from each lake and treatment were analysed every second day for DIC, DOC, dissolved O_2, fluorescence, and absorbance at 250 nm.

DIC analyses were performed as described above, and tubes were then immediately sampled for dissolved O_2 (Winkler titration). Water was aspirated with a 50-mL syringe connected to a silicone tubing that reached almost to the bottom of the quartz tube. Oxygen reagents were added into the filled syringe with cannulae attached to automatic micropipettes. Dissolved O_2 was analysed after dissolution of the precipitate using automatic potentiometric titration (Granéli and Granéli 1991).

Potential growth of microbes in the tubes during the experiments was monitored by flow cytometric analyses (Becton Dickinson FACSort) of samples preserved in 2% formaldehyde. Cells were stained with the nucleic acid stain SYTO® 13 (Molecular Probes, Eugene, Oreg.), and a standard solution containing fluorescent beads was used as reference (del Giorgio et al. 1996).

Statistical analyses were performed on log-transformed data. We applied ANOVA with Fisher's PLSD post hoc test and linear re-

© 2000 NRC Canada

Table 1. Characteristics of the two studied lakes during May 1995 to August 1996.

	Fiolen	Skärshultsjön
Lake area (km^2)[a] (% of catchment)	1.58 (31%)	0.36 (5%)
Catchment area (km^2)[a]	5.05	8
Forest (%)	50	90
Agriculture (%)	13	5
Pastures (%)	6	1
Bogs (%)	0	4
Retention time (theoretical)[a]	4 years	7 months
DIC ($mg \cdot L^{-1}$)	0.7 (0.5–1.6)	0.4 (0.2–1.9)
DOC ($mg \cdot L^{-1}$)	5.5 (4.1–6.5)	11.9 (8.2–13.6)
Absorbance at 430 nm (cm^{-1})	0.005 (0.003–0.008)	0.031 (0.024–0.042)
pH [b]	6.5	5.5
Fluorescence (QSU)	3.4 (1.2–5.5)	18.8 (5.7–29.2)
Secchi depth (m)[b]	5.5	1.8
Water color (mg $Pt \cdot L^{-1}$)[b]	5	90

Note: Values are medians (maximum and minimum values for the sampling period given in parentheses).
[a]From Bengtsson et al. (1965) and Meili (1992).
[b]From Granéli et al. (1996).

gression, unless otherwise stated. Each tube was considered to constitute one independent sample.

Results

Meteorological conditions and DOM in situ

Spring in 1995 was rainy, with a following summer (July and August) characterized by hot, sunny weather with little precipitation (Fig. 2). At the end of August, solar radiation decreased and remained low (about 20% of summer values) from the end of October 1995 until February 1996. The solar radiation from April through August (spring and summer) constituted approximately 75% of the total radiation per calendar year. The ice cover lasted for 5 months (November 1995 until April 1996) due to an unusually cold, dry, and long winter. The solar radiation increased in spring, with a sunny April, but May 1996 was cloudy with little radiation and high precipitation. The radiation reached normal values at the end of July and remained so through August, but generally, the summer of 1996 was relatively rainy and cold with low sunlight intensities compared with the previous summer (Fig. 2).

DOC in Lake Fiolen varied from 4.1 to 6.5 $mg \cdot L^{-1}$ (median 5.5 $mg \cdot L^{-1}$) and in Lake Skärshultsjön from 8.2 to 13.6 $mg \cdot L^{-1}$ (median 11.9 $mg \cdot L^{-1}$) (Table 1). DOC-specific absorbance (at 250 nm) was rather constant for each individual lake during the complete sampling period but was approximately twice as high in the humic lake compared with the clearwater lake (Fig. 3).

Treatment effects

Generally, samples from the three different treatments (UV-A+B, UV-A, and dark) differed significantly in DIC concentration, fluorescence, and absorbance ($p < 0.0001$). These differences were observed for both lakes and for each individual sampling occasion, with the exception of some sampling occasions in Lake Fiolen, where no significant differences in DIC concentration could be found between UV-A+B-exposed and UV-A-exposed samples (see Fig. 4). Photooxidative DIC production in water from Lake Fiolen (samples exposed to full radiation) varied between 3.5 and 8.9 $\mu g \cdot L^{-1} \cdot h^{-1}$ (median 6.5 $\mu g \cdot L^{-1} \cdot h^{-1}$), and the corresponding rates for Lake Skärshultsjön were between 28.5 and 56.7 $\mu g \cdot L^{-1} \cdot h^{-1}$ (median 47.2 $\mu g \cdot L^{-1} \cdot h^{-1}$) (Table 2; Fig. 4). The production in UV-A-irradiated water from Lake Fiolen corresponded to 57% (median) of DIC production in samples exposed to the total radiation (range 41–73%), while for Lake Skärshultsjön water, the median was 74% (range 62–83%). Thus, for the radiation source used, UV-B radiation was responsible for 43 and 26% of total DIC production in water from Lakes Fiolen and Skärshultsjön, respectively. DIC production was positively related to initial DOC content, fluorescence, and absorbance at 250 nm ($p < 0.005$) in both lakes and for both irradiation treatments (UV-A+B and UV-A alone).

The decrease in DOC could not be measured with the same precision as the increase in DIC (cf. Granéli et al. 1996). In water from Lake Fiolen, we rarely found any significant decrease in DOC after light exposure, and there was no significant correlation between irradiation-induced DIC production and changes in DOC ($p > 0.05$). We did not observe any correlation between DIC production and decreased fluorescence or absorbance at any of the measured wavelengths ($p > 0.05$). On the other hand, the DOC concentrations differed significantly between the UV-irradiated samples and the dark controls in water from Lake Skärshultsjön ($p < 0.001$). There were rarely any significant differences between the two types of irradiation (UV-A+B and UV-A alone). DIC production was positively related to the decrease in DOC in water from Lake Skärshultsjön ($p < 0.0001$) as well as to loss of fluorescence ($p < 0.005$) and loss of absorbance at 250 nm ($p < 0.005$) for this lake.

The pooled concentrations of the four analysed carboxylic acids (oxalic, malonic, formic, and acetic acids) differed significantly between dark controls and the two irradiation treatments for water from both Lakes Fiolen and Skärshultsjön ($p < 0.0001$). Generally, the pooled concentration of these acids in dark controls was less than 10% of the concentration observed in water exposed to full radiation. Among the four analysed carboxylic acids, formic and acetic

© 2000 NRC Canada

Fig. 2. Solar radiation measurements at Växjö airport, situated 30 km southeast from the two sampled lakes, lakes Fiolen and Skärshultsjön. Global radiation represents energy from the complete solar spectrum (300–3000 nm), while sun hours represent the number of hours per month with total solar radiation of more than 120 $W \cdot m^{-2}$ (summertime, normally between 09:00 and 17:00). Arrows indicate approximate date of sampling. Solid lines, 1995–1996; broken lines, average for 1983–1994. (Data from SMHI 1995, 1996.)

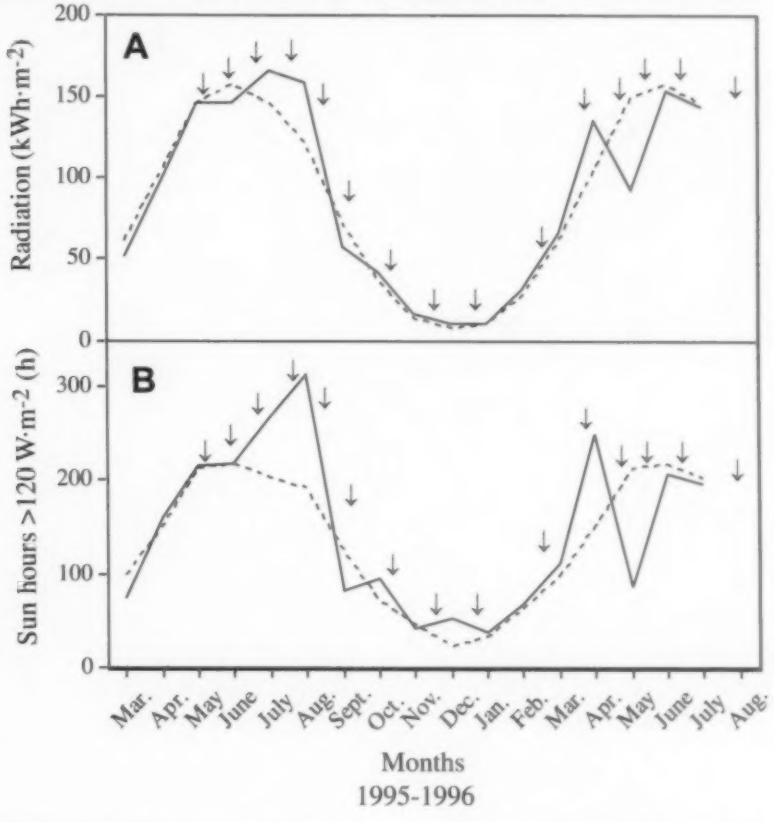

Fig. 3. DOC-specific absorbance of surface water during the sampling period in Lakes Skärshultsjön (squares) and Fiolen (diamonds).

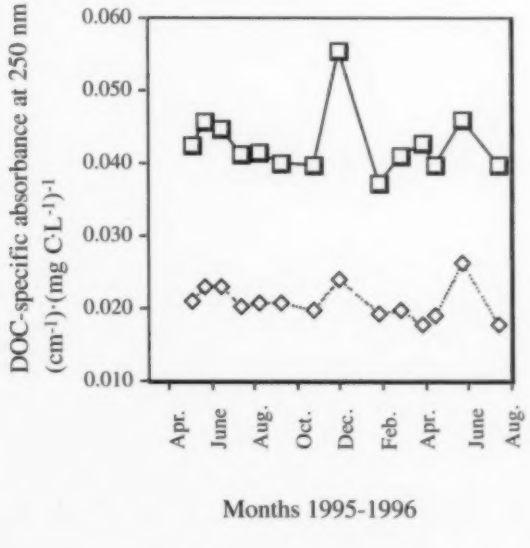

acids were the major intermediates produced (Table 3). Combined, they accounted for approximately 80% of the total carbon retrieved in the four analysed compounds for both Lakes Fiolen and Skärshultsjön (median throughout the sampling period). The pooled production of the four carboxylic acids in water from Lake Fiolen ranged between 1.7 and 3.7 μg $C \cdot L^{-1} \cdot h^{-1}$ (UV-A+B-exposed samples), while for Lake Skärshultsjön, corresponding production rates were between 6.2 and 21.4 μg $C \cdot L^{-1} \cdot h^{-1}$ (Table 2). UV-A radiation alone explained 49% (median) (range 19–83%) of the production in Lake Fiolen water and 62% (median) (range 48–79%) in water from Lake Skärshultsjön.

Seasonal variations in DOC photoreactivity

Photooxidative DIC production and photoproduction of the four measured LMW carboxylic acids varied with sampling occasion for both Lakes Fiolen and Skärshultsjön ($p < 0.0001$). DIC production was lowest in late summer for both lakes, while this rate was higher in winter and early spring (Fig. 4A). This pattern was also observed for carboxylic acid production in Lake Skärshultsjön, while no such strong seasonal pattern was observed for Lake Fiolen (Fig. 5A). DOC-normalized DIC production was 3.2 times higher (median) in Lake Skärshultsjön water compared with water from Lake

© 2000 NRC Canada

Fig. 4. (A) Potential DIC production rates in samples exposed to an artificial light source during May 1995 to August 1996, (B) DOC-normalized rates, and (C) absorbance-normalized (250 nm) rates. Open symbols indicate samples exposed to both UV-A and UV-B radiation, and half-solid symbols indicate Mylar-covered samples (i.e., exposed only to UV-A). The interval for silicone stoppers has been corrected for silicone contamination (see text). Error bars indicate 95% confidence intervals (fell within symbols) of arithmetric means (n = 5).

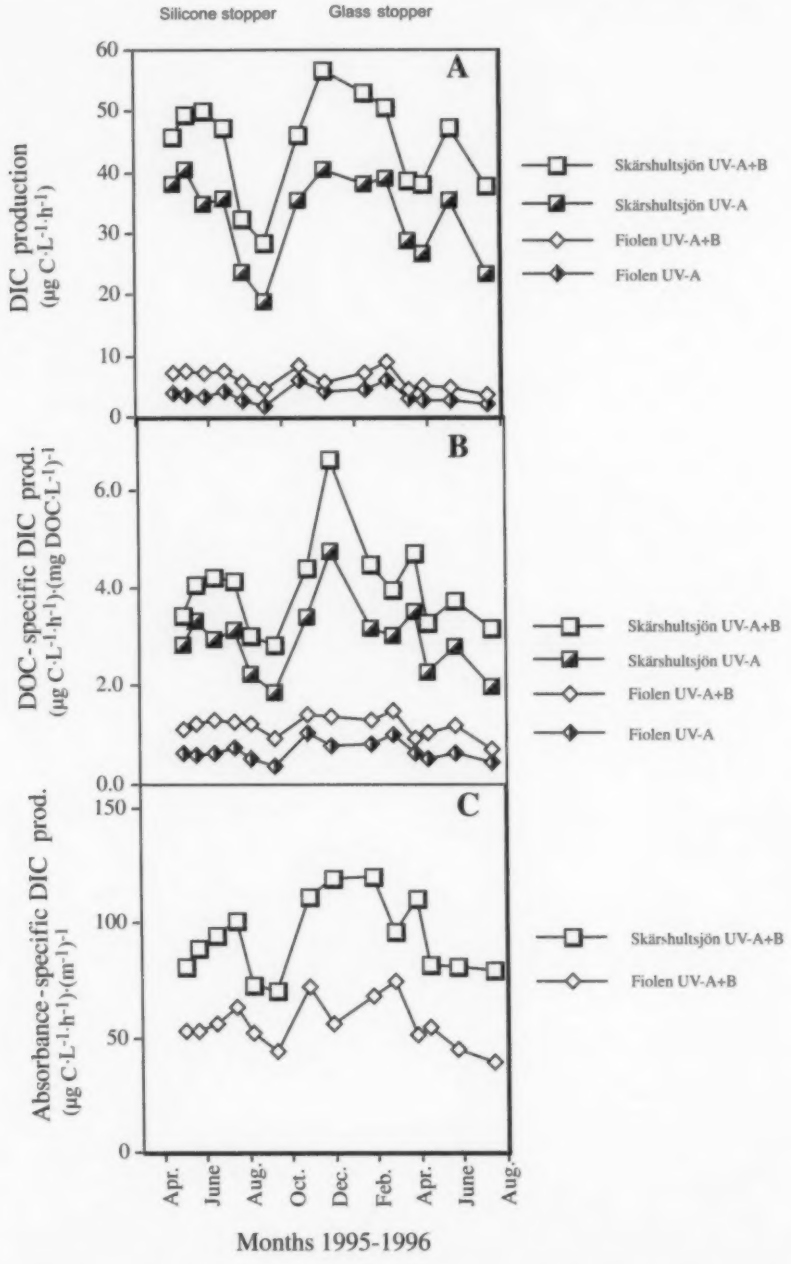

Fiolen (Fig. 4B). The DOC-normalized, pooled production of oxalic, formic, malonic, and acetic acids was approximately 2.7 times higher in water from the humic Lake Skärshultsjön compared with water from the clearwater Lake Fiolen (median through the period) (Fig. 5B). Since the DOC-specific absorbance did not change markedly in any of the lakes during the experimental period (Fig. 3), seasonal trends in DOC- and absorbance-normalized photoproduction of DIC and pooled carboxylic acids were rather similar (cf. Figs. 4 and 5). The normalization for absorbance did, how-

© 2000 NRC Canada

Table 2. Rates of photochemical DIC production, LMW carboxylic acid release, and DOC consumption in UV-A+B-exposed samples of the two investigated lakes during May 1995 to August 1996.

	Fiolen	Skärshultsjön
DIC production (μg $C \cdot L^{-1} \cdot h^{-1}$) ($n$ = 15)	6.5 (3.5–8.9)	47.2 (28.5–56.7)
LMW carboxylic acid production (μg $C \cdot L^{-1} \cdot h^{-1}$) ($n$ = 8)	2.1 (1.7–3.7)	12.9 (6.2–21.4)
DOC consumption (μg $C \cdot L^{-1} \cdot h^{-1}$) ($n$ = 15)	5 (–25–18)	50 (9.5–93)

Note: Values are medians (ranges for the sampling period are given in parentheses).

Table 3. Photoproduction of some LMW carboxylic acids in UV-A+B-exposed samples of the two investigated lakes during May 1995 to August 1996.

	Fiolen	Skärshultsjön
Formic acid (μg $C \cdot L^{-1} \cdot h^{-1}$)	0.97 (0.56–1.86, 41%)	5.86 (2.50–9.98, 46%)
Acetic acid (μg $C \cdot L^{-1} \cdot h^{-1}$)	0.92 (0.54–1.86, 39%)	3.72 (1.68–7.97, 29%)
Malonic acid (μg $C \cdot L^{-1} \cdot h^{-1}$)	0.35 (0.14–0.48, 15%)	2.69 (1.66–3.73, 21%)
Oxalic acid (μg $C \cdot L^{-1} \cdot h^{-1}$)	0.11 (0.00–0.34, 5%)	0.51 (0.28–0.79, 4%)

Note: Values are medians (minimum–maximum range and percentage of total carboxylic acid production for the sampling period are given in parentheses).

ever, even out the differences in photoreactivity between the two lakes.

Long time exposure

In the long time exposure, DIC increased, while dissolved O_2 decreased with increasing light exposure (Fig. 6). For water from Lake Fiolen, DIC had increased by 0.58 $mg \cdot L^{-1}$ at the end of the 11-day incubation, while DOC had decreased by 0.71 $mg \cdot L^{-1}$. Corresponding figures for irradiated water from Lake Skärshultsjön were 3.2 and 3.4 mg $C \cdot L^{-1}$. Approximately 13 and 25%, respectively, of the initial DOC content in the samples from Lakes Fiolen and Skärshultsjön had been photooxidized to DIC after 11 days. These are probably not maximal values for DOC photooxidation to DIC, since DIC increased continously for the Lake Fiolen samples during the course of the incubation, albeit with a decreasing rate (Fig. 6). On the other hand, DIC accumulation ceased abruptly for water from Lake Skärshultsjön after some 100 h of UV exposure, which was likely due to O_2 limitation (Fig. 6). Dissolved O_2 never decreased below 80% saturation in Lake Fiolen, while a 25% O_2 saturation was reached after 100 h of exposure in Lake Skärshultsjön (equal to 8700 $kJ \cdot m^{-2}$). No additional photooxidation was observed after reaching this low O_2 concentration. The pooled data sets from the two lakes were used for comparison between DIC production and O_2 consumption, since the linear relationship between these parameters did not differ between the systems (t test of slopes, $p > 0.05$). The loss of dissolved O_2 after irradiation was linearly correlated with DIC production for the pooled data set ($p < 0.0001$). The molar ratio of O_2 consumption to CO_2 evolution was close to 1 (slope = 0.86, $r^2 = 0.974$). Changes in DIC and O_2 concentrations in the dark controls during the 261-h exposure were small compared with changes in irradiated tubes (Fig. 6).

For both lakes, fluorescence and absorbance at 250 nm decreased markedly with irradiation time, while changes were small in dark controls (Fig. 7). For the pooled data set, a significant correlation was observed between loss of absorbance at 250 nm and loss of fluorescence ($p < 0.005$, $r^2 = 0.92$). Furthermore, both of these parameters were correlated with DIC production ($p < 0.0001$, $r^2 = 0.99$ and 0.94 for fluorescence and absorbance, respectively). No further bleaching of optical properties occurred at the low O_2 concentrations obtained after some 100 h of irradiation of Lake Skärshultsjön water (Fig. 7). For dark controls, changes in absorbance and fluorescence were small compared with irradiated samples.

At the end of the 11-day incubation, we observed small numbers of bacteria in the dark controls. No such growth of bacteria could be observed in irradiated treatments. The numbers of bacteria were always less than 100 000 $cells \cdot mL^{-1}$, and the counted cells were also very small and had a signal close to the detection limit of the flow cytometer. Final cell numbers in the seasonal 24-h incubations were always lower compared with the 11-day experiment. Both DIC and O_2 increased somewhat in dark controls in the long time exposure, contrary to what would have been expected if bacterial respiration had been significant. The increase in DIC and O_2 could be due to a small diffusion of gases into the tubes during the course of the long incubation.

Discussion

Seasonal trends and differences between lakes

Potential of lake water DOC to undergo photodegradation varied throughout the 16-month-long sampling period of the present study. Seasonal changes in potential photodegradation were more noticeable for the humic than for the clearwater lake. Furthermore, photochemical DIC and carboxylic acid formation rates were about eight and six times higher, respectively, in the humic lake. These differences can only partially be explained by the twofold higher DOC concentration in Lake Skärshultsjön. In addition, the quality of the organic matter and in particular the DOC-specific UV absorbance would be a plausible regulator of photochemical reaction rates, since the absorption of photons is a prerequisite for photochemical reactions to occur. Accordingly, a normalization for absorbance at 250 nm decreased the apparent differences in photochemical reactivity between Lakes Skärshultsjön and Fiolen markedly, even if seasonal variations were not affected to any major extent. In conclusion, neither DOC nor absorbance could satisfactorily

© 2000 NRC Canada

Fig. 5. (A) Potential production rates of pooled oxalic, malonic, formic, and acetic acids in samples exposed to an artificial radiation source during May 1995 to August 1996, (B) DOC-normalized rates, and (C) absorbance-normalized (250 nm) rates. Open symbols indicate samples exposed to both UV-A and UV-B radiation, and half-solid symbols indicate Mylar-covered samples (i.e., exposed only to UV-A). Error bars (occassionally hidden in the symbols) are 95% confidence intervals of aritmetric means (n = 3). Note that only every second sampling occassion has been analysed.

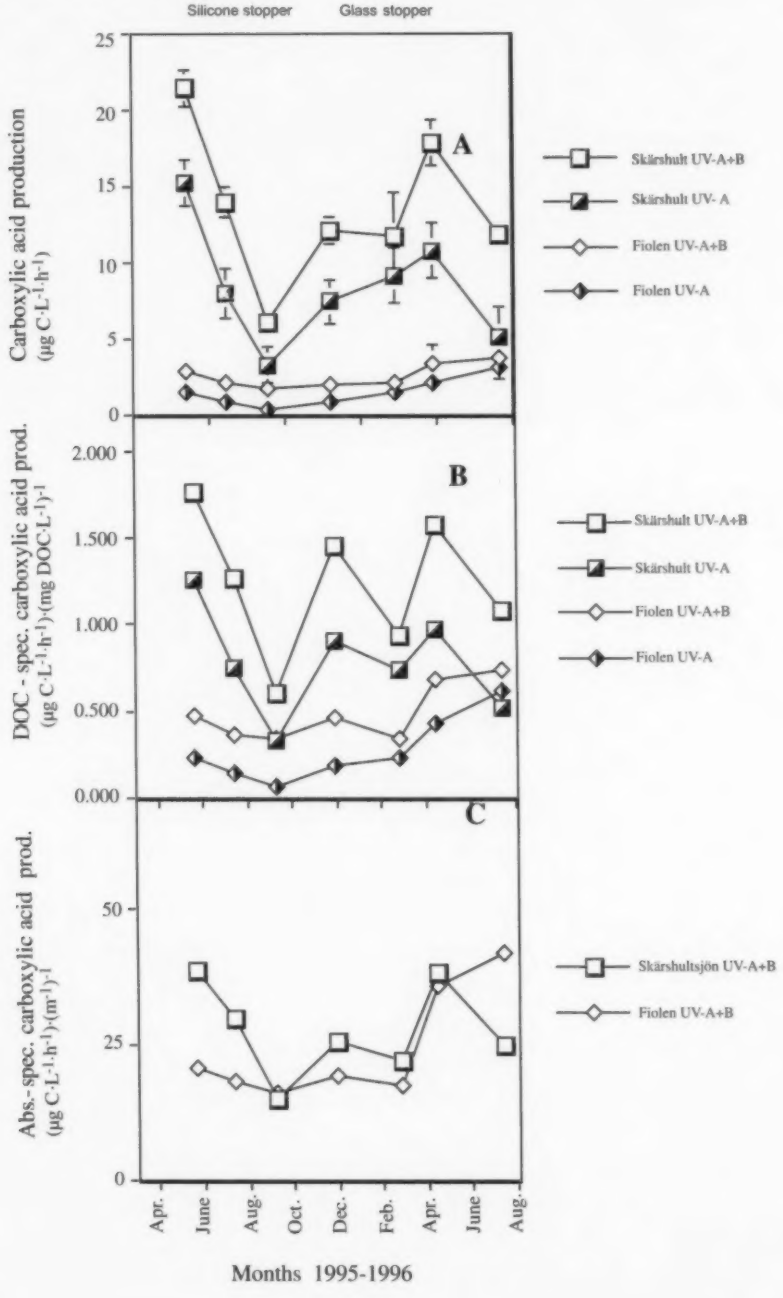

explain within-lake changes in photochemical reactivity potential but could be useful for evaluation of cross-system differences.

The observation that DOC may have variable photosensitivity, not only between systems of different humic content but also during a season within a single lake, is in accordance with Clair and Sayer (1997), who observed similar seasonal trends in chromophoric groups in DOC from

© 2000 NRC Canada

Fig. 6. DIC and dissolved O_2 for samples from lakes Skärshultsjön and Fiolen in relation to duration of continuous long-term irradiation. Squares represent DIC concentrations and circles dissolved O_2. Solid symbols represent dark-incubated samples and open symbols represent samples incubated in UV-A+B radiation. Dashed lines were drawn by eye, while continous lines were best fits (linear or second-order polynomial).

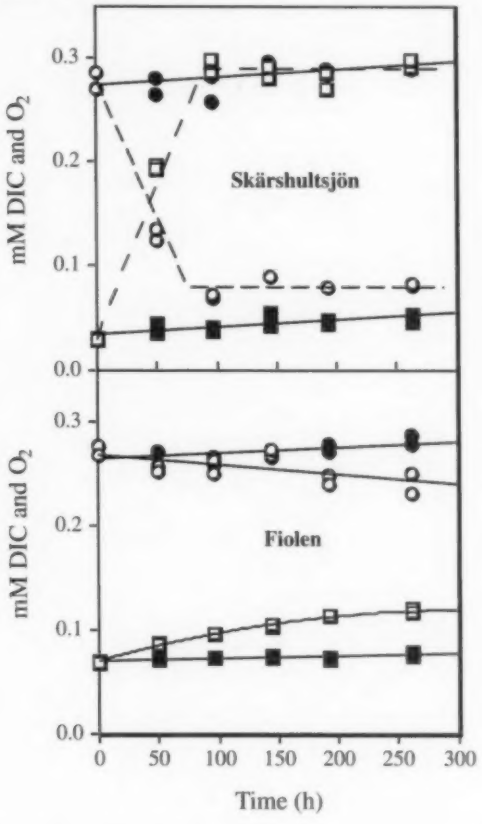

Fig. 7. Absorbance at 250 nm and fluorescence for long-term-incubated samples under continous UV radiation. Squares represent data points for Lake Fiolen samples, and circles retresent data for Lake Skärshultsjön samples. Solid symbols represent dark-incubated controls and open symbols represent samples incubated in UV-A+B radiation. Dashed lines were drawn by eye, while continous lines were best fits (linear).

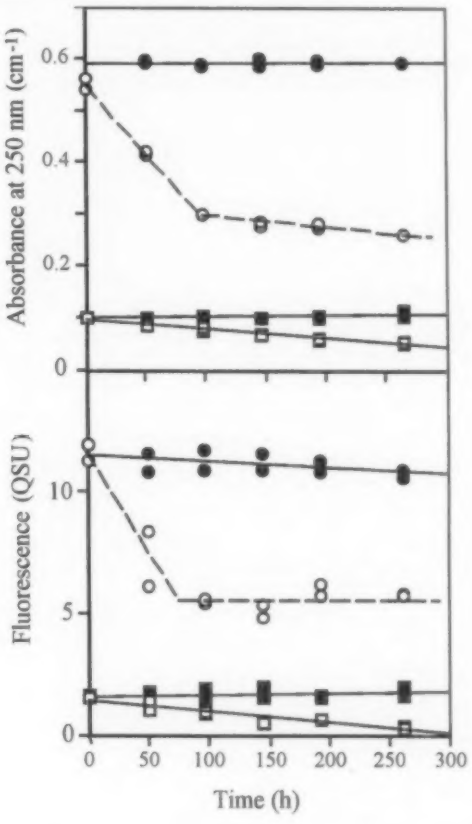

Canadian lakes. One possible reason for the observed variation in photoreactivity could be that a prolonged exposure to solar radiation might result in a gradual increase in the fraction of more photorecalcitrant DOC (Thomas and Lara 1995), presumably of low bacterial availability (Geller 1986; Lindell et al. 1995). Hence, the longer the hydraulic residence time, the longer the exposure of each individual organic molecule to solar radiation. The consequences for Lake Fiolen, which has a relatively long hydraulic recidence time (4 years), would be a low DOC-specific photoreactivity in the surface layer. This is in agreement with the results obtained in the present study. This is also in accordance with earlier studies in some Canadian lakes, where long residence times were correlated with a decrease in DOC-specific absorbance and fluorescence (Curtis and Schindler 1997). Still, the suggested importance of hydraulic residence time in the present study is based on results from no more than two lakes, and we do not highlight other potentially important variables, such as differences in DOC origin as well as the more detailed quality of the organic material.

Granéli et al. (1996) measured depth-integrated photooxidation rates in Lake Fiolen, Lake Skärshultsjön, and some other lakes of varying humic content. They found that depth-integrated DIC production was similar among most studied lakes, irrespective of humic content. This may seem contradictory given the lower DOC-specific photoreactivity reported for the oligohumic lake in the present study. However, the results in the present study only consider surface processes, while the study of Granéli et al. (1996) involved in situ incubations at several depths during a whole summer day, thus taking into account the vertical attenuation of sunlight, which is not the focus of the present study. The lower rate of photooxidation at the surface of the clear lake is compensated for by a much deeper layer of photooxidation.

DIC production and O_2 consumption

In the extended exposure experiment, photochemical O_2 consumption was proportional to DOC content, and the molar O_2 consumption to CO_2 evolution ratio was close to 1 (0.84). This is in agreement with earlier studies (Miles and Brezonik 1981; Lindell and Rai 1994). In Lake Skärshultsjön, DIC production and O_2 consumption continued

© 2000 NRC Canada

until dissolved O_2 concentration reached 25% of saturation. Below 25% saturation, no photooxidation could be detected. Oxygen availability appears to be a limiting factor for photodegradation of DOC (Miles and Brezonik 1981; Lindell and Rai 1994). This could explain the observed decrease in photoproduction of DIC for Lake Skärshultsjön after the prolonged exposure in experimental enclosures. However, such an O_2 depletion effect would not influence the photoreactivity rates obtained in the seasonal study to any larger extent, since employed incubation times in the seasonal study were significantly shorter (22 ± 2 h).

Photoproduction of LMW carboxylic acids

The average pooled photoproduction of oxalic, malonic, formic, and acetic acids in water from Lakes Fiolen and Skärshultsjön was close to 30% of the DIC photoproduction (in carbon units). Thus, photooxidation of DOC to DIC (Salonen and Vähätalo 1994; Granéli et al. 1996) appears to be a quantitatively dominant process compared with photoproduction of biologically labile LMW substrates. Still, the amount of LMW substrates produced relative to DIC was probably an underestimate, since we only measured the photoproduction of four different LMW carboxylic acids (oxalic, malonic, formic, and acetic acids). Several additional LMW organic acids, as well as other LMW organic molecules, are also likely to be formed photochemically (Kieber et al. 1990; Wetzel et al. 1995; Corin et al. 1996; Moran and Zepp 1997). Therefore, the reported quantities of photochemically produced LMW organic substances are likely underestimates.

The production of LMW carboxylic acids was generally highest in spring with a lower photoreactivity potential during the summer season. These results support previously reported observations of an irradiation-induced stimulation of bacterial secondary growth in lake water collected during early summer, while no such effects could be observed later in the season (Geller 1986). Lindell et al. (1995) observed a strong increase in bacterial growth potential after exposing humic lake water to artificial UV radiation. However, a plateau in the bacterial growth response was reached after a prolonged exposure, with no further increase in growth potential. According to Wetzel et al. (1995), these combined findings may be explained by an initially high but rapidly diminishing photorelease of LMW organic substances, potentially involving a sequential, further photooxidation of formed LMW substances into inorganic forms. Indeed, photochemically produced oxalic acid can easily be oxidized further into DIC (Kulovaara and Backlund 1993; Bertilsson and Allard 1996; Bertilsson and Tranvik 1998). In the present study, oxalic acid generally comprised less than 5% of the total carbon retrieved in the analysed LMW carboxylic acids. The samples were exposed for 22 ± 2 h, a period that could be long enough for a complete oxidation of photochemically released oxalic acid (Bertilsson and Tranvik 1998). The detailed study of such a process was beyond the scope of the present study, but it should be acknowledged that such further photooxidation processes might influence measured photoproduction rates of LMW organic substances relative inorganic forms (Moran and Zepp 1997). If bacteria were present during the exposure, a fraction of such photolabile LMW organic substances could be assimilated before being further photooxidized to DIC.

The analysed acids are readily available substrates for heterotrophic bacterial utilization in pelagic environments (Robinson et al. 1973; Wetzel et al. 1995; Bertilsson and Tranvik 1998), and a significant photochemical production of these compounds could positively influence bacterial activity and abundance. In contrast, the photochemical formation of DIC could represent a removal of potential substrates from the organic carbon pool, with an associated negative effect on bacterial growth. Thus, bacterial growth response to solar radiation might be a complex interaction between several concurrent photoreactions.

Relative importance of spectral wavelength bands

The relative effects of UV-B irradiation on photooxidation and photoproduction of LMW carboxylic acids varied between 25 and 50% (Figs. 4 and 5). This production is considerable, taking into account the low total energy in UV-B compared with UV-A radiation. These results are consistent with the findings of Granéli et al. (1998), who reported that 30% of total UV-mediated DIC production could be related to UV-B in waters exposed to natural solar radiation. However, none of these calculations include the effects of PAR, which, together with UV-A, may account for more than 80% of the photochemical oxidation of DOC into DIC in lake water under natural sunlight (Granéli et al. 1998). Indeed, PAR alone may account for roughly twice the photochemical DIC production originating from UV-B irradiation. UV-B radiation was more important for photochemical DIC production in water from Lake Fiolen compared with Lake Skärshultsjön (average 43 and 26%, respectively, of total production), which could be due to a higher proportion of relatively photorecalcitrant DOM in Lake Fiolen. Such DOM may need the more energy-rich UV-B photons to become photooxidized compared with the relatively "fresh" and thus photoreactive DOM in Lake Skärshultsjön, which may be photooxidized by the less energy-rich UV-A photons.

Conclusions

Our findings have several implications for the assessement of the importance of photochemical reactions occurring in lakes. We showed that the potential for complete photooxidation and photochemical carboxylic acid production varies seasonally, being highest in late winter and spring (cf. Figs. 4 and 5). We also showed that the carbon-specific photoreaction potential of DOC in a humic lake was higher compared with a clearwater lake. The systems differed in that the humic system had a considerably shorter retention time and a higher input of allochthonous organic material. We therefore suggest that the origin of DOC as well as the past light history are two important regulators of the potential of DOC to undergo photoreactions. Thus, solar radiation could be a significant regulator of the recalcitrance of DOC, and such an effect would be most pronounced in clear waters with long retention times and an associated extensive light treatment of DOC in situ.

Acknowledgements

Financial support from the Swedish Natural Science Re-

© 2000 NRC Canada

search Council to H. Wilhelm Granéli (G-AA/GU 04969-315) and to Stefan Bertilsson (G-AA/GU 03596-314 grants to Bert Allard) are gratefully acknowledged. Additional financial support was also given by the EC-WET project to Måns J. Lindell. Several people helped with sampling and analysis, among whom Alexandre Magno Anesio, Måns Denward, and Lars Tranvik are especially acknowledged. Dr. P.E.K. Symons and two anonymous referees had constructive comments on earlier versions of the manuscript. Dr. Tom Nielsen kindly helped us with spectral measurements in the laboratory.

References

Amon, R.M.W., and Benner, R. 1996. Bacterial utilisation of different size classes of dissolved organic matter. Limnol. Oceanogr. **41**: 41–51.

Bengtsson, R., Karlberg, S., and Müller, C. 1965. Excursion guide to the Aneboda area. Lund University, Lund, Sweden. (In Swedish.)

Bertilsson, S., and Allard, B. 1996. Sequential photochemical and microbial degradation of refractory dissolved organic matter in a humic freshwater system. Arch. Hydrobiol. Adv. Limnol. **48**: 133–141.

Bertilsson, S., and Tranvik, L.J. 1998. Photochemically produced carboxylic acids as substrates for frshwater bacterioplankton. Limnol. Oceanogr. **43**: 885–895.

Chrost, R.H., and Faust, M.A. 1983. Organic carbon release by phytoplankton: its composition and utilization by bacterioplankton. J. Plankton Res. **4**: 477–493.

Clair, T.A., and Sayer, B.G. 1997. Environmental variability in the reactivity of freshwater dissolved organic carbon to UV-B. Biogeochemistry, **36**: 89–97.

Cole, J.J., Caraco, N.F., Kling, G.F., and Kratz, T.K. 1994. Carbon dioxide supersaturation in the surface waters of lakes. Science (Washington, D.C.), **265**: 1568–1570.

Corin, N., Backlund, P., and Kulovaara, M. 1996. Degradation products formed during UV-irradiation of humic waters. Chemosphere, **33**: 245–255.

Curtis, P.J., and Schindler, D.W. 1997. Hydrologic control of dissolved organic matter in low-order Precambrian Shield lakes. Biogeochemistry, **36**: 125–137.

del Giorgio, P.A., Bird, D.F., Prairie, Y.T., and Planas, D. 1996. Flow cytometric determination of bacterial abundance in lake plankton with the green nucleic acid stain SYTO 13. Limnol. Oceanogr. **41**: 783–789.

Fenchel, T., and Blackburn, T.H. 1979. Bacteria and mineral cycling. Academic Press, London, U.K.

Geller, A. 1986. Comparison of mechanisms enhancing biodegradability of refractory lake water constituents. Limnol. Oceanogr. **31**: 755–764.

Granéli, W., and Granéli, E. 1991. Automatic potentiometric determination of dissolved oxygen. Mar. Biol. **108**: 341–348.

Granéli, W., Lindell, M.J., and Tranvik, L.J. 1996. Photooxidative production of dissolved inorganic carbon in lakes of different humic content. Limnol. Oceanogr. **41**: 698–706.

Granéli, W., Lindell, M.J., de Faria, B.M., and Estevez, F. 1998. Photoproduction of dissolved inorganic carbon in temperate and tropical lakes — dependence of wavelength band and dissolved organic carbon concentration. Biogeochemistry, **43**: 175–195.

Keil, R.G., and Kirchman, D.L. 1994. Abiotic transformation of labile protein to refractory protein in sea water. Mar. Chem. **45**: 187–196.

Kieber, R.J., Zhou, X., and Mopper, K. 1990. Formation of carbonyl compounds from UV-induced photodegradation of humic substances in natural waters: fate of riverine carbon in the sea. Limnol. Oceanogr. **35**: 1503–1515.

Kulovaara, M., and Backlund, P. 1993. Effects of simulated sunlight on aquatic humic matter. Vatten, **49**: 100–103.

Lindell, M.J., and Rai, H. 1994. Photochemical oxygen consumption in humic waters. Arch. Hydrobiol. Beih. Ergeb. Limnol. **43**: 145–155.

Lindell, M.J., Granéli, W., and Tranvik, L. 1995. Enhanced bacterial growth in response to photochemical transformation of dissolved organic matter. Limnol. Oceanogr. **40**: 195–199.

Meili, M. 1992. Sources, concentrations and characteristics of organic matter in softwater lakes and streams of the Swedish forest region. Hydrobiologia, **29**: 23–41.

Miles, C.J., and Brezonik, L. 1981. Oxygen consumption in humic-colored waters by a photochemical ferrous–ferric catalytic cycle. Environ. Sci. Technol. **15**: 1089–1095.

Miller, W.L., and Zepp, R.G. 1995. Photochemical production of dissolved inorganic carbon from terrestrial organic matter: significance to the oceanic organic carbon cycle. Geophys. Res. Lett. **22**: 417–420.

Moran, M.A., and Zepp, R.G. 1997. Role of photreactions in the formation of biologically labile compounds from dissolved organic matter. Limnol. Oceanogr. **42**: 1307–1316.

Naganuma, T., Konish, S., Inoue, T., Nakane, T., and Sukizaki, S. 1996. Photodegradation or photoalteration? Microbial assay of the effect of UV-B on dissolved organic matter. Mar. Ecol. Prog. Ser. **135**: 309–310.

Robinson, G.G.C., Hendzel, L.L., and Gillespie, D.C. 1973. A relationship between heterotrophic utilization of organic acids and bacterial populations in West Blue Lake, Manitoba. Limnol. Oceanogr. **18**: 264–269.

Salonen, K., and Vähätalo, A. 1994. Photochemical mineralisation of dissolved organic matter in Lake Skjervatjern. Environ. Int. **20**: 307–312.

Schindler, D.W., Curtis, P.J., Bayley, S.E., Parker, B.R., Beaty, K.G., and Stainton, M.P. 1997. Climate-induced changes in the dissolved organic carbon budgets of boreal lakes. Biogeochemistry, **36**: 9–28.

Scully, N.M., McQuenn, D.J., Lean, D.R.S., and Cooper, W.J. 1996. Hydrogen peroxide formation: the interaction of ultraviolet radiation and dissolved organic carbon in lake waters along a 43–75°N gradient. Limnol. Oceanogr. **41**: 540–548.

SMHI. 1995. Väder och Vatten. Väderåret 1995. Swedish Meterologic and Hydrological Institute. CA Tryck AB Norrköping, Sweden. (In Swedish.)

SMHI. 1996. Väder och Vatten. Väderåret 1996. Swedish Meteorologic and Hydrological Institute. CA Tryck AB Norrköping, Sweden. (In Swedish.)

Thomas, D.N., and Lara, R.J. 1995. Photodegradation of algal derived dissolved organic carbon. Mar. Ecol. Prog. Ser. **116**: 309–310.

Tranvik, L. 1990. Bacterioplankton growth on fractions of dissolved organic carbon of different molecular weights from humic and clear waters. Appl. Environ. Microbiol. **56**: 1672–1677.

Valentine, R.L., and Zepp, R.G. 1993. Formation of carbon monoxide from the photodegradation of terrestrial dissolved organic carbon in natural waters. Environ. Sci. Technol. **27**: 409–412.

Wetzel, R.G., Hatcher, P.G., and Bianchi, T.S. 1995. Natural photolysis by ultraviolet irradiance of recalcitrant dissolved organic matter to simple substrates for rapid bacterial metabolism. Limnol. Oceanogr. **40**: 1369–1380.

© 2000 NRC Canada

Bias in survival estimates from tag-recovery models where catch-and-release is common, with an example from Atlantic striped bass (*Morone saxatilis*)

David R. Smith, Kenneth P. Burnham, Desmond M. Kahn, Xi He, Cynthia J. Goshorn, Kathryn A. Hattala, and Andrew W. Kahnle

Abstract: Survival rate is underestimated when tag-recovery models include tags recovered from harvested and caught-and-released fish. The magnitude of the bias depends on tag-recovery rate, proportion of catch released alive, and reporting rate; changes in these factors over time confound temporal changes in survival. The bias is of potential concern for any tagging study where catch-and-release is mandatory or practiced voluntarily. The bias is of concern particularly for the Atlantic striped bass (*Morone saxatilis*) tagging study where catch-and-release is common and anglers commonly remove the tag upon capture regardless of fish disposition. Biased estimates of striped bass survival did not change with changes in harvest regulation during the mid-1990s. However, bias-adjusted estimates of survival showed a decrease, which corresponds to the regulatory change made in 1995. Year-specific reporting rate is critical to bias adjustment, underscoring the need for reward tags in fish tagging studies. Tag-recovery modeling allows for a diverse set of models, each of which can produce widely different estimates with far-reaching consequences for management. We applied model averaging to base inference on a weighted average of parameter estimates and to account for model selection uncertainty.

Résumé : Le taux de survie est sous-estimé lorsque les modèles de récupération des marques incluent les marques récupérées sur des poissons capturés et sur des poissons remis à l'eau. L'ampleur du biais dépend du taux de récupération des marques, de la proportion des poissons pris qui sont remis à l'eau vivants et du taux de déclaration; des changements dans ces facteurs au fil du temps brouillent les changements temporels dans la survie. Le biais peut causer des problèmes dans une étude de marquage lorsque la remise à l'eau est obligatoire ou pratiquée de façon volontaire. Ce biais est particulièrement préoccupant dans l'étude de marquage du bar rayé (*Morone saxatilis*) de l'Atlantique, car la remise à l'eau est courante, et les pêcheurs enlèvent généralement la marque du poisson dès la capture, qu'ils gardent ou non le poisson. Les estimations biaisées de la survie du bar rayé n'ont pas changé malgré la modification du règlement de capture au milieu des années 90. Toutefois, les estimations de la survie ajustées en fonction du biais ont montré une baisse, ce qui correspond aux changements dans la réglementation adoptés en 1995. Le taux de déclaration d'une année donnée est critique pour l'ajustement en fonction du biais, ce qui fait ressortir la nécessité de donner des primes en échange des marques dans les études de marquage des poissons. La modélisation de la récupération des marques permet d'avoir recours à des modèles divers, dont chacun peut produire des estimations très différentes, ce qui peut avoir des conséquences d'une grande ampleur dans la gestion. Nous avons appliqué un moyennage aux modèles pour fonder nos inférences sur la moyenne pondérée des estimations des paramètres et pour prendre en compte l'incertitude dans le choix du modèle.

[Traduit par la Rédaction]

Received August 24, 1999. Accepted January 5, 2000.
J15329

D.R. Smith.[1] U.S. Geological Survey, Biological Resources Division, Leetown Science Center, 1700 Leetown Road, Kearneysville, WV 25430, U.S.A.
K.P. Burnham. U.S. Geological Survey, Colorado Cooperative Fish and Wildlife Research Unit, Colorado State University, Fort Collins, CO 80523, U.S.A.
D.M. Kahn. Delaware Division of Fish and Wildlife, P.O. Box 330, Little Creek, DE 19961, U.S.A.
X. He.[2] Division of Marine Fisheries, 30 Emerson Avenue, Gloucester, MA 01930, U.S.A.
C.J. Goshorn. Maryland Department of Natural Resources, 580 Taylor Avenue, Annapolis, MD 21401, U.S.A.
K.A. Hattala and A.W. Kahnle. New York State Department of Environmental Conservation, Hudson River Fisheries, 21 S. Putt Corners Road, New Paltz, NY 12561, U.S.A.

[1]Author to whom all correspondence should be addressed. e-mail: david_r_smith@usgs.gov
[2]Present address: CSIRO Marine Research, GPO Box 1538, Hobart, Tasmania 7001, Australia.

© 2000 NRC Canada

Introduction

Brownie et al. (1985) published an influential handbook that presented methods of tag-recovery modeling and synthesized important early work. Hunted populations of waterfowl provided much of the motivation for Brownie et al. (1985). However, lake trout (*Salvelinus namaycush*) was the focus during early development of tag-recovery models (Youngs and Robson 1975), and the methods of Brownie et al. (1985) have been applied and extended to studies of fish populations (e.g., Schwarz and Arnason 1990; Dorazio 1993; Hoenig et al. 1998*b*). One important difference between waterfowl and fish populations involves the disposition of recaptured animals. Although the tag-recovery process for waterfowl (i.e., hunting) results only in dead recoveries, the recovery process for fish can result in dead recoveries (i.e., harvest) or live recaptures (i.e., catch-and-release). The extent of live recaptures (i.e., live release after tag recovery) in a fish tagging study depends on fishing methods and regulations. Analysis of tag recoveries that include live recaptures violates an underlying assumption of the tag-recovery models: the fate of the tag corresponds to the fate of the fish. If a tag is recovered (i.e., the tag "dies") and the recaptured fish is released (i.e., the fish lives), then the connection between the tag and fish is broken. This limitation of tag-recovery models was recognized early on by Youngs and Robson (1975, p. 2365) who stated that "this model is appropriate only for recaptures that are removed from the population."

We were motivated by analysis of Atlantic striped bass (*Morone saxatilis*) tagging data to assess bias in tag-recovery estimates when live recaptures are treated as dead recoveries. Although there are other tagging programs, we have been involved in the cooperative state and federal tagging effort initially funded through the "Emergency Striped Bass Study" (Richards and Rago 1999). In this program, anglers commonly remove the tag, regardless of the disposition of the recaptured fish, prior to reporting the tag's number to the U.S. Fish and Wildlife Service. Tag removal promotes accurate reporting of the tag's number. Unfortunately, tag removal from live recaptures also causes a lack of correspondence between the fate of the tag and the fate of the striped bass. Tag-recovery models have been applied to these data to estimate survival of striped bass, although some tags were recovered from fish caught and released alive (Dorazio 1993, 1997).

Youngs and Robson (1975) ignored live recaptures in their analysis of angler tag recoveries. Their strategy applied to Atlantic striped bass would lead to ignoring a significant amount of data, especially during years when harvest was severely restricted. Burnham (1991) and Barker (1997) developed models to analyze simultaneously dead recoveries and live recaptures. However, the models do not allow for the removal of the tag prior to release, as is the case for the Atlantic striped bass and, perhaps, other tagging programs. Bias in survival estimates based on tag recoveries pooled from both harvested and released fish has not been assessed previously. This bias is of potential concern for any fish tagging study where anglers practice catch-and-release or where regulations on fish length or fishing season cause a portion of the catch to be released.

The purpose of this paper is to discuss estimation of survival and mortality from tag-recovery data, with emphasis on bias due to tags recovered from fish caught and released. We begin with a brief review of the basic tag-recovery model and follow with discussion of a recently presented model selection technique, called model averaging (Burnham and Anderson 1998), and its application to tag-recovery modeling. (Through model averaging, inference is not conditional on one "best" model, but rather, estimates are weighted across a set of models and model selection uncertainty is incorporated as a variance component.) We then derive formulae for the bias due to recovery of tags from live recaptures, and we present methods to assess the bias. We apply the methods to estimate survival and mortality for Atlantic coast striped bass tagged in the Hudson River, the Maryland portion of the Chesapeake Bay, and the Delaware River during the period 1988–1997.

Materials and methods

Basic tag-recovery models

The building blocks of tag-recovery models are the expected probabilities of tag recoveries, which arise from the potential fates of tagged animals. After release of a tagged fish in year i, a tag is recovered during year $j = i, i + 1, i + 2$, and so on until the final year of the study or the tag is not recovered at all. The expected probability (π_{ij}) that a tag is released in year i and recovered in year j is modeled as a function of annual survival and recovery rates. This relationship provides the basis for estimating animal survival (or its complement, mortality) from tag releases and recoveries. In the models presented by Brownie et al. (1985), the recovery rate, which is interpreted as a measure of sampling intensity, is a function of tagging-induced mortality, tag retention, catch rate, and tag reporting rate (Hoenig et al. 1998*a*).

Consider a simple model where survival (S) and recovery rates (f) are equal among years, N_i fish are tagged and released in year i, and all fish caught are killed. For a tag to be recovered during the first year after release, the tagged fish must survive the tagging process with tag intact, be caught, and have its tag reported (i.e., $\pi_{i,i} = f$). For the tag to be recovered during the second year, the tagged fish must survive the first year after release with tag intact and then be recovered (i.e., $\pi_{i,i+1} = S \cdot f$). For the tag to be recovered during the third year, the tagged fish must survive the first and the second year after release with the tag intact and then be recovered (i.e., $\pi_{i,i+2} = S \cdot S \cdot f$). In this way, a tag-recovery model is developed and could be generalized to allow survival and recovery rates to vary, by time for example.

By releasing multiple batches (or cohorts) of tagged fish and making certain assumptions (such as tagged cohorts share the same recovery and survival rates, and fates of tagged fish are independent) the set of releases $\{N_i\}$ and recoveries $\{R_{ij}\}$ can be modeled using a product multinomial distribution with likelihood function

$$(1) \qquad L(\pi_{ij}; R_{ij}, N_i) = \prod_{i=1}^{k} \left[\binom{N_i}{R_{ii}, \ldots, R_{il}, R_{i,l+1}} \right] \prod_{j=i}^{l+1} \pi_{ij}^{R_{ij}}$$

The π_{ij} in the likelihood function are the expected probabilities of recovery and are functions of the recovery and survival rates (f_j and S_j). This model representing a theoretical expectation can be compared with the number of tags released in year i and recovered in year j (R_{ij}). Consequently, the maximum likelihood estimates are those values of S and f that maximize the likelihood function. Brownie et al. (1985) listed the important assumptions underlying these models.

© 2000 NRC Canada

Fig. 1. Potential fates of tagged fish alive at the start of the tagging occasion. Fishing capture probability is denoted by c, and K denotes probability that a caught fish is killed. Survival probabilities of fish caught but rereleased and fish never caught are denoted by S_c and S_{nc}, respectively.

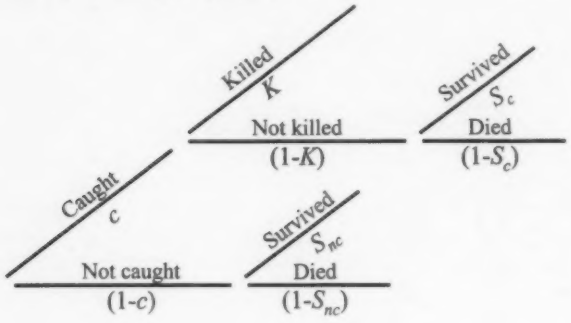

Model averaging

The basic tag-recovery model is generalized by allowing parameters to vary across time, space, and demographic characteristics. The result is a set of candidate models, some of which will be selected for estimation of survival rates. The approach for model selection presented by Brownie et al. (1985) combines goodness-of-fit (GOF) statistics with likelihood ratio tests (LRT) to arrive at a "best-fitting" model. However, there are a couple of shortcomings with this approach. First, LRT can be used only with "nested" models. A thorough analysis will often include models that are not nested. Second, it is common for more than one model to be equal, or essentially equal, in their fit to the data, which frustrates the goal of selecting the "best" model.

Recent work indicates that greater reliance should be placed on other measures of model fit that are useful for nonnested models, e.g., Akaike's information criteria (AIC), over LRTs for model selection (Burnham et al. 1995). Also, Buckland et al. (1997) considered the problem of model selection and presented methods to estimate parameters by a weighted average of the "better-fitting" models, with the weights being a function of the AIC (also see Burnham and Anderson 1998). Thus, by use of model averaging, the need to select one model for estimating parameters is avoided and model selection uncertainty is incorporated into the variance of parameter estimates.

Estimates of model-averaged survival rates are obtained by (Buckland et al. 1997)

$$(2) \qquad \hat{S}_t = \sum_{i=1}^{C} w_i \hat{S}_{t,i}$$

where $\hat{S}_t$ is estimated survival rate for year t, C is total number of candidate models, $\hat{S}_{t,i}$ is estimated survival rate for year t and model i, and w_i is relative weight for model i. Buckland et al. (1997) recommend that the weight be a function of the AIC. The number of estimable parameters and model likelihood are used to compute the AIC for a given model by AIC = $-2 \ln L + 2np$, where $\ln L$ is the natural log of the likelihood and np is the number of estimated model parameters. Then the weight w_i is calculated by

$$(3) \qquad w_i = \frac{e^{-\frac{\Delta AIC_i}{2}}}{\sum_{j=1}^{C} e^{-\frac{\Delta AIC_j}{2}}}$$

where ΔAIC_i is the difference between the AIC for the ith model and the minimum AIC, $i = 1,\ldots, C$ (Burnham and Anderson 1998). Thus, the better the model fit, the smaller the AIC and the larger the value of w_i. Burnham and Anderson (1998) used the term "Akaike weight" for w_i and recommended AICc, a small-sample version of AIC, which is compatible with model averaging.

An approximate standard error for $\hat{S}_t$ is given by Buckland et al. (1997):

$$(4) \qquad \sigma_t = \sum_{i=1}^{C} w_i (V_{t,i} + [\hat{S}_{t,i} - \hat{S}_t]^2)^{1/2}$$

where $V_{t,i}$ is estimated variance from model i. We computed approximate $(1 - \alpha)$% confidence intervals based on a logit transformation of $\hat{S}_t$, i.e., $y_t = \ln\left(\frac{\hat{S}_t}{1 - \hat{S}_t}\right)$ (Burnham et al. 1987, p. 214). The confidence limits for $\hat{S}_t$ were calculated by

$$(5) \qquad \left[\frac{\exp\left(y_t - Z_{1-\frac{\alpha}{2}} \frac{\sigma_t}{\hat{S}_t(1-\hat{S}_t)}\right)}{1+\exp\left(y_t - Z_{1-\frac{\alpha}{2}} \frac{\sigma_t}{\hat{S}_t(1-\hat{S}_t)}\right)}, \frac{\exp\left(y_t - Z_{1-\frac{\alpha}{2}} \frac{\sigma_t}{\hat{S}_t(1-\hat{S}_t)}\right)}{1+\exp\left(y_t - Z_{1-\frac{\alpha}{2}} \frac{\sigma_t}{\hat{S}_t(1-\hat{S}_t)}\right)}\right]$$

where $Z_{1-\frac{\alpha}{2}}$ is the $(1 - \frac{\alpha}{2})$ percentile of the standard normal distribution.

Bias due to release of recaptured fish

White and Burnham (1999) reparameterized recovery rate in tag-recovery models to create a consistent framework for modeling mark–recapture data. The framework provided the basis for the program MARK, which is a comprehensive software program for the analysis of capture–recapture data (White and Burnham 1999). In their formulation, recovery rate was redefined as $f = (1 - S)r$, where r is the rate at which tags are reported from dead fish, regardless of the source of mortality. The parameterization of tag recovery, $(1 - S)r$, makes clear the implicit assumption that the tagged animal dies before the tag is reported. The assumption is violated when tags are recovered from fish caught and released. This can be demonstrated when we consider the extreme case where no fish from a tagged cohort die from any cause (i.e., $S = 1$) and some fish are caught but released (tags are recovered and the fish suffered no ill effect from catch-and-release). If the resulting releases and recoveries are used for the tag-recovery models, then the estimate of S will be <1, even though S is in fact 1. Heuristically, there is a bias due to including recoveries from live recaptures, and the tag-based estimates of survival underestimate true survival.

Let c be fishing capture probability and K be the probability that a caught fish is killed. Let S_c and S_{nc} be the survival probabilities of a fish caught but rereleased and a fish never caught, respectively. Then the fate of each fish alive at the start of a time interval falls into one of five categories (Fig. 1). Tags can be recovered from fish caught and killed (cK) or from fish caught and released alive ($c(1 - K)$), subject to reporting rates for killed fish (λ_K) and fish released alive (λ_L). The λ_K and λ_L are the rates that anglers report tags recovered from captured fish; these rates are distinguished from the

© 2000 NRC Canada

Table 1. Expected probabilities of recovery for tag recoveries arising from fish that were harvested or released alive after recapture but with the tag removed.

Release year	Fate of catch	Expected probabilities of recovery for year: 1	2	3
1	Released	f_{L1}	$S_1\left\{\frac{\lambda_1-(f_{L1}+f_{K1})}{\lambda_1-[(1-\theta_1)f_{L1}+f_{K1}]}\right\}f_{L2}$	$S_1\left\{\frac{\lambda_1-(f_{L1}+f_{K1})}{\lambda_1-[(1-\theta_1)f_{L1}+f_{K1}]}\right\}S_2\left\{\frac{\lambda_2-(f_{L2}+f_{K2})}{\lambda_2-[(1-\theta_2)f_{L2}+f_{K2}]}\right\}f_{L3}$
	Harvested	f_{K1}	$S_1\left\{\frac{\lambda_1-(f_{L1}+f_{K1})}{\lambda_1-[(1-\theta_1)f_{L1}+f_{K1}]}\right\}f_{K2}$	$S_1\left\{\frac{\lambda_1-(f_{L1}+f_{K1})}{\lambda_1-[(1-\theta_1)f_{L1}+f_{K1}]}\right\}S_2\left\{\frac{\lambda_2-(f_{L2}+f_{K2})}{\lambda_2-[(1-\theta_2)f_{L2}+f_{K2}]}\right\}f_{K3}$
2	Released		f_{L2}	$S_2\left\{\frac{\lambda_2-(f_{L2}+f_{K2})}{\lambda_2-[(1-\theta_2)f_{L2}+f_{K2}]}\right\}f_{L3}$
	Harvested		f_{K2}	$S_2\left\{\frac{\lambda_2-(f_{L2}+f_{K2})}{\lambda_2-[(1-\theta_2)f_{L2}+f_{K2}]}\right\}f_{K3}$
3	Released			f_{L3}
	Harvested			f_{K3}

Note: Information on fate of catch is supplied by those who report the tag. To estimate survival and recovery rates, independent estimates of year-specific reporting rate (λ_i) and survival immediately after catch-and-release (θ_i) must be added as constants. A superior approach is to specify likelihoods for λ_i and θ_i and construct a full likelihood, i.e., $L(\pi_{ij};R_{ij},N_i)L(\theta)L(\lambda)$, so that all relevant parameters can be estimated simultaneously.

reporting rate r of the MARK formulation. Survival conditioned on the event that the fish was caught (S_c) applies to the entire time interval, but only for fish caught and rereleased.

Fish survival rate is $S_{fish} = c(1 - K)S_c + (1 - c)S_{nc}$, but tag survival rate is $S_{tag} = (1 - c)S_{nc}$. The rate that fish are caught and killed is finite exploitation rate, $cK = f_K/\lambda_K$. Similarly, the rate that fish are caught and released is $c(1 - K) = f_L/\lambda_L$. Thus, the relationship between fish survival and tag survival is

$$(6)\quad S_{tag} = S_{fish} - c(1-K)S_c = S_{fish} - \left(\frac{f_L}{\lambda_L}\right)S_c$$

Capture is known to affect survival (Diodati and Richards 1996), leading to the possibility that $S_c < S_{nc}$. On the other hand, the conditioning event of capture is relevant because the fish must have survived to capture. Consequently, it is possible that $S_c > S_{nc}$. However, to make the problem tractable, we proceed by assuming $S_c = S_{nc}$ and rearranging $S_{fish} = c(1 - K)S_c + (1 - c)S_{nc}$, which leads to $S_{fish}/(1 - cK) = S_c = S_{nc}$. Thus, we have

$$(7)\quad S_{tag} = S_{fish}\left(1 - \frac{f_L/\lambda_L}{1 - f_K/\lambda_K}\right)$$

An alternative form relies on the recovery rate ($f = f_L + f_K$) and the proportion of tags recovered from fish caught and released alive ($P_L = f_L/f$):

$$(8)\quad S_{tag} = S_{fish}\left[1 - \frac{P_L f/\lambda_L}{1-(1-P_L)f/\lambda_K}\right]$$

Typically, λ_L and λ_K are unknown and there is no information in the recovery data about these reporting rates. We might assume they are the same, $\lambda_L = \lambda_K = \lambda$, and hence:

$$(9)\quad S_{tag} = S_{fish}\left[1 - \frac{P_L f/\lambda}{1-(1-P_L)f/\lambda}\right]$$

One unknown parameter, λ, remains. If all fish are harvested upon capture, then $P_L = 0$ and $S_{tag} = S_{fish}$.

From the tag-recovery models, $E(\hat{S}_{tag}) \cong S_{tag}$, so we can correct for the bias by

$$(10)\quad \hat{S}_{fish} = \hat{S}_{tag}\left[\frac{1-(1-\hat{\theta}\hat{P}_L)\hat{f}/\hat{\lambda}}{1-\hat{f}/\hat{\lambda}}\right]$$

where $\hat{S}_{fish}$ is the adjusted survival rate (i.e., an estimate of fish survival), $\hat{\theta}$ is estimated survival immediately after the capture–release event (or the complement of mortality due to catch-and-release), and other estimators are of parameters defined previously. We obtained the variance for the adjusted survival by the delta method (Appendix A). An alternative parameterization can be used to specify cell probabilities for recovery models (Table 1). The models presented in Table 1 require independent, year-specific estimates of λ and θ. Ideally, given studies to estimate reporting and acute mortality rates (which are concurrent with the tagging study), likelihoods for λ and θ can be specified, and a full likelihood can be constructed, i.e., $L(\pi_{ij};R_{ij},N_i)L(\theta)L(\lambda)$, so that all relevant parameters can be estimated simultaneously.

We can assess approximate relative bias (i.e., $(S_{tag} - S_{fish})/S_{fish}$) by

$$(11)\quad -\frac{\theta P_L (f/\lambda)}{1-(1-\theta P_L)f/\lambda}$$

which approximates the relative error when $\hat{S}_{tag}$ is used to estimate S_{fish}. Diodati and Richards (1996) reported that 9% (SE = 2%) of striped bass die shortly after release because of hooking and handling. Thus, a possible value for θ is 0.91.

To adjust for the bias, reporting rate (λ) must be estimated. Pollock et al. (1991) discussed study designs to estimate reporting rate independently from the tagging study, and Hoenig et al. (1998*a*) discussed ways to incorporate tag reporting rate into tag-recovery modeling. We present an ad hoc method to estimate reporting rate from tag recovery based estimates of survival and recovery rate and assumed rates of natural mortality and survival immediately after catch-and-release. Given finite survival (S) and instantaneous natural mortality (M), instantaneous fishing mortality (F) can be found by $F = -\ln(S) - M$. Alternatively, fishing mortality can be based on rates of finite exploitation (u) and survival (Ricker 1975):

© 2000 NRC Canada

$$(12)\quad u = \frac{F}{-\ln(S)}(1 - S)$$

Exploitation is a function of recovery rate, proportion released alive, survival immediately after catch-and-release, and reporting rate, i.e.,

$$(13)\quad u = \frac{f_K}{\lambda} = \frac{(1 - \theta P_L)f}{\lambda}$$

Thus, based on eqs. 12 and 13, an alternative formula for fishing mortality is

$$(14)\quad F = -\ln(S)\frac{(1 - \theta P_L)f}{\lambda(1 - S)}$$

At this point, neither $F = -\ln(S) - M$ nor eq. 14 will yield an unbiased estimate of fishing mortality because we lack an unbiased estimate of survival and the tagging data alone provide no estimate of natural mortality, reporting rate, or survival immediately after catch-and-release. Bias-adjusted survival ($\hat{S}_{fish}$) from eq. 10 is a function of reporting rate and survival immediately after catch-and-release. Thus, a strategy to assess bias in fishing mortality is to set θ and M to widely accepted values (say, $\theta^*$and M^*) and solve iteratively for λ using

$$(15)\quad -\ln(\hat{S}_{fish})\frac{(1 - \theta^* \hat{P}_L)\hat{f}}{\lambda(1 - \hat{S}_{fish})} = -\ln(\hat{S}_{fish}) - M^*$$

where is $\hat{f}$ and $\hat{P}_L$ are estimated from tagging data and $\hat{S}_{fish}$ is found by eq. 10. Although the ad hoc method permits time-specific rates, widely accepted values are likely to be constant values derived from theory or estimates averaged over a range of conditions. Unfortunately, the assumption of constant rates in this ad hoc method is untestable.

Application: Atlantic striped bass

Between 1987 and 1997, over 175 000 wild Atlantic striped bass were tagged through a cooperative coastwide tagging study involving 15 state and federal agencies. Recreational and commercial anglers and researchers recapture tagged fish and report the tags to the U.S. Fish and Wildlife Service, which manages the tagging database. The initial purpose of the cooperative coastwide tagging study, with its genesis during the stock collapse of the mid-1980s, was to evaluate efforts to restore stocks of Atlantic striped bass (Wooley et al. 1990). Currently, fishery biologists use the tagging data to monitor mortality and migration of striped bass in a restored fishery.

Harvest regulations have been liberalized in a stepwise fashion during the tagging study (Richards and Rago 1999), providing an opportunity to study effects of management on mortality. Harvest regulations can be summarized into three distinct periods: a period of highly restricted fishing from 1985 to 1989, an interim fishery from 1990 to 1994, and a restored fishery, which took effect in 1995. At the beginning of the tagging study, a moratorium on fishing had been in effect in the Maryland portion of Chesapeake Bay and the Delaware River, which remained through 1989. A moratorium on commercial striped bass fishing was in effect throughout the study in the Hudson River because of PCB contamination. From 1990 to 1994, fishing was permitted coastwide under an interim level of fishing mortality (i.e., target $F = 0.25$). Then in 1995, the Atlantic striped bass stock was declared restored and harvest regulation was relaxed again to achieve an increased target fishing mortality (i.e., target $F = 0.31$).

We modeled tag recoveries of striped bass ≥ 711 mm that were tagged in the Maryland portion of Chesapeake Bay, Hudson River, and Delaware River (Appendix B). Striped bass ≥ 711 mm are considered by the Atlantic States Marine Fisheries Commission to be fully recruited to the fishery. Because a major objective of the tagging program has been stock-specific estimates of mortality, tagging has been conducted in areas where spawning occurs. These efforts are best represented by decade-long spring tagging programs in the Maryland portion of the Chesapeake Bay and in the Hudson River that began in 1987 and 1988, respectively, and by a more recent tagging program in the Delaware River that began in 1991. We did not include 1987 releases for the Maryland portion of Chesapeake Bay or 1991 and 1992 for Delaware River because of low numbers of releases of striped bass ≥ 711 mm in those years.

Tags and tagging methods are standardized among tagging programs, but methods and timing of capture differ. Internal anchor tags with external streamers, supplied by the U.S. Fish and Wildlife Service, are inserted into an incision made in the left ventral side of healthy fish slightly behind and below the tip of the smoothed back pectoral fin. In the Hudson River, haul seines are used to catch striped bass for tagging primarily during May. In the Maryland portion of Chesapeake Bay, experimental drift gill nets are used to catch striped bass primarily during April and May. In the Delaware River, electrofishing is used to capture striped bass on the spawning grounds during April and May.

Dunning et al. (1987) studied tag retention and tag-induced mortality in striped bass. They reported that retention of internal anchor tags, over 1 year, was 98% and that tagged and control fish survived equally over 180 days after tagging. Thus, we did not attempt to adjust for bias due to these sources. For a tagged fish to be included in the release cohort, it must have been at large for at least 7 days prior to recapture unless it was recaptured within 7 days and released with the tag intact. To account for lengthy tagging periods (>1 month), we first defined the median week of tagging as the week at which 50% of the tags were released in that year. If the difference between the median weeks of tagging in successive years exceeded 4 weeks, then we used a feature in program MARK to adjust survival estimate by $\hat{S}_i^{52/t}$, where $\hat{S}_i$ is the survival estimate for the ith year and t is the number of weeks between the median week of tagging in successive years.

Following the procedures outlined by Buckland et al. (1997) and Burnham and Anderson (1998), prior to data analysis, we specified a set of candidate models. The model parameters were functions of two factors: stock (i.e., Chesapeake Bay, Hudson River, or Delaware River) and time. We allowed model parameters to be either fully stock specific or equal for all stocks. In addition, because of the small sample size for the Delaware River and its proximity to Chesapeake Bay, we allowed model parameters to be equal for the Delaware River and Chesapeake Bay but different from the Hudson River. We specified models allowing parameters to be year specific or constant across time. Because we hypothesized that harvest regulation affects survival and catch rates, we specified models allowing parameters to differ among the three periods of harvest regulation (i.e., 1988–1989, 1990–1994, and 1995–1997). For models including both stock and time effects, we specified models where (*i*) temporal changes in parameters depended on stock (i.e., there was an interaction between stock and time effects) and (*ii*) temporal changes in parameters were equal among stocks but parameters were stock specific (i.e., there was an additive stock and time effect).

For the purpose of assessing bias due to catch-and-release, we calculated the proportion released alive and recovery rate; we then assumed values for natural mortality and survival immediately after catch-and-release and solved for reporting rate. We calculated proportion released alive as the ratio of striped bass released alive to striped bass caught in a recovery period; this information is supplied by the angler who reports the tag. We estimated f from the fully time-specific tag-recovery models of Brownie et al. (1985). We assumed natural mortality to be 0.15, which is the value used in the Atlantic States Marine Fisheries Commission striped bass

© 2000 NRC Canada

Table 2. Statistics for the set of tag-recovery models that do not account for recoveries coming from live recaptures and harvested fish.

Model label[a]	ΔAIC*c*[b]	*np*	GOF *P* value	Akaike weight
$S(\{CB = DR,HR\} \times p)r(g + p)$	0.00	11	0.237	0.413
$S(\{CB = DR,HR\} \times p)r(g \times p)$	1.63	14	0.306	0.183
$S(\{CB = DR,HR\} \times t)r(g)$	2.01	24	0.581	0.151
$S(g \times p)r(g + p)$	3.88	13	0.179	0.059
$S(\{CB = DR,HR\} \times t)r(g + p)$	3.90	26	0.615	0.059
$S(\{CB = DR,HR\} \times p)r(g)$	4.36	9	0.127	0.047
$S(g \times p)r(g \times p)$	4.94	16	0.266	0.035
$S(\{CB = DR,HR\} + p)r(g + p)$	7.61	9	0.111	0.009
$S(\{CB = DR,HR\} + p)r(g \times p)$	7.83	12	0.118	0.007
$S(g \times p)r(g)$	8.15	11	0.089	0.006
$S(g \times t)r(g + p)$	8.43	32	0.536	0.006
$S(g \times t)r(g)$	8.56	31	0.470	0.006
$S(\{CB = DR,HR\} \times t)r(g \times p)$	8.61	29	0.574	0.005
$S(p)r(g \times p)$	8.77	11	0.110	0.005
$S(g + p)r(g + p)$	9.59	10	0.087	0.003
$S(g + p)r(g \times p)$	9.78	13	0.107	0.003

Note: A total of 84 models were proposed, and only those with ΔAIC*c* < 10 are shown here. See table footnote *a* for a description of the notation to interpret the model label. AIC*c* is a small sample size adjusted version of AIC, ΔAIC*c* is the difference between the model AIC*c* and the minimum AIC*c*, *np* is the number of estimable parameters, GOF *P* value is the probability of a larger Pearson chi-square statistic to test goodness-of-fit, and Akaike weight is the value for w_i used in model averaging from Buckland et al. (1997) and Burnham and Anderson (1998).

[a]Model notation: $S(\cdot)$ and $r(\cdot)$ indicate that survival and reporting rate parameters are functions of factors specified in parentheses. The letters *g*, *t*, and *p* denote that parameters are stock specific, year specific, and specific to harvest regulation period, respectively. The notation {CB = DR,HR} indicates a type of stock-specific restriction where Chesapeake Bay (CB) and the Delaware River (DR) have equal survival but that survival differs from survival in the Hudson River (HR). If either stock- or time-specific notation is not included in the parentheses, then parameters are assumed constant in that respect. When parameters are simultaneously a function of stock and time, then stock and time effects can interact fully (e.g., denoted $g \times t$) or the effects can be additive (e.g., denoted $g + t$).

[b]For this best model, AIC*c* = minimum AIC*c* = 16725.736.

stock assessment, and survival immediately after catch-and-release to be 0.91 (Diodati and Richards 1996). We then found the reporting rate that satisfied eq. 15 and applied that reporting rate to calculate a bias-adjusted fishing mortality.

We used program SURVIV (White 1983) to compute survival based on the model structure presented in Table 1, which incorporates the bias-adjustment factor (eq. 10). We assumed that reporting rate (λ) and survival immediately after catch-and-release (θ) were known constants. We took λ from the iterative procedure discussed above and θ from the results of Diodati and Richards (1996). We ran the model using data from the Maryland portion of Chesapeake Bay for 1991–1997 because reporting rate appeared to be relatively constant for that program during that time span. We fit models that incorporated year-specific and regulation-specific parameters.

Results

A total of 84 tag-recovery models, which assume that tags are recovered only from dead fish, were proposed and fit to the data; of these, 16 had ΔAIC*c* < 10 (Table 2). GOF statistics indicated that the 16 models with the lowest AIC*c* were plausible summaries of the data (i.e., GOF *P* values > 0.05). Temporal changes in estimates of survival depended on stock; however, survival of Delaware River striped bass was similar to that of the Chesapeake Bay stock, at least from 1993 to 1997. Models that structured time into harvest regulation periods were among the better-fitting models, thus indicating that estimates of survival changed with regulation changes.

We averaged model parameters across the 16 best-fitting models and found that 76% of the weighting came from the top three best-fitting models (Table 2). Sixty one percent of the weight came from models with time categorized according to periods of harvest regulation and with survival of the Delaware River stock equal to that of the Chesapeake Bay stock.

Model-averaged estimates of survival were highest during the moratorium (1988–1989) and then declined and remained relatively stable during the transitional fishery (1990–1994) and the full fishery (1995–1997) (Table 3). Model-averaged estimates of survival in the Maryland portion of Chesapeake Bay were significantly higher during the moratorium and slightly higher during the transitional fishery than in the Hudson River.

Recovery rates increased slightly during the tagging study, whereas proportion of catch released alive decreased (Fig. 2; Table 4). These trends caused the bias in estimates of survival to decrease over the course of the tagging study. Consequently, the temporal pattern in bias-adjusted *F* differed from the *F* calculated directly from model-averaged estimates of survival (Fig. 3; Table 4). Unadjusted *F* increased in a stepwise fashion after the moratorium and then leveled off; however, bias-adjusted *F* increased throughout the tagging study (Fig. 3). Bias was greatest in 1990 immediately

© 2000 NRC Canada

Fig. 2. Recovery rate (circles) and proportion released alive (triangles) for striped bass >711 mm in three tagging programs: (*a*) Hudson River, 1988–1997, (*b*) Delaware River, 1993–1997, and (*c*) the Maryland portion of Chesapeake Bay, 1988–1997. Recovery rate was estimated from the stock- and time-specific survival and recovery rate model under the model parameterization of Brownie et al. (1985). The proportion of catch released alive was calculated using all recaptures in a given recovery year, regardless of release year.

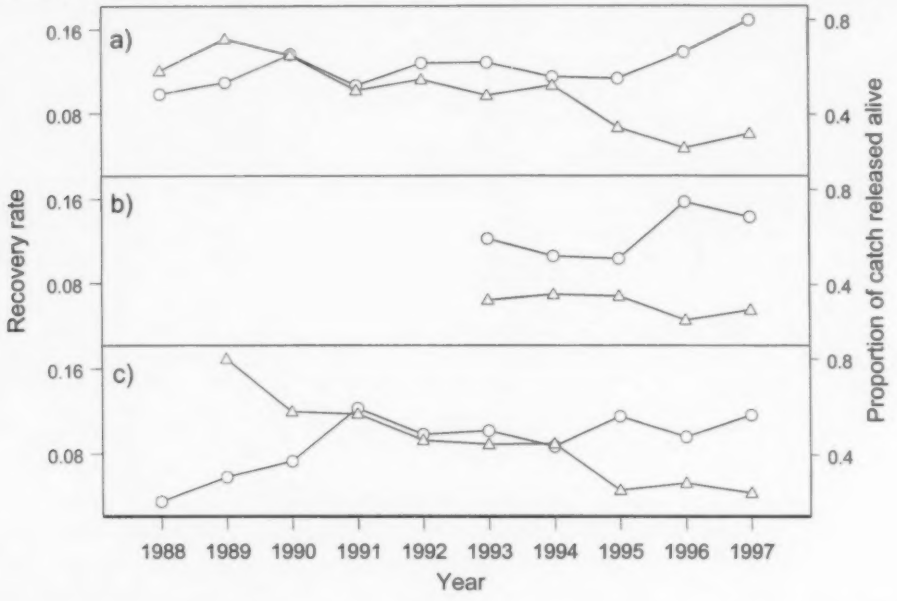

Table 3. Model-averaged estimates of biased survival ($\hat{S}_{tag}$) for spring tagging programs conducted in the Maryland portion of Chesapeake Bay, the Hudson River, and the Delaware River, 1988–1997.

	Maryland portion of Chesapeake Bay			Hudson River			Delaware River		
Year	$\hat{S}_{tag}$	SE	95% CI	$\hat{S}_{tag}$	SE	95% CI	$\hat{S}_{tag}$	SE	95% CI
1988	0.90	0.098	(0.52, 0.99)	0.75	0.087	(0.54, 0.88)			
1989	0.88	0.098	(0.55, 0.98)	0.72	0.093	(0.51, 0.86)			
1990	0.66	0.063	(0.53, 0.77)	0.62	0.053	(0.51, 0.72)			
1991	0.63	0.062	(0.51, 0.74)	0.63	0.060	(0.51, 0.74)			
1992	0.65	0.057	(0.53, 0.75)	0.62	0.052	(0.52, 0.72)			
1993	0.66	0.059	(0.53, 0.76)	0.62	0.052	(0.52, 0.72)	0.66	0.070	(0.52, 0.77)
1994	0.66	0.063	(0.53, 0.77)	0.63	0.059	(0.51, 0.74)	0.66	0.071	(0.51, 0.77)
1995	0.63	0.074	(0.48, 0.76)	0.66	0.073	(0.51, 0.78)	0.64	0.081	(0.47, 0.77)
1996	0.64	0.074	(0.50, 0.77)	0.65	0.076	(0.49, 0.78)	0.64	0.081	(0.47, 0.78)
1997	0.64	0.075	(0.48, 0.77)	0.63	0.089	(0.44, 0.78)	0.64	0.082	(0.47, 0.78)

Note: These estimates underestimate survival because the basic tag-recovery models do not allow for tag recoveries from fish caught and released alive, which occurs frequently with Atlantic striped bass. Confidence intervals are based on a logit transformation of $\hat{S}_{tag}$.

following the moratorium and decreased thereafter. Reporting rate dropped after the moratorium (Table 4). In the Hudson River and Delaware River, reporting rate increased during the two most recent years. In the Maryland portion of Chesapeake Bay, reporting rate remained level at around 40% after 1991.

Hypothetically, relative bias was most severe (–0.51) when reporting rate was low (0.25), recovery rate was high (0.15), and the proportion of catch released alive was high (0.75). Relative bias ranged from –0.02 to –0.51 for reporting rates from 0.25 to 0.75, recovery rates from 0.05 to 0.15, and proportions released alive from 0.25 to 0.75 (Table 5). Relative bias was –0.02 to –0.15 in all cases when reporting rate was high (0.75), which suggests that efforts to increase reporting rate would help minimize the bias. In 1997, proportions of catch released alive were 0.32, 0.21, and 0.29 for the Hudson River, Chesapeake Bay, and Delaware River tagging programs, respectively. Recovery rates in those same programs were 0.17, 0.12, and 0.14 during 1997. If we assume a reporting rate approaching 0.50 and recent values for recovery rates and proportion released alive, then we expect that the relative bias in recent estimates of striped bass survival is between –0.13 and –0.07. For example, for true survival of 0.70, relative bias of –0.13 to –0.07 would lead to estimates of survival between 0.61 and 0.65 from traditional tag-recovery models.

Nine tag-recovery models, based on recovery probabilities in Table 1, were fit to data from the Maryland tagging study

© 2000 NRC Canada

Table 4. Bias-adjusted estimates of survival and fishing morality and related parameters.

Stock and year	$\hat{f}$	$\hat{P}_L$	Biased $\hat{S}_{tag}$	Biased $\hat{F}_{tag}$	Bias adjusted $\hat{S}_{fish}$	Bias adjusted $\hat{F}_{fish}$	$\hat{\lambda}$
Hudson River							
1988	0.10	0.56	0.75	0.14	0.81	0.07	0.76
1989	0.11	0.72	0.72	0.18	0.81	0.06	0.68
1990	0.14	0.63	0.62	0.33	0.76	0.13	0.50
1991	0.11	0.51	0.63	0.31	0.73	0.16	0.42
1992	0.13	0.56	0.62	0.32	0.74	0.15	0.48
1993	0.13	0.49	0.62	0.32	0.72	0.18	0.48
1994	0.11	0.50	0.63	0.31	0.74	0.16	0.45
1995	0.11	0.34	0.66	0.27	0.72	0.18	0.50
1996	0.14	0.26	0.65	0.29	0.69	0.22	0.58
1997	0.17	0.32	0.63	0.32	0.69	0.22	0.65
Maryland portion of Chesapeake Bay							
1988	0.03	0.60	0.90	0.00	0.91	0.00	1.00
1989	0.06	0.79	0.88	0.00	0.91	0.00	1.00
1990	0.07	0.59	0.66	0.27	0.76	0.12	0.32
1991	0.12	0.60	0.63	0.31	0.75	0.13	0.48
1992	0.10	0.47	0.65	0.28	0.74	0.16	0.41
1993	0.10	0.45	0.66	0.27	0.74	0.16	0.44
1994	0.09	0.44	0.66	0.27	0.74	0.16	0.38
1995	0.11	0.25	0.63	0.31	0.68	0.23	0.46
1996	0.10	0.29	0.64	0.29	0.70	0.21	0.40
1997	0.12	0.21	0.64	0.30	0.68	0.24	0.47
Delaware River							
1993	0.12	0.40	0.66	0.27	0.73	0.16	0.55
1994	0.11	0.38	0.66	0.26	0.73	0.17	0.48
1995	0.10	0.35	0.64	0.30	0.70	0.20	0.41
1996	0.16	0.25	0.64	0.29	0.69	0.22	0.65
1997	0.14	0.29	0.64	0.30	0.69	0.22	0.58

Note: Recovery rate ($\hat{f}$) is estimated from the stock- and time-specific model using Brownie et al. (1985) parameterization. The estimate of proportion of catch released alive is denoted by $\hat{P}_L$. Biased survival ($\hat{S}_{tag}$) is the standard tag-recovery estimates of survival rate that are biased due to tag recoveries from caught-and-released striped bass. Biased fishing mortality rate is computed from $\hat{S}_{tag}$ and by assuming a natural mortality of 0.15, i.e., biased $\hat{F}_{tag} = -\ln(\hat{S}_{tag}) - 0.15$. Bias-adjusted survival ($\hat{S}_{fish}$) and fishing mortality are computed iteratively by assuming that natural mortality is 0.15 and survival immediately after catch-and-release is 0.91 and by finding a reporting rate (λ) that satisfies eq. 15.

during 1991–1997. Reporting rate and survival immediately after catch-and-release were assumed known and constant, 0.43 and 0.91, respectively. Models that structured survival or recovery rates by regulatory period accounted for 97.6% of the Akaike weights (Table 6). Survival dropped in conjunction with regulatory change made in 1995 (Table 7). In addition, regulatory change had an effect on recovery rates. Harvest recovery rates diverged dramatically from live-recapture recovery rates after 1994.

Discussion

Survival rate was underestimated when tag-recovery models included tags from harvested and caught-and-released striped bass. And the magnitude of the bias changed over time. Thus, temporal changes in survival estimates were confounded by temporal changes in recovery rate, proportion released alive, and possibly reporting rate (although we do not have independent, time-specific estimates of reporting rate). Unadjusted estimates of survival decreased immediately after the moratorium but then leveled off and remained relatively constant through 1997. This pattern, however, was misleading because changes in recovery rate and proportion released alive caused bias to decrease during the tagging study. After adjusting for the bias, we found that survival decreased with regulatory changes that occurred after the moratorium was lifted. An important additional consideration is that the bias can differ among subpopulations if proportion released alive, recovery rate, or reporting rate depends on subpopulation. For example, striped bass < 711 mm are not fully recruited to the fishery. Proportion released alive is likely to be higher for these smaller striped bass. As a result, the magnitude of bias, in absolute terms, will be higher for the prerecruited segment of the population.

Bias in survival estimates from tag-recovery models due to recoveries from live recaptures is an important finding that affects interpretation of previous tag-based estimates of striped bass survival. Implications are less clear for other tagging studies. When all catch is harvested, this bias is not an issue. However, catch-and-release, which is increasingly popular, can result in live recapture of large numbers of tagged fish. For example, high proportions of striped bass

© 2000 NRC Canada

Fig. 3. Fishing mortality for striped bass > 711 mm tagged during spring in (*a*) the Hudson River, 1988–1997, (*b*) the Delaware River, 1993–1997, and (*c*) the Maryland portion of Chesapeake Bay, 1988–1997. Unadjusted fishing mortality (squares) is calculated as $F = -\ln(\hat{S}_{tag}) - M$, where $\hat{S}_{tag}$ is the tag-based estimate of biased survival and M is assumed to be 0.15. Bias-adjusted fishing mortality (diamonds) accounts for bias due to catch-and-release and is calculated using an iterative method (explained in the text).

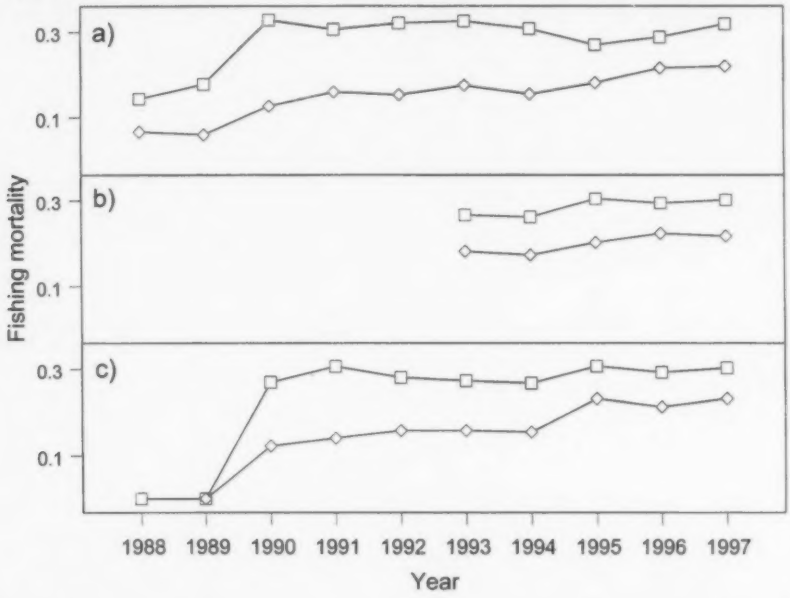

Table 5. Approximate relative bias (i.e., $(S_{tag} - S_{fish})/S_{fish}$) calculated for a range of reporting rates, recovery rates, and proportion of catch released alive and with survival immediately after catch-and-release fixed at 0.91.

	Proportion of catch released alive		
Recovery rate	0.25	0.50	0.75
Reporting rate = 0.25			
0.05	–0.05	–0.10	–0.15
0.10	–0.13	–0.23	–0.31
0.15	–0.25	–0.41	–0.51
Reporting rate = 0.50			
0.05	–0.02	–0.05	–0.07
0.10	–0.05	–0.10	–0.15
0.15	–0.09	–0.16	–0.23
Reporting rate = 0.75			
0.05	–0.02	–0.03	–0.05
0.10	–0.03	–0.07	–0.10
0.15	–0.05	–0.10	–0.15

Table 6. Statistics for tag-recovery models that incorporate a correction for tags recovered from live recaptures.

Model label[a]	ΔAIC*c*[b]	*np*	GOF *P* value	Akaike weight
$S(p)f_L(p)f_K(p)$	0.00	6	0.257	0.607
$S(\cdot)f_L(p)f_K(p)$	1.25	5	0.197	0.325
$S(t)f_L(p)f_K(p)$	5.25	10	0.213	0.044
$S(\cdot)f_L(t)f_K(t)$	7.72	15	0.279	0.013
$S(p)f_L(t)f_K(t)$	8.05	16	0.301	0.011

Note: Model structure is presented in Table 1. Nine models were fit to data from the Maryland portion of Chesapeake Bay from 1991 to 1997, and only those with ΔAIC*c* < 10 are shown here. Reporting rate (λ) and survival immediately after catch-and-release (θ) were fixed at 0.43 and 0.91, respectively. See table footnote *a* for a description of the notation to interpret the model label. AIC*c* is a small sample size adjusted version of AIC, ΔAIC*c* is the difference between the model AIC*c* and the minimum AIC*c*, *np* is the number of estimable parameters, GOF *P* value is the probability of a larger Pearson chi-square statistic to test goodness-of-fit, and Akaike weight is the value for w_i used in model averaging from Buckland et al. (1997).

[a]There are three types of parameters: fish survival (S), live-recapture recovery rate (f_L), and harvest recovery rate (f_K). Each type of parameter can be constant (·), year specific (t), or regulatory period specific (p). For example model "$S(t)f_L(p)f_K(p)$" denotes a model with year-specific survival and regulatory period specific recovery rates.

[b]For this best model, AIC*c* = minimum AIC*c* = 291.861.

tags were reported from fish caught and released (Table 4; Appendix B). These live recaptures, which are of fish not intended for harvest, can be released with or without the tag intact. Typically, published tagging studies do not report the proportion of catch released alive or the frequency that anglers remove tags prior to release. Thus, it is difficult to assess the generality of this bias, which clearly affected the striped bass tagging study.

In the event that tagged fish are subject to harvest and catch-and-release, we considered three basic approaches to survival estimation. Live recaptures can be excluded from the analysis, as was done by Youngs and Robson (1975). Alternatively, recoveries and multiple live recaptures can be analyzed jointly (Burnham 1991; Barker 1997). Finally, recoveries and first live recapture can be analyzed using tag-recovery models with a bias adjustment. We discuss these approaches in order with emphasis on the striped bass tagging study.

Youngs and Robson (1975) did not include live recaptures

© 2000 NRC Canada

Table 7. Model-averaged estimates of bias-adjusted survival, live-recapture recovery rate, and harvest recovery rate for the spring tagging program conducted in the Maryland portion of Chesapeake Bay, 1991–1997.

	Bias-adjusted survival			Live-recapture recovery rate			Harvest recovery rate		
Year	$\hat{S}_{fish}$	SE	95% CI	f_L	SE	95% CI	f_K	SE	95% CI
1991	0.75	0.033	(0.68, 0.81)	0.045	0.005	(0.04, 0.06)	0.051	0.004	(0.04, 0.06)
1992	0.75	0.032	(0.69, 0.81)	0.044	0.004	(0.04, 0.05)	0.051	0.004	(0.04, 0.06)
1993	0.76	0.030	(0.69, 0.81)	0.045	0.004	(0.04, 0.05)	0.051	0.004	(0.04, 0.06)
1994	0.76	0.037	(0.68, 0.82)	0.045	0.004	(0.04, 0.05)	0.051	0.004	(0.04, 0.06)
1995	0.69	0.052	(0.58, 0.78)	0.027	0.003	(0.02, 0.03)	0.080	0.005	(0.07, 0.09)
1996	0.69	0.051	(0.59, 0.78)	0.027	0.003	(0.02, 0.03)	0.080	0.005	(0.07, 0.09)
1997				0.027	0.003	(0.02, 0.03)	0.080	0.005	(0.07, 0.09)

Note: Estimates are based on the model structure presented in Table 1. Several models were fit to the data and used to estimate parameters. Model statistics are presented in Table 6. Reporting rate (λ) and survival immediately after catch-and-release (θ) were fixed at 0.43 and 0.91, respectively. Confidence intervals are based on a logit transformation.

in their analyses; they only used tags recovered from harvested lake trout. The strategy of excluding live recaptures from tag-recovery analysis works only if (*i*) tags are not removed prior to release and (*ii*) catch-and-release does not affect survival. In the Atlantic striped bass fishery, anglers commonly remove tags prior to release, and catch-and-release affects survival (Diodati and Richards 1996). Thus, this approach is not valid for tagging studies of Atlantic striped bass.

Burnham (1991) developed a theory for joint analysis of combined recovery and recapture data; however, it did not account for live recaptures between release periods (i.e., "tag resightings" that occur when anglers catch-and-release fish). Barker (1997) extended Burnham's (1991) work and developed a modeling framework allowing for recaptures, resightings, and recoveries. However, in the striped bass case, the removal of the tag permanently affects the probability of subsequent capture (the tag can be removed entirely or, more commonly, the tag's external streamer can be removed while the internal anchor is left in place). Also, catch-and-release affects survival (Diodati and Richards 1996), further complicating the probability structure for the model. Permanent changes in probability of subsequent capture are not part of the Barker (1997) model. Thus, the Barker (1997) model would need to be generalized to accommodate the striped bass tagging study, and large numbers of multiple recaptures would be required to support the extensive parameterization. We did not feel that the number of multiple recaptures of striped bass was sufficient to warrant generalizing the Barker (1997) model.

Estimation of reporting rate is the weak link in adjusting for bias in tag recovery based survival estimates using live recaptures. We used an ad hoc procedure to estimate reporting rate and adjust for bias in survival estimates. However, this procedure depends on knowing natural mortality rate, another parameter that is difficult to estimate and one that is often assumed to be constant, which may not be justified.

We computed maximum likelihood estimates of "bias-adjusted" survival with the program SURVIV (White 1983) assuming recovery probabilities presented in Table 1. However, the method requires independent year-specific estimates of reporting rate that account for nonreporting from commercial, charter boat, and recreational anglers. Such estimates are currently not available, and we assumed that reporting rate was known and constant. Thus, we overestimated precision (underestimated variance) of the survival estimates that appear in Table 7.

Studies to estimate time-specific reporting rate for striped bass should receive high priority. Pollock et al. (1991) reviewed ways to estimate reporting rate. If estimation of time-specific reporting rate (e.g., annual reward tag studies) were a routine component of the striped bass tagging study, then a full likelihood could be specified and uncertainty regarding reporting rate estimates could be included in bias-adjusted estimates of survival rate.

Finally, we note our application of the method of model averaging (Buckland et al. 1997; Burnham and Anderson 1998) to base inference on a weighted average of parameter estimates and to account for model selection uncertainty. The flexibility of tag-recovery modeling, and capture–recapture modeling in general, allows for a diverse set of models, each model representing a unique proposition for the biological and sampling processes that result in the observed tag recoveries. Different tag-recovery models can produce widely different estimates of vital parameters. Thus, model selection can have far-reaching consequences on management decisions. However, model selection is less certain when several models seem to fit the data equally well (i.e., have similar AIC or likelihood values). Furthermore, selection of the "true" model is not a realistic goal, and model selection uncertainty is a component of estimator variance, which is not accounted for when a single model is selected for inference. By model averaging, models contribute to the estimate according to how well the model serves as a parsimonious descriptor of the data. Inference is affected in two ways as a result. The model-averaged estimates reflect, in a balanced way, the patterns that emerge from the set of models, and variance of the model-averaged estimate includes a component for model selection uncertainty.

Acknowledgements

The Atlantic States Marine Fisheries Commission, through support of the Striped Bass Tagging Workgroup, fostered the cooperative coastwide striped bass tagging study and encouraged methodological advances. We thank Tina McCrobie and the U.S. Fish and Wildlife Service for managing striped bass tagging data, Beth Rodgers for assisting with Maryland's striped bass tagging program, and Penelope Pooler for assisting with tag-recovery modeling. Comments

© 2000 NRC Canada

from Gary Shepherd, Penelope Pooler, and Stuart Welsh on earlier drafts resulted in an improved manuscript.

References

Barker, R.J. 1997. Joint modeling of live-recapture, tag-resight, and tag-recovery data. Biometrics, **53**: 666–677.

Brownie, C., Anderson, D.R., Burnham, K.P., and Robson, D.S. 1985. Statistical inference from band recovery data — a handbook. 2nd ed. U.S. Fish Wildl. Serv. Resour. Publ. No. 156.

Buckland, S.T., Burnham, K.P., and Augustin, N.H. 1997. Model selection: an integral part of inference. Biometrics, **53**: 603–618.

Burnham, K.P. 1991. On a unified theory for release–resampling of animal populations. *In* Proceedings of the 1990 Taipei Symposium in Statistics. *Edited by* M.T. Chao and P.E. Cheng. Institute of Statistical Science, Academia Sinica, Taipei. pp. 11–35.

Burnham, K.P., and Anderson, D.R. 1998. Model selection and inference: a practical information theoretical approach. Springer-Verlag, New York.

Burnham, K.P., Anderson, D.R., White, G.C., Brownie, C., and Pollock, K.H. 1987. Design and analysis methods for fish survival experiments based on release–recapture. Am. Fish. Soc. Monogr. No. 5.

Burnham, K.P., White, G.C., and Anderson, D.R. 1995. Model selection strategy in the analysis of capture–recapture data. Biometrics, **51**: 888–898.

Diodati, P.J., and Richards, A.R. 1996. Mortality of striped bass hooked and released in salt water. Trans. Am. Fish. Soc. **125**: 300–307.

Dorazio, R.M. 1993. Prerelease stratification in tag-recovery models with time dependence. Can. J. Fish. Aquat. Sci. **50**: 535–541.

Dorazio, R.M. 1997. Modelling heterogeneity in the recoveries of marked animal populations with covariates of individual animals, groups of animals or recovery time. Environ. Ecol. Stat. **4**: 235–246.

Dunning, D.J., Ross, Q.E., Waldman, J.R., and Mattson, M.T. 1987. Tag retention by, and tagging mortality of, Hudon River striped bass. N. Am. J. Fish. Manage. **7**: 535–538.

Hoenig, J.M., Barrowman, N.J., Hearn, W.S., and Pollock, K.H. 1998*a*. Multiyear tagging studies incorporating fishing effort data. Can. J. Fish. Aquat. Sci. **55**: 1466–1476.

Hoenig, J.M., Barrowman, N.J., Pollock, K.H., Brooks, E.N., Hearn, W.S., and Polacheck, T. 1998*b*. Models for tagging data that allow for incomplete mixing of newly tagged animals. Can. J. Fish. Aquat. Sci. **55**: 1477–1483.

Pollock, K.H., Hoenig, J.M., and Jones, C.M. 1991. Estimation of fishing and natural mortality when a tagging study is combined with a creel survey or port sampling. Am. Fish. Soc. Symp. **12**: 423–434.

Richards, R.A., and Rago, P.J. 1999. A case history of effective fishery management: Chesapeake Bay striped bass. N. Am. J. Fish. Manage. **19**: 356–375.

Ricker, W.E. 1975. Computation and interpretation of biological statistics of fish populations. Bull. Fish. Res. Board Can. No. 191.

Schwarz, C.J., and Arnason, A.N. 1990. Use of tag-recovery information in migration and movement studies. Am. Fish. Soc. Symp. **7**: 588–603.

White, G.C. 1983. Numerical estimation of survival rates from band-recovery and biotelemetry data. J. Wildl. Manage. **47**: 716–728.

White, G.C., and Burnham, K.P. 1999. Program MARK — survival estimation from populations of marked animals. Bird Study, **46**: 120–138.

Wooley, C.M., Parker, N.C., Florence, B.M., and Miller, R.W. 1990. Striped bass restoration along the Atlantic coast: a multistate and federal cooperative hatchery and tagging program. Am. Fish. Soc. Symp. **7**: 775–781.

Youngs, W.D., and Robson, D.S. 1975. Estimating survival rates from tag returns: model tests and sample size determination. J. Fish. Res. Board Can. **32**: 2365–2371.

Appendix A. Variance for estimate of survival adjusted for release of recaptured fish using eq. 10.

Bias-adjusted survival, $\hat{S}_{\text{fish}}$ (eq. 10), can be written

$$\hat{S}_{\text{fish}} = \hat{S}_{\text{tag}}\left[\frac{\hat{\lambda} - (1-\hat{\theta})\hat{f}_{\text{L}} - \hat{f}_{\text{K}}}{\hat{\lambda} - \hat{f}_{\text{L}} - \hat{f}_{\text{K}}}\right]$$

where $\hat{S}_{\text{tag}}$ is the estimate of survival from standard tag-recovery modeling, f_{L} and f_{K} are tag-recovery rates for live recaptures and harvested fish, respectively, θ is survival immediately after catch-an-release, and λ is the reporting rate. The variance, as derived using the delta method and assuming that λ and θ are estimated independently from other parameters, is

$$\text{var}(\hat{S}_{\text{fish}}) = \left[\frac{S_{\text{fish}}}{S_{\text{tag}}}\right]^2 \text{var}(\hat{S}_{\text{tag}}) + [S_{\text{fish}} - S_{\text{tag}}]^2 Q$$

where Q is

$$Q = \left[\frac{\lambda - f_{\text{K}}}{f_{\text{L}}(\lambda - f_{\text{L}} - f_{\text{K}})}\right]^2 \text{var}(\hat{f}_{\text{L}}) + \left[\frac{1}{\lambda - f_{\text{L}} - f_{\text{K}}}\right]^2 \text{var}(\hat{f}_{\text{K}}) + \left[\frac{1}{\theta}\right]^2 \text{var}(\hat{\theta})$$

$$+\left[\frac{-1}{\lambda - f_{\text{L}} - f_{\text{K}}}\right]^2 \text{var}(\hat{\lambda}) + 2\left[\frac{S_{\text{fish}}}{S_{\text{tag}}}\right]\left[\frac{\lambda - f_{\text{K}}}{f_{\text{L}}(\lambda - f_{\text{L}} - f_{\text{K}})}\right]^2 \text{cov}(\hat{S}_{\text{tag}}, \hat{f}_{\text{L}})$$

$$+2\left[\frac{S_{\text{fish}}}{S_{\text{tag}}}\right]\left[\frac{-1}{\lambda - f_{\text{L}} - f_{\text{K}}}\right] \text{cov}(\hat{S}_{\text{tag}}, \hat{f}_{\text{K}}) + 2\left[\frac{\lambda - f_{\text{K}}}{f_{\text{L}}(\lambda - f_{\text{L}} - f_{\text{K}})^2}\right] \text{cov}(\hat{f}_{\text{L}}, \hat{f}_{\text{K}})$$

© 2000 NRC Canada

Appendix B. Release and recovery matrices of striped bass for tagging programs in the Maryland portion of Chesapeake Bay (1988–1997), the Hudson River (1988–1997), and the Delaware River (1993–1997).

Year of release	Number released	Disposition of catch	Number recaptured									
			1988	1989	1990	1991	1992	1993	1994	1995	1996	1997
Maryland portion of Chesapeake Bay												
1988	128	Released	3	8	5	9	0	1	1	0	0	0
		Harvested	2	2	3	5	4	1	1	0	0	0
1989	219	Released		7	10	13	2	2	2	0	0	0
		Harvested		2	7	3	4	2	1	5	2	0
1990	304	Released			14	7	5	2	1	1	0	0
		Harvested			10	8	5	3	1	3	0	3
1991	392	Released				26	10	6	1	2	0	1
		Harvested				21	11	13	5	6	3	4
1992	404	Released					21	12	5	3	3	1
		Harvested					19	12	8	11	5	7
1993	626	Released						28	19	9	2	1
		Harvested						32	27	30	11	15
1994	538	Released							24	12	4	0
		Harvested							24	29	19	16
1995	523	Released								16	6	5
		Harvested								44	23	19
1996	854	Released									34	16
		Harvested									57	34
1997	336	Released										9
		Harvested										30
Hudson River												
1988	277	Released	15	20	11	2	4	2	2	0	0	1
		Harvested	12	10	8	10	6	3	3	0	3	1
1989	382	Released		32	13	7	4	1	1	0	0	0
		Harvested		10	17	8	3	6	5	5	0	0
1990	442	Released			47	15	16	6	2	0	0	0
		Harvested			16	15	11	9	3	5	1	3
1991	362	Released				24	16	5	4	0	0	3
		Harvested				14	13	10	7	9	7	0
1992	692	Released					49	32	14	10	3	3
		Harvested					37	26	16	11	11	12
1993	534	Released						37	21	13	4	5
		Harvested						34	16	7	15	11
1994	377	Released							24	7	6	2
		Harvested							17	25	20	19
1995	460	Released								20	11	10
		Harvested								34	20	11
1996	676	Released									27	24
		Harvested									72	37
1997	184	Released										7
		Harvested										24
Delaware River												
1993	52	Released						2	2	0	0	0
		Harvested						3	5	2	4	2
1994	79	Released							3	3	2	0
		Harvested							3	6	4	1
1995	88	Released								4	3	4
		Harvested								5	5	0
1996	72	Released									2	3
		Harvested									8	3
1997	77	Released										0
		Harvested										11

Note: Total lengths of all fish were ≥ 711 mm. Fish were tagged during the spawning run in each tagging program.

© 2000 NRC Canada

Reconstruction of pinniped diets: accounting for complete digestion of otoliths and cephalopod beaks

W.D. Bowen

Abstract: The recovery of sagittal fish otoliths and cephalopod beaks from fecal samples is an important source of information about the diets of marine mammals. Nevertheless, diet reconstructions are biased to some extent because of the partial and complete digestion of these prey structures. Although some authors have used correction factors to account for partial digestion of otoliths, none to date have corrected for the number of otoliths and cephalopod beaks that are completely digested, termed number correction factors (NCFs). Data from nine studies of captive pinnipeds show that corrections for the complete digestion of otoliths and cephalopod beaks range from 1.0 to 25.0 in the 28 prey species. Correction factors ranged from 1.0 to 10.0 in cases where seals could exercise by swimming during the experiment. In several species, NCFs vary inversely with prey length. The effect of applying NCFs will depend on the relative proportion of prey species in the diet and the NCFs of these species. Nevertheless, estimates of the species composition of marine mammal diets will benefit from the use of NCFs. Finally, standardization of experimental protocols and attention to the estimation of variability are needed to provide more reliable NCFs.

Résumé : La récupération d'otolithes (sagitta) de poissons et de becs de céphalopodes dans des échantillons de fèces de mammifères marins constitue une importante source d'information sur l'alimentation de ces animaux. Toutefois, les reconstitutions sont biaisées dans une certaine mesure du fait que ces structures peuvent être partiellement ou complètement digérées. Bien que certains auteurs aient eu recours à des facteurs de correction pour tenir compte de la digestion partielle des otolithes, aucun n'a pour le moment apporté une correction pour le nombre d'otolithes et de becs de céphalopodes qui sont complètement digérés; nous avons calculé ces facteurs (facteurs de correction numérique ou NCF). Les données fournies par 9 études sur des pinnipèdes en captivité montrent que les corrections pour la digestion complète des otolithes et des becs de céphalopodes va de 1,0 à 25,0 chez les 28 espèces proies. Les facteurs de correction allaient de 1,0 à 10,0 dans des cas où les phoques pouvaient faire de l'exercice en nageant pendant l'expérience. Chez plusieurs espèces, les NCF varient en fonction inverse de la longueur de la proie. L'effet de l'application des NCF dépendra de la proportion relative des espèces proies dans l'alimentation et des NCF de ces espèces. Toutefois, les estimations de la composition spécifique de l'alimentation des mammifères marins tirera profit de l'usage des NCF. Enfin, pour avoir des NCF plus fiables, il faudra normaliser les protocoles expérimentaux et se pencher sur l'estimation de la variabilité.

[Traduit par la Rédaction]

Introduction

Increasing awareness of the value of an ecosystem approach to the management and conservation of marine animals has underscored the importance of understanding trophic relationships. In the case of marine mammals, our knowledge of diet varies considerably among species, and, with few exceptions, indirect methods are used to reconstruct what was eaten. The most common methods rely on the identification of prey structures that are resistant to digestion and can be collected from stomachs, intestines, feces, and spewings. In piscivorous marine mammal species, sagittal otoliths are most commonly used, but other structures such as bones, scales, and lenses also provide a means of prey identification (Fitch and Brownell 1968; Pierce and Boyle 1991; Pierce et al. 1993). Where cephalopods are eaten, beaks can be used for prey identification (e.g., Clarke 1986). Recovered otoliths and cephalopod beaks can be used to estimate both the number and size of the prey consumed. Stomach contents and fecal samples have been used as the main sources of prey hard parts. However, feces are being increasingly used for this purpose because they are often less expensive to collect, a high proportion of samples contain identifiable prey, and estimates of diet from fecal data are less affected by differential rates of digestion than are estimates from stomachs (Hammond and Prime 1990).

Despite their widespread use, estimates of species composition and the size of prey consumed derived from recovered otoliths and cephalopod beaks may be seriously biased (e.g., Murie and Lavigne 1985; Harvey 1989; Pierce and Boyle 1991). One difficulty is that otoliths and cephalopod beaks erode during digestion, such that the size and number of prey consumed may be underestimated, and, in some cases, prey identification is not possible. A further complication is that the degree of erosion is species specific and is often a function of prey size within species. Otoliths from some spe-

Received August 25, 1999. Accepted January 17, 2000.
J15330

W.D. Bowen. Department of Fisheries and Oceans, Bedford Institute of Oceanography, Marine Fish Division, Dartmouth, NS B2Y 1A4, Canada. e-mail: bowend@mar.dfo-mpo.gc.ca

© 2000 NRC Canada

cies (e.g., Atlantic salmon (*Salmo salar*)) are quickly digested and thus are rarely found in stomach or fecal contents (Boyle et al. 1990). Differential rates of digestion among species may seriously bias stomach content analyses in favor of species with large and robust hard parts.

Using these methods, there is generally little that can be done about the potential biases caused by nonrepresentative sample collection and the consumption of species without hard parts. However, a number of studies have attempted to experimentally measure in vivo the reduction in the size of otoliths that occurs during digestion and to apply correction factors to estimates of diet composition (e.g., Bigg and Fawcett 1985; Harvey 1989; Tollit et al. 1997). Although this is desirable, a correction for the complete digestion of ingested otoliths should also be made (Jobling 1987). Estimates of these prey-number correction factors (NCFs) come from the same studies in which partial-erosion correction factors have been derived. Nevertheless, corrections for the complete digestion of otoliths have not been routinely used. The purpose of this paper is to show that these correction factors usually exceed 1.0, to briefly illustrate their effect on estimates of marine mammal diets, and to encourage well-designed experimental studies to better determine the magnitude of these factors.

Methods

The data were obtained from nine papers (Table 1). An experiment by Gales and Cheal (1992) on two captive Australian sea lion (*Neophoca cinerea*) were not included in Table 1, as the number of otoliths of each prey species fed and recovered was not provided and thus correction factors could only be approximated from percentages in their fig. 2. Furthermore, the recovery rate was based on otoliths recovered from an aggregate of meals over a period of 4–7 days rather than from individual meals as in the other studies. Given this experimental design, it was not clear that the recovery rate calculated by Gales and Cheal (1992) were comparable with the other studies. Nevertheless, their results do help to shed light on some of the factors that may affect correction factors (see Discussion).

Otoliths not recovered from experimental meals may have been lost because they were completely digested or because the method used to recover otoliths was ineffective. Ineffective otolith recovery will introduce a positive bias in estimates of the number of otoliths lost to digestion. Thus, prior to analyses, I evaluated the quality and comparability of the data from each of these nine studies. The effectiveness of otolith recovery was tested in only five of the nine studies (Table 2.) Testing was done by distributing in the pool or feeding to the animals glass beads or by distributing marked otoliths of various sizes in the tank before draining the water and feces. The rate of recovery of these glass beads or otoliths was then used to infer the recovery of otoliths and cephalopod beaks from experimental meals. Essentially all test glass beads or otoliths were recovered in three of the five studies, indicating that all otoliths that survived digestion were likely recovered. In the study by Tollit et al. (1997), all test English whiting otoliths were recovered, but only 70–73% of sand eel otoliths were recovered. As the Atlantic cod fed in the Tollit et al. (1997) study were of similar size to the English whiting, I assumed that all Atlantic cod and English whiting otoliths were recovered. However, I corrected the number of otoliths recovered from other prey, with smaller otoliths, by applying the reciprocal of the mean sand eel otolith recovery test results (i.e., 1.40) to these species. Similarly, Dellinger and Trillmich (1988) recovered on average only 74% of test glass beads. Thus, I corrected their data by a factor of 1.35.

Four studies did not test the effectiveness of otolith recovery. In three of these, however, the conditions in which the animals were held suggested that few otoliths would have been missed. However, in the study by Prime and Hammond (1987), the authors noted that some fecal material could have been lost and thus the effect of digestion on otolith disappearance was confounded by effectiveness of otolith recovery. Thus, data from this study may overestimate the effect of digestion on otolith recovery rate.

NCFs were calculated as the inverse of the proportion of the number of sagittal otoliths/beaks fed that were recovered in fecal samples. Some of the NCFs from Tollit et al. (1997) were recalculated from the data given in the paper, as the reported NCFs did not agree with the data. However, in all but one case (i.e., Atlantic herring), the differences between the recalculated factors and those presented in Table 3 were insignificant. NCFs were calculated from the data in Harvey and Antonelis (1994) by combining feeding trials across the two seals before calculating the proportion recovered.

Approximate 95% confidence limits of the NCFs were calculated assuming a binomial distribution with otoliths as the sampling unit. In most cases, these limits are too small, as they assume that each otolith was involved in an independent trial. In reality, groups of otoliths were fed together to an individual seal or, in some cases, to a group of seals.

To examine the effect of prey size on NCFs, I used only values for each of the size-classes of prey fed to seals, excluding the overall average values from studies that fed more than one size-class. For example, there are nine estimates of NCFs for Atlantic cod in Table 1. Excluding the two average values left seven estimates to be used to examine the effect of prey size on NCFs.

One- and two-way ANOVAs were used to test for differences in NCFs among species and for the effect of pinniped species and prey type on NCFs of Atlantic herring. A Mann–Whitney test was used to test the effect of experimental housing (i.e., wet versus dry) on NCFs. An alpha level of 0.05 was used to establish statistical significance. Statistical analyses were performed using SPSS version 8.0. The standard error is given as a measure of variability about the mean.

Results

NCFs were available for 24 fish and four invertebrate species (Table 1). Although five species of pinnipeds (three phocids and two otariids) have been used in experiments to estimate these NCFs, most of the data were derived from experiments with harbour seals (*Phoca vitulina*) and to a lesser extent on grey seals (*Halichoerus grypus*). NCFs differed greatly among prey species, ranging from 1.0 to 25.0 (Table 1). For the subset of prey species with three or more estimates, NCFs varied significantly among species (one-way ANOVA on inverse transformed data, $F_{4,27} = 13.4$, $p < 0.001$) (Table 3). NCFs for Atlantic cod and English whiting did not differ significantly; however, these factors were significantly lower than the NCFs for Atlantic herring, sprat, and sand eel, which also did not differ from one another (Table 3). In 58 of 66 cases, the estimated confidence limits on the NCFs did not include 1.0 (Table 1). Marcus et al. (1998) found the NCF for Atlantic cod (mean length 25 cm) was 1.0 ($n = 120$ otoliths fed). However, in most cases where the 95% confidence limits included 1.0, sample size was small (i.e., 20–54 otoliths fed).

Some of the variation in NCFs among species may be an artifact of experimental housing conditions, namely whether the seals could exercise by swimming or not during the feeding trial. In three of the studies, the seals were held in dry

© 2000 NRC Canada

Table 1. Prey size (cm), pinniped species and age-class (ad, adults; juv, juveniles), and experimental condition (wet or dry, see text) used to estimate NCFs for fish and invertebrates.

Species			Prey		NCF				
Common name	Scientific name	Meal size	Length	Structures[a]	Mean[b]	95% CL	Pinniped species and age-class	No.	Condition
Fish									
Atlantic cod[e]	*Gadus morhua*	Average	17	54	1.1	1.0–1.3	Harbour, ad/juv	7	Wet
Atlantic cod[e]	*Gadus morhua*	Average[c]	22	148	1.2	1.1–1.4	Harbour, ad/juv	7	Wet
Atlantic cod[e]	*Gadus morhua*	Average	23	60	1.5	1.2–1.8	Harbour, ad/juv	7	Wet
Atlantic cod[f]	*Gadus morhua*	Average[c]	25	190	1.2	1.1–1.3	Grey, juv	8	Wet
Atlantic cod[f]	*Gadus morhua*	Half	25	70	1.5	1.3–1.8	Grey, juv	8	Wet
Atlantic cod[f]	*Gadus morhua*	1.5	25	120	1.0		Grey, juv	4	Wet
Atlantic cod[g]	*Gadus morhua*	Average	25	70	1.2	1.1–1.3	Grey, ad	2	Wet
Atlantic cod[e]	*Gadus morhua*	Average	27	34	1.1	1.0–1.4	Harbour, ad/juv	7	Wet
Atlantic cod[h]	*Gadus morhua*	Average	29	52	1.2	1.1–1.4	Harbour, juv	1	Dry
Haddock[h]	*Melanogrammus aeglefinus*	Average	24	20	1.1	1.0–1.5	Harbour, juv	1	Dry
Walleye pollock[i]	*Theragra chalcogramma*	Average	29	238	1.3	1.2–1.4	Harbour, ad/juv	4	Wet
Atlantic tomcod[j]	*Microgadus proximus*	Average	21	92	6.6	4.1–11.7	NES,[d] juv	2	Dry
Atlantic tomcod[k]	*Microgadus proximus*	Average	—	98	1.4	1.3–1.6	Harbour, ad/juv	6	Wet
English whiting[e]	*Merlangius merlangus*	Average	10	242	1.7	1.5–1.9	Harbour, ad/juv	7	Wet
English whiting[e]	*Merlangius merlangus*	Average	18	234	1.4	1.3–1.5	Harbour, ad/juv	7	Wet
English whiting[e]	*Merlangius merlangus*	Average[c]	18	744	1.4	1.3–1.5	Harbour, ad/juv	7	Wet
English whiting[e]	*Merlangius merlangus*	Average	22	102	1.3	1.2–1.5	Harbour, ad/juv	7	Wet
English whiting[h]	*Merlangius merlangus*	Average	25	23	1.2	1.1–1.6	Harbour, juv	1	Dry
English whiting[e]	*Merlangius merlangus*	Average	26	166	1.2	1.1–1.3	Harbour, ad/juv	7	Wet
English whiting[g]	*Merlangius merlangus*	Average	31	136	1.2	1.1–1.2	Grey, ad	2	Wet
Pout whiting[g]	*Trisopterus luscus*	Average	20	112	1.1	1.1–1.2	Grey, ad	2	Wet
Pacific hake[j]	*Merluccius productus*	Average	25	154	3.7	2.8–5.0	NES,[d] juv	2	Dry
Pacific hake[i]	*Merluccius productus*	Average	33	290	1.4	1.3–1.5	Harbour, ad/juv	4	Wet
Dover sole[k]	*Microstomus pacificus*	Average	—	24	1.2	1.0–1.6	Harbour, ad/juv	6	Wet
English sole[k]	*Pleuronectes vetulus*	Average	—	88	4.1	2.9–6.4	Harbour, ad/juv	6	Wet
Lemon sole[e]	*Microstomus kitt*	Average	19	76	3.8 (5.4)	2.6–6.0	Harbour, ad/juv	7	Wet
Lemon sole[e]	*Microstomus kitt*	Average[c]	23	108	2.3 (3.2)	1.9–3.0	Harbour, ad/juv	7	Wet
Lemon sole[e]	*Microstomus kitt*	Average	33	32	1.1 (1.6)	1.0–1.3	Harbour, ad/juv	7	Wet
Rex sole[k]	*Errex zachirus*	Average	—	188	1.3	1.2–1.4	Harbour, ad/juv	6	Wet
European plaice[e]	*Pleuronectes platessa*	Average	23	48	1.7 (2.4)	1.4–2.3	Harbour, ad/juv	7	Wet
European plaice[g]	*Pleuronectes platessa*	Average	17	134	1.6	1.4–1.9	Grey, ad	2	Wet
Dab[g]	*Limanda limanda*	Average	12	28	2.2	1.5–3.6	Grey, ad	2	Wet
Eulachon[k]	*Thaleichthys pacificus*	Average	—	152	2.9	2.3–3.7	Harbour, ad/juv	6	Wet
Sand eel[e]	*Ammodytes marinus*	Average	9	114	5.2 (7.1)	3.6–8.0	Harbour, ad/juv	7	Wet

© 2000 NRC Canada

Table 1 (*concluded*).

Species			Prey		NCF				
Common name	Scientific name	Meal size	Length	Structures[a]	Mean[b]	95% CL	Pinniped species and age-class	No.	Condition
Sand eel[e]	*Ammodytes marinus*	Average	14	314	4.7 (6.5)	3.8–5.8	Harbour, ad/juv	7	Wet
Sand eel[e]	*Ammodytes marinus*	Average[c]	15	1118	2.8 (4.0)	2.7–2.9	Harbour, ad/juv	7	Wet
Sand eel[e]	*Ammodytes marinus*	Average	16	400	2.1 (2.9)	2.0–2.3	Harbour, ad/juv	7	Wet
Sand eel[e]	*Ammodytes marinus*	Average	18	290	2.6 (3.6)	2.2–3.0	Harbour, ad/juv	7	Wet
Pacific herring[j]	*Clupea pallasi*	Average	18	3956	3.4	3.2–3.5	Harbour, ad/juv	4	Wet
Pacific herring[j]	*Clupea pallasi*	Average	20	126	21.0	9.9–56.7	NES,[d] juv	2	Dry
Pacific herring[k]	*Clupea pallasi*	Average	—	64	3.1	2.2–4.8	Harbour, ad/juv	6	Wet
Atlantic herring[f]	*Clupea harengus*	Average	21	590	1.4 (2.0)	1.4–1.5	Northern fur, ad	3	Dry
Atlantic herring[f]	*Clupea harengus*	Average	21	538	2.0 (2.9)	1.9–2.1	Sea lion, ad	2	Dry
Atlantic herring[f]	*Clupea harengus*	Average[c]	25	120	2.3	1.9–2.9	Harbour, juv	1	Wet
Atlantic herring[f]	*Clupea harengus*	Average[c]	25	334	4.1	3.4–5.0	Grey, juv	8	Wet
Atlantic herring[f]	*Clupea harengus*	Half	25	24	4.0	2.1–10.2	Harbour, juv	1	Wet
Atlantic herring[f]	*Clupea harengus*	Half	25	94	5.9	3.8–10.2	Grey, juv	8	Wet
Atlantic herring[f]	*Clupea harengus*	Double	25	96	1.6	1.4–1.9	Harbour, juv	1	Wet
Atlantic herring[f]	*Clupea harengus*	1.5	25	120	1.6	1.4–1.9	Grey, juv	4	Wet
Atlantic herring[f]	*Clupea harengus*	Double	25	120	2.1	1.8–2.6	Grey, juv	3	Wet
Atlantic herring[e]	*Clupea harengus*	Average	26	8732	3.3 (4.6)	4.4–4.8	Harbour	7	Wet
Atlantic herring[m]	*Clupea harengus*	Average	26	54	25.0	7.5–204	Harbour, ad	1	Dry
Sprat[f]	*Sprattus sprattus*	Average	12	564	1.5 (2.4)	1.4–1.6	Northern fur, ad	3	Dry
Sprat[f]	*Sprattus sprattus*	Average	12	570	3.0 (4.0)	2.9–3.3	Sea lion, ad	2	Dry
Sprat[e]	*Sprattus sprattus*	Average	13	252	10.0 (14.0)	6.9–15.0	Harbour, ad/juv	7	Wet
Rainbow trout[k]	*Oncorhynchus mykiss*	Average	—	146	1.6	1.4–1.8	Harbour, ad/juv	6	Wet
Chinook salmon[i]	*Oncorhynchus tshawytscha*	Average	14	148	1.6	1.4–1.9	Harbour, ad/juv	4	Wet
Shiner perch[k]	*Cymatogaster aggregata*	Average	—	240	1.7	1.5–1.9	Harbour, ad/juv	6	Wet
Surf smelt[i]	*Hypomesus pretiosus*	Average	17	3060	4.3	4.2–4.3	Harbour, ad/juv	4	Wet
Pacific staghorn sculpin[k]	*Leptocottus armatus*	Average	—	174	2.1	1.8–2.5	Harbour, ad/juv	6	Wet
Shortspine thornyhead[k]	*Sebastolobus alascanus*	Average	—	90	1.1	1.0–1.2	Harbour, ad/juv	6	Wet
Invertebrates									
Squid[e]	*Loligo forbesi*	Average	—	27	1.4	1.1–1.9	Harbour, ad/juv	7	Wet
Berryteuthis[j]	*Berryteuthis magister*	Average	17	33	1.1	1.0–1.4	NES,[d] juv	2	Dry
Loligo[j]	*Loligo opalescens*	Average	12	55	1.2	1.1–1.5	NES,[d] juv	2	Dry
Loligo[k]	*Loligo* sp.	Average	—	35	2.3	1.6–3.7	Harbour, ad/juv	6	Wet
Octopus[e]	*Eledone cirrhosa*	Average	—	36	1.2	1.1–1.5	Harbour, ad/juv	7	Wet

[a]Sagital otoliths or squid beaks.
[b]Original values in parentheses (see Methods).
[c]Average NCF calculated over all length-classes or meal sizes fed.
[d]Northern elephant seal.
[e]Tollit et al. (1997).
[f]Marcus et al. (1998).
[g]Prime and Hammond (1987).
[h]Prime (1979).
[i]Cottrell et al. (1996).
[j]Harvey and Antonelis (1994).
[k]Harvey (1989).
[l]Dellinger and Trillmich (1988).
[m]da Silva and Neilson (1985).

© 2000 NRC Canada

Table 2. Methods used to test the effectiveness of otolith recovery and to feed test prey in experiments on captive pinnipeds.

Effectiveness of recovery	Method to feed prey	Comments	% recovery	Source
Not tested	Atlantic herring as carrier	Animal held in dry compound; all feces recovered		Prime 1979
Not tested	1 otolith removed	Animal held in raised dry pen with mesh bottom; 95% of each fecal sample recovered based on visual estimate		da Silva and Neilson 1985
Not tested	Whole	Animals in water; not possible to distinguish loss during recovery from complete digestion		Prime and Hammond 1987
90 glass beads fed in 11 trials	Whole	Animals in dry room but given time each day to interact with other pinnipeds	74.0±37.7	Dellinger and Trillmich 1988
34 otoliths scattered in tank on 3 days	Whole	Pairs of seals held in water during feeding trial	97	Harvey 1989
Not tested	Whole	Animals held in dry cage; all fecal material collected twice daily		Harvey and Antonelis 1994
20–25 marked otoliths	Whole	Seals housed individually in water during feeding trials	100	Cotrell et al. 1996
36 marked otoliths on two occasions	Atlantic herring used as carrier	All seals held in same pool in water during the feeding trials	100 English whiting; 70–73 sand eel	Tollit et al. 1997
60 glass beads at each of 42 fecal collections	Atlantic herring whole; Atlantic cod heads in Atlantic herring	Seals housed individually in water during feeding trials	99.1±1.3	Marcus et al. 1998

surroundings for the duration of a feeding trial and were therefore relatively inactive, whereas in the other studies, the seals were able to swim during the feeding trials. Level of activity is known to affect the rate of digestion in mammals (see Harvey 1989), and thus, experimental condition might have effected estimates of NCFs. I examined the hypothesis that this difference might account for some of the variation in NCFs by comparing the NCFs for the same prey species using both the wet and dry protocols. In the case of Atlantic herring, the mean NCF from dry feeding trials was higher (12.5, $n = 4$) and more variable (CV = 94.5%) than those from wet feeding trials (mean = 3.3, CV = 40%, $n = 7$). However, this difference was not significant (Mann–Whitney test, $p = 0.65$). The dry protocol estimate of the NCF for Atlantic tomcod was about five times higher than the wet protocol estimate. However, this result is confounded by the fact that different seal species were used in the two studies. In species with more robust otoliths (e.g., Atlantic cod and English whiting), the data suggest that there is little difference among NCFs estimated in experiments using the wet or dry feeding protocol (Table 1). The data on sprat are unusual in this regard, as the estimate from Tollit et al. (1997) using the wet protocol was much higher than the two estimates using the dry protocol (Table 1). However, these results are further confounded, as three species of pinnipeds were used in these experiments.

Data were available for several prey species to examine the influence of prey size on NCFs. In English whiting, NCFs appear to vary inversely with prey length ($r = -0.96$, $p = 0.002$, $n = 6$); however, in Atlantic cod ($r = 0.06$, $p = 0.89$, $n = 7$) and Atlantic herring ($r = -0.31$, $p = 0.42$, $n = 10$), there was no correlation between prey length and NCF.

Differences in digestive efficiency among pinniped species might result in different NCFs within prey species. To examine this, I compared the NCFs of Atlantic cod and Atlantic and Pacific herring fed to grey seals and harbour seals. There was no difference in the NCFs of either prey species between seal species (Table 4). However, the mean NCF of Atlantic tomcod fed to two northern elephant seals (*Mirounga angustirostris*) (6.6, 95% CI = 4.1–11.7) was higher than that found in six harbour seals (1.4, 95% CI = 1.3–1.6), suggesting a predator digestion effect on NCF (Table 1). This conclusion is somewhat confounded, as the northern elephant seals were held in dry conditions during the feeding experiment, whereas the harbour seals were held in water. The mean NCFs for sprat also differed among three pinnipeds species, as the 95% confidence intervals did not overlap: northern fur seal (*Callorhinus ursinus*), 1.4–1.6; California sea lion (*Zalophus californianus*), 2.9–3.3; harbour seal, 6.9–15.0. Here again, different holding conditions were used with the northern fur seals and sea lions during the feeding experiment compared with the harbour seal. However, the direction of the effect (i.e., lower NCF in dry conditions) appears to be the reverse of that expected if experimental conditions were the source of the difference (Table 1).

Discussion

It has been known for some time (e.g., Prime 1979; Frost and Lowry 1980) that prey hard structures, used to both

© 2000 NRC Canada

Table 3. NCFs for prey species with three or more observations from captive feeding experiments with several species of pinnipeds (see Table 1).

	Atlantic cod	English whiting	Atlantic herring	Sprat	Sand eel
Mean	1.2 *a*	1.3 *a*	6.6 *b*	4.8 *b*	3.5 *b*
SE	0.07	0.08	2.48	2.62	0.62
n	7	6	11	3	5

Note: One-way ANOVA: $F_{4,27} = 13.4$, $p < 0.001$. Means followed by the same letter are not significantly different at the 5% level (Sidak multiple-comparisons test).

Table 4. NCFs of Atlantic cod and Atlantic and Pacific herring fed to grey and harbour seals.

	Atlantic cod		Atlantic and Pacific herring	
	Grey seal	Harbour seal	Grey seal	Harbour seal
Mean	1.2	1.2	4.0	6.1
SE	0.26	0.16	1.90	8.37
n	3	4	3	7

Note: Two-way ANOVA, main effects: prey species, $p = 0.22$; seal species, $p = 0.73$.

identify and determine the size and number of prey consumed by marine mammals, are eroded and in some cases completely dissolved during digestion. Thus, in most cases, the number of recovered otoliths underestimates the number of ingested otoliths and therefore the number of ingested prey. The biases produced by the complete and partial digestion of otoliths/beaks also have been appreciated for some time (e.g., Jobling and Breiby 1986). As a result, a growing number of studies have attempted to estimate prey-specific factors to correct for these two biases (see Introduction). However, in practice, authors have corrected only for partial erosion of otoliths in the reconstruction of marine mammal diets. Given the results presented in Tables 1 and 5, there can be little doubt that the use of NCFs to account for the complete digestion of otoliths and cephalopod beaks could have a significant effect on estimates of the number of prey consumed by marine mammals.

The implications of complete digestion of otoliths for estimates of marine mammal diet have been previously explored (Jobling 1987). For example, if equal numbers of haddock and herring were ingested, Jobling (1987) showed that one would conclude that the marine mammal consumed 3.6 times as many haddock as herring, based on recovered otoliths. In the case of grey seals on Sable Island, sand lance dominate the number of prey eaten (Bowen and Harrison 1994). Application of NCFs to the July 1991 sample of otoliths resulted in an increase in the estimated number of sand lance eaten to 95.3% from 88.1% with a corresponding decrease in the percentage of other prey. Clearly, the impact of NCFs on estimates of diet composition will vary with the mixture of prey species consumed and their relative NCFs. In general, however, the use of NCFs will tend to decrease the importance of gadoids in the diets of pinnipeds. As such, their use could have implications with respect to the importance of pinniped predation on the dynamics of many

Table 5. Mean NCFs for fish and invertebrates.

Prey species	Prey length range (cm)	Mean NCF
Atlantic cod	16–33	1.2
Haddock	22–32	1.1
Walleye pollock	20–38[a]	1.3
Atlantic tomcod	na	1.4
English whiting	9–31	1.3
Pout whiting	na	1.1
Pacific hake	27–39[a]	1.4
Dover sole	na	1.2
English sole	na	4.1
Lemon sole	16–35	2.1
Rex sole	na	1.3
European plaice	21–24	1.6
Dab	na	2.2
Eulachon	na	2.9
Sand eel	8–19	3.6
Atlantic herring	13–28[b]	3.0
Sprat	12–14	4.8
Rainbow trout	na	1.6
Chinook salmon	12–17[a]	1.6
Shiner perch	na	1.7
Surf smelt	14–20[a]	4.3
Pacific staghorn sculpin	na	2.1
Shortspine thornyhead	na	1.1
Berryteuthis	14–20	1.1
Loligo forbesi	na	1.4
Loligo opalescens	9–15	1.3
Loligo sp.	na	2.3
Octopus	401–1025[c]	1.2

Note: na, not available.
[a]Range estimated as ±3 SD.
[b]Excluding values from dry condition experiments.
[c]Mass in grams.

groundfish species. Given these implications, it would be unwise to continue to assume that NCFs are not required.

There is little evidence from the recent literature that investigators are aware of this bias. Part of the reason why NCFs have not been regularly used may stem from the fact that, until recently, too few prey species and marine mammals had been studied to provide much confidence in their use. However, recent studies (Cottrell et al. 1996; Tollit et al. 1997; Marcus et al. 1998) combined with earlier work provide a firmer empirical basis for the use of NCFs. A broad range of prey species, representing those with small, fragile otoliths and those with large, robust otoliths, now have been used in feeding studies. Thus, as a first approximation, authors will generally be able to find NCFs from an analogous prey species to fill gaps.

Although I would argue that the use of NCFs will improve estimates of the species composition of marine mammal diets, the existing estimates of NCFs are not satisfactory in several respects. There is evidence that at least five factors affect NCFs within a prey species: meal size (Marcus et al. 1998), the condition in which the animal is held (i.e., in water versus dry; see Results), the size of prey used (Tollit et

© 2000 NRC Canada

al. 1997), the species of pinniped, and the effectiveness of hard part recovery. Yet for none of these factors have experiments been conducted across a range of prey types and pinnipeds species under standardized experimental conditions. Although data on the effect of experimental housing on NCFs are conflicting, exercise likely affects digestive efficiency in pinnipeds, and thus, it would seem prudent to provide pinnipeds with the opportunity to exercise during feeding trials. The length-specific NCFs for Eglish whiting and lemon sole are quite convincing. However, despite the evidence that NCFs in some prey species may vary as a function of length, there is not enough data at this time to use size-specific NCFs in most cases. The influence of pinniped species on NCFs within prey species is also unclear. There appears to be little difference in the NCFs of prey consumed by harbour and grey seals, but the northern elephant seal data suggests that even within phocids, there may be pinniped species effects. Although not included in Table 1, the high NCFs (i.e., >25) in six prey species fed to the otariid *N. cinerea* (Gales and Cheal 1992) differ from the results of Dellinger and Trillmich (1988) for two other otariids, again suggesting pinniped species effects on NCFs. Lack of standardization also applies to the method of feeding otoliths and cephalopod beaks to pinnipeds (Table 2). Whole prey should be used in these experiments. Although this may not be possible in all cases, we need to understand the effect on NCFs of using a carrier species, such as Atlantic herring, to present otoliths of other prey species to pinnipeds. Until this is done, comparisons among studies will be problematic.

Recent developments in the use of telemetry and animal-borne video to determine feeding frequency, meal size, and the size of prey eaten by free-ranging marine mammals suggest that it may be possible to greatly improve estimates of diet composition by using NCFs that account for these variables. Thus, future experimental studies should systematically investigate the relationships between NCFs, meal size, and prey size for a range of species differing in otolith architecture. It is also important to obtain estimates of the variability of NCFs such that this variability can be used to estimate confidence limits associated with diet composition (Hammond and Rothery 1996).

There is also the issue of whether to use NCFs derived from hard parts recovered in feces on hard parts recovered from stomach contents. Murie and Lavigne (1985) showed that the proportion of Atlantic herring otoliths recovered from the stomachs of harp (*Phoca groenlandica*) and grey seals decreased inversely with time since feeding. Up to 3 h postfeeding, 100% of the otoliths were recovered from the stomachs, indicating an NCF of 1.0. However, beyond 3 h, the percentage of otoliths recovered in the stomach decreased rapidly, reaching 0% after 12 h. The clearance and digestion rate will undoubtedly differ among prey species. Thus, it would not seem possible to apply the NCFs derived from recovery of otoliths and cephalopod beaks in feces to hard parts recovered from stomach contents. However, Murie and Lavigne's (1985) work does indicate that, with the exception of quite recently ingested meals, the number of recovered otoliths from stomach contents will not accurately estimate the number of prey consumed.

Acknowledgements

I would like to thank Debbie Austin, Carrie Beck, and Margi Cooper for commenting on an earlier draft of the paper. The paper was improved by the valuable suggestions made by Andrew Trites and two anonymous reviewers.

References

Bigg, M.A., and Fawcett, I.F. 1985. Two biases in diet determination of northern fur seals (*Callorhinus ursinus*). *In* Maine mammals and fisheries. *Edited by* J.R. Beddington, R.J.H. Beverton, and D.M. Lavigne. George Allen & Unwin, London, England. pp. 284–291.

Bowen, W.D., and Harrison, G.D. 1994. Offshore diet of grey seals *Halichoerus grypus* near Sable Island, Canada. Mar. Ecol. Prog. Ser. **112**: 1–11.

Boyle, P.R., Pierce, G.J., and Diack, J.S.W. 1990. Sources of evidence for salmon in the diet of seals. Fish. Res. **10**: 137–150.

Clarke, M.R.1986. A handbook for the identification of cephalopod beaks. Clarendon Press, Oxford, England.

Cottrell, P.E., Trites, A.W., and Miller, T.E. 1996. Assessing the use of hard parts in faeces to identify harbour seal prey: results of captive-feeding trials. Can. J. Zool. **74**: 875–880.

da Silva, J., and Neilson, J.D. 1985. Limitation of using otoliths recovered in scats to estimate prey consumption in seals. Can. J. Fish. Aquat. Sci. **42**: 1439–1442.

Dellinger, T., and Trillmich, F. 1988. Estimating diet composition from scat analysis in otariid seals (Otariidae): is it reliable? Can. J. Zool. **66**: 1865–1870.

Fitch, J.E., and Brownell, R.L. 1968. Fish otoliths in cetacean stomachs and their importance in interpreting feeding habits. J. Fish. Res. Board Can. **25**: 2561–2575.

Frost, K.J., and Lowry, L.F. 1980. Feeding of ribbon seal (*Phoca fasciata*) in the Bering Sea in spring. Can. J. Zool. **58**: 1601–1607.

Gales, N.J., and Cheal, A.J. 1992. Estimating diet composition of the Australian sea-lion (*Neophoca cinerea*) from scat analysis: an unreliable technique. Wildl. Res. **19**: 447–456.

Hammond, P.S., and Prime, J.H. 1990. The diet of British grey seals (*Halichoerus grypus*). *In* Population biology of sealworm (*Psuedoterranova decipiens*) in relation to its intermediate and seal hosts. *Edited by* W.D. Bowen. Can. Bull. Fish. Aquat. Sci. No. 222. pp. 243–254.

Hammond, P.S., and Rothery, P. 1996. Estimating seal diet using computer sampling. J. Appl. Stat. **23**: 1–15.

Harvey, J.T. 1989. Assessment of errors associated with harbour seal (*Phoca vitulina*) feacal sampling. J. Zool. (Lond.), **219**: 101–111.

Harvey, J.T., and Antonelis, G.A. 1994. Biases associated with non-lethal methods of determining the diet of northern elephant seals. Mar. Mammal Sci. **10**: 178–187.

Jobling, M. 1987. Marine mammal faecal samples as indicators of prey importance — a source of error in bioenergetics studies. Sarsia, **72**: 255–260.

Jobling, M., and Breiby, A. 1986. The use and abuse of fish otoliths in studies of feeding habits of marine piscivores. Sarsia, **71**: 265–274.

Marcus, J., Bowen, W.D., and Eddington, J.D. 1998. Effects of meal size on otolith recovery from fecal samples of gray and harbor seal pups. Mar. Mammal Sci. **14**: 789–802.

Murie, D.J., and Lavigne, D.M. 1985. Digestion and retention of Atlantic herring otoliths in the stomachs of grey seals. *In* Marine mammals and fisheries. *Edited by* J.R. Beddington, R.J.H.

© 2000 NRC Canada

Beverton, and D.M. Lavigne. George Allen & Unwin, London, England. pp. 292–299.

Pierce, G.J., and Boyle, P.R. 1991. A review of methods for diet analysis in piscivorous marine mammals. Oceanogr. Mar. Biol. **29**: 409–486.

Pierce, G.J., Boyle, P.R., Watt, J., and Grisley, M. 1993. Recent advances in diet analysis of marine mammals. Symp. Zool. Soc. Lond. **66**: 241–261.

Prime, J.H. 1979. Observations on the digestion of some gadoid fish otoliths by a young common seal. ICES Mar. Mammals Comm. CM 1979/N:14.

Prime, J.H., and Hammond, P.S. 1987. Quantitative assessment of gray seal diet from fecal analysis. *In* Approaches to marine mammal energetics. *Edited by* A.C. Huntley, D.P. Costa, G.A.J. Worthy, and M.A. Castellini. Allen Press, Lawrence, Kans. pp. 165–181.

Tollit, D.J., Steward, M.J., Thompson, P.M., Pierce, G.J., Santos, M.B., and Hughes, S. 1997. Species and size difference in the digestion of otoliths and beaks: implications for estimates of pinniped diet composition. Can. J. Fish. Aquat. Sci. **54**: 105–119.

© 2000 NRC Canada

Effects of increasing winter rearing habitat on abundance of salmonids in two coastal Oregon streams

M.F. Solazzi, T.E. Nickelson, S.L. Johnson, and J.D. Rodgers

Abstract: We used a BACI (before–after–control–impact) experimental design to examine the effects of increasing winter habitat on the abundance of downstream migrant salmonids. Two reference streams and two treatment streams were selected in the Alsea and Nestucca basins of Oregon. Population parameters for juvenile coho salmon (*Oncorhynchus kisutch*), age-0 trout (*Oncorhynchus* spp.), steelhead (*Oncorhynchus mykiss*), and coastal cutthroat trout (*Oncorhynchus clarki*) were estimated each year for 8 years in each stream. Stream habitat was modified to increase the quality and quantity of winter habitat during the summers of 1990 (Nestucca Basin) and 1991 (Alsea Basin). Complex habitat was constructed by adding large woody debris to newly created alcoves and dammed pools. Numbers of coho salmon summer juveniles and smolts increased in the treatment streams relative to the control streams during the posttreatment period. Overwinter survival of juvenile coho salmon also increased significantly in both treatment streams posttreatment. Summer trout populations in the treatment streams did not change, but downstream migrant numbers the following spring did increase. These increases suggest that winter habitat was limiting abundance of all three species.

Résumé : On a utilisé la méthode expérimentale CAA (comparaison avant–après) pour examiner les effets de l'extension des habitats d'hiver sur l'abondance des salmonidés en dévalaison. On a choisi deux cours d'eau de référence et deux cours d'eau expérimentaux dans les bassins de l'Alsea et de la Nestucca, en Oregon. On a estimé les paramètres de population du saumon coho (*Oncorhynchus kisutch*) juvénile, de truites (*Oncorhynchus* spp.) d'âge 0, du saumon arc-en-ciel (*O. mykiss*) et de la truite fardée côtière (*O. clarki*) chaque année pendant huit ans dans chacun des cours d'eau. Pendant les étés 1990 (bassin de la Nestucca) et 1991 (bassin de l'Alsea), l'habitat lotique a été modifié pour augmenter la qualité et la quantité des habitats d'hiver. On a construit un habitat complexe en ajoutant de gros débris ligneux dans des fosses latérales et des retenues artificielles nouvellement créées. Le nombre de juvéniles d'été et de smolts de coho dans les cours d'eau expérimentaux a augmenté par rapport à celui des cours d'eau de référence après l'aménagement. La survie hivernale des cohos juvéniles a aussi augmenté considérablement dans les deux cours d'eau après l'aménagement. Au cours du premier été, la population de truites dans les cours d'eau expérimentaux n'a pas changé, tandis que le nombre de migrateurs en dévalaison a augmenté au printemps suivant. Ces augmentations semblent indiquer que l'habitat d'hiver limite l'abondance chez ces trois espèces de poissons.

[Traduit par la Rédaction]

Introduction

Recent declines in abundance of coho salmon (*Oncorhynchus kisutch*) populations in Oregon coastal streams have resulted in increased recognition of the need for quantitative assessments of the effectiveness of methods used to restore habitat for juvenile salmon and trout (*Oncorhynchus* spp.). Various methods to improve freshwater habitat have been practiced in trout fishery management for several decades (Hubbs et al. 1932; Tarzwell 1937; Shetter et al. 1949). More recently, some of these techniques have been modified for Pacific salmon and trout (House and Boehne 1985; Nickelson et al. 1992*b*; Beechie et al. 1994).

Received January 28, 1999. Accepted February 10, 2000. J14989

M.F. Solazzi,[1] T.E. Nickelson, S.L. Johnson, and J.D. Rodgers. Oregon Department of Fish and Wildlife, 28655 Highway 34, Corvallis, OR 97333, U.S.A.

[1]Author to whom all correspondence should be addressed. e-mail: solazzim@ucs.orst.edu

A review of the literature reveals a lack of quantitative information on whether habitat restoration affects the freshwater production of anadromous salmonid populations. Smokorowski et al. (1998) concluded that documentation of habitat projects was generally poor and that success was often measured by evaluating the desired changes in habitat without determining biological benefit. When evaluations of instream habitat restoration projects have examined the impacts on fish populations, the studies have usually focused only on estimating the number of fish rearing in the vicinity of the restoration project (Nickelson et al. 1992*b*; House 1996). They generally have not included reference streams or reaches with which to compare changes in fish abundance in the treated area. As a result, it is difficult to determine if changes in fish abundance near the restoration project represent an actual increase in production due to the effects of the habitat project or a redistribution of fish. Also, most past studies were completed during the summer low-flow period (Crispin et al. 1993; House 1996), leaving unresolved the question of survival during winter rearing prior to ocean migration.

Results of salmonid habitat restoration projects have been

© 2000 NRC Canada

mixed. For example, Scruton et al. (1997) evaluated a variety of habitat projects aimed at increasing the production of Atlantic salmon (*Salmo salar*) in Newfoundland, Canada. These authors concluded that "Generally, the projects evaluated have been successful in increasing salmonid abundance and (or) production." Cederholm et al. (1997), comparing coho salmon and age-1 steelhead (*Oncorhynchus mykiss*) abundance from treatment and reference reaches in Washington, found that coho salmon smolt abundance, but not steelhead, increased significantly following the addition of large wood. An evaluation of a spawning habitat rehabilitation project on the Merced River, California (Kondolf et al. 1996), showed that the project failed to consider the erosion and transport potential. Consequently, the gravel placements were quickly transported downstream. These conflicting results coupled with the growing interest in the use of habitat modification techniques by federal, state, and private organizations underscore the need for careful evaluations of habitat enhancement projects.

We present the results of an experiment designed to evaluate the effects of habitat restoration projects on coho salmon smolt abundance in two coastal Oregon streams. The intent of the habitat modification was to increase the amount and complexity of winter habitat, which has been suggested to limit coho salmon populations in Oregon (Nickelson et al. 1992*a*). This experiment was originally designed to examine changes in abundance of coho salmon smolts. However, we collected information on two sympatric but less abundant species, steelhead and coastal cutthroat trout (*Oncorhynchus clarki*), as well.

Our experimental design combined a preproject and postproject evaluation with a treatment and reference stream approach. This allowed us to account for changes in the number of migrants produced in a given length of stream that could be due to factors other than the experimental treatment. We monitored the summer population size and estimated the number of spring migrants produced each year for 8 years in each of four study streams. This type of quantitative evaluation is critical for fishery managers trying to determine if artificial habitat manipulation projects are a viable tool for restoring salmonid habitat.

Materials and methods

Study area

Our paired study streams were of similar size and located largely on land managed by the U.S. Bureau of Land Management (Fig. 1). One pair was in the Alsea Basin, East Fork Lobster Creek and Upper Lobster Creek, and the other was in the Nestucca Basin, East Creek and Moon Creek. Upper Lobster Creek and East Creek were designated treatment streams. Study reaches established on each of the four streams ranged from a downstream smolt trap site to the upper limits of coho salmon distribution. Physical characteristics of these stream reaches are shown in Table 1. Both the Nestucca and Alsea basins receive between 150 and 250 cm of rain each year. Typical summer water temperatures ranges between 11 and 17°C and winter temperatures occasionally drop to as low as 4°C. Aquatic species present in the study streams included coho salmon, steelhead, coastal cutthroat trout, sculpins (*Cottus* spp.), Pacific lamprey (*Lampetra tridentata*), and giant salamanders (*Dicamptodon tenebrosus*). The riparian vegetation consists of an overstory of red alder (*Alnus rubra*), bigleaf maple (*Acer macrophyllium*), western redcedar (*Thuja plicata*), Douglas-fir (*Pseudotsuga menziesii*), and western hemlock (*Tsuga heterophylla*) as well as an understory of salmonberry (*Rubus spectabilis*), salal (*Gaultheria shallon*), vine maple (*Acer circinatum*), and sword fern (*Polystichum munitum*).

Summer and winter habitat surveys

During August and September of each year, we used Hankin and Reeves' (1988) methodology to estimate the amount of available habitat within the study reach of each stream. We classified habitat using the methods of Bisson et al. (1982), as modified by Nickelson et al. (1992*a*). Surface area for each habitat unit in each stream was visually estimated, and every tenth unit was measured to calibrate the visual estimates.

Habitat surveys were also conducted during winter. These surveys were completed in December and January during winter base flows. During the pretreatment period, surveys were completed twice in the Alsea study streams and once in the Nestucca study streams. During the posttreatment period, surveys were completed twice in all four streams.

Estimating summer fish populations

A combination of snorkeling and electrofishing was used during August and September of each year to estimate the number of juvenile coho salmon, age-0+ trout, steelhead and cutthroat trout (<90 mm combined), and yearling and older (≥90 mm) steelhead and cutthroat trout (designated age 1+). In pool habitats, divers counted the number of each species in every third pool. This value was then adjusted by a calibration factor derived from electrofishing population estimates in a subset of these snorkeled pools (Hankin and Reeves 1988). To determine the number of fish rearing in glide, riffle, and rapid habitats, we estimated the average fish density for a subset of each habitat type by electrofishing. For each habitat type, we then multiplied this average density by the surface area of the habitat type in the entire stream reach above the trap (Hankin 1984).

For the electrofishing sampling, we estimated the number of each species and age group using either a mark–recapture estimate (Chapman 1951) or a removal estimate with two or more passes (Seber and LeCren 1967). Mark–recapture estimates were generally used only in pool habitat characterized by a high degree of wood complexity or that presented special sampling problems where removal estimation methods have been shown to be less accurate (Rodgers et al. 1992). Every habitat unit was blocked by seines on both ends and then sampled using 1000-V DC backpack electrofishers. Specific protocols for sampling intensity were established to control the size of the confidence interval derived from the population estimate and to prevent exposing the fish to unnecessary repeated electrofishing. In each study stream each summer, we generally sampled 10 pools for snorkel calibrations and 10 glides and 10 riffles or rapids for electrofishing expansion.

Estimating the number of downstream migrants

We estimated the number of downstream-migrating coho salmon, steelhead, and cutthroat trout in each stream each spring for 8 years using modified incline plane traps (McLemore et al. 1989). Sampling began by the first week in March and continued until we no longer captured fish, usually by 1 June. Traps generally operated 24 h per day. Captured fish were removed daily from the trap, anesthetized with buffered MS 222, and measured. Population estimates were made for coho salmon ≥60 mm. Scale samples collected from coho salmon migrants ≥60 mm in 1991 and 1992 revealed that this size-class averaged 98% age-1+ fish and 2% age-2+ fish. Juvenile coho salmon in Oregon typically spend about a year in freshwater before migrating to the ocean as smolts during their second spring (Moring and Lantz 1975; Bradford et al. 1997).

© 2000 NRC Canada

Fig. 1. Location of the four study streams in the Alsea and Nestucca basins, Oregon.

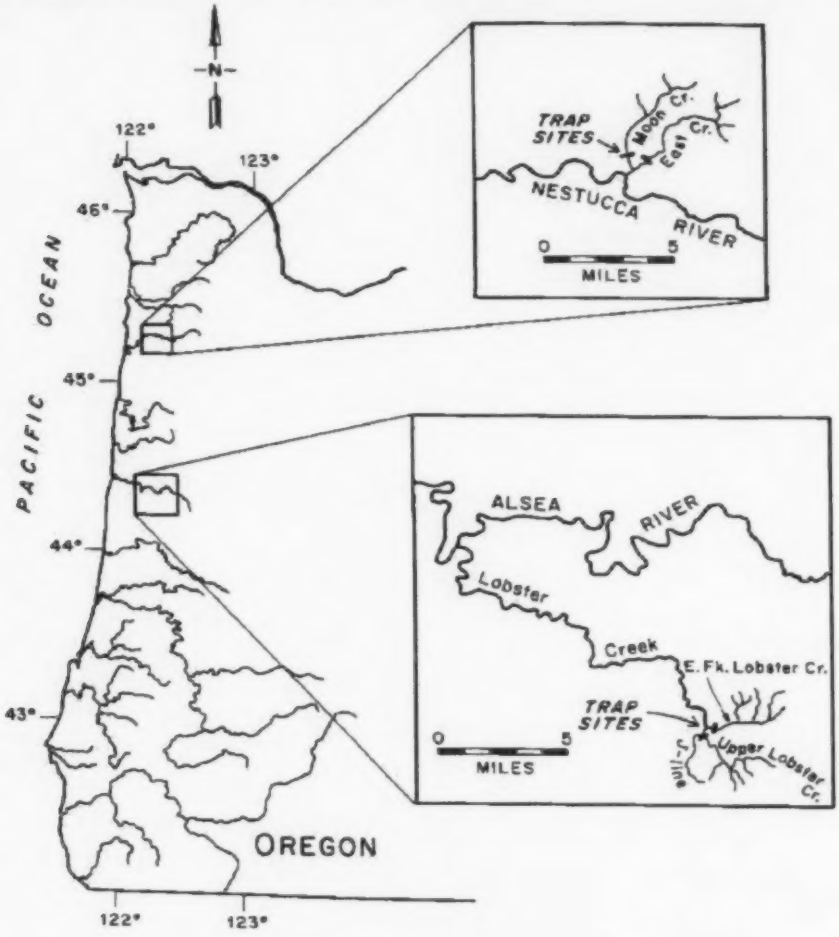

Table 1. Physical characteristics of the four study streams above the smolt traps.

Stream	Basin area (km^2)	Stream length (km)	Mean summer wetted width (m)	Average gradient (%)
Alsea Basin				
East Fork Lobster Creek	14.2	3.5	3.5	4.0
Upper Lobster Creek	12.4	4.7	3.2	2.6
Nestucca Basin				
Moon Creek	13.2	3.8	3.6	1.8
East Creek	17.5	5.0	4.0	2.4

Thus, our estimates of the number of coho salmon migrants ≥60 mm encompasses the smolt population. We made population estimates for steelhead and cutthroat trout migrants ≥90 mm. Scale analyses and length–frequency histograms indicated that fish of this size were age 1+ and older.

To estimate trap efficiency, up to 25 fish from each species were removed from the trap each day, given a caudal fin notch mark, and released into an area of quiet water 50–100 m above the trap site. Weekly trap efficiency estimates were calculated by dividing the number of marked fish recaptured by the number of marked fish released.

For coho salmon, the total number of unmarked fish captured was divided by the estimated trap efficiency to estimate the number of fish passing the trap site each week. Weekly estimates were summed to estimate the total number of fish passing the trap site each spring. Overwinter survival rates for coho salmon were calculated by dividing the estimate of the total number of coho salmon migrating past the trap site each season by the summer population estimate.

We did not attempt to calculate weekly estimates of the number of trout passing the trap because of the low numbers of migrants captured. A population estimate for trout was usually calculated by dividing the total number of trout captured during the trapping season by the seasonal estimate of trap efficiency.

© 2000 NRC Canada

Habitat modification

The habitat modification was completed during the summer of 1990 in East Creek (Nestucca Basin) and during the summer of 1991 in Upper Lobster Creek (Alsea Basin). Work on both streams was funded and constructed by the U.S. Bureau of Land Management in consultation with the Oregon Department of Fish and Wildlife. Total installation cost was about US$80 000. A track hoe was used to place full-spanning logs into the stream channel (to create large dam pools) and to excavate off-channel rearing ponds (alcoves). Erosion cloth and chain-link fence were attached to the upstream side of most full-spanning logs to reduce undercutting. Most of the large logs were anchored to the substrate with rebar. Large wood was added to each dam pool to act as scour agents. Rootwads and smaller trees were added to increase habitat complexity within the pools.

Sites for alcove construction were selected by using natural springs or seeps whenever possible. Full-spanning logs were generally placed immediately below the mouth of the alcove to insure that water flooded the entrance. Alders were uprooted and added to the alcoves to provide cover. We created 23 dam pools and eight alcoves in Upper Lobster Creek along a 3.2-km reach. Twenty-nine dam pools and 13 alcoves were constructed in East Creek along a 2.4-km reach. The constructed pools averaged 160 m^2 in surface area compared with an average of about 50 m^2 for natural pools.

Study design and analysis

The study was designed to assess changes in habitat and fish population parameters in a treatment stream by using a reference stream to account for changes due to factors other than the treatment. This approach has been referred to as a BACI (before–after–control–impact) design by Stewart-Oaten et al. (1986), who recommended it to address the problem of pseudoreplication often encountered in ecological impact studies (Hurlbert 1984). For each habitat or fish population parameter, we (*i*) calculated the ratio of treatment to reference each year, (*ii*) estimated the mean ratios for the pretreatment and posttreatment periods, and (*iii*) used a *t* test to compare the means. For coho salmon, our null hypothesis was that the ratio during the posttreatment period was not greater than the ratio during the pretreatment period because the habitat modification was expected to increase coho salmon populations. Thus, a one-tailed test was employed. For trout, our null hypothesis was that the posttreatment ratio was not different from the pretreatment ratio because the possible effects of habitat modification were unknown. Therefore, a two-tailed test was used. In each case, a logarithmic transformation of the ratios was used to equalize variances.

Due to the presumed importance of winter habitat to coho salmon survival, we focused on changes in winter habitat. These parameters included the surface area of coho salmon winter rearing habitat (i.e., slow-water habitat), the surface area of fast-water habitat, and total surface area. Winter rearing habitat was defined as the combined area of alcoves, dammed pools, and beaver ponds. The restoration modifications were designed to increase this habitat type. Fast-water habitat, the combined area of cascades, rapids, riffles, and glides, was expected to decrease because habitat modification tended to convert fast water to slow water (i.e., winter rearing habitat). The statistical analysis of winter habitat was only possible for the Alsea study streams because the Nestucca study streams had only one winter habitat survey during the pretreatment period.

The parameters used to assess changes in coho salmon populations were summer population, overwinter survival rate, and estimated numbers of smolts. For trout populations, we analyzed summer populations of age-0+ trout, age-1+ steelhead, and age-1+ cutthroat trout and numbers of downstream-migrating steelhead and cutthroat trout. We did not compare overwinter survival rate for trout because the populations contained multiple year-classes.

Potentially, the first effects of the habitat modification should have been on overwinter survival during the winter following construction. This would have occurred following summer rearing of the 1989 brood coho salmon in the Nestucca study streams and the 1990 brood coho salmon in the Alsea study streams. The organization of the pre–post comparisons of the habitat and population parameters is described in Table 2.

Results

Habitat

The amount of winter rearing habitat in Upper Lobster Creek (Alsea treatment) was significantly greater (one-tailed *t* test: $p = 0.025$) following habitat modification relative to that in East Fork Lobster Creek (Alsea reference). The average area of winter rearing habitat increased by about 700% in the treatment stream, whereas it decreased by about 30% in the reference stream (Fig. 2). The average area of fast-water habitat decreased by about 5000 m^2 (30%) in the treatment stream, while that in the reference stream remained about the same (Fig. 2). However, the decrease was not significant (one-tailed *t* test: $p = 0.16$).

Average area of winter rearing habitat in East Creek (Nestucca treatment) following habitat modification increased 13 times over that in the previous year (Fig. 2). During the same years, winter rearing habitat in Moon Creek (Nestucca reference) remained about the same. Fastwater habitat in the treatment stream decreased by about 6000 m^2 after the habitat modification, whereas it remained relatively constant in the reference stream (Fig. 2).

Total surface area during winter remained relatively constant in both reference streams (Fig. 2). The range of values represented only about 10% of the total area. Total surface area of the Alsea treatment was not changed significantly by the habitat modification (two-tailed *t* test: $p = 0.47$), most of which occurred within the stream channel. In the Nestucca treatment stream, total surface area increased by about 25% the first winter following habitat modification because of extensive construction of off-channel alcoves (Fig. 2). The area decreased somewhat the next winter when channel changes isolated some of these alcoves.

Fish populations

Following habitat modification, summer populations of juvenile coho salmon in the Alsea treatment stream increased relative to populations in the reference stream (one-tailed *t* test: $p = 0.02$). Mean summer population in the treatment stream increased by 50% in the posttreatment period compared with the pretreatment period, while the mean population in the reference stream decreased by 25% (Fig. 3). Mean summer populations of coho salmon in both of the Nestucca study streams were lower during the posttreatment period than during the pretreatment period (Fig. 2). However, because the populations in the treatment stream declined to a lesser degree (20%) than did those in the reference stream (50%), the ratio between the two increased (one-tailed *t* test: $p = 0.01$).

The number of coho salmon smolts in the treatment streams after habitat modification increased relative to the number of coho salmon migrants in the reference streams (one-tailed *t* test: Alsea, $p = 0.024$; Nestucca, $p = 0.005$).

© 2000 NRC Canada

Table 2. Analytical layout of the habitat and population parameters.

		Alsea study streams comparisons		Nestucca study streams comparisons	
Parameter	First data collected	Pretreatment	Posttreatment	Pretreatment	Posttreatment
Winter physical habitat	Winter 1988–1989	Winter 1988–1989 Winter 1990–1991	Winter 1991–1992 Winter 1993–1994	Winter 1988–1989	Winter 1990–1991 Winter 1991–1992
Coho salmon summer population	Summer 1988	1987–1990	1991–1993	1987–1989	1990–1993
Coho salmon overwinter survival	Winter 1988–1989	1987–1989	1990–1993	1987–1988	1989–1993
Coho salmon smolts	Spring 1988	1986–1989	1990–1993	1986–1988	1989–1993
Trout summer populations	Summer 1988	1987–1990[a]	1991–1993[a]	1987–1989	1990–1993
Steelhead migrants	Spring 1988	1986–1989[a]	1990–1993[a]	1986–1988	1989–1993
Cutthroat trout migrants	Spring 1988	1986–1989[a]	1990–1993[a]	1986–1988	1989–1993

Note: For habitat comparisons, years represent calendar years. For population comparisons, years represent brood years.
[a]For consistency, brood year designations are based on coho salmon smolts. Thus, brood year 1987 would have a summer population estimated in 1988 and a migrant population in spring 1989, regardless of trout age.

Fig. 2. Surface area of winter rearing habitat, fast-water habitat, and total habitat in the treatment and reference streams in the Alsea and Nestucca basins, pretreatment and posttreatment. Winter rearing habitat areas in the Nestucca reference stream were too small to display on the graph and are therefore shown as numeric values. Solid bars, treatment pre; open bars, reference pre; diagonally hatched bars, treatment post; horizontally hatched bars, reference post.

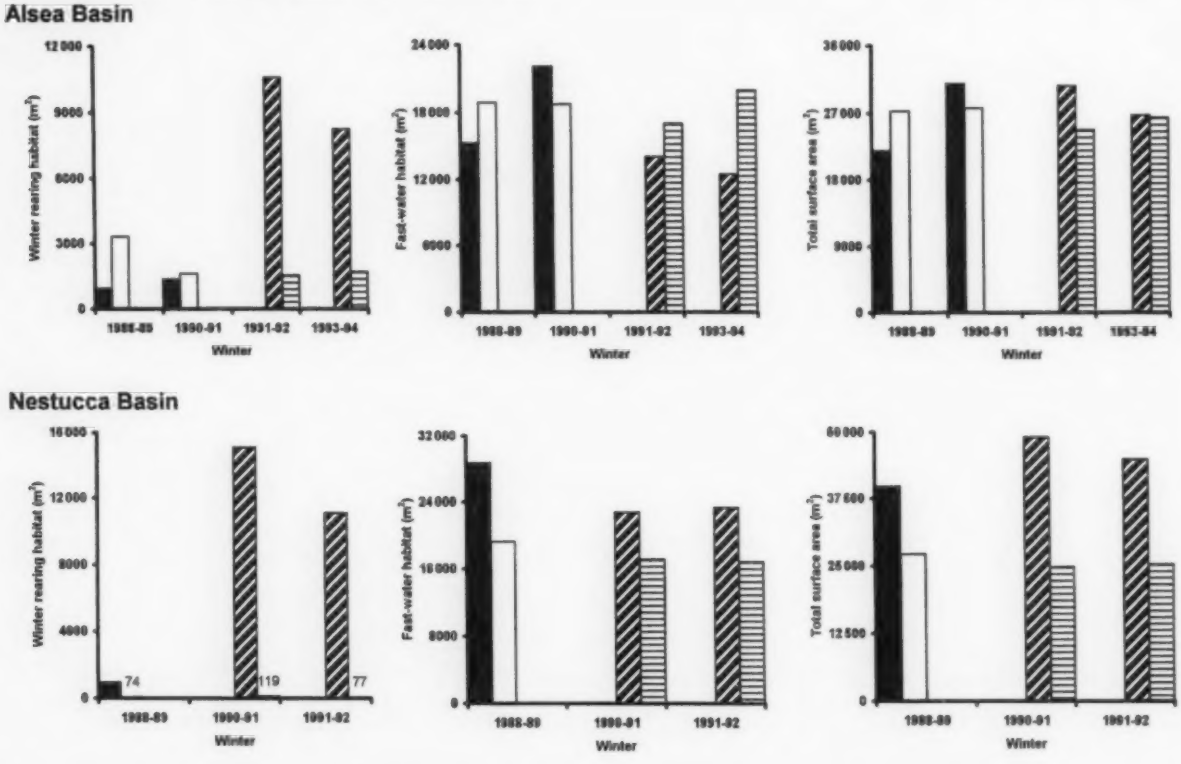

Mean number of coho salmon smolts increased by over 200% in the Alsea treatment stream, while the mean for the reference stream remained the same (Fig. 3). Similarly, the mean number of coho salmon migrants in the Nestucca treatment stream doubled, whereas the mean in the reference stream decreased by 75% (Fig. 3).

Overwinter survival of coho salmon also increased in both treatment streams after habitat modification relative to survival in the reference streams (one-tailed t test: Alsea, p = 0.04; Nestucca, p = 0.007). Survival in the Alsea treatment stream increased from a pretreatment mean of 0.13 to a posttreatment mean of 0.38 (Fig. 3). Mean survival in the reference stream increased slightly from 0.17 to 0.20 (Fig. 3). In the Nestucca treatment stream, mean overwinter survival increased 250% from 0.11 to 0.39, whereas in the reference stream, survival fell from a mean of 0.19 to a mean of 0.10 (Fig. 3).

Summer populations of trout did not change significantly in the treatment streams following habitat modification relative to populations in the reference streams in either the

© 2000 NRC Canada

Fig. 3. Coho salmon summer populations, spring migrants, and overwinter survival for the treatment and reference streams in the Alsea and Nestucca basins, pretreatment and posttreatment. Solid bars, treatment pre; open bars, reference pre; diagonally hatched bars, treatment post; horizontally hatched bars, reference post.

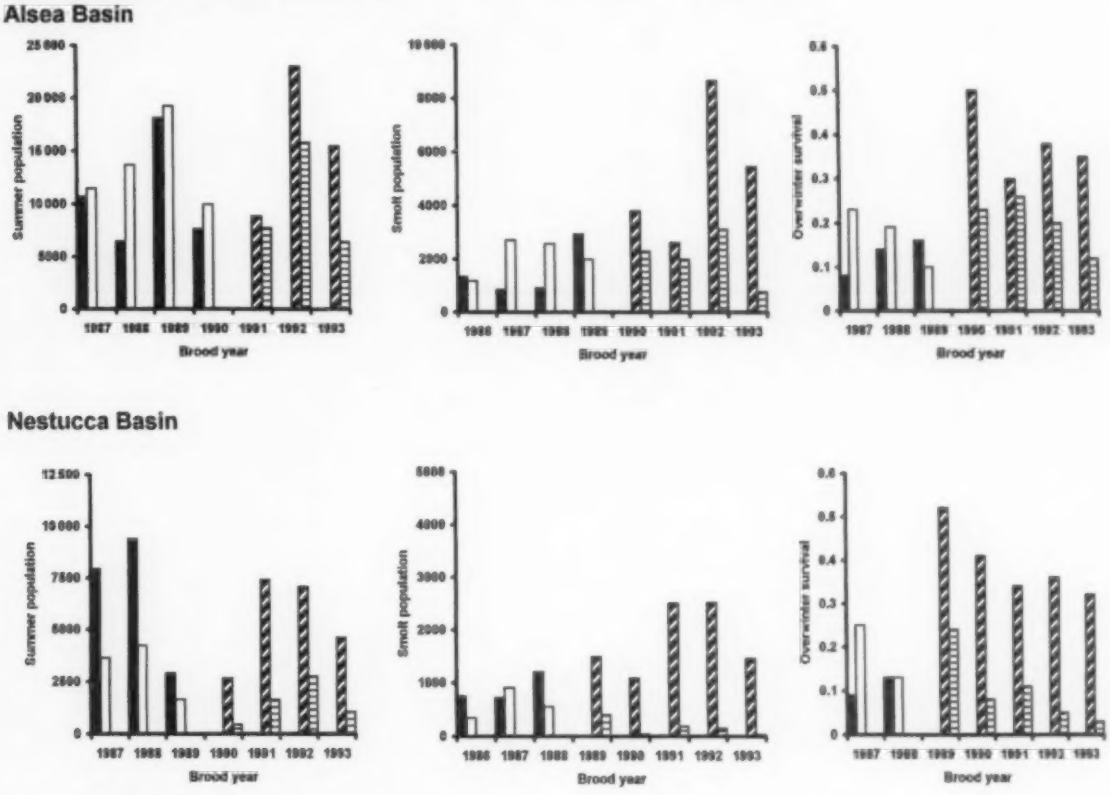

Alsea (two-tailed t test: 0+ trout, $p = 0.78$; 1+ steelhead, $p = 0.26$; 1+ cutthroat, $p = 0.20$) or the Nestucca (two-tailed t test: 0+ trout, $p = 0.62$; 1+ steelhead, $p = 0.63$; 1+ cutthroat, $p = 0.33$). Populations of age-0+ trout and age-1+ steelhead in the Alsea study streams had similar levels of abundance and variability, whereas age-1+ cutthroat trout were more variable (Fig. 4). The opposite tended to be the case in Nestucca study streams, where the age-0+ trout and age-1+ steelhead populations tended to be more variable than the cutthroat trout populations (Fig. 4). Because of the interannual variability in these populations, the power of these tests was low.

Following habitat modification, migrant populations of steelhead increased in the two treatment streams relative to the reference streams (two-tailed t test: Alsea, $p = 0.005$; Nestucca, $p = 0.037$). The mean number of steelhead migrants increased by over 800% in the Alsea treatment stream, whereas the mean number of steelhead migrants in reference stream increased by 65% (Fig. 5). Similarly, in the Nestucca treatment stream, steelhead migrants increased by about 400%, while in the reference stream, they declined by about 40% (Fig. 5).

Cutthroat trout migrants increased in both of the Alsea study streams during the posttreatment period (Fig. 5). Although there was about a fivefold increase in cutthroat trout migrants in the treatment stream and a doubling of migrants in the reference stream (Fig. 5), the difference was not significant (two-tailed t test: $p = 0.25$). Following habitat modification, the number of migrants in the Nestucca treatment stream increased relative to that in the reference stream (two-tailed t test: $p = 0.024$). Cutthroat trout migrants in the treatment stream increased by 275%, whereas migrants in the reference stream decreased by 75% (Fig. 5).

Discussion

Habitat modification in two Oregon coastal streams resulted in increased winter rearing habitat for anadromous salmonids. The increases in winter rearing habitat resulted from a combination of improvement of marginal in-channel habitats and the creation of new off-channel habitats. The creation of slow-water habitat and the addition of large quantities of wood to the stream were critical elements of the habitat modification.

The increase in winter habitat resulted in increased coho salmon smolt abundance. In the summers following habitat modification, there were significantly more juveniles in the treatment streams compared with the reference streams. However, our study demonstrates that overwinter survival was the key to the increased smolt abundance. In the Alsea treatment stream, the summer juvenile population increased by about 50%; however, the overwinter survival increased

© 2000 NRC Canada

Fig. 4. Summer populations of 0+ trout and 1+ steelhead and cutthroat trout in the treatment and reference streams in the Alsea and Nestucca basins, pretreatment and posttreatment. Solid bars, treatment pre; open bars, reference pre; diagonally hatched bars, treatment post; horizontally hatched bars, reference post.

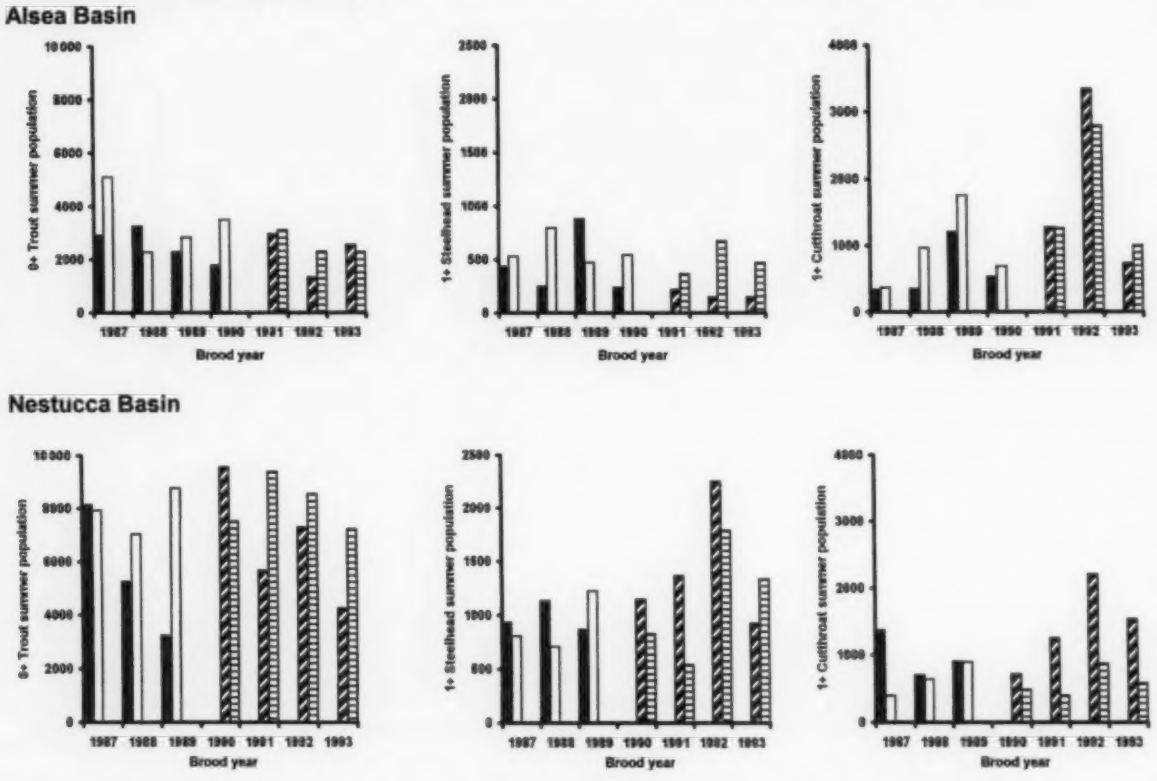

300% after habitat modification. Likewise, the Nestucca treatment stream produced twice as many coho salmon smolts despite a 20% decrease in summer juveniles; overwinter survival increased approximately 3.5 times. The alcoves and complex dammed pools constructed in these two streams provided the coho salmon with refuge from the high-velocity conditions that characterize most Oregon coastal streams during winter. These results further support the conclusion of Nickelson et al. (1992*a*) that winter habitat limits production of coho salmon smolts in many Oregon coastal streams.

Because the habitat modification in our study streams was targeted at coho salmon, the question arises as to possible impacts on other salmonids, such as trout, which might prefer different habitat (Bisson et al. 1982). Cederholm et al. (1997) examined this question for the addition of large wood to a stream. Except for a decrease in age-0 steelhead at one treatment site during spring, they found no changes in age-0 or age-1 steelhead during spring, autumn, or winter following treatment. The one exception may have been an artifact of the difficulty of estimating abundance of very small fish. House and Boehne (1985) reported that abundance of trout fry, steelhead parr, and cutthroat trout parr increased during summer as a result of placing boulders and rock-filled gabions in East Fork Lobster Creek. The results suggest no negative impacts of habitat enhancement on trout populations. However, neither of these studies examined steelhead or cutthroat trout migrants.

We found increases in steelhead migrants in both treatment streams and increases in cutthroat trout migrants in one treatment stream following creation of winter habitat for coho salmon. Changes in summer populations were not detectable. This implies that, like coho salmon, overwinter survival of trout was increased by the habitat modification. Habitat modification that creates complex slow-water habitat appears to benefit not only coho salmon but steelhead and cutthroat trout as well.

The increases in population size for all three salmonid species were probably due to the increase in habitat that had a combination of depth, velocity, and cover sufficient to provide an increase in winter refuge or rearing space. In species such as coho salmon, steelhead, and cutthroat trout, which have evolved in sympatry, the ability to partition the available habitat to minimize competition has been documented (Facey and Grossman 1992). In our study, the increase in habitat complexity was sufficient to increase the abundance of all three species.

The inclusion of the reference streams was critical to the design of this study. Without the reference streams to help account for interannual variation, two of our conclusions would have been different. If we had looked only at the treatment streams, we would have concluded that summer

© 2000 NRC Canada

Fig. 5. Steelhead and cutthroat trout spring migrants for the treatment and reference streams in the Alsea and Nestucca basins, pretreatment and posttreatment. Solid bars, treatment pre; open bars, reference pre; diagonally hatched bars, treatment post; horizontally hatched bars, reference post.

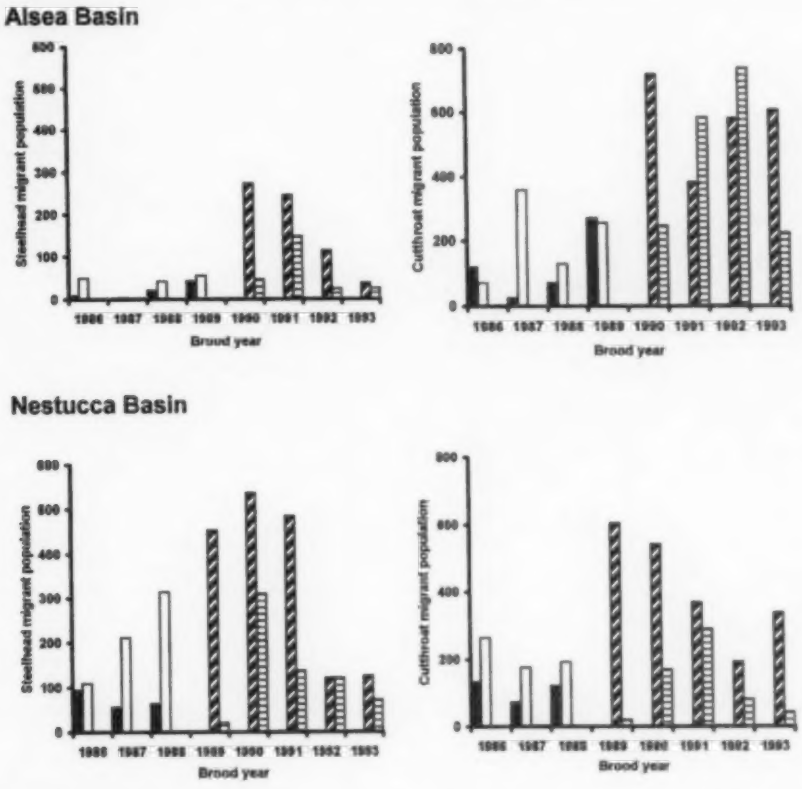

populations did not differ between pretreatment and posttreatment. However, because summer populations in the reference streams decreased posttreatment, the relationship between populations in treatment streams and the reference streams changed significantly. Similarly, without knowing that cutthroat trout migrants increased in East Fork Lobster Creek posttreatment, we would have concluded that the treatment had resulted in an increase in cutthroat trout migrants in Upper Lobster Creek. It is therefore difficult to interpret the results of studies of the effects of habitat modification that do not include reference streams to account for the effects of factors other than the treatment.

Our study also provides insights into the construction details of habitat restoration. For example, when alcoves are constructed, we recommend that they only be located in areas where springs, seeps, or temporary streams can be incorporated. Water flowing through the alcoves helps control the accumulation of fine sediment that tends to block the entrance. Even so, periodic maintenance will probably be necessary in most cases to keep constructed alcove habitat available for winter use by juvenile salmonids. We also do not recommend that full-spanning structures be anchored to the substrate or incorporate the use of rebar, chain-link fence, or erosion cloth. When the channel moves or the structure fails, the nonnatural materials are left exposed in the stream channel and do not provide much in the way of habitat. Instead, we recommend that large wood be placed in the stream to establish itself in the channel as a function of natural processes.

We believe that the results of this study are specific to the particular type of habitat created (i.e., deep, complex dammed pools and excavated alcoves with large amounts of wood). They should not be interpreted as a general justification for all types of instream habitat restoration. This type of restoration project would be inappropriate and probably have little beneficial impact on salmonid migrant production if, for example, the stream was subject to extreme summer temperatures due to the lack of an adequate riparian area. In addition, these types of projects have substantial impact on the landscape (due to the use of heavy equipment and the large volumes of excavated material) and are only appropriate for unconstrained stream reaches with poor-quality habitat.

Although the restoration efforts that we describe were located relatively high in the drainage basins, we believe that even larger benefits could be derived from projects to increase the amount of available winter rearing areas in the lower reaches of coastal basins. These areas, where historically the largest numbers of juvenile coho salmon probably overwintered, are now used primarily for agricultural production. Many of the streams have been channelized and the sloughs and wetlands drained, resulting in large-scale reductions in potential overwinter rearing space (Lichatowich

© 2000 NRC Canada

1987). We do not recommend that this type of habitat restoration be used ubiquitously. There are, however, some key areas where it can give immediate help to salmonid populations threatened by the lack of adequate winter rearing habitat.

Acknowledgements

We thank the many dedicated seasonal employees who assisted with the field sampling and data summary chores throughout the 8 years of this project. We also thank Linda Ashkenas and two anonymous reviewers whose suggestions greatly improved the quality of the manuscript. We thank Mary Buckman for advice on statistical treatment and interpretation. Funding was provided by the Sport Fish and Wildlife Restoration Program administered by the U.S. Fish and Wildlife Service.

References

Beechie, T., Beamer, E., and Wasserman, L. 1994. Estimating coho salmon rearing habitat and smolt production losses in a large river basin, and implications for habitat restoration. N. Am. J. Fish. Manage. **14**: 797–811.

Bisson, P.A., Nielson, J.L., Palmason, R.A., and Grove, L.E. 1982. A system of naming habitat types in small streams, with examples of habitat utilization by salmonids during low stream flow. *In* Acquisition and utilization of aquatic habitat inventory information. *Edited by* N.B. Armantrout. American Fisheries Society, Bethesda, Md. pp. 62–73.

Bradford, M.J., Taylor, G.C., and Allan, J.A. 1997. Empirical review of coho salmon smolt abundance and the prediction of smolt production at the regional level. Trans. Am. Fish. Soc. **126**: 49–64.

Cederholm, C.J., Bilby, R.E., Bisson, P.A., Bumstead, T.W., Fransen, B.R., Scarlett, W.J., and Ward, J.W. 1997. Response of juvenile coho salmon and steelhead to placement of large woody debris in a coastal Washington stream. N. Am. J. Fish. Manage. **17**: 947–963.

Chapman, D.G. 1951. Some properties of the hypergeometric distribution with applications to zoological sample census. Univ. Calif. Publ. Stat. **1**: 131–160.

Crispin, V., House, R., and Roberts, D. 1993. Changes in instream habitat, large woody debris, and salmon habitat after the restructuring of a coastal Oregon stream. N. Am. J. Fish. Manage. **13**: 96–102.

Facey, D.E., and Grossman, G.D. 1992. The relationship between water veloity, energetic costs, and microhabitat use in four North American stream fishes. Hydrobiologia, **239**: 1–6.

Hankin, D.G. 1984. Multistage sampling designs in fisheries research: applications in small streams. Can. J. Fish. Aquat. Sci. **41**: 1575–1591.

Hankin, D.G., and Reeves, G.H. 1988. Estimating total fish abundance and total habitat area in small streams based on visual estimation methods. Can. J. Fish. Aquat. Sci. **45**: 834–844.

House, R.A. 1996. An evaluation of stream restoration structures in a coastal Oregon stream, 1981–1993. N. Am. J. Fish. Manage. **16**: 272–281.

House, R.A., and Boehne, P.L. 1985. Evaluation of instream enhancement structures for salmon spawning and rearing in a coastal Oregon stream. N. Am. J. Fish. Manage. **6**: 38–46.

Hubbs, C.L., Greenley, J.R., and Tarzwell, C.M. 1932. Methods for the improvement of Michigan trout streams. Univ. Mich. Inst. Fish. Res. Bull. 1, University of Michigan, Ann Arbor, Mich.

Hurlbert, S.H. 1984. Pseudoreplication and the design of ecological field studies. Ecol. Monogr. **54**: 187–211.

Kondolf, G.M., Vick, J.C., and Ramirez, T.M. 1996. Salmon spawning habitat rehabilitation on the Merced River, California: an evaluation of project planning and performance. Trans. Am. Fish. Soc. **125**: 899–912.

Lichatowich, J.A. 1987. Habitat alteration and changes in abundance of coho salmon (*Oncorhynchus kisutch*) and chinook (*O. tshawytscha*) salmon in Oregon's coastal streams. *In* Proceedings of the National Workshop on Effects of Habitat Alteration on Salmonid Stocks. *Edited by* C.D. Levings, L.B. Holtby, and M.A. Henderson. Can. Spec. Publ. Fish. Aquat. Sci. No. 105. pp. 92–99.

McLemore, C.E., Everest, F.H., Humphreys, W.R., and Solazzi, M.F. 1989. A floating trap for sampling downstream migrant fishes. U.S. Dep. Agric. For. Serv. Pac. Northwest Res. Stn. PNW-RN-490.

Moring, J.R., and Lantz, R.L. 1975. The Alsea watershed study: effects of logging on the aquatic resources of three headwater stream of the Alsea River, Oregon. Part I. Biological studies. Oreg. Dep. Fish Wildl. Fish Div. Fish. Res. Rep. No. 9.

Nickelson, T.E., Rodgers, J.D., Johnson, S.L., and Solazzi, M.F. 1992*a*. Seasonal changes in habitat use by juvenile coho salmon (*Oncorhynchus kisutch*) in Oregon coastal streams. Can. J. Fish. Aquat. Sci. **49**: 783–789.

Nickelson, T.E., Solazzi, M.F., Johnson, S.L., and Rodgers, J.D. 1992*b*. Effectiveness of selected stream improvement techniques to create suitable summer and winter rearing habitat for juvenile coho salmon (*Oncorhynchus kisutch*) in Oregon coastal streams. Can. J. Fish. Aquat. Sci. **49**: 790–794.

Rodgers, J.D., Solazzi, M.F., Johnson, S.L., and Buckman, M.A. 1992. A comparison of three population estimation techniques to estimate juvenile coho salmon populations in small streams. N. Am. J. Fish. Manage. **12**: 79–86.

Scruton, D.A., Clarke, K.D., Anderson, T.C., Hoddinott, A.S., Van Zyll De Jong, M.C., and Huston, K.A. 1997. Evaluation of habitat improvement and restoration initiatives for salmonids in Newfoundland, Canada. Can. MS Rep. Fish. Aquat. Sci. 2413.

Seber, G.A.F., and LeCren, E.D. 1967. Estimating population parameters from catches large relative to the population. J. Anim. Ecol. **36**: 631–643.

Shetter, D.S., Clark, O.H., and Hazzard, A.S. 1949. The effects of deflectors in a section of a Michigan trout stream. Trans. Am. Fish. Soc. **76**: 248–278.

Smokorowski, K.E., Withers, K.J., and Kelso, J.R.M. 1998. Does habitat creation contribute to management goals? An evaluation of literature documenting freshwater habitat rehabilitation or enhancement projects. Can. Tech. Rep. Fish. Aquat. Sci. No. 2249.

Stewart-Oaten, A., Murdoch, W.W., and Parker, K.R. 1986. Environmental impact assessment: "pseudoreplication" in time? Ecol. **67**: 929–940.

Tarzwell, C.M. 1937. Experimental evidence on the value of trout stream improvement in Michigan. Trans. Am. Fish. Soc. **66**: 177–187.

© 2000 NRC Canada

Analysis of microsatellite DNA resolves genetic structure and diversity of chinook salmon (*Oncorhynchus tshawytscha*) in California's Central Valley

Michael A. Banks, Vanessa K. Rashbrook, Marco J. Calavetta, Cheryl A. Dean, and Dennis Hedgecock

Abstract: We use 10 microsatellite DNA markers to assess genetic diversity within and among the four runs (winter, spring, fall, and late fall) of chinook salmon (*Oncorhynchus tshawytscha*) in California's Central Valley. Forty-one population samples are studied, comprising naturally spawning and hatchery stocks collected from 1991 through 1997. Maximum likelihood methods are used to correct for kinship in juvenile samples and run admixture in adult samples. Through simulation, we determine the relationship between sample size and number of alleles observed at polymorphic microsatellite markers. Most samples have random-mating equilibrium proportions of single and multilocus genotypes. Temporal and spatial genetic heterogeneity is minimal among samples within subpopulations. An F_{ST} of 0.082 among subpopulations, however, indicates substantial divergence among runs. Thus, with the exception of our discovery of two distinct lineages of spring run, genetic structure accords with the diverse chinook life histories seen in the Central Valley and provides a means for discrimination of protected populations.

Résumé : Nous nous sommes servis de dix marqueurs microsatellites de l'ADN pour estimer la diversité génétique dans et entre les quatre remontes (hiver, printemps, automne et fin de l'automne) de quinnat (*Oncorhynchus tshawytscha*) dans la vallée centrale de la Californie. Nous avons étudié 41 échantillons de populations, représentant des poissons à reproduction naturelle et des stocks d'écloserie, prélevés entre 1991 et 1997. Les méthodes du maximum de vraisemblance ont servi à faire la correction pour la parenté génétique dans les échantillons de juvéniles et pour le mélange des remontes dans les échantillons d'adultes. Par la simulation, nous déterminons la relation entre la taille de l'échantillon et le nombre d'allèles observés aux marqueurs polymorphes microsatellites. La plupart des échantillons présentent des proportions équilibrées d'appariement aléatoire de génotypes à un et à plusieurs locus. L'hétérogénéité génétique temporelle et spatiale est minime entre les échantillons au sein des sous-populations. Un F_{ST} de 0,082 entre les sous-populations indique toutefois une divergence substantielle entre les remontes. Ainsi, à l'exception de notre découverte de deux lignées distinctes dans la remonte du printemps, la structure génétique concorde avec les divers cycles biologiques du quinnat observés dans la vallée centrale et fournit un moyen de distinguer les populations protégées.

[Traduit par la Rédaction]

Introduction

Many salmon populations throughout the Pacific Northwest have been extirpated and, of those remaining, the majority is at risk of extinction (Nehlsen 1994). At the southern limit of its range in North America, the Pacific salmon *Oncorhynchus* is particularly vulnerable, owing primarily to dry climate and human competition for water but also to intensive exploitation and habitat disturbance. In California, three salmonid stocks are already protected, and listing of all remaining stocks has been proposed (National Marine Fisheries Service (NMFS) 1998, 1999). Salmon conservation concerns are particularly acute in California's Central Valley, habitat for four spawning runs of the chinook salmon (*Oncorhynchus tshawytscha*) and the source of water for two thirds of the state's inhabitants and its enormous agricultural industry. The stock at greatest risk, the Sacramento River winter-run chinook salmon, was listed as threatened by the state of California in 1989, when run size fell below 200, and as endangered by the federal government in 1994 (NMFS 1994).

Population genetic data are increasingly important in managing salmonid populations on the brink of extinction (Waples 1995). There is a need to identify protected stocks in mixed ocean harvests and in rivers or estuaries where dams or water diversions imperil out-migrating juveniles. Identification of broodstock in propagation programs is

Received March 8, 1999. Accepted February 17, 2000. J15051

M.A. Banks,[1] V.K. Rashbrook, M.J. Calavetta,[2] C.A. Dean, and D. Hedgecock. Bodega Marine Laboratory, University of California at Davis, P.O. Box 247, Bodega Bay, CA 94923, U.S.A.

[1]Author to whom all correspondence should be addressed. e-mail: mabanks@ucdavis.edu

[2]Current address: Hitachi Genetic Systems, 1201 Harbor Bay Parkway, Suite 150, Alameda, CA 94502, U.S.A.

© 2000 NRC Canada

required to avoid admixture and hybridization among spawning runs. Genetic markers are useful for confirming parentage and relatedness in hatchery-bred fish and for verifying models of hatchery impacts on genetic diversity of naturally spawning stocks. In the case of Central Valley chinook salmon, however, a study of 39 allozyme loci revealed very slight divergence among fall- and winter-run chinook salmon, with Wright's standardized allele frequency variance F_{ST} = 0.01 (Bartley et al. 1992). Nielsen et al. (1994) reported substantially more divergence in frequencies of six mtDNA haplotypes, F_{ST} = 0.24, but the probability of any two Central Valley chinook haplotypes being identical is 0.7, precluding use of this marker for individual identification. Highly variable nuclear DNA markers, such as microsatellites, make possible genealogical analyses or genetic discrimination among closely related fish populations (Wright and Bentzen 1996). Thus, Banks et al. (1999) cloned microsatellite DNA markers from winter-run chinook salmon, developed polymerase chain reaction (PCR) methods for rapid genotyping, and verified Mendelian inheritance in families produced in a captive breeding program.

Here, we report the results of a genetic analysis of 41 naturally spawning and hatchery populations of California's Central Valley chinook salmon using 10 microsatellites. We use maximum likelihood methods to correct for family structure among samples comprising juveniles as well as to correct for run admixture in adult samples and demonstrate increased accuracy and precision as a result of these corrections. Our objective is to provide a baseline genetic profile of chinook salmon in the Central Valley that will allow the distinction of endangered stocks from their less threatened close relatives. The study reveals substantial diversity of chinook salmon at the southern limit of their North American range despite 150 years of major ecological disturbances (Yoshiyama et al. 1998). It also illustrates the power of microsatellite DNA markers to resolve the complex genetic structure of salmon populations within a major river basin.

Materials and methods

Sample collections

Between 1991 and 1997, tissue samples from 3032 chinook salmon were collected from 20 Central Valley sites by the California Department of Fish and Game (CDFG) and the U.S. Fish and Wildlife Service (Table 1). Samples comprised all four runs of chinook salmon and, for 11 sites, multiple year-classes. A complete list of all samples used in this study, their accession numbers if taken from the CDFG tissue archive (The Resource Agency, CDFG, 1701 Nimbus Rd, Rancho Cordova, CA 95670), and their genotypes are available at http://www-bml.ucdavis.edu/cvdataset.htm. Winter-run samples comprised both spawned carcasses (1995–1997) collected from the Sacramento River and broodstock collections (1991–1995) trapped at Keswick and Red Bluff diversion dams near Redding (Fig. 1). Owing to the inaccessibility of spring-run spawning habitat and consequent difficulties of collecting a sufficient number of spawned carcasses, out-migrating juveniles were sampled in addition to carcasses from Butte, Deer, and Mill creeks (1994–1997). The fall run, presently the most abundant chinook run in the Central Valley, is the only run found in the lower Sacramento – San Joaquin watershed (Yoshiyama et al. 1998). Samples from eight naturally spawning and five hatchery fall-run populations were collected from 1993 to 1996. Like the winter run, late-fall-run stocks are confined to the Sacramento River where both hatchery (1993 and 1995) and naturally spawning (1995) adults were sampled.

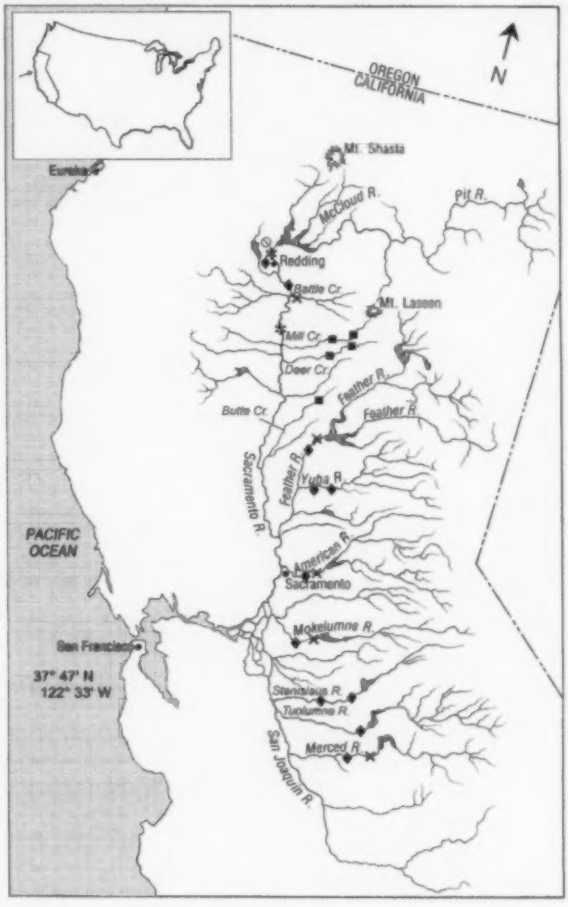

Fig. 1. The Sacramento and San Joaquin rivers and their tributaries. Sampling sites per run are indicated as follows: *, winter; ■, spring; ◆, fall; open circle with diagonal line, late fall; ×, hatcheries. See Table 1 for temporal and life history stage details for each population sample.

Microsatellite typing

Tissue samples (caudal fin clips) were placed in a storage buffer (10 mM Tris–HCl, pH 8.0, 25 mM EDTA, 100 mM NaCl) and frozen until processed. Genomic DNA extraction varied according to whether tissue was obtained from live fish or degraded carcasses. With fresh tissue, 0.5 mm^2 was placed in 200 µL of 5% Chelex®100 (BioRad) in 96-well PCR trays (0.2 mL) (Corning-Costar). Tissue extracts were covered with a silicone-sealing mat (Corning-Costar), heated for 30 min at 60°C, and then boiled for 30 min at 103°C in a thermocycler (M.J. Research). Trays were centrifuged for 5 min at 3000 rpm to pellet fin debris and Chelex® beads. One hundred microlitres of supernatant was removed and transferred to a new 96-well tray to be used as template for PCR, leaving the rest of the DNA for long-term storage. DNA was extracted from carcass fin clips using the Puregene® DNA isolation kit (Gentra Systems).

Individuals were genotyped at up to 10 previously described unlinked microsatellite loci: *Ots-1*, *-2*, *-3*, *-5*, *-9*, and *-10* (Banks et al.

© 2000 NRC Canada

Table 1. California's Central Valley chinook salmon scored at up to 10 microsatellite loci: collection data and within-population genetic parameters for adjusted samples (see text).

Run	Year	Collection site	Life stage	L	N	H_e	H_o	A	F_{IS}	H-W-C
Winter										
W1	1991	Keswick and Red Bluff dams	Adult	10	18	0.48	0.48	3.7	0.05	0.84
W2	1992	Keswick Dam	Adult	10	29	0.51	0.50	4.7	–0.01	0.99
W3	1993	Keswick and Red Bluff dams	Adult	10	11	0.52	0.66	3.6	–0.25	0.78
W4	1994	Keswick Dam	Adult	10	26	0.53	0.54	4.3	0.00	0.14
W5	1995	Keswick Dam	Adult	10	37	0.52	0.57	5.4	–0.11	0.61
W6	1995	Sacramento River	Spawned carcass	10	32	0.50	0.52	4.5	–0.01	0.79
W7	1996	Sacramento River	Spawned carcass	10	36	0.49	0.55	4.1	–0.11	0.95
W8	1997	Sacramento River	Spawned carcass	10	103	0.50	0.51	4.7	–0.02	0.86
Mean					37	0.51	0.54	4.4		
Spring										
S1	1994	Butte Creek	Spawned carcass	10	67	0.60	0.59	7.3	0.03	0.12
S2	1996	Butte Creek	Spawned carcass	5	41	0.66	0.65	4.4	0.06	0.81
S3	1996	Butte Creek	Juvenile	5	35	0.68	0.71	5.8	–0.02	0.68
S4	1997	Butte Creek	Spawned carcass	10	117	0.59	0.54	7.2	0.13*	0.00*
Mean					65	0.63	0.62	6.18		
S5	1994	Deer Creek	Juvenile	10	30	0.52	0.52	5.8	0.03	0.64
S6	1995	Deer Creek	Spawned carcass	10	25	0.56	0.57	6.9	0.04	0.20
S7	1996	Deer Creek	Juvenile	6	73	0.73	0.76	9.7	–0.03	0.89
S8	1997	Deer Creek	Spawned carcass	10	49	0.60	0.57	8.3	0.12*	0.04*
S9	1995	Mill Creek	Spawned carcass	10	15	0.54	0.65	4.7	–0.14	1.00
S10	1996	Mill Creek	Juvenile	10	40	0.54	0.57	6.6	0.00	0.73
Mean					51	0.61	0.61	6.6		
Fall		Hatchery								
F1	1993	Coleman Hatchery	Adult	10	144	0.62	0.62	9.8	–0.04	0.16
F2	1994	Coleman Hatchery	Adult	8	95	0.53	0.56	6.5	–0.06	0.07
F3	1995	Coleman Hatchery	Adult	10	95	0.63	0.65	9.9	0.01	0.56
F4	1995	Feather River Hatchery	Adult	10	95	0.62	0.61	10.3	0.00	0.19
F5	1996	Feather River Hatchery	Adult	7	94	0.72	0.72	10.8	0.01	0.76
F6	1995	Merced River Hatchery	Adult	10	95	0.63	0.59	9.5	0.067*	0.02*
F7	1995	Mokelumne River Hatchery	Adult	10	95	0.61	0.61	9.6	0.01	0.79
F8	1995	Nimbus Hatchery	Adult	10	95	0.60	0.61	10.2	0.01	0.75
Mean					101	0.62	0.62	9.58		
Fall		Naturally spawning								
F9	1995	American River	Spawned carcass	8	90	0.57	0.60	5.9	–0.07	0.89
F10	1995	Feather River	Spawned carcass	7	75	0.56	0.53	5.4	0.07	0.14
F11	1996	Feather River	Spawned carcass	5	53	0.68	0.72	6.6	–0.04	0.48
F12	1995	Merced River	Spawned carcass	8	88	0.54	0.54	6.3	0.00	0.04*
F13	1995	Mokelumne River	Spawned carcass	10	94	0.60	0.60	9.7	0.00	0.12
F14	1994	Stanislaus River	Spawned carcass	8	26	0.50	0.46	5.0	0.12*	0.27
F15	1995	Stanislaus River	Spawned carcass	8	27	0.54	0.54	4.9	0.05	0.09
F16	1994	Toulumne River	Spawned carcass	8	15	0.52	0.55	4.5	–0.07	0.65
F17	1995	Toulumne River	Spawned carcass	8	29	0.54	0.52	5.1	0.08	0.49
F18	1996	Toulumne River	Spawned carcass	5	78	0.63	0.65	6.2	–0.02	0.24
F19	1995	Sacramento River	Spawned carcass	10	94	0.61	0.60	9.3	0.02	0.08
F20	1996	Yuba River	Spawned carcass	5	54	0.64	0.63	7.4	–0.03	0.77
Mean					60	0.58	0.58	5.94		
Fall grand mean					77	0.59	0.59	7.33		
Late fall										
LF1	1993	Coleman Hatchery	Adult	10	143	0.55	0.55	8.9	0.02	0.25
LF2	1995	Keswick Dam	Adult	10	90	0.56	0.53	8.9	0.07*	0.00*
LF3	1995	Coleman Hatchery	Adult	10	90	0.55	0.58	8.6	–0.04	0.17
Mean					108	0.56	0.55	8.8		
Grand mean					64	0.58	0.59	6.7		
Total					2638					

Note: L, number of loci; N, adjusted sample size; H_e, expected heterozygosity; H_o, observed heterozygosity; A, average number of alleles per locus; *significant ($\alpha = 0.05$).

© 2000 NRC Canada

Table 2. Classification and examples of hypotheses for observed arrays of progeny phenotypes and their associated probabilities.

Classes of hypotheses	Genotype		F_1 phenotype[a]				Probability[b]
	Parent 1	Parent 2	I	II	III	IV	
Two alleles	AA	AB	n_1	n_2			$[n_T!/(n_1!n_2!)](0.5)^{n1}(0.5)^{n2}$
	AB	AB	n_1	n_2	n_3		$[n_T!/(n_1!n_2!n_3!)](0.25)^{n1}(0.25)^{n2}(0.5)^{n3}$
Three alleles	AA	BC	n_1	n_2			$[n_T!/(n_1!n_2!)](0.5)^{n1}(0.5)^{n2}$
	AB	AC	n_1	n_2	n_3	n_4	$[n_T!/(n_1!n_2!n_3!n_4!)](0.25)^{n1}(0.25)^{n2}(0.25)^{n3}(0.25)^{n4}$
Four alleles	AB	CD	n_1	n_2	n_3	n_4	$[n_T!/(n_1!n_2!n_3!n_4!)](0.25)^{n1}(0.25)^{n2}(0.25)^{n3}(0.25)^{n4}$

[a]Full-sib progeny can have from one to four phenotypes, depending on parental genotypes; the n_i are the numbers of progeny observed in each phenotypic category.

[b]Terms of the relevant bi-, tri-, or tetranomial probability distributions; n_T is the sum of the n_i.

1999), *Ots-104* and *-107* (Nelson and Beacham 1999), *One*μ*13* (Scribner et al. 1996), and *Omy-77* (Morris et al. 1996). The forward PCR primer was labeled with a fluorescent phosphoamidite (HEX or fluorescein). PCR products were electrophoresed, 96 at a time with allelic controls, on a 45.0 cm wide by 22.5 cm high 8% denaturing polyacrylamide gel at 50 W for 60–150 min. DNA fragments were visualized on the FMBIO® fluorescent imaging system (Hitachi Software Engineering America Ltd.). Gels were manually scored and independently verified by at least one other researcher. The data were entered into a relational database (Paradox®, Borland, version 7) and double-checked for accuracy. Individuals that did not produce repeatable genotypes were not included in the analyses. Variation in the quality of DNA extracted from carcass tissues made genotypes difficult to score; consequently, fewer than 10 loci were assayed in many carcass samples (Table 1).

Statistical analyses

We developed and applied methods to address three sampling issues: relatedness among juveniles, run admixture, and limits to precision of allele frequency estimates for highly polymorphic loci. Each of the methods is described below.

Correcting for kinship in samples of juveniles

Four samples of the spring run (Deer Creek, 1994 and 1996, Mill Creek, 1996, and Butte Creek, 1996) comprised juveniles only. We investigated and attempted to correct for kinship in these samples because the presence of full- or half-sibs could bias allele frequency estimates (Allendorf and Phelps 1981).

The odds of two individuals being full-siblings rather than unrelated can be calculated using the program Kinship 1.2 (Goodnight and Queller 1999). We first explored the power of this approach using 53 winter-run offspring comprising seven full-sib and three half-sib families in a captive breeding program (Banks et al. 1999). These fish afforded 393 pairwise comparisons among known full-sibs, 307 comparisons among known half-sibs, and 678 comparisons among unrelated individuals. Odds for a full-sib relationship were calculated with both five and nine loci to mimic the information available in the spring-run juvenile samples. Significance thresholds for the full-sib LOD score (the log of the odds ratio) were taken from simulation results at an empirical level of $\alpha = 0.01$. Threshold LODs were 1.04 and 1.14 for five and nine loci, respectively, corresponding to Type II errors of 0.72 and 0.50. Percentages of known full-sib, half-sib, and unrelated pairs yielding significant full-sib LOD scores when scored at five loci are 42.2, 5.6, and 0.4%, respectively. The comparable percentages using nine loci are 57.2, 6.8, and 0.6%, respectively, showing the expected improvement in power with more loci. This exercise suggests that LOD score classification of a full-sib relationship between two winter-run individuals is conservative. The test has low power, detecting a little more than half of true full-sibs when nine loci are used, but suitable protection against Type I error, classifying very few truly unrelated pairs as full-sibs.

To analyze the spring-run juvenile samples, we first deleted individuals missing more than one or two loci (depending on the number of loci sampled) to avoid potentially spurious results in evaluating kinship. Adult spring-run samples for Mill and Deer creeks and from Butte Creek were pooled into two reference populations for calculation of genotypic probabilities under the two kinship hypotheses (full-sib versus unrelated). We selected and grouped pairs of individuals for which full-sib LOD scores were significant ($p < 0.01$), as above, removing them from their sample. The Type II errors were approximately 0.6 for the two samples studied at five loci (Deer Creek, 1996, and Butte Creek, 1996) and 0.4 for the two samples studied at eight or nine loci (Deer Creek, 1994, and Mill Creek, 1996).

We next examined the genotypes of these kin groups for evidence against a simple full-sib hypothesis, i.e., more than four alleles per locus or impossible genotypic combinations, and identified the largest subset of potential full-sibs for further analysis. The remaining individuals in a kinship group could be explained as half-sibs, although this sometimes constrained the genotype of the common parent. For each putative full-sib group, we calculated the probability for the observed array of progeny genotypes under one or more mating-type hypotheses. For example, if there were one AA and two AB in a full-sib group with three members, we would calculate the relevant terms of the binomial probability distribution for {0.5, AA : 0.5, AB}, implying a mating type AA × AB, the trinomial probability distribution for {0.25, AA : 0.5, AB : 0.25, BB}, implying an AB × AB mating, and the tetranomial probability distribution for {0.25, AA : 0.25, AB : 0.25, AC : 0.25, BC}, implying an AB × AC mating (Table 2). The probabilities for each mating type, given the observed progeny, were then multiplied by the frequency of the implied mating type, given baseline allelic frequencies and assuming Hardy–Weinberg–Castle (H-W-C) equilibrium, to yield the likelihood for each possible mating type. The mating type with the maximum likelihood was selected, and the inferred parental genotypes were then substituted into the data set for the juveniles.

Correction for run admixture

Because different spawning runs of chinook salmon can overlap in space and time, a given collection of adults can comprise a mixture of two or more runs. Such an admixture of spring run in broodstock collected for hatchery propagation of winter run (samples W1–W5, Table 1) was first suspected on phenotypic grounds in 1995. Extensive genetic analyses subsequently confirmed this admixture based on linkage disequilibrium (D. Hedgecock et al., unpublished data), a well-known feature of admixed populations (Waples and Smouse 1990). Linkage disequilibrium was measured using the program GENETIX version 3.3 (available at http://www.univ-montp2.fr/~genetix/genetix.htm) and found to be significant for 60% of the dilocus combinations. Nonwinter contaminants were identified and removed from the winter-run broodstock sample by the following procedure: (*i*) individuals with uncommon gametic types contributing to the significance of multiple pairwise

© 2000 NRC Canada

Fig. 2. UPGMA phenogram derived from CSE using raw data at five microsatellite loci (*Ots-2*, *-3*, *-9*, and *-10* and *Oneμ13*) for 41 chinook salmon population samples (see Table 1) from California's Central Valley. The scale indicates genetic distance; numbers at nodes indicate clusters with bootstrap results greater than 50%.

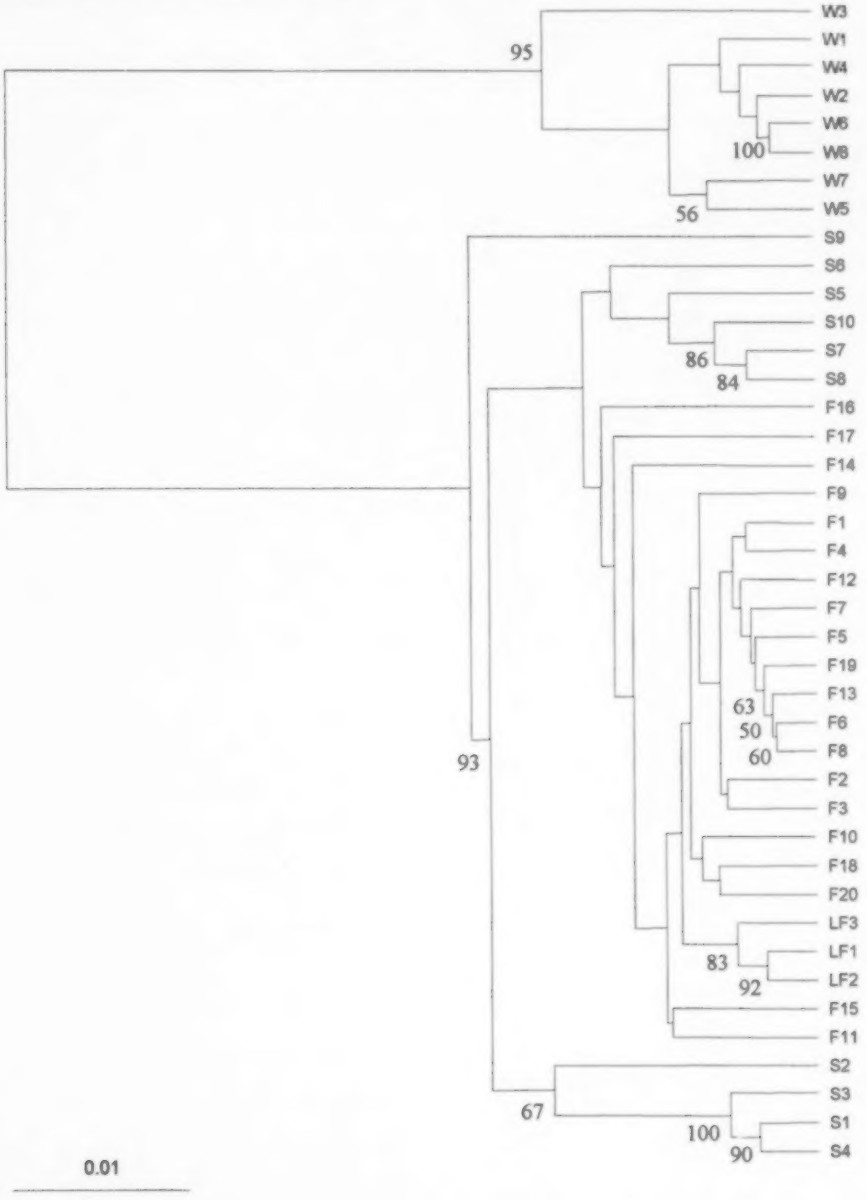

disequilibria were identified, (*ii*) these individuals were removed from the broodstock sample and the linkage equilibrium of the remainder of the broodstock was verified, (*iii*) the culled individuals were reassigned to run on the basis of their multilocus genotypes by a maximum likelihood method implemented in the program WHICHRUN (Banks and Eichert 2000), and (*iv*) individuals with better than even odds of belonging to the winter-run broodstock were returned to that sample, and linkage equilibrium was again verified. This procedure resulted in the removal of 19 of the 140 winter-run broodstock before the present study (i.e., W1–W5 samples comprise 121 fish in Table 1). A similar procedure was applied here to each of the remaining samples for which more than 10% of all pairwise disequilibrium tests were significant at the 5% level. Smaller genetic distances among the spring, fall, and late-fall runs, however, reduce the power of assignment of individual genotypes to run.

Bootstrap analyses of number of alleles per locus

To compare the numbers of microsatellite alleles observed in different populations, we used the program BOOTSTRAP (M.

© 2000 NRC Canada

Table 3. Sizes of spring-run juvenile chinook salmon samples before and after adjustment for missing data and kinship.

Spring-run sample	No. original sample	No. loci typed	Individuals removed for missing data[a]	No. kin groups[b]	No. parents inferred[c]	Net adjustment for kinship[d]	Size of adjusted sample
Deer Creek, 1994	53	9	–17	4	13	–6	30
Deer Creek, 1996	81	5	–3	14	28	–5	73
Mill Creek, 1996	64	8	–14	11	26	–10	40
Butte Creek, 1996	74	5	–32	7	19	–7	35

[a]Individuals were removed if they were missing more than one of five loci or more than two of eight or nine loci.
[b]Groups of individuals among which there was significant probability of being full-sibs, as determined by kinship (Goodnight and Queller 1999).
[c]Each kin (full-sib) group has at least two parents; in some kin groups, the presence of more than four alleles or impossible genotype combinations suggested half-sib relationships requiring additional parents to be inferred.
[d]Net adjustment is removal of juveniles belonging to kin group followed by substitution with their inferred parents.

Table 4. Heterogeneity testing within four subpopulations of chinook salmon from California's Central Valley with stepwise removal of samples to determine the largest subset of samples with homogeneous allelic frequencies.

Before adjustment[a]			After adjustment[a]		
Pool	Samples[b]	F_{ST}	Pool	Samples[b]	F_{ST}
Central Valley chinook	41 samples	0.0637*	Central Valley chinook[c]	38 samples	0.0745*
Winter	W1, 2, 3, 4, 5, 6, 7, 8	0.0172*	Winter	W1, 2, 3, 4, 5, 6, 7, 8	0.0087*
	W4, 5	0.0047		W1, 2, 3, 4, 5, 6, 8	0.0035
Spring	S1, 2, 3, 4, 5, 6, 7, 8, 9, 10	0.0175*	Spring	S1, 2, 3, 4, 5, 6, 7, 8, 9, 10	0.0171*
Spring Deer and Mill creeks	S5, 6, 7, 8, 9, 10	0.0038*	Spring Deer and Mill creeks	S5, 6, 7, 8, 9, 10	0.0017
	S6, 7, 8, 9, 10	0.0009			
Spring Butte Creek	S1, 2, 3, 4	0.0065*	Spring Butte Creek	S1, 2, 3, 4	0.0045*
	S1, 4	0.0053*		S2, 3, 4	0.0018
Fall and late fall	F1, 2, 3, 4, 5, 6, 7, 8, 9, 10, 11, 12, 13, 14, 15, 16, 17, 18, 19, 20, LF1, 2, 3	0.0072*	Fall and late fall[c]	F2, 4, 5, 6, 7, 8, 9, 10, 11, 12, 13, 14, 15, 16, 17, 18, 20, LF1, 2, 3	0.0078*
	F4, 5, 6, 7, 8, 10, 13, 15, 17, 18, 19	0.0011		F4, 5, 6, 7, 8, 10, 11, 13, 15, 16, 17, 18, 20	0.001
Late fall	LF1, 2, 3	0.0032*	Late fall	LF1, 2, 3	0.0034*
	LF1, 2	0.0011		LF1, 2	0.0015
			Central Valley chinook (homogeneous pools)[c]	—	0.0819*

Note: *results significant ($\alpha = 0.05$).
[a]Adjustment refers to correction for kinship or run admixture (see text).
[b]See Table 1 for sample names.
[c]Excluding fall naturally spawning sample from the Sacramento River, 1995, and Coleman Hatchery, 1993 and 1995.

Barré, Laboratoire Génétique et Pathologie, IFREMER BP 133, 17390 La Tremblade, France, personal communication) to simulate the relationship between sample size and number of alleles by bootstrap sampling for each of 10 loci. For this analysis, population samples were combined within each of the winter, spring from Butte Creek, spring from Deer and Mill creeks, fall naturally spawning, fall hatchery, and late-fall runs. At each sample size (from $n = 1$ to the total number of fish in a given run at a given locus), the program performed 1000 randomized samplings, counting the number of alleles and calculating the mean and standard error. Sign tests were then used to compare allelic diversity among runs at a common sample size of 50.

Population genetic analyses

Allelic frequencies and population genetic statistics — observed and expected heterozygosities, mean number of alleles per locus, pairwise linkage disequilibrium, Wright's *F* statistics, Nei's (1972) distance (D), and Nei's (1987) minimum distance (D_m) — were calculated using the program GENETIX version 3.3. Tests for random mating proportions of genotypes within samples (H-W-C equilibrium) were calculated using the program GENEPOP version 3.1 (Raymond and Rousset 1995). The significance of F_{IS} and F_{ST} ($\alpha = 0.05$) was determined by performing 500 permutations in GENETIX at five loci (*Ots-2*, *-3*, *-9*, and *-10* and *Oneμ13*). Significance of F_{ST} was also determined for a subset of 26 samples that were scored at all 10 loci (*Ots-1*, *-2*, *-3*, *-5*, *-9*, *-10*, *-104*, and *-107*, *Oneμ13*, and *Omy77*, Table 1). We did not calculate any distance measures that assume the stepwise mutation model, as recent studies have demonstrated that this model is often falsified by complex microsatellite mutational events and does not perform any better than more traditional infinite allele measures (e.g., Paetkau et al. 1997; Estoup et al. 1998; Colson and Goldstein 1999). Four major subpopulations were evident from the unweighted paired group method using arithmetic averages (UPGMA) phenogram derived from raw data (see below and Fig. 2): all winter, spring from Butte Creek, and spring from Deer and Mill creeks and, lastly, all fall and late-fall population samples as a single clade. Heterogeneity among samples within subpopulations was assessed by signifi-

© 2000 NRC Canada

cance of F_{ST}. When a subpopulation was heterogeneous, sets of homogeneous samples were determined by stepwise removal of samples until F_{ST} for the remaining subpopulation pool was nonsignificant ($\alpha = 0.05$). The order of sample removal was determined by rank of average F_{ST} for within-pool pairwise comparisons. The above tests were repeated using Nei's D_m to explore whether an alternative distance measure resulted in the same findings.

Nei's D and the Cavalli-Sforza and Edwards (1967) chord measure (CSE) were calculated using GENDIST in the program PHYLIP (Felsenstein 1993) for data from five loci and repeated for the 26 population samples that were characterized at 10 loci. Neighbor-joining (Saitou and Nei 1987) and UPGMA trees (Sneath and Sokal 1973) were calculated using NEIGHBOR in PHYLIP. Maximum likelihood trees (Cavalli-Sforza and Edwards 1967) were calculated using CONTML in PHYLIP. Bootstrap results for assessing the frequency of occurrence, and thus significance, of each tree cluster were attained using SEQBOOT and CONSENSE in PHYLIP with 1000 replicates. Trees were visualized using TREEVIEW (Page 1996). We investigated phenetic distances using four alternative distance measures: F_{ST}, D, D_m, and CSE.

Results

Sample adjustments

Adjustments for relatedness were made to four spring-run juvenile samples (Deer Creek, 1994 and 1996, Mill Creek, 1996, and Butte Creek, 1996). Sixty-six of the original 272 individuals in these samples were removed before kinship analysis because of missing genotypic data. Of the remaining 206 individuals, 114 were involved in pairwise comparisons for which the hypothesis of a full-sib relationship was significantly more likely ($p < 0.01$) than the hypothesis that they were unrelated. These related individuals were removed from their samples and replaced with 86 parents whose genotypes were inferred by maximum likelihood methods, resulting in the adjusted sample sizes shown in Tables 1 and 3. Before adjustment for kinship, Butte Creek, 1996, and Mill Creek, 1996, had significant F_{IS} and Mill Creek, 1996, was not in random-mating (H-W-C) equilibrium; after adjustment, these populations have single-locus genotypic proportions that conform to random-mating expectations. Kinship adjustments also reduced the number of significant pairwise linkage disequilibria from 11 to four, over all four samples. More importantly, kinship adjustments changed the allelic frequencies in these samples. In the most extreme case, the frequency of the *Oneμ13*^{150} allele increased from 0.333 to 0.456 for the spring Butte Creek, 1996, sample after kinship adjustment. The cumulative effects of these allele frequency shifts on F_{ST} estimates are discussed below.

Previously, we found that 60% of pairwise linkage disequilibria were significant in winter-run samples W1–W5, owing to admixture of spring run in broodstock collections (see Materials and methods section). Likewise, 35% of pairwise linkage disequilibria were significant in two of the winter-run carcass samples, W7 and W8. Removing 17 individuals determined to be likely of nonwinter origin (odds ratios ranging from 1.03 to 9.68) from these samples restored equilibrium conditions. Of the 33 nonwinter samples examined in this study, six had more than 10% of pairwise linkage disequilibria significant at the 5% level, indicating potential admixture although at a lower level than winter run. These included spring Butte Creek, 1994 and 1997, fall Coleman Hatchery, 1993 and 1995, Sacramento River, 1995, and late-fall Coleman Hatchery, 1993. Removing three individuals likely to have been of nonspring origin (odds ratios ranging from 1.50 to 1.55×10^5) from spring Butte Creek, 1994 and 1997, samples brought them into linkage equilibrium. However, significant linkage disequilibrium remained in two hatchery (Coleman Hatchery, 1993 and 1995) and one naturally spawning fall-run sample (Sacramento River, 1995) despite removal of 10, 24, and 10 individuals determined to be of nonfall origin, respectively. These three fall-run samples were thus dropped from further analyses. Two individuals determined to be non-late-fall (odds ratios of 3.50 and 4.10) were removed from the Coleman Hatchery, 1993, sample.

Adjustments for relatedness and run admixture increased the F_{ST} estimated among all samples from 0.0637 to 0.0745 and decreased the F_{ST} estimated within three of the four subpopulations adjusted (0.0172 versus 0.0087 for winter run, 0.0038 versus 0.0017 for spring run from Deer and Mill creeks, 0.0065 versus 0.0045 for spring run from Butte Creek, Table 4). The number of samples having homogeneous allele frequencies also increased. Only two of eight winter-run samples (W4 and W5) were homogeneous before adjustment, whereas seven were homogeneous after adjustment. The juvenile spring-run sample from Deer Creek, 1994, joined a homogenous pool of seven samples from Deer and Mill creeks after correction for kinship. Finally, none of the four Butte Creek samples were homogeneous prior to corrections for kinship and admixture, whereas three were homogeneous after adjustment (Table 4).

Genetic diversity within population samples

We now focus exclusively on results from adjusted samples, excluding the three fall samples with persistent linkage disequilibrium. Expected and observed heterozygosities within population samples are in close agreement, with means ranging from 0.51 to 0.63 and from 0.54 to 0.62, respectively (Table 1). Thirty-three of 38 tests for H-W-C equilibrium and significance of F_{IS} values within populations conform to random-mating expectations (Table 1). We note the few exceptions: significant F_{IS} values for two of 10 spring-run samples (Butte and Deer creeks, 1997), two of 20 fall-run samples (Stanislaus River, 1994, and Merced Hatchery, 1995), and one of three late-fall samples (Keswick, 1995). These results are supported by exact probability tests for H-W-C equilibrium, except that the test for the Stanislaus, 1994, fall sample is not significant and the test for the naturally spawning Merced River, 1995, fall-run sample is significant. Only one of 38 population samples had more than 10% of pairwise loci combinations in linkage disequilibrium (late-fall Coleman Hatchery, 1993) despite adjustment for admixture. The sample was retained because it was homogeneous with the late-fall Keswick, 1995, sample and the pooled samples were in linkage equilibrium.

Genetic heterogeneity within subpopulations

Samples within the four subpopulations determined from the major nodes of Fig. 2 come from different geographical sites and collection years and from naturally spawning or hatchery populations. Tests of homogeneity within these subpopulations resulted in the following population groupings (Table 4). Seven winter-run samples are homogeneous

© 2000 NRC Canada

Fig. 3. Results from bootstrap simulations for (A) dinucleotide and (B) tetranucleotide microsatellites illustrating the number of alleles detected in chinook salmon population samples as a function of sample size. Each curve was generated using 1000 iterations for each successive sample size. Homogeneous subpopulations were used except for spring run, where Butte, Deer, and Mill Creek samples were combined.

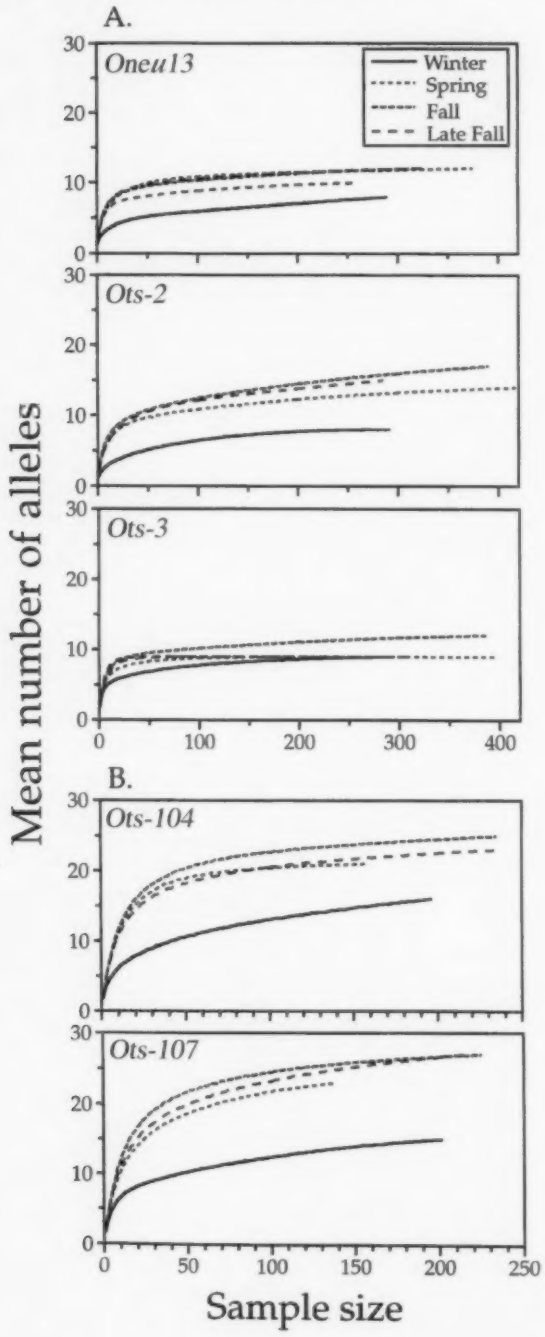

if the carcass sample of 1996 is removed. Three spring-run samples from Butte Creek are homogenous if the 1994 sample is removed. All six spring-run samples from Deer and Mill creeks are homogeneous. Thirteen fall samples are homogeneous after American River, 1995, Stanislaus River, 1994, Merced River, 1995, Coleman Hatchery, 1994, and all three late-fall samples are removed. No subset of the fall anomalies is homogeneous, but two late-fall population samples are homogeneous (Coleman Hatchery, 1993, and Keswick, 1995). The anomalous late-fall sample (Coleman Hatchery, 1995) is more closely related to the homogeneous late-fall subpopulation (F_{ST} = 0.0072) than to the homogeneous fall subpopulation (F_{ST} = 0.0174). Similar tests using D_m rather than F_{ST} resulted in the same homogeneous pools as above with one exception; it was not necessary to remove the fall Coleman Hatchery, 1994, sample before attaining a homogeneous subpopulation for fall run. Likewise, F_{ST} homogeneity tests performed for the 26 population samples scored at 10 loci affirm the same sample components among the five subpopulations except that two additional anomalous fall populations were identified; hatchery samples from the Feather and Merced rivers, 1995, were dropped to allow homogeneity among the remaining fall populations. This series of within-subpopulation tests of homogeneity define five major, more or less homogeneous subpopulations of chinook salmon in the Central Valley: winter, spring from Butte Creek, spring from Deer and Mill creeks, fall, and late fall. We note that temporal samples from the same geographic location are generally contained within the homogeneous pool for their respective subpopulation. The exceptions are distributed over different subpopulations (winter Sacramento River, 1996, spring Butte Creek, 1994, fall Stanislaus, 1994, and late-fall Coleman Hatchery, 1995). Thus, temporal variation within geographic site is not significant relative to the greater differences among subpopulations.

Comparisons among subpopulations

Bootstrapping results illustrating the number of alleles as a function of sample size are shown for the five most polymorphic loci (*Ots-2*, *-3*, *-104*, and *-107* and *Oneμ13*, Fig. 3). Both the locus concerned and run sampled are important with respect to the number of alleles observed. For example, a sample size of 100 is sufficient to encounter 90% of the alleles at *Ots-3* in spring, fall, or late-fall runs, but in winter run, the minimum sample size required is 124. Likewise, a sample size of 137 is required for nonwinter runs at *Oneμ13*, but winter requires 207. For the three more polymorphic loci, even larger samples sizes are necessary.

The simulated allele richness curves (Fig. 3) suggest that winter run consistently has fewer alleles per locus than do the other three runs. Winter run also has lower observed and expected heterozygosity and lower mean number of alleles per locus (4.4) than any of the other runs (6.7, 7.7, and 8.8 for spring, fall, and late fall, respectively, Table 1). Table 5 compares the number of alleles per locus for different populations at a common sample size of 50. In comparing winter with the other populations, fewer alleles are observed at eight or nine of 10 loci, which is significant by sign test. Likewise, within spring run, the pooled Butte Creek sample

© 2000 NRC Canada

has fewer alleles at seven of 10 loci than the pooled sample from Mill and Deer creeks.

Pooling of homogeneous samples within the five major subpopulations discussed in the preceding section increases the F_{ST} estimate for Central Valley chinook from 0.075 (calculated from 38 independent samples) to 0.082 ($p = 0.00$). Diversity among these five major subpopulations is illustrated by a UPGMA phenogram of relative genetic distance (Fig. 4). All four distance measures (F_{ST}, CSE, D, and D_m) resulted in topographically equivalent trees. Moreover, three methods of phenetic tree construction (neighbor-joining, UPGMA, and maximum likelihood estimation) yielded the same branching topology. Bootstrap values for the tree based on CSE were often higher than for the other trees (Fig. 4). Bootstrap values greater than 70% are obtained for all branch clusters, indicating statistically defined distinction of all five major subpopulations (Hillis and Bull 1993). Greater genetic distinctiveness of winter run is illustrated by the markedly larger genetic distance values in pairwise comparisons with all other runs. Spring Butte Creek samples are next most distinct, followed by spring Mill Creek and Deer Creek samples. Fall and late-fall runs have the lowest genetic distance estimate indicated by their inner cluster (Fig. 4).

Individual loci make markedly different contributions to average genetic distance among subpopulations, and different measures of genetic distance rank loci differently (Table 6). Spearman rank correlations indicate that F_{ST} is negatively, although not significantly, correlated with heterozygosity. Nei's D, on the other hand, is positively and significantly ($p < 0.05$) correlated with heterozygosity. Nei's D and D_m are both positively and significantly ($p < 0.05$) correlated with CSE, but their positive correlation with each other is not significant.

Discussion

The most important finding of this study is that chinook salmon of the Central Valley in California have substantial genetic diversity and structure. Analysis of microsatellite DNA variation reveals five distinct subpopulations that, with the exception of our discovery of two distinct lineages of spring run, are congruent with the winter, spring, fall, and late-fall spawning runs that have long been recognized (Fisher 1994). That such biological diversity has survived more than 100 years of massive habitat destruction, exploitation, and artificial propagation (Yoshiyama et al. 1998) is perhaps surprising but at the same time encouraging of efforts to protect these populations. Our data retrospectively support the designation of winter run and spring run as evolutionary significant units protected under the U.S. Endangered Species Act (NMFS 1994, 1999; Waples 1995). Winter run, whose blend of ocean- and stream-type life history characteristics is unique among all chinook salmon (Healey 1991), is the most distinctive of the subpopulations in the Central Valley. The next most distinctive subpopulations are the spring runs, particularly those in Butte Creek, which have unique life history adaptations (Yoshiyama et al. 1996). Formerly the most abundant chinook salmon throughout the Central Valley, spring runs are presently found in only a few tributaries of the Sacramento River, primarily those considered in this study (Fisher 1994; Yoshiyama et al. 1996, 1998). Finally, fall and late-fall runs, although closely related, are significantly different at 10 microsatellite markers and differ in geographic range, run timing, and size at maturity (Fisher 1994).

The two most divergent runs in the Central Valley, winter run and spring run from Butte Creek, show signs of having experienced past reductions in size (bottleneck). Winter run has significantly fewer alleles at most loci and lower average heterozygosity than all other runs. Spring run from Butte Creek also has fewer alleles than spring run from Mill and Deer creeks. Thus, bottlenecks and genetic drift, which can affect highly polymorphic microsatellite markers in particular (Hedrick 1999), may have accelerated the genetic divergence measured for these spawning runs (Nei 1987). Whether the bottlenecks and reductions in genetic diversity coincided with precipitous declines of these stocks within the last 100 years (Yoshiyama et al. 1998) or resulted from earlier events is a matter for speculation. We note, however, that drift might also explain heterogeneity among samples from Butte Creek, as the abundance of spring run in this creek ranged from a high of 8700 adults in 1960 to a low of 10 fish in 1979 (CDFG 1998). Because mean age at reproduction is 3 years in spring-run chinook (Fisher 1994), the 1994 and 1997 samples were drawn from a weak year-class tracing back to the 1979 low.

Despite spatial and temporal overlap of chinook salmon spawning runs in the Central Valley, we have no evidence for natural hybridization among runs. A commonly held view is that most spring-run populations have hybridized with fall run and that Butte Creek spring run in particular has hybridized with the Feather River fall hatchery stock (Yoshiyama et al. 1998). Genotypic proportions in the Butte Creek spring run conform to random-mating expectations, however, and this subpopulation clusters farther from the fall run than does the spring run from Deer and Mill creeks, not closer as expected under the hybridization hypothesis. Admixture of runs can nevertheless occur in samples and appears to be a likely cause for significant linkage disequilibrium in broodstock collected for a winter-run hatchery supplementation program as well as in eight other samples from naturally spawning populations. Our ability to detect run origin among mixed samples is well defined for winter run owing to the genetic distinctiveness of this run. Identifying the provenance of individuals from runs other than the winter run is more difficult, however, owing to their greater similarity. Tests of linkage equilibrium nevertheless remain useful for detecting admixture in population samples (Waples and Smouse 1990).

Artificial hybridization in hatcheries, where mating choices are not made by the fish, could pose a risk to conservation of chinook salmon diversity in the Central Valley. Spring run were unwittingly hybridized with winter run in the early years of a hatchery supplementation program for the latter (D. Hedgecock et al., unpublished data). Broodstock are now typed for microsatellites upon collection, and only those with significant genotypic odds of being winter run are used in the hatchery. Here, we present evidence for significant linkage disequilibrium in two samples from the Coleman Hatchery fall stock (1993 and 1995), suggesting admixture and possible hybridization between fall and spring runs. Temporal overlap of both runs in Battle Creek

© 2000 NRC Canada

makes simultaneous capture of adults from both runs highly likely, and morphology does not provide reliable discrimination between them. This problem was first identified in the early operation of the Coleman Hatchery (Cope and Slater 1957) and remains a challenging problem, given limited power for individual genetic identification of non-winter-run fish. Admixture or hybridization of fall into late fall might also explain the significant linkage disequilibrium and failure of random-mating equilibrium in samples from the Coleman Hatchery late-fall stock. However, we have even less power for identifying non-late-fall individuals, given the smaller genetic distance apparent between late fall and fall. Finally, the Feather River Hatchery has long been suspected of hybridizing spring and fall runs on the basis of coded-wire tag returns (Yoshiyama et al. 1998). Yet, we observe neither linkage disequilibrium nor failure of random-mating equilibrium in samples from the hatchery or naturally spawning populations of fall chinook in the Feather River. In addition, the Feather River Hatchery samples considered in this study are not significantly different from the fall run, providing no evidence for past hybridization with Central Valley spring run.

Evaluating the extent of spatial and temporal heterogeneity within runs is critical to the successful development and implementation of conservation and management plans (Small et al. 1998; Nielsen et al. 1999; Tessier and Bernatchez 1999). Neither spatial nor temporal variation within runs appears to be important, however, compared with the much larger differences among the runs. Fall run, which was sampled extensively in both the Sacramento River and San Joaquin River drainages of the Central Valley, including both hatchery and naturally spawning populations, is largely homogeneous. Spring run from Deer and Mill creeks is homogeneous (although distinct from the second spring-run subpopulation in Butte Creek). Spatial variation is not an issue for the remaining runs, which presently have very restricted geographic ranges. On a temporal scale, overall homogeneity within the major subpopulations of chinook salmon in the Central Valley affirms a general lack of significant year-to-year variation within runs. Samples of winter run from 1991 to 1997 were homogeneous, with the exception of the 1996 carcass sample. Samples of spring run from Deer and Mill creeks were likewise homogeneous over a 4-year period, from 1994 through 1997. Fall run and late-fall run were each homogeneous over a 3-year period.

Finally, we find that local populations of chinook salmon in the Central Valley have proportions of microsatellite genotypes that conform to those expected from random mating among individuals. Random mating has, of course, been confirmed by innumerable studies in the vast literature on salmonid population genetics. The importance of confirming random mating for microsatellite markers in this study lies in the contrast that it provides for those exceptional failures of equilibrium genotypic distribution that we have attributed to kinship among juveniles or run admixture in samples.

Although substantial genetic structure of chinook salmon in the Central Valley was apparent from a cluster analysis of raw population data, the picture was brought into sharper focus by adjusting samples for kinship and run admixture. Relatedness of individuals within juvenile samples has long been recognized as a problem for estimation of population allelic frequencies (Allendorf and Phelps 1981). In the past, geneticists have simply tried to avoid such samples, but today, we have the problem of sampling threatened populations whose juvenile life stages may be more abundant and more readily collected than adults. In the case of spring-run chinook in the Central Valley, for example, the inaccessibility of much of the spawning habitat greatly limits collection of spawning adults or postspawned carcasses (Yoshiyama et al. 1996, 1998). Fortunately, highly polymorphic microsatellite DNA markers now provide more statistical power for detecting kinship than was previously afforded by allozymes (O'Reilly et al. 1998; Fontaine and Dodson 1999). Thus, to maximize population genetic information for the threatened spring run, we corrected for relatedness in juvenile samples by replacing the genotypes of likely siblings with the most likely genotypes of their parents.

The second type of sample adjustment was for admixture of different spawning populations, which has also long been recognized as an issue in delineating spawning stocks that are incompletely isolated in space and time (Campton and Johnston 1985; Waples and Smouse 1990; Estoup et al. 1998). Again, microsatellite DNA markers now provide more statistical power than was previously afforded by allozymes, both for detecting linkage disequilibrium, a signal of sample admixture (Waples and Smouse 1990), and for assigning individuals to populations of origin (Banks and Eichert 2000). For samples with unusual levels of linkage disequilibrium, we first identified and removed individuals responsible for the disequilibrium and then reassigned them to their sample only if they were more likely to belong to the remainder of their sample than to any other run.

Although the difference in population structure before and after these adjustments appears small (cf. Figs. 2 and 4), the increase in the precision and accuracy of the population genetic analysis is significant and important for future applications of microsatellites to conservation. The two types of adjustments resulted in the net removal of 116 individuals, less than 5% of individuals genotyped in the study, with the following consequences. The number of populations displaying departure from single and multilocus equilibrium at a nominal significance level of 5% was reduced from 12 to five and from eight to one, respectively, further increasing confidence in the application of the H-W-C principle in mixed-stock analyses and individual assignment. Variation among samples within runs was also reduced, as evidenced by reductions in numbers of alleles and within-run F_{ST} values, resulting in an increase in the sizes of homogeneous pools of samples and the precision of allele frequency estimates for runs. Finally, genetic distance among runs was dramatically increased, as evidenced by an increase in F_{ST} from 0.064 to 0.082. These changes all favor the further application of these markers in conservation efforts.

Average allele frequency variance among the runs of chinook salmon in the Central Valley (F_{ST} = 0.082 for five loci or 0.078 for 10 loci) is substantial compared with the genetic divergence detected by microsatellite studies of other anadromous salmonids. Based on five microsatellite loci, Olsen et al. (1998) reported F_{ST} values of 0.026 and 0.032 for comparisons within and between odd- and even-year populations of pink salmon (*Oncorhynchus gorbuscha*), respectively. Small et al. (1998) estimated an F_{ST} of 0.058, based

© 2000 NRC Canada

Table 5. Means and standard errors obtained from bootstrap simulations of the number of alleles observed at a common sample size of 50.

	Winter		Spring				Fall					
			Butte Creek		Mill and Deer creeks		Naturally spawning		Hatchery		Late fall	
	Mean	SE	Mean	SE	Mean	SE	Mean	SE	Mean	SE	Mean	SE
Ots-1	2.37	0.02	3.35	0.02	3.22	0.02	2.95	0.01	3.71	0.02	3.60	0.02
Ots-2	5.20	0.03	8.08	0.03	10.49	0.03	10.74	0.04	12.76	0.04	10.53	0.04
Ots-3	6.86	0.03	7.97	0.01	8.06	0.02	9.50	0.02	8.85	0.01	8.97	0.01
Ots-5	2.00	0.00	1.32	0.01	1.99	0.00	2.78	0.02	2.59	0.02	2.37	0.02
Ots-9	3.00	0.00	3.00	0.00	3.00	0.00	3.00	0.00	3.00	0.00	3.00	0.00
Ots-10	2.42	0.02	4.59	0.02	4.32	0.02	4.74	0.01	5.00	0.02	3.69	0.02
Ots-13	5.23	0.03	8.64	0.03	10.16	0.02	9.47	0.03	9.72	0.03	8.11	0.02
Omy-77	1.63	0.02	3.37	0.02	3.51	0.02	4.83	0.01	4.44	0.02	3.27	0.03
Ots-104	10.67	0.04	16.18	0.02	17.69	0.02	20.17	0.03	26.16	0.07	18.10	0.04
Ots-107	10.33	0.04	15.88	0.04	20.42	0.02	23.48	0.03	21.76	0.05	19.95	0.05

Fig. 4. UPGMA phenogram derived from CSE using adjusted data from 10 microsatellite loci (*Ots-1*, *-2*, *-3*, *-5*, *-9*, *-10*, *-104*, and *-107*, *Oneμ13*, and *Omy-77*) for 26 chinook salmon population samples from California's Central Valley. Populations were grouped in homogeneous subpopulations as defined in the Results section for 10 loci. Numbers in parentheses indicate mean sample sizes; numbers at nodes indicate the percentage of bootstrap simulations supporting a given cluster (1, CSE–UPGMA; 2, *D*–UPGMA; 3, CSE–neighbor joining; 4, *D*–neighbor joining). The scale indicates genetic distance.

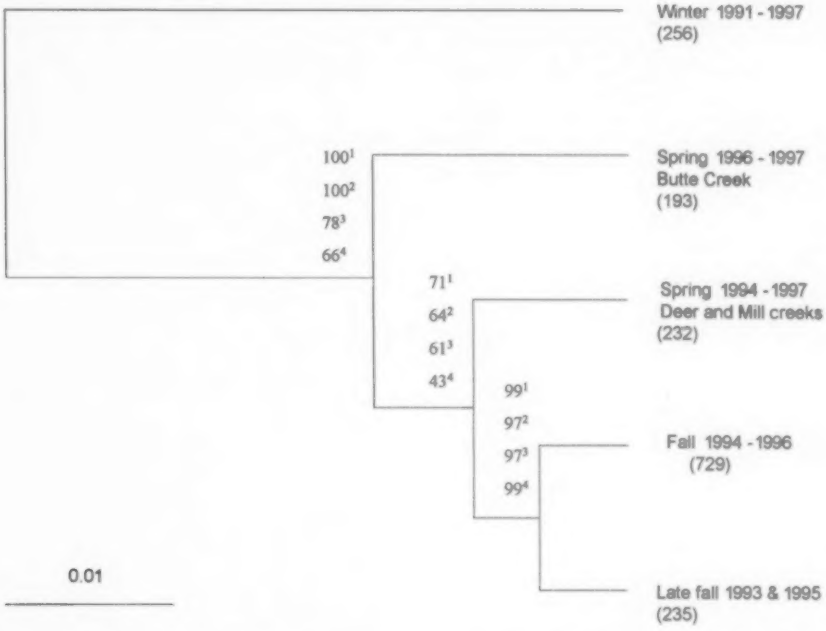

on three microsatellite loci, for coho salmon (*Oncorhynchus kisutch*) in the Fraser River. McConnell et al. (1997), in a survey of eight microsatellite loci of Atlantic salmon (*Salmo salar*), reported an F_{ST} of 0.072 among populations in the Inner Bay of Fundy having different life histories.

Divergence among Central Valley chinook salmon runs has also been estimated using allozymes, mtDNA, and sequence variation in a major histocompatibility (MHC) gene. In a study of variation at 39 allozyme-coding loci, Bartley et al. (1992) estimated F_{ST} to be only 0.01 among five samples of chinook salmon from the Central Valley. However, the allozyme-based estimate includes more shared monomorphic loci than were allowed in our selection of polymorphic microsatellite markers. In addition, the identity of the winter-run sample in the Bartley et al. (1992) study has been questioned, and a recent allozyme study has detected substantial divergence among runs (D. Teel and G. Winans, NMFS, Seattle, Wash., personal communication). Thus, protein and microsatellite DNA markers may paint more similar pictures of divergence of salmon runs in the Central Valley than presently appreciated. On the other hand, mtDNA and MHC markers appear, at first glance, to show greater divergence among runs than do microsatellite markers. Our average F_{ST} estimate for 10 microsatellite loci (0.078) is notably less than the F_{ST} of 0.24 calculated from the mtDNA data of Nielsen et al. (1994) or the 0.129 estimate from the MHC class II β1 exon (Kim et al. 1999). However, these last two marker types have substantially fewer alleles than is typical

© 2000 NRC Canada

Table 6. Single-locus average genetic distance and heterozygosity estimates for chinook salmon from California's Central Valley.

Locus	H_e	F_{ST}	CSE	D	D_m
Ots-104	0.87884	0.0473	0.3308	0.5735	0.0258
Ots-107	0.86563	0.0573	0.4355	0.7009	0.0348
Ots-3	0.80355	0.0299	0.2086	0.2592	0.0156
Oneμ13	0.71252	0.1172	0.3720	0.3895	0.0481
Ots-2	0.66378	0.1687	0.4753	0.4872	0.0808
Ots-10	0.52825	0.0512	0.1428	0.1955	0.0204
Ots-1	0.4732	0.0227	0.1276	0.1429	0.0074
Ots-9	0.46908	0.1053	0.1932	0.2368	0.0229
Omy-77	0.19023	0.0531	0.1222	0.1309	0.0066
Ots-5	0.13883	0.1611	0.1415	0.1393	0.0139

Note: Population samples were combined into heterogeneous pools as defined for 10 loci. Loci were ranked according to the magnitude of heterozygosity.

of microsatellites. A number of researchers (Hedrick 1999 and references therein) have shown that, for highly variable loci such as microsatellites, F_{ST} is constrained by high within-population diversity. As gene diversities within subpopulations and the total population approach 1.0, the difference between them, which should represent the diversity among subpopulations, approaches zero. Thus, F_{ST} estimates for polymorphic marker types may be lower than those obtained from less variable marker types, as we observe when comparing our average estimate from microsatellites with those from mtDNA and MHC data. F_{ST} ranges from 0.023 to 0.169 for our microsatellite loci (Table 6) and is negatively, although not significantly, correlated with heterozygosity. In contrast, Nei's D is positively and significantly correlated with heterozygosity, which suggests that this measure may not be as affected by high heterozygosity as F_{ST}. Nei's D values of 0.395 for mtDNA (from data in Nielsen et al. 1994) and 0.648 for MHC (from data in Kim et al. 1999) are within the range that we observe for microsatellite loci (0.131–0.701). All markers suggest that winter run is the most distinctive subpopulation, followed by spring run and then fall and late fall, so there is general concordance among different types of markers concerning divergence among chinook salmon runs in the Central Valley.

In conclusion, we find substantial genetic diversity revealed by microsatellite DNA markers among California's Central Valley chinook salmon populations. Despite well-justified concern for the irreversible loss of genetic heterogeneity, owing to substantial habitat loss, water diversion, harvest pressure, and significant hatchery influence (Yoshiyama et al. 1998), we are impressed with the genetic diversity and structure that remain. Evidence for run admixture and resultant hybridization in hatcheries remains a pressing concern, and there is need for increased genetic power for verifying the run identity of hatchery broodstock. However, the potential for discrimination among the five chinook subpopulations with microsatellite loci has obvious importance for management and protection of specific stocks. With increasing numbers of salmon being listed as endangered species, we have urgent need for the best possible resolution among populations. Water policy, fishing quotas, and other regulatory decisions require precise information on specific stocks at risk. We report sufficient genetic diversity among Central Valley chinook spawning runs to enable estimation of contributions to mixed samples and individual identification of winter run. The increase in precision offered by microsatellite loci, together with the sample adjustment methods developed in this study, demonstrates great promise for resolving closely related populations in a conservation context.

Acknowledgements

We thank S. Hamelberg and associates of the U.S. Fish and Wildlife Service and J. Navicky and associates of the California Department of Fish and Game for providing samples used in this study. We also thank R. Brown, S. Greene and associates of the California Department of Water Resources for supporting this research, and members of the salmon project at the Bodega Marine Laboratory for their assistance. We thank K. Belkhir (Laboratoire Génome et Populations, CNRS UPR 9060, Université de Montpellier II, Montpellier, France) for various modified versions of GENETIX. We also thank two anonymous reviewers whose comments substantially improved this paper. This study was supported by funds from the Department of Water Resources, CALFED, and the U.S. Fish and Wildlife Service. This paper is dedicated to the memory of Nat Bingham, who recruited us to the cause of salmon conservation and fostered this work.

References

Allendorf, F.W., and Phelps, S.R. 1981. Use of allelic frequencies to describe population structure. Can. J. Fish. Aquat. Sci. **38**: 1507–1514.

Banks, M.A., and Eichert, W. 2000. WHICHRUN (version 3.2): a computer program for population assignment of individuals based on multilocus genotype data. J. Hered. **91**: 87–89.

Banks, M.A., Blouin, M.S., Baldwin, B.A., Rashbrook, V.K., Fitzgerald, H.A., Blankenship, S.M., and Hedgecock, D. 1999. Isolation and inheritance of novel microsatellites in chinook salmon (*Oncorhynchus tshawytscha*). J. Hered. **90**: 281–288.

Bartley, D., Gall, G.A.E., Bentley, B., Brodziak, J., Gomulkiewicz, R., and Mangel, M. 1992. Geographic variation in population genetic structure of chinook salmon from California and Oregon. Fish. Bull. U.S. **90**: 77–100.

California Department of Fish and Game (CDFG). 1998. A status review of the spring-run chinook salmon (*Oncorhynchus tshawytscha*) in the Sacramento River drainage. Candidate Species Status Rep. 98-01.

Campton, D.E., and Johnston, J.M. 1985. Electrophoretic evidence for admixture of native and nonnative rainbow trout (*Salmo gairdneri*) in the Yakima River, Washington, (USA). Trans. Am. Fish. Soc. **114**: 782–793.

Cavalli-Sforza, L.L., and Edwards, A.W.F. 1967. Phylogenetic analysis: models and estimation procedures. Evolution, **32**: 550–570.

Colson, I., and Goldstein, D.B. 1999. Evidence for complex mutations at microsatellite loci in *Drosophila*. **152**: 617–627.

Cope, O.B., and Slater, D.W. 1957. Role of Coleman Hatchery in maintaining a king salmon run. U.S. Dep. Inter. Fish Wildl. Serv. Res. Rep. 47. pp. 1–22.

Estoup, A., Rousset, F., Michalakis, Y., Cornuet, J.-M., Adriamanga, M., and Guyomard, R. 1998. Comparative analysis of microsatellite and allozyme markers: a case study investigating microgeographic differentiation in brown trout (*Salmo trutta*). Mol. Ecol. **7**: 339–353.

© 2000 NRC Canada

Felsenstein, J. 1993. PHYLIP (Phyologeny Inference Package), version 3.57c. Department of Genetics, University of Washington, Box 357360, Seattle, WA 98105, U.S.A.

Fisher, F.W. 1994. Past and present status of Central Valley chinook salmon. Conserv. Biol. **8**: 870–873.

Fontaine, P.M., and Dodson, J.J. 1999. An analysis of the distribution of juvenile Atlantic salmon (*Salmo salar*) in nature as a function of relatedness using microsatellites. Mol. Ecol. **8**: 189–198.

Goodnight, K.F., and Queller, D.C. 1999. Computer software for performing likelihood tests of pedigree relationship using genetic markers. Mol. Ecol. **8**: 1231–1234.

Healey, M.C. 1991. The life history of chinook salmon. *In* Pacific life histories. *Edited by* C. Groot and L. Margolis. University of British Columbia Press, Vancouver, B.C. pp. 39–52.

Hedrick, P.W. 1999. Perspective: highly variable genetic loci and their interpretation in evolution and conservation. Evolution, **53**: 313–318.

Hillis, D.M., and Bull, J.J. 1993. An empirical test of bootstrapping as a method for assessing confidence in phylogenetic analysis. Syst. Biol. **42**: 182–192.

Kim, J.T., Parker, K.M., and Hedrick, P.W. 1999. MHC differentiation in Sacramento River chinook salmon. Genetics, **151**: 1115–1122.

McConnell, S.K.J., Ruzzante, E.D., O'Reilly, P.T., Hamilton, L., and Wright, J.M. 1997. Microsatellite loci reveal highly significant genetic differentiation among Atlantic salmon (*Salmo salar* L.) stocks from the east coast of Canada. Mol. Ecol. **6**: 1075–1089.

Morris, D.B., Richard, K.R., and Wright, J.M. 1996. Microsatellites from rainbow trout (*Oncorhynchus mykiss*) and their use for genetic study of salmonids. Can. J. Fish. Aquat. Sci. **53**: 120–126.

National Marine Fisheries Service (NMFS). 1994. Endangered and threatened species; status of Sacramento River winter-run chinook salmon. Fed. Register **59**(No. 2): 440–450.

National Marine Fisheries Service (NMFS). 1998. Endangered and threatened species; west coast chinook salmon; listing status change; proposed rule. Fed. Register **63**(No. 45): 11482.

National Marine Fisheries Service (NMFS). 1999. Endangered and threatened species; threatened status for two chinook salmon evolutionary significant units (ESUs) in California. Fed. Register **64**(No. 179): 50 394 – 50 415.

Nehlsen, W. 1994. Salmon stocks at risk: beyond 214. Conserv. Biol. **8**: 867–869.

Nei, M. 1972. Genetic distance between populations. Am. Nat. **106**: 283–292.

Nei, M. 1987. Molecular evolutionary genetics. Columbia University Press, New York.

Nelson, R.J., and Beacham, T.D. 1999. Isolation and cross species amplification of microsatellite loci useful for study of Pacific salmon. Anim. Genet. **30**: 228–229.

Nielsen, J.L., Tupper, D., and Thomas, W.K. 1994. Mitochondrial DNA polymorphism in unique runs of chinook salmon (*Oncorhynchus tshawytscha*) from the Sacramento – San Joaquin River basin. Conserv. Biol. **8**: 882–884.

Nielsen, E.E., Hansen, M.M., and Loeschcke, V. 1999. Genetic variation in time and space: microsatellite analysis of extinct and extant populations of Atlantic salmon. Evolution, **53**: 261–268.

Olsen, J.B., Seeb, L.W., Bentzen, P., and Seeb, J. 1998. Genetic interpretation of broad-scale microsatellite polymorphism in odd-year pink salmon. Trans. Am. Fish. Soc. **127**: 535–350.

O'Reilly, P.T., Herbinger, C., and Wright, J.M. 1998. Analysis of parentage determination in Atlantic salmon. Anim. Genet. **29**: 363–370.

Paetkau, D., Waits, L., Clarkson, P., Craighead, L., and Strobeck, C. 1997. An empirical evaluation of genetic distance statistics using microsatellite data from bear (Ursidae) populations. Genetics, **147**: 1943–1957.

Page, R.D.M. 1996. TREEVIEW: an application to display phylogenetic trees on personal computers. Comp. Appl. Biosci. **12**: 357–358.

Raymond, M., and Rousset, F. 1995. GENEPOP (version 1.2): population genetics software for exact tests and ecumenicism. J. Hered. **86**: 248–249.

Saitou, N., and Nei, M. 1987. The neighbor-joining method: a new method for reconstructing phylogenetic trees. Mol. Biol. Evol. **4**: 406–425.

Scribner, K.T., Gust, J.R., and Fields, R.L. 1996. Isolation and characterization of novel salmon microsatellite loci: cross-species amplification and population genetic applications. Can. J. Fish. Aquat. Sci. **53**: 833–841.

Small, M.P., Beacham, T.D., Withler, R.E., and Nelson, R.J. 1998. Discriminating coho salmon (*Oncorhynchus kisutch*) populations within the Fraser River, British Columbia, using microsatellite DNA markers. Mol. Ecol. **7**: 141–155.

Sneath, P.H.A., and Sokal, R.R. 1973. Numerical taxonomy. Freeman Press, San Francisco, Calif.

Tessier, N., and Bernatchez, L. 1999. Stability of population structure and genetic diversity across generations assessed by microsatellites among sympatric populations of landlocked Atlantic salmon (*Salmo salar* L.). Mol. Ecol. **8**: 169–179.

Waples, R.S. 1995. Evolutionary significant units and the conservation of biological diversity under the Endangered Species Act. Am. Fish. Soc. Symp. **17**: 8–27.

Waples, R.S., and Smouse, P.E. 1990. Gametic disequilibrium analysis as a means of identifying mixtures of salmon populations. Am. Fish. Soc. Symp. **7**: 439–458.

Wright, J.M., and Bentzen, P. 1996. Microsatellites — genetic markers of the future. Rev. Fish Biol. Fish. **4**: 384–388.

Yoshiyama, R.M., Gerstung, E.R., Fisher, F.W., and Moyle, P.B. 1996. Historical and present distribution of chinook salmon in the Central Valley drainage of California. Sierra Nevada Ecosystem Project: final report to Congress. *In* Assessments, commissioned reports, and background information. Center for Water and Wildlife Resources, University of California at Davis, Davis, Calif. pp. 309–362.

Yoshiyama, R.M., Fisher, F.W., and Moyle, P.B. 1998. Historical abundance and decline of chinook salmon in the Central Valley region of California. N. Am. J. Fish. Manage. **18**: 487–521.

© 2000 NRC Canada

Spatial variability of stream bed scour and fill: a comparison of scour depth in chum salmon (*Oncorhynchus keta*) redds and adjacent bed

Colin D. Rennie and Robert G. Millar

Abstract: Scour depth in egg pockets of chum salmon (*Oncorhynchus keta*) egg nests (redds) in a short gravel-bed spawning reach (45 × 20 m) of Kanaka Creek, British Columbia, was not significantly different from that in the adjacent bed during 1997–1998 winter flood events, whereas the scour depth in tailspills of redds was greater. Over the course of the incubation period, none of the egg pocket locations (zero of four), all of the tailspills (three of three), and 17% of the immediately adjacent bed locations (three of 18) scoured to the assumed egg burial depth of 15 cm below the initial postspawning surface elevation. Egg pocket scour depth has not previously been monitored, and the reliance of earlier studies on tailspill monitoring as an indication of redd scour may have led to faulty assessment of embryo loss. Only one flood event, which exceeded bankfull, caused widespread and deep scour and fill. Despite implementation of the most spatially intensive array of wiffle-ball scour monitors to date, scour was so variable that there was no spatial autocorrelation of scour depths.

Résumé : Le niveau d'affouillement dans les poches d'œufs des nids de fraye du saumon kéta (*Oncorhynchus keta*) dans un tronçon de gravières (45 × 20 m) du ruisseau Kanaka, en Colombie-Britannique, ne différait pas beaucoup de celui mesuré dans les portions adjacentes du lit pendant les crues de l'hiver 1997–1998. Par contre, le niveau d'affouillement le gravier déplacé par le creusement des nids était supérieur. Au cours de la période d'incubation, 0% des sites où se trouvaient des poches d'œufs (0 sur 4), 100% du gravier déplacé (3 sur 3) et 17% des sites surveillés dans le lit adjacent (3 sur 18) ont été affouillés à la profondeur de 15 cm, qui doit correspondre à la position des œufs au-dessous de la surface du nid recouvert. Le niveau d'affouillement dans les poches d'œufs n'ayant jamais été surveillé auparavant, les études antérieures sur la surveillance du gravier déplacé comme moyen d'indication de l'affouillement des nids de fraye ont peut-être mené à des évaluations erronées de la perte d'embryons. Une seule crue, qui a dépassé le niveau de débordement, a causé un affouillement et un colmatage importants et profonds. Malgré la mise en place du système le plus serré de surveillance de l'affouillement par balles de plastique jamais employé, l'affouillement était tellement variable qu'aucune autocorrélation spatiale des niveaux d'affouillement n'a pu être établie.

[Traduit par la Rédaction]

Introduction

The mobilization depth of riverbed substrate below the initial bed surface (scour depth) during high flows is an important constraint on salmon spawning habitat. Salmon embryos can be swept out and washed away if scour depth at the site of the redd (egg nest) exceeds the depth of egg burial. Montgomery et al. (1996) speculated that salmon tend to lay their eggs at depths just below typical scour levels for their natal stream. However, it has been shown that changes in flow and sediment regimes can increase scour to exceed egg burial depths with a correlated reduction in fry abundance (Tripp and Poulin 1986, 1992). Also, scour depths tend to vary spatially in a reach due to variability in hydraulics and bed texture (Hassan 1990; Schuett-Hames 1996); thus, redds may be subjected to scour even if mean scour depth is less than egg burial depth.

To assess the likelihood of embryo loss, the architecture and construction process of a redd must be considered. A redd (Fig. 1) consists of an upstream hole called the pit, a constructed central egg pocket area, and an elevated downstream mound of loose cast-off material termed the tailspill (Bjornn and Reiser 1991). Vertical architecture at the central egg pocket area consists of four texturally distinct layers from the surface down: cover, bridge, egg pocket (where the eggs are placed), and undisturbed (Peterson and Quinn 1996). In chum salmon (*Oncorhynchus keta*) redds, Peterson and Quinn (1996) found that the egg pocket layer is texturally coarser than all the other layers, being composed of surface armour particles and purged of materials <15 mm. Based on a review of literature data, DeVries (1997) suggested that a chum salmon egg pocket layer is typically 20 cm deep beginning at 15 cm below the original streambed elevation. Thus, scour at the central egg pocket area to a depth of about 15 cm could result in embryo loss.

Redd construction influences local morphology, grain size, and particle packing, all of which may affect scour

Received April 1, 1999. Accepted February 4, 2000. J15095

C.D. Rennie[1] and R.G. Millar. Department of Civil Engineering, The University of British Columbia, Vancouver, BC V6T 1Z4, Canada.

[1]Author to whom all correspondence should be addressed. e-mail: millar@civil.ubc.ca

© 2000 NRC Canada

Fig. 1. Longitudinal and vertical architecture of a typical chum salmon redd. The tailspill is unconsolidated. At the egg pocket, the cover, bridge, and egg pocket are purged of sand. The bridge consists of granules and pebbles, the cover is slightly coarser, and the coarsest is the egg pocket, which includes surface cobbles.

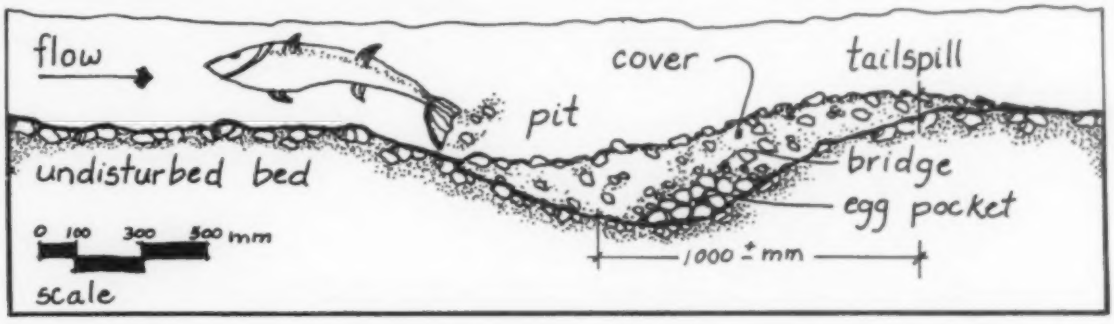

Table 1. Spatial monitoring intensity of scour studies and monitoring location with respect to spawning.

Reach	Monitor type[a]	Number of monitors	Reach length (m)	Reach width (m)	Monitor spatial intensity (no.·m^{-2})	Spawning area, in redds?
Bonanza Creek[b]	WB	18	311	23	0.0025	Yes, no
Haans Creek[b]	WB	18	312	19	0.0030	Yes, no
Hangover Creek[b]	WB	18	400	20	0.0022	Yes, no
MacMillan Creek[b]	WB	30	680	13	0.0034	Yes, no
Miller Creek[b]	WB	18	660	20	0.0014	Yes, no
Piper Creek[b]	WB	30	806	10	0.0037	Yes, no
Riley Creek[b]	WB	18	247	20	0.0036	Yes, no
Sachs Creek[b]	WB	18	500	13	0.0028	Yes, no
Saltspring Creek[b]	WB	30	292	17	0.0060	Yes, no
Schomar Creek[b]	WB	30	507	12	0.0049	Yes, no
Southbay Dump Creek[b]	WB	30	260	18	0.0064	Yes, no
Tarundi Creek[b]	WB	27	473	12	0.0053	Yes, no
Jacoby Creek (1978–1979)[c]	SC	36	1 600	15	0.0015	Yes, no
Jacoby Creek (1979–1980)[c]	SC	46	1 600	15	0.0019	Yes, no
Prairie Creek[c]	SC	14	360	10	0.0039	Yes, no
North Fork Caspar Creek (1979–1980)[c]	SC	11	230	5	0.0096	Yes, no
North Fork Caspar Creek (1980)[c]	SC	8	230	5	0.0070	Yes, no
Nahal Og[d]	SC	18	1 000	5–12 (estimated 9)	0.0020	No
Nahal Hebron[d]	SC	24	900	3–5 (estimated 4)	0.0067	No
Dungeness River[e]	WB	29	25 600	10?	0.00011	Yes, yes
Kennedy Creek[f]	WB	104	Four 100-m reaches	11	0.024	Yes, no
Carnation Creek subreach 1[g]	SC	26	100	22	0.012	Likely, no
Carnation Creek subreach 2[g]	SC	21	90	14	0.017	Likely, no
Carnation Creek subreach 3[g]	WB	49	100	16	0.031	Likely, no
Carnation Creek subreach 4[g]	SC	9	30	30	0.010	Likely, no
Carnation Creek subreach 5[g]	SC	15	40	10	0.038	Likely, no
Present study	WB	53	45	20	0.059	Yes, yes

[a]Wb, wiffle-ball sliding bead type; SC, scour chain.
[b]Tripp and Poulin (1986).
[c]Lisle (1989).
[d]Hassan (1990).
[e]Orsborn and Stephen C. Ralph Consultants (1994).
[f]Montgomery et al. (1996).
[g]Haschenburger (1996).

depth. The small local dunelike form of a redd may increase local grain mobility due to convective acceleration over the crest at the tailspill. Convective acceleration will increase shear stress imposed upon the grains on the upstream side of the bedform, with the maximum experienced at the crest (Thibodeaux and Boyle 1987; Kinfu and Quick 1998). The act of digging a redd during spawning both loosens and coarsens the substrate at the redd, since the bed is disturbed and fines are removed (Peterson and Quinn 1996). Looser gravel should be more mobile due to reduced particle im-

© 2000 NRC Canada

Fig. 2. Study site location map.

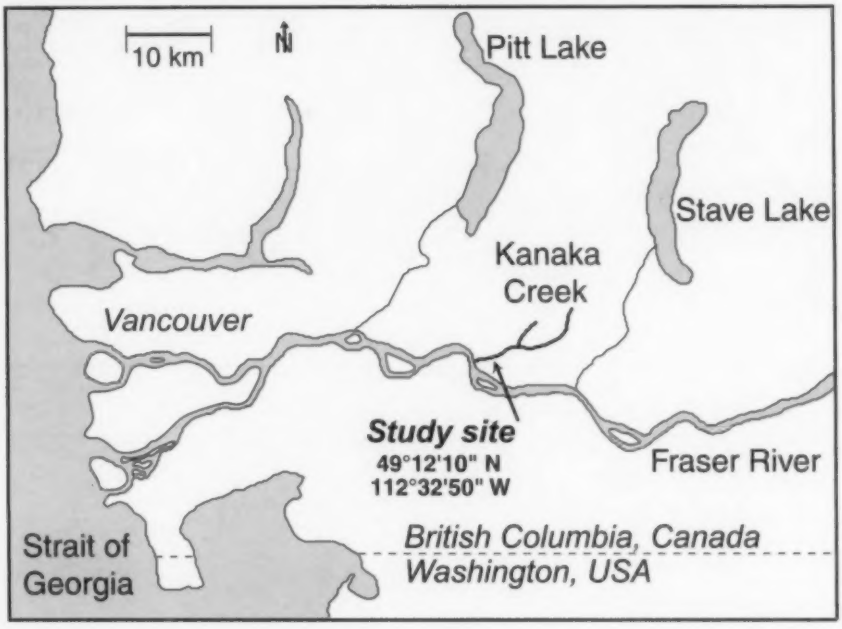

Table 2. Kanaka Creek study reach characteristics.

Mean bankfull width (m)	20
Mean bankfull depth (m)	1.0
Bed slope	
Full reach	0.002
Scour reach	0.01
Surface D_{16} (mm)	14.5
Surface D_{50} (mm)	58
Surface D_{84} (mm)	110
Surface sorting (σ_ϕ)	1.51
Subsurface D_{16} (mm)	6.5
Subsurface D_{50} (mm)	29
Subsurface D_{84} (mm)	67
Mean Corey shape factor	0.58
Approximate average Powers roundness	Subrounded
Mean daily flow ($m^3 \cdot s^{-1}$)	2.8
Mean annual peak daily flow ($m^3 \cdot s^{-1}$)	42.2
Approx. bankfull flow ($m^3 \cdot s^{-1}$)	25
Drainage area at gauge (km^2)	48

brication, yet coarser gravel should be less mobile due to greater particle mass and increased friction angles in better-sorted sediment (Montgomery et al. 1996). Furthermore, different locations within the redd display varying degrees of loosening and coarsening. The mobility of a redd, or parts of a redd, relative to the surrounding bed will depend on which of the above mechanisms are most important. At present, it is not possible to quantify all of the factors. In particular, quantification of bed packing remains illusive (Montgomery et al. 1996). Thus, scour depth in a redd cannot presently be predicted analytically.

Only a few studies have focused on scour depth in spawning areas (Table 1). One group (Orsborn and Stephen C. Ralph Consultants 1994) measured scour in the tailspill of redds. In general, scour depths were found to be highly spatially variable and at some locations were observed to exceed egg deposition depths. However, scour depth in redd egg pockets has not previously been measured. Thus, because scour depth at egg pockets may differ from that in the surrounding bed, the likelihood of scour-induced loss of embryos remains uninvestigated.

This paper reports the results of a field study that was conducted primarily to determine whether scour depth in redd egg pockets is different from that in the the surrounding bed. A short spawning reach was instrumented with a spatially intensive array of scour monitors. Monitors were also placed in the egg pockets and tailspills of all chum salmon redds within the reach. Scour in redd locations was compared with that in the adjacent bed. The spatial variability of scour was also examined, since, while mean scour depth may be less than egg burial depth, there remains the possibility that excessive local scour can wash away embryos. Quantification of the full distribution of scour depths can give an indication of the likelihood of scour-induced embryo loss.

Methods

Study site

Kanaka Creek flows into the Fraser River east of Haney (in the outer suburbs of Vancouver) in the southwestern mainland of British Columbia, Canada (Fig. 2). It flows from headwaters in the steep, forested Coast Range mountains to the lower catchment in the agricultural Fraser Valley. The floodplain is protected by parkland, but there has been increasing suburban development in the lower parts of the catchment in recent years. The climate is coastal temperate and dominated by heavy winter rains. Snow occurs at

© 2000 NRC Canada

higher elevations surrounding the headwaters, resulting in the potential for rain-on-snow events.

A 210-m-long study reach was established in a gravel-bed section 3 km upstream from the confluence with the Fraser River. The study reach was a single-thread alluvial channel and contained good salmonid spawning habitat. A Water Survey Canada flow gauge (WSC-08MH076) is located 1 km upstream of the study reach, and no major tributaries enter Kanaka Creek between the flow gauge and the study reach. Reach characteristics are summarized in Table 2. A short 45-m subreach that contained the most suitable spawning habitat was established within the study reach for scour monitoring. The subreach was essentially a riffle unit. A diagonal bar composed of loose gravel filled most of the channel, and the thalweg flowed over a clay and cobble bed next to a steep clay bank on the right side (facing upstream). The clay extended out under the channel and was covered with varying depths of alluvial gravel. The left bank was low (about 1 m), sandy, and secured with vegetation.

Reach characteristics

A longitudinal thalweg profile and four cross sections were surveyed in the long reach. Furthermore, 12 subreach cross sections were surveyed three times during the 1997–1998 winter. Bankfull elevations were estimated for each cross section using either perennial vegetation root lines or changes in bank slope as indicators (Harrelson et al. 1994). All surveying was performed using a tripod-mounted level. Substrate surface and subsurface grain size distributions were determined by bulk sampling, with sample volumes conforming to the criterion that a clast of size D_{90} accounted for ≤1% of the total sample weight (Church et al. 1987). The D_{90} particle size is defined such that 90% of a sample mass comprises particles smaller than D_{90}. A reach pebble count (Wolman 1954) of 200 grains was also conducted to determine D_{90} and to compare with the estimated surface size distribution. The pebble count was performed at two pace intervals using a pointer lowered to the streambed with eyes averted.

Flow and shear stress

Shear stress for each flood peak was estimated to relate observed scour depths to event magnitude. Rating curves for water stage and surface slope were established using manual staff gauge readings and the corresponding Water Survey Canada hourly flow gauge data. The slope rating curve suggested that water surface slope approached the long reach bed slope at higher (bankfull) stages. This was reasonable, as the flow visually appeared to be uniform during bankfull events. Thus, for each flood event of the 1997–1998 winter, reach average bed shear stress at the flood peak (τ_o) was estimated using the reach average event peak flow depth (Y) and the study reach bed slope (S), i.e., $\tau_o = \gamma YS$, where γ is the specific weight of water.

Scour and fill measurements

Scour and fill were monitored during each 1997–1998 winter flood event at 53 scour monitors (Fig. 3). To assess the local variability of scour and fill, monitor density almost doubled that of any previously reported studies and exceeded some previous studies by an order of magnitude or more (Table 1). Forty-three of the monitors were installed in an approximate 4 × 3 m grid throughout the alluvial bed sections of the subreach (Fig. 4). An additional 10 monitors were installed in all of the four active chum redds in the subreach, including a monitor in the egg pocket (four redds) and tailspill (three redds).

Monitors were of the wiffle-ball sliding bead type (Tripp and Poulin 1986; Nawa and Frissell 1993). All monitors were installed in mid-November 1997, subsequent to the chum spawning that occurred in the first half of November but prior to the coho salmon (*Oncorhynchus kisutch*) spawning that occurred in late November and early December. Coho spawning activity was concentrated at the second from most upstream cross section: monitor 41 was sufficiently disturbed that this monitor was excluded from further analysis. The study period coincided with the period of chum incubation: chum fry emerged at the Kanaka Creek fish hatchery on March 5, 1998, and the final survey occurred on March, 12 1998. Each monitor could record scour depths of up to 0.98 m. Fill depths were estimated by surveying bed surface elevation after each flood event. Scour was assumed to equal zero when deep fill buried a scour monitor. Scour at such locations in subsequent events was estimated by surveying changes in bed surface elevation. Thus, burial of a scour monitor reduced the reliability of subsequent scour measurement, but this was unavoidable, since the monitor could not be exhumed if the bed was to remain undisturbed for ensuing flood events. Further details on installation techniques can be found in Rennie (1998).

Comparison of redd scour with adjacent bed scour

Scour depth in redds was recorded with respect to the initial redd surface elevation, not the original streambed elevation. However, surveyed differences in initial elevation between redds and immediately adjacent bed were small (less than a few centimetres). This compared favourably with DeVries (1997), who suggested that the difference between initial redd surface and the original bed elevation is approximately 0–5 cm. Thus, there was little difference between the initial surface and the original streambed elevation as datum. It was therefore assumed that embryos were subject to destruction if scour depth exceeded 15 cm below the initial egg pocket surface.

A statistical test was required to compare scour in redds with scour in the adjacent bed. Parametric procedures could not be used, since measured scour depths displayed nonnormal probability distribution functions. The functions resembled negative exponential distributions (cf. Montgomery et al. 1996; Haschenburger 1999) (Fig. 5), although if zero values were excluded, the distributions for individual flood periods appeared lognormal. Also, the flood periods produced very different degrees of scour (Fig. 6), and redd bedform morphology tended to diminish in amplitude with each successive flood (cf. Lisle 1989); thus, it was necessary to use a procedure that reduced the variability due to different flood periods.

The maximum scour depth below the initial bed surface observed over the entire flood season was compared in the three treatments of egg pocket of redds, tailspill of redds, and riverbed immediately adjacent to redds. Maximum scour depth over the flood season was a useful metric because (*i*) this factor determined the viability of incubating embryos and (*ii*) variability due to different flood periods was avoided. Monitors immediately adjacent to redds were used to represent the surrounding bed, since scour depths within the reach were highly variable and were affected by local factors such as woody debris and collapsing banks. Limiting the surrounding bed monitors to immediately adjacent locations provided a better test of the effect of redds on scour depth, since immediately adjacent monitoring points were subjected to hydraulic conditions similar to those of the redd location. The nonparametric multiple comparison Nemenyi–Dunn test following the Kruskal–Wallis test (Zar 1996) was used to compare mean scour depth in the three treatments. This test only requires that the underlying probability distribution be similar for all the treatments.

Spatial variability of scour

Surface contour plots were generated for channel survey, scour, and fill data by interpolation using a linear kriging algorithm in the software package Surfer™. Interpolation procedures such as kriging assume that site values are spatially autocorrelated and vary smoothly across the area (Haining 1990). The interpolations for bed surface elevations were more successful than for scour and (or) fill, due to the greater density and spatial similarity of survey

© 2000 NRC Canada

Fig. 3. Hourly flows at Kanaka Creek WSC-08MH076 for the period August 1, 1997, to April 8, 1998. Vertical bars denote scour monitor survey dates, with flood periods between survey dates. The scour survey on December 10, 1997, did not involve bed elevation surveying; thus, the first two flood periods are grouped together as flood period 1.

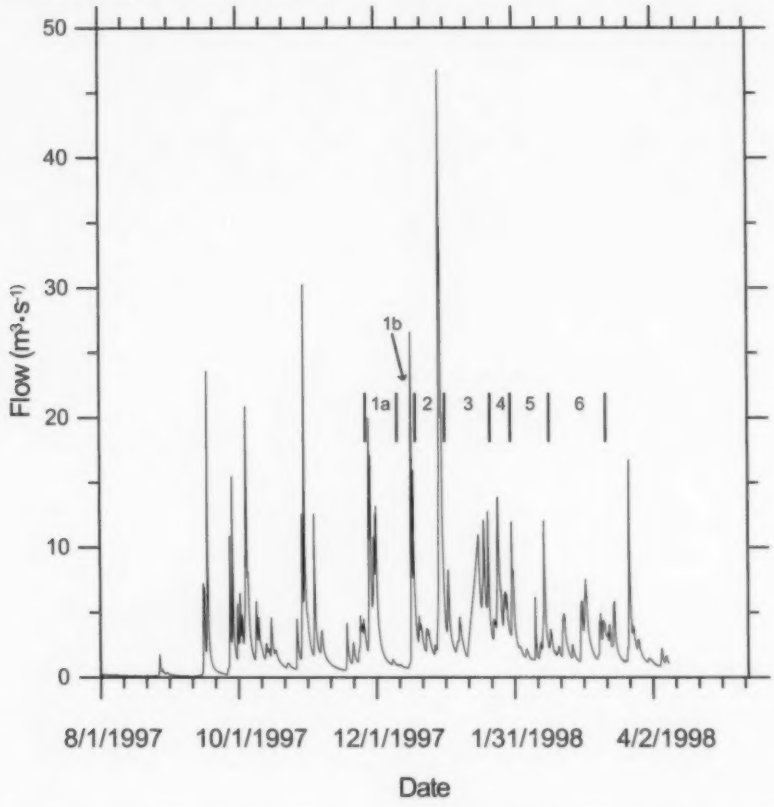

data. In fact, as shown in the Results, the scour data did not show spatial autocorrelation.

The 3 × 4 m grid scour data were analyzed for spatial autocorrelation using both the Moran coefficient (I) and the Geary ratio (c) (Cliff and Ord 1981; Goodchild 1986):

$$I = \frac{n\sum_{i=1}^{n}\sum_{j=1}^{n} w_{ij}(x_i - \bar{x})(x_j - \bar{x})}{\sum_{i=1}^{n}\sum_{j=1}^{n} w_{ij}\sum_{i=1}^{n}(x_i - \bar{x})^2}$$

$$c = \frac{(n-1)\sum_{i=1}^{n}\sum_{j=1}^{n} w_{ij}(x_i - x_j)^2}{2\sum_{i=1}^{n}\sum_{j=1}^{n} w_{ij}\sum_{i=1}^{n}(x_i - \bar{x})^2}$$

where n is the sample size (number of scour monitors), x_i is the scour depth at monitor i, $\bar{x}$ is the mean scour depth of the n monitors, and w_{ij} is the weighting value for the interaction between monitors i and j (in this case, $w_{ij} = 1$ if the monitors were adjacent to each other and $w_{ij} = 0$ otherwise). Positive spatial autocorrelation ($I = 1$, $c = 0$) suggests that similar values of scour occur close together. Negative spatial autocorrelation ($I = -1$, $c = 2$) indicates that dissimilar values are closely spaced. A lack of spatial autocorrelation ($I \rightarrow 0$, $c = 1$) suggests a random pattern of scour. Scour depth sample populations were tested for each of the six flood periods, for the average of the flood periods, and for the maximum scour depth below the initial bed surface.

A graphical method was also used to test scour depths for spatial autocorrelation. A correlation coefficient was generated for all possible pairs of scour monitors by correlating the 5 × 1 matrix of scour depths observed for the first five flood periods at a monitoring location with the corresponding matrix at another location. The correlation coefficient for each monitor pair was plotted versus the distance between the monitors. Correlation coefficients were expected to be greater for smaller distances, since neighbouring monitors were expected to display similar trends in scour depths over the flood season. All monitors that recorded zero values of scour for all five flood periods were excluded from the analysis, since correlation coefficients could not be calculated from values of zero.

Results

Scour and fill measurements

Of the six monitored flood periods, only flood period 2 caused deep and widespread scour and fill (Fig. 6). Peak daily flow for flood period 2 was 31.3 $m^3 \cdot s^{-1}$, which has an estimated return period of about 0.9 year. Based on field indicators of leaf-litter wash lines, the peak stage for flood period 2 was 0.4–0.5 m above bankfull. No other events during the scour monitoring period were observed to exceed bankfull. During this event, a large tree (0.8-m-diameter

© 2000 NRC Canada

Fig. 4. Contour plot of the Kanaka Creek scour monitoring reach. (*a*) Initial condition (November 26, 1997, survey); (*b*) following flood period 2 (December 31, 1997, survey). Contour interval is 0.2 m. Numbered labels correspond to scour monitors (+, redd; ×, nonredd). Bankfull elevation is approximately 0 m, with a mean bankfull depth of 1.03 m (Fig. 4*a*) and 1.06 m (Fig. 4*b*).

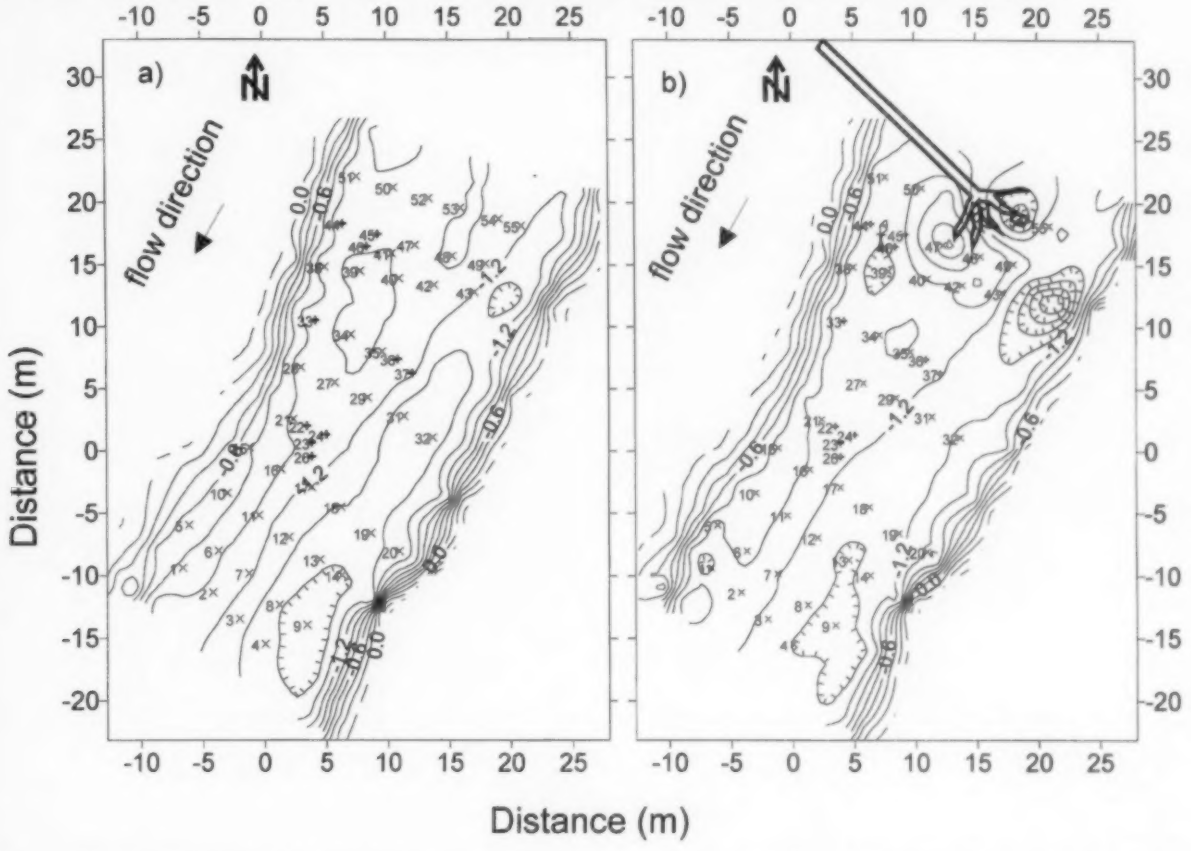

trunk, about 4-m-diameter root wad) floated down into the monitoring reach (Fig. 4*b*) and caused adjacent local scour and fill in the three most upstream cross sections. Also, the upstream end of the steep clay bank eroded laterally more than 1 m (not directly measured). This bank material was deposited in the right side of the channel as fill. It is plausible that flow deflection by the root wad caused the bank to collapse. Several monitors were buried under fill material or under the tree itself. Finally, a sandy bar on the lower left side of the reach (monitors 1 and 5) scoured out. The mean scour depth for flood period 2 was 8.5 cm. Excluding the large scour hole around the root wad, the mean scour depth was 6.9 cm. The subsequent flood periods caused relatively little scour and (or) fill.

Comparison of redd scour with adjacent bed scour

The primary concern of this study was to determine if redds were more or less likely than the surrounding bed to scour to sufficient depth to expose incubating embryos. The maximum scour depth below the initial bed surface at the three treatments (Table 3) was compared using the Nemenyi–Dunn test. There was a significant difference (α = 0.10) between mean scour depth in tailspills versus adjacent monitors but not between egg pockets and the adjacent bed or between the tailspill and egg pockets. It was also noteworthy that none of the egg pockets (zero of four), yet all of the tailspills (three of three), scoured to depths greater than the assumed egg burial depth of 15 cm. This result was sensitive to uncertainty in the egg burial depth: chum egg burial depths observed in other studies range from 5 to 45 cm, depending on real variability in depth as well as variable sampling methodology (DeVries 1997). However, if the egg burial depth was more conservatively considered to be 10 cm in the egg pockets and 20 cm in the tailspills, one of four egg pockets and two of three tailspills would have scoured to egg pocket depth. It appears that embryos in egg pockets may not have been subjected to scour.

Spatial variability of scour

Flood period 2 produced major changes in reach geometry (Figs. 4 and 7). Zones of scour appeared around the root wad, the left bank (facing upstream) sandy bar deposit, at one redd, and downstream of another redd. Zones of fill were apparent along the collapsed right bank and immediately downstream of the root wad.

Despite the apparent zoning of scour, tests of the Moran coefficient and Geary ratio did not reveal significant spatial autocorrelation (α = 0.05) in any of the individual flood

© 2000 NRC Canada

Fig. 5. Frequency distribution of maximum scour depths observed at all monitors over the flood season for the present study and at Kennedy Creek (Montgomery et al. 1996). Zero values are isolated from the 0- to 5-cm bin in the present study but are included in the 0- to 5-cm bin for the Kennedy Creek data.

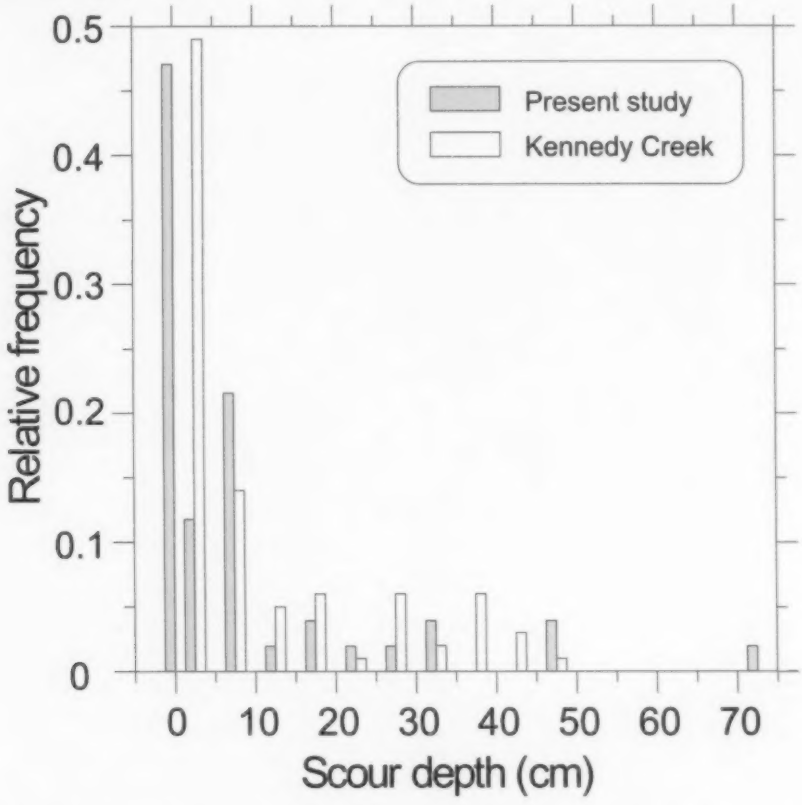

period nonredd scour data sets. The maximum scour depth below the initial bed surface observed during the entire monitoring period showed significant (α = 0.05) spatial autocorrelation (positive) by the Moran coefficient but not by the Geary ratio. It should be noted that spatial autocorrelation is scale dependent, and the lack of observed spatial autocorrelation is for the established monitor spacing of an approximate 3 × 4 m grid.

Similarly, a plot of correlation coefficients for all scour monitor pairs versus the distance between the monitors did not reveal any trend with distance (Fig. 8). The correlation coefficients close to 1.0 indicate that scour monitor pairs displayed similar trends of scour over the five flood periods. This was fairly common, since many monitors had significant scour for flood period 2 and little or no scour for all other flood periods. A small negative correlation usually occurred between monitors when one scoured during flood period 2 and the other did not.

Discussion

Implications for scour monitoring

The results confirmed previous studies, which indicated that scour and fill are extremely spatially variable. Despite implementation of the most spatially intensive scour monitoring to date, no spatial autocorrelation of scour depths could be detected. Given the high spatial variability in scour depths, it behooves the scour depth investigator to justify his or her choice of sampling intensity. If extreme values are of interest, as is the case with quantification of the potential for scour-induced loss of embryos, then the full distribution must be characterized and sufficient monitors must be installed to properly sample the scour depth population. If the shape and variance of the distribution are known or assumed a priori, then a suitable sampling protocol can be designed (Haschenburger 1999). Alternatively, a monitor spacing similar to the lateral dimension of an egg pocket should be sufficient to capture scour depth spatial variability relevant to redd mobilization.

Full characterization of the spatial distribution of scour may require even more intensive sampling. If particles are mobilized in patches as opposed to individually, it seems reasonable to assume that at some finite spatial scale, scour depths should be spatially autocorrelated. The entrainment of a patch of particles should cause a spatially continuous lowering of the bed surface elevation. Thus, neighbouring points within the patch should show positive autocorrelation. It would be worthwhile to collect scour data, by some appropriate method, with sufficient spatial intensity to determine the degree of monitoring intensity required to capture scour

© 2000 NRC Canada

Fig. 6. Bed mobilization depth (scour) and fill for each monitor (monitor number increasing from left to right) for the six observed flood periods.

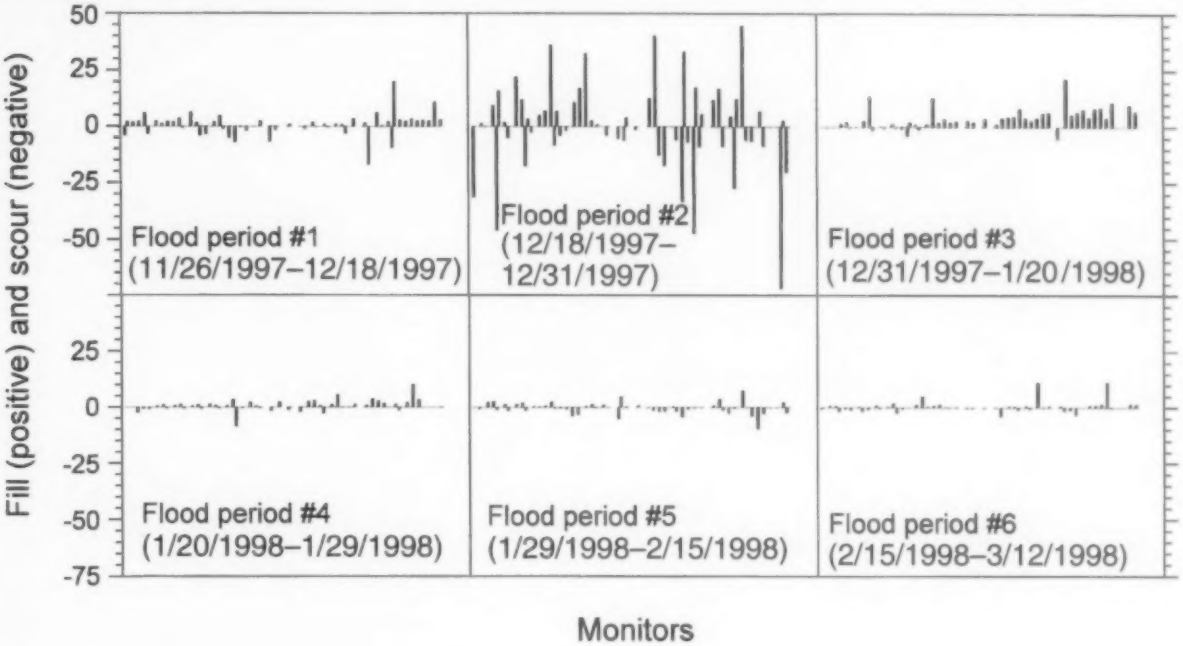

Table 3. Maximum scour depths from the initial bed surface over the entire flood season.

Monitor location	*n*	Range (cm)	Mean (cm)	SD (cm)	Percentage >15 cm
All nonredd	42	0–61	9	15	17
Immediately adjacent to redds	18	0–51	8	12	17
All redd	10	0–32	11	11	30
Egg pockets	4	0–12.5	6	5	0
Tailspills	3	17–32	25	8	100

variability. This could be accomplished by testing for spatial autocorrelation at varying monitoring point separation distances (i.e., test (x_i, x_{i+1}), then (x_i, x_{i+2}), and so on) to establish the minimum monitor spatial intensity required to observe spatial autocorrelation.

Entrainment of the entire bed

The question can be raised as to whether spatial variability of scour would be observed at Kanaka Creek during larger flood flows that produce higher shear stresses. As shear stress increases, a greater proportion of the bed area becomes mobilized (cf. Wilcock and McArdell 1997; Haschenburger 1999). At the highest shear stresses, it has been postulated that complete mobilization of the bed surface occurs, a condition that has been referred to as a "traction carpet" (Tacconi and Billi 1987). During traction carpet transport, one could speculate that scour depths would become more uniform throughout a reach, since the entire bed is in motion, as opposed to the mobilization of discrete patches at lower shear stresses.

Nondimensional bed shear stress can be defined as $\tau^* = \frac{\tau_o}{d_{50}\gamma(S_s - 1)}$, where τ_o is the bed shear stress, γ is the specific weight of water, S_s is the specific gravity of the bed material, and D_{50} is the 50th percentile particle size of the bed surface. The peak τ^* estimated for flood period 2 was 0.036, and at Kanaka Creek, scour was not observed below τ^* values of about 0.019; thus, shear stresses during flood period 2 never greatly exceeded threshold conditions for bed transport. It could be argued that a higher flood stage would have produced less spatial variability of scour. Two scenarios are possible: (*i*) a traction carpet or (*ii*) an event of some duration that eventually mobilizes the entire bed surface through entrainment of individual, discrete patches of comparable depth. The likelihood of each scenario will be discussed through both empirical evidence and physical arguments.

Theoretical and empirical evidence suggests that attainable shear stresses in alluvial gravel-bed rivers may be far below that necessary to induce a traction carpet. Bagnold (1966, his fig. 4) predicted theoretically that, for a gravel bed, τ^* would have to exceed a value of about 0.25 for a traction carpet to occur. On Kanaka Creek, the peak τ^* estimate of 0.036 is almost an order of magnitude less than is necessary for a traction carpet to develop according to Bagnold's (1966) criterion. It is hardly surprising, then, that traction carpet transport was not evident in the present study. Furthermore, nondimensional shear stresses computed for gravel-bed rivers worldwide typically do not exceed 0.1. Data for 176 stable, alluvial gravel-bed rivers in the United

© 2000 NRC Canada

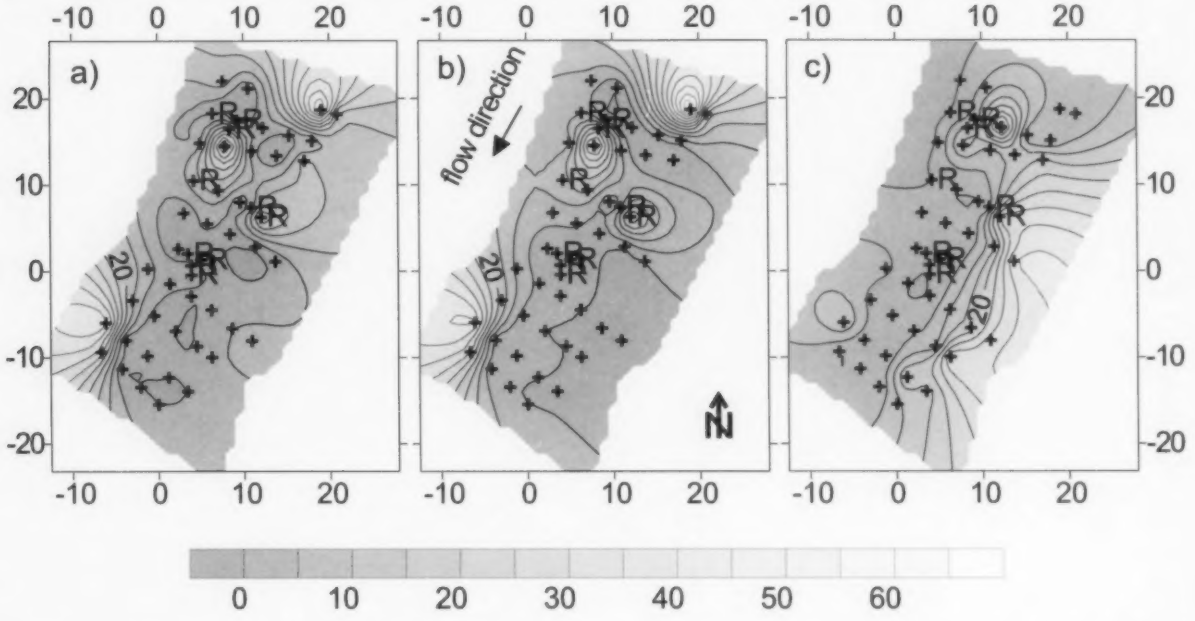

Fig. 7. Scour and fill depths observed in the Kanaka Creek scour monitoring reach. (*a*) Maximum scour depth below the initial bed surface observed over the entire monitoring period (November 26, 1997, to March 12, 1998); (*b*) scour depth observed during flood period 2; (*c*) fill depth observed during flood period 2. The scour and fill contour interval is 5 cm. +, scour monitors; R, monitors in redds.

Kingdom and North America were compiled from Charlton et al. (1978), Bray (1979), Andrews (1984), and Hey and Thorne (1986). Estimates of bankfull τ^* ranged from 0.009 to 0.14, with a mean and standard deviation of 0.047 and 0.027, respectively. Only six of the 176 rivers had values of bankfull τ^* that exceeded 0.1, and all of these were described as having banks that were stabilized by dense riparian forest. Also, average computed τ^* for 100-year flood discharges was 0.068 in 24 Colorado gravel-bed rivers (Andrews 1984). Greater shear stresses are not produced because rivers will convey large flows by eroding banks instead of cutting deeper channels (Ikeda et al. 1988). We conclude that traction carpet transport is unlikely in gravel-bed rivers.

However, the question remains whether the entire bed surface could eventually be mobilized through entrainment of individual, discrete patches of comparable depth. If every area of the bed scoured to an equal depth, then data from typical scour monitors would reveal little spatial variability in scour. Existing evidence does not support this scenario. Scour and particle tracer studies have failed to reveal entrainment of the entire bed surface. Scour depth populations tend to follow negative exponential distributions, with a large number of bed locations displaying zero values (Haschenburger 1999). Particle tracer studies also show many immobile bed locations (cf. Hassan and Church 1992). Furthermore, scour populations for larger floods (about an 8-year flood, maximum τ^* of 0.11) still show negative exponential distributions, with some areas of zero scour (20–30% of monitors) and a few patches of deep scour (Haschenburger 1999).

The spatial distributions of bed shear stress and particle entrainability may explain these observations. Local bed shear stress tends to vary through a reach due to channel curvature and variable bed roughness and topography (Dietrich and Whiting 1989). Similarly, bed particle size distributions and structuring vary between locations in a reach, which results in areas of variable particle entrainability. These spatial patterns both create and are formed by channel morphology. Spatial variations in bed entrainability and shear stress produce spatially variable entrainment. Thus, as long as channel riffle–pool morphology is maintained, patchy spatial patterns of scour should be expected.

Implications for salmon mortality

The majority of salmonid lifetime mortality takes place during in-gravel stages of incubation. Egg to fry survival is typically estimated to be 10%, with values for chum in natural streams ranging from 0.7 to 85.9% in the studies summarized by Salo (1991). Scour of redds has been identified as a contributor to this mortality, but the relative importance of scour versus other factors, including superimpositioning of redds, burial, siltation, and poor water quality, is not very well known. Certainly, dominance of factors will vary from stream to stream. Previous investigators have found scour to be an important element in embryo mortality based on measurements of scour in spawning areas (e.g., Tripp and Poulin 1986; Lisle 1989), but their studies lacked direct measurement of egg pocket scour. The present study attempted to verify their conclusions by examining if scour in redds is similar to surrounding bed scour.

The evidence indicated that tailspills were more susceptible to scour than the surrounding bed, but egg pockets were not. The unconsolidated, elevated tailspill material was more

© 2000 NRC Canada

Fig. 8. Test of spatial autocorrelation. The correlation coefficient for scour monitor pairs is plotted versus the distance between the monitors. Scour data from the five flood periods up to February 15, 1998 were used to generate the correlation coefficient between monitor pairs.

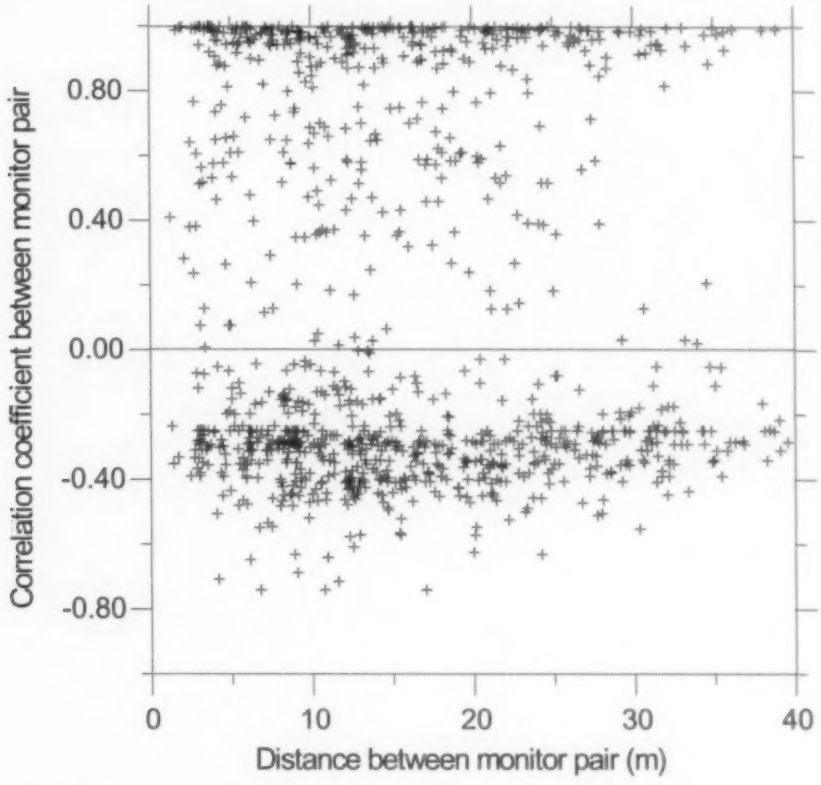

readily mobilized than the surrounding bed, yet the relatively well-constructed and coarser egg pocket material maintained a mobility similar to that of the surrounding bed. Investigators of scour in redds should be aware that, even if scour is observed at tailspills of redds, embryos in the relatively immobile egg pockets may not be exposed. In fact, if an investigator does not wish to install monitors in egg pockets for fear of disturbing embryos, scour in the immediately adjacent bed may be better than tailspill scour as an indication of scour in egg pockets. However, these conclusions are limited by the fact that, due to conservation concerns, only a small number of redds were observed in a single reach during a single flood season.

Furthermore, the mean scour depth was slightly less in egg pockets than in the adjacent bed, although the small sample size precluded a finding of significant difference. It is possible that embryos are protected from scour in the coarser, less erodible egg pocket. If so, scour may be less of a factor in incubation mortality than indicated by previous studies of scour in spawning areas that did not monitor egg pocket scour. Further, direct investigation of egg pocket scour is warranted.

In conclusion, based on this field study of a single reach over a single season, it appears that scour and fill are spatially oriented and depend on local factors such as debris, banks, and surface texture. However, despite the most spatially intensive monitoring to date, spatial autocorrelation of scour depths was not observed; thus, even more spatially intensive monitoring is necessary. Scour depths in the tailspills of redds were found to exceed significantly the scour depths in the spawning bed immediately adjacent to redds. There was no significant difference between scour depth in egg pockets versus that in the adjacent bed. Thus, it appears that developing embryos in the egg pockets of redds were no more susceptible to scour than the spawning bed itself.

Acknowledgements

This research was supported financially by the Natural Sciences and Engineering Research Council of Canada. We wish to thank Paul DeVries and Michael Church for advice regarding data collection methods. Dave Strajt provided many field hours of thoughts and labour. The manuscript was improved by suggestions from Paul DeVries, Chris Frissell, and an anonymous Associate Editor. Jennifer Shepherd drafted Fig. 1.

References

Andrews, E.D. 1984. Bed material entrainment and hydraulic ge-

© 2000 NRC Canada

ometry of gravel-bed rivers in Colorado. Geol. Soc. Am. Bull. **95**: 371–378.

Bagnold, R.A. 1966. An approach to the sediment transport problem from general physics. Physiographic and hydraulic studies of rivers. Geol. Surv. Prof. Pap. 422.1, United States Government Printing Office, Washington, D.C.

Bjornn, T.C., and Reiser, D.W. 1991. Habitat requirements of salmonids in streams. *In* Influences of forest and rangeland management on salmonid fishes and their habitats. *Edited by* W.R. Meehan. Am. Fish. Soc. Spec. Publ. No. 19. pp. 83–138.

Bray, D.I. 1979. Estimating average velocity in gravel-bed rivers. J. Hydraul. Eng., ASCE, **105**: 1103–1122.

Charlton, F.G., Brown, P.M., and Benson, R.W. 1978. The hydraulic geometry of some gravel rivers in Britain. Rep. IT 180, Hydr. Res. Stn., Wallingford, U.K.

Church, M.A., McLean, D.G., and Wolcott, J.F. 1987. River bed gravels: sampling and analysis. *In* Sediment transport in gravel-bed rivers. *Edited by* C.R. Thorne, J.C. Bathurst, and R.D. Hey. John Wiley & Sons Ltd., Chichester (West Sussex), U.K. pp. 43–79.

Cliff, A.D., and Ord, J.K. 1981. Spatial processes: models and applications. Pion Limited, London, U.K.

DeVries, P. 1997. Riverine salmonid egg burial depths: review of published data and implications for scour studies. Can. J. Fish. Aquat. Sci. **54**: 1685–1698.

Dietrich, W.E., and Whiting, P. 1989. Boundary shear stress and sediment transport in river meanders of sand and gravel. *In* River meandering. *Edited by* S. Ikeda and G. Parker. American Geophysical Union, Washington, D.C. pp. 1–50.

Goodchild, M.F. 1986. Spatial autocorrelation. CATMOG — Concepts and Techniques in Modern Geography No. 47. Institute of British Geographers. Geo Books, Norwich, U.K.

Haining, R. 1990. Spatial data analysis in the social and environmental sciences. Cambridge University Press, Cambridge, U.K.

Harrelson, C.C., Rawlins, C.L., and Potyondy, J.P. 1994. Stream channel reference sites: an illustrated guide to field technique. U.S. For. Serv. Gen. Tech. Rep. RM-245.

Haschenburger, J.K. 1996. Scour and fill in a gravel-bed channel: observations and stochastic models. Ph.D. thesis, Department of Geography, University of British Columbia, Vancouver, B.C.

Haschenburger, J.K. 1999. A probability model of scour and fill depths in gravel-bed channels. Water Resour. Res. **35**: 2857–2869.

Hassan, M.A. 1990. Scour, fill, and burial depth of coarse material in gravel bed streams. Earth Surf. Processes Landforms, **15**: 341–356.

Hassan, M.A., and Church, M. 1992. The movement of individual grains on the streambed. *In* Dynamics of gravel-bed rivers. *Edited by* P. Billi, R.D. Hey, C.R. Thorne, and P. Tacconi. John Wiley & Sons Ltd., Chichester, U.K. pp. 159–173.

Hey, R.D., and Thorne, C.R. 1986. Stable channels with mobile gravel beds. J. Hydraul. Eng., ASCE, **112**: 671–689.

Ikeda, S., Parker, G., and Kimura, Y. 1988. Stable width and depth of straight gravel rivers with heterogeneous bed materials. Water Resour. Res. **24**: 713–722.

Kinfu, Y., and Quick, M.C. 1998. Efficiency of bedload transport under non-uniform flow conditions. *In* Mountains to sea: human interaction with the hydrologic cycle. Proceedings of the 51st Annual Conference, Canadian Water Resources Association, June 10–12, 1998, Victoria, B.C. *Edited by* Y. Alila. Canadian Water Resources Association, Cambridge, Ont. pp. 320–325.

Lisle, T.E. 1989. Sediment transport and resulting deposition in spawning gravels, north coastal California. Water Resour. Res. **25**: 1303–1319.

Montgomery, D.R., Buffington, J.M., Peterson, N.P., Schuett-Hames, D., and Quinn, T.P. 1996. Stream-bed scour, egg burial depths, and the influence of salmonid spawning on bed surface mobility and embryo survival. Can. J. Fish. Aquat. Sci. **53**: 1061–1070.

Nawa, R.K., and Frissell, C.A. 1993. Measuring scour and fill of gravel streambeds with scour chains and sliding-bead monitors. N. Am. J. Fish. Manage. **13**: 634–639.

Orsborn, J.F., and Stephen C. Ralph Consultants. 1994. An aquatic resource assessment of the Dungeness River system. Phase II — physical channel analysis, hydrology and hydraulics. Phase III — fisheries habitat survey. Report prepared for the Jamestown S'Klallam Tribe, Sequim, Wash., and the Quilcene Ranger District Olympic National Forest, Quilcene, Wash. Available at RALPH.STEVE@EPAMAIL.EPA.GOV

Peterson, N.P., and Quinn, T.P. 1996. Persistence of egg pocket architecture in redds of chum salmon, *Oncorhynchus keta*. Environ. Biol. Fishes, **46**: 243–253.

Rennie, C.D. 1998. Bed mobility of gravel rivers: mobilization (scour) depth of chum salmon redds, and equilibrium bedload transport. M.A.Sc. thesis, Department of Civil Engineering, The University of British Columbia, Vancouver, B.C.

Salo, E.O. 1991. Life history of chum salmon (*Oncorhynchus keta*). *In* Pacific salmon life histories. *Edited by* C. Groot and L. Margolis. University of British Columbia Press, Vancouver, B.C. pp. 231–309.

Schuett-Hames, D.E. 1996. Patterns of scour and fill and their effects on salmonid incubation habitat in Kennedy Creek, a low gradient alluvial channel in Mason and Thurston counties, Washington. M.S. thesis, Evergreen State College, Olympia, Wash.

Tacconi, P., and Billi, P. 1987. Bed load transport measurements by the vortex-tube trap on Virginio Creek, Italy. *In* Sediment transport in gravel-bed rivers. *Edited by* C.R. Thorne, J.C. Bathurst, and R.D. Hey. John Wiley & Sons Ltd., Chichester, U.K. pp. 583–606.

Thibodeaux, L.J., and Boyle, J.D. 1987. Bedform-generated convective transport in bottom sediment. Nature (Lond.), **325**: 341–343.

Tripp, D.B., and Poulin, V.A. 1986. The effects of logging and mass wasting on salmonid spawning habitat in streams on the Queen Charlotte Islands. Report by V.A. Poulin & Associates for the B.C. Ministry of Forests and Lands. Land Manage. Rep. 50. B.C. Ministry of Forests and Lands, Vancouver, B.C.

Tripp, D.B., and Poulin, V.A. 1992. The effects of logging and mass wasting on juvenile salmonid populations in streams on the Queen Charlotte Islands. Report by V.A. Poulin & Associates for the B.C. Ministry of Forests. Land Manage. Rep. 80. B.C. Ministry of Forests, Victoria, B.C.

Wilcock, P.R., and McArdell, B.W. 1997. Partial transport of a sand/gravel sediment. Water Resour. Res. **33**: 235–245.

Wolman, M.G. 1954. A method of sampling coarse river-bed material. Trans. Am. Geophys. Union, **35**: 951–956.

Zar, J.H. 1996. Biostatistical analysis. 3rd ed. Prentice-Hall, Upper Saddle River, N.J.

© 2000 NRC Canada

Coho salmon (*Oncorhynchus kisutch*) transgenic for a growth hormone gene construct exhibit increased rates of muscle hyperplasia and detectable levels of differential gene expression

James A. Hill, Anders Kiessling, and Robert H. Devlin

Abstract: Transgenic coho salmon (*Oncorhynchus kisutch*) containing a growth hormone gene construct were compared with nontransgenic coho salmon in terms of gross anatomy, muscle cellularity, muscle enzyme activity, and differential gene expression. Transgenic fish were found to have significantly higher numbers of small-diameter muscle fibres in both the dorsal and lateral region of the somitic muscle, suggesting that they grow by greater rates of hyperplasia relative to slower growing nontransgenic fish. Higher levels of activity were found for phosphofructokinase and cytochrome oxidase in white muscle of the transgenic fish. This difference indicates a higher glycolytic and aerobic requirement in the muscle of transgenic fish. Subtractive hybridisation of muscle RNA of transgenic fish from control fish provided a library of cDNAs whose expression is upregulated in the transgenic fish. This library contains genes that may be involved in, or related to, both high growth rates and muscle hyperplasia. We have sequenced a number of fragments and have found a preponderance of myosin light chain 2 mRNAs, consistent with a putative high level of expression in the early stages of muscle fibre construction.

Résumé : On a comparé des saumons cohos (*Oncorhynchus kisutch*) transgéniques contenant un gène chimère d'hormone de croissance à des saumons cohos non transgéniques aux chapitres de l'anatomie générale, de la cellularité musculaire, de l'activité d'enzymes des muscles et de l'expression génique différentielle. On a observé que les poissons transgéniques renfermaient des quantités significativement supérieures de fibres musculaires de faible diamètre dans les régions dorsale et latérales du muscle somitique, ce qui indique que leur croissance est tributaire de taux d'hyperplasie plus élevés que chez les poissons non transgéniques à croissance plus lente. Les activités de la phosphofructokinase et de la cytochrome oxydase étaient plus élevées dans le muscle blanc des poissons transgéniques. Cette différence indique que le muscle des poissons transgéniques exige une glycolyse et une consommation d'oxygène plus intenses. Grâce à l'hybridation soustractive d'ARN musculaire des poissons transgéniques à partir du matériel de poissons témoins, on a obtenu une banque d'ADNc dont l'expression est régulée en amont chez les poissons transgéniques. Cette banque contient des gènes déterminant directement ou indirectement les taux de croissance élevés et l'hyperplasie musculaire. Nous avons séquencé certains fragments et observé une prépondérance d'ARNm de chaînes légères de myosine de type 2, ce qui va dans le sens de notre supposition selon laquelle il y aurait une forte expression dans les premiers stades de la construction des fibres musculaires.

[Traduit par la Rédaction]

Introduction

Muscle development and growth in vertebrates occurs by two fundamental growth processes: recruitment of new muscle fibres (hyperplasia) and increase in size of existing fibres (hypertrophy) (Goldspink 1972). In higher vertebrates, hyperplasia ceases shortly after birth (Goldspink 1972; Campion 1984) and postnatal growth continues by hypertrophy of already existing fibres (Goldspink 1972), making the number of fibres formed during embryosis one of the main factors determining postnatal growth dynamics of muscle in mammals. In teleosts, muscle hyperplasia may continue beyond embryogenesis (Greer-Walker 1970; Stickland 1983; Weatherley et al. 1988). This allows growth potential of muscle in fish to be affected postnatally, making growth dynamics of skeletal muscle of adult fish remarkably plastic compared with that of mammals and birds. Growth strategy (hypertrophy versus hyperplasia) has been shown to be influenced by both exogenous and endogenous factors (Carpene and Veggetti 1981; Weatherley and Gill 1982; Higgins and Thorpe 1990). There are also marked species differences in the contribution of hyperplastic and hypertrophic processes to muscle growth in fish. Weatherley et al. (1988) examined 10 different species of teleost fish and

Received September 24, 1998. Accepted October 13, 1999. J14794

J.A. Hill[1] **and A. Kiessling.**[2] Departments of Aquaculture and Food Science, Swedish University of Agricultural Sciences, 901 83 Umeå, Sweden.
R.H. Devlin. Fisheries and Oceans Canada, 4160 Marine Dr., West Vancouver, BC V7V 1N9, Canada.

[1]Current address: Institute of Molecular Agrobiology, 1, Research Link, National University of Singapore, Singapore 117604.
[2]Author to whom all correspondence should be sent at the following address: Matre Research Station, Institute of Marine Research, 5198 Matredal, Norway.

© 2000 NRC Canada

found that the largest and fastest growing species showed sustained recruitment of fibres to a large body size, in contrast with the slowest growing species, where cessation of recruitment led to slow growth and small size. Large variations in muscle fibre growth within populations of fish also occur in many fish species (Higgins and Thorpe 1990; Rowlerson et al. 1995). Weatherley and Gill (1982) demonstrated that fast-growing rainbow trout (*Oncorhynchus mykiss*) achieved a greater proportion of their growth by recruiting new fibres than did slow-growing fish. It therefore seems likely that high growth rates are linked to hyperplasia in postlarval muscle growth of fish.

Kiessling et al. (1991*a*) presented contradicting results in that the disappearance and appearance of small and large fibres in white muscle of rainbow trout (growth by hyperplasia) was related to body length independent of growth rate. However, in the study of Weatherley and Gill (1982), a much smaller size and growth range of the experimental fish and a shorter time period were used than in the study of Kiessling et al. (1991*a*). It is therefore possible that the importance of hyperplastic versus hypertrophic growth is different in growth spurts of more limited time periods compared with muscle growth over longer time periods.

Supplementation of growth hormone (GH) has been shown to promote hyerplastic growth in rainbow trout (Weatherley and Gill 1982) and common carp (*Cyprinis carpio*) (Fauconneau et al. 1996). However, the genetic control of fish muscle growth is poorly understood. For example, although muscle regulatory factors are known to transcribe contractile proteins (for a review, see Buckingham 1994), little is known about genes (or cellular factors) that influence the choice of muscle stem cells to form new fibres or to fuse with existing fibres.

White muscle in fish is composed of a mixture of small diameter fibres dispersed between large diameter fibres, giving the muscle a mosaic appearance (Greene 1913). The presence of small diameter fibres has been related to hyperplasia, and has been used as a method to identify continuing hyperplastic growth (Greer-Walker 1970; Weatherley et al. 1980; Stickland 1983). Strong indications exist suggesting that fibre size composition of muscle in fish is an important factor in flesh quality in terms of texture. In addition, other influences of accelerated growth on muscle, for example lipid deposition, enzyme titres and differential expression of structural protein isoforms may result in significant quality changes of farmed products (Johansson et al. 1995).

Transgenic coho salmon (*Oncorhynchus kisutch*) have been produced using the all-salmon GH/metallothionen (MT) gene construct (OnMTGH1) (Devlin et al. 1994). These fish are extremely fast growing relative to controls, averaging a size more than 11-fold larger than that of controls by the age of 15 months (Devlin et al. 1994). In swimming stamina tests (U_{crit} swimming test in a standard Brett-type swimming tunnel), transgenic fish showed a significantly lower performance compared with control fish (Farrell et al. 1997), suggesting that there may be a number of important biochemical and structural differences in the transgenic fish muscle. The extent to which transgenic fish provide a model for the study of fast growth has not been established.

In this paper, we present a study of muscle cellularity analysis of growth-enhanced transgenic coho salmon relative to older controls of the same size. The aim was to establish whether there was an increase in hyperplasia under the influence of the transgene. A number of other comparative techniques were also used to examine other factors that might be altered. These included enzyme substrate assays and differential gene transcription through production of a subtracted library of cDNAs. In order to produce such a library, we have employed the technique of subtractive hybridisation. This technique reveals the difference in expression between transgenic versus nontransgenic fish of all activated genes. The advantage of such an approach is that unexpected differences are revealed, giving much better coverage of the true effect of the insertion of a gene complex that leads to major differences in growth rate. This differs markedly from earlier work where only expected effects have been monitored, as the technique to monitor gene or protein expression by an untargeted approach has been lacking. This study therefore provides a unique comparison with earlier studies of fish in which high growth rate was stimulated through other factors, e.g., environmental or physiological. The data presented in this paper will also provide a starting point for the use of transgenic coho salmon as an experimental model in studies of fish growth and development and the effects of rapid growth on farmed fish products.

Methods

Fish

Transgenic coho salmon were produced using a strain derived from the Chehalis River in southwestern British Columbia, Canada. The F_2 progeny were generated by mating a single F_1 transgenic male with wild Chehalis River females to yield both control animals and their heterozygous transgenic siblings. The animals utilised in this study contained the GH gene construct OnMTGH1, which we have previously shown results in approximately an 11-fold increase in size in the first year of growth (Devlin et al. 1994). Animals were reared in 10°C freshwater until sampling. Alevins and fry were determined to be transgenic or control using the polymerase chain reaction (PCR), similar to that described in Devlin et al. (1995): DNA was extracted from a small piece of fin tissue and subjected to PCR using primers MT-1 (5′-CTGATTAAGTTTTGTATAGT-3′) and GH-19 (5′-GTTAAATTGTATTAAATGGT-3′).

Transgenic and nontransgenic fish were reared according to Devlin et al. (1995). In brief, this comprised indoor flow-through 200-L glassfibre aquaria supplied with fresh well water (10 ± 1°C) under simulated natural light conditions. Fish were fed ad libatum with a standard commercial feed (Moore-Clarke Ltd., Vancouver, B.C.).

The control fish used in this experiment were offspring of the same family of transgene-carrying fish spawned 1 year earlier. Both groups of fish were sampled on the same day at an approximate fork length of 10 mm. At this length, control fish were aged 14 months post-first-feeding and transgenic fish were aged 2 months post-first-feeding. At present, coho salmon made transgenic with an inactive form of the construct are not available; such fish will, in the future, provide an additional control for comparative experiments analysing transgenic fish, although differences in age will remain an experimental artifact.

Sampling

Fish were sampled by netting and sedated by submersion into water containing 5 ppm Marinil® (metomidate hydrochloride) (Syndel Laboratories, Vancouver, B.C.). The fish were killed by decapitation and two cross sections were immediately cut, one an-

© 2000 NRC Canada

terior to the dorsal fin and one anterior to the adipose fin of the whole fish (Fig. 1). These cross sections were photographed together with a ruler, allowing measurement of whole-body and whole-muscle morphometrics by computerised digitising techniques (Kiessling et al. 1991*a*). Muscle blocks for fibre measurements were cut from the most rostral of these cross sections. Two blocks of tissue were obtained, one just dorsal to the lateral line region containing mediolateral white (MLW) and red muscle (MLR) and the second from the dorsal part of the epaxial muscle denoted dorsolateral white (DLW) (Fig. 1). The muscle block was mounted in Tissue Tek® (Miles Laboratories Inc., Elkhart, Ind.), frozen in isopentane, and cooled to its freezing point in liquid nitrogen. Samples were then packed and stored in liquid nitrogen after a maximum delay of 5 min after decapitation. Concurrently (<1 min after decapitation), muscle samples for measurement of enzymatic activity and purification of total RNA were removed anterior to the rostral chop (Fig. 1). Samples for enzymatic activity were wrapped in aluminium foil and immediately frozen in liquid nitrogen, while samples for RNA were stabilised in guanidine thiocyanate buffer (4 M guanidine thiocyanate, 25 mM sodium citrate, pH 7.0, 0.5% sarcosyl, 0.1 M 2-mercaptoethanol (Chomczynski and Sacchi 1987)) before freezing in liquid nitrogen. All samples were then stored at –80°C until analyses.

Enzymatic and histochemical analysis

The activity of the three enzymes studied were measured as described in Shonk and Boxer (1964) for phosphofructokinase (PFK, EC 2.7.1.11, indicative of glycolysis), in Bass et al. (1969) for 3-hydroxyacyl-CoA dehydrogenase (HAD, EC 1.1.1.35, indicative of fat oxidation), and in Whereat et al. (1969) for cytochrome oxidase (Cytox, EC 1.9.3.1, indicative of aerobic ATP formation). For enzyme activity determinations, muscle samples (100 mg) were homogenised in an ice-cold, all-glass Potter–Elvehjem homogenise, and the crude homogenate was incubated at 15°C as described in Kiessling and Kiessling (1984). The activity, measured on frozen samples, was converted to fresh tissue values by multiplying by the following factors: 1.0 for PFK, 2.9 for HAD, and 0.6 for Cytox (Kiessling et al. 1990).

Muscle samples were sectioned into slices (10 μm) and stained with acid–Schiff reagent for glycogen and NADH dehydrogenase activity (Novikoff et al. 1961). These two stains were chosen because they produce the overall best results in red and white muscle, respectively (Kiessling et al. 1990).

Statistical evaluation

An analysis of variance model was used where anatomical measurements, mean muscle fibre cross-sectional area, theoretical fibre numbers, and enzyme activities were dependent variables and transgenesis was the fixed factor. Extended models (i.e., analyses of covariance models) were carried out with the above-mentioned factors and two continuous variables, body weight and fork length, as covariates. The purpose of these models was to correct the comparisons between factor levels for differences in the continuous variables.

Muscle fibre frequency distribution was compared by paired *t* test (including the following size-classes: DLW, 200 to +4400 μm^2; MLW, 200 to 1300 μm^2; MLW, 1300 to +4400 μm^2; MLR, 500 to +4400 μm^2). This test was used because white muscle fibre size has a skewed distribution, making a comparison by variance doubtful. Further, if the paired *t* test revealed a significant difference, the means of single size-classes were also tested by variance.

The statistical calculations were processed by the statistical program package SAS (version 6.12 for PC-DOS, GLM procedure). All tests were two-tailed. In white muscle, 400 fibres were measured per sample site and fish. In samples of red muscle, 300 fibres were measured. A total of 1100 fibres were counted per fish.

Fig. 1. Graphic of coho salmon sampling sites. "A" represents the dorsolateral sampling area at which white muscle fibres were measured, and "B" represents the mediolateral sampling area at which both red and white muscle fibres were measured. Other samples were taken as indicated by the labels (not to scale).

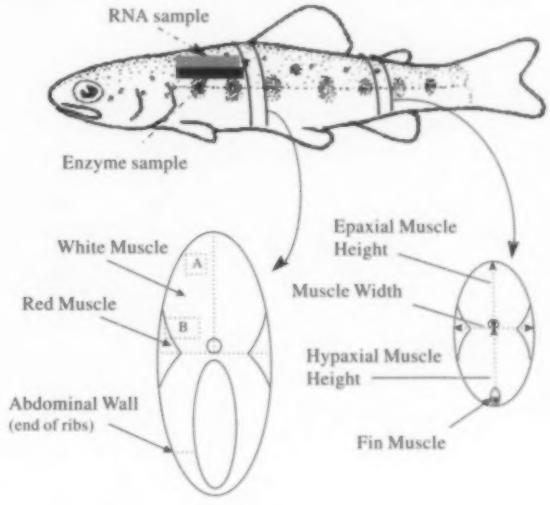

Subtractive hybridisation

Total RNA was isolated from muscle samples from the dorsal proliferative zone of GH-transgenic and nontransgenic coho salmon according to the method of Chomczynski and Sacchi (1987). Samples (approximately 1 g each) from three individual fish were pooled separately for transgenic and nontransgenic (wild type) and homogenised in 400 μL guanidine thiocyanate buffer·g^{-1} followed by the addition of 30 μL of 2 M sodium acetate (pH 4.5). RNA was extracted twice with one volume of water-saturated phenol (pH5.5) – chloroform – isoamyl alcohol (25:24:1) and precipitated with one volume of isopropanol. After centrifugation, the pellet was washed with one volume of 96% ethanol, dried, and redissolved in 50 μL of distilled water. One microlitre of each was run on an agarose gel and the samples were observed to contain approximately the same amount of total RNA at a concentration of about 1 mg·mL^{-1}.

cDNA synthesis was performed on 1 μL (approximately 1 μg) of the total RNA solution for transgenic and wild type using the Clontech SMART™ cDNA Synthesis Kit (Chenchik et al. 1996), which enables proportionate amplification of full-length cDNA during the exponential phase of a PCR. First-strand cDNA was produced in a 10-μL reaction (50 mM Tris–HCl (pH 8.3), 75 mM KCl, 6 mM $MgCl_2$, 1 μM cDNA synthesis primer, 1 μM SMART™ II oligonucleotide, 2 mM DTT, 1 mM dNTP, 20 units of Superscript™ II reverse transcriptase (Gibco BRL)), 1 h, 42°C. This was diluted with 40 μL of 10 mM Tris – 1 mM EDTA buffer (pH 7.6). Two microlitres of each was amplified in a 200-μL reaction volume (40 mM tricine–KOH (pH 9.2), 15 mM KOAc, 3.5 mM $Mg(OAc)_2$, 75 μg bovine serum albumen·mL^{-1}, 200 μM dNTP, 200 nM PCR primer, 1× Advantage Klentaq Polymerase mix) with the following program: 95°C for 1 min and 21 cycles of 95°C for 15 s, 65°C for 30 s, and 68°C for 6 min. The PCR product was extracted once with Tris (pH 7.6) saturated phenol – chloroform – isoamyl alcohol (25:24:1) and once with chlorofrom – isoamyl alcohol (24:1), precipitated, and redissolved in water. The cDNA was digested overnight with *Rsa*I in the appropriate buffer at 37°C. The digested

© 2000 NRC Canada

cDNA was extracted as before, precipitated, and redissolved in 5.5 μL of distilled water.

The digested transgenic cDNA was divided into two samples (2 μL), TG1 and TG2, and each ligated to a different adapter (adapters 1 and 2, respectively, from the Clontech PCR-select cDNA subtraction kit) in a 10-μL reaction volume (400 units of T4 DNA ligase, 1× standard ligation buffer, appropriate adapter at 1 μM) and incubated at 16°C overnight. The reaction was stopped with 1 μL of 0.2 M EDTA and 1 mg glycogen mix·mL^{-1} and heated to 72°C for 5 min to inactivate the ligase. One microlitre was removed from each reaction for use as an unsubtracted control for PCR.

TG1 and TG2 were separately hybridised to digested wild-type cDNA (denatured at 98°C for 1.5 min, hybridised at 68°C for 8 h in 1× hybridisation buffer supplied with the Clontech kit); the two reactions were then mixed and treated to additional hybridisation in the presence of fresh denatured digested wild-type cDNA and hybridised overnight at 68°C (Diatchenko et al. 1996). The hybridisation reactions were diluted with 200 μL of dilution buffer (20 mM HEPES–HCl (pH 8.3), 50 mM NaCl, 0.2 mM EDTA (pH 8.0)).

Subtracted cDNAs in the hybridisation reactions were then amplified along with the unsubtracted adapter ligated transgenic cDNA with two rounds of PCR. PCR reaction conditions were as before; the first round used a general primer with priming sites present in both adaptors and the following cycling parameters: 75°C for 5 min and 27 cycles of 94°C for 30 s, 66°C for 30 s, and 72°C for 1.5 min. One microlitre from the first PCR was diluted 1:1000 in the second PCR reaction mixture (components as before, except primers) with 400 nM of each of nested primer 1 (priming site built into adapter 1) and nested primer 2 (priming site built into adapter 2). The product of this PCR was analysed on a 2.0% agarose gel in 1× TAE buffer. In addition, a control reaction was run using human skeletal muscle total RNA, half of which was mixed with *Hae*III digested ΦX174 DNA prior to adapter ligation; after the control subtraction, only the *Hae*III-digested bands were present in the sample, indicating a good subtraction. The transgenic subtracted PCR amplification (2 μL) was ligated to a pT-Adv cloning vector (Clontech) in a 10-μL reaction volume (1× standard ligation buffer; 4 units of T4 DNA ligase, 50 ng of pT-Adv vector) overnight at 14°C. Competent cells (TOP10F' *Escherichia coli*) were transformed with 5 μL of the ligation reaction in the presence of 20 mM β-mercaptoethanol. The transforming cells were taken through the following temperature regime: ice for 30 min, 42°C for 30 s, and ice for 2 min. SOC (250 μL, 2% tryptone, 0.5% yeast extract, 10 mM NaCl, 2.5 mM KCl, 10 mM $MgCl_2$, 10 mM $MgSO_4$, 20 mM glucose) was added and the cells incubated at 37°C for 1 h. Fifty and 200 μL were plated onto LB agar white/blue selection plates (1% tryptone, 0.5% yeast extract, 1.0% NaCl, 1.5% agar, 50 μg ampicillin·mL^{-1}, 0.2 mg X-gal·mL^{-1}, 4 mM IPTG) and incubated overnight. Plate 1 (infected with 50 μL of cells) contained 84 positive colonies and plate 2 (infected with 200 μL of transformed cells) contained >200 positive colonies. Each colony from plate 1 was picked with a sterile cocktail stick and used to infect 2.5 mL of LB broth (1% tryptone, 0.5% yeast extract, 1.0% NaCl) containing 50 μg ampicillin·mL^{-1}, grown overnight at 37°C with shaking (200 rpm), and vector DNA purified by lysing with alkaline and centrifuging at 14 000 rpm in a bench-top microcentrifuge. The supernatant was extracted once with phenol – chloroform – isoamyl alcohol (25:24:1), precipitated in ethanol, air dried, and redissolved in 50 μL of water containing DNase-free RNase.

Dot blots

To test subtraction, 2 μL of each miniprep was denatured in a reaction volume of 250 μL (1 M NaCl, 10 mM EDTA) and was arrayed on a Hybond N+ nylon filter (Amersham). Each blot was rinsed with 0.4 M NaOH, and the filter was rinsed in 2× SSC and air dried. Three such dot blots were tested with probes produced from GH-transgenic muscle total cDNA and nontransgenic muscle total cDNA. Template cDNA (1 μg, transgenic, wild type) was added to 4 μL of DIG High Prime (Boehringer Mannheim) in a 20-μL total reaction volume and incubated overnight at 37°C. Concentration of each probe was determined using DNA standards on test strips (Boehringer Mannheim). The membranes were incubated in hybridisation buffer (5× SSC, 0.1% *N*-laurosarcosinate, 0.02% SDS, 1% blocking reagent (Boehringer Mannheim)) for 30 min at 68°C. The respective DIG-labelled probes were denatured by boiling for 5 min diluted in preheated hybridisation buffer (2 μL of probe in 20 mL of hybridisation buffer). The prehybridisation solution was replaced with hybridisation buffer containing probe, and the filters were incubated overnight at 68°C. The membranes were then washed twice for 5 min in 2× SSC, 0.1% SDS at room temperature and twice for 15 min in 0.5× SSC, 0.1%SDS at 68°C. The filters were washed for 2 min in wash buffer (maleic acid buffer (0.1 M maleic acid, 0.15 M NaCl (pH 7.5), 0.3% Tween 20)), 30 min in blocking solution (1× blocking reagent in maleic acid buffer), 30 min in blocking solution containing 1 : 20 000 anti-DIG-alkaline phosphatase conjugate antibody, twice for 15 min in wash buffer, 2 min in detection buffer (0.1 M Tris–HCl, 0.1 M NaCl (pH 9.5)), and 5 min in CSPD (Boehringer Mannheim), incubated at 37°C for 10 min, and exposed to X-ray film for 10 s. The X-ray film was developed using standard photographic chemicals and rephotographed onto black and white Polaroid film.

Sequencing

Each clone was sequenced by dye terminator cycle sequencing (Lee et al. 1992; Prober et al. 1992) using the Thermo Sequenase (Amersham) premix, 2 μL (0.4 μg) of the appropriate miniprep, and nested primer 1 (0.5 μM) from adapter 1 of the subtractive hybridisation kit in a 20-μL reaction volume. Thermal cycling parameters were as follows: 96°C for 1 min followed by 28 cycles of 96°C for 30 s, 45°C for 15 s, and 60°C for 4 min. The reaction was then precipitated in 70% ethanol in the presence of 2 M ammonium acetate, redissolved in loading dye, and run on an ABI Prism 377 sequencer according to the manufacturer's instructions.

Results

General characterisation of transgenic coho salmon

Controls (1994 nontransgenic fish) and the transgenic fish (of the 1995 year-class) were not significantly different in size when comparing fork length, body weight, condition factor, or slaughter yield (carcass weight percentage) (Table 1). However, significant differences were found in the body conformation variables abdominal wall thickness, area of total chop, muscle width, and muscle height (shown indirectly by the quota of width/height) (Table 1).

Muscle frequency distribution

Muscle fibre average cross-sectional area differed significantly between transgenic and nontransgenic fish in the two white muscle sample sites (Table 2). No difference in mean fibre size was evident in red muscle, even though an increase in variation of fibre sizes (occurrence of larger fibres in transgenic fish, $p < 0.0027$) (Fig. 2) was observed. This difference was abolished by including body weight in the model. In white muscle, body size, described by body weight (BW) and fork length (FL), asserted no significant effect on either average cross-sectional area or fibre size distribution (DLW: BW, $p < 0.26$; FL, $p < 0.28$; MLW: BW, $p <$

© 2000 NRC Canada

Table 1. Anatomical measurements of transgenic and nontransgenic control coho salmon.

	Transgenic group	Control group	p
Body weight (BW, g)	8.9±0.6	9.6±0.5	<0.447
Carcass weight (% of BW)	79±1.0	88.0±0.6	<0.060
Fork length (FL, mm)	9.5±0.2	9.8±0.2	<0.395
Condition factor	1.02±0.04	1.03±0.04	<0.5
Abdominal wall (AW, mm)	0.57±0.04	1.13±0.04	<0.0001*
AW/FL (%)	0.60±0.05	1.16±0.05	<0.0001*
Chop anterior (mm^2)	76.8±3.9	101.5±5.2	<0.0001*
Chop posterior (mm^2)	36.8±2.1	43.6±1.4	<0.01*
Height epaxial anterior (mm)	6.4±0.40	7.08±0.20	<0.14
Height epaxial posterior (mm)	4.9±0.16	5.04±0.20	<0.57
Width/FL anterior (%)	9.3±0.28	10.2±0.34	<0.0001*
Width/FL posterior (%)	5.3±0.27	5.49±0.14	<0.45
Width/height anterior (%)	1.42±0.10	1.40±0.01	<0.83
Width/height posterior (%)	1.02±0.05	1.07±0.04	<0.51
Red muscle anterior (%)	1.61±0.16	0.96±0.16	<0.007*
Red muscle posterior (%)	1.98±0.20	0.97±0.22	<0.002*

Note: The majority of anatomical measurements were not significantly different between transgenic and nontransgenic control fish. The fish from each group were of similar weight and length (top section, whole-body measurements). Among the anatomical measurements taken (lower section, see Fig. 1), abdominal wall thickness, cross-sectional area, and the percentage of red muscle showed significant differences (*$p < 0.05$, errors are standard errors).

Table 2. Mean muscle fibre cross-sectional area in transgenic and nontransgenic control coho salmon.

	Transgenic group	Control group	p
DLW (μm^2)	735±61	1645±5 ($n = 5$)	<0.0001*
MLW (μm^2)	1267±112	1941±155 ($n = 5$)	<0.006*
MLR (μm^2)	771±115	953±142 ($n = 3$)	<0.364

Note: In white fibre, but not in red fibre, transgenic fish have significantly smaller fibres (*$p < 0.05$, errors are standard errors).

0.60; FL, $p < 0.94$). On the contrary, a strong effect of body weight was observed for both average red muscle fibre cross-sectional area and fibre size distribution (MLR: BW, $p < 0.001$; FL, $p < 0.45$).

Comparing fibre size distribution (Fig. 2) with a paired t test indicated a significant difference in sizes-classes of DLW (size classes >200 μm^2, $p < 0.04$) and of MLW (size-class <1.300 μm^2, $p < 0.048$; size-class >1.300 μm^2, $p < 0.036$) but not of MLR (size-class >500 μm^2, $p < 0.17$). Comparing variance in individual size-classes indicated a significant difference between DLW (size-class 0–200 μm^2, $p < 0.0025$ with 42.1 ± 4.9 and 10.9 ± 2.4 of transgenic and nontransgenic fish, respectively) and MLW (size-class 0–500 μm^2, $p < 0.0071$ with 68.0 ± 3.7 and 45 ± 4.0% of transgenic and nontransgenic fish, respectively). A corresponding comparison between size-class 0–500 μm^2 in MLR yielded no significant difference ($p < 0.97$) with an average of 36.8 ± 10.3 and 36.0 ± 11.5% of transgenic and nontransgenic fish, respectively. Body size did not seem to influence this variable (BW, $p < 0.91$; FL, $p < 0.68$).

Comparison of average fibre size in the smallest size class (0–200 μm^2) yielded a significant difference in this class of DLW (transgenic fish, 126 ± 2.3 μm^2; nontransgenic fish, 186 ± 4.0 μm^2 ($p < 0.0001$)), while no such differences were observed in any other sample site (MLW: transgenic fish, 170 ± 4 μm^2; nontransgenic fish, 176 ± 8 μm^2 ($p < 0.83$); MLR: transgenic fish, 167 ± 6 μm^2; nontransgenic fish, 170 ± 9 μm^2 ($p < 0.80$)).

Analysis of muscle structure

Comparing the relative composition of white versus red muscle in the total cross section of the fish revealed highly significant differences. Transgenic fish had more red muscle than the nontransgenic controls (Table 1). This difference in total amount of red muscle was most prominent in the caudal region.

The anatomical positions of muscle blocks taken for fibre area measurements within the white muscle (Fig. 1) represent zones of prolific growth in growing adult fish, established by traditional histological techniques in a number of species (Kiessling et al. 1990, 1991*a*, 1993). DLW and MLW fibres were both significantly smaller than controls on the basis of mean fibre area (Table 2); however, in an analysis of the difference in the distribution curve of fibre size, only the fibre frequency pattern from DLW fibres was significantly different (Figs. 2 and 3). This is consistent with previous observations that the distribution curve of fibre size in the mediolateral muscle reflects a more prominent hypertrophic growth (Kiessling et al. 1990, 1991*a*), indicating lower recruitment of small fibres and an increase in fibres in larger size groups. Average fibre size and size distribution of the MLR did not show any significant difference between transgenic fish and controls.

Enzyme analysis

Of the three enzymes analysed during the study, PFK and Cytox were significantly higher in activity in the transgenic fish (Table 3). PFK levels were approximately fourfold higher, while Cytox levels were increased by approximately 20%. No difference was found in activity of the third investi-

© 2000 NRC Canada

Fig. 2. Distribution of fibre cross-sectional area transgenic coho salmon (solid bars) and nontransgenic control coho salmon (open bars). (A) DLW muscle in transgenic fish has a greater number of small fibres than that in control fish (paired t test comparison of distribution, $p < 0.0064$ by variation in standard error). (B) MLW muscle also has a higher number of small fibres in transgenic fish than in the control group ($p < 0.0009$ by variation in standard error). (C) MLR fibres from transgenic fish show more similarity in distribution but are significantly different by variation in standard error ($p < 0.0027$).

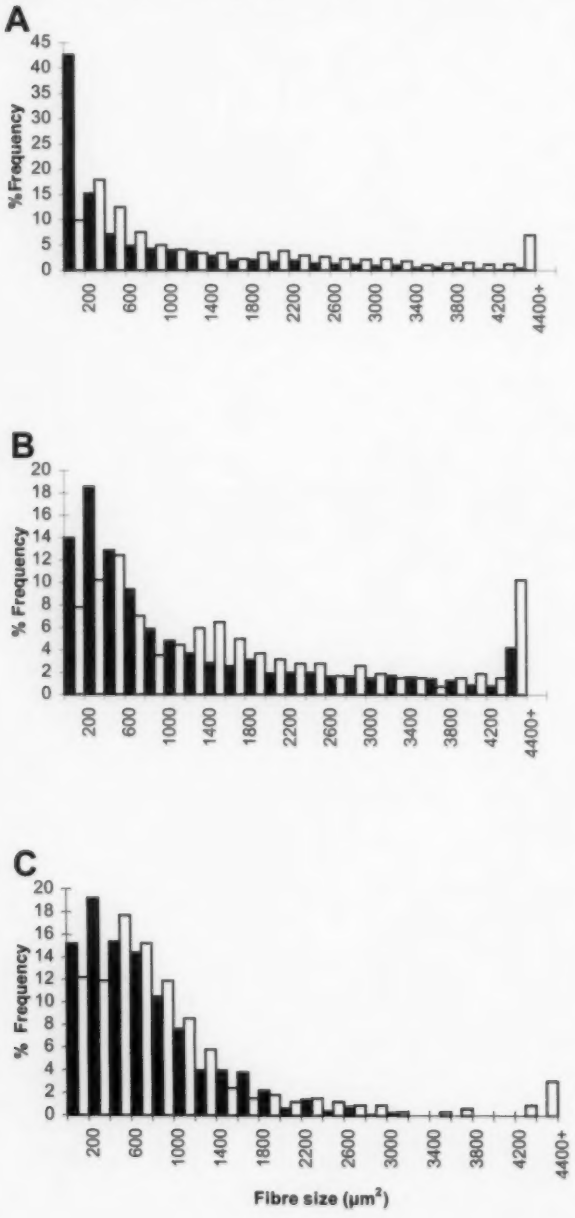

gated enzyme, HAD, between transgenic and nontransgenic fish.

Differential expression of myosin light chain 2 (MLC2) in GH-transgenic coho salmon

Differences in gene expression were detectable between the transgenic fish and the controls using subtractive hybridisation. A number of cDNA clones isolated from the subtracted cDNA (Fig. 4A) library are differentially expressed when tested with probes generated from total cDNA from nontransgenic (Fig. 4B) or transgenic (Fig. 4C) coho salmon. This analysis was repeated several times with different concentrations of probe and different exposures to X-ray sensitive film. Results were consistent throughout, and all clones (with the exception of the negative control) were found to hybridise to both probes (results not shown). All of the differences in expression indicated higher expression in transgenic fish than in nontransgenic fish. No differences were observed when the two probes were hybridised against cDNA pools of transgenic and nontransgenic coho salmon. A negative control of a miniprep containing no insert was negative to both probes.

A number of these clones were sequenced, and several cDNAs with high homology to vertebrate MLC2 were identified along with a number of others (summarised in Table 4). Two different-sized fragments were identified that resulted from the *Rsa*I digestion of the initial cDNA pool, and we were able to identify the ends of each fragment, allowing us to construct a single continuous cDNA fragment. The combined cDNA fragment of 683 base pairs aligns with zebrafish (*Danio rerio*) MLC2 (Xu et al. 1998) mRNA with a homology of 88% for a region of 528 base pairs, which includes the entire coding region (Fig. 5A), and a homology of 89% at the amino acid level (Fig. 5B). The only major difference between the two proteins appears to be the insertion of a glycine at position 16 on the chain.

Discussion

In this experiment, we tested the effect of growth rate on muscle tissue by measuring muscle architecture and the titres of three important muscle enzymes. We have also isolated a number of genes by subtractive hybridisation that are more highly expressed in the transgenic fish. There are a number of points that must be remembered during discussion of these results. Firstly, we have no evidence that the muscle architecture observed in transgenic fish is causal to fast growth rates or growth efficiency but only that fibre distribution changes fast-growing transgenic fish. Secondly, we have no way to assess whether the differences seen between slow-growing nontransgenic fish and fast-growing transgenic fish are a result of growth rate or are a direct result of high levels or ectopic expression of the transgene. Also, this paper addresses changes in muscle under the influence of the GH transgene; no attempt has been made to address the effects on other tissues that are also an important component of whole-body growth.

Observations in rainbow trout suggest that submaximal growth is not expressed as more large and fewer small fibres when compared with maximally growing fish. In fact, an identical fibre distribution was found in fish of the same

© 2000 NRC Canada

Fig. 3. Cross-sectional view of muscle fibres from the DLW sampling site in (A) nontransgenic control coho salmon clearly showing that muscle fibres are larger than those in (B) transgenic coho salmon. M indicates a muscle fibre and the fibre boundary is indicated by arrowheads. Magnification 1075×.

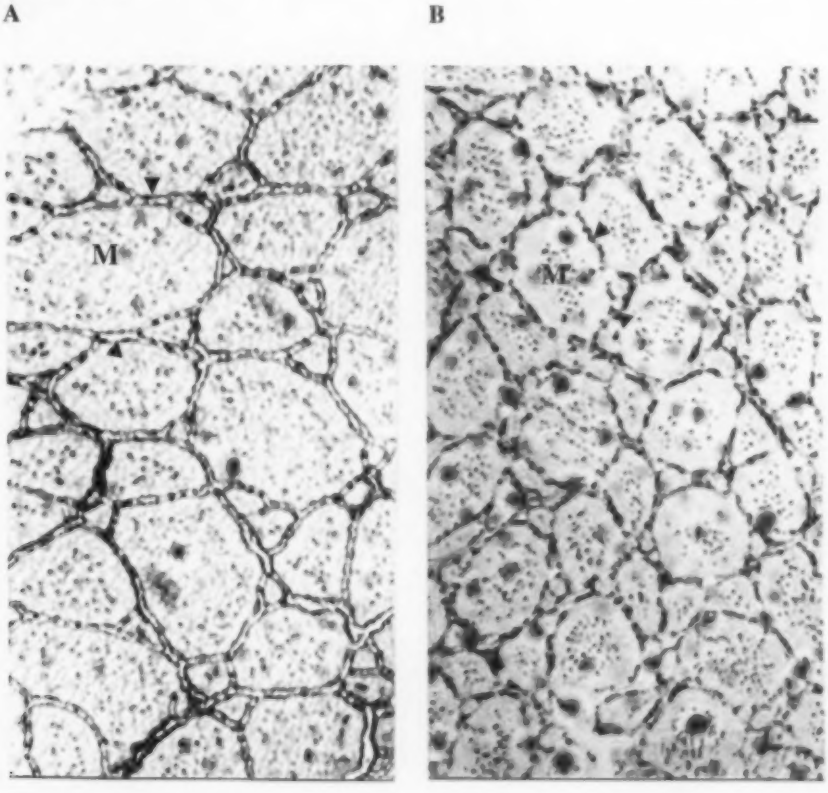

Table 3. Enzyme analysis of transgenic and nontransgenic control coho salmon muscle.

Enzyme ($\mu mol \cdot g^{-1} \cdot min^{-1}$)	Transgenic	Control	p
PFK	9.33 ±2.23	2.49±0.58	<0.014*
HAD	4.08±1.11	4.30±0.85	<0.879
Cytox	7.22±0.55 (n = 5)	5.53±0.49	<0.047*

Note: Transgenic fish muscle has significantly higher activity levels of PFK and Cytox (*p < 0.05, errors are standard errors).

weight but of widely different age (Kiessling et al. 1991*a*). However, the latter study was conducted over a much longer time period with larger sampling intervals. A possibility therefore exists that rapid muscle growth supported by hyperplasia is limited in time and its contribution to growth is replaced by hypertrophy when measured over longer time periods. This cyclic growth pattern is supported by our own observations (Kiessling et al. 1991*a*), with a "burst" of small fibre production occurring in large fish but only during the autumn. The same phenomenon with small fibres occurring only during autumn was reported by Carpene et al. (1982) in mullet.

Transgenic fish have a greater percentage population of small white fibres compared with large white fibres (fibre area <200 mm^2 = 42% of the total fibres compared with 22% for the controls) (Fig. 2), and the anatomical region with the greatest difference is the dorsolateral area (Fig. 3). This was most prominent, not only as a larger difference in mean average cross-sectional area, but also as a more marked difference in number of small fibres in the smallest size-class (Figs. 2 and 3) and the mean average size of the fibres within this smallest size-class. Not only are many more small fibres found in DLW of transgenic fish, but the average size of these fibres is significantly smaller. This has been shown to be the major area of new fibre production in a number of teleost species (see Kiessling et al. 1990, 1991*a*, 1993). These observations are consistent with those of (Weatherley and Gill (1982) and Fauconneau et al. (1996), which show that exogenous GH induces hyperplasia in fish muscles. It is therefore possible that the constant and elevated level of GH in the transgenic fish replaces a cyclic shift between which growth type, hypertrophy or hyperplasia, dominates. In transgenic fish, hyperplastic growth may dominate constantly.

We observed no effect of body size on either white muscle mean cross-sectional area or fibre distribution within the size range used in this study. This tallies well with earlier published data on rainbow trout (Kiessling et al. 1991*a*). Further, in the same study, red muscle fibre cross-sectional area was found to relate more to growth rate (measured as feed level) than to attained body size. Our data agree with this

© 2000 NRC Canada

Fig. 4. (A) A 1.2% agarose gel electrophoresis of the result of the subtractive hybridisation. Lane 1, ΦX174 *Hae*III digest DNA marker (603 base pair band indicated); lane 2, subtracted control human skeletal muscle cDNA showing amplification of ΦX174 *Hae*III digest DNA bands, which are slightly longer than the marker lane due to the ligation of adapters during the experiment; lane 3, unsubtracted control human skeletal muscle cDNA with little amplification of specific bands; lanes 4 and 6, independent duplicate subtracted coho salmon muscle cDNA; amplified bands are differentially expressed cDNA in the transgenic fish; lanes 5 and 7, independent duplicated unsubtracted cDNA from coho salmon muscle showing additional bands that are subtracted out by the experiment. (B) Dot blot of 44 minipreps from the subtracted library probed with wild-type cDNA probe. Minipreps containing MLC2 identified by sequencing are circled. Also shown are the negative control (within a square), transgenic cDNA (underlined in black), and wild-type cDNA (underlined in white). (C) Dot blot identical to that in Fig. 4B probed with transgenic cDNA probe. Note that the majority of the minipreps are differentially expressed in the two cDNA populations and that this is true for all of the MLC2 clones.

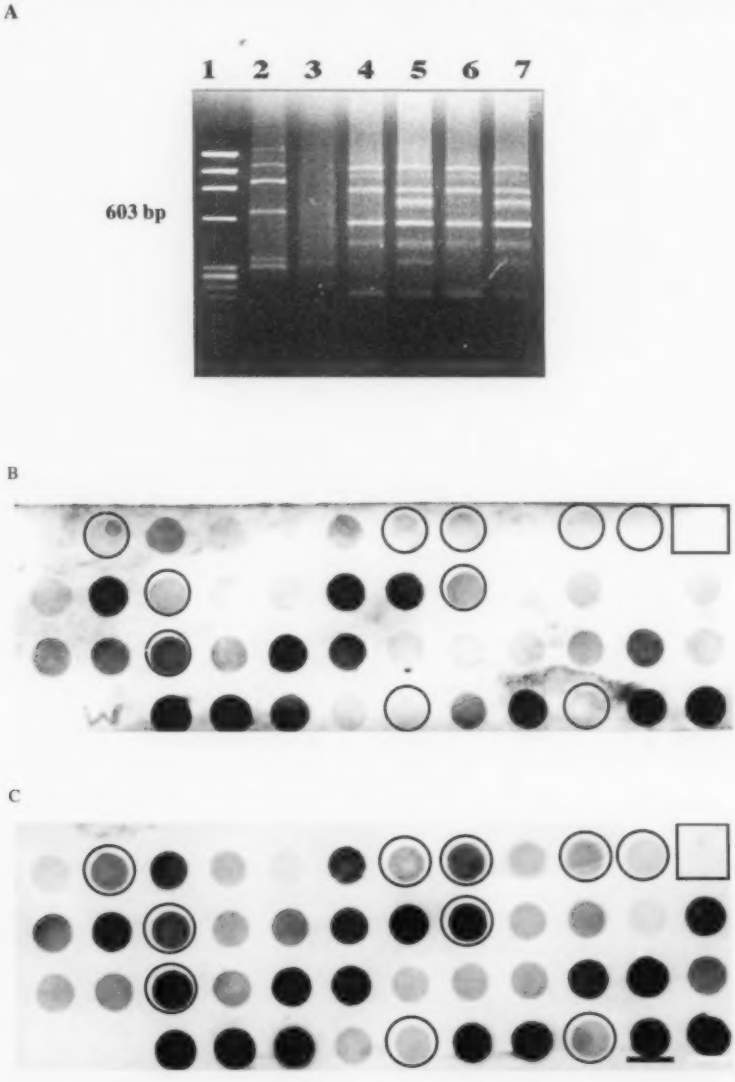

observation in that only in red muscle was any significant relationship found between muscle fibres and body size, indicating that growth of red muscle fibres by hyperplasia or hypertrophy is more plastic than in white muscle, at least during earlier life stages.

The most prominent difference in body conformation between transgenic and nontransgenic fish is a leaner body in relation to fork length of the transgenic fish. Also the abdominal wall of the transgenic fish is much thinner, again indicating a less stout body conformation. Whether this difference is a result of altered growth rates between muscle and other tissues such as skeleton or whether it is caused by a shift in muscle growth between hyperplasia and hypertrophy cannot be deduced from these data. What is apparent is

© 2000 NRC Canada

Table 4. Identified genes from the subtracted library.

cDNA fragment similar to:	Homology	NCBI database accession No.	Comment
MLC2	Significant	AF251130	High representation, two fragments
Parvalbumin-β	Significant	—	High representation, two fragments
Skeletal α-actin	Significant	—	
Myosin heavy chain	Significant	—	
Ribosomal protein S17	Significant	—	
Nucleolar protein B23	Significant	—	
tRNA	Significant	—	
Plasmodium gene		—	Possible parasite?
Hs myoblast KIAA0005		—	Similar to human myoblast gene

Note: Genes were assessed for significant homology using online BLAST database homology searching (see Altschul et al. 1990).

that a much higher total number of fibres in the anterior region (Table 1) still results in a reduced total cross section of the muscle.

Comparing the enzyme activities found in this study with those in rainbow trout of equivalent size (approximately 40 $\mu mol \cdot g^{-1} \cdot min^{-1}$, Kiessling et al. 1991*b*) indicates that the activity of PFK is much lower. The level of PFK measured for transgenic fish resembles that of rainbow trout exposed to severe underfeeding (Kiessling et al. 1989), and that of the controls is well below any value reported earlier for salmonids (based on crude homogenate). However, distinct species and age differences exist in activity of this enzyme, indicative of muscle glycolytic capacity. In rainbow trout, a marked increase in activity of this enzyme was reported in white muscle during the first winter, increasing from 40 $\mu mol \cdot g^{-1} \cdot min^{-1}$ to a level close to 90 $\mu mol \cdot g^{-1} \cdot min^{-1}$ as the fish reached the size of saltwater tolerance (Kiessling et al. 1991*c*). This is the same activity level found in white muscle of sea-running sockeye salmon (*Oncorhynchus nerka*) (Kiessling et al. 1994*b*). An activity level of 10 $\mu mol \cdot g^{-1} \cdot min^{-1}$ was measured in the white muscle of adult seawater-adapted chinook salmon (*Oncorhynchus tshawytscha*), much higher than the activity level (2.49 $\mu mol \cdot g^{-1} \cdot min^{-1}$) measured in the control fish (Kiessling et al. 1994*a*). From this, it is clear that widely different levels of glycolytic activity exist in white muscle between different species of Pacific salmon.

The higher activity level of PFK found in the transgenic fish, relative to controls, and the less marked increase in the mitochondrial-bound enzyme Cytox (indicative of aerobic potential) may indicate that transgenic fish have a higher basal metabolic level than controls. This difference is intriguing, considering the observation that transgenic fish have a lower sustained swimming capacity than non-transgenic fish (Farrell et al. 1997), in spite of a white muscle metabolic profile normally associated with a higher capacity for sustained and burst activity. The superior sustained swimming capacity of the control fish is even more puzzling, considering the difference in muscle type profile (amount of red versus white muscle) between the transgenic and control fish. The muscle type profile of the control fish would, if found in humans, be indicative of a sprinter, while that of the transgenic fish would be indicative of a long-distance runner. This may be explained by physical limitations outside the muscle, perhaps differential growth rates between muscle and other organ systems such as circulation or skeletal development, although small white muscle fibres have been shown, by semiquantitative histochemical staining techniques, to contain higher levels of glycogen and a higher density of mitochondria (Kiessling et al. 1990).

Another explanation is that metabolic performance and swimming performance are affected by ectopic expression of the transgene in muscle cells. Such expression may stimulate genetic responses within the muscle cells, altering the performance profile of the muscle in unexpected ways. With no previous studies available for experimental design, we decided upon an untargeted approach in order to assess whether a broad-scale difference in genetic expression exists between the fast muscle of the transgenic fish and that of the nontransgenic fish.

Subtractive hybridisation is a powerful technique that isolates and identifies mRNA (as cDNA) present at an abundance of 2.5-fold or higher in the tester sample, in this case, fast muscle from the transgenic fish. Analysis of the clones isolated from the subtracted library showed that there was a significant increase in expression of a number of genes in the library. We have yet to isolate a clone in the library that suggests that GH mRNA is present in the library, which is surprising, since the promoter included in the construct is general. The analysis of clones in the library has, however, produced a number of identified cDNAs that are upregulated in transgenic fish fast muscle. The upregulation of some of these genes can be explained by increased growth rate or observed muscle architectural changes, whereas that of others is harder to explain due to the lack of previous studies linking them to growth rate, muscle cellularity, or GH blood titres.

MLC2 has not previously been fully sequenced and characterised in salmonids, and we have included the full sequence of the coding region in this paper. The mRNA has been cloned in zebrafish (Xu et al. 1998); however, there is not yet enough information to indicate how many isoforms of MLC2 are likely to be expressed in fish during development and growth of muscle.

One recent study of Atlantic herring (*Clupea harengus*) development (Johnston et al. 1997) showed by two-dimensional polyacrylamide gel electrophoresis that there are at least two detectable protein isoforms of MLC2, which are expressed in a temporal pattern during development. This indicates that there is at least one MLC2 isoform that is associated with developing muscle fibres and that another (adult) isoform is switched on in existing, growing fibres.

© 2000 NRC Canada

Fig. 5. (A) Nucleic acid sequence analysis and comparison of MLC2 from coho salmon with zebrafish MLC2. The solid line above the sequence indicates the coding region, and an asterisk indicates sequence identity. (B) Deduced amino acid sequence of coho salmon MLC2 compared with zebrafish MLC2. An asterisk indicates identity, a colon indicates fully conserved functionality, and a period indicates partially conserved functionality.

A

```
D. rerio      ----------------------------CTCTTCTTGATCTTCTTAGACTTCACACATAC 32
O. kisutch    CCCCTTGGGGCGGTTCCATCAGTCTCTTCTCTTGTTGACCATCCAAACCTCCATACATAC 60
                                          ***** **** * **  *  ** ** *******

D. rerio      CGTCTCGACATGGCACCCAAGAAGGCCAAGAGGAGGGCAGCAGGAGGAGAGGG---TTCC 89
O. kisutch    CGTCTCGAGATGGCACCCAAGAAGGCCAAGAGGAGGGGAGCAGCAGCAGAGGGCGGTTCC 120
              ******** ***************************** ***** ** ******    ****

D. rerio      TCCAACGTCTTCTCCATGTTTGAGCAGAGCCAGATTCAGGAGTACAAAGAGGCTTTCACA 149
O. kisutch    TCCAACGTGTTCTCCATGTTTGAGCAGAGCCAGATCCAGGAGTACAATTCAGGTTTCCCA 180
              ******** ***************************** ************     * **** **

D. rerio      ATCATTGACCAGAACAGAGACGGTATCATCAGCAAAGACGACCTTAGGGACGTGTTGGCC 209
O. kisutch    ATCACTGATCAGAACAGAGACGGTATCATCAGCAAGGATGACTTGAGGGACGTGCTGGCC 240
              **** *** ***************************** ** *** * ********** *****

D. rerio      TCAATGGGCCAGCTGAATGTGAAGAATGAGGAGCTGGAGGCCATGATCAAGGAAGCCAGC 269
O. kisutch    TCAATGGGCCAGTTGAATGTGAAGAATGAGGAGCTGGAAGCTATGGTCAAGGAGGCCAGC 300
              ************ ************************** ** *** ******* ******

D. rerio      GGCCCAATCAACTTCACCGTTTTCCTCACCATGTTCGGAGAGAAGTTGAAGGGTGCTGAC 329
O. kisutch    GGCCCCATCAACTTCACCGTCTTCCTCACCATGTTCGGAGAGAAGCTCAAGGGGGCTGAT 360
              ***** *************** ************************* * ***** *****

D. rerio      CCCGAAGACGTCATCGTGTCTGCCTTCAAGGTGCTGGACCCTGAGGGCACTGGATCCATC 389
O. kisutch    CCCGAGGATGTCATCGTTAGTGCTTTCAAGGTCCTGGACCCCGATGCTACCGGTTTCATC 420
              ***** ** ********   *** ******** ******** ** *  ** ** * ****

D. rerio      AAGAAGGAATTCCTTGAGGAGCTTTTGACCACTCAGTGCGACAGGTTCACCGCAGAGGAG 449
O. kisutch    AAGAAGGACTTCCTTCAGGAGCTCCTGACCACTCAGTGCGACAGGTTCTCTGCAGAGGAG 480
              ******** ****** *******  ************************ * *********

D. rerio      ATGAAGAATCTGTGGGCCGCCTTCCCCCCAGATGTGGCTGGCAATGTTGACTACAAGAAC 509
O. kisutch    ATGAAGAACCTGTGGGCTGCCTTCCCCCCAGATGTGGCCGGCAACGTAAACTACAAGCAA 540
              ******** ******** ********************** ***** **  ******** *

D. rerio      ATCTGCTACGTCATCACACACGGAGAGGAGAAGGAGGAGTAAACAACCTTGGAATCAAGA 569
O. kisutch    ATCTGCTACGTCATCACACACGGAGAGGAGAAGGAGGAGTAA-------TGAAACCGACA 593
              ******************************************       ** ** * * *
```

B

```
D. rerio      MAPKKAKRRAAGGEG-SSNVFSMFEQSQIQEYKEAFTIIDQNRDGIISKDDLRDVLASMG 59
O. kisutch    MAPKKAKRRGAAAEGGSSNVFSMFEQSQIQEYNSGFPITDQNRDGIISKDDLRDVLASMG 60
              *********.*..** ****************:..*.* **********************

D. rerio      QLNVKNEELEAMIKEASGPINFTVFLTMFGEKLKGADPEDVIVSAFKVLDPEGTGSIKKE 119
O. kisutch    QLNVKNEELEAMVKEASGPINFTVFLTMFGEKLKGADPEDVIVSAFKVLDPDATGFIKKD 120
              ************:****************************************:.** ***:

D. rerio      PLEELLTTQCDRFTAEEMKNLWAAFPPDVAGNVDYKNICYVITHGEEKEE 169
O. kisutch    FLQELLTTQCDRFSAEEMKNLWAAFPPDVAGNVNYKQICYVITHGEEKEE 170
              **:**********:********************:**:*************
```

Future studies will establish whether the isoform described in this study is expressed in embryonic muscle or is expressed as a juvenile or adult isoform only. The division of labour of MLC2 isoforms between embryonic and adult muscle has been established in higher vertebrates (Bandman 1992), and the high homology suggests that there may be very little evolution of functional difference. The increased expression of MLC2 in transgenic fish is therefore concordant with the increased emphasis on hyperplastic growth, and this gene may provide a valuable molecular method for monitoring hyperplastic growth in salmonids.

In addition, we identified a number of other clones from the subtracted library (Table 4) that are consistent with elevated levels of transcription (ribosomal proteins and tRNA) and changes in muscle ultrastructure (myosin heavy chain and skeletal α-actin). One interesting finding was that the

© 2000 NRC Canada

Ca^{2+} transport protein parvalbumin-β was subtracted into the library. This gene has been identified as a major human allergen in food fish (Lindstrom et al. 1996), and this finding implies that increased growth rates in salmonids may have unexpected meat quality consequences. This remains to be tested in other experiments on fast growth, for example, temperature or diurnal light cycle studies, since it may be a direct response to the presence of the transgene. However, this result displays the value of the untargeted approach, since parvalbumin has not previously been linked to growth rate changes and can now be monitored in growth rate experiments. A potential risk to consumer health, through increased levels of a strong allergen due to modern farming methods, has been identified.

A number of clones in the library have not yet been identified through homology searches of genetic databases. Cellular analysis of the expression of these genes will provide novel data on genetic expression of muscle cells. For example, one of the clones has some homology to a currently unidentified clone isolated from a human myocyte cell line. We will characterise this cDNA in future studies, since it may prove to be a marker of muscle stem cells. Such a marker has not yet been cloned in salmonids but has great potential for analysis of salmon growth.

In conclusion, increased growth rates, caused by transgenesis, in coho salmon have resulted in changes to muscle architecture consistent with increased rates of hyperplasia. This identifies a meat quality effect of growth rate that can be considered in future studies. Changes in levels of the muscle enzymes PFK and Cytox suggest effects on metabolism that can also lead to changes in meat quality due to postmortality effects. The subtracted library contains genes that are differentially expressed in salmon with high growth rates. These can be used as markers, increasing the analytical tools available for future studies of salmon growth under experimental farming conditions. Our future work will continue to analyse the cDNAs in the library with a view to understanding their relationship to growth processes and to developing diagnostic tests that will enhance growth experiments. In summary, a number of the effects of GH transgene mediated increases in growth rates have been identified. Future experiments will also determine which of these effects can be attributed to growth processes and which, if any, are a direct result of the presence of the transgene.

Acknowledgements

The economic contribution of the Faculty of Agricultural, Landscape Planning and Horticulture, Swedish University of Agricultural Sciences (SLU), Umeå, Sweden, as well of the Department of Fisheries and Oceans, Pacific Region, Canada, is greatly appreciated. We are also in great debt to Dr. Jan Nilsson, Department of Aquaculture, SLU, for valuable discussion and advice during the laboratory work with expression techniques and for assistance during sampling.

References

Altschul, S.F., Gish, W., Miller, W., Myers, E.W., and Lipman, D.J. 1990. Basic local alignment search tool. J. Mol. Biol. **215**: 403–410.

Bandman, E. 1992. Contractile protein isoforms in muscle development. Dev. Biol. **154**: 273–283.

Bass, A., Brdiczka, D., Eyer, P., Hofer, S., and Pette, D. 1969. Metabolic differentiation of distinct muscle types at the level of enzymic organisation. Eur. J. Biochem. **10**: 198–206.

Buckingham, M. 1994. Molecular biology of muscle development. Cell, **78**: 15–21.

Campion, R.D. 1984. The satellite cell; a review. Int. Rev. Cytol. **87**: 225–251.

Carpene, E., and Veggetti, A. 1981. Increase in muscle fibres in the lateralis muscle white portion of Mugilidae (Pisces, Teleostei). Experientia, **37**: 191–193.

Carpené, E., Veggetti, A, and Mascarello, F. 1982. Histochemical fibre types in the lateral muscle of fishes in fresh, brackish and salt water. J. Fish. Biol. **20**: 379–396.

Chenchik, A., Moquadam, F., and Siebert, P.D. 1996. A new method for full length cDNA cloning by PCR. *In* A laboratory guide to RNA isolation, analysis and synthesis. *Edited by* P.A. Kreig, Wiley-Liss, Inc., New York. pp. 273–321.

Chomczynski, P., and Sacchi, N. 1987. Single step method of RNA isolation by acid guanidium thiocyanate – phenol – chloroform extraction. Anat. Biochem. **162**: 156–159.

Devlin, R.H., Yesaki, T.Y., Biagi, C.A., Donaldson, E.M., Swanson, P., and Chan, W.-K. 1994. Extraordinary salmon growth. Nature (Lond.), **371**: 209–210.

Devlin, R.H., Yesaki,T.Y., Donaldson, E.M., and Hew, C.-L. 1995. Transmission and phenotypic effects of antifreeze/GH gene construct in coho salmon (*O. kisutch*). Aquaculture, **137**: 161–169.

Diatchenko, L., Campbell, Y.-F.C., Chenchik, A., Moqadam, F., Huang, B., Lukyanov, S., Lukyanov, K., Gurskaya, N., Sverdlov, E.D., and Siebert, P.D. 1996. Suppression subtractive hybridisation: a method for regulating differentially regulated or tissue specific cDNA probes and libraries. Proc. Natl. Acad. Sci. U.S.A. **93**: 6025–6030.

Farrell, A.P., Bennet, W., and Devlin, R.H. 1997. Growth-enhanced transgenic salmon can be inferior swimmers. Can. J. Zool. **75**: 335–337.

Fauconneau, B., Mady, M.P., and LeBail, P.Y. 1996. Effect of growth hormone on muscle protein synthesis in rainbow trout *Oncorhynchus mykiss* and Atlantic salmon *Salmo salar*. Fish Physiol. Biochem. **15**: 49–56.

Goldspink, G. 1972. Post-embryonic growth and differentiation of striated muscle. *In* Structure and function of muscle. Vol. 1. *Edited by* G.H. Bourne. Associated Press, New York. pp. 179–236.

Greene, C.W. 1913. The storage of fat in the muscular tissue of the king salmon and its resorbtion during the fast of the spawning migration. Bull. Bur. Fish No. 33.

Greer-Walker, M. 1970. Growth and development of the skeletal muscle fibres of the cod *Gadus morhua* L. J. Cons. Cons. Int. Explor. Mer, **33**: 228–244.

Higgins, P.S., and Thorpe, J.E. 1990. Hyperplasia and hypertrophy in the growth of skeletal muscle in juvenile Atlantic salmon, *Salmo salar*. J. Fish Biol. **37**: 505–519.

Johansson, L., Kiessling, A., Åsgård, T., and Berglund, L. 1995. Eating quality of rainbow trout — effects of ration level on sensory characteristics, lipid content and fatty acid composition. Aquacult. Nutr. **1**: 59–66.

Johnston, I.A., Viera, V.L.A., and Abercrombie, M. 1995. Temperature and myogenesis in embryos of the Atlantic herring *Clupea harengus*. J. Exp. Biol. **198**: 1389–1403.

Johnston, I.A., Cole, N.J., Vieira, V.L.A., and Davidson, I. 1997. Temperature and developmental plasticity of muscle phenotype in herring larvae. J. Exp. Biol. **200**: 849–868.

Kiessling, K.-H., and Kiessling, A. 1984. Fibre composition and enzyme activities in five different muscles from Svalbard reindeer. Comp. Biochem. Physiol. A, **77**: 75–78.

© 2000 NRC Canada

Kiessling, A., Storebakken, T., Åsgård, T., Andersson, I.-L., and Kiessling, K.-H. 1989. Physiological changes in muscle of rainbow trout fed different ration levels. Aquaculture, **79**: 293–301.

Kiessling, A., Johansson, L., and Kiessling, K.-H. 1990. Effects of starvation on rainbow trout muscle. I: Histochemistry, metabolism and composition of white and red muscle in mature and immature fish. Acta Agric. Scand. **40**: 909–924.

Kiessling, A., Kiessling, K.-H., Storebakken, T., and Åsgård, T. 1991*a*. Changes in the structure and function of the epaxial muscle of rainbow trout *Oncorhynchus mykiss* in relation to ration and age. I: Growth dynamics. Aquaculture, **93**: 335–356.

Kiessling, A., Kiessling, K.-H., Storebakken,T., and Åsgård, T. 1991*b*. Changes in the structure and function of the epaxial muscle of rainbow trout *Oncorhynchus mykiss* in relation to ration and age. II: Activity of key enzymes in the energy metabolism. Aquaculture, **93**: 357–372.

Kiessling, A., Åsgård, T., Storebakken, T., Johansson, L., and Kiessling, K.-H. 1991*c*. Changes in the structure and function of the epaxial muscle of rainbow trout *Oncorhynchus mykiss* in relation to ration and age. III: Chemical composition. Aquaculture, **93**: 373–387.

Kiessling, A., Hung, S., and Storebakken, T. 1993. Differences in protein mobilization between ventral and dorsal parts of white epaxial muscle, from fed, fasted and re-fed white sturgeon (*Acipenser transmontanus* Rich.). J. Fish Biol. **43**: 401–408.

Kiessling, A, Gallaugher, P., Thorarensen, H., Kolok, A., Eales, J.G., Sweeting, R., Gong, B., McKeown, B.A., Dosanjh, B., Farrell, A.P., and Higgs, D. 1994*a*. Influence of sustained exercise and endurance training on growth, muscle physiology, cardiovascular parameters, and plasma levels of metabolic hormones of seawater adapted all-female chinook salmon. *In* Proc. Int. Fish Physiol. Symp., Vancouver, B.C. *Edited by* D. Mackinlay. Trans. Am. Fish. Soc. **1**: 300–305.

Kiessling, A., Kiessling, K.-H., and Lindahl-Kiessling, K. 1994*b*. Changes in muscle energy metabolism and mobilisation of protein and fat from different parts of the somatic muscle and lipid depots during the spawning run of early Stuart sockeye salmon. *In* Proc. Int. Fish Physiol. Symp., Vancouver, B.C. *Edited by* D. Mackinlay. Trans. Am. Fish. Soc. **1**: 335.

Lee, L.G., Connell, C.R., Woo, S.L., Cheng, R.D., McArdle, B.F., Fuller, C.W., Halloran, N.D., and Wilson, R.K. 1992. DNA sequencing with dye-labelled terminators and t7 DNA-polymerase effect of dyes and dNTPs on incorporation of dye-terminators and probability analysis of termination fragments. Nucleic Acids Res. **20**: 2471–2483.

Lindstrom, C.D., van Do, T., Hordvik, I., Endresen, C., and Elsayed, S. 1996. Cloning of two distinct cDNAs encoding parvalbumin, the major allergen of Atlantic salmon *Salmo salar*. Scand. J. Immunol. **44**: 335–344

Novikoff, A.B., Shin, W.Y., and Drucker, J. 1961. Mitochondrial localization of oxidative enzymes: staining results with two tetrazolium salts. J. Biophys. Biochem. Cytol. **9**: 47–61.

Prober, J.M., Trainor, G.L., Dam, R.J., Hobbs, F.W., Robertson, C.W., Zagursky, R.J., Cocuzza, A.J., Jensen, M., and Baumeister, K. 1992. A system for rapid DNA sequencing with fluorescent chain-terminating dideoxynucleotides. Science (Washington, D.C.), **238**: 336–341.

Rowlerson, A., Mascarello, F., Radaelli, G., and Veggetti, A. 1995. Differentiation and growth of muscle in the fish *Sparus aurata* L.: II. Hyperplastic and hypertrophic growth of lateral muscle from hatching to adult. J. Muscle Res. Cell Motil. **16**: 223–236.

Shonk, C.E., and Boxer, G.E. 1964. Enzyme patterns in human tissue. I. Methods for determination of glycolytic enzymes. Cancer Res. **24**: 709–724.

Stickland, N.C. 1983. Growth and development of muscle fibres in rainbow trout *O. mykiss*. J. Anat. **137**: 323–333.

Weatherley, A.H., and Gill, H. 1982. Influence of bovine growth hormone on the growth dynamics of mosaic muscle in relation to somatic growth of rainbow trout *O. mykiss*. J. Fish Biol. **20**: 165–172.

Weatherley, A.H., Gill, H., and Rogers, S.C. 1980. The relationship between mosaic muscle fibres and size in rainbow trout *O. mykiss*. J. Fish Biol. **17**: 603–610.

Weatherley, A.H., Gill, H.S., and Lobo, A.F. 1988. Recruitment and maximal diameter of axial muscle fibres in teleost and their relationship to somatic growth and ultimate size. J. Fish Biol. **33**: 851–859.

Whereat, A.F., Orishimo, M.W., Nelson, J., and Phillips, S.J. 1969. The location of different synthetic systems for fatty acids in inner and outer mitochondrial membranes from rabbit heart. J. Biol. Chem. **44**: 6498–6506.

Xu, Y., He, J., Tian, H.L., Chan, C.H., Liao, J., Yan, T., Lam, T.J., and Gong, Z. 1998. Fast skeletal muscle specific expression of a zebrafish myosin light chain 2 gene and characterisation of its promoter by direct injection into skeletal muscle. Genbank Submission, Accession No. AF081462.

© 2000 NRC Canada

Predicting fish abundance using single-pass removal sampling

Matthew G. Mitro and Alexander V. Zale

Abstract: Three-pass removal data for juvenile rainbow trout (*Oncorhynchus mykiss*) along bank areas of the Henrys Fork of the Snake River, Idaho, were used to construct a mean capture probability (MCP) model to predict abundance from single-pass catch data. We evaluated the MCP model by simulation. The precision of the MCP model was poor when predicting abundance within a specific bank unit. MCP model prediction intervals were about 7.5 times greater than three-pass removal intervals. However, the MCP model performed about the same as three-pass removal for predicting total abundance in a river section from multiple bank samples. We evaluated how the MCP model can be used to improve precision of total abundance estimates. Reallocating effort to sample 150 bank units by single-pass removal rather than 50 bank units by three-pass removal resulted in a 48% increase in prediction interval precision for a simulated population of 10 000 fish. Precision also increased when allocating effort to sampling more bank units of smaller length versus fewer bank units of longer length. Sampling 1500 m of bank as one hundred 15-m bank units increased precision by about 28% versus sampling fifty 30-m bank units and by about 50% versus sampling twenty-five 60-m bank units.

Résumé : À partir de données de prélèvement de juvéniles de truite arc-en-ciel (*Oncorhynchus mykiss*) par triple passage sur des portions de berges du secteur de Henrys Fork, sur la rivière Snake (Idaho), nous avons construit un modèle de probabilité moyenne de capture (PMC) pour prédire l'abondance à partir des données de capture par passage unique. Nous avons évalué le modèle par simulation. La précision du modèle était médiocre lorsqu'on voulait prédire l'abondance pour une unité de berge donnée. Les intervalles de prédiction du modèle étaient d'environ 7,5 fois supérieurs à ceux du prélèvement par triple passage. Toutefois, la performance était à peu près équivalente pour la prédiction de l'abondance totale dans un tronçon de cours d'eau à partir d'échantillons d'unités de berge multiples. Nous avons évalué la façon dont le modèle PMC pourrait servir à améliorer la précision des estimations de l'abondance totale. En réaffectant l'effort de façon à échantillonner 150 unités de berge par prélèvement par passage unique plutôt que 50 unités de berge par prélèvement par triple passage, nous avons obtenu une augmentation de 48% de la précision de l'intervalle de prédiction pour une population simulée de 10 000 poissons. La précision augmentait également lorsqu'on allouait l'effort à l'échantillonnage d'un plus grand nombre d'unités de berge de longueur inférieure plutôt qu'à un petit nombre d'unités de berge de longueur supérieure. C'est ainsi que l'échantillonnage de 1 500 m de berge sous forme de 100 unités de 15 m a accru la précision d'environ 28% par rapport à l'échantillonnage de 50 unités de 30 m, et d'environ 50% par rapport à l'échantillonnage de 25 unités de 60 m.

[Traduit par la Rédaction]

Introduction

Three-pass removal sampling is a common methodology used to estimate fish abundances in streams. A group of fish is numerically depleted by physical removal or marking on successive capture occasions such that catch per unit effort decreases proportionately to the number of fish remaining. An estimate of abundance is obtained using a maximum likelihood estimator (Zippin 1956; Otis et al. 1978; Rexstad and Burnham 1991).

Three-pass removal sampling can be labor intensive and costly when applied to many areas in a watershed or to a random selection of sampling units for the purpose of estimating abundance for a larger area (Strange et al. 1989; Kruse et al. 1998). For example, we were interested in using three-pass removal sampling to estimate juvenile rainbow trout (*Oncorhynchus mykiss*) abundance along the banks of a 4-km section of the Henrys Fork of the Snake River, Idaho. The river section was too large to sample as a whole and therefore required division into bank sampling units from which a subset could randomly be selected to sample. The overall precision of an abundance estimate for such an area depends on the number of units sampled and the precision of the estimate from each sample. The abundance estimate should include measures of within-unit and among-unit variability and an extrapolation error term. Extrapolation error is

Received April 12, 1999. Accepted February 2, 2000.
J15103

M.G. Mitro[1] and A.V. Zale. Montana Cooperative Fishery Research Unit, U.S. Geological Survey, Department of Biology, Montana State University, Bozeman, MT 59717, U.S.A.

[1]Author to whom all correspondence should be sent at the following address: Atlantic States Marine Fisheries Commission, c/o Rhode Island Division of Fish and Wildlife, Coastal Fisheries Laboratory, 1231 Succotash Rd., Wakefield, RI 02879, U.S.A.

© 2000 NRC Canada

related to the percentage of units sampled out of the total population of units in the area of interest. This error can be quite large when a small subset of units is sampled.

Some interest has been directed at reducing, from three to two, the number of passes required to obtain an abundance estimate (Seber 1982; Heimbuch et al. 1997). If the effort required to obtain an abundance estimate for a sampling unit could be reduced, the overall effort could be directed towards sampling more units to reduce among-unit variability and extrapolation error. However, if a large proportion of fish are captured on the first pass, then we should be able to reduce sampling effort to a single pass. This would require additional information to predict abundance from the single-pass catch, i.e., if a statistical relationship could be developed between total abundance and a single-pass removal sample, it could be used to predict abundance (Jones and Stockwell 1995; Kruse et al. 1998). We could then, for example, sample 60 units by single-pass removal with the same effort required to sample 20 units by three-pass removal. The loss in estimate precision would be compensated by a gain in precision among sample units and in the extrapolation error term for estimating total abundance in a larger area.

Strange et al. (1989) proposed a statistical relationship to predict abundances of juvenile Atlantic salmon (*Salmo salar*) and brown trout (*Salmo trutta*) in small streams. They first obtained a "semiquantitative" sample by electrofishing a single pass through a 50-m block-netted stream section, excluding 10 m near each net. The entire section was subsequently sampled by three-pass removal and the "quantitative" estimate was the sum of the semiquantitative single-pass catch and the three-pass removal estimate. Predictions were made from a model of the quantitative estimate as a function of the semiquantitative sample. Crozier and Kennedy (1994) used a similar method for juvenile salmonids in streams but only excluded 5 m near each net for their semiquantitative single-pass sample. Lobon-Cervia and Utrilla (1993) proposed estimating abundance of trout in streams by relating a three-pass abundance estimate to the catch in the first pass. Kruse et al. (1998) used such a relationship to predict trout abundance in mountain streams with sparse habitat. Jones and Stockwell (1995) proposed the same method and compared it with a relationship between a single-pass sample and an independent three-pass abundance estimate obtained 3–5 weeks later.

An alternative approach is the use of a capture probability estimate from a previous multiple-pass removal sample(s) to estimate abundance from a single-pass catch (Seber and Le Cren 1967). Here, it is assumed that the estimate of capture probability from the previous sample is similar to the expected capture probability for the new sample. Capture probability is also assumed to remain constant as a population is depleted. Abundance is estimated by dividing a single-pass catch by the estimate of capture probability. Mitro (1999) compared this approach, using a mean capture probability from multiple samples, with the simple linear regression approach.

We constructed and evaluated a predictive model, using the mean capture probability approach, for obtaining abundance estimates from single-pass catch data. Three-pass removal data for juvenile rainbow trout along bank areas of the Henrys Fork were used to construct a model using a mean capture probability for all bank units sampled by three-pass removal. Simulation was used to evaluate bias and interval coverage properties for predicting abundance in a bank sampling unit, mean abundance per bank sampling unit, and total abundance in a river section.

Methods

Henrys Fork study

Three-pass removal sampling in bank sampling units was used to collect data for the estimation of juvenile rainbow trout (i.e., ≤200 mm total length) abundance in the Box Canyon section of the Henrys Fork. Box Canyon is a 4-km-long river section that has an average width of 75 m, a high gradient (0.45%), and a cobble–boulder substrate. Mean annual discharge during the study was 23 m^3/s (range 5.9–78.4 m^3/s). Bank areas are characterized by an abundance of rocks and woody debris. A bank sampling unit (hereafter referred to as bank unit) was defined as a known-length section of bank extending out into the channel a minimum of 2 m, or further to encompass any structure associated with the bank, such as a fallen tree. Bank units were about 15 m in length. A subset of the total population of bank units in the river section was randomly selected and sampled.

Juvenile trout were immobilized using a hand-held probe operated from boat-mounted electrofishing gear (continuous DC, 250 V) and collected with a dip net. Each removal pass was performed by wading upstream from the boat. All habitat was thoroughly sampled on each pass such that effort remained constant. Blocking nets could not be used to physically close bank units; an attempt to install a blocking net caused excessive disturbance and a seal could not be maintained between the net and the substrate. We assumed that bank units were biologically closed such that juvenile rainbow trout were not entering or leaving the area. Unlike adult rainbow trout, which typically fled outside a bank unit as we approached, juvenile rainbow trout moved to nearby cover within a unit during electrofishing.

Maximum likelihood estimates of abundance with $\log_e$-based confidence intervals were obtained using the Zippin removal estimator in the program CAPTURE (Rexstad and Burnham 1991). Bank unit estimates were used to obtain an estimate of the mean number of juvenile rainbow trout per bank unit and an extrapolated estimate of total abundance for the river section. Samples were collected from 154 bank units during nine seasons (spring, summer, or autumn) from summer 1995 to spring 1998.

Mean capture probability model

A mean capture probability (MCP) model was constructed in which the mean capture probability $\hat{\bar{p}}$ for all bank units sampled by three-pass removal was used to estimate abundance from single-pass removal data (Seber and Le Cren 1967):

$$\hat{n} = \frac{c_1}{\hat{\bar{p}}}$$

We constructed 95% prediction intervals assuming a log-odds transformation:

$$\left[\frac{c_{1\text{pred}}}{\hat{\bar{p}}_{\text{log-odds(upper)}}}, \frac{c_{1\text{pred}}}{\hat{\bar{p}}_{\text{log-odds(lower)}}} \right]$$

where

$$\hat{\bar{p}}_{\text{log-odds(lower)}} = \frac{\hat{\bar{p}}}{\hat{\bar{p}} + (1 - \hat{\bar{p}}) \cdot d}$$

© 2000 NRC Canada

$$\hat{\hat{p}}_{\text{log-odds(upper)}} = \frac{\hat{\hat{p}}}{\hat{\hat{p}} + \frac{(1-\hat{\hat{p}})}{d}}$$

$$d = \exp\left[\frac{1.96\,\text{SE}(\hat{\hat{p}})}{\hat{\hat{p}}(1-\hat{\hat{p}})}\right]$$

and $\hat{\hat{p}}_{\text{log-odds(lower)}}$ is the lower bound of the log-odds 95% confidence interval for $\hat{\hat{p}}$, $\hat{\hat{p}}_{\text{log-odds(upper)}}$ is the upper bound of the log-odds 95% confidence interval for $\hat{\hat{p}}$, and $\text{SE}(\hat{\hat{p}})$ is the standard error of $\hat{\hat{p}}$ (Burnham et al. 1987). The model and prediction intervals were programmed in MATLAB version 5 (MathWorks, Inc. 1998).

Model evaluation

Simulated data were used to construct an MCP model and to evaluate the bias of model predictions and the coverage properties of prediction intervals. All simulations were programmed in MATLAB version 5 (MathWorks, Inc. 1998). A simulated 4-km river section was divided into five hundred and thirty-three 15-m bank units. A population of known size was randomly selected from a range of 7500 to 12 500 and distributed among the bank units following a normal distribution with a standard deviation of 50% of the mean number of individuals per bank unit (i.e., normal(μ, σ^2), where $\mu = N/533$ (N is population size) and $\sigma = 0.50\mu$). (We use the term "population" to refer to the aggregate of individuals of interest, e.g., juvenile rainbow trout.) A subset of 15 bank units was randomly selected and sampled using three-pass removal. This procedure was repeated 10 times to obtain a total sample of 150 bank units.

A capture probability p_{beta} was randomly selected from a beta($\alpha = 11.14, \beta = 4.0341$) distribution for each bank unit sampled (Rexstad and Burnham 1991). The estimated parameters of the beta distribution were maximum likelihood estimates obtained by fitting the distribution to the capture probability estimates for field data (excluding observations of $\hat{p} = 1$). The capture probability p_{beta} remained constant for each removal occasion. A random number p_{unif} was selected from uniform(0,1) for each individual in the bank unit. If $p_{\text{unif}} \leq p_{\text{beta}}$, then the individual was considered captured and removed from the bank unit; otherwise, the individual was not captured and remained in the bank unit. This procedure was repeated for second- and third-pass removals for individuals remaining in the bank unit. The three-pass removal data were checked to determine if the group of individuals in a bank unit was sufficiently depleted (i.e., the number of fish captured in the third pass was less than the number captured in the first pass (Seber and Whale 1970; Otis et al. 1978)). If a group was not sufficiently depleted, the sampling failed and an estimate of abundance could not be obtained for that bank unit; another bank unit was then sampled in its place. The three-pass removal data were analyzed using the Zippin maximum likelihood removal estimator to estimate abundance $\hat{n}_i$ for i = 1–150. The capture probability $\hat{p}_i$ was estimated from the catch data and $\hat{n}_i$ (Zippin 1956).

The 150 observations were used to construct an MCP model as described above. Single-pass catch data were simulated from bank units and river sections of known abundance to evaluate the ability of the MCP model to predict (*i*) abundance in a bank unit, (*ii*) mean abundance per bank unit, and (*iii*) abundance in a river section. Second- and third-pass catch data were also simulated to evaluate the Zippin removal estimator and compare it with the model predictions.

Abundance in a bank unit

One hundred groups of known size ranging from 1 to 100 were each sampled by three-pass removal using a randomly selected p_{beta} for a group and p_{unif} for each individual in a group on each removal pass as described above. The three-pass removal data were used to estimate group size using the Zippin removal estimator and to construct $\log_e$-based confidence intervals. (Three-pass removal samples that failed to sufficiently deplete the group could not be analyzed using the Zippin removal estimator.) The first-pass catch data were used in the MCP model to estimate group size and to construct log-odds prediction intervals. This procedure was replicated 1000 times for each group size. The following bias and interval statistics were computed: mean bias, bias standard error, percent interval coverage, mean lower bound, mean upper bound, mean interval length, and interval length standard error.

Mean abundance per bank unit

A population of known size N = 10 000 was distributed normal (μ = 10 000/533, $\sigma^2 = (0.50\mu)^2$) in a 4-km river section comprising five hundred and thirty-three 15-m bank units. Two hundred bank units were randomly selected for sampling by three-pass removal. A randomly selected p_{beta} was used for each bank unit and p_{unif} for each individual in a bank unit on each removal pass as described above. The three-pass removal data were used to estimate abundance and its associated variance for each bank unit using the Zippin removal estimator. (Three-pass removal samples that failed to sufficiently deplete the group could not be analyzed using the Zippin removal estimator.) The first-pass catch data were used in the MCP model to estimate abundance and its associated variance (including an error term for making a prediction). These data were used to estimate the mean abundance per bank unit for 191 sample sizes ranging from 10 to 200. Normal confidence intervals were constructed for three-pass removal estimates and normal prediction intervals were constructed for MCP model predictions. This sampling and evaluation procedure was replicated 1000 times. Bias and interval statistics were computed as described above.

Abundance in a river section

The procedure to estimate mean abundance per bank unit for a population of known size N = 10 000 was extended to estimate abundance for the river section as a whole. Estimates of river section abundance were obtained by multiplying the mean abundance per bank unit times the total number of bank units in the river section. Prediction intervals assuming normality were constructed for three-pass removal and MCP model predictions. Variance estimates included error terms for within-bank unit error (i.e., variation associated with making an estimate or model prediction), among-bank unit error (i.e., spatial variation), and extrapolation error:

$$\hat{\text{var}}_{\text{total}} = \frac{U}{m}(U-m)\,\hat{\text{var}}_{\text{among}} + \frac{U}{M}\,\hat{\text{var}}_{\text{within}}$$

where

$$\hat{\text{var}}_{\text{among}} = \frac{\sum_{i}^{m}(\hat{n}_i - \hat{\bar{n}})^2}{m-1}$$

$$\hat{\text{var}}_{\text{within}} = \sum_{i}^{m}\hat{\text{var}}(\_)_i$$

and $\hat{\text{var}}(\_)$ is $\hat{\text{var}}_{\text{est}}$ for three-pass estimates and $\hat{\text{var}}(\text{MCP})_{\text{pred}}$ for MCP model predictions, U is the total number of bank units in the river section, and m is the sample size (Bohlin et al. 1989). This procedure was also performed for the 1000 replicates. Bias and interval statistics were computed as described above.

© 2000 NRC Canada

Bank unit size

We also investigated the effect of bank unit length on sample size (i.e., the number of bank units sampled) and the estimation of abundance in a river section. An MCP model was constructed from three-pass removal data from one hundred and fifty 30-m bank unit samples from the 10 simulated populations of known size described earlier. A population of known size $N = 10\,000$ was distributed normal($\mu = 10\,000/266$, $\sigma^2 = (0.50\mu)^2$) in a 4-km river section comprising two hundred and sixty-six 30-m bank units. One hundred bank units were randomly selected and sampled by three-pass removal as described above. These data were used to estimate the abundance in a river section for 91 sample sizes ranging from 10 to 100.

An MCP model was also constructed from three-pass removal data from one hundred and fifty 60-m bank unit samples from the 10 simulated populations of known size described earlier. A population of known size $N = 10\,000$ was distributed normal($\mu = 10\,000/133$, $\sigma^2 = (0.50\mu)^2$) in a 4-km river section comprising one hundred and thirty-three 60-m bank units. Fifty bank units were randomly selected and sampled by three-pass removal. These data were used to estimate abundance in a river section for 41 sample sizes ranging from 10 to 50.

Each abundance estimation procedure was replicated 1000 times. Bias and interval statistics were computed as described above. MCP models for the Henrys Fork and for simulations of 15-, 30-, and 60-m bank units were compared by analysis of variance on ranked capture probabilities (SAS Institute Inc. 1994).

Results

Henrys Fork study

Maximum likelihood estimates of abundance were obtained for 147 bank units; five bank units were not sufficiently depleted and abundance could not be estimated (3.4% failure rate) and no rainbow trout were captured in two samples. Five observations were considered influential points (Sen and Srivastava 1990) and were excluded from the data set for model construction. Sixteen observations of $\hat{p} = 1$ were removed from the data set containing 142 observations to estimate $\bar{\hat{p}}$ for the MCP model (Table 1).

Model evaluation by simulation

Simulating capture probabilities

There was no linear relationship between capture probability $\hat{p}$ and estimated abundance $\hat{n}$ for the 142 observations from the Henrys Fork ($r^2 = 0.16$) (Fig. 1*a*). Most observations of $\hat{p}$ were between 0.6 and 0.9. A beta distribution fit to the 142 observations (including 16 observations of $\hat{p} = 1$) was strictly increasing on the interval (0, 1) (beta($\alpha = 2.4884$, $\beta = 0.6675$)) (Fig. 1*b*). (The observations of $\hat{p} = 1$ were in practice analyzed as values close to 1, i.e., 0.9999, when fitting the beta distribution.) This indicated that there was a higher probability of selecting random values of $\hat{p}$ greater than 0.9 than values of $\hat{p}$ between 0.6 and 0.9 from this beta distribution. A beta distribution fit to 126 observations (excluding the 16 observations of $\hat{p} = 1$) was not strictly increasing on the interval (0, 1) and indicated a higher probability of selecting random values of $\hat{p}$ between 0.6 and 0.9 (beta($\alpha = 11.14$, $\beta = 4.0341$)) (Fig. 1*c*). A plot of $\hat{p}$ and $\hat{n}$, each estimated from simulated three-pass removal data collected using a p_{beta}, showed no linear relationship and estimates of $\hat{p} = 1$ were observed as in data from the Henrys Fork ($r^2 = 0.14$) (Fig. 1*d*).

Models for 15-, 30-, and 60-m bank unit samples

Thirty-four observations of $\hat{p} = 1$ were removed from the data set containing 150 observations to estimate $\bar{\hat{p}}$ for the 15-m bank unit MCP model; 24 and 21 observations were removed for the 30- and 60-m bank unit MCP models (Table 1). There was no significant difference among mean capture probabilities used in MCP models for the Henrys Fork and for simulated data ($P = 0.53$).

Sample failures

There were 755 failures out of 100 000 samples for estimating abundance in a bank unit. Three-pass removal estimates could not be calculated for failed samples. Most failures occurred for samples of smaller abundances: 608 failures for abundances less than or equal to 5 and 703 failures for abundances less than or equal to 10.

There were 7228 failures out of 200 000 samples of 15-m bank units. The failure rate was about 3.6% for a given sample size ranging from 10 to 200. Therefore, actual sample sizes used for three-pass removal estimates of mean abundance per bank unit or abundance in a river section were on average about 3.6% less than the stated sample size.

There were 3817 failures out of 100 000 samples of 30-m bank units. The failure rate was about 3.8% for a given sample size ranging from 10 to 100. There were 1586 failures out of 50 000 samples of 60-m bank units. The failure rate was about 3.2% for a given sample size ranging from 10 to 50.

Abundance in a bank unit

The $\log_e$-based confidence intervals for three-pass removal estimates of abundance achieved a coverage level of 93–95% (Fig. 2*a*). The percent coverage remained relatively constant with increasing abundance. The log-odds prediction intervals for the MCP model achieved a coverage level between about 90 and 95% for abundances up to about 40 and achieved the nominal coverage level thereafter (Fig. 2*b*). (See Appendix for interval statistics for 10 sample sizes ranging from 10 to 100.)

Mean bias (expressed as a percentage of known abundance) for three-pass removal estimates and MCP model predictions was negative and relatively small and constant. The average percent mean bias for abundances between two and 100 was –1.4% (SD = 0.6) for three-pass estimates and –3.6% (SD = 0.9) for MCP model predictions. (See Appendix for bias statistics for 10 sample sizes ranging from 10 to 100.)

Mean interval length and the standard error of interval length (each expressed as a percentage of known abundance) were large for small abundances and rapidly declined asymptotically to stable levels as abundance increased (Fig. 3). Percent mean interval length for three-pass removal $\log_e$-based confidence intervals decreased asymptotically to about 10% for abundances up to 100 (Fig. 3*a*). The percent standard error of interval length was variable and greater than percent mean interval length (Fig. 3*a*).

Percent mean interval length for MCP log-odds prediction intervals was greater than 90% for abundances less than five and decreased asymptotically to about 75% for abundances up to 100 (Fig. 3*b*). The percent standard error of interval length was less than percent mean interval length and de-

© 2000 NRC Canada

Table 1. MCP models for Henrys Fork data and simulations of 15-, 30-, and 60-m bank units.

MCP model		$\hat{\bar{p}}$ (SE)	$\hat{\bar{p}}$ log-odds 95% confidence interval	N
Henrys Fork	$\hat{n} = \frac{c_1}{0.7334}$	0.7334 (0.1071)	[0.4845, 0.8895]	126
Simulation (15 m)	$\hat{n} = \frac{c_1}{0.7620}$	0.7620 (0.1161)	[0.4773, 0.9182]	116
Simulation (30 m)	$\hat{n} = \frac{c_1}{0.7546}$	0.7546 (0.1168)	[0.4717, 0.9137]	126
Simulation (60 m)	$\hat{n} = \frac{c_1}{0.7436}$	0.7436 (0.1205)	[0.4566, 0.9092]	129

Fig. 1. (*a*) Scatter plot of abundance and capture probability estimates from Henrys Fork data, beta distribution fit to Henrys Fork capture probability estimates (*b*) including and (*c*) excluding 16 values of $\hat{p} = 1$, and (*d*) scatter plot of abundance and capture probability estimates from simulated data collected from 15-m bank units using p_{beta} from beta distribution excluding values of $\hat{p} = 1$.

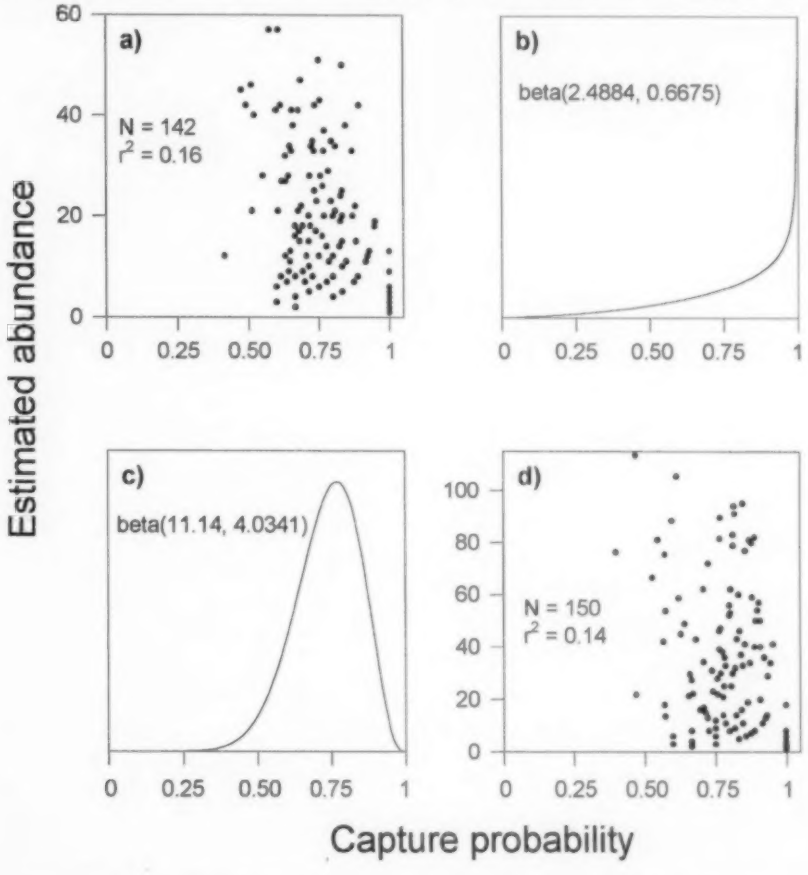

creased asymptotically to about 12% (Fig. 3*b*). The log-odds prediction intervals for the MCP model achieved the nominal coverage level of 95% when percent mean interval length was greater than 75% (Figs. 2*b* and 3*b*).

Mean abundance per bank unit

The mean abundance per 15-m bank unit for a population of 10 000 in a 4-km river section was 18.762. Three-pass removal estimates had a positive bias and MCP model predictions had a negative bias. Percent mean bias for three-pass removal estimates decreased from 7% ($N = 10$) to 0.2% ($N = 200$). Percent mean bias was least for MCP model predictions and decreased from −5% ($N = 12$) to −0.35% ($N = 200$).

Normal confidence intervals for three-pass removal estimates of mean abundance per 15-m bank unit achieved the nominal coverage level of 95% at a sample size of about 190 (Table 2). Normal prediction intervals for the MCP model achieved the nominal coverage level at a sample size of

© 2000 NRC Canada

Fig. 2. Percent coverage of the true abundance (range 1–100) for (*a*) 95% confidence intervals for three-pass removal estimates and (*b*) 95% prediction intervals for MCP model predictions. The solid line indicates intervals and the broken line indicates the 95% nominal level.

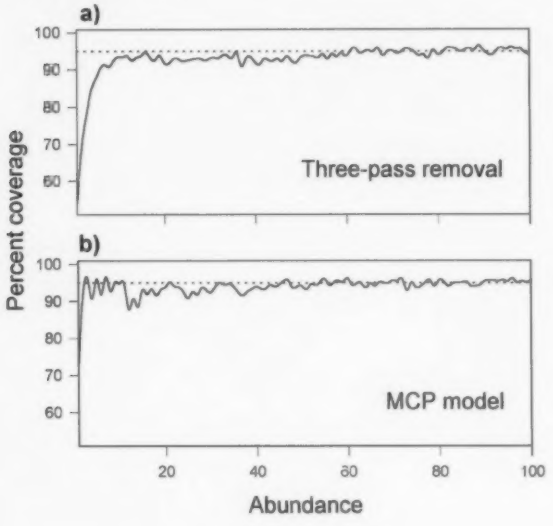

about 75. Mean interval length for three-pass removal estimates gradually increased with sample size from 5 at $N = 10$ to 6.6 at $N = 200$ (Table 2). Mean interval length was larger for MCP model predictions and remained relatively constant at 9.3–9.4 as sample size increased. The standard error of interval length decreased for all intervals as sample size increased and was largest for three-pass removal intervals (Table 2).

Abundance in a river section

Three-pass removal estimates of abundance in a river section from sampling 15-m bank units had a positive bias; the mean estimate of abundance $\hat{N}$ was 10 253 (Fig. 4*a*). There was a negative bias in MCP model predictions ($\hat{N} = 9652$) (Fig. 5*a*).

Three-pass removal and MCP model predictions performed about equally well at a given sample size (Figs. 4 and 5; Table 3). Prediction interval coverage for three-pass removal increased from about 90% at $N = 10$ to about 94–95% at $N = 25$–200 (Fig. 4*b*; Table 3). Prediction interval coverage for the MCP model increased from about 90% at $N = 10$ to about 93–95% at $N = 25$–135 and decreased to about 90% at $N = 200$ (Fig. 5*b*; Table 3). Mean interval length decreased as sample size increased (e.g., from about 6150 at $N = 50$ to about 3200 at $N = 150$) (Figs. 4*a* and 5*a*; Table 3).

The reallocation of an equal amount of effort applied to three-pass removal sampling to single-pass sampling and the use of the MCP model increased the precision of prediction intervals (Table 3). Sampling with 150 removal passes as single passes rather than as 50 sets of three-pass samples resulted in a 48% increase in prediction interval precision (i.e., mean interval length decreased from 6279 (three-pass removal) to 3134 (MCP model)).

Fig. 3. Mean interval length (solid line) and interval length standard error (broken line) (each expressed as a percentage of abundance) for (*a*) three-pass removal $\log_e$-based 95% confidence intervals and (*b*) MCP model log-odds 95% prediction intervals.

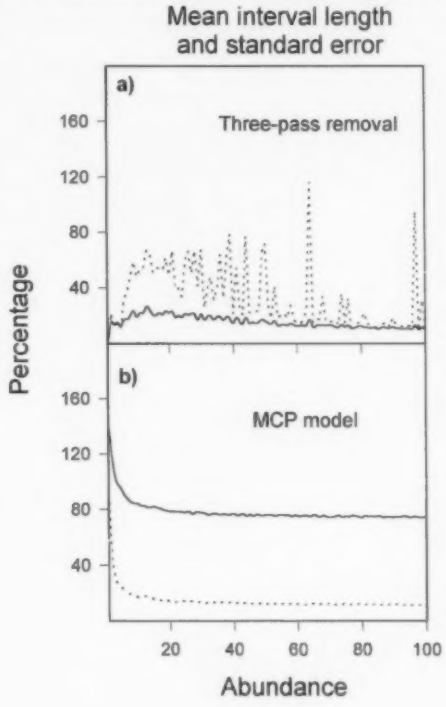

Bank unit size

Doubling or quadrupling the area sampled by doubling or quadrupling the length of bank units provided a marginal increase in prediction interval precision (Table 3). Precision increased by about 6% when sampling fifty 30-m bank units and by about 16% when sampling fifty 60-m bank units versus sampling fifty 15-m bank units.

Doubling the number of bank units sampled by halving the length of bank units (while total length of bank sampled remained constant) provided a large increase in prediction interval precision (Table 3). Sampling 1500 m of bank as one hundred 15-m bank units increased precision by about 28% versus sampling fifty 30-m bank units and by about 50% versus sampling twenty-five 60-m bank units. Precision also increased by about 28 and 50% when sampling 3000 m of bank as two hundred 15-m bank units versus one hundred 30-m bank units and fifty 60-m bank units.

Discussion

Abundance in a river section

The precision of total abundance estimates for a river section can be significantly improved by allocating a given amount of effort (i.e., for three-pass removal sampling) to sampling more bank units by single-pass removal and using the MCP model to predict abundance. The loss of precision by predicting abundance for a given bank unit using single-

© 2000 NRC Canada

Table 2. Bias and interval statistics for three-pass estimates and MCP model predictions of mean abundance per 15-m bank unit (1000 replications).

Sample size	Mean bias	SE bias	% coverage	Mean lower bound	Mean upper bound	Mean interval length	SE interval length
Three-pass estimates (normal 95% confidence intervals)							
25	0.5	4.3	40.8	16.6	22.1	5.5	5.3
50	0.5	3.0	59.3	16.3	22.2	5.9	4.8
75	0.5	2.3	73.5	16.2	22.4	6.2	4.6
100	0.5	1.9	80.7	16.1	22.3	6.2	4.2
125	0.5	1.7	85.6	16.1	22.4	6.3	3.9
150	0.4	1.5	90.7	16.0	22.5	6.5	4.2
175	0.5	1.4	93.5	16.0	22.5	6.5	4.0
200	0.4	1.2	94.8	15.9	22.5	6.6	4.1
MCP model predictions (normal 95% prediction intervals)							
25	–0.6	4.1	71.9	13.5	22.8	9.3	1.1
50	–0.7	2.9	87.1	13.4	22.7	9.3	0.8
75	–0.6	2.3	94.9	13.5	22.8	9.3	0.6
100	–0.7	1.9	97.2	13.4	22.8	9.3	0.5
125	–0.6	1.7	98.2	13.4	22.8	9.4	0.4
150	–0.7	1.5	99.2	13.4	22.8	9.3	0.4
175	–0.7	1.3	99.7	13.4	22.8	9.4	0.3
200	–0.7	1.2	99.9	13.4	22.8	9.4	0.3

Note: The true mean abundance per bank unit was 18.762.

Fig. 4. (*a*) Three-pass removal predicted abundance and 95% prediction intervals and (*b*) percent coverage of the true river section abundance $N = 10\,000$ for sample sizes ranging from 10 to 100.

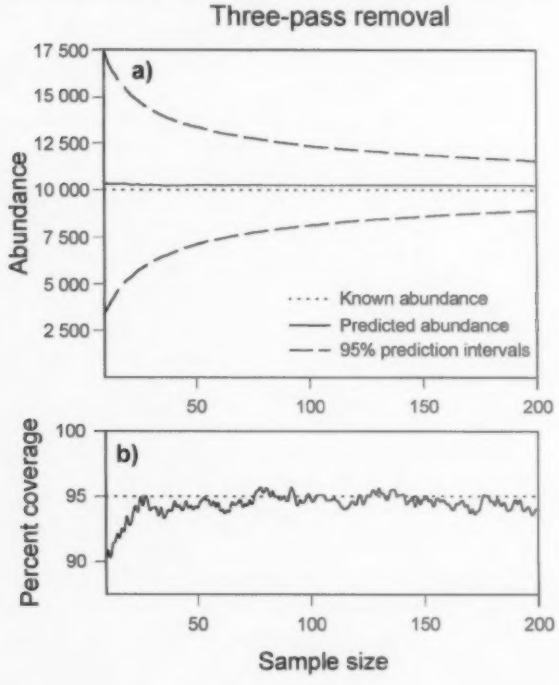

Fig. 5. (*a*) MCP model predicted abundance and 95% prediction intervals and (*b*) percent coverage of the true river section abundance $N = 10\,000$ for sample sizes ranging from 10 to 100.

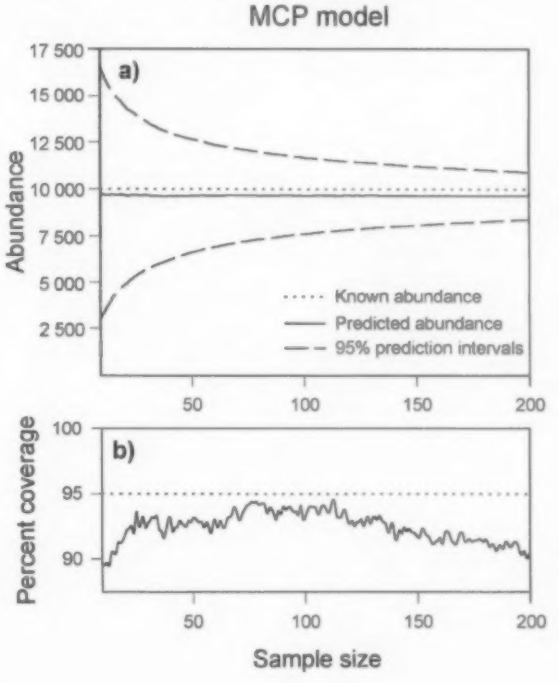

pass data was more than compensated for by reductions in among-bank unit variability and extrapolation error because of increased sample size. Strange et al. (1989) and Crozier and Kennedy (1994) proposed using such a sampling strategy along with a regression model to construct indices of abundance for a large area. Jones and Stockwell (1995) went further in stating that actual abundance estimates could be obtained. We explicitly showed by simulation that abun-

© 2000 NRC Canada

Table 3. Interval statistics (normal 95% prediction intervals) for three-pass estimates and MCP model predictions for population size = 10 000 (1000 replications).

	% coverage	Mean lower bound	Mean upper bound	Mean interval length	SE interval length
Sample size = 50 (15-m bank units)					
Three-pass	94.1	7105	13 383	6279	516
MCP model	93.1	6612	12 665	6053	542
Sample size = 150 (15-m bank units)					
Three-pass	94.8	8610	11 869	3259	136
MCP model	91.7	8075	11 209	3134	142
Sample size = 100 (15-m bank units) (1500 m of bank sampled)					
Three-pass	94.8	8132	12 355	4223	222
MCP model	93.2	7615	11 686	4071	237
Sample size = 50 (30-m bank units) (1500 m of bank sampled)					
Three-pass	94.8	7329	13 226	5897	448
MCP model	93.7	6839	12 540	5701	480
Sample size = 25 (60-m bank units) (1500 m of bank sampled)					
Three-pass	94.8	6121	14 345	8224	866
MCP model	92.6	5785	13 870	8085	977
Sample size = 200 (15-m bank units) (3000 m of bank sampled)					
Three-pass	93.9	8917	11 561	2645	94
MCP model	90.7	8374	10 910	2536	98
Sample size = 100 (30-m bank units) (3000 m of bank sampled)					
Three-pass	93.6	8436	12 123	3687	178
MCP model	92.3	7926	11 473	3547	187
Sample size = 50 (60-m bank units) (3000 m of bank sampled)					
Three-pass	94.7	7631	12 778	5147	326
MCP model	94.5	7290	12 335	5045	368

dance estimates for a large area, with prediction intervals that achieved the nominal level of coverage, could be obtained using an MCP model.

The actual sample size for three-pass removal estimates of total abundance was on average 3.6% less than the stated sample size. If 200 three-pass removal samples were taken, maximum likelihood estimates of abundance could be calculated for about 196 of those samples. Sample failures often occur in field situations. About 3.4% of bank samples from the Henrys Fork failed. Time constraints may preclude obtaining additional field samples in the event of sample failure; the simulation procedure mimicked that scenario. This type of sample failure is not a problem for the MCP model because the model only uses the catch from the first pass to predict abundance. Failures cannot be identified because second and third passes are not performed. Therefore, if 200 single-pass samples were taken, 200 samples were used to predict total abundance.

Lobon-Cervia and Utrilla (1993) expressed caution concerning the use of a mean capture probability to predict abundance from single-pass catch, but no one has explicitly considered an MCP model as an alternative to a simple linear regression model. We found that the MCP model performed well for predicting total abundance in a river section. We recommend the use of the MCP model for predicting total abundance in a river section. The MCP model could also be used in watershed-wide monitoring programs. A network of small streams in a watershed could be divided into segments, of which a subset is sampled. If three-pass removal sampling had previously been used, sampling effort in the future could be allocated to sampling more stream segments by single-pass removal. If single-pass sampling had previously been used for collecting presence and absence data, the model could be used to now obtain abundance estimates.

The MCP model constructed for Henrys Fork data will be used in the future for monitoring juvenile rainbow trout recruitment in the Henrys Fork. This model may or may not be robust such that it can be used in other systems. We recommend constructing and calibrating models for rivers or watersheds in which they will be used and recalibrating models if gear or other design features change. This entails randomly selecting and sampling by three-pass removal a subset of bank units or stream segments in a system to obtain data to construct models. The parameter estimates for the MCP models for simulated data stabilized at a sample size of about 30, which can therefore be considered a minimum number of valid three-pass removal samples for constructing a model. After models have been constructed, a hybrid sampling strategy may be used that includes both three-pass and single-pass removal. Three-pass samples can be used for model validation and calibration while using single-pass sampling to increase the number of areas sampled.

Bank unit size

There was no significant difference among MCP models (comparisons of $\hat{\bar{p}}$) constructed from samples from 15-, 30-, and 60-m bank units. Sampling larger bank units resulted in sampling some larger groups of fish and hence obtaining some larger values of $\hat{n}$ and c_1. There was a marginal increase in precision for predictions of total abundance in a

© 2000 NRC Canada

river section when sampling an equal number of larger bank units, e.g., fifty 30-m bank units (i.e., 1500 m of bank) versus fifty 15-m bank units (i.e., 750 m of bank). This increase in precision results from sampling a larger portion of the bank in a river section, thereby decreasing extrapolation error. Precision was actually lost for abundance estimates for individual bank units when using an MCP model constructed from samples of larger bank units. Capture probability tends to vary more when sampling larger groups of fish, resulting in larger variation in the estimate of $\hat{\bar{p}}$ in the MCP model.

Precision of total abundance estimates increased greatly when sampling a larger number of small bank units versus a smaller number of large bank units (e.g., one hundred 15-m bank units (1500 m of bank) versus fifty 30-m bank units (1500 m of bank)). In this case, the gain in precision is a result of a reduction in among-bank unit variation. Sampling smaller bank units means encountering a smaller size range of groups of fish. This reduces the size of the difference between any abundance estimate and the mean estimate of abundance for all bank units sampled, which is squared and summed in calculating $\text{var}_{\text{among}}$.

Mean abundance per bank unit

The MCP model was also useful for obtaining an estimate of mean abundance per bank unit. Such an estimate is a precursor to estimating total abundance in a river section but may also be used by itself as an index. The nominal coverage level was achieved at a relatively small sample size of about 75 for the MCP model. Three-pass removal estimation required a sample size of about 190 to achieve the same nominal coverage level. This was a result of small interval length rather than bias.

Abundance in a bank unit

Lobon-Cervia and Utrilla (1993) and Jones and Stockwell (1995) suggested that a regression model and single-pass removal data could be used as an alternative to three-pass removal sampling for predicting site-specific abundance. Our simulation results for predicting abundance in a single bank unit using the MCP model were not encouraging because of the great loss in precision (bias was minimal). Mitro (1999) obtained similar results in simulations using the simple linear regression approach. These results were in accordance with Crozier and Kennedy's (1994) recommendation not to use a regression model and single-pass removal data to predict site-specific abundance. We found the performance of the MCP model to be unsatisfactory because prediction intervals were large, about 7.5 times those of three-pass removal intervals.

Simulating capture probabilities

A beta distribution fit to a set of capture probability estimates excluding all $\hat{p} = 1$ better represented the observed capture probabilities than had all $\hat{p} = 1$ been included. Likewise, estimates of $\hat{p} = 1$ were excluded from calculations of a mean capture probability for an MCP model. Estimates of $\hat{p} = 1$ were an artifact of small abundances. If the actual probability of capture is high, all individuals in a small group are often captured, sometimes in the first pass. The concept is similar to that of demographic stochasticity: stochastic effects decrease in magnitude with increasing population size (Nations and Boyce 1997). Simulations showed that estimates of $\hat{p} = 1$ could be obtained from analyses of sample data collected using a $p_{\text{beta}} \neq 1$.

Removal methodology assumptions

Population closure

Population closure is an important condition for the use of the removal methodology. The loss or addition of juvenile trout during sampling could bias estimates of abundance (Otis et al. 1978; White et al. 1982; Pollock et al. 1990). Bank units in the Henrys Fork were physically open when sampled because the use of blocking nets was impractical. The installation and maintenance of efficient blocking nets would be labor intensive, and any advantage of a physically closed system may have been offset by the disturbance of fish while installing the nets (Bohlin et al. 1989). However, physically open populations can sometimes be treated as closed, contingent on a short study period (Pollock 1982). It can also be argued that the sample areas are biologically closed when the species of interest restricts its activities to a defined area (Bohlin et al. 1989). When disturbed, juvenile rainbow trout in the Henrys Fork concealed themselves in the interstitial space of the rocky substrate, in woody debris, and in macrophytes. The slow, methodical process of electrofishing upstream was particularly effective at capturing juvenile rainbow trout because of this tendency towards concealment. (Such an approach to sampling large rainbow trout would not work because large rainbow trout were typically observed fleeing sample areas, except when water temperatures were low and fish response time was slow.) Any loss of juvenile rainbow trout from bank units during sampling was likely minimal. Movement of juvenile rainbow trout into bank units during the short sampling duration (e.g., 1 h) was also likely minimal, as groups of fish in bank units were consistently depleted.

Equal catchability of individuals

Temporal variation in capture probability was controlled because effort was equal for each pass. Effort remained constant by thoroughly sampling all habitat in a bank unit on each pass (Riley and Fausch 1992). Trout may exhibit a behavioral response to electrofishing (Cross and Stott 1975; Mesa and Schreck 1989). This was not a concern for juvenile rainbow trout that were captured because they were removed from bank units and not subject to recapture. However, trout that escape capture in the electric field should be subject to recapture during a subsequent pass. The probability of recapture would decrease if these trout left the bank unit or better concealed themselves. We cannot say that this never occurred, but some juvenile rainbow trout were observed concealing themselves in the rocky substrate and were recaptured during the subsequent pass.

Decreasing catchability in multiple-pass removal sampling of fish populations is common and may result in the underestimation of abundance if catchability is modeled as remaining constant (Cross and Stott 1975; Bohlin and Sunderstrom 1977; Peterson and Cederholm 1984; Riley and Fausch 1992). Henrys Fork removal data consisted of three passes and could therefore only be analyzed assuming a con-

© 2000 NRC Canada

stant capture probability model. MCP models constructed from simulated data with a known constant capture probability did not significantly differ from models constructed for Henrys Fork data. This suggests that if capture probability did decrease on the second and third passes in the Henrys Fork, the decrease was not severe such that abundance was greatly underestimated.

Conclusions

We do not recommend the use of an MCP model to predict abundance for a bank unit or stream segment if that area is the only area of interest. The extra effort required for the second and third pass greatly improves estimate precision. This model has the greatest utility for predicting total abundance from multiple samples. The MCP model can be used to reduce data collection effort for the estimation of total abundance in a river section or network of streams. The models can also be used to improve precision by reallocating a given amount of effort from three-pass sampling to single-pass sampling. A hybrid sampling protocol may be used that includes both three-pass and single-pass sampling. The three-pass samples could be used to construct a new model for the present sampling situation or to check model adequacy (i.e., model validation) and to further calibrate a previously constructed model; single-pass samples can be analyzed using the MCP model.

Acknowledgements

This study was supported by a grant from the Idaho Department of Fish and Game. We thank Mark Gamblin, Bruce Rich, and Jeff Dillon of the Idaho Department of Fish and Game for their logistic support and general facilitation of this study. We thank the following individuals for their field assistance: Richard Dykstra, Katherine Ellsworth, Michael Enk, Daniel Gustafson, Richard Henderson, John Jorgenson, Douglas Megargle, Gregory Pavellas, John Perry, Steven Ritter, Adam Sahnow, Stan Van Sickle, Brian Vaughn, Eldon Volk, and Seth Zimmerman. We also thank John Borkowski for critically reviewing an earlier version of this manuscript. The Montana Cooperative Fishery Research Unit is jointly sponsored by the U.S. Geological Survey, Biological Resources Division; Montana State University; and the Montana Department of Fish, Wildlife, and Parks.

References

Bohlin, T., and Sundstrom, B. 1977. Influence of unequal catchability on population estimates using the Lincoln index and the removal method applied to electro-fishing. Oikos, **28**: 123–129.

Bohlin, T., Hamrin, S., Heggberget, T.G., Rasmussen, G., and Saltveit, S.J. 1989. Electrofishing — theory and practice with special emphasis on salmonids. Hydrobiologia, **173**: 9–43.

Burnham, K.P., Anderson, D.R., White, G.C., Brownie, C., and Pollock, K.H. 1987. Design and analysis methods for fish survival experiments based on release–recapture. Am. Fish. Soc. Monogr. No. 5.

Cross, D.G., and Stott, B. 1975. The effect of electric fishing on subsequent capture of fish. J. Fish Biol. **7**: 349–357.

Crozier, W.W., and Kennedy, G.J.A. 1994. Application of semi-quantitative electrofishing to juvenile salmonid stock surveys. J. Fish Biol. **45**: 159–164.

Heimbuch, D.G., Wilson, H.T., Weisberg, S.B., Volstad, J.H., and Kazyak, P.F. 1997. Estimating fish abundance in stream surveys by using double-pass removal sampling. Trans. Am. Fish. Soc. **126**: 795–803.

Jones, M.L., and Stockwell, J.D. 1995. A rapid assessment procedure for the enumeration of salmonine populations in streams. N. Am. J. Fish. Manage. **15**: 551–562.

Kruse, C.G., Hubert, W.A., and Rahel, F.J. 1998. Single-pass electrofishing predicts trout abundance in mountain streams with sparse habitat. N. Am. J. Fish. Manage. **18**: 940–946.

Lobon-Cervia, J., and Utrilla, C.G. 1993. A simple model to determine stream trout (*Salmo trutta* L.) densities based on one removal with electrofishing. Fish. Res. **15**: 369–378.

MathWorks, Inc. 1998. MATLAB version 5. MathWorks, Inc., Natick, Mass.

Mesa, M.G., and Schreck, C.B. 1989. Electrofishing mark–recapture and depletion methodologies evoke behavioral and physiological changes in cutthroat trout. Trans. Am. Fish. Soc. **118**: 644–658.

Mitro, M.G. 1999. Sampling and analysis techniques and their application for estimating recruitment of juvenile rainbow trout in the Henrys Fork of the Snake River, Idaho. Ph.D. thesis, Montana State University, Bozeman, Mont.

Nations, C.S., and Boyce, M.S. 1997. Stochastic demography for conservation biology. *In* Structured-population models in marine, terrestrial, and freshwater systems. *Edited by* S. Tuljapurkar and H. Caswell. Chapman and Hall, New York. pp. 451–469.

Otis, D.L., Burnham, K.P., White, G.C., and Anderson, D.R. 1978. Statistical inference from capture data on closed animal populations. Wildl. Monogr. No. 62.

Peterson, N.P., and Cederholm, C.J. 1984. A comparison of the removal and mark–recatpure methods of population estimation for juvenile coho salmon in a small stream. N. Am. J. Fish. Manage. **4**: 99–102.

Pollock, K.H. 1982. A capture–recapture design robust to unequal probability of capture. J. Wildl. Manage. **46**: 752–757.

Pollock, K.H., Nichols, J.D., Brownie, C., and Hines, J.E. 1990. Statistical inference for capture–recapture experiments. Wildl. Monogr. No. 107.

Rexstad, E., and Burnham, K. 1991. User's guide for interactive program CAPTURE. Colorado Cooperative Fish and Wildlife Research Unit, Colorado State University, Fort Collins, Colo.

Riley, S.C., and Fausch, K.D. 1992. Underestimation of trout population size by maximum likelihood removal estimates in small streams. N. Am. J. Fish. Manage. **12**: 768–776.

SAS Institute Inc. 1994. SAS/STAT user's guide, version 6, edition 4. SAS Institute Inc., Cary, N.C.

Seber, G.A.F. 1982. The estimation of animal abundance and related parameters. 2nd ed. Macmillan, New York.

Seber, G.A.F., and Le Cren, E.D. 1967. Estimating population parameters from catches large relative to the population. J. Anim. Ecol. **36**: 631–643.

Seber, G.A.F., and Whale, J.F. 1970. The removal method for two and three samples. Biometrics, **26**: 393–400.

Sen, A., and Srivastava, M. 1990. Regression analysis: theory, methods, and applications. Springer-Verlag, New York.

Strange, C.D., Aprahamian, M.W., and Winstone, A.J. 1989. Assessment of a semi-quantitative electric fishing sampling technique for juvenile Atlantic salmon, *Salmo salar* L., and trout, *Salmo trutta* L., in small streams. Aquacult. Fish. Manage. **20**: 485–492.

White, G.C., Anderson, D.R., Burnham, K.P., and Otis, D.L. 1982. Capture–recapture and removal methods for sampling closed

© 2000 NRC Canada

populations. Los Alamos National Laboratory, LA 8787-NERP, Los Alamos, N.M.

Zippin, C. 1956. An evaluation of the removal method of estimating animal populations. Biometrics, **12**: 163–189.

Appendix. Bias and interval statistics for three-pass estimates and MCP model predictions for 10 groups of known size (n) ranging from 10 to 100 (1000 replications).

n	$\hat{\bar{n}}$	Mean bias	SE bias	% coverage	Mean lower bound	Mean upper bound	Mean interval length	SE interval length
Three-pass estimates ($\log_e$ 95% confidence intervals)								
10	9.8	–0.2	0.6	93.5	9.7	11.5	1.9	4.8
20	19.6	–0.4	1.3	92.0	19.4	23.8	4.4	9.8
30	29.6	–0.4	2.1	93.0	29.1	35.4	6.3	20.3
40	39.4	–0.6	1.7	92.1	38.9	44.9	5.9	8.6
50	49.5	–0.5	3.7	93.2	48.7	56.8	8.1	36.0
60	59.2	–0.8	2.1	93.7	58.4	66.1	7.6	8.7
70	70.2	–0.8	2.5	95.3	69.1	78.2	9.2	11.2
80	79.3	–0.7	2.8	94.3	77.9	88.0	10.1	13.2
90	89.2	–0.8	3.8	95.4	87.6	98.1	10.6	16.8
100	99.3	–0.7	3.8	94.2	97.7	108.0	10.3	14.9
MCP model predictions (log-odds 95% prediction intervals)								
10	9.7	–0.3	2.2	94.8	7.4	15.9	8.4	1.7
20	19.2	–0.8	3.8	93.8	15.5	31.2	15.7	2.8
30	29.1	–0.9	5.4	92.4	23.7	47.0	23.3	4.1
40	38.8	–1.2	6.7	94.0	31.7	62.5	30.8	5.1
50	48.4	–1.6	8.0	94.2	39.7	77.9	38.1	6.2
60	57.9	–2.1	9.4	96.3	47.6	92.9	45.3	7.2
70	66.9	–3.1	11.2	95.7	55.0	107.3	52.3	8.6
80	76.4	–3.6	12.7	95.7	62.9	122.4	59.5	9.8
90	86.2	–3.8	14.4	95.5	71.1	138.1	67.1	11.0
100	96.7	–3.3	14.9	95.6	79.8	154.9	75.1	11.4

Note: $\hat{\bar{n}}$, mean estimated size of group.

© 2000 NRC Canada

A Bayesian decision analysis to set escapement goals for Fraser River sockeye salmon (*Oncorhynchus nerka*)

Jon T. Schnute, Al Cass, and Laura J. Richards

Abstract: This paper illustrates a complete Bayesian decision analysis for evaluating multistock harvest goals in the fishery on Fraser River sockeye salmon (*Oncorhynchus nerka*). We identify four key steps necessary to assess a resource production system. Each step entails choices that can alter the perceived consequences of management decisions. A Markov chain Monte Carlo sample captures uncertainty in the population dynamics. The Bayesian formalism then translates this uncertainty into uncertain policy outcomes. We examine a relatively simple control law, designed to protect stocks at low abundance. We restrict our attention to retrospective policy analysis by investigating what might have happened to sockeye stocks if management had proceeded differently during years for which historical data are available. A formal objective function quantifies societal values associated with a range of policy options. To confine the paper to manageable scope, we consider only relatively simple assumptions. Our analytical framework offers an iterative route to policy design, where managers play an active role in formulating policy options and evaluating their consequences.

Résumé : Le présent article illustre une analyse de décision bayésienne complète visant à évaluer les objectifs d'exploitation de plusieurs stocks de saumon rouge (*Oncorhynchus nerka*) du Fraser. Nous avons déterminé quatre étapes importantes pour évaluer un système de production de la ressource. Chaque étape comporte des choix susceptibles de modifier la perception des conséquences des décisions de gestion. Une simulation de Monte Carlo chaîne de Markov donne l'incertitude dans la dynamique des populations. Le formalisme bayésien convertit ensuite cette incertitude en résultats décisionnels incertains. Nous étudions une loi de contrôle assez simple, conçue pour protéger les stocks peu abondants. Nous limitons notre examen à une analyse décisionnelle rétrospective en étudiant ce qui aurait pu se produire si les stocks avaient été gérés différemment au cours des années pour lesquelles nous possédons des données historiques. Une fonction formelle objective mesure les valeurs sociétales associées à diverses options décisionnelles. Pour garder à notre article une portée gérable, nous prenons en compte uniquement des hypothèses assez simples. Notre cadre d'analyse offre une démarche itérative pour la conception de politiques, où les gestionnaires jouent un rôle actif en formulant des options stratégiques et en évaluant leurs conséquences.

[Traduit par la Rédaction]

Introduction

Fraser River sockeye salmon (*Oncorhynchus nerka*) provide the backbone of the Canadian commercial salmon fishery (Roos 1991). They also contribute substantially to the culture and economy of aboriginal peoples in the region. More than 150 sockeye stocks have been identified by adult migratory patterns and spawning location within the watershed. Most stocks are still recovering from catastrophic mortality inflicted in the early twentieth century from river blockages and overfishing. In addition, sockeye returns to the Fraser River vary markedly over the 4-year cycle representing different brood lines (Ricker 1950, 1987, 1997). The persistence of cycles has contributed to large variability in annual catches and ultimately to economic instability. Previous stock collapses and the propensity to cycle are the two principal factors that shape the present-day fishery.

In this paper, we present a complete Bayesian decision analysis for assessing multistock harvest goals in the fishery on Fraser sockeye. We identify four key steps necessary to assess a resource production system. Each step entails choices that can alter the perceived consequences of management decisions. We make a particular set of choices and examine their implications for management. Thus, our analysis illustrates the range of choices available, but does not propose a definitive policy. Where possible, we use intuitive arguments to articulate relationships between model assumptions and management decisions.

Uncertainty plays a major role in this analysis. Fraser sockeye typically experience a 4-year life cycle with highly variable population dynamics. We use a version of the stock–recruitment model proposed by Schnute and Kronlund (1996) to represent these dynamics, where parameter uncertainty is captured by sampling the Bayes posterior distribution. Essentially, the model produces estimates of productivity and capacity for each stock. The dimensionless

Received June 21, 1999. Accepted December 22, 1999. J15201

J.T. Schnute,[1] A. Cass, and L.J. Richards. Fisheries and Oceans Canada, Science Branch, Pacific Region, Pacific Biological Station, Nanaimo, BC V9R 5K6, Canada.

[1]Author to whom all correspondence should be addressed. e-mail: schnutej@pac.dfo-mpo.gc.ca

© 2000 NRC Canada

productivity parameter relates to the number of recruits per spawner. Capacity, a dimensioned scale parameter, corresponds to the number of fish that can be sustained by the ecosystem. The data reveal that Fraser sockeye are highly productive, with a capacity poorly defined for stocks that are still rebuilding.

Results from any proposed management strategy must reflect uncertainty in the system dynamics. The Bayes formalism provides a straightforward transition from uncertain population dynamics into uncertain policy outcomes. We restrict our attention to retrospective policy analysis. Thus, we examine what might have happened to sockeye stocks if management had proceeded differently during the years for which data are available. This approach offers a realistic, intuitive framework for managers and stakeholders familiar with the historical conduct of the fishery. We consider a range of policy options and evaluate their consequences with a formal objective function that quantifies societal values, such as a sustained fishery during a period of stock rebuilding.

Section 1 describes sockeye population dynamics, identifies the data used here, and presents an exploratory data analysis. Section 2 outlines the four key steps in our resource analysis and illustrates their relevance to Fraser sockeye. Section 3 articulates the dynamic model and uses Bayes posterior sampling to express parameter uncertainty. Section 4 presents the retrospective policy analysis, along with an objective function for evaluating possible outcomes. In the final section, we discuss advantages and limitations of our analysis. We sometimes compile equations into tables and indicate the table number in equation references. For example, (T2.1) and (2.1) refer to the first equation in Table 2 and section 2, respectively.

1. Biology and data

Strong homing behavior of adult sockeye salmon brings them back to the natal area for spawning. Most Fraser sockeye (about 94%) mature and die at age 4, after an initial winter as eggs, 1 year as juveniles in nursery lakes, and 2 years as adults at sea. Fisheries take place on migratory adults returning to spawn. Each stock i ($i = 1,...,m$) is defined by (A) the natal lake or stream and (B) the timing pattern for returning to the natal area within a year.

Because of the 4-year life cycle, stocks also have four distinct cycle lines j ($j = 1,...,4$) associated with particular years of return. For example, sockeye that spawned in 1949 produced adult descendants in 1953, 1957, 1961, and so on. We denote that particular sequence of ancestors and descendants as "cycle 1". Similarly, sockeye in cycles 2, 3, and 4 have ancestors or descendants in the years 1950, 1951, and 1952, respectively. We use the index t ($t = 1,...,n$) to denote a sequence of years starting in 1949 ($t = 1$). Thus, the cycle j associated with year t is

$$(1.1) \quad j = t - 4\,\mathrm{int}\left(\frac{t-1}{4}\right),$$

where int(x) denotes the integer part of x.

Some Fraser stocks exhibit cyclic dominance, which occurs when stock abundance in one cycle substantially dominates the abundance in other cycles. Such a persistently high cycle line is called the "dominant" cycle for the stock. An extensive literature documents potential reasons for cyclic dominance (Ricker 1950, 1997; Ward and Larkin 1964; Larkin 1971; Collie and Walters 1987; Eggers and Rogers 1987; Walters and Staley 1987; Collie et al. 1990; Welch and Noakes 1990, 1991; Levy and Wood 1992; Cass and Wood 1994; Myers et al. 1998). Despite the long-standing investigation of this problem, scientists have not achieved consensus on the explanation.

For management purposes, Fraser stocks are grouped into four migratory timing patterns or runs called the Early Stuart, Early Summer, Summer, and the Late runs. The Summer run is now the largest of these four management groups. In data compiled by the Pacific Salmon Commission, the Summer run consists of four major component stocks: (1) the "Quesnel" component from the Mitchell and Horsefly rivers, (2) the "Late Stuart" component from late returns to the Stuart Lake system, (3) the "Chilko" component from Chilko Lake, and (4) the "Stellako" component from the Stellako River. Our analysis focuses entirely on the Summer run, so that we have $m = 4$ stocks with indices i specified in the list above.

The spawning escapement S_{it} of stock i in year t can be estimated by a field program at the appropriate time of year in the watershed of interest (Schubert 1998). In the catch removed by the fishery, migratory timing patterns, scale characteristics, and other indicators can be used to identify individual stocks (Gable and Cox-Rogers 1993). Thus, the total catch of sockeye from the Summer run can be divided among stocks to estimate the catch C_{it} of stock i in year t. Estimates of recruitment R_{it} and harvest rate h_{it},

$$(1.2) \quad R_{it} = C_{it} + S_{it},$$

$$(1.3) \quad h_{it} = \frac{C_{it}}{C_{it} + S_{it}},$$

follow from the estimated catch and escapement.

Each cycle line for each stock follows a conceptually simple population dynamics. In year t, a spawning escapement S_{it} reaches the natal area, spawns, and dies. Four years later, the subsequent generation of $R_{i,t+4}$ recruited adults begins the return migration. From these, a catch $C_{i,t+4}$ is removed and $S_{i,t+4}$ spawners escape to continue the cycle. Productivity from year t to $t + 4$ can be estimated as the ratio

$$(1.4) \quad p_{it} = \frac{R_{i,t+4}}{S_{it}}.$$

Our analysis uses Pacific Salmon Commission Summer-run spawner data S_{it} from years 1949–1997 and recruitment data R_{it} from years 1953–1997. This compilation gives spawner–recruitment observations $\{S_{it}, R_{i,t+4}\}$ for each stock $i = 1,..., m$ and year $t = 1,..., n$, where $m = 4$ and $n = 45$. Thus, spawners S_{it} from the 45 brood years 1949–1993 produce recruits R_{it} in the corresponding return years 1953–1997. The available data allow us to infer catches $C_{it} = R_{it} - S_{it}$ and harvest rates h_{it} in all return years, as well as productivities p_{it} from all brood years.

A conceptual link between spawners S_{it} and recruits $R_{i,t+4}$ ignores the fact that not all Fraser sockeye return at age 4. According to the current database, 151.5 million sockeye

© 2000 NRC Canada

Fig. 1. Total returns $R_{i,t+4}$ (10^6 fish) from spawners S_{it} in brood years 1949–1993 for the (A) Quesnel, (B) Late Stuart, (C) Chilko, and (D) Stellako stocks $i = 1,...,4$. A logarithmic scale on the vertical axis shows contrasting magnitudes for cycles 1–4, indicated by the symbols □, ○, △, and +, respectively.

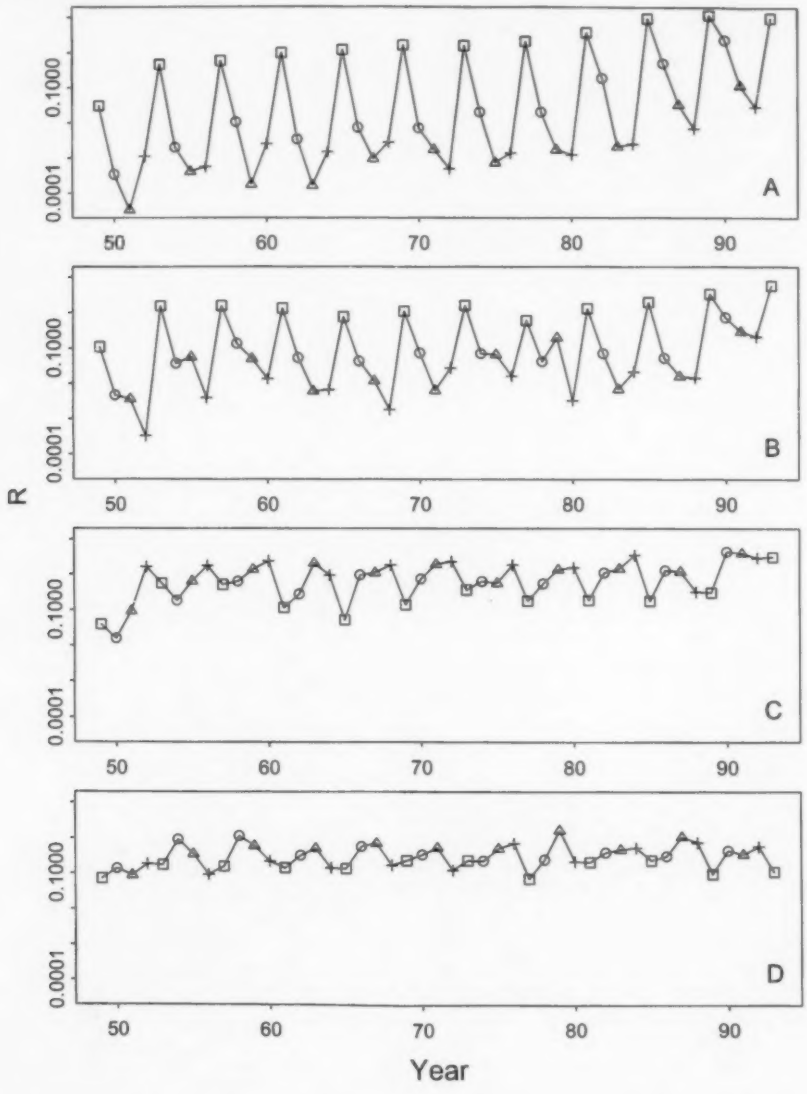

from the Summer-run stocks have returned during the historical period mentioned above. These include fish at ages 3 (0.6%), 4 (94.0%), 5 (5.4%), and 6 (0.03%). For simplicity, we use data from age 4 fish only; thus, our analysis ignores the presence of fish at other ages.

Figure 1 shows total annual returns for each of the four stocks considered here, where a logarithmic scale highlights the contrast between high and low cycle lines. Stocks 1 and 2 each have a dominant cycle 1 (□) and a subdominant cycle 2 (○). The low cycles 3 (△) and 4 (+) for these stocks represent much smaller runs by comparison. Stock 1 shows considerable evidence of rebuilding in all cycles during the time period depicted. A similar pattern for stock 2 suggests rebuilding particularly in the 1980s and 1990s. Stocks 3 and 4 show less variability between highs and lows, with no obvious trend upward or downward. Furthermore, stocks 3 and 4 typically experience low returns in cycle 1, the dominant cycle for stocks 1 and 2.

The Summer-run stocks have been remarkably productive (Fig. 2), rarely dropping below the replacement level $p_{it} = 1$. Summing across all stocks and years, each spawner produces 5.6 recruits on average. Although a logarithmic scale in Fig. 2 allows for extreme values, high outliers p_{it} have been truncated at 100. Stocks 1 and 2 have productivities near the average for most years in the dominant cycles, with a suggestion of reduced productivity in recent years. Stock 4 appears to have a stable productivity, with relatively low variance.

Because Summer-run stocks occur simultaneously in the

© 2000 NRC Canada

Fig. 2. Productivities p_{it} from spawners S_{it} in brood years 1949–1993 for the (A) Quesnel, (B) Late Stuart, (C) Chilko, and (D) Stellako stocks $i = 1,...,4$. A logarithmic scale on the vertical axis shows contrasting magnitudes, where values p_{it} above 100 are plotted at the maximum 100. A dotted line emphasizes the replacement productivity level $p = 1$. Cycles 1–4 are indicated by the symbols □, ○, △, and +, respectively.

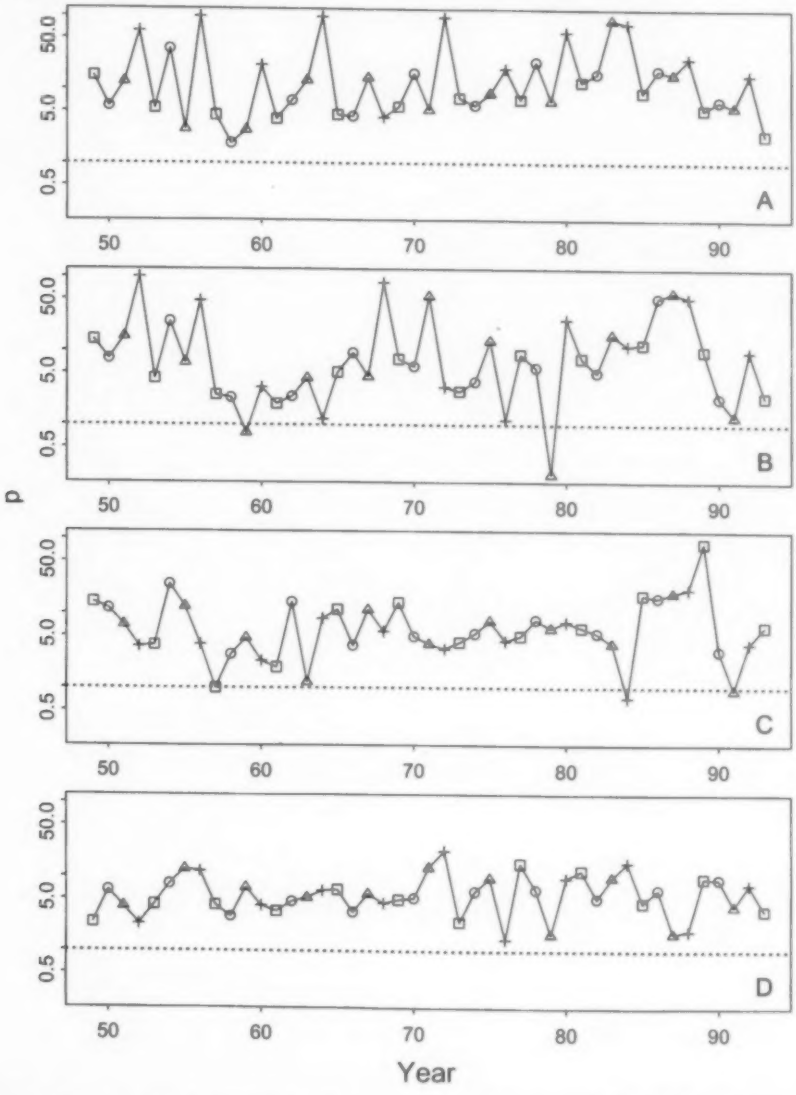

same mixed-stock fishery, harvest rates h_{it} tend to be similar in each year t for all stocks i (Fig. 3). Scatter plots show particularly strong relationships for two stock pairs: (1,2) = (Quesnel,Late Stuart) and (3,4) = (Chilko,Stellako). Furthermore, in cycle 1 (□), all four stocks show coherent patterns of harvest rates. This coherence poses a potential management problem because protection of some stocks might require fishery restrictions, even when other stocks could sustain a higher harvest rate.

2. System analysis

As mentioned in the introduction, our analysis of Summer-run stocks proceeds through four steps toward a formal evaluation of management policy options. Table 1 summarizes these steps and provides a technical outline of the paper. The previous section completes step 1 by defining stocks i ($i = 1,...,m$) with available spawner–recruit data in years t ($t = 1,...,n$), where $m = 4$ and $n = 45$. Based partly on exploratory data analysis (EDA), we focus entirely on age 4 fish. Four-year cycles appear clearly in Fig. 1, with other aspects of cyclic dependence revealed in Figs. 2 and 3.

Step 2 (Table 1) requires translating the conceptual model described earlier into a quantitative model of the form

$$R_{i,t+4} = g(S_{it}, \theta_i) \quad (2.1)$$

© 2000 NRC Canada

Fig. 3. Pairs plot of harvest rates h_{it} in return years 1953–1997 for the Summer-run stocks. Cycles 1–4 are indicated by the symbols □, ○, △, and +, respectively. A line in each panel shows points where the two harvest rates are equal.

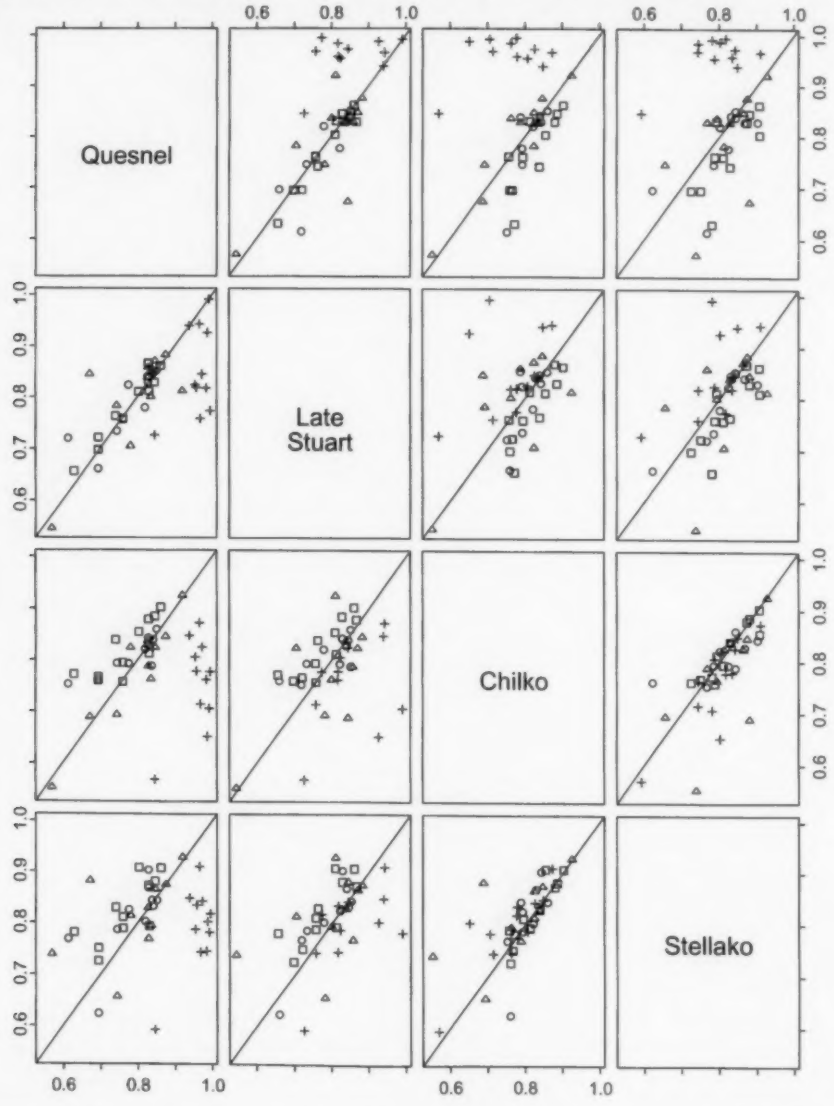

with suitable parameters θ_i for stock i. The complete recruitment parameter vector

$$\phi = (\theta_1, \theta_2, \theta_3, \theta_4)$$

includes parameters from all four stocks. Model (2.1) must also be extended to include the noise inherent in the data. A particular stochastic model implies an inference function, such as a likelihood or Bayes posterior, that can be used to estimate the parameters. We adopt a Bayes perspective and capture uncertainty by drawing an approximately random sample of K parameter vectors

$$(2.2) \quad \Phi_K = \{\phi_k\}_{k=1}^K$$

from the posterior distribution.

Each sample vector ϕ_k in (2.2) represents one possible version of the system dynamics (2.1). Collectively, the sample Φ_K portrays the full spectrum of possibilities, given the data and the chosen model. Both the deterministic function g and the statistical extension of (2.1) involve model choices. We examine various options in section 3 and illustrate their influence on the perceived system dynamics. For example, some models imply much greater certainty in the system dynamics than others.

The analysis so far reflects only an uncertain dynamics, without regard to policy alternatives. To address the policy issue (Table 1, step 3), the space of management options must first be defined. For example, if each catch C_{it} is considered an independent control, then policy space includes $4n$ quantities, one for each stock i and year t. In practice, it

© 2000 NRC Canada

Table 1. Key steps in the analysis of a resource management system.

Step 1. Define the system
Identify components (stocks, space, time)
Compile relevant data
Conduct exploratory data analysis (EDA)
Step 2. Model the dynamics
Devise stochastic model
Construct inference function
Estimate parameters and uncertainty
Conduct model diagnostics and sensitivity analysis
Step 3. Simulate harvest policies
Define policy space
Simulate policy outcomes
Incorporate system uncertainty
Step 4. Evaluate policy results
Define value function
Assign values to policy outcomes
Assess distribution of values

would be difficult to examine fully such a high-dimensional set of controls. Furthermore, as illustrated in Fig. 3, harvest rates in a given year tend to be similar for all four stocks in the mixed-stock fishery. In section 4, we consider a two-dimensional policy space (T, f), dependent on a minimal target escapement T and a removal fraction f applied to the excess population above the target level (Cass and Riddell 1999).

Simulation gives a distribution of outcomes for each policy (T, f), but offers no criterion for choosing an optimal policy. Formal decision theory requires an objective function (Table 1, step 4) that assigns relative values to trajectories of the dynamic system (Keeney and Raiffa 1976). We consider a value function V that depends only on the catch sequence C_{it}. The function includes penalties attached to years in which the fishery drops to low levels. Each policy (T, f) and sample parameter vector ϕ_k in (2.2) gives a simulated trajectory with value $V(T, f|\phi_k)$. Thus, the sample (2.2) implies a distribution of K values V for each policy (T, f). In effect, the value of a policy can be known only within the limits of an uncertain population dynamics.

This overview of the analysis reveals many critical points where choices must be made. We have selected Summer-run stocks of fish at age 4. Given the cyclic character of these stocks, which data are germane to the dynamics (2.1)? Should data from all cycles be used, or only some cycles? For example, we could employ a cycle-dependent model with parameters θ_{ij}, thus multiplying the number of parameters by 4. Alternatively, we could extend the simple stock recruitment model (2.1) to include cross-cycle interactions (Larkin 1971). We could adopt numerous recruitment functions g in (2.1), such as the classical functions of Ricker (1954, 1958), Schaefer (1954, 1957), and Beverton and Holt (1957). The residuals in (2.1) could be normal or lognormal. Consistent with state space model design (Schnute 1994), measurement error could be introduced into the data C_{it} and S_{it}. We could examine more complex policy spaces than the one proposed here, which we apply only to the dominant cycle for stocks 1 and 2 (Quesnel and Late Stuart). The objective function could be tailored to favor either conservation or high exploitation of the fish stocks. Even at a theoretical level, we have made a fundamental choice by adopting a Bayes, rather than frequentist, approach to the decision problem. We restrict the paper's scope by confining ourselves to relatively few cases that illustrate the range of possibilities.

3. Bayesian estimation

Formal parameter estimates require an explicit form of the stock–recruitment function $g(S,\theta)$ in (2.1). Table 2 presents the model applied here. We use the variant (T2.1) of a family of curves proposed by Schnute and Kronlund (1996). These depend on the parameter vector θ in (T2.3). To interpret the components of θ, let $C(S)$ denote the surplus production from the recruitment function (T2.1) for an equilibrium escapement S; that is,

$$C(S) = g(S, \theta) - S.$$

The function $C(S)$ is maximized when $S = S^*$, so that $C^* = C(S^*)$ is the maximum sustainable yield (MSY). Furthermore, the corresponding harvest rate is $h^* = C^*/(S^* + C^*)$. Thus, the parameters S^* and h^* in (T2.1) automatically represent the escapement and harvest rate, respectively, associated with MSY. The third parameter γ defines a range of potential curve shapes, including those proposed by Beverton and Holt ($\gamma = -1$), Ricker ($\gamma = 0$), and Schaefer ($\gamma = 1$). In (T2.1), the Ricker case with $\gamma = 0$ can be obtained from the general case ($\gamma \neq 0$) as the limit when $\gamma \to 0$.

To be mathematically meaningful, the model (T2.1) requires the parameter constraints (T2.4) and (T2.5). Essentially, these restrict the parameters to biologically meaningful ranges, although when $\gamma < -1$, h^* must be even smaller than the obvious upper limit 1. Furthermore, when $\gamma > 0$, the function (T2.1) becomes 0 for sufficiently large values of S, as indicated in (T2.2).

Parameter estimates depend not only on the choice of function g, such as (T2.1), but also on the error structure introduced into the dynamic equation (2.1). We adopt a lognormal error model. A given stock i and data points $\{S_{it}, R_{i,t+4}\}_{t=1}^{n}$ define the residuals (T2.6). We assume that these are independently normally distributed with mean 0 and variance σ_i^2.

Inference functions for θ_i depend on the residual sum of squares Q_i in (T2.7), where the set Y_i denotes a particular set of years used in the analysis. This formulation allows parameter estimates to be based on a restricted set of data points $\{S_{it}, R_{i,t+4}\}$ with $t \in Y_i$. For example, data might be confined to selected cycles. Let N_i denote the number of years in Y_i. Thus, if all available data are used, then $N_i = n$.

We adopt the simple prior distribution $P_0(\theta_i)$ indicated in (T2.8), where the prior on each parameter is uniform across an admissible range and 0 elsewhere (Appendix B, last paragraph). From (T2.4), the prior $P_0(h_i^*|\gamma_i)$ for h_i^* depends on γ_i. Thus, if $\gamma_i \geq -1$, h^* is confined only to the unit interval (0,1) of possible harvest rates; otherwise, a more restrictive interval applies. We confine γ to the somewhat arbitrary interval (–3,3) because this allows for extreme possible shapes of the recruitment function g (Schnute 1985, his figs. 2–4). Based on past history and informal data from the watersheds, we set an upper escapement limit E_i for each stock i, where

$$(E_1, E_2, E_3, E_4) = (5.0, 3.0, 2.0, 0.5) \times 10^6 \text{ fish}. \quad (3.1)$$

© 2000 NRC Canada

Table 2. Recruitment model and Bayesian analysis applied in this paper.

Recruitment model

$$\text{(T2.1)}\quad g(S,\theta)=\begin{cases}\dfrac{S}{1-h^*}\left[1+\gamma h^*\left(1-\dfrac{S}{S^*}\right)\right]^{1/\gamma}; & \gamma\neq 0\\[2ex] \dfrac{S}{1-h^*}\exp\left[h^*\left(1-\dfrac{S}{S^*}\right)\right]; & \gamma=0\end{cases}$$

$$\text{(T2.2)}\quad g(S,\theta)=0;\quad \gamma>0,\quad S\geq S^*\left(1+\frac{1}{\gamma h^*}\right)$$

$$\text{(T2.3)}\quad \theta=(h^*,S^*,\gamma)$$

$$\text{(T2.4)}\quad 0<h^*<\begin{cases}1; & \gamma\geq -1\\ -1/\gamma; & \gamma<-1\end{cases}$$

$$\text{(T2.5)}\quad 0<S^*$$

Residuals

$$\text{(T2.6)}\quad \eta_{it}(\theta_i)=\log R_{i,t+4}-\log g(S_{it},\theta_i)$$

$$\text{(T2.7)}\quad Q_i(\theta_i)=\sum_{t\in Y_i}\eta_{it}(\theta_i)^2$$

Bayes distributions

$$\text{(T2.8)}\quad P_0(\theta_i)\propto P_0(h_i^*\mid\gamma_i)\,P_0(S_i^*)P_0(\gamma_i)$$

$$\text{(T2.9)}\quad P(\theta_i,\sigma_i)\propto\frac{1}{\sigma_i^{N_i+1}}\exp\left[-\frac{1}{2\sigma_i^2}Q_i(\theta_i)\right]P_0(\theta_i)$$

$$\text{(T2.10)}\quad P(\theta_i)\propto[Q_i(\theta_i)]^{-N_i/2}P_0(\theta_i)$$

$$\text{(T2.11)}\quad \hat{\sigma}_i^2=\frac{1}{N_i+1}Q_i(\theta_i)$$

The prior $P_0(S_i^*)$ then restricts S_i^* to the interval $(0,E_i)$.

We choose the standard noninformative prior $P_0(\sigma_i)\propto 1/\sigma_i$ for the scale parameter σ_i, so that $P_0(\log\sigma_i)\propto 1$. Then, (T2.9) specifies the posterior distribution $P(\theta_i,\sigma_i)$. Appendix A shows that the nuisance parameter σ_i can be integrated analytically from the right-hand side of (T2.9) to give the posterior distribution (T2.10) for the recruitment parameter θ_i alone. Furthermore, (T2.11) gives the modal estimate of σ_i, obtained by maximizing (T2.9) with respect to σ_i for fixed θ_i.

We use two methods to estimate parameters and their uncertainty from (T2.10). First, we employ the normal approximation, in which the modal estimate $\hat{\theta}_i$ corresponds to the maximum value of $P(\theta_i)$. Also, if $\mathbf{H}$ denotes the Hessian matrix of second partial derivatives of $\log P(\theta_i)$ evaluated at $\hat{\theta}_i$, then the inverse $\mathbf{H}^{-1}$ approximates the posterior covariance matrix for the parameter vector θ_i. In practice, both $\hat{\theta}_i$ and $\mathbf{H}$ can be computed from the right-hand side of (T2.10) because the constant of proportionality cancels in the approximation

$$\text{(3.2)}\quad \log P(\theta_i)-\log P(\hat{\theta}_i)\approx-\frac{1}{2}\,t(\theta_i-\hat{\theta}_i)\mathbf{H}(\theta_i-\hat{\theta}_i),$$

where the function $t(\cdot)$ denotes the transpose of a column vector.

Our second method of assessing the posterior distribution (T2.10) uses a posterior sample obtained by the Metropolis version of the Markov chain Monte Carlo (MCMC) algorithm (Gelman et al. 1995, chap. 11). In our MCMC implementation (Appendix B), we always start at the modal estimate $\hat{\theta}_i$. The Markov chain moves in step sizes proportional to the standard error for each parameter computed from $\mathbf{H}^{-1}$. We adjust each step with a fixed scale factor s, chosen from trial runs to give about a 50% acceptance rate. An excessively high value s results in a low acceptance rate because steps typically extend beyond regions of reasonable posterior probability. By contrast, a small s leads to a high acceptance rate along a path that wanders too slowly to cover the entire relevant area of parameter space. In our analyses, a suitable value s typically lies between 1 and 2, and diagnostic tests (Appendix B) indicate reasonable convergence when the acceptance rate is about 50%.

Figure 4 illustrates two stock–recruitment curves (γ = –1, 1) estimated from the posterior mode for each of the four stocks, where data for the Quesnel and Late Stuart runs are restricted to cycles 1 and 2. For these two stocks, returns in cycles 3 and 4 have been much smaller than returns from cycles 1 and 2 (Figs. 1A and 1B), and data from the low cycles are subject to considerable measurement error. A diamond symbol on each curve indicates the estimated MSY point $(\hat{S}^*,\hat{R}^*)$, where $R^*=g(S^*,\theta)$ denotes equilibrium MSY recruitment. At this point, the curve has slope 1, that is, its tangent line is parallel to the line $R=S$. For each stock, the Schaefer curve (dashed line) reaches a maximum within the observed data range, and this is also true for estimated Ricker curves (γ = 0, not shown). The asymptotic Beverton–Holt curve (solid line) never reaches a maximum and typically suggests a higher estimate $\hat{S}^*$ than the Schaefer curve. For the Quesnel stock (Fig. 4A), the estimated MSY point from the Beverton–Holt model lies outside the range of historical data.

Table 3 illustrates a sensitivity analysis to the shape parameter γ in a model for the Chilko stock (Fig. 4C), where cases 1–3 correspond to the Beverton–Holt, Ricker, and Schaefer models (γ = –1, 0, 1), respectively. We examine modal estimates $(\hat{h}^*,\hat{S}^*)$ computed from (T2.10) and means $(\bar{h}^*,\bar{S}^*)$ obtained from a posterior sample of size 10 000. These have standard errors SE_H and SE_M obtained, respectively, from the modal Hessian and the MCMC sample. In this example, all estimates of h^* have similar values, although estimates of S^* exhibit greater variability. Consistent differences occur between modal estimates and means:

$$\text{(3.3)}\quad \hat{h}^*>\bar{h}^*,\quad \hat{S}^*<\bar{S}^*,$$

with particularly marked differences in the second inequality (3.3). Standard errors from the MCMC sample are consistently higher than those obtained from the modal Hessian. Again, differences are most striking for standard errors of S^*. In practice, the MCMC estimate $(\bar{h}^*,\bar{S}^*)$ suggests a more conservative policy with a lower harvest rate and higher escapement target than the modal estimate $(\hat{h}^*,\hat{S}^*)$.

© 2000 NRC Canada

Fig. 4. Stock–recruitment curves of the form (T2.1) fitted to data for the (A) Quesnel, (B) Late Stuart, (C) Chilko, and (D) Stellako stocks $i = 1,...,4$. Solid and dashed curves indicate the Beverton–Holt ($\gamma = -1$) and Schaefer ($\gamma = 1$) formulations, respectively. For each model, the diamond symbol indicates the MSY point where $S = S^*$. A dotted line shows the equilibrium replacement condition $R = S$. Analyses of the Chilko and Stellako stocks include all available data points (S_{it}, $R_{i,t+4}$) from years $t = 1,...,45$ (1949–1993). Data for the Quesnel and Late Stuart stocks are restricted to cycles 1 and 2 only.

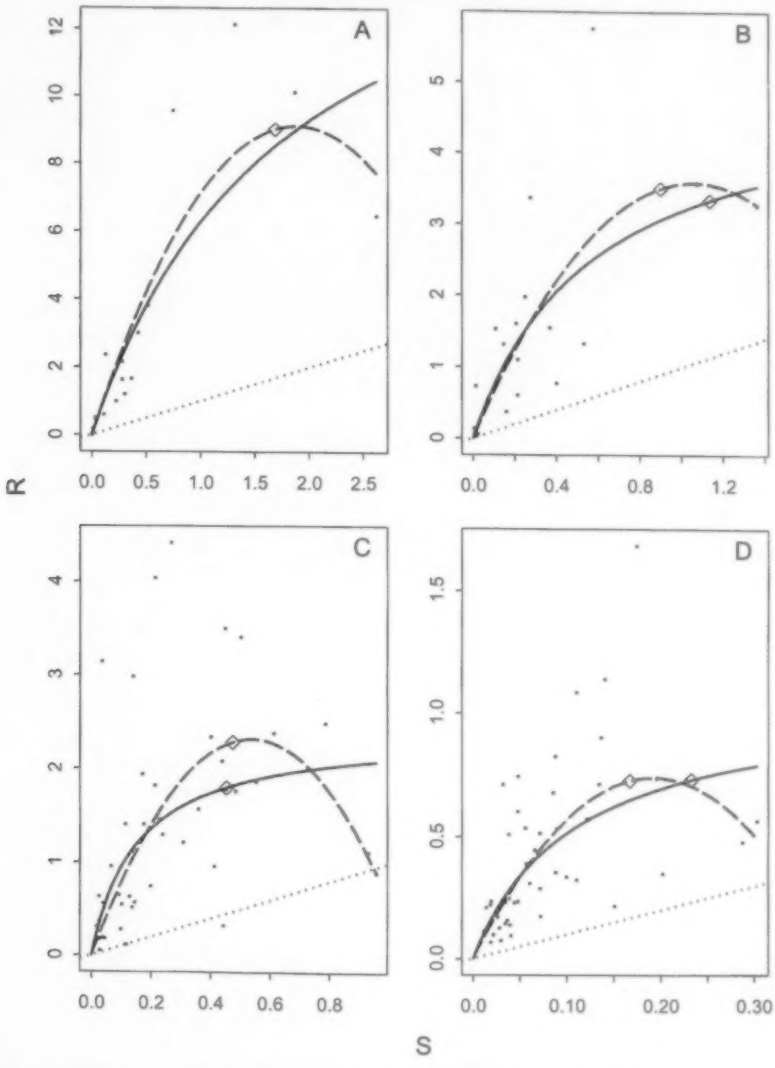

Each result in Table 3 depends on a fixed parameter γ. Table 4 gives similar results for a model of the Chilko stock ($i = 3$) in which all three parameters $\theta = (h^*, S^*, \gamma)$ are estimated. The MCMC sample includes 40 000 points. Figure 5 portrays 3000 points extracted systematically from this sample, where pairs plots include the value $P(\theta)$ for each sample point θ. The posterior probability profiles (bottom panels of Fig. 5) visually identify the modal estimate $\hat{\theta}$ in Table 4, as discussed further in Appendix B. These profiles also explain the inequalities (3.3) because modes occur at the high and low ends, respectively, of the h^* and S^* distributions. The profile for γ is more nearly symmetric. Although the mode ($\hat{\gamma} = 0.15$) and the mean ($\bar{\gamma} = -0.54$) estimates differ somewhat, the discrepancy is modest compared with the estimated standard error. For γ, the Hessian and MCMC sample methods give similar error estimates ($SE_H(\gamma) = SE_M(\gamma) = 0.91$). By contrast, for h^* and S^*, the error estimate from the MCMC sample is larger than the modal Hessian estimate, similar to results in Table 3. Thus, highly skewed distributions of h^* and S^* (Fig. 5) produce greater variability than suggested by the normal approximation at the mode.

Three scatter plots in Fig. 5 reveal a rather complex correlative structure in the posterior distribution (T2.10) of $\theta = (h^*, S^*, \gamma)$. First, the (h^*, S^*) plot shows a comet-like distribution with a slight negative correlation. The dense comet head occupies a region of relatively low values S^* and high values h^*, consistent with the skewed probability profiles discussed above. The prior constraint $S^* < 2$, associated with

© 2000 NRC Canada

Table 3. Modal estimates (^), sample means (¯), standard errors from the posterior Hessian (SE_H) and an MCMC sample (SE_M), fixed scale factors s chosen by experimentation, and corresponding acceptance rates for three choices of the shape parameter ($\gamma = -1, 0, 1$), based on data from the Chilko stock ($i = 3$) and MCMC samples of size 10 000 from the posterior (T2.10).

	Case 1	Case 2	Case 3
γ	−1.00	0.00	1.00
$\hat{h}^*$	0.71	0.78	0.79
$\bar{h}^*$	0.69	0.76	0.77
$SE_H(h^*)$	0.04	0.03	0.02
$SE_M(h^*)$	0.04	0.04	0.03
$\hat{S}^*$	0.49	0.37	0.47
$\bar{S}^*$	0.68	0.49	0.56
$SE_H(S^*)$	0.17	0.08	0.03
$SE_M(S^*)$	0.32	0.22	0.14
s	1.50	1.60	2.00
Rate	0.50	0.54	0.54

the Chilko escapement limit $E_3 = 2$ defined in (3.1), restricts the extent of the comet's tail.

Second, the (γ, h^*) plot shows a thin limb descending toward the lower left. This corresponds to the constraint (T2.4). Thus, when $\gamma < -1$, probable values h^* lie at the high end of the admissible range $h^* < -1/\gamma$. As γ increases from −2 to 0, the distribution of h^* increases almost linearly, followed by a more gradual increase in h^* as γ moves through the range 0 to 3. This trend agrees with that shown for the estimates $\hat{h}^*$ and $\bar{h}^*$ in Table 3.

Third, the (γ, S^*) plot shows the influence of prior upper bounds for γ and S^*: $\gamma < 3$ and $S^* < 2$. The majority of points lie in a boomerang-shaped distribution oriented to give a decreasing variance of S^* as γ increases. This feature, also evident in the estimates $SE_H(S^*)$ and $SE_M(S^*)$ (Table 3), has an intuitive geometric explanation. As discussed above, the MSY point (S^*, R^*) on the recruitment curve has an associated tangent line with slope 1. (Mathematically, the equilibrium catch $C(S) = g(S,\theta) - S$ is maximized when $dC/dS = 0$ or $dg/dS = 1$.) Figure 4 shows that this point (◇) occurs on a relatively flat section of the curve when $\gamma = -1$, compared with a section of higher curvature when $\gamma = 1$. In general, as γ increases, the curvature at (S^*, R^*) increases, thus giving better definition to the point where the slope is 1.

The modal value of γ in Fig. 5 suggests that a Ricker curve ($\gamma = 0$) might be representative for the Chilko stock. To illustrate a Bayesian decision analysis in the next section, we consider a Ricker model for each stock $i = 1,..., 4$. As in Fig. 4, data for the Quesnel and Late Stuart stocks ($i = 1, 2$) are restricted to cycles 1 and 2. Figure 6 shows the four corresponding comet-shaped distributions (h^*, S^*), where each scatter plot portrays 1000 points taken systematically from an MCMC sample of size 20 000. The influence of prior constraints $S_i^* < E_i$ from (3.1) can be seen for three stocks ($i = 1, 2, 4$; Figs. 6A, 6B, and 6D). All four distributions indicate high uncertainty in S^*, with h^* relatively well defined in a region centered near 0.75.

Contours in Fig. 6 are computed directly from the posterior function (T2.10) with $\gamma = 0$, based on probability quantiles from the MCMC sample. For instance, the sample used to produce Fig. 6A includes 20 000 values $P(h^*, S^*)$. If these are scaled to a maximum value 1 at the mode, then the 20, 40, 60, and 80% quantiles for $P(h^*, S^*)$ are, respectively, 0.13, 0.30, 0.50, and 0.73. Contours in Fig. 6A correspond to these scaled values of the posterior function (T2.10). Thus, points external to the outermost contour occur with probability 20%, and points occur inside this contour with probability 80%. Similarly, the innermost contour defines two regions: an exterior with probability 80% and an interior with probability 20%.

Table 4. Parameter estimates and standard errors for the model with three free parameters $\theta = (h^*, S^*, \gamma)$, based on data from the Chilko stock ($i = 3$) and an MCMC sample of size 40 000 from the posterior (T2.10).

Quantity	h^*	S^*	γ
$\hat{\theta}$	0.79	0.38	0.15
$\bar{\theta}$	0.70	0.74	−0.54
$SE_H(\theta)$	0.03	0.09	0.91
$SE_M(\theta)$	0.08	0.41	0.91

4. Policy evaluation

Scatter plots and contours in Fig. 6 portray the range of uncertainty in system dynamics for each of the four Summer-run stocks (Table 1, step 2). In this section, we define a policy space (step 3) and evaluate policy results (step 4). Table 5 formalizes the definition of a two-dimensional policy (T, f) mentioned earlier in section 2. Special cases (T, 1) and (0, f) correspond, respectively, to setting a fixed escapement target T or a fixed harvest rate f. Equations (T5.1) and (T5.2) partition the total escapement target T into separate targets for each stock, based on ratios ρ_i defined by the escapement limits (3.1). These stock-dependent targets are held constant through time, so that (T5.2) specifies a target escapement T_{it} for each stock i and year t. Similarly, (T5.3) applies the harvest fraction f to all stocks and years. We interpret (T_{it}, f_{it}) as simple control rules. The fishery is opened in year t only if the target escapement T_{it} can be achieved for each stock i. Thus, a weak stock i with returns R_{it} in year t causes fishery closure if $R_{it} \leq T_{it}$. When the fishery is open, a maximum fraction f_{it} of the surplus production $R_{it} - T_{it}$ can be removed as catch.

As discussed in the introduction, we restrict our policy analysis to years for which historical data are available. In this context, we examine potential consequences of policies different from those pursued historically. Perhaps the simplest retrospective simulations would apply the observed productivities p_{it}, calculated from the raw data in (1.4). This approach would bypass the need for modeling and uncertainty analysis, as in section 3, but it would fail to address an important issue. If we choose a restrictive harvest policy that allows rapid stock rebuilding, can historical productivities p_{it} be maintained? As stocks become large, we might expect carrying capacity to become a limitation, thus reducing the number of recruits per spawner from observed historical lev-

© 2000 NRC Canada

Fig. 5. Pairs plot of 3000 estimates (h^*, S^*, γ) taken from an MCMC sample of length 40 000 for the Chilko stock $i = 3$. Each estimate has an associated posterior value $P(h^*, S^*, \gamma)$ from (T2.10), scaled here to a maximum value 1.

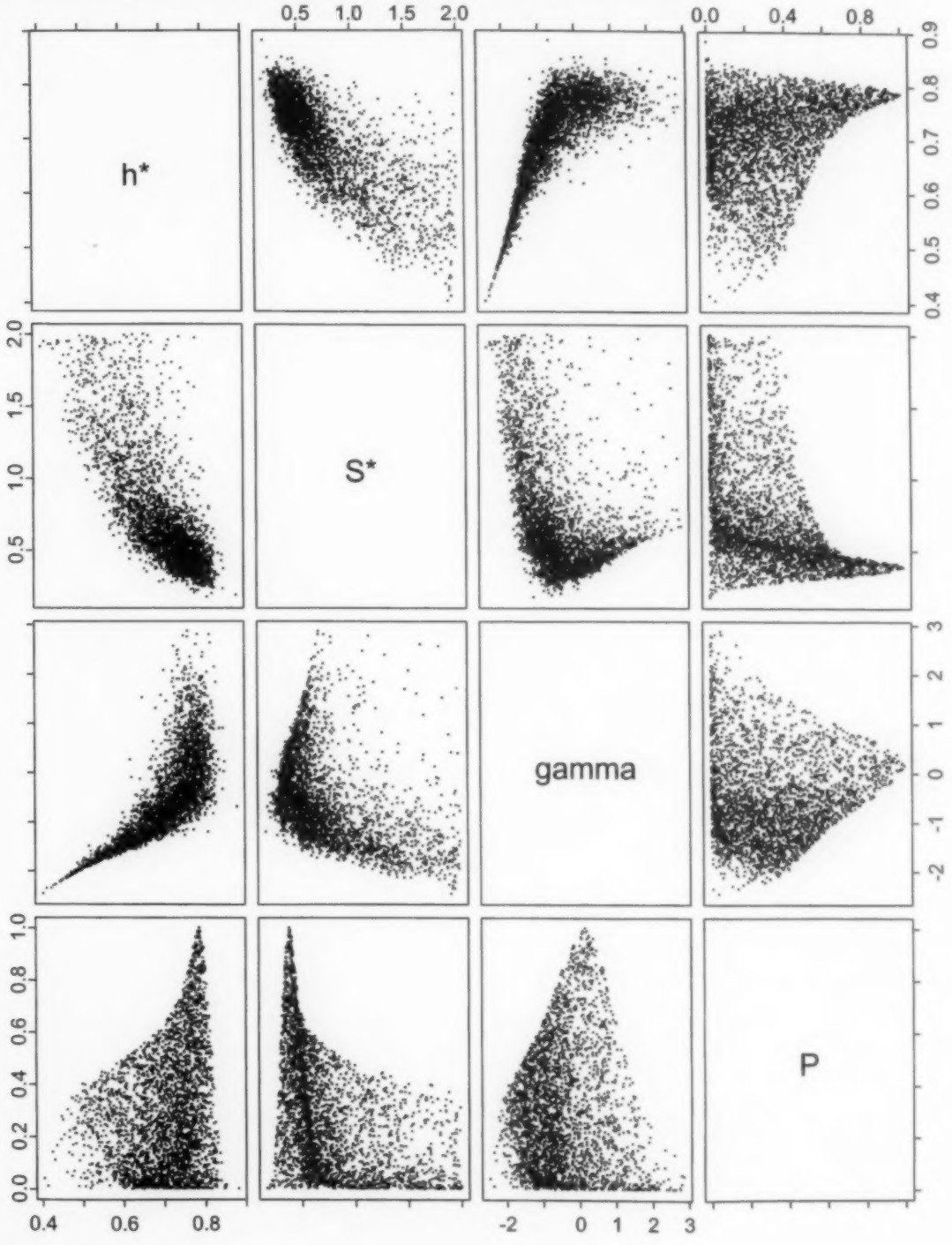

© 2000 NRC Canada

Fig. 6. (A–D) Scatter plots of 1000 estimates (h^*, S^*) with fixed $\gamma = 0$ taken from an MCMC sample of length 20 000 for each stock as specified in Fig. 4. Contour lines in each panel are computed exactly from the posterior function (T2.10), corresponding to 20, 40, 60, and 80% posterior confidence regions.

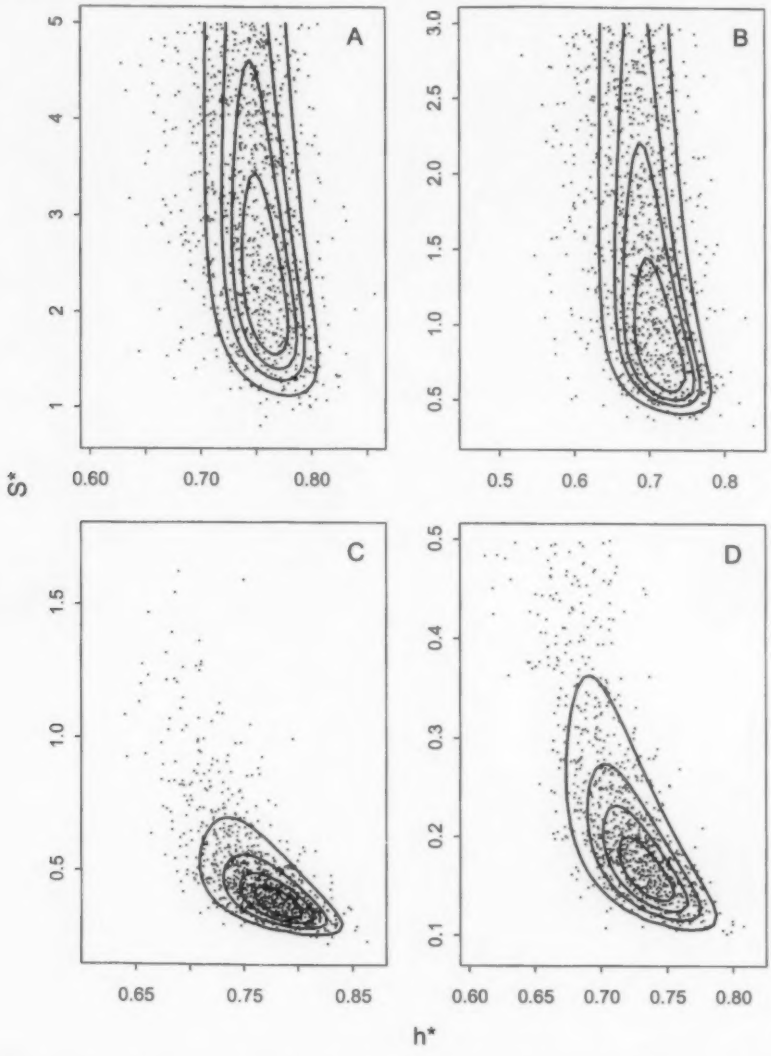

els. A more realistic approach would consider existing evidence of limited capacity for each stock. The comet-shaped distributions in Fig. 6 precisely capture this evidence, where modest capacities S^* in the comet head have higher probability than extreme values S^* in the tail.

Equations (T5.4)–(T5.9) describe a retrospective simulation of the policy (T, f), based on the recruitment model (2.1). We use a prime accent (′) to distinguish reconstructed values from their historical counterparts. Thus, S'_{it} denotes a simulated number of spawners for the given policy, in contrast with the observed historical number S_{it}. Each policy has an uncertain outcome associated with the unknown parameter vectors θ_i $(i = 1,...,4)$. We capture this uncertainty by taking sample vectors θ'_i from the MCMC samples used to create Fig. 6. A single reconstruction (T5.4)–(T5.9) depends on the sample $\phi' = \{\theta'_i\}_{i=1}^4$ and the policy (T, f).

Equation (T5.4) initializes the number of spawners in each cycle to their numbers at the start of the historical time series. Subsequently, (T5.5)–(T5.9) define an iterative calculation for $t \geq 5$. Residuals $\eta'_{i,t-4}$ associated with θ'_i are calculated from the observed historical data and then used to predict recruits R'_{it} in the next generation. For each stock i and year t, (T5.6) adjusts the simulated recruitment curve up or down to pass through the historical data point $(S_{i,t-4}, R_{it})$. It follows from (T5.5) and (T5.6) that

$$(4.1) \quad R'_{it} = R_{it} \frac{g(S'_{i,t-4}, \theta'_i)}{g(S_{i,t-4}, \theta'_i)}.$$

Thus, the simulated recruitment equals the historical recruitment $(R'_{it} = R_{it})$ whenever the simulated and historical spawners match in the previous generation $(S'_{i,t-4} = S_{i,t-4})$. Ef-

© 2000 NRC Canada

Table 5. Harvest policy, retrospective simulation, and value function for Bayesian decision analysis.

Harvest policy (T, f)

(T5.1) $\rho_i = \dfrac{E_i}{E_1 + E_2 + E_3 + E_4}$

(T5.2) $T_{it} = \rho_i T$

(T5.3) $f_{it} = f$

Simulation with $\phi' = \{\theta_i'\}_{i=1}^4$

(T5.4) $S'_{it} = S_{it}$: $1 \le t \le 4$

For $t \ge 5$:

(T5.5) $\eta'_{i,t-4} = \log R_{it} - \log g(S_{i,t-4}, \theta_i')$

(T5.6) $R'_{it} = g(S'_{i,t-4}, \theta_i') \exp(\eta'_{i,t-4})$

(T5.7) $h'_t = \min_i \max\left[0, f_{it}\left(1 - \dfrac{T_{it}}{R'_{it}}\right)\right]$

(T5.8) $C'_{it} = h'_t R'_{it}$

(T5.9) $S'_{it} = R'_{it} - C'_{it}$

Harvest value for $t \in Y$

(T5.10) $C'_t = \sum_{i=1}^{4} C'_{it}$

(T5.11) $\delta'_t = \begin{cases} 0, & \text{if } C'_t \ge D \\ 1, & \text{if } C'_t < D \end{cases}$

(T5.12) $V(T, f \mid \phi', v, w, D) = \dfrac{1}{N} \sum_{t \in Y} (v C'_t - w \delta'_t)$

fectively, the model uses the nonlinear recruitment function $g(S, \theta_i')$ to set a relative scale between simulated and historical spawners. By contrast, a linear scaling

$$(4.2) \quad R'_{it} = R_{it} \frac{S'_{i,t-4}}{S_{i,t-4}} = p_{i,t-4} S'_{i,t-4}$$

gives the historical productivity model mentioned above, which does not depend on θ_i'.

Equation (T5.7) translates the policy (T_{it}, f_{it}) into a single harvest rate h'_t for all stocks. The allowable rate for a given stock i is the product of two factors, f_{it} and $1 - T_{it}/R'_{it}$, where the second assures that the target T_{it} is achieved. If recruitment R'_{it} is inadequate (i.e., $R'_{it} < T_{it}$), this factor is negative, and the maximum function defines a zero harvest rate. The minimum function restricts the overall harvest rate so that no stock i is overharvested. Straightforward equations (T5.8) and (T5.9) give the projected catch C'_{it} and escapement S'_{it}, after which the iteration proceeds to the next year t. In the analysis here, we confine our reconstructions to the single cycle $j = 1$. Thus, we examine only years corresponding to the dominant cycle line for the Quesnel and Late Stuart stocks.

In summary, a single reconstruction (T5.4)–(T5.9) depends on a policy (T, f) and a sample parameter vector ϕ'. The simulation gives a complete population trajectory for every stock, including the catches C'_{it}. Step 4 (Table 1) requires an objective function to evaluate the chosen policy. We adopt the simple value function V defined by (T5.10)–(T5.12). Our notation allows V to be associated with a particular set Y of N years. In the example here, $Y = (1953, 1957, \ldots, 1993, 1997)$ consists of $N = 12$ years from cycle 1. To reflect a possible loss associated with a closed fishery, V depends on a specified minimum catch level D. The quantity δ'_t in (T5.11) serves as an indicator of whether or not the total reconstructed catch C'_t in (T5.10) drops below D. The function V in (T5.12) assigns a value v to each unit of catch and a loss w to each instance of a fishery with catch less than D. If $w = 0$, no penalty is attached to a minimal fishery, so that the value of D becomes irrelevant. For example, when $(v, w) = (1, 0)$, V represents the average annual catch. Similarly, when $(v, w) = (0, -1)$, V gives the proportion of years in which the catch fell below the acceptable level D.

For a fixed policy (T, f) and specified quantities (v, w, D), an MCMC sample of parameters ϕ' gives a spectrum of values $V(T, f \mid \phi', v, w, D)$. Based on 250 samples ϕ' from the runs used to produce Fig. 6, Fig. 7 shows mean values of V across a range of policies in the two cases mentioned above when $D = 0.5$. Thus, the top and bottom panels represent, respectively, the mean catch and the probability of a fishery below 0.5 million fish.

In Fig. 7 (top panel), contours suggest a correlated influence between T and f. A low escapement target T with a low harvest rate f on the surplus can give an average catch similar to that achieved by a high T with a high f. The figure shows a diagonal ridge with a maximum average annual catch of above 11 million fish, in comparison with the historical average catch of 5.3 million fish per year in cycle 1. A steep decline from the ridge in the upper left corresponds to a combined low T and high f that drives the population to extinction, thus giving a low average catch. The ridge drops more gradually to the lower right, where reduced fishing pressure produces less catch. As mentioned earlier, the policy $(0, f)$, i.e., the f-axis where $T = 0$, corresponds to a policy with a fixed harvest rate f. Along this axis, the mean catch V reaches a maximum of 9.3 million fish per year when f is between 0.6 and 0.7. Similarly, the policy $(T, 1)$, i.e., the line $f = 1$ parallel to the T-axis, corresponds to the removal of all fish above the escapement target T. Along this line, V reaches a maximum of 11.2 million fish per year for T near 1.5 million fish.

Figure 7 (bottom panel) shows contours of probability that the fishery will be effectively closed, here defined as a fishery that produces fewer than 0.5 million fish. In the middle range of the graph, vertical contours suggest that closure probability increases primarily with T, where a target T = 1.5 million fish gives almost a 30% closure probability. Close contours in the upper left correspond to high fishing mortalities that drive the population to extinction. Higher rates of mortality produce extinction earlier in the time series and, consequently, more frequent closures. At the lower right of the figure, for high escapement targets $T > 2$ million fish, it appears that the probability of closure is actually reduced by increasing f. This feature results from the Ricker stock–recruitment curve, which implies low returns R from very high spawner abundance levels S. Within this framework, some harvest from a very large run gives improved returns in the next generation.

Figure 7 (top panel) suggests that the maximum annual catch can be achieved by setting an escapement target $T >$ 0.6 million fish. However, Fig. 7 (bottom panel) indicates a cost associated with high escapement targets: more frequent

© 2000 NRC Canada

Fig. 7. Mean contours of the value function V in relation to policy choices (T, f), based on values V corresponding to 250 parameter vectors ϕ' drawn from the MCMC runs used in Fig. 6. The top and bottom panels correspond, respectively, to the cases $(v, w, D) = (1, 0, 0.5)$ and $(v, w, D) = (0, -1, 0.5)$.

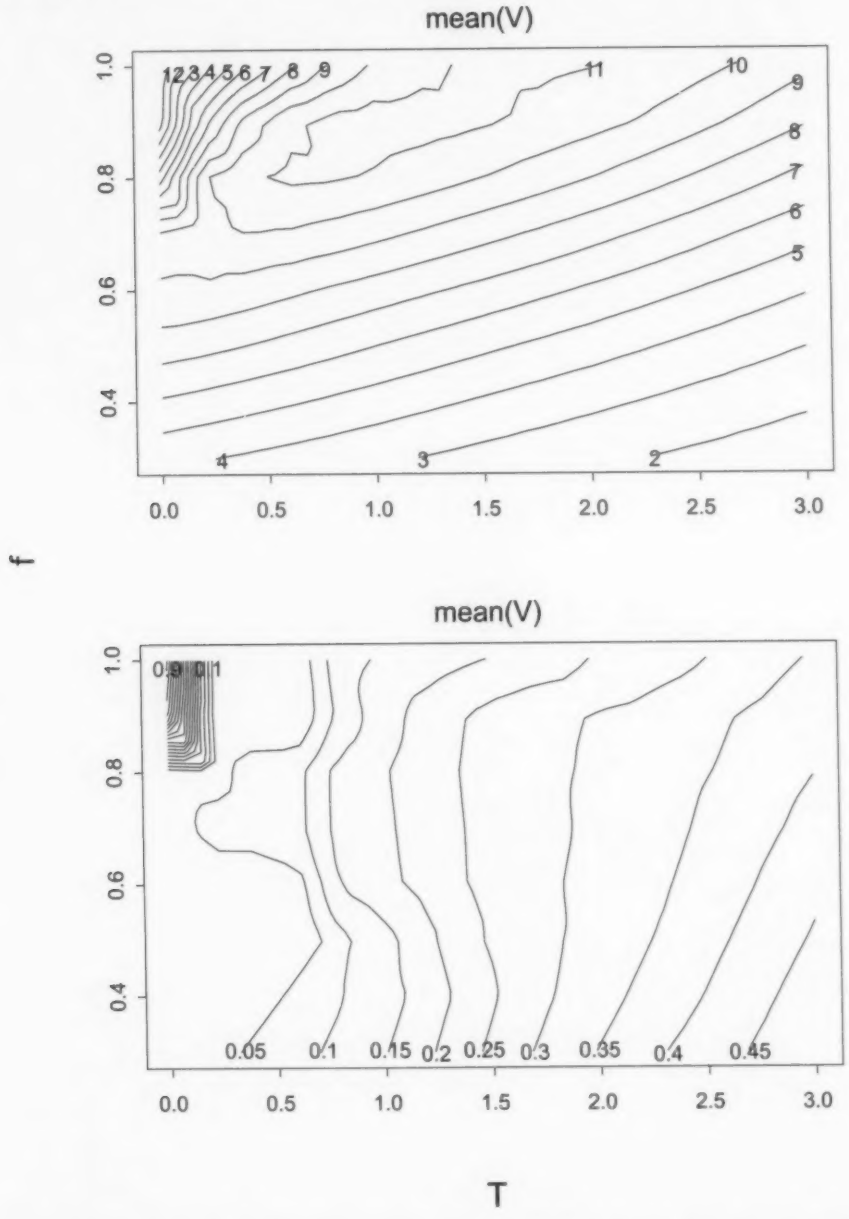

fishery closures. Figure 8 (top panel) seeks a compromise between benefits and costs, where the value $v = 1$ for each million fish caught is offset by a penalty $w = 10$ for each instance of effective fishery closure. In this case, a maximum penalized average catch of about 10 million fish per year is achieved with policies (T, f) near (0.6, 0.85). As in Fig. 7 (top panel), contours here follow a diagonal from lower left to upper right. Thus, a range of options (T, f) appear to give similar harvest values V. In Fig. 8 (bottom panel), however, it appears that policies with high T and high f typically give more variation in V (i.e., a higher standard error) than policies in which T and f are low. The higher variation results partly from more frequent fishery closures. At the other extreme, low variation associated with low T and high f results from consistently low catches as the stocks collapse from overfishing.

In practice, a manager might examine Fig. 8 (top panel) to find a policy (T, f) that gives high value, without coming too

© 2000 NRC Canada

Fig. 8. Contours of the mean and standard error (SE) for the value function V in relation to policy choices (T, f) when $(v, w, D) = (1, 10, 0.5)$. The V distribution comes from 250 sample parameters vectors ϕ' used in Fig. 7.

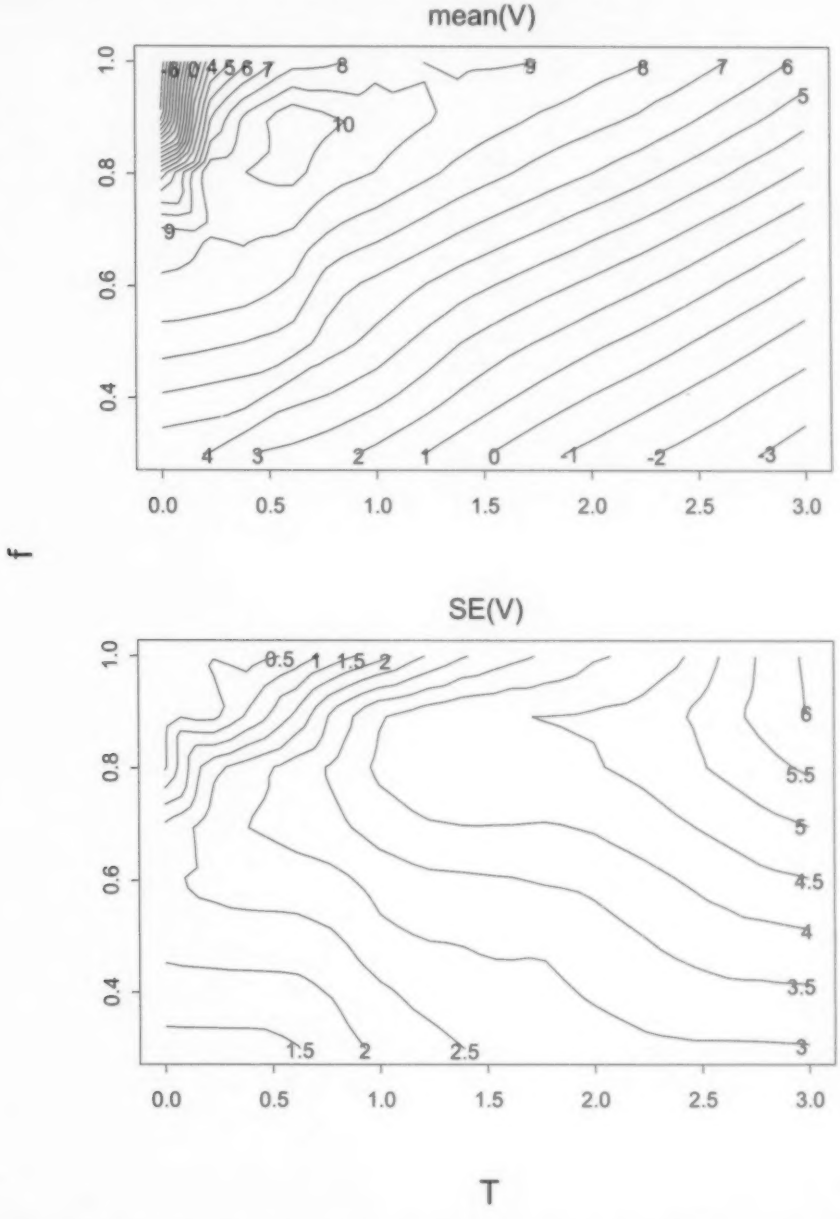

close to the steep decline at the upper left. The choice might also be guided by seeking a low standard error in Fig. 8 (bottom panel), particularly if a steady fishery from year to year is desirable. Figure 7 offers further detail, by showing separately the effects of policy on catch and fishery closures.

Discussion

Modern posterior sampling techniques make Bayesian theory tractable for complex applied problems (Gelman et al. 1995; Gilks et al. 1996). Recent fishery literature illustrates the use of sampling with importance resampling (McAllister et al. 1994; Kinas 1996; McAllister and Ianelli 1997), Gibbs samplers (Meyer and Millar 1999), and MCMC methods (Patterson 1999). In this paper, we follow the outline in Table 1 to illustrate a complete system analysis for a multistock fishery on Fraser River sockeye salmon. Scatter plots in Fig. 5 portray highly nonnormal parameter distributions, typical of those encountered in realistic fishery models. The Bayesian approach offers the advantage that

© 2000 NRC Canada

such complex distributions can be readily incorporated into the policy analysis.

To confine our paper to manageable scope, we have made numerous simplifying assumptions. We consider our analysis illustrative, rather than definitive, as a guide to Fraser sockeye management. Each step in the analysis (Table 1) necessitates choices that can influence the outcome. Choices made in one step can alter the options available in subsequent steps. For example, if step 1 includes additional data sources, then more possibilities exist for the dynamic model in step 2. Similarly, greater model complexity in step 2 may give a wider range of policy options in step 3. In practice, policy development proceeds iteratively by examining the consequences of different assumptions.

In step 1, we restrict our analysis to specific data sets, stocks, cycle lines, and ages. Fraser sockeye have been intensively studied and a number of alternative data sets are available. For the Chilko stock, smolt abundance has been measured for most years since 1948 and could be incorporated as a covariate in the recruitment model. Spawning habitat data available for Quesnel and Chilko stocks could provide independent estimates of carrying capacity (Hume et al. 1996). Various climate indices could be examined in relation to rates of survival and spawning success.

In step 2, we apply a simple dynamic model with one age-class. A more complex age-structured model could be used to explore interactions among stocks and cycle lines, or (given appropriate data in step 1) the value of environmental indices as explanators of survival. Alternative error structures could also be examined. For example, a square root transformation, rather than the logarithm in (T2.6), would give more weight to high points in the stock–recruitment relationship. The model could also acknowledge measurement error in estimates of catch and spawning escapement. Current stock identification methods applied to multistock catches result in underestimates for large stocks and overestimates for small stocks (Cass and Wood 1994). Furthermore, overlap of stocks from other timing groups with the Summer-run stocks can make identification even more difficult. A thorough sensitivity analysis of alternative models lies beyond the scope of this paper. We do, however, examine model sensitivity to the shape parameter γ in Table 3 and Fig. 5.

In step 3, we examine only a simple two-dimensional policy. This could be extended to higher dimensional policies that vary in time and depend on stock size. Adaptive strategies (Walters 1986) could probe higher escapement levels to reduce uncertainty in S^*. Current management of Fraser sockeye is adaptive and adjusts the harvest rate to achieve stock-specific escapements within a fixed range, based on circumstances particular to each year t. For example, in 1997 and 1998, estimates of returning sockeye declined during their river migration, possibly due to high mortality from adverse environmental conditions, Thus, harvest rates in these years were reduced during the fishing season. On a broader scale, the policy here must be extended to consider other salmon species and sockeye stocks captured in the fishery on Summer runs. Furthermore, if the model in step 2 accounts for interactions among stocks and cycle lines, then the policy should look beyond the single cycle 1 considered here. For example, if strong stocks in cycle 1 act to suppress stocks in other cycles, then it might even be advisable to fish cycle 1 more heavily to create greater biological opportunity for stocks in other cycles.

In general, a policy (T, f) cannot be implemented precisely, due to noisy measurements and variable behavior of fish and fishers. Our analysis makes no attempt to consider implementation error; thus, the simulation model in Table 5 assumes that the harvest rate (T5.7) is achieved exactly. Furthermore, our retrospective study uses observed process error, that is, the actual pattern of historical residuals (T5.5) to simulate outcomes consistent with historical sockeye productivity. This calculation hides the role of the parameter σ, which is implicit in (T5.5). Futuristic policy evaluations would need to simulate process error using explicit estimates $\hat{\sigma}$ obtained from an MCMC sample of the full posterior distribution (T2.9). Such simulations might even attempt to capture ecosystem changes. For example, our data come from a period of stock rebuilding under climatic conditions perhaps more favorable than current conditions.

The value function in step 4 must incorporate trade-offs among potentially conflicting demands. Even our simple choice (T5.12), based solely on the simulated catch trajectory C_t', offers a range of alternative choices (v, w, D). Other forms of the value function could be chosen to reflect a nonlinear scale for the catch. For example, a logarithmic scale (log C_t) would decrease the relative value of high catches and favor harvest policies that avoid low catches (Deriso 1985; Walters and Ludwig 1987). The Bayesian framework here captures the full range of probable parameters, including long comet tails for S^*. The choice of scale in the value function influences the balance between potential losses and gains. Ultimately, the value function must be tailored to reflect societal values and tolerance to risk. In practice, policy makers need to establish targets or reference points (Schnute and Richards 1998) and the acceptable probability of exceeding them, as advocated by the precautionary approach to fisheries management (Richards and Maguire 1998).

Our analysis at least offers a framework for investigating the influence of model assumptions on policy design. A value function, such as (T5.12), translates results from the statistics of population models into the practical realm of public policy. We have investigated a rather complex multistock fishery with a control rule (T5.7) that protects stocks with low abundance. In spite of numerous simplifications, contours of the value function in Figs. 7 and 8 suggest a compromise between the spawning target T and the harvest rate f on surplus fish. Such broad conclusions can guide the development of more complex scenarios, in which managers play an active role in the development of policies and value functions analogous to (T5.7) and (T5.12).

Acknowledgements

We thank two anonymous reviewers for suggestions leading to an improved final draft.

References

Beverton, R.J.H., and Holt, S.J. 1957. On the dynamics of exploited fish populations. U.K. Minist. Agric. Fish. Food, Fish. Invest. Ser. 2. No. 19.

© 2000 NRC Canada

Cass, A., and Riddell, B. 1999. A life history model for assessing alternative management policies for depressed chinook salmon. ICES J. Mar. Sci. **56**: 414–421.

Cass, A.J., and Wood, C.C. 1994. Evaluation of the depensatory fishing hypothesis as an explanation for population cycles in Fraser River sockeye salmon (*Oncorhynchus nerka*). Can. J. Fish. Aquat. Sci. **51**: 1839–1854.

Collie, J.S., and Walters, C.J. 1987. Alternative recruitment models of Adams River sockeye salmon, *Oncorhynchus nerka*. Can. J. Fish. Aquat. Sci. **44**: 1551–1561.

Collie, J.S., Peterman, R.M., and Walters, C.J. 1990. Experimental harvest policies for a mixed stock fishery: Fraser River sockeye salmon, *Oncorhynchus nerka*. Can. J. Fish. Aquat. Sci. **47**: 145–155.

Deriso, R.B. 1985. Risk averse harvesting strategies. *In* Lecture notes in biomathematics. Vol. 61. *Edited by* M. Mangel. Resource Management: Proceedings of the Second Ralf Yorque Workshop, Ashland, Oregon, 1984. Springer-Verlag, New York. pp. 65–73.

Eggers, D.M., and Rogers, D.E. 1987. The cycle of runs of sockeye salmon (*Oncorhynchus nerka*) to the Kvichak River, Bristol Bay, Alaska: cyclic dominance of depensatory fishing? *In* Sockeye salmon (*Oncorhynchus nerka*) population biology and future management. *Edited by* H.D. Smith, L. Margolis, and C.C. Wood. Can. Spec. Publ. Fish. Aquat. Sci. No. 96. pp. 343–366.

Gable, J., and Cox-Rogers, S. 1993. Stock identification of Fraser River sockeye salmon: methodology and management application. Pac. Salmon Comm. Tech. Rep. No. 5.

Gelman, A., Carlin, J.B., Stern, H.S., and Rubin, D.B. 1995. Bayesian data analysis. Chapman and Hall, London, U.K.

Gilks, W.R., Richardson, S., and Spiegelhalter, D.J. 1996. Markov chain Monte Carlo in practice. Chapman and Hall, London, U.K.

Hume, J.M.B., Shortreed, K.S., and Morton, K.F. 1996. Juvenile sockeye rearing capacity of three lakes in the Fraser River system. Can. J. Fish. Aquat. Sci. **53**: 719–733.

Keeney, R.L., and Raiffa, H. 1976. Decisions with multiple objectives. Wiley, New York.

Kinas, P.G. 1996. Bayesian fishery stock assessment and decision making using adaptive importance sampling. Can. J. Fish. Aquat. Sci. **53**: 414–423.

Larkin, P.A. 1971. Simulation studies of the Adams River sockeye salmon, *Oncorhynchus nerka*. J. Fish. Res. Board Can. **28**: 1493–1502.

Levy, D.A., and Wood, C.C. 1992. Review of proposed mechanisms for sockeye salmon population cycles in the Fraser River. Bull. Math. Biol. **54**: 241–261.

McAllister, M.K., and Ianelli, J.N. 1997. Bayesian stock assessment using catch–age data and the sampling-importance resampling algorithm. Can. J. Fish. Aquat. Sci. **54**: 284–300.

McAllister, M.K., Pikitch, E.K., Punt, A.E., and Hilborn, R. 1994. A Bayesian approach to stock assessment and harvest decisions using the sampling/importance resampling algorithm. Can. J. Fish. Aquat. Sci. **51**: 2673–2687.

Meyer, R., and Millar, R.B. 1999. Bayesian stock assessment using a state–space implementation of the delay difference model. Can. J. Fish. Aquat. Sci. **56**: 37–52.

Myers, R.A., Mertz, G., Bridson, J.M., and Bradford, M.J. 1998. Simple dynamics underlie sockeye salmon (*Oncorhynchus nerka*) cycles. Can. J. Fish. Aquat. Sci. **55**: 2355–2364.

Patterson, K.R. 1999. Evaluating uncertainty in harvest control law catches using Bayesian Markov chain Monte Carlo virtual population analysis with adaptive rejection sampling and including structural uncertainty. Can. J. Fish. Aquat. Sci. **56**: 208–221.

Richards, L.J., and Maguire, J.-J. 1998. Recent international agreements and the precautionary approach: new directions for fisheries management science. Can. J. Fish. Aquat. Sci. **55**: 1545–1552.

Ricker, W.E. 1950. Cyclic dominance among the Fraser River sockeye. Ecology, **31**: 6–26.

Ricker, W.E. 1954. Stock and recruitment. J. Fish. Res. Board Can. **11**: 559–623.

Ricker, W.E. 1958. Handbook of computations for biological statistics of fish populations. Bull. Fish. Res. Board Can. No. 119.

Ricker, W.E. 1987. Effects of the fishery and of obstacles to migration on the abundance of Fraser River sockeye (*Oncorhynchus nerka*). Can. Tech. Rep. Fish. Aquat. Sci. No. 1522.

Ricker, W.E. 1997. Cycles of abundance among Fraser River sockeye salmon (*Oncorhynchus nerka*). Can. J. Fish. Aquat. Sci. **54**: 950–968.

Roos, J.F. 1991. Restoring Fraser River salmon. Pacific Salmon Commission, Vancouver, B.C.

Schaefer, M.B. 1954. Some aspects of the dynamics of populations important to the management of the commercial marine fisheries. Inter.-Am. Trop. Tuna Comm. Bull. **1**: 26–56.

Schaefer, M.B. 1957. A study of the dynamics of the fishery for yellowfin tuna in the eastern tropical Pacific Ocean. Inter.-Am. Trop. Tuna Comm. Bull. **1**: 245–285.

Schnute, J. 1985. A general theory for the analysis of catch and effort data. Can. J. Fish. Aquat. Sci. **42**: 414–429.

Schnute, J.T. 1994. A general framework for developing sequential fisheries models. Can. J. Fish. Aquat. Sci. **51**: 1676–1688.

Schnute, J.T., and Kronlund, A.R. 1996. A management oriented approach to stock recruitment analysis. Can. J. Fish. Aquat. Sci. **53**: 1281–1293.

Schnute, J.T., and Richards, L.J. 1998. Analytical models for fishery reference points. Can. J. Fish. Aquat. Sci. **55**: 515–528.

Schubert, N.D. 1998. The 1994 Fraser River sockeye salmon (*Oncorhynchus nerka*) escapement. Can. Tech. Rep. Fish. Aquat. Sci. No. 2210.

Walters, C.J. 1986. Adaptive management of renewable resources. MacMillan, New York.

Walters, C.J., and Ludwig, D. 1987. Adaptive management of harvest rates in the presence of a risk averse utility function. Nat. Resour. Model. **1**: 321–337.

Walters, C.J., and Staley, M.J. 1987. Evidence against the existence of cyclic dominance in Fraser River sockeye salmon (*Oncorhynchus nerka*). *In* Sockeye salmon (*Oncorhynchus nerka*) population biology and future management. *Edited by* H.D. Smith, L. Margolis, and C.C. Wood. Can. Spec. Publ. Fish. Aquat. Sci. No. 96.

Ward, F.J., and Larkin, P.A. 1964. Cyclic dominance in Adams River sockeye salmon. Int. Pac. Salmon Fish. Comm. Prog. Rep. No. 11.

Welch, D.W., and Noakes, D.J. 1990. Cyclic dominance and optimal escapement of Adams River sockeye salmon (*Oncorhynchus nerka*). Can. J. Fish. Aquat. Sci. **47**: 838–849.

Welch, D.W., and Noakes, D.J. 1991. Optimal harvest rate policies for rebuilding the Adams River sockeye salmon (*Oncorhynchus nerka*). Can. J. Fish. Aquat. Sci. **48**: 526–535.

Appendix A. Proof of (T2.10) and (T2.11)

For simplicity, we omit subscripts i in this appendix. The proof of (T2.10) follows from the definite integral

$$\text{(A.1)}\quad \int_0^\infty \frac{1}{\sigma^{N+1}} e^{-Q/(2\sigma^2)}\, d\sigma = \frac{1}{2}\,\Gamma\left(\frac{N}{2}\right)\left(\frac{Q}{2}\right)^{-\frac{N}{2}} \propto Q^{-\frac{N}{2}},$$

© 2000 NRC Canada

where $\Gamma(z) = \int_0^\infty x^{z-1} e^{-x} dx$ denotes the gamma function. To prove (A.1), transform the integration variable from σ to $x = Q/(2\sigma^2)$. The integral then reduces to various constants multiplied by $\Gamma(N/2)$. Dependency on θ comes entirely through $Q(\theta)$, so that the integrated posterior is proportional to the expression on the right.

The proof of (T2.11) follows from the derivative of log P in (T2.9) with respect to σ:

$$\text{(A.2)} \quad \frac{\partial \log P}{\partial \sigma} = \frac{1}{P}\frac{\partial P}{\partial \sigma} = -\frac{N+1}{\sigma} + \frac{Q}{\sigma^3}.$$

Setting $\partial \log P/\partial t = 0$ and solving for σ^2 in (A.2) gives the modal estimate (T2.11).

Appendix B. MCMC implementation

As described in section 3, we begin the sample Markov chain at the modal estimate $\hat{\theta}_i$ for stock i obtained from (T2.10). The method requires defining a random movement from a current point θ_i to a new trial point θ_i'. For each component θ_{ij} of the vector θ_i, we compute θ_{ij}' by the simple rule

$$\text{(B.1)} \quad \theta_{ij}' = \theta_{ij} + su\Delta_j,$$

where u is a uniform random variate on the interval (–1,1), Δ_j denotes the standard deviation obtained from the square root of the jth diagonal entry in $\mathbf{H}^{-1}$, and s is a fixed scale factor. The trial point θ_i' is accepted with probability

$$\text{(B.2)} \quad \min\left[\frac{P(\theta_i')}{P(\theta_i)}, 1\right],$$

where the posterior ratio is independent of the proportionality constant in (T2.10). If θ_i' is accepted, it becomes the next point in the sequence; otherwise, θ_i is repeated. The algorithm then continues with a new trial point defined by (B.1).

Most of our analyses depend on software written in S-PLUS (www.mathsoft.com/splus/) explicitly for this paper. For example, we find posterior modes with the S-PLUS function `nlminb`, and we compute the Hessian in (3.2) with a customized algorithm based on central second differences. Output from these procedures links directly into code that implements the MCMC algorithm (B.1) and (B.2). For computational efficiency, we conduct the retrospective simulations in Table 5 using Pascal code written in the Borland Delphi (www.borland.com/delphi/) environment with ASCII files as data links to S-PLUS. We check our code using tests from examples with known results.

Based on software that directly implements the algorithms described here, we can report the following results. First, the `nlminb` algorithm works reasonably efficiently for the low-dimensional problems here, after appropriate scaling to give parameter values in a range within two orders of magnitude of 1 (0.01 to 100). Second, after experimentally choosing a fixed scale factor s that gives about a 50% acceptance rate, sample chains generally appear to converge. Third, chains that start at the posterior mode and use the Hessian for scaling parameter step sizes show no evidence of an initial burn-in phase before convergence.

Figure B1 illustrates diagnostic tests on the sample used to produce Fig. 5, where 3000 points are extracted systematically from a chain of length 40 000. We reduce the number of points in both figures to produce legible results, although properties of the sample closely mirror properties of the entire chain. Trace plots in Figs. B1A, B1C, and B1E for parameters (h^*, S^*, γ) show reasonable mixing near the mode of each distribution, with episodic excursions to the tails. Kernel density plots in Figs. B1B, B1D, and B1F suggest modal values of the marginal distributions somewhat different from the overall posterior mode portrayed in Fig. 5. For example, the posterior mode occurs near $\gamma = 0$ (Fig. 5, P versus γ), but the marginal distribution for γ appears to have a mode near $\gamma = -1$ (Fig. B1F). This occurs because the posterior probability function represents a hill with a broad ridge on the left, when viewed from the γ direction. Thus, Fig. 5 (P versus γ) shows a higher density of points to the left of the mode for γ than to the right.

Conceptually, panels in the bottom row and right column of Fig. 5 represent posterior profiles, which reveal the highest posterior value for a fixed value of each parameter. These are akin to likelihood profiles, where nuisance parameters are eliminated by maximization. In fact, the MCMC sampling method could be applied in this way to obtain individual parameter profiles from the likelihood function itself. By contrast, the kernel density plots in Fig. B1 represent Bayes marginal distributions, where nuisance parameters are eliminated by integration. We include the profile plots in Fig. 5 partly to emphasize the role of the posterior mode in our MCMC implementation.

Prior distributions provide a key component of any Bayesian analysis, and we typically adopt simple priors uniform across a prescribed range and zero elsewhere. Obviously, we could have chosen more complex priors designed to taper off gradually between acceptable and unacceptable parameter values. For this example, however, we prefer to retain a knife-edged approach because it clearly reveals the role of the prior in the posterior analysis. For example, scatter plots in Figs. 6A, 6B, and 6D extend to the prescribed upper bound for S^*, although the scatter plot in Fig. 6C does not. A more tapered choice of prior might mask this central feature in the analysis, where the data define an upper limit to the capacity for some stocks but not for others.

© 2000 NRC Canada

Fig. B1. Trace plots (A, C, and E) and kernel density plots (B, D, and F) for the sample of 3000 points (h^*, S^*, γ) used in Fig. 5. The traces show parameter values in relation to the index (1,...,3000). Density curves are computed from the sample with a triangular kernel function that spans 20% of the observed parameter range. Jittered parameter values from a 15% subsample (450 points) provide another illustration of parameter density.

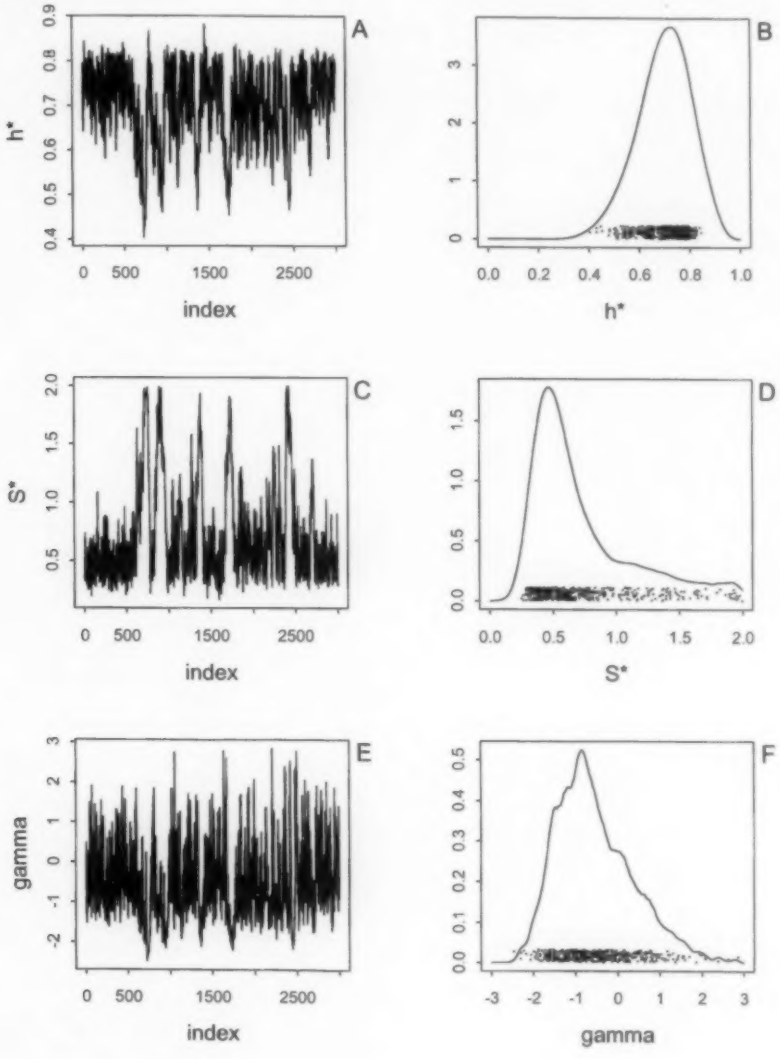

© 2000 NRC Canada

Spatial variability in growth and mortality of the red sea urchin, *Strongylocentrotus franciscanus*, in northern California

Lance E. Morgan, Louis W. Botsford, Stephen R. Wing, and Barry D. Smith

Abstract: Natural and fishing mortality rates of the red sea urchin, *Strongylocentrotus franciscanus*, in northern California were estimated from growth increment and size distribution data under the assumption of a constant recruitment rate. Mean asymptotic test diameter, standard deviation of asymptotic test diameter, growth rate coefficient, and natural mortality rate were first estimated for three nominally unharvested sites, Bodega Marine Reserve, Caspar Closure, and Salt Point. These estimated growth and mortality parameters differed among sites, leading to substantially different yield-per-recruit surfaces. Estimates of fishing mortality rate from size distributions collected at 11 harvested sites were then calculated based on the growth and natural mortality estimates obtained from the Caspar Closure and Bodega Marine Reserve sites. Estimates of fishing mortality rate ranged from 0.11 to 1.87·year^{-1}. The alongshore pattern of fishing mortality rate was moderately correlated with landings and effort, but the spatial pattern of rare, strong recruitment events also appeared to influence values of fishing mortality rate. The positive bias in estimates of fishing mortality rate due to recruitment variability indicated that our observed pattern in estimated values for fishing mortality rate could have been caused by the historical spatial pattern of interannual variability in recruitment.

Résumé : Les taux de mortalité naturelle et par pêche de l'oursin rouge dans le nord de la Californie ont été estimés à partir de données sur les incréments de croissance et la distribution des tailles d'après l'hypothèse d'un taux de recrutement constant. Nous avons d'abord estimé le diamètre asymptotique moyen du test, l'écart-type du diamètre asymptotique du test, le coefficient de croissance et le taux de mortalité naturelle pour trois sites pratiquement inexploités, la réserve marine de Bodega, la zone fermée Caspar Closure et la zone de Salt Point. Ces paramètres estimés de la croissance et de la mortalité différaient d'un site à l'autre, ce qui donnait des courbes nettement différentes de la production par recrue. Nous avons ensuite calculé le taux de mortalité par pêche (F) à partir des distributions de tailles recueillies à 11 sites exploités, en fonction des estimations de la croissance et de la mortalité naturelle obtenues pour les sites de Caspar Closure et de la réserve de Bodega. Les estimations de F allaient de 0,11 à 1,87·an^{-1}. Le régime de F le long du littoral était modérément corrélé aux débarquements et à l'effort, mais le patron spatial d'épisodes rares de fort recrutement semblait aussi influer sur les valeurs de F. Le biais positif observé dans les estimations de F à cause de la variabilité du recrutement indiquait que le patron que nous avons observé dans les valeurs estimées de F a pu être causé par le régime spatial historique de variabilité du recrutement d'une année à l'autre.

[Traduit par la Rédaction]

Introduction

The red sea urchin *Strongylocentrotus franciscanus* is a dominant member of subtidal marine communities along the west coast of North America and is a valuable commercial species (Kato and Schroeter 1985; Tegner 1989; Estes and Duggins 1995). In recent years, demand for red sea urchins in Asian markets has led to intensive harvesting in northern California. The California fishery began in 1972, and landings peaked in 1988 at over 23 000 t with a monetary value of US$20 million (Kalvass and Hendrix 1997). Landings in the northern California fishery increased rapidly in the mid-1980s followed by an 80% decline from 1988 to 1994. Catch-per-unit-effort, defined as landings per vessel trip, declined from a high of 1901 kg in 1986 to 515 kg in 1995 (Kalvass and Hendrix 1997). The number of permittees in northern California (an indication of effort) also declined, from 112 in 1990 to 69 in 1995 (Kalvass and Hendrix 1997). Red sea urchin fishery management has consisted of a minimum legal size (89 mm), limited entry, and seasonal closures. In spite of these measures, catch-per-unit-effort has declined and independent fishery surveys have shown a decrease in densities (0.4–1.1 individuals·m^{-2} in recent years) (Kalvass and Hendrix (1997), which are near the minimum believed necessary for successful reproduction by a broad-

Received May 20, 1999. Accepted February 10, 2000.
J15152

L.E. Morgan[1] **and L.W. Botsford.** Department of Wildlife, Fish, and Conservation Biology, University of California, Davis, CA 95616, U.S.A.
S.R. Wing. Department of Marine Science, University of Otago, Dunedin, New Zealand.
B.D. Smith. Environment Canada, Pacific Wildlife Research Centre, 5421 Robertson Rd., Delta, BC V4K 3N2, Canada.

[1]Author for all correspondence at the following address: National Marine Fisheries Service, Southwest Fisheries Science Center, Santa Cruz/Tiburon Laboratory, 3150 Paradise Dr., Tiburon, CA 94920, U.S.A. (e-mail: lancem@tib.nmfs.gov). After June 1, 2000: Marine Conservation Biology Institute, 15 806 NE 47th Court, Redmond, WA 98052, U.S.A. (e-mail: lance@mcbi.org).

© 2000 NRC Canada

cast spawner (<1 spawning adult·m^{-2}) (Pennington 1985; Levitan 1991; Levitan et al. 1992). There is now concern over the long-term viability of this fishery (Kalvass and Hendrix 1997).

The development of better management of the red sea urchin fishery is hampered by a lack of knowledge of growth and mortality rates. Even the most rudimentary management analysis, such as the use of yield-per-recruit calculations to evaluate size limits and fishing mortality rates, requires accurate estimates of growth rates (Beverton and Holt 1957). Attempts to design more comprehensive management policies in the red sea urchin fishery have included spatially explicit policies based on temporary or permanently closed areas (e.g., Botsford et al. 1993, 1999; Quinn et al. 1993). Studies of both a rotating spatial harvest management strategy (Botsford et al. 1993) and permanent harvest refugia (Quinn et al. 1993) indicate that the results of such management schemes are sensitive to growth and mortality rates. In addition, spatial management provides the opportunity to take advantage of differences in productivity, such as spatially varying growth, mortality, and recruitment rates.

The approach to estimating growth and mortality rates taken here is based on the size-structured von Foerster equation (Botsford et al. 1994). It describes how a size distribution changes with time, assuming deterministic growth and mortality functions. Based on this model, a maximum likelihood method was developed to estimate growth and mortality rates from size distribution and growth increment data under the assumption that final asymptotic size varies among individuals and that recruitment of new individuals to the population is constant (Smith and Botsford 1998; Smith et al. 1998). Because observed sea urchin size distributions rarely included recruitment pulses at small size, they (Smith et al. 1998) developed a steady-state recruitment model rather than a model that relies on cohort modes to estimate growth. The model requires growth increment data in addition to the size distribution data to avoid confounding the estimation of mortality and growth rates (Barry and Tegner 1990; Smith et al. 1998). Using simulation, Smith et al. (1998) evaluated the effect of sample size, measurement error, and random monthly recruitment on the precision and bias of model estimates. They found the precision and bias of most parameters to be less than 10%, using as few as 30 growth increments and 300 individuals in the size distribution. Smith et al. (1998) also concluded that in practice, natural and fishing mortality rates were unlikely to be confidently estimated using only data from a harvested size distribution. Rather, estimation of population parameters from fished populations is best done by first estimating the growth and natural mortality rates from a comparable unfished population and then calculating the estimates of fishing mortality rate in fished populations.

Here, we use this estimation method (Smith and Botsford 1998; Smith et al. 1998) to estimate natural mortality rates and parameters of the von Bertalanffy growth equation from field measurements of growth increments and size distributions at three nominally unharvested sites. We compare growth and natural mortality at these locations to determine spatial variability in these vital rates. These growth and natural mortality estimates are then used to calculate fishing mortality rate estimates for individuals greater than the minimum legal size using size distribution data from 11 harvested sites distributed along the coast of northern California. Finally, we interpret these results with regard to recruitment dynamics and management of the northern California red sea urchin fishery.

Materials and methods

Growth increment data were obtained from a series of visits to each site that involved tagging sea urchins and checking others to determine whether and when they had been tagged. Sea urchins were tagged with passive interrogatable responders (PIT tags) by injecting the tags through the soft mesentery around the oral opening. We collected and tagged red sea urchins at Salt Point State Park (38°26.3′N) (Fig. 1) during October 1993, September 1994, and May 1996, at Bodega Reserve (38°19.2′N) in April and October of 1996 and May and August of 1997, and at Caspar Closure (39°21.5′N) in May of 1996 and July of 1997. We also include growth increments from sea urchins tagged and recovered by the California Department of Fish and Game at Caspar Closure between September 1996 and October 1997 (P. Kalvass, California Department of Fish and Game, 19160 S. Harbor Dr., Ft. Bragg, CA 95437, U.S.A., personal communication). Tagged sea urchins ranged in size from approximately 35 to 100 mm test diameter.

Tagging involved SCUBA divers bringing sea urchins to the surface where they were measured with calipers to the nearest 0.25 mm and implanted with PIT tags. For each sea urchin, we averaged three measurements of test diameter taken across the oral surface and recorded it along with the unique 11-digit PIT tag code. Sea urchins were released at a depth of 8–12 m at sites marked with anchored lines. Sixty-seven to 421 days later, divers returned to the marked sites and brought sea urchins to the surface where they were identified with a Destron miniportable PIT tag reader. PIT-tagged individuals were measured and growth increments calculated. Growth increments were converted to normalized growth rates by dividing the growth increment by the number of days between measurements (release and recapture).

Divers also collected size distribution data at Salt Point and Bodega Reserve in 1994, 1995, 1996, and 1997 and at Caspar Closure in 1995, 1996, and 1997. Sea urchins were collected by hand at a depth of 7–12 m and placed in canvas bags. Sampling was done without altering the physical structure of the bottom. Because juvenile sea urchins typically seek out adults for shelter (Tegner and Dayton 1977; Breen et al. 1985), and all sea urchins observed were collected, we believe that juveniles were well sampled. However, the abundance of very small sea urchins (<15 mm) may have been underrepresented due to divers' inability to locate them. We measured the collected sea urchins in small boats at the surface immediately following each dive. Additional sites were sampled during the late summer and early fall (August–October) of 1995 and 1996 at 11 locations in northern California (Fig. 1). These size distribution data were used in the estimation of fishing mortality rate (F).

The von Bertalanffy growth equation typically used to model growth in a variety of finfish and shellfish species (von Bertalanffy 1957) is

$$(1) \qquad l_t = L_\infty(1 - e^{-Kt})$$

where l_t is size (millimetres) at age t years, L_∞ is asymptotic test size (millimetres), and K (t^{-1}) is the instantaneous rate of change in growth rate with time. Sainsbury (1980) expanded this definition of von Bertalanffy growth to allow for growth variability among individuals.

The maximum likelihood method developed by Smith et al. (1998) builds on Sainsbury's (1980) assumptions and includes parameters that describe growth variability by allowing L and K to be random variables as captured in the parameters μ_L, σ_L, μ_K, and σ_K.

© 2000 NRC Canada

Fig. 1. Location of sampling sites in northern California. PIT tag sites are indicated with open circles; harvested sites are indicated with solid diamonds. Arrows indicate the two headlands discussed in the text (Point Arena to the north and Point Reyes to the south). Horizontal lines indicate the approximate boundaries of California Department of Fish and Game management sectors.

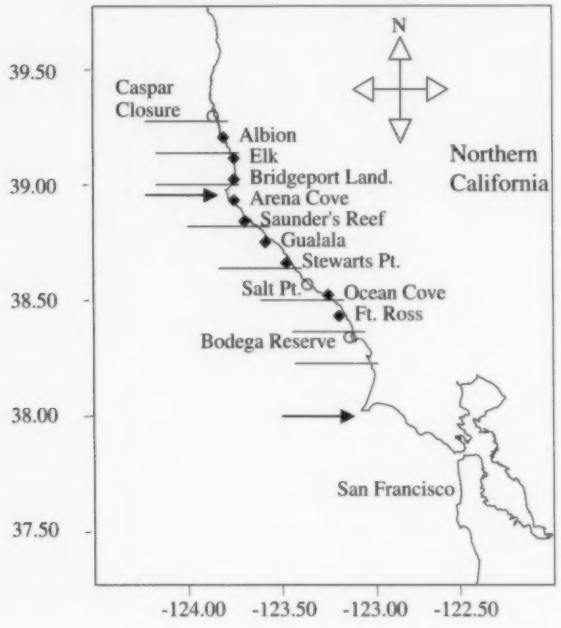

The Smith et al. (1998) model includes a parameter for measurement error, and if size distribution data are analyzed, parameters for natural mortality rate (M) and F and size selectivity. Their method assumes a constant rate of recruitment of new individuals into a size distribution recruitment, i.e., it is a steady-state model, although the method is robust to modest departures from this assumption (Smith et al. 1998).

The objectives of this paper require that we estimate only some of these parameters. For example, Smith and Botsford (1998) found no evidence of random variability in von Bertalanffy's K parameter for red sea urchins, and so, we treat K to be constant. We set the value for measurement error to 2% of test diameter based on repeated blind measurements of sea urchins taken by independent observers. Our confidence that divers adequately sampled sea urchins larger than 15 mm test diameter prompted us to set the mean and standard deviation of a cumulative Gaussian size selectivity function to 15 and 7.5 mm, respectively. Therefore, we estimate only five parameters: μ_L, σ_L, K, M, and F.

The maximum likelihood method sums two negative ln likelihood functions, one for the growth increment data and one for the size distribution data. The objective function for the growth increment data is related to least squares and includes the effects of measurement error. This objective function is incorrectly represented by eq. 13 in Smith et al. (1998). We report the correct formulation in the Appendix. The objective function for the size distribution data is based on the separation statistic of Schnute and Fournier (1980), as implemented by Smith et al. (1998). This objective function evaluates the fit of the predicted proportions-at-length to the observed proportions-at-length.

Comparisons of growth rate and M among sites were made by constructing full (multisite) models using all data from various combinations of locations and then estimating the growth and mortality parameters for these multisite data sets. We compared parameter estimates obtained by analyzing size frequency and growth increment data for the full models (multisite data) with those obtained from the individual analyses for each location.

Values of F were then estimated for the size distributions from the harvested sites using the parameter estimates obtained for μ_L, σ_L, K, and M estimated from the unharvested size distributions. Our estimates of F were obtained by fitting the size frequency data only to individuals in the size-classes above 90 mm in the harvested size distributions to reduce the influence of recent recruitment variation on abundance at smaller sizes.

To examine potential influences on the pattern of spatial variation in F, we calculated correlations between the estimated values for F (the mean of the 1995 and 1996 estimates) and (*i*) a recruitment index, calculated as the sum of individuals in the first three year-classes (<60 mm) divided by the number of unfished adult sea urchins (individuals between 70 and 90 mm) (Morgan et al. 2000), (*ii*) total landings by the California Department of Fish and Game management sector (10′ of latitude) between 1992 and 1994, (*iii*) effort in diver hours per management sector from 1992 and 1994, and (*iv*) site location (minutes of latitude north of a prominent headland, either Point Reyes or Point Arena). Consideration of this last variable is motivated by a potential mechanism by which circulation influences recruitment (Morgan et al. 2000).

The red sea urchin fishery operates from four major ports in northern California. These ports have accounted for over 70% of the catch landed from 1988 to 1994. Catch-and-effort data from fishers' logbooks (available from California Department of Fish and Game, 19160 S. Harbor Dr., Ft. Bragg, CA 95437, U.S.A.) are available for each management sector for the years 1988–1994. However, we focus on the last three years. This time frame (1992–1994) is more likely to reflect an influence on the state of the fishery during this study.

Sensitivity to recruitment variability

Examination of our results suggested that occasional recruitment pulses could affect our model results in two different ways: (*i*) as a bias in the growth estimates produced and (*ii*) as variation in F. The first of these would result in poor estimates of growth and (or) mortality, while the second would result in a true, well-measured estimate of F that varies in relation to the change in availability of individuals entering the fishery from cohorts of different magnitudes. The latter occurs because despite constant harvest effort; it is due to changes in the annual percentage of individuals available to the fishery relative to prefishery-sized individuals.

While the maximum likelihood method assumes constant recruitment, and this appears to be true over longer time frames, we were concerned that these occasional modes at smaller sizes may unduly influence our growth parameter estimates. Therefore, we used simulation to test the sensitivity of our estimates of the growth parameters and M to annual pulses of unusually large and unusually small recruitment. Smith et al. (1998) tested sensitivity to random monthly variability in recruitment but did not explicitly test sensitivity to annual variability (i.e., variability correlated over months). Our simulations were designed to measure the bias specifically associated with large annual variation in recruitment. Size distributions with constant recruitment and with annual pulses either one half, two, or four times the constant recruitment rate in one of the first 3 years of age were simulated. We then estimated the values for μ_L, σ_L, K, and M from these simulated data sets and compared our estimates with their true values.

We then explored the effect of random variability in annual recruitment on estimates of F, since unusually large cohorts sporadically entering the fishable size-classes could subtly alter the shape of the upper mode in the size distribution. We estimated temporal variability in F by simulating size distribution data for a 50-year period of variable recruitment, but with a constant F. These distri-

© 2000 NRC Canada

butions were created using a true F of 0.7 and a 5-year interval between large recruitment events. We then estimated the growth and mortality parameters for distributions representing the last 10 of those 50 years to measure the effect of transient fluctuations in the numbers of individuals in the legally fishable size class (>89 mm) on the estimate of F.

Finally, as a test of the robustness of our growth parameter estimates, we visually checked our estimates of growth rate by comparing the progress of a simulated strong recruitment pulse through an otherwise constant recruitment size distribution with the modes present at small sizes in size distributions collected from the Bodega Reserve, Salt Point, and Caspar Closure sites over successive years. We used data on the monthly distribution of settlement observed by Wing et al. (1995*a*) to characterize the simulated recruitment pulse.

Results

Parameter estimates from the three sites where sea urchins were PIT tagged showed among-site and among-year variation (Fig. 2; Table 1). We report growth parameters only for the combined analyses of growth increment and size frequency data, since the growth increment data lack information on growth for the largest sea urchins collected in the sizes distributions. The estimates obtained for size distributions from individual years at each location (but including growth increments from all years at that location) demonstrate the sampling and interannual variability typical of these data and its consequences on the consistency of the estimates (Table 1). We include estimates from Salt Point, even though specific parameter values are difficult to interpret. Salt Point is a reserve; however, we are suspicious that the population may have been harvested. At each location, there is greater variability in estimates among years than is expected from the estimates of precision given in Table 1. This indicates that the data are from different "populations" and are not just different random samples from the same population. Examination of the individual distributions in Fig. 3 indicates that these differences are not solely due to pulses in recruitment. They may originate from slight differences in size distributions from year to year due to either movement of sea urchins or errors in our ability to locate the exact site each year.

Comparisons among values for the Akaike information criterion (AIC, Burnham and Anderson 1998) indicate that growth and mortality rates differ among locations (Table 1; Fig. 2). The AIC that results from fitting data from all three locations is greater than the sum of AICs that result from fitting each location separately. Examination of the size distributions from individual years (Fig. 3) indicates that the population from Salt Point declines for sizes greater than the legal size limit of 89 mm from 1995 to 1997, while size distributions from Caspar Closure and Bodega Reserve do not decline until larger sizes. In the 4 years of size distributions from Salt Point, the size distribution from the first year, 1994, declines for sizes greater than about 110 mm, while in subsequent years, it begins to decline near 90 mm (Fig. 3). Comparing the objective functions from only the Bodega Reserve and the Caspar Closure populations without Salt Point (Table 1) still indicates that there is a difference in growth and mortality parameters between those two sites.

These estimates could also have been biased by the growth increments from the two locations being taken over different times of the year and growth being seasonal. Although it is not known whether growth of this species is seasonal, it is possible that the growth increments from Caspar Closure were from a season of higher growth rate. We tested this by randomly removing subsets of the growth increment data from the combined data set for Bodega Reserve so that the intraannual distributions of times-at-large were essentially the same at both locations. These revised estimates of growth were virtually identical to the previous ones.

Values for F based on the best fit of data to the two unharvested size distributions (Caspar Closure and Bodega Reserve) range from a low of 0.11 at Bridgeport Landing to a high of 1.87 at Saunder's Reef (Table 2). We did not use estimates from Salt Point to calculate F because of our limited confidence that this site was unharvested. In general, estimates of F using Caspar Closure growth rate and M were higher than those using Bodega Reserve data. Estimates based on Caspar Closure parameters varied from 0.16 to 1.87 (1995: $\mu = 0.52$, $\sigma = 0.07$; 1996: $\mu = 0.76$, $\sigma = 0.16$). Values for F estimated from Bodega Reserve parameters var-

Fig. 2. Normalized growth increment (GI) data (diamonds) and model fits (lines) (Table 1) to the data using the maximum likelihood procedure with size distribution data. (*a*) Caspar Closure (n = 50); (*b*) Salt Point (n = 48); (*c*) Bodega Reserve (n = 157).

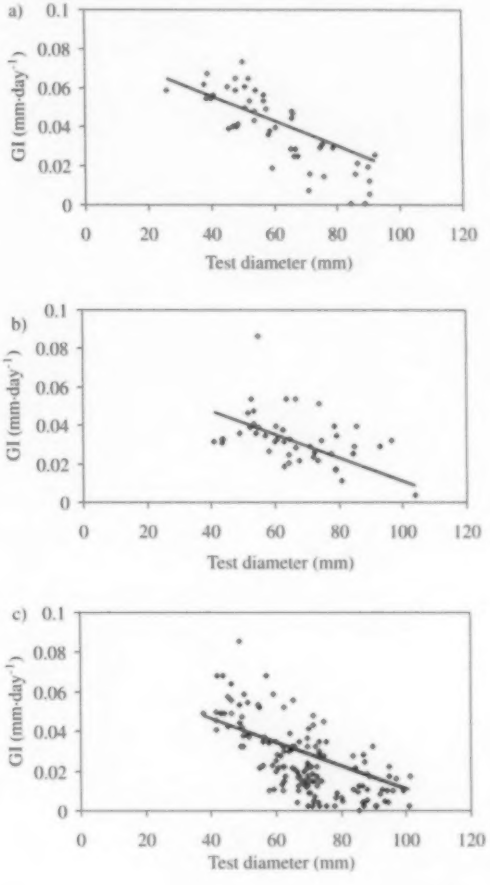

© 2000 NRC Canada

Table 1. Maximum likelihood estimates of growth and mortality parameters from red sea urchin data from three locations in northern California plus combinations over several locations.

Location	Growth increment (N)	Size distribution (N)	μ_L	σ_L	Growth coefficient K	Natural mortality M	Objective function: Size frequency	Objective function: Growth increment	AIC
Full models									
CC	50	1636	126.6 (1.3)	9.7 (0.8)	0.27 (0.01)	0.21 (0.01)	91.9	217.4	317.3
SP	48	2628	102.0 (0.6)	13.5 (0.4)	0.32 (0.03)	0.00 (0.01)	54.1	238.5	300.6
BMR	157	2251	118.1 (0.6)	10.0 (0.4)	0.22 (0.01)	0.08 (0.01)	316.6	602.9	927.5
CC/SP/BMR	255	6515	112.5 (0.6)	12.8 (0.4)	0.28 (0.01)	0.09 (0.01)	1094.9	1072.9	2175.8
CC/BMR	207	3887	120.6 (0.6)	10.3 (0.4)	0.25 (0.01)	0.13 (0.01)	530.3	851.2	1389.5
CC									
1995	50	666	108.0 (2.7)	15.8 (1.5)	0.34 (0.02)	0.12 (0.02)	50.3	222.7	281.0
1996	50	651	126.3 (1.8)	8.4 (1.1)	0.27 (0.01)	0.23 (0.02)	153.0	217.9	378.9
1997	50	319	136.9 (2.3)	7.6 (1.5)	0.24 (0.01)	0.20 (0.02)	184	222.5	414.5
SP									
1994	48	663	102.4 (1.3)	15.3 (0.7)	0.31 (0.03)	–0.02 (0.02)	106.4	240.6	355.0
1995	48	648	95.4 (1.4)	13.4 (0.8)	0.38 (0.02)	0.06 (0.02)	64.4	243.9	316.3
1996	48	653	102.6 (0.98)	13.1 (0.6)	0.31 (0.02)	–0.10 (0.02)	45.7	237.7	291.4
1997	48	664	102.0 (0.88)	10.8 (0.6)	0.32 (0.01)	–0.04 (0.02)	32.5	236.1	276.6
BMR									
1994	157	657	113.0 (1.1)	7.9 (0.7)	0.25 (0.01)	0.10 (0.008)	114.6	598.0	720.6
1995	157	592	121.8 (1.0)	9.1 (0.7)	0.21 (0.01)	0.05 (0.01)	91.1	605.8	704.9
1996	157	670	111.5 (1.4)	13.5 (0.9)	0.25 (0.01)	–0.003 (0.01)	94.4	602.0	704.4
1997	157	332	126.3 (2.1)	4.4 (1.8)	0.19 (0.01)	0.17 (0.01)	461.2	611.7	1080.9

Note: Full models include all of the data collected at those sites in all years. Fits from individual-year size distribution data are listed separately. Standard errors are given in parentheses. The estimates of standard errors were obtained using a reliable numerical method (see Smith et al. 1998). CC, Caspar Closure; SP, Salt Point; BMR, Bodega Reserve.

© 2000 NRC Canada

Fig. 3. Size distributions collected at PIT tag sites for each year (solid line). The first column contains the sequential years 1995–1997 from Caspar Closure: (*c*) 1995 (n = 666), (*f*) 1996 (n = 651), and (*i*) 1997 (n = 319). The second column shows the years 1994–1997 from Salt Point: (*a*) 1994 (n = 663), (*d*) 1995 (n = 648), (*g*) 1996 (n = 653), and (*j*) 1997 (n = 664). The third column shows the years 1994–1997 from Bodega Reserve: (*b*) 1994 (n = 657), (*e*) 1995 (n = 592), (*h*) 1996 (n = 670), and (*k*) 1997 (n = 332). A recruitment cohort modeled on growth parameters estimated from the multiple-year size distribution is included (broken line). TD, test diameter (mm); *N*, number.

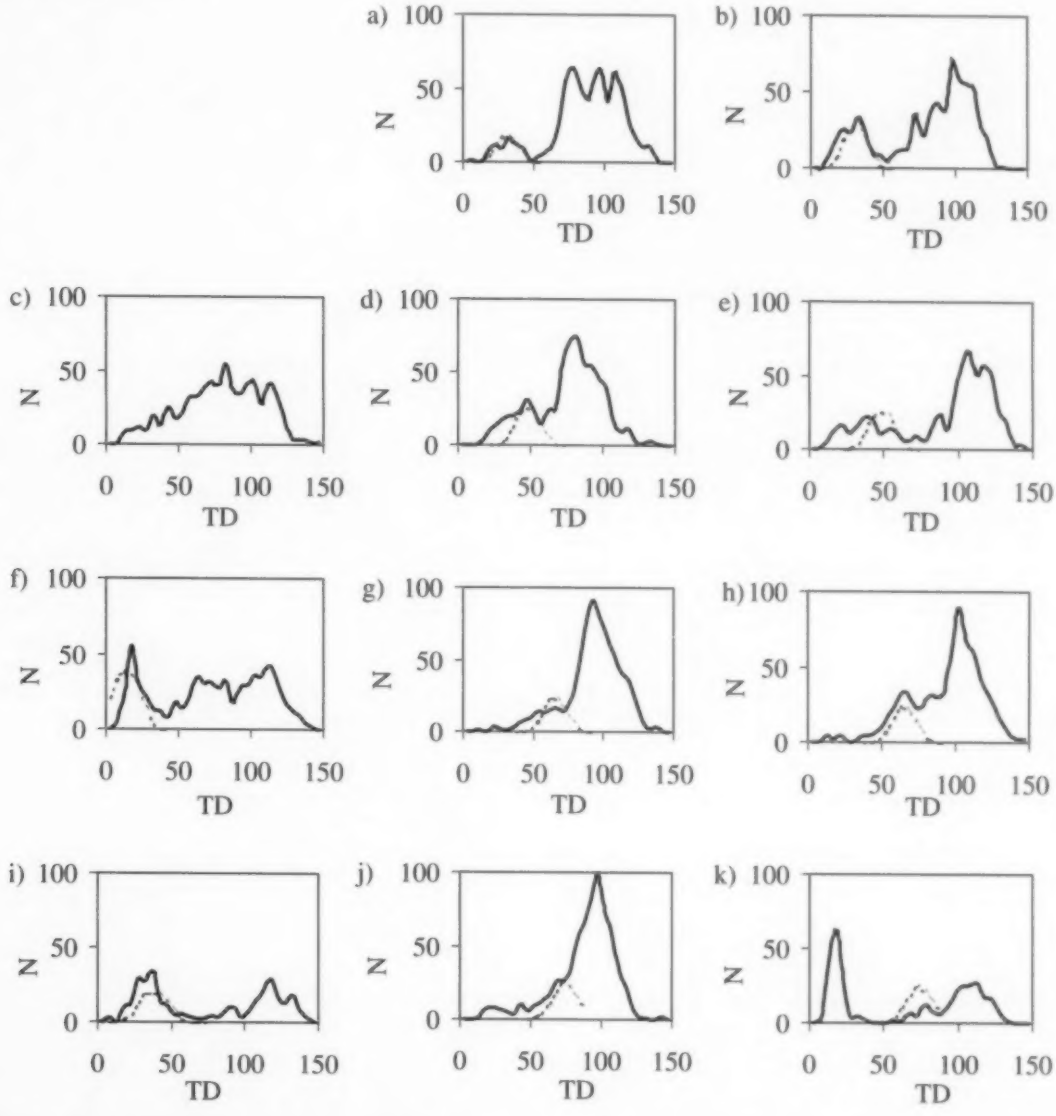

ied from 0.11 to 1.2 (1995: μ = 0.35, σ = 0.05; 1996: μ = 0.49, σ = 0.1). Sites further to the north of headlands had higher values of F and also showed greater variability. Estimated rates in 1996 were either similar or slightly higher at most sites. Sites that have higher estimates of F appear to decline more rapidly at sizes above the legal size limit (Fig. 4).

Values of F were most strongly correlated with latitude to the north of either Point Arena or Point Reyes (Table 3), with estimates of F increasing at locations further to the north of either point. This pattern is inversely correlated with the history of recent recruitment (Morgan et al. 2000). Where recent recruitment is higher, i.e., to the north of Point Arena and Point Reyes, F is lower. Where recent recruitment is lower, i.e., to the south of Point Arena, F is higher and more variable. There is also a moderate correlation between estimates of F and both landings and diver hours.

Sensitivity to recruitment variability

Tests of the sensitivity of the maximum likelihood method

© 2000 NRC Canada

Table 2. Maximum likelihood estimates of F based on growth and natural mortality estimates from two unharvested sites, Caspar Closure and Bodega Reserve.

	1995				1996				
Site	n total	$n > 90$ mm	Caspar	Bodega	n total	$n > 90$ mm	Caspar	Bodega	Mean F
Caspar	414	195	0.74	0.49	276	78	0.87	0.57	0.67
Albion	464	112	0.32	0.21	562	149	0.59	0.39	0.38
Elk	723	407	0.37	0.24	444	162	0.39	0.26	0.32
Bridgeport Landing	274	136	0.17	0.11	378	208	0.16	0.11	0.14
Point Arena	737	454	0.47	0.32	545	265	0.75	0.49	0.51
Saunders	802	502	0.88	0.58	270	188	1.87	1.20	1.13
Gualala	638	429	0.83	0.54	293	189	0.82	0.53	0.68
Stewart's Point	612	424	0.74	0.48	263	164	1.75	1.13	1.03
Ocean Cove	577	319	0.50	0.33	445	242	0.49	0.33	0.41
Fort Ross	372	225	0.63	0.42	340	242	0.72	0.47	0.56
Bodega Head	208	139	0.21	0.13	287	197	0.51	0.33	0.30

Note: Mean F is the mean of both estimates from both 1995 and 1996, n total represents the total number of individuals in the size distribution collected, and $n > 90$ mm is the number of individuals used in the estimate of F (see text).

to the effects of recruitment variation using size distributions distorted by levels of annual recruitment one half, two, and four times the assumed constant value indicated that these had the greatest influence on estimates of M and μ_L. Effects on estimates of K and μ_L are less than 15 and 10%, respectively, of their true values (Table 4). Positive pulses have a positive bias on mortality estimates, being highest for pulses at age 1 (from 33 to 92% for pulses two and four times normal, respectively) and then declining with age. Negative pulses have a negative effect on natural mortality (–17% for recruitment half of normal) that also declines with age. Both positive and negative recruitment pulses positively bias estimates of μ_L, and their maximum effect is at midages, the ages when a cohort grows into the peak in the size distribution.

We examined the suspected influence of annual variability in recruitment on estimates of F as well as on the correlation between our index of recruitment and F using simulated size distributions with recruitment variability. Our examination showed that episodic recruitment on the order of once every 5 years can lead to widely ranging estimates of F as individual cohorts pass through the fishable size-classes (Fig. 5*a*–5*e*). The observed pattern of F is biased very high as the cohort first reaches the minimum legal size-class (more sea urchins in the smallest fishable size and very few in larger size-classes, resulting in a steeply declining size distribution). This bias declines as the cohort spreads across the range of unfishable and fishable size-classes, and estimates are closer to the simulated value of F. As the cohort grows into the fishable size-classes, the estimates are biased slightly low, i.e., no new recruitment to the fishery results in a shallow declining slope to the upper half of the size distribution. This demonstrates that F varies with recruitment pulses as frequently as every 5 years (Fig. 5*f*).

The change over time in the position of the simulated cohort in otherwise constant recruitment size distributions compared favorably with the observed shift in size of the lower mode at Salt Point and Bodega Reserve (Fig. 3). The observed modes for the first, second, third, and fourth years of a cohort from a model based on the parameter estimates of Bodega Reserve (Table 1) approximate the observed modes at lower sizes from Bodega Reserve and Salt Point size distributions from 1994, 1995, 1996, and 1997 (Fig. 3). The observed modes shift similarly from year to year at both sites. At both Bodega Reserve and Salt Point in 1994, 1995, and 1996, the predicted mode is on the leading edge of the mode in the data that apparently results from a large settlement in 1993. The large lower mode observed at Caspar Closure in 1996 (Fig. 3) also shifts in a way similar to the calculated growth trajectory of this cohort over 1 year.

Discussion

The estimates obtained here establish a range of growth rate and M for red sea urchins in northern California and indicate that there may be spatial variability within that range. These differences are consistent with our interpretation of the visual appearance of the size distributions and growth increments from each location. Growth increments from the Caspar Closure site are also greater than those from Bodega Reserve. Estimates for both μ_L and K at Caspar Closure are consistent with this difference in growth. The slopes of the size distributions at sizes between those affected by selectivity at small sizes and the peak at large sizes ($\approx\mu_L$) are proportional to 1 minus the ratio of M to K (see Botsford et al. 1994). Caspar Closure has a lower slope than Bodega Reserve, which leads to a greater mortality rate so that the ratio of M to K is closer to unity. The differences between the reserve sites of Caspar Closure and Bodega Reserve are also consistent with growth conditions; Caspar Closure has an extensive kelp forest canopy of *Nereocystis luetkeana* in a relatively protected bay, while Bodega Reserve is wave exposed and devoid of any attached brown macroalgae. In support of our results, growth estimates from these sites approximate the change in size of the lower mode in the size distribution from one year to the next.

Bias from recent recruitment pulses could explain some of the difference between the Caspar Closure and Bodega Reserve estimates of M, if there were several sequential recruitment pulses. The estimate of M at Caspar Closure is more than twice the rate for Bodega Reserve. Although there is a large recruitment pulse in the 1997 Bodega Reserve data, in all other years, recruitment appears to be more constant, and the aggregate size distribution has only a small mode at lower size. At Caspar Closure, high levels of recruitment oc-

© 2000 NRC Canada

Fig. 4. Size distribution data from 1996 (solid line) and maximum likelihood fits of F (broken line) based on Bodega Reserve growth and mortality estimates for sea urchins greater than the legal size limit (F values in Table 2). Locations are, from north to south, (*a*) Caspar Bay, (*b*) Albion, (*c*) Elk, (*d*) Bridgeport Landing, (*e*) Point Arena Cove, (*f*) Saunder's Reef, (*g*) Gualala, (*h*) Stewart's Point, (*i*) Ocean Cove, (*j*) Fort Ross, and (*k*) Bodega Head. TD, test diameter (mm); N, number.

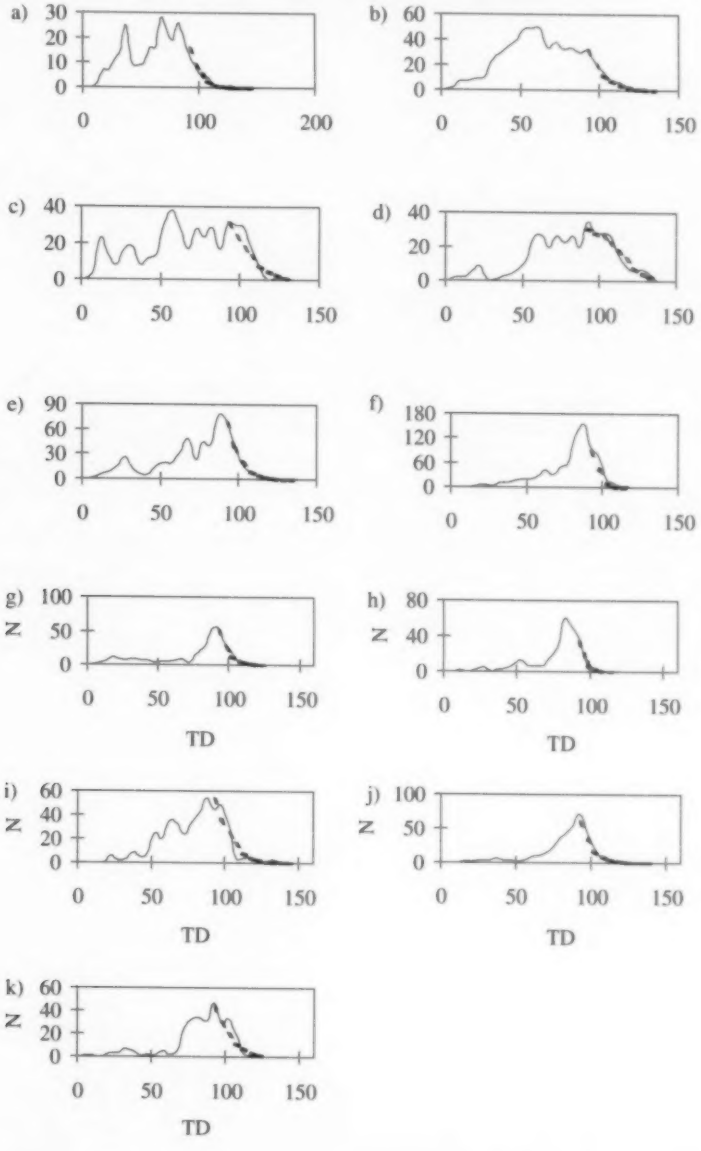

cur in 1996 and 1997. If these levels represent unusually large recruitment over the long-term average, then a bias up to 90% is possible. The estimates of M for individual years 1996 and 1997 are 0.23 and 0.20, respectively. From these observations, we conclude that the combination of 2 years of high recruitment could be responsible for a substantial amount of the difference between the estimates of M at the Caspar Closure site and the Bodega Reserve site. However, the differences in growth increments between the two sites indicate that at least part of the difference in growth parameters between sites is not due solely to recruitment. To determine whether recruitment levels at Caspar Closure during this study are unusually high or representative of an area with higher average levels of recruitment will require longer term study.

The significance of such differences in growth and mortality patterns rests on the practical difference they make with regard to (*i*) their influence on our estimates of F and (*ii*) whether or not they indicate changes in present management of the fishery. Our analysis of F based on the parame-

© 2000 NRC Canada

Table 3. Correlations between F (1995–1996), recruitment index (1995–1996), sector landings (1992–1994), diver hours (1992–1994), and location relative to a major headland.

Site	Mean F	Recruitment index	Sector landings (kg)	Diver hours	Minutes of latitude north of headland
Caspar	0.67	2.17	994 506	10 384	22
Albion	0.38	2.94	1 553 607	13 762	17
Elk	0.32	1.83	670 138	4 867	8
Bridgeport Landing	0.14	1.21	670 138	4 867	6
Pt Arena	0.51	0.68	1 990 194	15 298	55
Saunders	1.13	0.24	1 990 194	15 298	51
Gualala	0.68	0.74	699 507	5 122	47
Stewart's Point	1.03	0.29	1 307 509	9 845	38
Ocean Cove	0.41	0.67	1 307 509	9 845	33
Fort Ross	0.56	0.34	210 106	1 428	30
Bodega Head	0.30	1.84	459 766	2 167	18
Mean F	1.00				
Recruitment index	–0.53	1.00			
Landings	0.46	–0.12	1.00		
Diver hours	0.45	0.01	0.98	1.00	
Latitude	0.70	–0.67	0.58	0.50	1.00

Note: Correlations greater than 0.52 are significant at $p < 0.1$.

Table 4. Sensitivity of maximum likelihood estimates of von Bertalanffy growth parameters and M to simulated annual variation in recruitment.

		Magnitude of recruitment variation					
		0.5 times		2 times		4 times	
Years since recruitment	Parameter	Estimate	Bias	Estimate	Bias	Estimate	Bias
1	μ_L	120	0.02	123	0.01	128	0.05
	σ_L	12.5	0.25	12	0.20	12.1	0.21
	K	0.28	0.00	0.27	0.04	0.25	0.11
	M	0.1	0.17	0.16	0.33	0.23	0.92
2	μ_L	120	0.02	122	0.00	125	0.02
	σ_L	12.2	0.22	12.2	0.22	12.1	0.21
	K	0.28	0.00	0.27	0.04	0.26	0.07
	M	0.11	0.08	0.15	0.25	0.19	0.58
3	μ_L	121	0.01	121	0.01	122	0.00
	σ_L	12.1	0.21	12.4	0.24	12.8	0.28
	K	0.28	0.00	0.28	0.00	0.27	0.04
	M	0.12	0.00	0.14	0.17	0.17	0.42
5	μ_L	122	0.00	119	0.02	110	0.10
	σ_L	12	0.20	13.4	0.34	17.4	0.74
	K	0.28	0.00	0.29	0.04	0.32	0.14
	M	0.12	0.00	0.11	0.08	0.07	0.42
7	μ_L	121	0.01	118	0.03	115	0.06
	σ_L	12.3	0.23	12.7	0.27	13.3	0.33
	K	0.28	0.00	0.29	0.04	0.3	0.07
	M	0.12	0.00	0.11	0.08	0.08	0.33
10	μ_L	121	0.01	120	0.02	120	0.02
	σ_L	12.4	0.24	11.9	0.19	12.4	0.24
	K	0.28	0.00	0.28	0.00	0.28	0.00
	M	0.12	0.00	0.11	0.08	0.12	0.00

Note: Parameters used to simulate size distributions: mean asymptotic test diameter (μ_L) = 122 mm, SD of asymptotic test diameter (σ_L) = 10 mm, growth coefficient K = 0.28, and M = 0.12. Growth increments from Caspar Closure were used in the estimation procedure. Bias is the fractional bias.

© 2000 NRC Canada

Fig. 5. Simulated size distributions (shaded bars) based on Bodega Reserve growth and natural mortality parameters and with $F = 0.7$ demonstrating the influence of one recruitment pulse every 5 years on the estimate of F. The line represents the maximum likelihood estimate for F and the abundance-at-size of legal-sized sea urchins. If a recruitment event reaches the minimum legal size (89 mm) (*a*) in year 1, then $F = 1.56$, (*b*) in year 2, then $F = 1.18$, (*c*) in year 3, then $F = 0.67$, (*d*) in year 4, then $F = 0.47$, and (*e*) in year 5, then $F = 0.60$. (*f*) Plot of the cycle in estimates of F (solid line) with a 5-year interval between unusually large recruitment events. The broken line represents the simulated F; recruitment occurs in years 1, 6, and 11. TD, test diameter (mm); N, number; F, instantaneous fishing mortality rate.

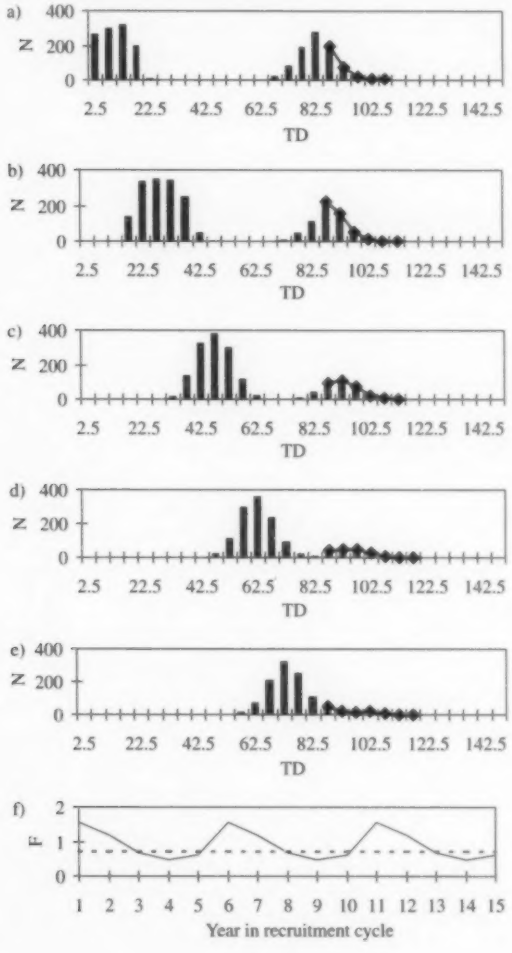

ters from unharvested sites indicates that values of F from estimates of growth and mortality at Bodega Reserve are approximately one third lower than estimates from Caspar Closure parameters. The spatial pattern of F is the same regardless of the origin of the growth and natural mortality estimates (correlation coefficients >0.99). In earlier assessments of the maximum likelihood method, Smith et al. (1998) found estimates of F to be highly sensitive to estimates of K, F increasing dramatically as estimates of K increased.

We can get a sense of the potential management implications of differences in growth and mortality estimates by noting that the ideal optimal size limit for an intensely harvested population (i.e., $F = \infty$) is 100 mm using the values of μ_L, K, and M estimated for Caspar Closure and 105 mm using the parameters from Bodega Reserve (Smith and Botsford 1998). However, we are more interested in the management implications of these potential differences over our observed range of F. A plot of yield-per-recruit for growth and mortality parameters from Caspar Closure indicates that the size limit that produces maximum yield goes from 85 to 90 mm as F goes from 0.5 to 1.0-year^{-1} (Fig. 6*a*). For Bodega Reserve growth and natural mortality parameters, these values are approximately 93 to 96 mm as F goes from 0.5 to 1.0 (Fig. 6*b*). Using Caspar Closure growth and natural mortality estimates, the present size limit for northern California of 89 mm would maximize yield-per-recruit. However, the growth and mortality rates obtained for Bodega Reserve indicate a higher minimum legal size limit for maximizing yield-per-recruit.

The spatial pattern in estimated values of F is particularly intriguing because it is inversely related to an observed pattern in recent recruitment, which in turn is related to coastal circulation (Morgan et al. 2000). A thorough analysis of data from settlement collectors, plankton tows, and concurrent ocean conditions (Wing et al. 1995*a*, 1995*b*, 1998) has shown that the spatial distribution of settlement of a number of invertebrates is determined by circulation associated with alternating periods of upwelling and relaxation. In particular, during strong upwelling in the spring, larvae between Point Reyes and Point Arena appear to be swept south and retained in the upwelling shadow to the south of Point Reyes (Wing et al. 1998). When the upwelling winds relax, on weekly time scales, these warmer, less saline waters flow northward along the coast north of Point Reyes (Kosro 1987; Send et al. 1987), leading to larval settlement. Variability in the strength of these flows leads to a spatial pattern of recruitment in which points just to the north of promontories receive more frequent recruitment, while points further north receive less frequent recruitment (Wing et al. 1995*a*, 1995*b*). A similar upwelling–relaxation mechanism is believed to occur near Point Arena, although the retention mechanism would be different (discussed in Morgan et al. 2000). The area around Point Arena has been less studied, but during the upwelling season, poleward flows have been observed (Huyer and Kosro 1987), and drifter studies have shown onshore flow to the north of Point Arena (Davis 1985). Additionally, Washburn et al. (1993) described a persistent anticyclonic eddy in this region which could retain larvae and transport them shoreward during relaxation. This upwelling–relaxation mechanism operating at these two promontories is also evident in the spatial pattern of recent recruitment to size distributions of red sea urchins, leading to their significant negative correlation with distance north of promontories (Morgan et al. 2000).

While the covariability between recruitment and F is intriguing, there is no obvious biological way by which higher recruitment can lead to lower values of F, which leaves two other possibilities: (*i*) an influence on F that is independent

© 2000 NRC Canada

Fig. 6. Yield-per-recruit curves based on growth and natural mortality parameters from (*a*) Caspar Closure and (*b*) Bodega Reserve. LSL, lower legal size limit; *F*, instantaneous fishing mortality rate.

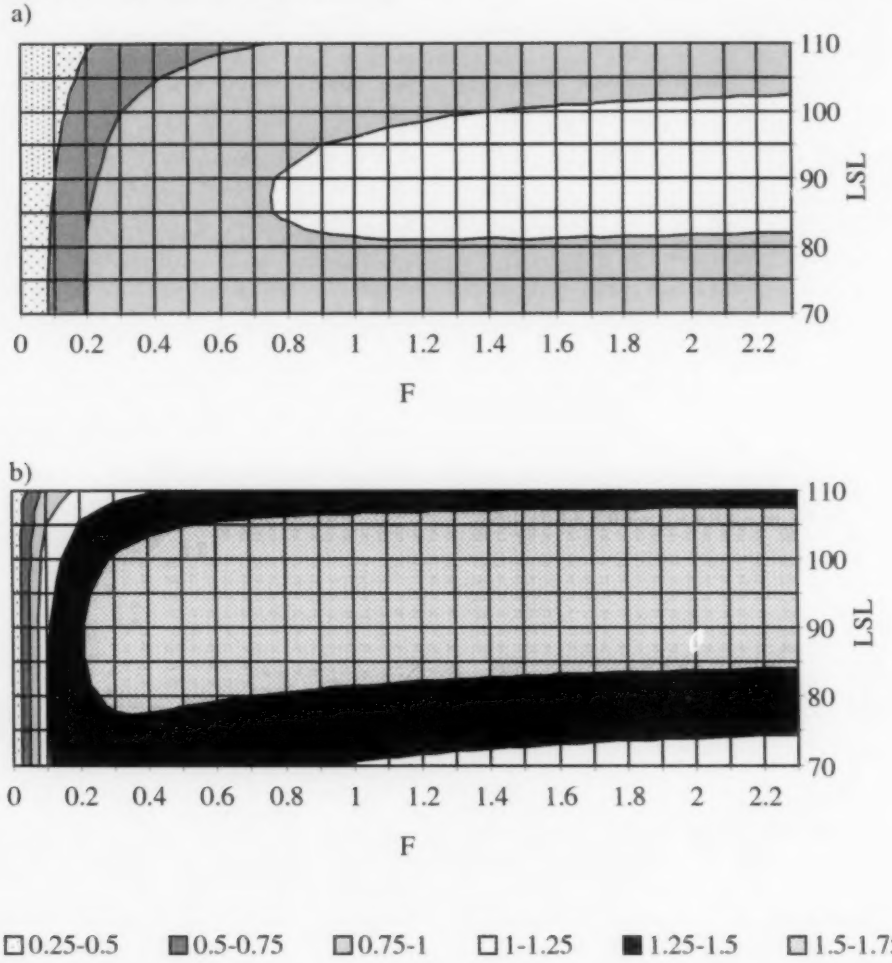

of red sea urchin biology, but driven by the same geographic factors that affect recruitment variability, and (*ii*) a relationship between the spatial pattern in recruitment variability and estimates of *F*. With regard to the former possibility, both landings and effort show a positive correlation with distance (latitude) north of a headland, suggesting that fishing conditions might be better in these areas. This interpretation is consistent with wind exposure in northern California. Headlands typically protect areas just to the south from the strong northerly winds during spring and early summer. With regard to the latter possibility, the bias in estimates due to recruitment variability is asymmetrical, resulting in sometimes highly positive and at other times slightly negative estimates. If sites just to the north of promontories receive more reliable recruitment, then they would tend to have minimal bias relative to sites further north that had greater variability due to only occasional settlement.

The conclusion that growth rate and *M* differ among locations would be influenced by any harvesting that has occurred in these reserve populations. Illicit harvesting of reserves represents a significant loss of information for evaluating harvest rates in populations that are necessarily analyzed using size-structured models in addition to the direct loss to the resource. The decline in sizes greater than 90 mm at Salt Point strongly suggests that it has been harvested, although we cannot rule out other unknown causes of adult mortality. Not being able to use Salt Point as an unharvested site significantly reduces our ability to assess spatial variability in productivity and underscores the value of no-take reserves. In addition to their use as a practical management option, reserves provide (*i*) unfished populations that are highly desirable for reliable estimation of growth and mortality parameters using our size-structured model (Smith et al. 1998) and (*ii*) an unperturbated locale for the study of the behavior and dynamics of a natural population (Murray et al. 1999).

Comparison of the growth rates obtained here with growth rates obtained by others is complicated by the fact that different growth models have been used. Ebert and Russell (1993) and Ebert et al. (1999) modeled growth using the

© 2000 NRC Canada

Tanaka function, which describes growth with an early period of slow growth followed by an accelerated phase and a final phase of slowly declining growth. The von Bertalanffy growth equation describes growth as a monotonically declining rate with increasing size as individuals approach an asymptotic size and, as implemented in our study, incorporates individual variation in L (Sainsbury 1980; Smith et al. 1998). Despite these differences, calculated growth rates are similar for red sea urchins greater than 4 cm test diameter.

The influence of handling and tagging on sea urchin growth may have biased our estimates of growth; however, 2 years of growth under laboratory conditions did not result in differences in growth or survival between PIT-tagged and non-PIT-tagged individuals (L.E. Morgan, unpublished data). However, this does not rule out the possibility that handling alone may have influenced sea urchin growth.

Our estimates indicate that M is relatively low for red sea urchins, similar to previous estimates of M in northern California. Kalvass and Hendrix (1997) estimated M at 0.077·year^{-1}, based on the assumption that recruitment would be balanced by mortality in an unfished, stable population. Ebert et al. (1999) estimated M at three sites in northern California to range from 0.05 to 0.204·year^{-1}. In general, these rates are lower than rates calculated for southern California, which have ranged from 0.088 to 0.4 (Ebert and Russell 1993; Ebert et al. 1999). These regional differences may be related to the greater abundance of the sea urchin predators spiny lobster, *Panulirus interruptus*, and California sheephead, *Semicossyphus pulcher*, in southern California (Tegner and Levin 1983; Tegner 1989) or the warmer ocean conditions of southern California, which may increase the prevalence of disease outbreaks (Ebert et al. 1999).

In summary, the growth and mortality rates reported in this study provide information that is useful in management in several ways: (*i*) as an indication of spatial variability in productivity, (*ii*) as an estimate of the time delay between changes in recruitment and these effects being observed in the fishery, (*iii*) as an indication of a possible spatial pattern in fishing effort and mortality, and (*iv*) as an example of the potential biases associated with spatially and temporally varying recruitment on calculation of these rates. Further analysis is needed to determine whether spatially explicit harvesting strategies, through either closed areas (Quinn et al. 1993; Pfister and Bradbury 1996) or rotating spatial closures (Botsford et al. 1993), should take advantage of the potential spatial differences in productivity indicated here. MacCall (1990) has shown that including spatial variability in productivity in management plans can enhance fishery yields. Growth rates indicate that individuals may take as long as 5–7 years to reach the minimum legal size, suggesting caution when considering the influence of harvesting on recruitment. The length of this period indicates that recruitment failure, as might occur due to the presence of Allee effects (Tegner and Dayton 1977; Levitan et al. 1992; Quinn et al. 1993), will not be detectable in the catch until it is possibly too late to correct harvest rates.

Acknowledgements

The authors thank the staff of the Bodega Marine Laboratory for support of this project. Diving assistance by Carolyn Lundquist, Jennifer Diehl, James Leichter, Dave Nothhelfer, Todd Switzer, and Kelly Bachelor is also greatly appreciated. Pete Kalvass and the other members of the Ft. Bragg office of the California Department of Fish and Game were very helpful. This research was part of a doctoral dissertation by L.E.M. at the University of California at Davis. This research was funded under grant No. NA66RG0477, project No. R/F-169, from the California Sea Grant College Program, National Oceanic and Atmospheric Administration, U.S. Department of Commerce. The views expressed herein are those of the authors and do not necessarily reflect the view of the National Oceanic and Atmospheric Administration or any of its subagencies. The U.S. Government is authorized to reproduce and distribute for governmental purposes.

References

Barry, J.P., and Tegner, M.J. 1990. Inferring demographic processes from size–frequency distributions: simple models indicate specific patterns of growth and mortality. Fish. Bull. U.S. **88**: 13–19.

Beverton, R.J.H., and Holt, S.J. 1957. On the dynamics of exploited fish populations. Chapman and Hall, London, U.K.

Botsford, L.W., Quinn, J.F., Wing, S.R., and Brittnacher, J.G. 1993. Rotating spatial harvest of a benthic invertebrate, the red sea urchin *Strongylocentrotus franciscanus*. *In* Proceedings of the International Symposium on Management Strategies of Exploited Fish Populations. *Edited by* G. Kruse, D.M. Eggers, R.J. Marasco, C. Pautzke, and T.J. Quinn II. University of Alaska, Fairbanks, Alaska. pp. 408–429.

Botsford, L.W., Smith, B.D., and Quinn, J.F. 1994. Bimodality in population size distributions: the red sea urchin, *Strongylocentrotus franciscanus* as an example. Ecol. Appl. **4**: 42–50.

Botsford, L.W., Morgan, L.E., Lockwood, D.R., and Wilen, J.E. 1999. Marine reserves and management of the northern California red sea urchin fishery. Calif. Coop. Oceanic Fish. Invest. Rep. **40**: 87–93.

Breen, P.A., Carolsfeld, W., and Yamanaka, K.L. 1985. Social behavior of juvenile red sea urchins, *Strongylocentrotus franciscanus* (Agassiz). J. Exp. Mar. Biol. Ecol. **92**: 45–61.

Burnham, K.P., and Anderson, D.R. 1998. Model selection and inference: a practical information-theoretic approach. Springer, New York.

Davis, R.E. 1985. Drifter observations of coastal surface currents during CODE: the statistical and dynamical views. J Geophys. Res. **90**: 4756–4772.

Ebert, T.A., and Russell, M.P. 1993. Growth and mortality of subtidal red sea urchin *Strongylocentrotus franciscanus* at San Nicolas Island, California, USA. Mar. Biol. **117**: 79–89.

Ebert, T.A., Dixon, J.D., Schroeter, S.C., Kalvass, P.E., Richmond, N.T., Bradbury, W.A., and Woodby, D.A. 1999. Growth and mortality of red sea urchins (*Strongylocentrotus franciscanus*). Mar. Ecol. Prog. Ser. **190**: 189–209.

Estes, J.A., and Duggins, D.O. 1995. Sea otters and kelp forests in Alaska: generality and variation in a community ecological paradigm. Ecol. Monogr. **65**: 75–100.

Huyer, A., and Kosro, P.M. 1987. Mesoscale surveys over the shelf and slope in the upwelling region near Point Arena, California. J. Geophys. Res. **92**: 1655–1681.

Kalvass, P.A., and Hendrix, J.M. 1997. The California red sea urchin (*Strongylocentrotus franciscanus*) fishery: catch, effort and management trends. Mar. Fish. Rev. **59**(2): 1–17.

© 2000 NRC Canada

Kato, S., and Schroeter, S.C. 1985. Biology of the red sea urchin, *Strongylocentrotus franciscanus*, and its fishery in California. Mar. Fish. Rev. **47**(3): 1–20.

Kosro, P.M. 1987. Structure of the coastal current field off northern California during the Coastal Ocean Dynamics Experiment. J. Geophys. Res. **92**: 1637–1654.

Levitan, D.R. 1991. Influence of body size and population density on fertilization success and reproductive output in a free spawning invertebrate. Biol. Bull. (Woods Hole), **181**: 261–268.

Levitan, D.R., Sewell, M.A., and Chia, F.S. 1992. How distribution and abundance influence fertilization success in the sea urchin *Strongylocentrotus franciscanus*. Ecology, **73**: 248–254.

MacCall, A. 1990. Dynamic geography of marine fish populations. University of Washington Press, Seattle, Wash.

Morgan, L.E., Wing, S.R., Botsford, L.W., Lundquist, C.J., and Diehl, J.M. 2000. Spatial variability in red sea urchin (*Strongylocentrotus franciscanus*) recruitment in northern California. Fish. Oceanogr. **9**: 83–98.

Murray, S.N., Ambrose, R.F., Bohnsack, J.A., Botsford, L.W., Carr, M.H., Davis, G.E., Dayton, P.K., Gotshall, D., Gunderson, D.R., Hixon, M.A., Lubchenco, J., Mangel, M., MacCall, A., McArdle, D.A., Ogden, J.C., Roughgarden, J., Starr, R.M., Tegner, M.J., and Yoklavich, M.M. 1999. No-take reserve networks: sustaining fishery populations and marine ecosystems. Fisheries (Bethesda), **24**(11): 11–25.

Pennington, J.T. 1985. The ecology of fertilization of echinoid eggs: the consequence of sperm dilution, adult aggregation and synchronous spawning. Biol. Bull. (Woods Hole), **169**: 417–430.

Pfister, C.A., and Bradbury, A. 1996. Harvesting red sea urchins: recent effects and future predictions. Ecol. Appl. **6**: 298–310.

Quinn, J.F., Wing, S.R., and Botsford, L.W. 1993. Harvest refugia in marine invertebrate fisheries: models and applications to the red sea urchin *Strongylocentrotus franciscanus*. Am. Zool. **33**: 537–550.

Sainsbury, K.J. 1980. Effect of individual variability on the von Bertalanffy growth equation. Can. J. Fish. Aquat. Sci. **37**: 241–247.

Schnute, J., and Fournier, D. 1980. A new approach to length–frequency analysis: growth structure. Can. J. Fish. Aquat. Sci. **37**: 1337–1351.

Send, U., Beardsley, R.C., and Winant, C.D. 1987. Relaxation from upwelling in the coastal ocean dynamics experiment. J. Geophys. Res. **92**: 1683–1698.

Smith, B.D., and Botsford, L.W. 1998. Interpretation of growth, mortality and recruitment patterns from size-at-age, growth increment and size frequency data. *In* Proceedings of the North Pacific Symposium on Invertebrate Stock Assessment and Management. *Edited by* G.S. Jamieson and A. Campbell. Can. Spec. Publ. Fish. Aquat. Sci. No. 125. pp. 125–139.

Smith, B.D., Botsford, L.W., and Wing, S.R. 1998. Estimation of growth and mortality parameters from size frequency distributions lacking age patterns: the red sea urchin (*Strongylocentrotus franciscanus*) as an example. Can. J. Fish. Aquat. Sci. **55**: 1236–1247.

Tegner, M.J. 1989. The feasibility of enhancing red sea urchin, *Strongylocentrotus franciscanus*, stocks in California: an analysis of the options. Mar. Fish. Rev. **51**(2): 1–22.

Tegner, M.J., and Dayton, P.K. 1977. Sea urchin recruitment patterns and implications of commercial fishing. Science (Washington, D.C.), **196**: 324–326.

Tegner, M.J., and Levin, L.A. 1983. Spiny lobsters and sea urchins: analysis of a predator–prey interaction. J. Exp. Mar. Biol. Ecol. **73**: 125–150.

von Bertalanffy, L. 1957. Quantitative laws in metabolism and growth. Q. Rev. Biol. **32**: 217–231.

Washburn, L., Swenson, M.S., Largier, J.L., Kosro, P.M., and Ramp, S.R. 1993. Cross-shelf transport by an anticyclonic eddy off northern California. Science (Washington, D.C.), **261**: 1560–1564.

Wing, S.R., Largier, J.L., Botsford, L.W., and Quinn, J.F. 1995*a*. Settlement and transport of benthic invertebrates in an intermittent upwelling region. Limnol. Oceanogr. **40**: 316–329.

Wing, S.R., Botsford, L.W., Largier, J.L., and Morgan, L.E. 1995*b*. Spatial variability in settlement of benthic invertebrates in an intermittent upwelling system. Mar. Ecol. Prog. Ser. **128**: 199–211.

Wing, S.R., Botsford, L.W., Largier, J.L., and Ralston, S. 1998. Meroplankton distribution and circulation associated with a coastal retention zone in the northern California upwelling zone. Limnol. Oceanogr. **43**: 1710–1721.

Appendix

Equation A1 is the correct representation of eq. 13 of Smith et al. (1998), which was reported incorrectly in that paper:

$$\text{(A1)}\quad \Theta_2(\mu_L, \sigma_L, \mu_K, \sigma_K, \sigma_{M,l=100} | l, \Delta t) = \sum_{j=1}^{v} \ln(2\pi\sigma_{M,l_j}\sigma_{l_j}) - \ln\left(\int_{l_j=0}^{l_j=\infty} e^{-\left(\frac{(\bar{l}_j - l_j)^2}{2\sigma^2_{M,l_j}} + \frac{(l_j - \mu_{l_j})^2}{2\sigma^2_{l_j}}\right)}\right)^{r} + \ln(1-\zeta_l)$$

Appendix reference

Smith, B.D., Botsford, L.W., and Wing, S.R. 1998. Estimation of growth and mortality parameters from size frequency distributions lacking age patterns: the red sea urchin (*Strongylocentrotus franciscanus*) as an example. Can. J. Fish. Aquat. Sci. **55**: 1236–1247.

© 2000 NRC Canada

Regional differences in rates and patterns of North American inland lake invasions by zebra mussels (*Dreissena polymorpha*)

Clifford E. Kraft and Ladd E. Johnson

Abstract: Zebra mussels (*Dreissena polymorpha*) have spread rapidly in North America by dispersal within connected bodies of waters. This study provides the first systematic evaluation of rates of zebra mussel dispersal to inland lakes separated from source populations by functional dispersal barriers. Plankton samples were examined for this exotic species from 140 lakes during a 3-year period (1995–1997). Infestations were detected in 19% of lakes surveyed: seven of 28 Indiana lakes (25%), 15 of 49 Michigan lakes (31%), but only five of 63 Wisconsin–Illinois lakes (8%). Annual rates of infestation varied from 0 to 12%·year^{-1} among the three regions. Wisconsin–Illinois lake infestations were only detected in 1995 and 1996, whereas new Indiana and Michigan infestations were detected in all three years. Lakes with surface areas less than 100 ha had lower infestation rates than larger lakes. Incidental sightings of inland lake colonization within the study region qualitatively supported observed regional differences in rates and spatial patterns of colonization. These results demonstrate that the spread of zebra mussels into inland lakes is not occurring as rapidly as through connected waterways, and rates of inland lake colonization vary according to regional conditions and lake size.

Résumé : Les moules zébrées (*Dreissena polymorpha*) se sont rapidement répandues en Amérique du Nord en se dispersant au sein de masses d'eau interreliées. Notre étude est la première évaluation systématique des taux de dispersion de la moule zébrée dans les lacs intérieurs séparés des populations sources par des obstacles fonctionnels. Pendant une période de 3 ans (1995–1997), nous avons recherché cette espèce exotique dans des échantillons de plancton. Des infestations ont été détectées dans 19% des lacs étudiés : 7 sur 28 lacs en Indiana (25%), 15 sur 49 lacs dans le Michigan (31%), mais seulement 5 sur 63 lacs dans la région Wisconsin–Illinois (8%). Les taux annuels d'infestation variaient de 0 à 12%·an^{-1} entre les trois régions. Dans le Wisconsin–Illinois, des infestations ont été détectées seulement entre 1995 et 1996, tandis que de nouvelles infestations ont été détectées chacune des trois années dans l'Indiana et le Michigan. Les lacs à superficie de moins de 100 ha présentaient des taux d'infestation moindre que les lacs plus grands. Des observations occasionnelles de colonisation des lacs de l'intérieur dans la zone d'étude sont venues confirmer qualitativement les différences observées régionalement dans les taux et les régimes spatiaux de colonisation. Ces résultats montrent que la dispersion de la moule zébrée dans les lacs intérieurs n'est pas aussi rapide que dans le cas des masses d'eau interreliées, et que le taux de colonisation des lacs intérieurs varie selon les conditions régionales et la taille des lacs.

[Traduit par la Rédaction]

Introduction

Information on rates and patterns of invasion is essential to predict the geographic spread of exotic species (Shigesada and Kawasaki 1997). The North American zebra mussel (*Dreissena polymorpha*) invasion has been notorious (Vitousek et al. 1996), in part due to the unusually rapid range expansion of these nuisance molluscs (Neary and Leach 1992; Ludyanskiy et al. 1993; Hincks and Mackie 1997). By 1991, 3 years after their initial detection in Lake St. Clair, zebra mussels were already found throughout the Laurentian Great Lakes and connecting river systems as far away as Louisiana and Quebec. This rapid range expansion produced prominent warnings, such as that "by the year 2000, the zebra mussel can be expected to have colonized all North American rivers, lakes and reservoirs that fit its broad ecological requirements" (Ludyanskiy et al. 1993).

Lost in such predictions was the distinction between range boundaries and the internal structure of that range (Brown et al. 1996). Once the breadth of the North American range of zebra mussels was established, little attention was paid to the details of colonization inside that range boundary, especially with regard to inland lakes. The early North American distribution of zebra mussels closely matched the commercially navigable waters of the Great Lakes and Mississippi basins and included few inland lakes (Johnson and Carlton 1996). Differences in barriers to dispersal are likely to produce unequal colonization rates between connected bodies of water, such as large navigable rivers, relative to inland lakes that require overland transport for colonization (Carlton 1993; Johnson and Carlton 1996).

Downstream spread of zebra mussels occurs largely

Received June 2, 1999. Accepted February 2, 2000.
J15159

C.E. Kraft.[1] Department of Natural Resources, Cornell University, Ithaca, NY 14853-3001, U.S.A.
L.E. Johnson. Département de Biologie and GIROQ, Université Laval, Québec, QC G1K 7P4, Canada.

[1]Author to whom all correspondence should be addressed.
email: cek7@cornell.edu

© 2000 NRC Canada

through the advective transport of planktonic larvae (veligers) (Stoeckel et al. 1997), although in streams less than 30 m in diameter, downstream colonization appears to be limited to distances less than 10 km (Horvath et al. 1996). This distance may define a functional dispersal barrier. Upstream spread appears to require human-mediated vectors (Carlton 1993) such as boats (Keevin et al. 1992). Thus, for transport to inland lakes without navigable or nearby (<10 km) hydrological connections to infested waters, a dispersal barrier must be crossed. Many potential overland dispersal mechanisms exist (Carlton 1993), but in general, successful overland colonization is probably more difficult due to greater stress during periods out of water (Ricciardi et al. 1995) or to low numbers of individuals transported by any given dispersal event (Johnson and Padilla 1996).

Predictions of zebra mussel distributions have focused on their likely maximum range in North American waters (Strayer 1991; Neary and Leach 1992; Koutnik and Padilla 1994) based on environmental limits determined from European (Ramcharan et al. 1992*a*, 1992*b*) and North American studies (Hincks and Mackie 1997). Attempts to predict which suitable waters are likely to be first colonized are rare (Neary and Leach 1992), and no data have been published regarding the rates at which environmentally suitable North America lakes have become colonized.

In this study, we addressed two issues. First, we evaluated whether zebra mussels were colonizing North American inland lake districts as quickly as connected large lake and river systems. To do this, we examined zebra mussel colonization of inland lakes in a four-state region adjacent to the Great Lakes over a 3-year period. Second, we used our sampling results, in conjunction with verified incidental reports of inland lake colonization, to assess rates and spatial patterns of colonization over several geographical scales.

Methods

Data collection conducted in 1995, 1996, and 1997 consisted of determining the presence or absence of zebra mussels in 140 inland lakes in Illinois, Indiana, Michigan, and Wisconsin. Our sampling focused on 10 regional lake districts, which were defined as areas in which we could sample 50–100% of suitable lakes (defined below) in a 2- to 3-day sampling period. These districts included 89% of the lakes surveyed. Study lakes did not have navigable connections to other waters, and at the time of sampling, no lake was located downstream from any body of water known to be infested. During the course of the study, potential upstream source populations were found for two infested survey lakes.

Since we were specifically interested in rates and patterns of inland lake invasions, and not in environmental limitations, we only sampled lakes with water chemistry (pH > 7.3, Ca > 28 mg/L; Ramcharan et al. 1992*b*) and physical characteristics (>50 ha, >2 m mean depth, >4 m maximum depth; Strayer 1991) suitable for zebra mussel colonization. Prior to sampling, we did not know if zebra mussels were established in the study lakes. Public access was available to all study lakes, except for two Michigan lakes (Oakland district), and all lakes were located in areas with extensive recreational activity and residential development.

Relative proportions of surveyed lake sizes were similar in both Wisconsin–Illinois and Michigan–Indiana (Fig. 1). Overall, surveyed lakes included a smaller proportion of lakes between 50 and 100 ha in surface area than would be expected by randomly sampling all lakes in the study area and a larger proportion of lakes with surface areas greater than 600 ha (Fig. 1).

Plankton sampling provided the most efficient way to sample large numbers of lakes for zebra mussels and also offered early detection of recently colonized lakes, prior to widespread colonization of adult mussels (Kraft 1993). The field sampling program was established so that all lakes were surveyed with equal sampling effort. In a given year, we attempted to collect plankton samples from each lake on at least three dates at 3-week intervals. Most sampling was conducted from late May to mid-July, when veligers are most abundant in the plankton of small midwestern lakes (C. Kraft and L. Johnson, unpublished data), although Wisconsin and Illinois lakes were surveyed through mid-September. In rare instances, logistical difficulties (e.g., weather, equipment failure) limited sampling to two occasions during a given year. Plankton samples were collected from three sites within each lake on each sampling date. When selecting sites, we tried to include as many distinct areas of the lake as possible. For long narrow lakes, samples were collected at both ends and in the center of the lake. If a lake contained distinct basins, we tried to collect at least one sample from each basin. In lakes with one homogeneous basin, samples were collected at three locations spaced as far apart as possible.

Plankton samples were collected with a 0.5- or 0.3-m-diameter, 64-μm-mesh plankton net with a length to mouth ratio of 5:1. Depending on water depth and net diameter, one or two vertical tows were taken from depths of 4–6 m for a total sample volume of 800 L. Samples were preserved in ethanol. Plankton nets were bathed in vinegar (minimum period of 45 min) after sampling each lake to prevent sample contamination and veliger dispersal. Prior to this study, we examined the water used to wash nets after sampling infested waters. Veligers were never found in wash water from vinegar-soaked nets but were frequently found in water from nets not exposed to vinegar (C. Kraft, unpublished data).

After field preservation, samples were examined at 40× with a stereomicroscope under cross-polarized light (Johnson 1995). During the first year, laboratory protocols were established to determine efficient methods to analyze plankton samples to detect veligers. Initially, entire samples were examined for zebra mussel veligers. We subsequently determined that as few as four veligers could be detected in a 350 mL concentrated plankton sample (the average sample volume) by examining subsamples (50 mL total) of particulate material settled at the bottom of undisturbed jars. If low numbers of veligers (<10) were found in subsamples from a lake not previously known to contain zebra mussels, we verified the detection by examining the entire sample. Our effective detection limit was 5 veligers/m^3 water sampled. This threshold would represent a total of 25 million larvae in a 100-ha lake with a 5-m average depth, which could represent the maximal reproductive output of less than 100 female mussels (Borcherding 1991).

Sampling was discontinued following confirmation that zebra mussels were established in a lake (i.e., adult mussels were observed), and additional lakes were added to the sampling program in subsequent years to maximize the number of surveyed lakes. Because the presence of veligers does not necessarily mean that a lake has become colonized by adult zebra mussels, our estimate of zebra mussel inland lake infestations could be an overestimate. However, adult mussels were usually found later, often in the same season that veligers were detected. Because detections during the first year of sampling could result from an infestation occurring in any preceding year, annual infestation rates were only calculated from lakes sampled in consecutive years (i.e., for 1996 and 1997). However, given that we could only detect the presence of zebra mussels above a certain threshold (see above), we could not conclusively determine that colonization of these lakes occurred during the preceding year.

© 2000 NRC Canada

Fig. 1. Proportion of lakes greater than 50 ha in surface area in different size categories. Surveyed lakes in Wisconsin–Illinois and Michigan–Indiana are shown as distinct categories as well as all lakes in Wisconsin and the lower peninsula of Michigan that appear on U.S. Geological Survey 1 : 24 000 topographic maps.

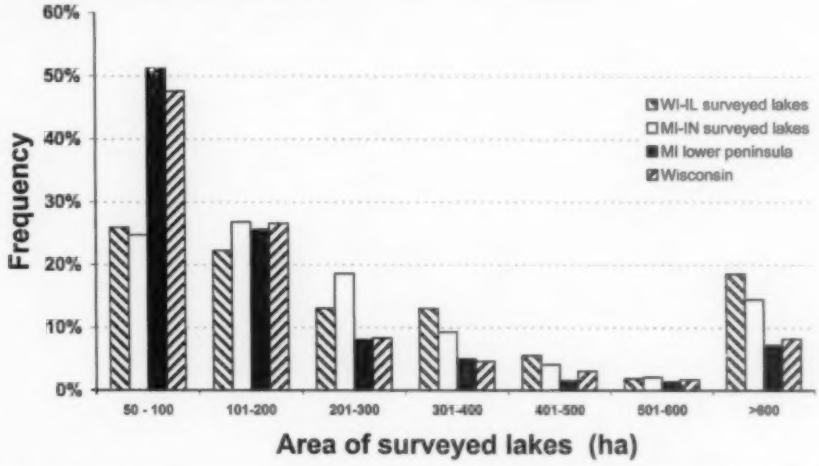

Both before and during the course of our study, adult zebra mussels were discovered within the study region in lakes that were not included in our planned sampling program. None of these lakes had navigable connections to Great Lakes waters. All incidental discoveries were verified by us or by state agencies and were used as auxiliary information to our sampling program to confirm regional patterns of lake infestation. These data were also used to compare the size distribution of infested lakes detected in a planned survey relative to the size distribution detected from unplanned observations.

Results

Zebra mussels were detected in 27 of the 140 lakes surveyed (19%) during this study, but the distribution of these detections was spatially variable (Fig. 2; Table 1). In general, the proportion of lakes found to be infested with zebra mussels was far greater in Michigan (15 of 49 = 31%) and Indiana (seven of 28 = 25%) than lakes surveyed in Wisconsin–Illinois (five of 63 = 8%; G test, $G = 10.51$, $p < 0.01$). Incidental discoveries of inland lake zebra mussel infestations also supported the observation that inland lake colonization was more prevalent in Michigan and Indiana by the end of 1997 than in Wisconsin and Illinois (Fig. 3).

Further variation was also apparent at the finer spatial scale of individual lake districts (Fig. 4; Table 2). In Michigan, infestations occurred in all three lake districts but at higher levels in Oakland County, north of Detroit. Similar levels were observed in Indiana with the exception of the Lagrange County district in which no infestations were detected, in spite of being located between two highly infested districts. In Wisconsin–Illinois, four of the five infestations occurred in the southeast Wisconsin district near the Wisconsin–Illinois border. Thus, 20–44% of lakes in five out of six Michigan and Indiana districts were infested, in contrast with consistently low proportions (<15%) in Wisconsin–Illinois districts.

Detections of new infestations were variable from year to year, and the Wisconsin–Illinois results again contrasted sharply with those from Michigan and Indiana. After the first year of the study (1995) during which four Wisconsin infestations were discovered, no additional infestations were found in the initial set of survey lakes during the second and third years of sampling (Table 1; one additional infestation was found in an Illinois lake added to the sampling program in 1996). Overall, using only lakes surveyed in consecutive years (Table 1), the annual infestation rate was 4.6% (3.0% (2/67) for 1995–1996 and 5.6% (6/108) for 1996–1997). Among these same lakes, annual infestation rates were consistent in Indiana (11–12%) while more variable in Michigan (5–12%). The annual infestation rate for Wisconsin study lakes was 0% during both periods.

Infested lakes were more likely to have surface areas between 100 and 500 ha, and lakes smaller than 100 ha and greater than 500 ha were less likely to be infested (Fig. 5A). By contrast, 25% of the incidental sightings came from lakes greater than 500 ha in surface area (Fig. 5B).

Discussion

The impact of any invasive species will depend on its geographic range, and other studies have predicted the ultimate range of zebra mussels at continental (Strayer 1991) and regional scales (e.g., Neary and Leach 1992; Koutnik and Padilla 1994). Unfortunately, simple range boundaries can be misleading, since most maps of geographic ranges ignore the area inside the range boundary (Brown et al. 1996). For invasive species, "jump" or long-distance dispersal often produces patchy patterns of colonization (Shigesada and Kawasaki 1997). Our results show that the colonization of inland lakes by zebra mussels is patchy at regional and district-level spatial scales, and inland lakes are becoming colonized more slowly than the initial range expansion through North American navigable waterways. This slower rate of spread is undoubtedly due to functional dispersal barriers that reduce dispersal to and within watersheds. A majority of the infestations detected either incidentally (73%) or as a part of our survey (93%) occurred in lakes without navigable connec-

© 2000 NRC Canada

Fig. 2. Lakes surveyed as part of this study in the lower peninsula of Michigan, Wisconsin, northern Indiana, and northern Illinois. Lakes infested with zebra mussels are shown with solid circles, and lakes that were uninfested as of 1997 are shown with open circles.

Table 1. Percentage of sampled lakes with zebra mussel infestations in three regions: lower peninsula of Michigan (MI), northern Indiana (IN), and Wisconsin – northern Illinois (WI–IL).

		Year first sampled			
Region	Year detected	1995	1996	1997	Row total
MI	1995	15% (4/26)	—	—	15% (4/26)
MI	1996	5% (1/22)*	14% (2/14)	—	8% (3/36)
MI	1997	19% (4/21)*	0% (0/12)*	44% (4/9)	19% (8/42)
MI	All years	35% (9/26)	14% (2/14)	44% (4/9)	31% (15/49)
IN	1995	25% (3/12)	—	—	25% (3/12)
IN	1996	11% (1/9)*	10% (1/10)	—	11% (2/19)
IN	1997	13% (1/8)*	11% (1/9)*	0% (0/6)	9% (2/23)
IN	All years	42% (5/12)	20% (2/10)	0% (0/6)	25% (7/28)
WI–IL	1995	10% (4/40)	—	—	10% (4/40)
WI–IL	1996	0% (0/36)*	4% (1/23)	—	2% (1/59)
WI–IL	1997	0% (0/36)*	0% (0/22)*	—	0% (0/58)
WI–IL	All years	10% (4/40)	4% (1/23)	—	8% (5/63)

Note: Data are cross-tabulated by the year in which infestations were detected and by the year in which lakes were first sampled. Values in parentheses represent the number of infested lakes per number of lakes sampled. Asterisks indicate values used to estimate annual rates of infestations.

tions to infested downstream waters or upstream source populations (C. Kraft and L. Johnson, unpublished data). We believe that these slow rates of spread are largely due to limitations in overland dispersal and that concerns over the rapid overland dispersal of zebra mussels (e.g., Griffiths et al. 1991; Ricciardi et al. 1995), although legitimate, may be overly fatalistic.

We have clearly documented that the inland spread of zebra mussels has been less extensive for Wisconsin–Illinois lakes than for either Michigan or northern Indiana lakes. Assuming other factors being equal, this pattern might be initially attributed to the way in which nearby source populations developed in the Great Lakes. Zebra mussels were first discovered in Lake St. Clair and western Lake Erie (1988), subsequently became established in eastern and southern Lake Michigan (1990), and finally colonized western Lake Michigan in 1991 (Griffiths et al. 1991; Kraft 1993; Cope et al. 1997). Consequently, nearby source populations for potential infestations of southeastern Michigan lakes developed 2–3 years earlier than for Wisconsin lake districts. Indiana districts were in an intermediate position: farther from Lake St. Clair and western Lake Erie shorelines but a similar distance from southeastern Lake Michigan. Additionally, Lake Wawasee, Indiana's largest inland lake, became infested relatively early (1991) and therefore could have served as a local source.

© 2000 NRC Canada

Fig. 3. Inland lakes (in the lower peninsula of Michigan, Wisconsin, northern Indiana, and northern Illinois) that had confirmed zebra mussel infestations through 1997. Detections shown include those resulting from this study (solid circles) as well as confirmed infestations from unplanned observations (open circles) made both during the course of this study (1995–1997) and prior to 1995.

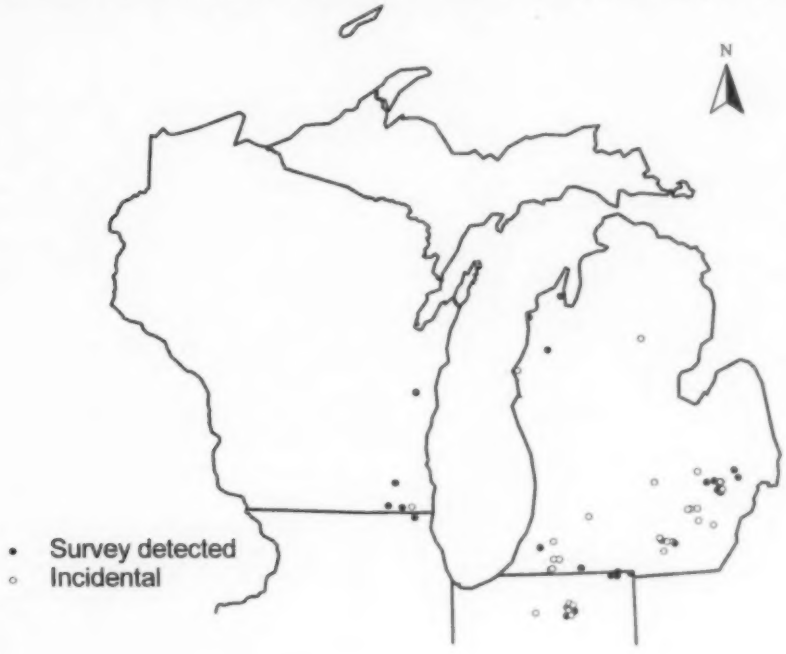

Fig. 4. Regional differences in relative rates of lake infestation by zebra mussels. The relative size of pie charts is proportional to the number of lakes surveyed within a region on which the pie chart is centered. The proportion of infested lakes is shown in black, and proportion of lakes remaining uninfested as of 1997 is shown in grey.

© 2000 NRC Canada

Table 2. Number of survey lakes in which zebra mussels were found according to survey districts. Not all lakes surveyed were included in these districts. Also shown is the number of lakes in each region from which zebra mussels were reported based on incidental discoveries reported through unplanned observations (1991–1997).

District	State	No Mussels (surveyed)	Mussels (surveyed)	Mussels (incidental)
Steuben	Indiana	5	4	0
Lagrange	Indiana	9	0	0
Kosciusko	Indiana	7	3	4
Oakland	Michigan	13	8	6
Jackson	Michigan	8	2	4
Leelanau	Michigan	8	2	0
Northeast	Wisconsin	5	0	0
Sheboygan	Wisconsin	7	1	0
Western Milwaukee	Wisconsin	15	0	0
Southeast	Wisconsin–Illinois	24	4	1

Although plausible, this scenario does not explain observed colonization patterns because it is inconsistent with the timing of the infestations observed within each region. Given the east–west time lag in the establishment of Great Lakes source populations, if the rates and patterns of dispersal were similar in all regions, we would have predicted fewer Wisconsin–Illinois inland lake infestations in 1995 than in subsequent years. Instead, four Wisconsin–Illinois infestations were found in 1995, one in 1996, and none in 1997.

Several alternative hypotheses may explain the observed differences between Michigan–Indiana and Wisconsin–Illinois. First, inland lakes might be less suitable for zebra mussels in Wisconsin–Illinois. Second, dispersal vectors might be less common or have different behaviors in Wisconsin–Illinois. Third, dispersal vectors might be less efficient at transporting zebra mussels in Wisconsin–Illinois.

Lake characteristics in the study region are similar and not restrictive for zebra mussel colonization. Summer total phosphorus levels in lakes within the study region exceed 15 g/L (Omernik et al. 1988), and total alkalinity exceeds 2000 μequiv./L (Omernik and Powers 1983; Omernik et al. 1988). Lakes surveyed as part of this study were located in regions with carbonate bedrock, which is a good predictor of lake types suitable for zebra mussel colonization (Neary and Leach 1992; Koutnik and Padilla 1994). Relative proportions of surveyed lake sizes were similar in both study regions.

Transient recreational boating is considered to be the primary mechanism for overland zebra mussel dispersal (Johnson and Carlton 1996; Schneider et al. 1998), and recreational boats are used sequentially between Great Lakes waters and inland waters (Padilla et al. 1996; Buchan and Padilla 1999). Although precise measures of boat use for each region are lacking, the number of recreational boats registered in the study region suggests that boat use cannot explain large differences in rates and patterns of colonization. In 1997, 760 000 boats were registered in Michigan, 490 000 in Wisconsin, 207 000 in northern Illinois, and 70 000 in northern Indiana (Bossenbroek 1999).

Differences may also exist in the efficiency by which mussels are transported upon recreational boats. One possible difference is the degree to which zebra mussels are transported on macrophytes entangled on boats leaving infested waters (Johnson and Carlton 1996). We have observed evidence of this type of dispersal at Great Lakes boat ramps in southeastern Michigan but never at ramps along Wisconsin's Lake Michigan shoreline (Johnson and Carlton 1996; C. Kraft and L. Johnson, unpublished data). Thus we speculate that zebra mussels might have been transported on entangled macrophytes in higher numbers or at greater frequency from source populations in Lake St. Clair and western Lake Erie than from source populations in western Lake Michigan.

However, even without knowing the precise mechanisms involved, we believe that observed regional differences were due to differences in rates of dispersal, not to differences in habitat features. A simulation model of zebra mussel dispersal in this region has shown that infested lake distributions within our study area can be predicted without invoking differences in lake habitat suitability (Bossenbroek 1999).

We do not have data to examine the characteristics of infested lakes, except that we observed that lakes larger than 100 ha were more likely to become infested. This is consistent with studies in Europe (Karataev and Burlakova 1995) and surveys of European data (Strayer 1991; Ramcharan et al. 1992*b*). Because the majority of lakes in Wisconsin and the lower peninsula of Michigan are smaller than 100 ha, overall lake infestation rates would be substantially lower than reported in this study, since we disproportionately sampled larger lakes. We believe that our observation of low infestation rates for large lakes (>600 ha) was an artifact of the distribution of large lakes within our lake districts, since 16 of 18 large lakes (>600 ha) sampled were located in districts that had low overall rates of infestation. Moreover, at the start of our study, many of the larger lakes in our lake districts were already infested and thus were not included in our survey.

The public is highly aware of zebra mussels, and people have been encouraged to report new sightings. Although data from such reports can be useful for general comparisons, they provide insufficient precision to examine rates and patterns of geographic spread. Unplanned sampling efforts cannot be standardized in either space or time and therefore may be biased. This problem is reflected in our observation that incidental discoveries of infestations occurred more frequently from lakes greater than 600 ha in surface area, where more people are likely to be looking for mussels. In addition, the absence of zebra mussels is not reported in such databases, and thus, neither rates nor proportions of infestations can be calculated. We established a systematic monitoring program with consistent sampling protocols to avoid such problems.

The recognition that many aquatic habitats across North America are ecologically suitable for zebra mussels, and the fact that this invader spread rapidly over a broad geographic range, has promoted the unfounded assumption among journalists, educators, the public, and even scientists that the invasion of all suitable habitats by zebra mussels is a "fait accompli." Indeed, journalists have so frequently reported the zebra mussel's rapid spread throughout North America

© 2000 NRC Canada

Fig. 5. (A) Proportion of surveyed inland lakes that were infested (solid bars) and uninfested (open bars) by zebra mussels as of 1997 according to lake surface area and (B) number of infested lakes discovered through surveys conducted as part of this study (surveyed 1995–1997, open bars) and incidental discoveries reported through unplanned observations (1991–1997, solid bars) according to lake surface area. All incidental discoveries were verified (see text).

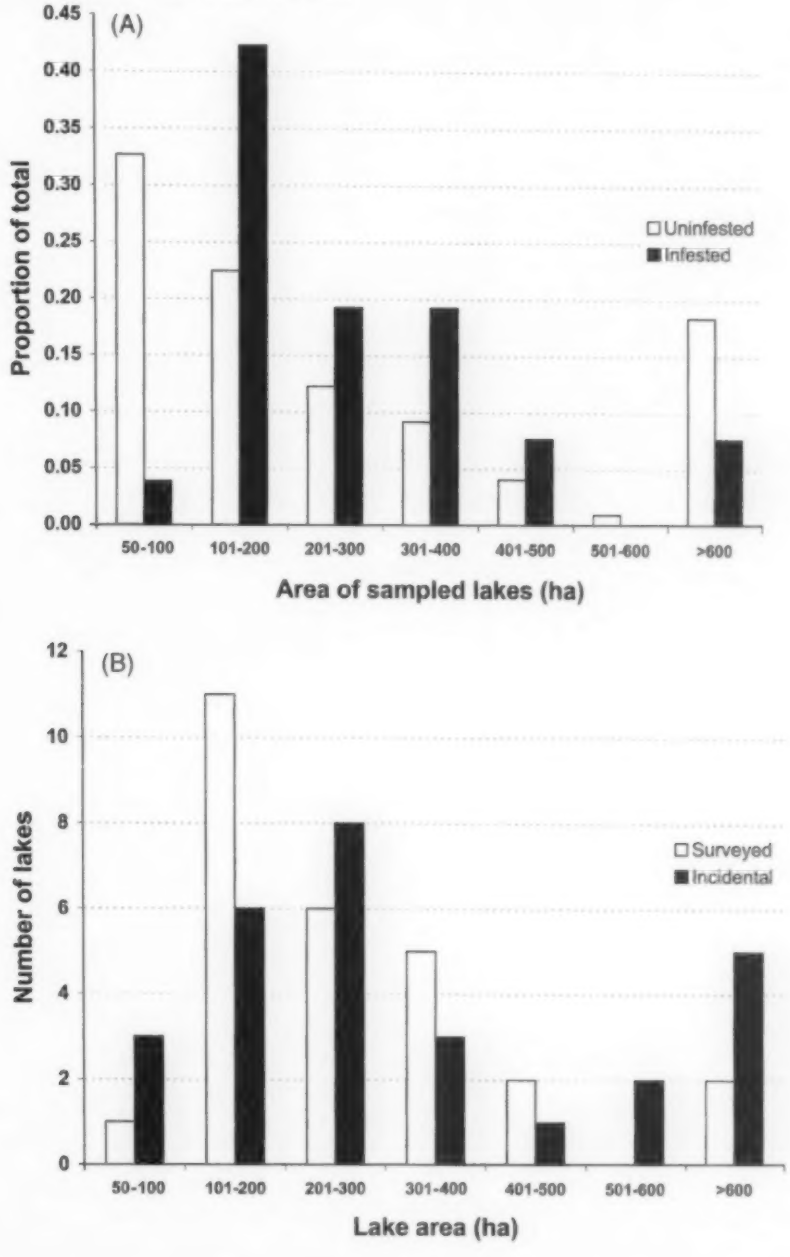

that it has become a metaphor for rapidly occurring events ("the data communications industry is growing faster than zebra mussels in a drainpipe..." (*Fortune*, March 7, 1995) "...brew pubs that have been spreading like zebra mussels across the country" (*Ithaca Journal*, December 5, 1998)). Yet zebra mussel dispersal involves two distinct methods that have produced vastly different rates of spread. Whereas the commercially navigable and connected inland waters of North America were quickly colonized by zebra mussels, our results demonstrate that dispersal to inland lakes has been taking place more slowly. When evaluating rates of zebra mussel dispersal, it will be critical to distinguish between dispersal occurring within connected and nonconnected waterways. Other scientists have implicitly made this dis-

© 2000 NRC Canada

tinction by only describing the rapid spread of zebra mussels through river systems (e.g., Mellina and Rasmussen 1994; Hincks and Mackie 1997) without referring to the subject of dispersal rates to inland lakes.

This distinction is particularly important for education and outreach efforts that have been initiated with the premise that zebra mussels are spreading rapidly throughout North America. The slower spread into inland lakes will provide more opportunities to mount an effective effort to diminish the overland spread of zebra mussels to inland lakes but will also require a long-term, sustained commitment focused on preventing dispersal to susceptible lakes.

Our results have documented the early stages of the colonization of inland North American lakes by zebra mussels and suggest that new inland lake infestations will continue for decades. Our data on rates and patterns of this invasion have already been used to forecast future inland lake distribution patterns (Bossenbroek 1999; J. Bossenbroek, Colorado State University, Fort Collins, Co., unpublished data). Since data sets suitable for evaluating spatial or temporal patterns of aquatic invasions are rare (Cohen and Carlton 1998), additional studies detailing spatial and temporal patterns of aquatic invasions will provide an improved predictive capability regarding the spread of aquatic invasive species.

Acknowledgements

We thank Jim Carlton for many helpful discussions in planning and implementing this project and two anonymous reviewers for their comments. We thank Jeffrey Hieb, Heidi Bunk, Jaime Corbisier, Eric Damkot, and Tamara Smith (Team Wisconsin) and Paul Marangelo, Sue Kersten, Steve Hart, Kristin Pirkola, Dan Lavoie, and Matt Bolang (Team Michigan) for dedicated assistance in collecting and analyzing plankton samples as well as data entry and organization. Ours thanks as well to those individuals and organizations who assisted us with sample collection: Ron Martin, Bob Wakeman, Scott Szymanski, and other personnel from the Wisconsin Department of Natural Resources, personnel from the Michigan Sea Grant Program and Oakland County Health Department, and many lakeshore residents in Michigan and Indiana. Special thanks to the Great Lakes Fishery Science Center for the use of their facilities. This work was funded in part by the University of Wisconsin Sea Grant Institute under grant No. NA46RG0481, by the National Sea Grant College Program, National Oceanic and Atmospheric Administration, U.S. Department of Commerce, by the State of Wisconsin, and by the Connecticut Sea Grant College Program, project R/ES-8.

References

Borcherding, J. 1991. The annual reproductive cycle of the freshwater mussel *Dreissena polymorpha* Pallas in lakes. Oecologia, **87**: 208–218.

Bossenbroek, J. 1999. Modeling the dispersal of *Dreissena polymorpha* (zebra mussel) into the inland lakes of the western Great Lakes region using a gravity model. M.S. thesis, University of Wisconsin-Green Bay, Green Bay, Wis.

Brown, J.H., Stevens, G.C., and Kaufman, D.M. 1996. The geographic range: size, shape, boundaries and internal structure. Annu. Rev. Ecol. Syst. **27**: 597–623.

Buchan, L.A.J., and Padilla, D.K. 1999. Estimating the probability of long-distance overland dispersal of invading aquatic species. Ecol. Appl. **9**: 254–265.

Carlton, J.T. 1993. Dispersal mechanisms of the zebra mussel. *In* Zebra mussels: biology, impacts and control. *Edited by* D. Schloesser and T. Nalepa. Lewis Publishers, Ann Arbor, Mich. pp. 677–697.

Cohen, A.N., and Carlton, J.T. 1998. Accelerating invasion rate in a highly invaded estuary. Science (Washington, D.C.), **279**: 555–558.

Cope, W.G., Bartsch, M.R., and Hayden, R.R. 1997. Longitudinal patterns in abundance of the zebra mussel (*Dreissena polymorpha*) in the Upper Mississippi River. J. Freshwater Ecol. **12**: 235–238.

Griffiths, R.W., Schloesser, D.W., Leach, J.H., and Kovalak, W.P. 1991. Distribution and dispersal of the zebra mussel (*Dreissena polymorpha*) in the Great Lakes region. Can. J. Fish. Aquat. Sci. **48**: 1381–1388.

Hincks, S.S., and Mackie, G.L. 1997. Effects of pH, calcium, alkalinity, hardness, and chlorophyll on the survival, growth, and reproductive success of zebra mussel (*Dreissena polymorpha*) in Ontario lakes. Can. J. Fish. Aquat. Sci. **54**: 2049–2057.

Horvath, T.G., Lamberti, G.A., Lodge, D.M., and Perry, W.L. 1996. Zebra mussel dispersal in lake–stream systems: source-sink dynamics. J. North Am. Benthol. Soc. **15**: 564–575.

Johnson, L.E. 1995. Enhanced early detection and enumeration of zebra mussel (*Dreissena* spp.) veligers using cross-polarized light microscopy. Hydrobiologia, **312**: 139–146.

Johnson, L.E., and Carlton, J.T. 1996. Post-establishment spread in large-scale invasions: dispersal mechanisms of the zebra mussel *Dreissena polymorpha*. Ecology, **77**: 1686–1690.

Johnson, L.E., and Padilla, D.K. 1996. Geographic spread of exotic species: ecological lessons and opportunities from the invasion of the zebra mussel *Dreissena polymorpha*. Biol. Conserv. **78**: 23–33.

Karataev, A.Yu., and Burlakova, L.E. 1995. The role of *Dreissena* in lake ecosystems. Russ. J. Ecol. **26**: 207–211.

Keevin, T.M., Yarbrough, R.E., and Miller, A.C. 1992. Long-distance dispersal of zebra mussels (*Dreissena polymorpha*) attached to hulls of commercial vessels. J. Freshwater Ecol. **7**: 437.

Koutnik, M.A., and Padilla, D.K. 1994. Predicting the spatial distribution of *Dreissena polymorpha* (zebra mussel) among inland lakes of Wisconsin: modeling with a GIS. Can. J. Fish. Aquat. Sci. **51**: 1189–1196.

Kraft, C.E. 1993. Early-warning detection of zebra mussels. *In* Zebra mussels: biology, impacts and control. *Edited by* D. Schloesser and T. Nalepa. Lewis Publishers, Ann Arbor, Mich. pp. 705–714.

Ludyanskiy, M.L., McDonald, D., and MacNeill, D. 1993. Impact of the zebra mussel, a bivalve invader. BioScience, **43**: 533–544.

Mellina, E., and Rasmussen, J.B. 1994. Patterns in the distribution and abundance of zebra mussel (*Dreissena polymorpha*) in rivers and lakes in relation to substrate and other physicochemical factors. Can. J. Fish. Aquat. Sci. **51**: 1024–1036.

Neary, B.P., and Leach, J.H. 1992. Mapping the potential spread of the zebra mussel (*Dreissena polymorpha*) in Ontario. Can. J. Fish. Aquat. Sci. **49**: 406–415.

Omernik, J.M., and Powers, C.F. 1983. Total alkalinity of surface waters — a national map. Ann. Assoc. Am. Geogr. **73**: 133–136.

Omernik, J.M., Larsen, D.P., Rohm, C.M., and Clarke, S.E. 1988. Summer total phosphorus in lakes: a map of Minnesota, Wisconsin, and Michigan, USA. Environ. Manage. **6**: 815–825.

Padilla, D.K., Chotkowski, M.A., and Buchan, L.A.J. 1996. Predicting the spread of zebra mussels (*Dreissena polymorpha*) to

© 2000 NRC Canada

inland waters using boater movement patterns. Global Ecol. Biogeogr. Lett. **5**: 353–359.

Ramcharan, C.W., Padilla, D.K., and Dodson, S.I. 1992*a*. A multivariate model for predicting population fluctuations of *Dreissena polymorpha* in North American lakes. Can. J. Fish. Aquat. Sci. **49**: 150–158.

Ramcharan, C.W., Padilla, D.K., and Dodson, S.I. 1992*b*. Models to predict potential occurrence and density of the zebra mussel *Dreissena polymorpha*. Can. J. Fish. Aquat. Sci. **49**: 2611–2620.

Ricciardi, A., Serrouya, R., and Whoriskey, F.G. 1995. Aerial exposure tolerance of zebra and quagga mussels (Bivalvia: Dreissenidae): implications for overland dispersal. Can. J. Fish. Aquat. Sci. **52**: 470–477.

Schneider, D.W., Ellis, C.D., and Cummings, K.S. 1998. Assessing the risk to native mussel communities of zebra mussel spread. Conserv. Biol. **12**: 788–800.

Shigesada, N., and Kawasaki, K. 1997. Biological invasions: theory and practice. Oxford University Press, New York.

Stoeckel, J.A., Schneider, D.W., Soeken, L.A., Blodgett, K.D., and Sparks, R.E. 1997. Larval dynamics of a riverine metapopulation: implications for zebra mussel recruitment, dispersal, and control in a large-river system. J. North Am. Benthol. Soc. **16**: 586–601.

Strayer, D.L. 1991. Projected distribution of the zebra mussel, *Dreissena polymorpha*, in North America. Can. J. Fish. Aquat. Sci. **48**: 1389–1395.

Vitousek, P.M., D'Antonio, C.M., Loope, L.L., and Westbrooks, R. 1996. Biological invasions as global environmental change. Am. Sci. **84**: 468–478.

© 2000 NRC Canada

Natural mortality rates in tropical tunas: size really does matter

John Hampton

Abstract: Important size-related variability in natural mortality rates has been revealed in populations of skipjack tuna (*Katsuwonus pelamis*), yellowfin tuna (*Thunnus albacares*), and bigeye tuna (*Thunnus obesus*) in the western tropical Pacific Ocean using a new, size-structured tagging model. The tagging data were classified into release groups by size at release, and a growth model was used to predict size at each time at liberty interval. Natural and fishing mortality rates were categorized by broad size-classes and estimated by maximum likelihood. The method incorporates a correction for incomplete mixing of new releases. For each population, the natural mortality rate declined by about an order of magnitude over the initial size-classes. For skipjack and yellowfin tuna, there was also evidence of elevated natural mortality for some of the larger size-classes. Size- or age-related variability in natural mortality is likely to have important implications for tropical tuna stock assessment in the western Pacific.

Résumé : On a observé que le taux de mortalité naturelle variait fortement en fonction de la taille chez des populations de bonite à ventre rayé (*Katsuwonus pelamis*), d'albacore (*Thunnus albacares*), et de thon obèse (*Thunnus obesus*), de l'ouest du Pacifique tropical, à l'aide d'un nouveau modèle des données de marquage structuré selon la taille. Les données de marquage ont été classées en groupes de lâchers en fonction de la taille au lâcher, et un modèle de croissance a été utilisé pour prédire la taille à chaque intervalle de temps en liberté. Les taux de mortalité naturelle et par pêche ont été répartis en catégories selon des grandes classes de taille et estimés par la technique de la probabilité maximale. La méthode comporte une correction pour le mélange incomplet des poissons nouvellement libérés. Pour chaque population, le taux de mortalité naturelle diminuait d'environ un ordre de grandeur par rapport aux classes de taille initiales. Dans le cas de la bonite à ventre rayé et de l'albacore, on a relevé des signes de mortalité naturelle élevée chez certaines classes de poissons de grande taille. La variabilité de la mortalité naturelle liée à la taille ou à l'âge aura vraisemblablement des effets importants pour l'évaluation des stocks de thons tropicaux dans l'ouest du Pacifique.

[Traduit par la Rédaction]

Introduction

The natural mortality rate (M) is the aggregate of several processes, including predation, starvation, and senescence, that can rarely be observed in natural fish populations. Consequently, it is difficult to estimate accurately and is frequently a major source of uncertainty in fish stock assessments (Vetter 1987).

It has been long recognized (e.g., Beverton and Holt 1957; Ricker 1975) that the biological processes producing natural mortality are likely to vary substantially over the life span of a fish. Most early studies of variability in M were based on catch-curve analyses of lightly exploited populations, which showed increases in total mortality with age over the exploited phase (for details, see Beverton and Holt 1957). Although the details may vary considerably among species, there seems to be general agreement that M is likely to be high during early juvenile stages, low during the onset of adulthood, and increasing with senescence to produce an overall U-shaped function (Vetter 1987). Despite the compelling logic of this theory, there is little evidence that estimates of size- or age-dependent M are routinely used in many fisheries stock assessments. For example, none of the approximately 400 M estimates reported in FishBase 97 (Froese and Pauly 1997) are size or age specific. However, given the difficulties in estimating even an average value of M, this is not altogether surprising.

In this paper, I present analyses of tagging data to derive size-specific estimates of M and fishing mortality rate (F) for three species of tuna in the western tropical Pacific Ocean: skipjack tuna (*Katsuwonus pelamis*), yellowfin tuna (*Thunnus albacares*), and bigeye tuna (*Thunnus obesus*). The method of analysis is new and is potentially applicable to other fish species for which suitable tagging data and information on growth are available. The results show that M for the small juvenile size-classes is up to an order of magnitude higher than for midsized fish. For skipjack and yellowfin tuna, there was also evidence of elevated M for some of the larger size-classes. Such size-related variability in M is likely to have important effects on stock assessments for these species.

Received August 23, 1999. Accepted December 10, 1999. J15328

J. Hampton. Oceanic Fisheries Programme, Secretariat of the Pacific Community, B.P. D5, 98848 Noumea Cedex, New Caledonia. e-mail: JohnH@spc.int

Materials and methods

Western Pacific tuna fishery

The western Pacific tuna fishery, which extends from the Philip-

© 2000 NRC Canada

pines to about 160°W longitude (Fig. 1), provides about 50% of the world's current tuna production. Since 1990, total annual catches have been about 1 500 000 t, comprising mainly skipjack (67%), yellowfin (25%), and bigeye tuna (6%) (Lawson 1998). The three species are caught by purse seiners operating in the equatorial band (60% of the total catch). Skipjack tuna are also caught by pole-and-line vessels (8%) and yellowfin and bigeye tuna by longliners (7%) in the same area. Small-scale fisheries in Indonesia and the Philippines catch mainly juvenile tuna and contribute about 25% of the total regional catch.

The diverse character of the western Pacific tuna fishery results in significant exploitation of the three species over much of their size range. Skipjack, yellowfin, and bigeye tuna as small as 20 cm fork length (FL) are captured by the small-scale fisheries in the Philippines. Purse seiners capture skipjack tuna over their entire adult size range (about 40–80 cm FL), yellowfin tuna as juveniles and younger adults (about 40–120 cm FL), and bigeye tuna mainly as juveniles (about 40–100 cm FL). Longliners capture yellowfin and bigeye tuna over their entire adult size range (about 100–180 cm FL). Assessment of the impacts of these components of the fishery on the stocks and on each other requires information on M and its variability over the exploited size ranges.

Tagging data

The data analyzed in this paper consisted of tag releases and returns of skipjack, yellowfin, and bigeye tuna tagged during the Secretariat of the Pacific Community's Regional Tuna Tagging Project (RTTP). Tuna were tagged during the period July 1989 to December 1992, with the tag releases and returns covering the main tuna fishing area of the western tropical Pacific (Fig. 2). Most of the tagging was carried out from a chartered pole-and-line vessel, supplemented in some countries by short-term charters on commercial pole-and-line vessels. Standard tuna tagging equipment and techniques (Hampton 1997) were used throughout. Most tuna were single tagged, with a sample double tagged to estimate tag-shedding rates (Hampton 1997). Tags and accompanying information (FL, date, location, fishing method, etc.) for recaptured tuna were reported by fleets throughout the fishery (for details, see Kaltongga 1998). The return of recovered tags was promoted by a widespread publicity campaign and attractive tag rewards. The tag-reporting rate was estimated independently by a tag-seeding experiment carried out on purse seiners (Hampton 1997).

In total, 98 401 skipjack, 40 075 yellowfin, and 8074 bigeye tuna were tagged during the RTTP. The percentage of tags returned was 12–13% for each species. Most skipjack tuna were recaptured within 3 years of release and most yellowfin tuna within 4 years of release, while small numbers of bigeye tuna were still being recaptured 7 years after release.

The data were screened to include only those records for which the tuna had been accurately measured at release (99% of releases). The release and recapture dates were also required for the analysis. The release dates were known for all releases and the recapture dates were known with an accuracy of calendar month or better for 91% of tag returns. For the returns with more uncertain recapture dates, the midpoint of the period during which recapture was considered most likely to have occurred was used. For some tag returns, an accurate FL measurement was taken soon after the fish had been recaptured. Where available, recapture FLs were also included in the data set for growth analysis. Details of the final, screened data set are provided in Table 1.

The size composition of RTTP tag releases was similar to those of purse-seine, pole-and-line, and other surface fisheries operating in the region (Fig. 3). In particular, the tag-release sample included considerable numbers of smaller tuna released during tagging cruises in the Philippines. Because pole-and-line gear is not effective in catching large yellowfin and bigeye tuna, relatively few tuna >100 cm FL were tagged. However, these larger fish are represented in the recaptured sample (Fig. 4).

Fig. 1. Average distribution of the catch of skipjack, yellowfin, and bigeye tuna, 1990–1997. The area of the circle in each 5° square is proportional to the catch; the largest circle size represents an average annual catch of 94 359 t.

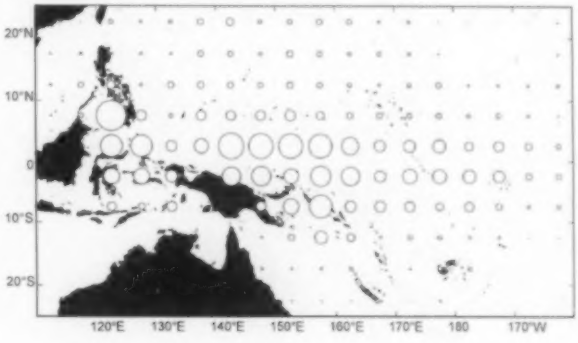

Analytical methods

Size-specific tagged population model

The size-specific tagged population model is a generalization of the size-aggregated model of tagged fish dynamics often referred to as the tag-attrition model (Kleiber et al. 1987; Hampton 1997). The size-aggregated model in its simplest form can be expressed as

$$(1)\qquad \hat{r}_{ij} = (1-\alpha)R_i \exp\left[-(F+M+\lambda)(j-1)\Delta t\right] \times \frac{F}{F+M+\lambda}\left[1-\exp(-F-M-\lambda)\Delta t\right]$$

where $\hat{r}_{ij}$ is the predicted number of tag returns from tag-release group i in the jth time period after release, α represents the type 1 tag loss rate (from tag shedding and nonreporting), R_i is the number of tag releases of group i, λ represents the continuous type 2 tag loss rate (from tag shedding), and Δt is the time step relative to the units of the instantaneous rates (normally, $\Delta t = 1$). The F and M are assumed to be constant over time, fish size, and age.

To add size structure to eq. 1, we define a tag-release group as all releases at a given size. I used 1-cm initial size-classes, resulting in 60 release groups (21–80 cm) for skipjack tuna, 100 release groups (21–120 cm) for yellowfin tuna, and 103 release groups (21–140 cm, some lengths not represented) for bigeye tuna. The F and M were then stratified by broad size intervals, appropriate to the distribution of the tag-return data, as follows. Skipjack tuna: 21–30, 31–40, 41–50, 51–60, 61–70, >70 cm FL; yellowfin tuna: 21–30, 31–40, 41–50, 51–60, 61–70, 71–80, 81–90, 91–100, >100 cm FL; bigeye tuna: 21–40, 41–60, 61–80, 81–100, 101–120, >120 cm FL. The size-structured version of eq. 1 is then

$$(2)\qquad \hat{r}_{ij} = (1-\alpha)R_i \exp\left[-\sum_{k=1}^{j-1}(F_{s(l_i,k)} + M_{s(l_i,k)} + \lambda)\Delta t\right] \times \frac{F_{s(l_i,j)}}{F_{s(l_i,j)} + M_{s(l_i,j)} + \lambda}\left[1-\exp(-F_{s(l_i,j)} - M_{s(l_i,j)} - \lambda)\Delta t\right]$$

© 2000 NRC Canada

Fig. 2. Geographical distribution of RTTP releases and returns of skipjack, yellowfin, and bigeye tuna. The area of the circle in each 5° square is proportional to the number of releases or returns.

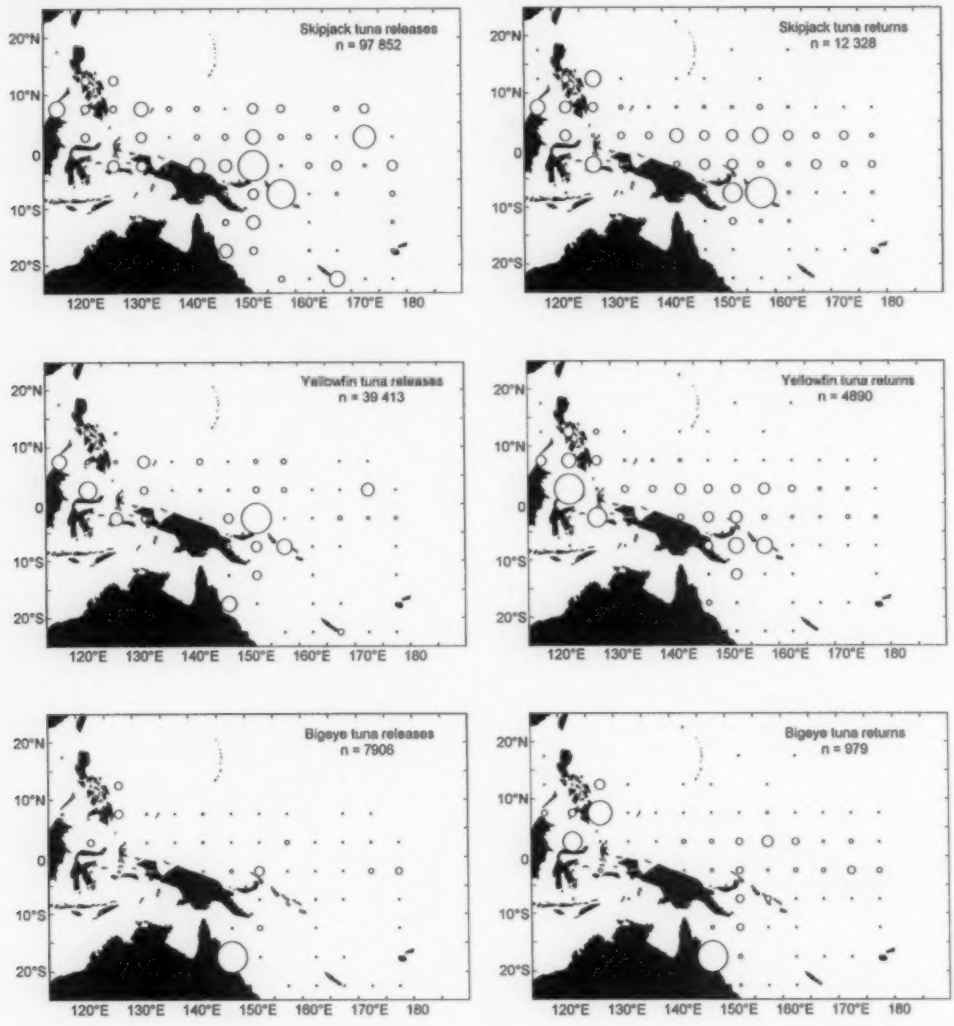

Size-class s is specified as a function of the initial size of release group i (l_i) and the time after release j. It is necessary to use a model to predict s from l_i and j, as we need to specify s for every time interval after release, and this cannot be observed directly. For these predictions, I used a simple von Bertalanffy model of the form

$$\hat{L}_j = [\bar{L}_\infty - l_i][1 - \exp(-Kt_j)] + l_i \quad (3)$$

where $\hat{L}_j$ is the predicted size at time t_j, the middle of the jth period after release, and $\bar{L}_\infty$ and K are the von Bertalanffy growth parameters mean maximum length and growth coefficient. The $\bar{L}_\infty$ and K were estimated by maximum likelihood from tag-return records in which accurate measurements of FL at recapture were available. The estimation model incorporated individual variation in L_∞ as well as observation error (model 3 in Hampton 1991*a*).

I assumed that α comprised instantaneous tag shedding and nonreporting of tags and used an estimate of 0.45 for the three species (Hampton 1997). Tagging mortality was assumed to be insignificant. Likewise, λ was assumed to consist only of type 2 tag shedding, and an estimate of 0.0023·month^{-1} (Hampton 1997) was used. These parameters were assumed to be independent of fish size.

Table 1. Tag releases and returns of skipjack, yellowfin, and bigeye tuna used in the analysis of size-specific mortality rates.

	Skipjack tuna	Yellowfin tuna	Bigeye tuna
Tag releases	97 852	39 413	7906
Tag returns	12 328	4 890	979
Tag returns with accurate recapture FL measurement	4 242	1 629	307

I made the simplifying assumption that F_s and M_s did not vary over time, enabling the tag releases to be aggregated over time. Effectively, the data were treated as if all tag releases occurred at the same time. This is a common assumption with respect to M_s and

© 2000 NRC Canada

Fig. 3. Length–frequency distributions of RTTP releases of tagged (*a*) skipjack, (*b*) yellowfin, and (*c*) bigeye tuna. The length-class labels refer to the lower boundaries of the 5-cm length-classes.

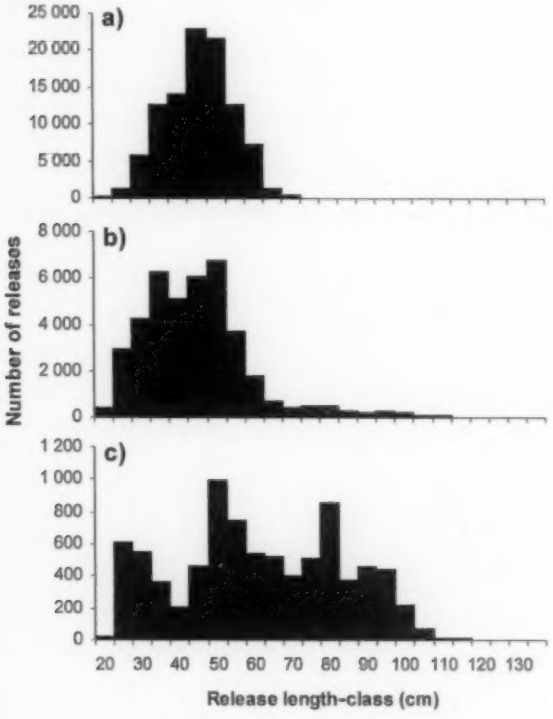

Fig. 4. Length–frequency distributions of RTTP returns of tagged (*a*) skipjack, (*b*) yellowfin, and (*c*) bigeye tuna. The length-class labels refer to the lower boundaries of the 5-cm length-classes.

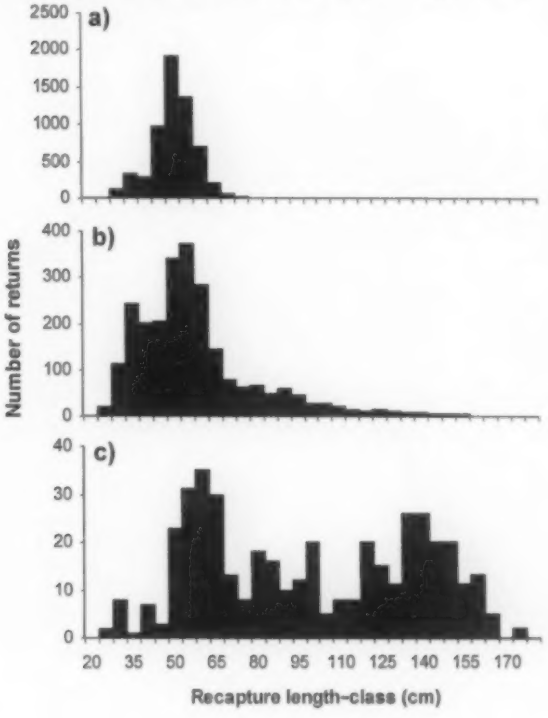

may not be unreasonable for F_s if the recapture fishery operated at a fairly constant level over the course of the recapture period. The time series of commercial catch data during the recapture period show seasonal and some lower frequency variation, but there are no consistent trends that might indicate a serious failure of this assumption (Fig. 5).

Some constraints on the selection of time interval and size-classes are necessary. Accuracy may suffer if the time strata j are large relative to the time taken to grow through the size-classes. In cases where j cannot be made sufficiently small, e.g., because of recapture date resolution, subiterations (whereby j is broken up into n subperiods of length $\Delta t = 1/n$ for computing eq. 2) may be used to increase accuracy. For the tuna analyses, rerunning the models with up to five subiterations demonstrated that acceptable accuracy was obtained using a single monthly computational time step.

Incomplete mixing of new releases

New tag releases are not immediately mixed throughout the range of the fishery and may therefore experience a different level of fishing mortality than the mixed population in that size-class. Such anomalous returns soon after release may bias the estimates of M_s and F_s for the fully mixed population unless explicitly dealt with in the model. This involves estimating the additional fishing mortality parameters F'_{im}, where m indexes a number of initial, premixing periods (Hoenig et al. 1998; Bertignac et al. 1999). The number of such "nuisance" parameters to be estimated is potentially large (the number of premixing periods times the number of release groups). The most efficient procedure is to set $\hat{r}_{ij} = r_{ij}$ for each of the premixing periods and to solve the equivalent of eq. 1 for F'_{im} using the Newton–Raphson technique (for details, see

Fig. 5. Estimated monthly catches of skipjack, yellowfin, and bigeye tuna in the western and central Pacific Ocean. The lines are 12-month moving averages.

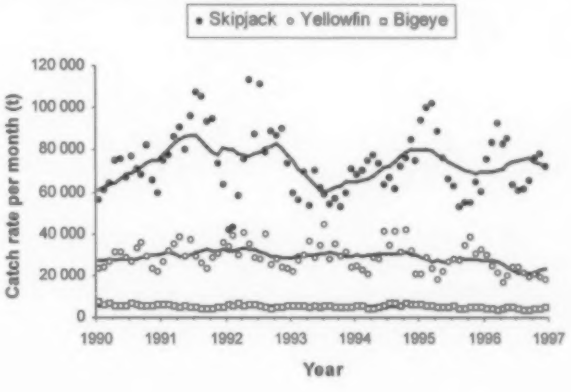

Press et al. 1988). As suggested by Hoenig et al. (1998), I used likelihood ratio tests to choose the optimal number of premixing periods for each data set. The number of premixing periods deemed to be optimal was the smallest number of periods for which the P value of the χ^2 test for adding a premixing period was >0.05.

Parameter estimation

The F_s, M_s, and F'_{im} were estimated by minimizing the negative

© 2000 NRC Canada

Fig. 6. Length increment and time at liberty data for (*a*) skipjack, (*b*) yellowfin, and (*c*) bigeye tuna used to estimate growth models.

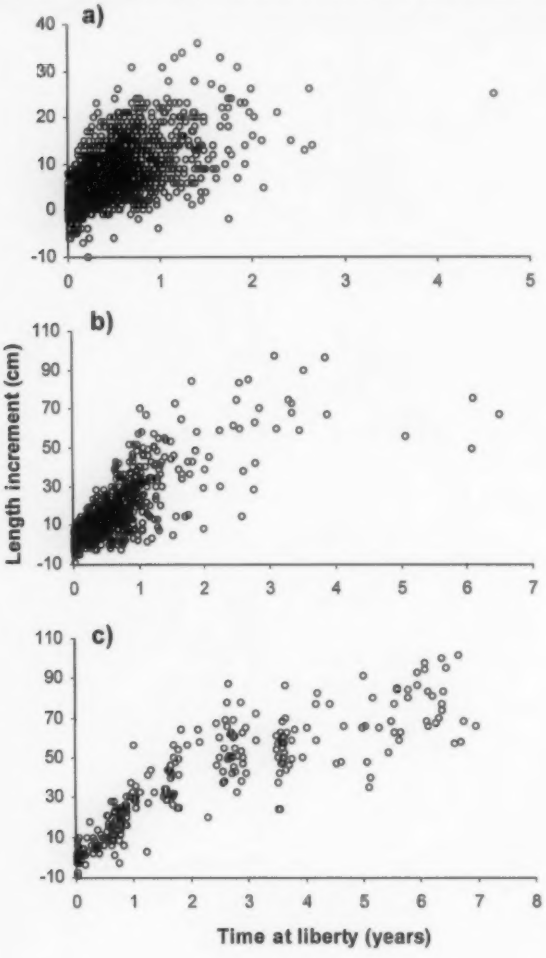

log of the multinomial likelihood function (omitting terms dependent only on the data):

$$(4) \qquad -\sum_i \left[(R_i - \sum_j r_{ij}) \ln\left(1 - \frac{\sum_j \hat{r}_{ij}}{R_i}\right) + \sum_j \ln\left(\frac{\hat{r}_{ij}}{R_i}\right) \right]$$

where r_{ij} is the observed number of tag returns from tag-release group i in the jth time period after release. Approximate 95% confidence intervals for F_s and M_s were obtained using the percentile method (Efron 1982) applied to distributions of the parameters generated from 1000 bootstrap replicates. Growth parameter estimation was included in the bootstrapping. For the analysis of each replicate data set, estimates of tag-shedding and tag-reporting parameters were obtained by the parametric bootstrap (or Monte Carlo) approach described in Hampton (1997). The confidence intervals for the mortality parameters therefore incorporated estimated uncertainty in growth, tag-shedding, and tag-reporting rates.

Table 2. Growth parameter estimate mean maximum length ($\bar{L}_\infty$) and growth coefficient (K) for skipjack, yellowfin, and bigeye tuna.

	$\bar{L}_\infty$ (cm)	K (year^{-1})
Skipjack tuna	65.1 (0.58)	1.30 (0.065)
Yellowfin tuna	166.4 (13.5)	0.250 (0.031)
Bigeye tuna	181.7 (6.88)	0.251 (0.028)

Note: The standard deviations of the estimates obtained from 1000 bootstrap replicates are given in parentheses.

Table 3. Statistical tests to determine the appropriate number of premixing periods.

	No. mixing periods	df	χ^2	P
Skipjack tuna	1	60	2 248.2	<0.001
	2	120	353.4	<0.001
	3	180	161.3	<0.001
	4	**240**	**133.0**	**<0.001**
	5	300	77.8	0.060
Yellowfin tuna	1	100	635.7	<0.001
	2	**200**	**160.8**	**<0.001**
	3	300	94.4	0.640
	4	400	118.9	0.096
	5	500	95.8	0.599
Bigeye tuna	**1**	**103**	**420.7**	**<0.001**
	2	206	116.8	0.167
	3	309	76.5	0.977
	4	412	74.1	0.986
	5	515	75.8	0.980

Note: The df corresponds to the increase in the number of F'_{im} parameters to be estimated for successive increases in the number of premixing periods. The χ^2 statistic is twice the difference between the negative log-likelihood values for the current model and the model with one fewer premixing period. P is the probability that the improvement in fit of the current model is due to chance. For each species, the selected model, based on a critical value of $P = 0.05$, is boldfaced.

Results

Growth

Growth parameter estimates for the three species were required so that the tagged tuna populations would be assigned to length-classes at each time step of the analysis using eq. 3. Subsets of the tag-return data were analyzed for this purpose (Table 1). Plots of length increment against time at liberty (Fig. 6) show evidence of the asymptotic growth characteristic of von Bertalanffy and other commonly applied growth functions. The estimates of $\bar{L}_\infty$ and K (Table 2) derived from these data imply growth rate estimates for the exploited size ranges that are consistent with the range of estimates obtained in other growth studies for these species in the Pacific Ocean (Miyabe 1994; Suzuki 1994; Wild and Hampton 1994).

Size-specific mortality

Likelihood ratio tests determined the optimal numbers of premixing periods to be four for skipjack tuna, two for yellow-

© 2000 NRC Canada

Fig. 7. Observed (circles) and predicted (line) (*a*) skipjack, (*b*) yellowfin, and (*c*) bigeye tuna tag returns by time at liberty.

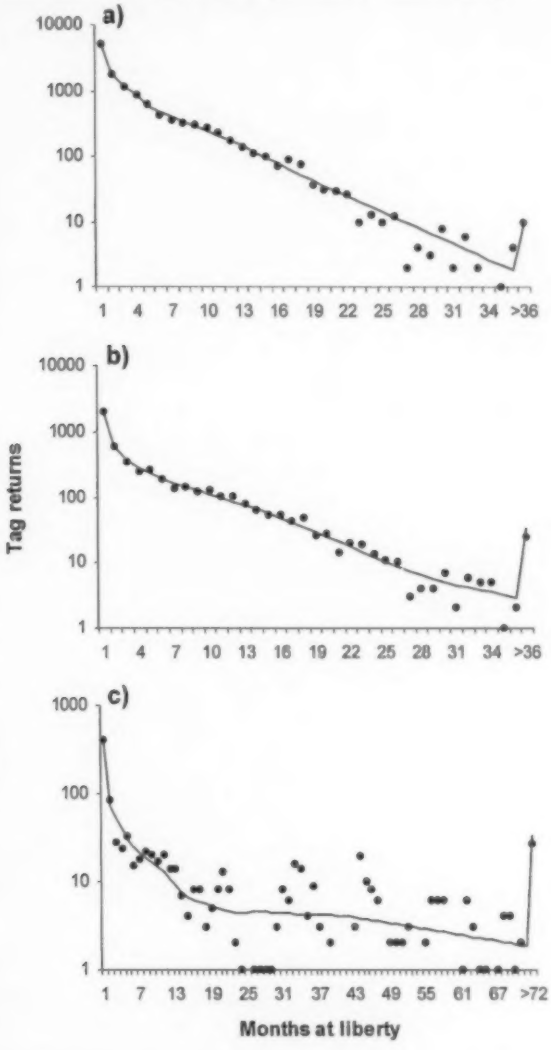

Fig. 8. Observed (circles) and predicted (line) (*a*) skipjack, (*b*) yellowfin, and (*c*) bigeye tuna tag returns by initial size of release groups.

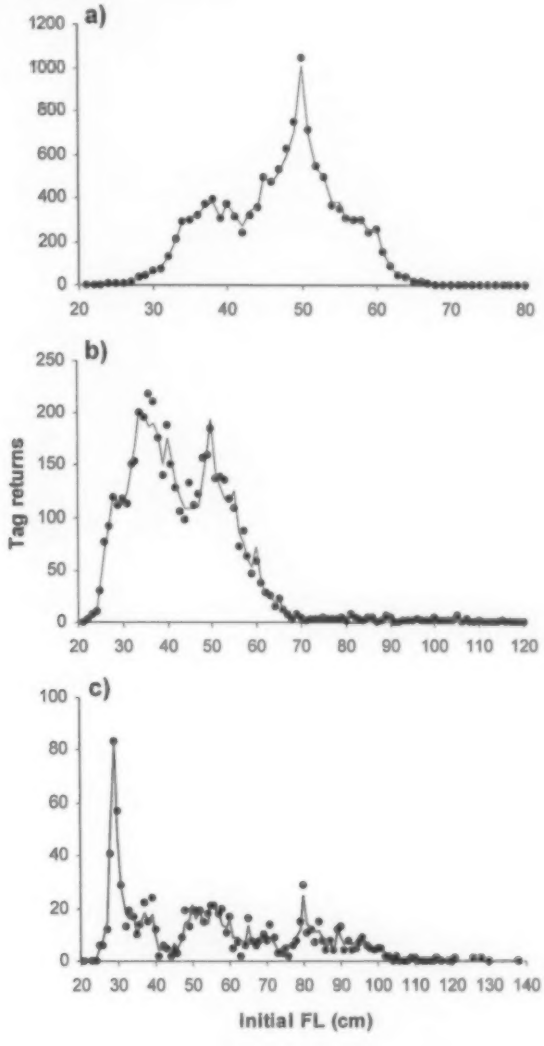

fin tuna, and one for bigeye tuna (Table 3). The results presented below incorporate these premixing periods.

For each species, the parameter estimation was stable, and the negative log likelihoods converged rapidly to their minima. Scatter plots of parameter estimates for the 1000 bootstrap replicates did not reveal any serious cases of high parameter correlation. Likewise, plots of observed and predicted tag returns aggregated by time at liberty (Fig. 7) and by size at release (Fig. 8) indicated that the models provided reasonably good descriptions of the data, particularly for skipjack and yellowfin tuna where the numbers of returns were large. In each case, reduced models assuming constant M (but size-dependent F) produced significant degradation of the fits (likelihood ratio test, $P < 0.001$).

Skipjack tuna M estimates show a classical U-shaped relationship with size (Fig. 9*a*), with the median estimates of M for the smallest (21–30 cm) and largest (>70 cm) size-classes approximately an order of magnitude higher than those for the 41–50, 51–60, and 61–70 cm size-classes. The estimates for these midsizes of skipjack tuna (which comprise the bulk of the exploited size range) are 1.6, 1.2, and 2.0·year^{-1}, respectively, which are similar to the size-aggregated estimate (about 1.9·year^{-1}) obtained from a previous skipjack tuna tagging experiment in the western tropical Pacific (Kleiber et al. 1987). The F for the mixed population tends to decline with increasing size (Fig. 9*b*). There are large 95% confidence intervals on F for the two smallest size-classes because most of the recaptures for these size-classes occur during the premixing periods.

Yellowfin tuna M estimates decline sharply with increasing size, but there is a significant increase in M for the 81–

© 2000 NRC Canada

Fig. 9. Estimates of skipjack tuna (*a*) natural mortality rates and (*b*) fishing mortality rates by size-class. The circles represent the medians of 1000 bootstrap replicates; the ranges are the 2.5–97.5 percentiles.

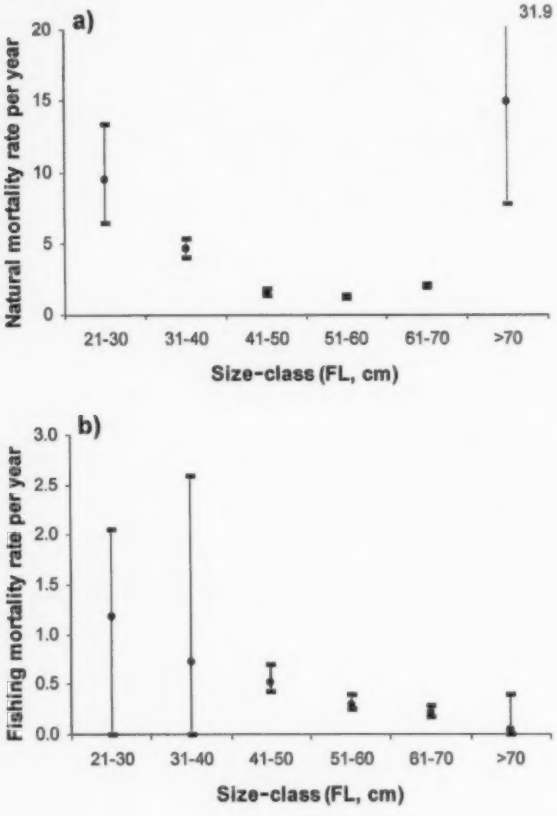

Fig. 10. Estimates of yellowfin tuna (*a*) natural mortality rates and (*b*) fishing mortality rates by size-class. The circles represent the medians of 1000 bootstrap replicates; the ranges are the 2.5–97.5 percentiles.

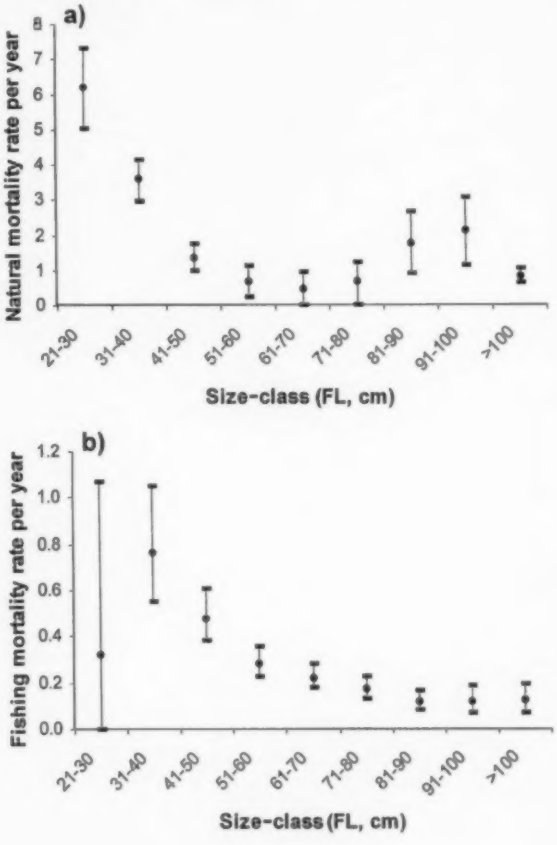

90 and 91–100 cm size-classes (Fig. 10*a*). As with skipjack tuna, the decline with increasing size is by an order of magnitude, with the lowest M estimates for the midsized fish, in this case the 51–60, 61–70, and 71–80 cm size-classes. These estimates (0.68, 0.44, and 0.69·year^{-1}) are somewhat lower than the value of 0.8·year^{-1}, which seems to be most commonly used in yellowfin tuna assessment (Wild 1994), although several estimates in the 0.4–0.6·year^{-1} range have been reported (e.g., Schaefer 1967; Francis 1977). Apart from a relatively low estimate of F for the smallest size-class (the 95% confidence interval of which is large because of few tag returns in the postmixing periods), F declines with increasing size (Fig. 10*b*).

Bigeye tuna M estimates are considerably lower than those for skipjack and yellowfin tuna (Fig. 11*a*). Again, there is an order of magnitude decline in M from the smallest (21–40 cm) to the larger size-classes, but there is no evidence of an increase in M at larger size. The M varies between 0.15 and 0.90·year^{-1} for size-classes >40 cm, which compares with the range of 0.4–0.8·year^{-1} most often used in bigeye tuna stock assessment (Anonymous 1998). The F estimates are highest for the smallest size-class and decline with increasing size (Fig. 11*b*).

Discussion

The method described for deriving size-specific estimates of M and F from tagging data is new and is potentially applicable to other fish species. The data requirements are tagging data (size at release and times of release and recapture), independent estimates of nuisance parameters such as tag-shedding and tag-reporting rates, and a means of predicting length increment as a function of initial size and time period. In some cases, as for the applications in this paper, growth estimates may be obtained using a model fitted to length increment and time at liberty data available from the same tagging data set. However, a growth model derived from other data could also be used. If such a model provided estimates of length at age (which are generally not available from growth models fitted to tagging data), it would be a simple matter to adapt the existing model to estimate M and F by age-class rather than by size-class.

An alternative model structure to that used in this study would be to parameterize a specific functional form for the relationship between M and size or age. This type of approach was adopted by Chen and Watanabe (1989), who

© 2000 NRC Canada

Fig. 11. Estimates of bigeye tuna (*a*) natural mortality rates and (*b*) fishing mortality rates by size-class. The circles represent the medians of 1000 bootstrap replicates; the ranges are the 2.5–97.5 percentiles.

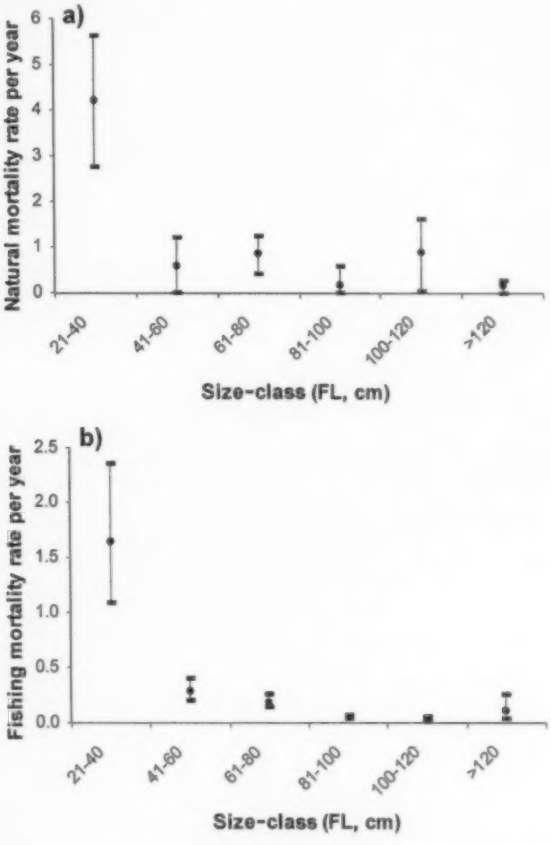

modeled *M* as an inverse function of growth rate. This approach may work in some cases, although a flexible functional relationship would be required to estimate, for example, the variation in yellowfin tuna *M* with size detected in this study.

I made the simplifying assumption that *F* for the fully mixed tagged population did not vary over time. This assumption may be justified if, as was the case here, the fisheries did not undergo significant changes during the period over which recaptures occurred. In cases where such an assumption cannot be made, it would be necessary to parameterize *F* as a function of fishing effort or catch (e.g., Kleiber et al. 1987; Hampton 1991*b*; Sibert et al. 1999) and to estimate the catchability coefficient (in the case of effort) or mean population size (in the case of catch) instead of *F*. This would be a straightforward adaptation of the present model.

The analyses of skipjack, yellowfin, and bigeye tuna tagging data revealed important size-related variation in *M*. For the three species, *M* for the smallest size-class was an order of magnitude higher than those for midsized fish. The transition from high to low *M* was around 40 cm FL, approximately the size at which the three species recruit to the western Pacific purse-seine fishery. However, other fisheries, notably the domestic tuna fisheries in the Philippines and Indonesia, catch significant quantities of tuna < 40 cm FL (around 25% of the total western Pacific tuna catch by weight). The question of the impact of these catches of small tuna on other western Pacific tuna fisheries is frequently raised in fishery management meetings. Estimates of the impact can be derived using yield per recruit or some other form of size- or age-structured model. Estimates of *M* are frequently critical to such assessments, and in this case, the higher *M* estimates for the small tuna would considerably dampen the estimated impacts of small tuna catches on fisheries targeting larger tuna.

For skipjack and yellowfin tuna, there was evidence of elevated *M* for some of the larger size-classes as well. In the case of skipjack tuna, high *M* for the >70 cm size-class possibly indicates the onset of senescence, as this is near the maximum size for this species. For yellowfin tuna, there was an increase in *M* over the 80–100 cm size range. The significance of this pattern is not fully understood, but it could be related to the onset of reproductive maturity and the associated high energetic demands of spawning, particularly for females (Schaefer 1996).

The size-related variation in *M* demonstrated in this study suggests that size- or age-dependent *M* should be a feature of future stock assessment models for these species. The length-based, age-structured model developed by Fournier et al. (1998) incorporates an option for estimating *M* by age-class from time series of commercial catch, effort, and size composition data. This model is currently being extended to include tagging data in the analysis. The information on *M* and its variability obtained from the analyses of tagging data presented here suggests that the extended length-based, age-structured model may be a useful tool for assessment of western Pacific tuna stocks.

Acknowledgments

The RTTP was funded by a grant from the Commission of the European Community Sixth European Development Fund. The cooperation of the fishing industry and many government agencies in the tagging project is gratefully acknowledged. I also thank Marc Labelle, National Marine Fisheries Service, Honolulu, Hawaii, and two anonymous referees for their comments on the manuscript.

References

Anonymous. 1998. Annual report of the Inter-American Tropical Tuna Commission 1996. Inter-American Tropical Tuna Commission, La Jolla, Calif.

Bertignac, M., Hampton, J., and Coan, A.L. 1999. Estimates of exploitation rates for north Pacific albacore, *Thunnus alalunga*, from tagging data. Fish. Bull. U.S. **97**: 421–433.

Beverton, R.J.H., and Holt, S.J. 1957. On the dynamics of exploited fish populations. U.K. Minist. Agric. Fish. Fish. Invest. Ser. 2, **19**.

Chen, S., and Watanabe, S. 1989. Age dependence of natural mortality coefficient in fish population dynamics. Nippon Suisan Gakkaishi, **52**: 205–208.

© 2000 NRC Canada

Efron, B. 1982. The jackknife, the bootstrap and other resampling plans. Society for Industrial and Applied Mathematics, Philadelphia, Pa.

Fournier, D.A., Hampton, J., and Sibert, J.R. 1998. MULTIFAN-CL: a length-based, age-structured model for fisheries stock assessment, with application to South Pacific albacore, *Thunnus alalunga*. Can. J. Fish. Aquat. Sci. **55**: 2105–2116.

Francis, R.C. 1977. TUNPOP: a simulation of the dynamics and structure of the yellowfin tuna stock and surface fishery of the eastern Pacific Ocean. Bull. Inter-Am. Trop. Tuna Comm. **17**: 233–279.

Froese, R., and Pauly, D. (*Editors*). 1997. FishBase 97: concepts, design and data sources. International Center for Living Aquatic Resources Management, Manila, Philippines.

Hampton, J. 1991*a*. Estimation of southern bluefin tuna *Thunnus maccoyii* growth parameters from tagging data, using von Bertalanffy models incorporating individual variation. Fish. Bull. U.S. **89**: 577–590.

Hampton, J. 1991*b*. Estimation of southern bluefin tuna *Thunnus maccoyii* natural mortality and movement rates from tagging experiments. Fish. Bull. U.S. **89**: 591–610.

Hampton, J. 1997. Estimates of tag-reporting and tag-shedding rates in a large-scale tuna tagging experiment in the western tropical Pacific Ocean. Fish. Bull. U.S. **95**: 68–79.

Hoenig, J.M., Barrowman, N.J., Pollock, K.H., Brooks, E.N., Hearn, W.S., and Polacheck, T. 1998. Models for tagging data that allow for incomplete mixing of newly tagged animals. Can. J. Fish. Aquat. Sci. **55**: 1477–1483.

Kaltongga, B. 1998. Regional Tuna Tagging Project: data summary. Tech. Rep. No. 35, Oceanic Fisheries Programme, Secretariat of the Pacific Community, Noumea, New Caledonia.

Kleiber, P., Argue, A.W., and Kearney, R.E. 1987. Assessment of Pacific skipjack tuna (*Katsuwonus pelamis*) resources by estimating standing stock and components of population turnover from tagging data. Can. J. Fish. Aquat. Sci. **44**: 1122–1134.

Lawson, T.A. (*Editor*). 1998. Secretariat of the Pacific Community tuna fishery yearbook 1997. Secretariat of the Pacific Community, Noumea, New Caledonia.

Miyabe, N. 1994. A review of the biology and fisheries for bigeye tuna, *Thunnus obesus*, in the Pacific Ocean. *In* Interactions of Pacific tuna fisheries. *Edited by* R.S. Shomura, J. Majkowski, and S. Langi. FAO Fish. Tech. Pap. 336/2. pp. 207–243.

Press, W.H., Flannery, B.P., Teukolsky, S.A., and Vetterling, W.T. 1988. Numerical recipes in C. Cambridge University Press, New York.

Ricker, W.E. 1975. Computation and interpretation of biological statistics of fish populations. Bull. Fish. Res. Board Can. No. 191.

Schaefer, K.M. 1996. Spawning time, frequency, and batch fecundity of yellowfin tuna, *Thunnus albacares*, near Clipperton Atoll in the eastern Pacific Ocean. Fish. Bull. U.S. **94**: 98–112.

Schaefer, M.B. 1967. Fishery dynamics and present status of the yellowfin tuna population of the eastern Pacific Ocean. Bull. Inter-Am. Trop. Tuna Comm. **12**: 87–136.

Sibert, J.R., Hampton, J., Fournier, D.A., and Bills, P.J. 1999. An advection-diffusion-reaction model for the estimation of fish movement parameters from tagging data, with application to skipjack tuna (*Katsuwonus pelamis*). Can. J. Fish. Aquat. Sci. **56**: 925–938.

Suzuki, Z. 1994. A review of the biology and fisheries for yellowfin tuna (*Thunnus albacares*) in the western and central Pacific Ocean. *In* Interactions of Pacific tuna fisheries. *Edited by* R.S. Shomura, J. Majkowski, and S. Langi. FAO Fish. Tech. Pap. 336/2. pp. 108–137.

Vetter, E.F. Estimation of natural mortality in fish stocks: a review. Fish. Bull. U.S. **86**: 25–43.

Wild, A. 1994. A review of the biology and fisheries for yellowfin tuna, *Thunnus albacares, in the eastern Pacific Ocean. In* Interactions of Pacific tuna fisheries. *Edited by* R.S. Shomura, J. Majkowski, and S. Langi. FAO Fish. Tech. Pap. 336/2. pp. 52–107.

Wild, A., and Hampton, J. 1994. A review of the biology and fisheries for skipjack tuna, *Katsuwonus pelamis*, in the Pacific Ocean. *In* Interactions of Pacific tuna fisheries. *Edited by* R.S. Shomura, J. Majkowski, and S. Langi. FAO Fish. Tech. Pap. 336/2. pp. 1–51.

© 2000 NRC Canada

Small-scale spatial and temporal patterns in spawning of Atlantic cod (*Gadus morhua*) in coastal Newfoundland waters

Gareth L. Lawson and George A. Rose

Abstract: Acoustic surveys were used to locate coastal Atlantic cod (*Gadus morhua*) spawning grounds and examine spatial and temporal patterns of spawning in Placentia Bay, Newfoundland, Canada. The same three grounds were used in 1997 and 1998 (Bar Haven in the inner bay and Cape St. Mary's and Oderin Bank in the outer bay). Grounds had densities >0.1 fish·m^{-2} over scales of 100 m and >13% of mature females in spawning condition. Ground use and spawning timing differed between years. Mean spawning female densities were highest at Cape St. Mary's in 1997 (1.6×10^{-2} fish·m^{-2}) and Oderin Bank in 1998 (1.0×10^{-2} fish·m^{-2}). At all grounds, spawning peaked earlier in 1997 (April) than in 1998 (June–July). In both years, cod spawned at sub- or near-zero temperatures. "Spawning columns" were observed at sites and times having high densities of spawning females. Sex ratios suggested that males arrived first and stayed later, while females followed when ready to spawn, accompanied by juveniles. Older females spawned earlier and later than younger females. Peaks in density of spawning females and the proportion of females spawning did not coincide. Hence, the location and timing of spawning cannot be quantified solely from the proportions of females in spawning condition.

Résumé : Nous avons eu recours à des relevés acoustiques pour localiser les frayères côtières de morue franche (*Gadus morhua*) et examiner les patrons spatiaux et temporels de la fraye dans la baie de Plaisance (Terre-Neuve), Canada. Les trois mêmes zones ont été étudiées en 1997 et 1998 (Bar Haven dans la portion intérieure de la baie, et le cap St. Mary's et le banc Oderin dans la portion extérieure de la baie). Les frayères présentaient des densités de >0,1 poisson·m^{-2} sur des échelles de 100 m et >13% de femelles matures prêtes à frayer. L'utilisation des frayères et le moment de la fraye différaient d'une année à l'autre. Les densités moyennes des femelles reproductrices étaient au plus haut au cap St. Mary's en 1997 ($1,6 \times 10^{-2}$ poissons·m^{-2}) et sur le banc Oderin en 1998 ($1,0 \times 10^{-2}$ poissons·m^{-2}). Dans toutes les zones, la fraye a atteint un sommet plus tôt en 1997 (avril) qu'en 1998 (juin–juillet). Les deux années, les morues frayaient à des températures inférieures à zéro ou proches de zéro. Des « colonnes de fraye » ont été observées aux endroits et aux moments où les densités de reproductrices étaient élevées. Les rapports des sexes semblent indiquer que les mâles arrivaient les premiers et restaient plus tard, alors que les femelles suivaient quand elles étaient prêtes à frayer, accompagnées par les juvéniles. Les femelles plus âgées frayaient plus tôt et plus tard que les jeunes. Les pics de densité des femelles reproductrices et la proportion de femelles en fraye ne coïncidaient pas. En conséquence, il n'est pas possible de quantifier le lieu et le moment de la fraye simplement à partir de la proportion de femelles reproductrices.

[Traduit par la Rédaction]

Introduction

In contrast with other major cod (*Gadus morhua*) stocks in the North Atlantic where spawning locations are well known (e.g., Icelandic, Jónsson 1982; Arcto-Norwegian, Bergstad et al. 1987; Faroe Island, Jakupsstovu and Reinert 1994), the historical locations of spawning in Newfoundland waters have been controversial (Taggart et al. 1994). Egg distributions, acoustic surveys directed at spawning cod, and analyses of commercial fishing catches from prespawning and spawning aggregations suggest a concentration of spawning at several locations on the outer parts of the Labrador and northeast Newfoundland shelves and Grand Banks (e.g., Serebryakov 1965; Rose 1993; Kulka et al. 1995). In contrast, Hutchings et al. (1993) employed bottom trawl survey data to argue that spawning was more widespread over the continental shelf and less concentrated on the outer shelf and in northern areas. Spawning in Newfoundland bays has also been reported (e.g., Thompson 1943; Hutchings et al. 1993; Smedbol and Wroblewski 1997), but the extent of spatial and temporal patterns of such coastal spawning is poorly understood.

Spawning location and timing in Newfoundland stocks have remained elusive for several reasons. These stocks appear to spawn over a protracted period (e.g., Myers et al. 1993), and some fish may spawn at varying locations during migration (Rose 1993) and over broad areas at diffuse densities (Hutchings et al. 1993). Nonetheless, there is also evidence that spawning occurs in large aggregations at re-

Received June 3, 1999. Accepted February 4, 2000.
J15171

G.L. Lawson and G.A. Rose.[1] Fisheries and Marine Institute of Memorial University of Newfoundland, P.O. Box 4920, St. John's, NF A1C 5R3, Canada.

[1]Author to whom all correspondence should be addressed.
e-mail: grose@caribou.mi.mun.ca

© 2000 NRC Canada

Fig. 1. Map of Newfoundland and NAFO subdivisions, with Placentia Bay indicated by a broken rectangle. The shelf break occurs near the 500-m depth contour, where depths drop sharply from 300 to >1000 m.

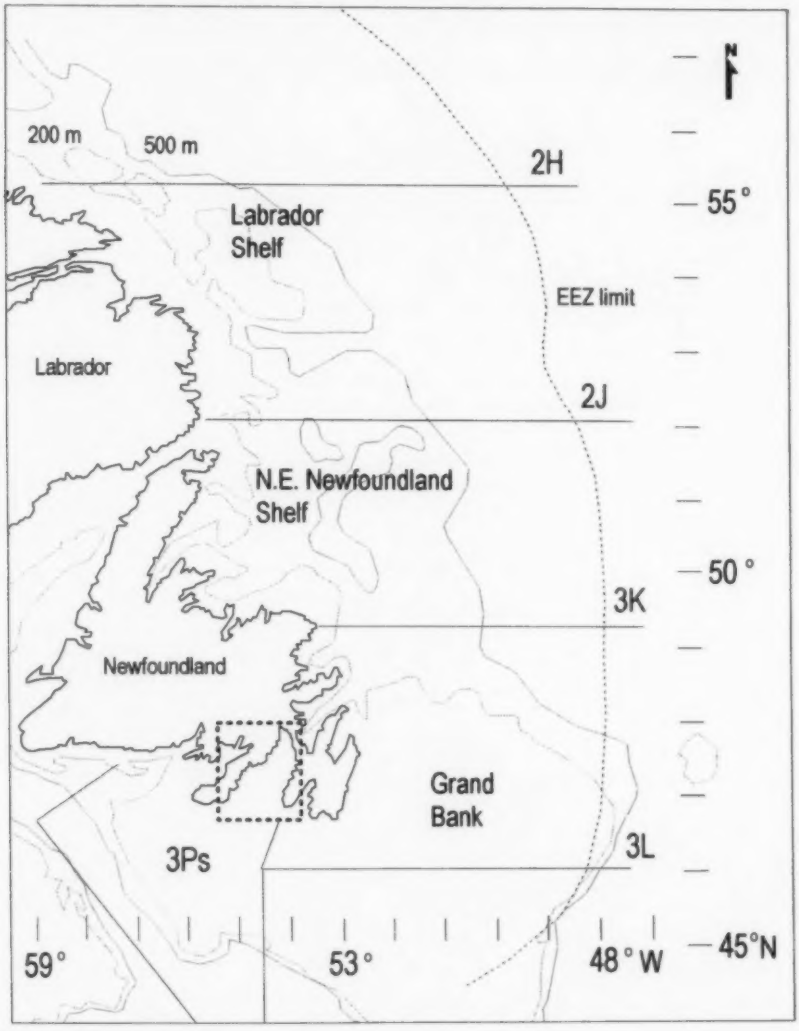

stricted locations and times (Rose 1993; Kulka et al. 1995), as in other North Atlantic stocks (Jónsson 1982; Bergstad et al. 1987; Jakupsstovu and Reinert 1994).

Both direct and indirect methods have been used to identify the location and timing of cod spawning. Commercial and research bottom trawl data have been used for this purpose (e.g., Hutchings et al. 1993; Kulka et al. 1995; Morgan and Trippel 1996) but are limited by low spatial resolution and uncertainties stemming from the possibility that major spawning locations and times were missed. In addition, bottom trawl data may be biased if fish distributions are at times pelagic or semipelagic, as documented for the Arcto-Norwegian stock (Sund 1935; Godo 1989) and Newfoundland and northern Gulf of St. Lawrence cod (Rose 1993; Ouellet et al. 1997). Surveys of egg and larval distributions have also been used to back-calculate spawning timing and location. However, such indirect methods are subject to uncertainties about drift patterns, mortality rates, and temperature-dependent developmental rates and an inability to distinguish early-stage cod eggs from haddock (*Melanogrammus aeglefinus*) and witch flounder (*Glyptocephalus cynoglossus*) (Ouellet et al. 1997). Acoustic surveys, assisted by biological sampling, can be used to directly locate spawning aggregations (e.g., Sund 1935; Rose 1993). Acoustic methods enable enhanced spatial (vertical and horizontal) and temporal resolution and allow quasi-continuous observation of behaviour (e.g., Ouellet et al. 1997). Problems with acoustic measures of semidemersal species, namely near-bottom detectability (Lawson and Rose 1999), and species identification (LeFeuvre et al. 2000) are likely to be minimal during spawning periods because of the semipelagic and monospecific composition of cod spawning aggregations (Godo 1989). Local fishers' knowledge can also be used to locate spawning areas (Neis et al. 1999) and to inform research surveys (this work).

Direct methods typically rely on an examination of female

© 2000 NRC Canada

Table 1. Dates of acoustic surveys of the Bar Haven, Oderin Bank, and Cape St. Mary's spawning grounds.

Bar Haven		Oderin Bank		Cape St. Mary's	
1997	1998	1997	1998	1997	1998
April 10	April 18				March 29
May 18	May 14			May 26	May 15
June 12	June 29	June 24	June 20*	June 30	June 20
August 5	July 27	August 9		August 12	
October 6	September 12	October 10		October 10	
November 12					

Note: All acoustic measurements were supported by biological data on fish caught with handlines. The asterisk indicates the single survey where a Campelen 1800 bottom trawl was used to catch cod.

gonad condition to identify spawning location and timing (e.g., Myers et al. 1993; Hutchings and Myers 1994; Smedbol and Wroblewski 1997). However, inferences drawn about population spawning location and timing may be biased if the distribution of abundance is not also quantified. For example, measuring a high proportion of females in spawning condition in an area of low fish density might not indicate where or when most cod spawned.

Spawning timing may be influenced by age, size, feeding history, and temperatures experienced during gonadal development (Hutchings and Myers 1993; Kjesbu 1994). Such individual effects, together with gender- and age-specific differences in behaviour and migration timing, could result in interannual variations in spawning timing (and perhaps location) and in intraannual variation in spawning shoal composition. For example, observations of unequal sex ratios in spawning shoals have led to the hypothesis that males arrive on the spawning grounds prior to females (McKenzie 1940; Morgan and Trippel 1996). Despite a potential importance to fisheries conservation, few studies have attempted to observe such behaviour through a complete spawning season.

In this paper, we use sequential acoustic surveys to document the location of cod spawning grounds in the largest embayment in coastal Newfoundland waters. On these grounds, small-scale intra- and inter-annual variation in the timing, intensity, and location of spawning in 1997 and 1998 is examined. The hypothesis that males arrive on spawning grounds prior to females is tested, and the age and gender composition of cod aggregations on the grounds throughout the spawning seasons is described. Finally, we compare quantifications of where and when cod spawn based solely on the proportion of females in spawning condition with those scaled by estimates of spawning fish density.

Methods

Study area

The study area was Placentia Bay (about 115 × 75 km, centred at 47°15′N, 54°30′W) (Fig. 1) on Newfoundland's south coast (NAFO subdivision 3Ps). In 1997, 3Ps became the first Newfoundland cod stock to reopen to commercial fishing after being under moratoria since 1993. An acoustic survey of Placentia Bay and the adjacent shelf region in 1998 indicated a cod biomass of approximately 70 000 t (Rose and Lawson 1999). Strong 1989, 1990, and 1992 year-classes have enriched the age composition and abundance since the moratorium (Anonymous 1999). However, the abundance and age structure of 3Ps cod were not reduced to the same extent as were other Newfoundland cod stocks from 1960 to 1990 (e.g., northern cod). There is no evidence of major distribution and migration change in the 1990s from historical patterns (P. Brown, commercial fisherman, Little Harbour, Placentia Bay, personal communication) as there is for the northern stock (Rose et al. 2000). However, age of maturity did decline in the 1980s and, at a present mean of 5, has not recovered to historical levels (Anonymous 1999). The population structure of 3Ps cod is poorly understood. Placentia Bay cod may belong to an Avalon stock complex (Templeman 1979) in which component populations spawn separately but intermingle during summer in coastal areas of 3Ps and 3L (Fig. 1). Recent tagging studies indicate that many cod emigrate from Placentia Bay in spring towards the east but remain in coastal areas, return in fall, and stray only rarely to the shelf (Lawson and Rose 2000).

Acoustic surveys

Two types of acoustic surveys were undertaken. Bay-scale surveys to locate spawning grounds were conducted in April, May, and June of 1997 and May and June of 1998 along a systematic grid of transects running east–west across the bay at intervals of 4 nautical miles (7.4 km) (see Fig. 2). An additional survey was conducted in March 1998 from the CCGS *Teleost*, with less complete coverage, but found no evidence of spawning. Spawning grounds were identified as sites of high-density cod aggregations with large proportions of sampled mature females in spawning condition. The second type of survey concentrated on the identified grounds. Each ground was surveyed several times during the spring, summer, and fall of 1997 and 1998 (see Table 1 for dates). For each survey, a single fixed transect (5–15 km) that bisected each ground was run in 1–3 h. Sampling with handlines accompanied each survey. In addition, a separate towed body housing a low-light video camera was deployed to assist in verification of species and behaviour. The video body was lowered or towed at approximately 1 kn (1.85 km·h^{-1}) through several cod spawning aggregations.

There were limitations to survey coverage. The inner bay could not be surveyed in June 1998 because the CCGS *Teleost* cannot effectively survey the shallow inner bay (Fig. 2). In both years, the deep (>150 m) trench in the middle of the outer bay was allocated less overall survey effort because exploratory surveys in 1996 and the initial April 1997 survey found few cod deeper than 150 m. In June 1998, cod were found in deeper waters (up to 200 m) but only in close proximity to Oderin Bank.

All acoustic surveys except for the bay-scale surveys in March and June of 1998 employed two BioSonics single-beam DT4000 echosounders (38 and 120 kHz, specifications in Lawson and Rose (1999)). Transducers were mounted on a "dead weight" body towed at 4 kn (7.4 km·h^{-1}) at a depth of 1.5 m alongside either the RV *Innovation*, RV *Mares* (<14 m), or CCGS *Shamook* (23 m). The March and June 1998 surveys employed the CCGS *Teleost* (63 m) and a Simrad EK500 38-kHz split-beam echosounder with hull-mounted transducer (specifications in Rose and Lawson (1999)). Calibrations were performed in situ according to Foote et al. (1987). Surveys were conducted during daylight to maximize

© 2000 NRC Canada

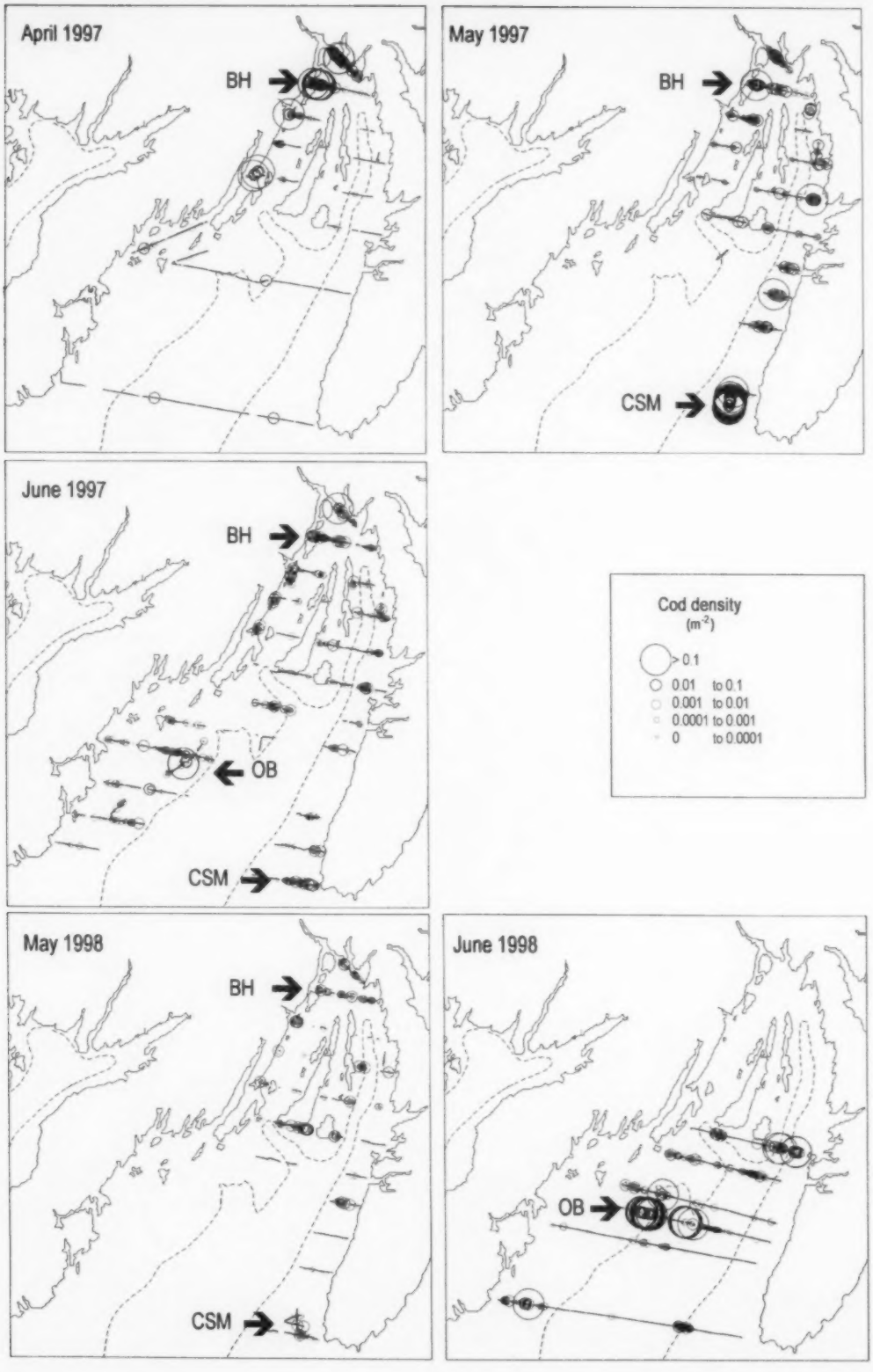

© 2000 NRC Canada

Fig. 2. Summary of acoustic surveys in April, May, and June of 1997 and May and June of 1998. Arrows indicate spawning grounds (in all cases, cod density achieved levels >0.1 fish·m^{-2}, and >10% of mature females were in spawning condition) at Bar Haven (BH), Oderin Bank (OB), and Cape St. Mary's (CSM). The broken line indicates the 160-m depth contour.

Fig. 3. Spawning at Bar Haven in (*a*) 1997 and (*b*) 1998 and at (*c*) Cape St. Mary's and (*d*) Oderin Bank. The bar plot (left axis) shows the percentage of mature females in spawning (solid bars), ripening (open bars), and spent condition (hatched bars). The number of mature females sampled is indicated on each bar (not the total number). The line graph (right axis) shows mean (with 95% confidence interval) acoustic estimates of cod density. Asterisks indicate CGSS *Teleost* transects. N.D., no data; 0, no fish present.

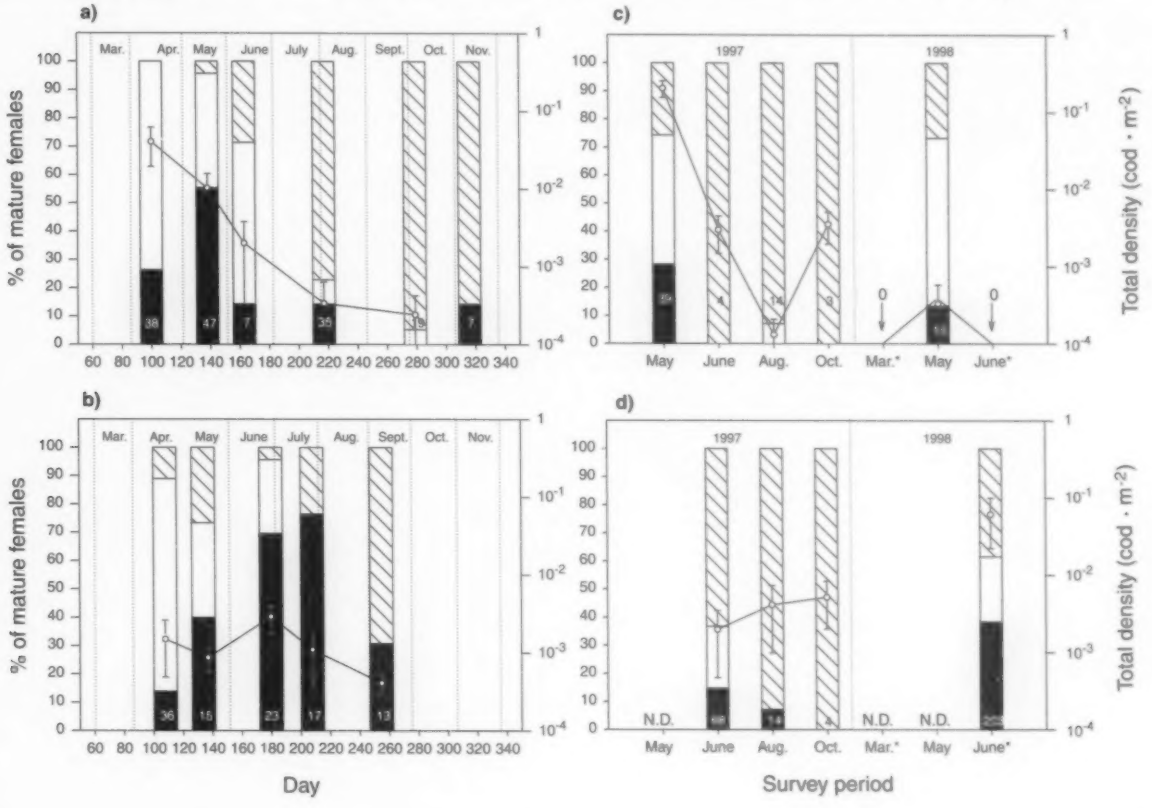

cod detectability (Lawson and Rose 1999), except from the CCGS *Teleost*, which surveyed over 24 h. On each spawning ground, several vertical temperature and salinity profiles were measured using a Seabird 19 or 25 conductivity–temperature–depth (CTD) instrument.

Sampling and analyses

In both bay-scale and ground surveys, cod aggregations located with echosounders were sampled using handlines with feather hooks to verify acoustic measurements and provide biological samples. Such handlines are thought to catch adult fish (>50 cm) with minimal size selectivity (G.A. Rose, unpublished data). Sampling over the entire water column was achieved by varying line length and was directed at those depths in which cod were observed with the echosounders. In June 1998, a single bottom trawl (Campelen 1800) was performed at Oderin Bank from the CCGS *Teleost*, as handlining was impractical from the large vessel. It is important to note that all sampling at Bar Haven in both 1997 and 1998 was done with identical gear (handlines) and that these data form the basis of size and age comparisons between months and years. For all cod caught, measures were made of sex, length, and weight and individual ages were determined from otoliths. Female gonad condition was categorized as either immature or mature, with mature gonads further divided into three stages according to Morrison (1990). Ripening females had visible opaque eggs. Spawning females had gonads with hydrated eggs, and possibly some eggs already extruded. Spent females had completed spawning and had no or very few hydrated eggs.

Acoustic and fishing surveys in Placentia Bay have suggested that cod form monospecific aggregations that are readily recognized acoustically (Rose and Lawson 1999). Species that might be acoustically mistaken for cod, such as pollock (*Pollachius virens*) and haddock, are rare. Acoustic data were manually edited to separate cod from pelagic backscatter (likely zooplankton, capelin (*Mallotus villosus*), or Atlantic herring (*Clupea harengus*)) and from bottom using FASIT software (LeFeuvre et al. 2000). Data were then integrated to produce areal backscatter values (s_A) in bins of 100 m horizontal length and of width defined by water depth and beam width. In 1997, 38-kHz data were analysed, while in 1998, 120-kHz data were used (the 38-kHz system malfunctioned). Densities derived from 38- and 120-kHz data collected concurrently did not differ ($p < 0.05$).

Survey s_A data were scaled to areal density (cod per square

© 2000 NRC Canada

metre) using a mean target strength (TS) for the mean length of cod caught by handline during each survey from the relationships after Rose and Porter (1996):

(1) $\text{TS at } 38\text{ kHz (dB)} = 20\log_{10}\text{length (cm)} - 66$

(2) $\text{TS at } 120\text{ kHz (dB)} = 20\log_{10}\text{length (cm)} - 65$

Spawning ground transect densities were subject to more detailed analyses. It was determined that random samples of 25% of the original acoustic data were free of autocorrelation ($p < 0.05$). Hence, 50 such independent samples were used to calculate a bootstrap mean s_A, with standard error. These s_A values were then scaled to fish density using a target strength based on the catch during each survey:

(3) $$\text{TS}_{\text{survey}} = 10\log_{10}\{\Sigma^n[(N_i/N_t)\sigma_i]\}(4\pi)^{-1}$$

where n is the number of 4-cm length bins, N_i is the number of fish in length bin i, N_t is the total number of fish caught, and σ_i the mean acoustic cross section of bin i.

The mean depth inhabited by cod was calculated by weighting the depth of each 100-m integration bin by the density of cod in that bin relative to mean survey density:

(4) $$\text{Mean occupied depth} = 1/n[\Sigma^n(y_i/\bar{y})x_i]$$

where n is the number of integration bins in the survey, x_i is the depth of bin i, and $y_i/\bar{y}$ is the ratio of bin density (y_i) to the mean cod density of all bins ($\bar{y}$). Probit analyses were employed to examine the effects of fish age, sample date, and year on individual female gonad condition. The relationship between these parameters and the probability of being in spawning condition was examined by defining females with maturing gonads as 0 and spawning females as 1. Cessation of spawning (i.e., the probability of being spent) was studied in a separate analysis by defining ripening and spawning females as 0 and spent females as 1. Binomial tests were used to test for differences between the observed ratio of adult females to males and a 1:1 sex ratio. Chi-square analyses were used to test for differences among surveys in the observed numbers of spawning and nonspawning mature females.

Results

Cod spawning aggregations were located by bay-scale surveys at three sites within Placentia Bay in the spring of 1997 (Bar Haven Island, Cape St. Mary's, and Oderin Bank; see Fig. 2). On these identified spawning grounds, mean densities averaged over 100 m were high, typically exceeding 0.1 fish·m^{-2} in places and at times exceeded 1 fish·m^{-2} during peak spawning. The percentage of mature females in spawning condition was also elevated (range of 13–75%). Cod were located at several other sites in the bay, but either at much lower densities, typically in the range of 0.0001–0.01 fish·m^{-2}, or if densities were comparable with those of the spawning grounds, aggregations contained mostly juveniles and nonspawning adults. Such areas were therefore not considered to be spawning grounds.

In April 1997, a spawning aggregation was present only at Bar Haven (Fig. 2). During May 1997, aggregations were found at both Bar Haven and Cape St. Mary's. The southwestern portion of the bay (including Oderin Bank) could not be surveyed at that time. In June 1997, densities at Bar Haven and Cape St. Mary's had declined, while high densities of spawning cod were present at Oderin Bank.

In 1998, identified cod spawning sites were the same as in 1997, with no new grounds located (Fig. 2). However, spawning aggregations were smaller and significantly less dense in 1998 than in 1997 at Bar Haven and Cape St. Mary's (t tests, $p < 0.05$) (Figs. 3*a*, 3*b*, and 3*c*). Monthly densities from June to September did not differ between years where comparisons were possible at either site ($p > 0.05$) In contrast, the spawning aggregation at Oderin Bank was larger and significantly more dense in June 1998 than in June 1997 ($p < 0.05$) (Fig. 3*d*). Note that all densities cited here are means over 100 m of transect distance and are not within-aggregation densities.

The mean depth inhabited by cod at Bar Haven in 1997 decreased from April to May and then increased over the summer (Fig. 4*a*). A similar pattern was evident in 1998. Despite the general warming of near-surface waters over the summer (Fig. 4*b*), spawning cod occupied waters at sub- or near-zero temperatures throughout the spawning season (Fig. 4*c*). The range of inhabited temperatures increased over the summer (delimited by the maximum and minimum depths where cod were present at densities >0.001 fish·m^{-2}).

Columnar aggregations of cod (e.g., Fig. 5) conforming to Rose's (1993) description of "spawning columns" were detected at Oderin Bank in June of 1997 and 1998, at Cape St. Mary's in May of 1997 and 1998, and at Bar Haven in April 1997. The occurrence of columns corresponded to times of highest spawning female density, and columns were never observed at any other time or location in the bay. Column dimensions were characterized by a much greater ratio of vertical to horizontal extension than nonspawning shoals. Volumetric densities within columns frequently exceeded 1 fish·m^{-3}. Columns most often extended from bottom upwards 10–40 m and ended 15–75 m from the surface. A few columns extended upwards from a dense cod shoal, and some were fully pelagic. Underwater video recorded through the areas occupied by the columns indicated the presence of only large cod and no other species.

In 1997, mean cod density on the Bar Haven spawning ground was highest in April (0.04 fish·m^{-2}) and then decreased by two orders of magnitude over the course of spring and summer (Fig. 3*a*). The proportion of females in spawning condition, by contrast, increased from 26% in April to a maximum of 55% in May and subsequently declined in June to remain at background levels (<15%) through late fall. Chi-square analysis suggested that this trend was significant: the numbers of spawning relative to nonspawning mature females differed significantly among surveys ($\chi^2 = 29.3$, $p < 0.001$, df = 5), largely as a consequence of the elevated proportion of spawners in May. In 1998, mean cod density at Bar Haven was less peaked than in 1997, but the highest densities occurred in late June at 0.003 fish·m^{-2} (Fig. 3*b*). The proportion of females that were spawning in 1998 was highest in July and again differed among surveys ($\chi^2 = 27.8$, $p < 0.001$, df = 4) (Fig. 3*b*). In neither year did the highest mean densities coincide with the peak in the proportion of females spawning. Note that densities were averaged over the entire transect covering the spawning ground. Hence, spawning aggregations were often identified on the ground (i.e., internal densities >0.1 fish·m^{-2}) when mean densities over the full transect were lower.

Spawning timing differed between years (Fig. 6). At the better-studied Bar Haven ground, peak spawning (spawning female density) occurred more than a month later in 1998

© 2000 NRC Canada

than in 1997. Peak densities in spawning females decreased from 3.5×10^{-3} fish·m^{-2} in April 1997 to 1.1×10^{-3} fish·m^{-2} in June 1998. The density of spawning females was calculated by multiplying total density by the sex ratio and the proportion of females that were in spawning condition. The 1997 peak was inferred from the initial survey of that year and may have occurred earlier. The spawning grounds at Oderin Bank and Cape St. Mary's were surveyed less frequently than was Bar Haven. The time of peak spawning at these sites is therefore not easily determined. At Cape St. Mary's, spawning was observed only in May of both years (Fig. 3*c*). In May 1997, a higher proportion of fish were spawning and a lower proportion still ripening than in May 1998. At Oderin Bank in June, the percentage of females in spawning condition was greater and a higher proportion of females were spent in 1997 than in 1998 (Fig. 3*d*).

Mean spawning female density at Cape St. Mary's was three orders of magnitude higher in May 1997 (mean 1.6×10^{-2} fish·m^{-2}, SE 2.0×10^{-3} fish·m^{-2}) than in May 1998 (mean 2.4×10^{-5} fish·m^{-2}, SE 1.9×10^{-5} fish·m^{-2}). In contrast, the density of spawning females at Oderin Bank in June 1998 (mean 9.7×10^{-3} fish·m^{-2}, SE 1.1×10^{-2} fish·m^{-2}) was two orders of magnitude greater than at any time in 1997 (maximum of 6.7×10^{-5} fish·m^{-2}, SE 6.1×10^{-5} fish·m^{-2}). Spawning female density determined acoustically in June 1998 was more than an order of magnitude greater at Oderin Bank than at the other sites. As such, any bias in acoustic measurements of density introduced by the effects of gear selectivity on estimates of mean length and thereby on target strength (biological sampling in June 1998 at Oderin Bank employed a bottom trawl whereas handlines were used in all other instances) is likely to be relatively small and not to restrict direct comparisons.

The mean age (and to a lesser extent length) of mature females on the Bar Haven spawning ground was high early in the spawning season and then declined until fall in both 1997 and 1998 (Table 2). Mean age was >7 years in April and May of 1997 but declined to <6 years by September. Mean age was approximately 8 in May and June of 1998 and then declined to approximately 6 by September. April 1998 ages were also low, but few fish were present at that time (e.g., Fig. 6). Probit analysis indicated that age had a significant and positive effect on the probability of mature females being in spawning condition ($p < 0.001$) (Table 3). Consequently, at a given date and year, an older female was more likely to have begun spawning than a younger fish. A significant interaction between survey year and date ($p < 0.05$) confounded individual effects of these factors. The proportion of females that was spent was negatively affected by age ($p < 0.001$), indicating that at a given time, an older female was less likely to have ceased spawning than a younger one. Again, a significant year by date interaction precluded the interpretation of individual effects. Interactions likely arose from the change in time of peak spawning between years.

In 1997, the sex ratio (females to males) of adult fish at Bar Haven estimated from handline samples increased from 0.8 in April to 1.2 in May and then decreased over the summer (Fig. 7*a*). In 1998, the sex ratio followed the same trend, from a minimum of 0.2 in April to a peak of 1.3 in May, followed by a decrease. Sex ratios differed significantly from 1:1 in September and November 1997 and in April 1998 ($p < 0.05$). The proportion of cod at the Bar Haven spawning ground that were immature followed a trend similar to that of the sex ratio, increasing in both years from April to a peak in May and then subsequently declining (Fig. 7*b*).

Discussion

This study indicates that cod spawn at specific grounds in the coastal waters of Placentia Bay but that substantial variation exists in spawning intensity and timing between grounds and years. Although there have been previous reports of cod spawning in Newfoundland coastal waters (e.g., Thompson 1943; Hutchings et al. 1993; Smedbol and Wroblewski 1997), this study provides descriptions of intra- and interannual variations in the spatial and temporal patterns of spawning behaviour.

All available evidence suggests that spawning in both 1997 and 1998 occurred in large aggregations at three main grounds within Placentia Bay and that no major grounds existed elsewhere in the bay. Densities of spawning cod on the grounds were one to two orders of magnitude higher than in the remainder of the bay and are high relative to historical measures of cod density. For example, the typical ranges of density observed (e.g., 0.1 fish·m^{-2}) are equivalent to a total availability of approximately 5 t of demersally oriented 2-kg adult cod to a 15-min Campelen research standard bottom trawl. If cod were distributed semipelagically, correspondingly fewer would be available. The single trawl undertaken on a ground with a semipelagic distribution caught the equivalent of approximately 6 t of cod. Such acoustic densities and catch rates are quite high compared with most published accounts from these waters (e.g., Hutchings et al. 1993; Rose 1993; Rose and Kulka 1999). In the spawning aggregations, the proportions of females spawning were also high, reaching 76%. More widespread spawning occurred at much lower densities or where few females were in spawning condition. There is additional evidence that spawning took place primarily on the identified grounds. In a companion study, high concentrations of cod eggs were observed in bay-wide ichthyoplankton surveys only at and adjacent to these grounds (Bradbury et al. 1999). We conclude that the majority of egg production resulted from the large aggregations spawning at discrete grounds within this coastal ecosystem.

The location of the spawning grounds may relate to larval retention (e.g., Sinclair 1988; deYoung and Rose 1993). Mean flows within Placentia Bay are counterclockwise, with waters entering at Cape St. Mary's, flowing around the bay, then exiting to the west (Bradbury et al. 1999). Of the three grounds, Cape St. Mary's and Bar Haven are well positioned for retention of eggs and larvae in the bay (Bradbury et al. 1999). Oderin Bank may be better positioned for more broad-scale retention on the adjacent shelf. Alternate use of these grounds may enhance the distribution of juveniles to different areas within the stock range. Temperature regimes and depth are likely to influence ground location, but the similar depths (<100 m) and temperatures (subzero) were widespread in areas of the bay where little spawning occurred. Substrate type might influence ground location at

© 2000 NRC Canada

Fig. 4. For the Bar Haven spawning ground surveys, (*a* and *b*) mean weighted depth inhabited by cod in 1997 and 1998 (solid circles) and maximum (open circles) and minimum (triangles) depths at which cod were present at densities >0.001 fish·m^{-2}, (*c* and *d*) temperature profiles at indicated depths during 1997 and 1998, and (*e* and *f*) temperature at the mean (solid circles), maximum (open circles), and minimum (triangles) depths inhabited by cod.

smaller spatial scales, but there is no evidence that substrates at the grounds were unique.

Our data suggest that the usage of the three spawning grounds appears to vary greatly between years, as may be typical of cod (Brander 1994). The highest spawning intensity (spawning female density) occurred at Cape St. Mary's in 1997 but shifted to Oderin Bank in 1998. Tagging of fish from the spawning aggregations in 1997 and 1998 suggests that most cod return to the bay to spawn again in subsequent years but that some cod may stray outside the bay, especially to the north (Lawson and Rose 2000; D. Robichaud, Memorial University of Newfoundland, unpublished data). Movement between spawning grounds either inside or outside the bay could account for the observed interannual variation in spawning intensity between grounds. However, an alternative hypothesis is that the grounds represent discrete populations with individual site affinity and that varying proportions of fish from each population may not spawn every year (Burton et al. 1997). In either case, interannual variations in currents, temperatures, and other ocean properties may influence ground usage (Godo 1989). For example, water temperatures were generally warmer in 1998 than in 1997. Interannual temperature variations could favour specific grounds. Wind conditions that likely result in small-scale flow variations also varied between years, although there was no evidence for interannual differences in mean flows (Bradbury et al. 1999).

Our data provide direct evidence that cod spawn at subzero temperatures. This result is not consistent with the hypothesis that cod spawning in coastal Newfoundland occurs only after waters warm above 0°C (Smedbol and Wroblewski 1997) or with the range of spawning temperatures of 25 north Atlantic stocks (including Newfoundland) reviewed by Brander (1994). Nevertheless, spawning at subzero temperatures may be more common than previously thought. For example, Morgan and Trippel (1996) reported a mean bottom temperature of –0.3°C during bottom trawl sets where spawning cod were present on the Grand Banks. In addition, spawning at subzero temperatures has been repeatedly observed in embayments on the Newfoundland northeast coast (G.A. Rose, unpublished data). It is possible that recent changes in Newfoundland cod distribution (Rose et al. 2000) have led to changes in spawning relative to temperature. However, the spawning distributions observed here are consistent with limited historical data (e.g., Hutchings et al. 1993) and with the more extensive local knowledge of historical patterns within our study area, which leads us to conclude that coastal spawning in cold waters is neither recent nor anomalous in this region.

Rose (1993) first observed so-called "spawning columns" associated with aggregations of spawning cod on the northeast Newfoundland shelf. In coastal Placentia Bay, the repeated observation of columns at sites and times of spawning, coupled with their absence at all other places and times where cod aggregated, strengthens the hypothesis that columns are associated with spawning behaviour. However, the function and gender composition of the columns cannot be determined from our data. It is noteworthy that the present observations, together with previous reports of pelagic distributions of cod during the spawning season (e.g., Rose 1993; Ouellet et al. 1997; O.R. Godø, Institute of Marine Research, Bergen, Norway, personal communication), suggest that a component of the reproductive process occurs pelagically. In the laboratory, cod have been reported to engage in courtship rituals near the bottom of 1.3- to 3-m-deep experimental tanks (Brawn 1961; Hutchings et al. 1999). However, Brawn (1961) also reported that behaviours immediately preceding spawning involve substantial vertical movement (even in such shallow tanks) and that egg and sperm extrusion occurs in a "ventral mount" position near the surface. Templeman (1958) similarly reported ventral mounts occurring at the surface of cod hatchery spawning ponds. It is not straightforward to infer from shallow-tank experiments what cod might do in 50–450 m of water where they spawn. However, it is possible that such coordinated vertical movements could be the basis of the observed columns. It is also possible that the vertical segregation between male and female cod in experimental tanks observed by Hutchings et al. (1999) leads to columns in the wild, although this hypothesis does not account for the pronounced columnar structure that is only a few fish wide in many cases (e.g., Fig. 5).

Trends in the density of spawning females suggest that spawning at Bar Haven peaked at least a month earlier in 1997 than in 1998 (sample sizes are inadequate to define peaks with greater resolution). Gonadal development rates increase with ambient temperature (Kjesbu 1994). However, temperatures were warmer in 1998 (later spawning) than in 1997 (earlier spawning) at all grounds and throughout 3Ps (Colbourne 1999). Hence, earlier spawning did not coincide with generally warmer conditions (also reported for offshore 3Ps cod by Hutchings and Myers (1994)). Feeding and resultant condition differences might also influence spawning timing (Kjesbu 1994). However, cod in 1997 and 1998 did not differ in condition (G.A. Rose, unpublished data).

Our data suggest that older females initiate spawning earlier, cease spawning later, and hence have a longer spawning period than younger individuals. These results are in general agreement with Bergstad et al. (1987) and earlier Norwegian references therein for Arcto-Norwegian cod, Ouellet et al. (1997) for northern Gulf of St. Lawrence cod, and Marteinsdottir and Petursdottir (1995) for Icelandic cod. In contrast, Hutchings and Myers (1993) in a study of Newfoundland cod and Jónsson (1982) in an earlier study of Icelandic cod reported the opposite trend of older cod initiating spawning later than younger cod. The differences among these studies are not easy to resolve. However, Kjesbu (1994) suggested that older cod might overwinter in warmer waters than younger cod, so that any increased time requirements of higher fecundity might be counteracted by enhanced gonad devel-

© 2000 NRC Canada

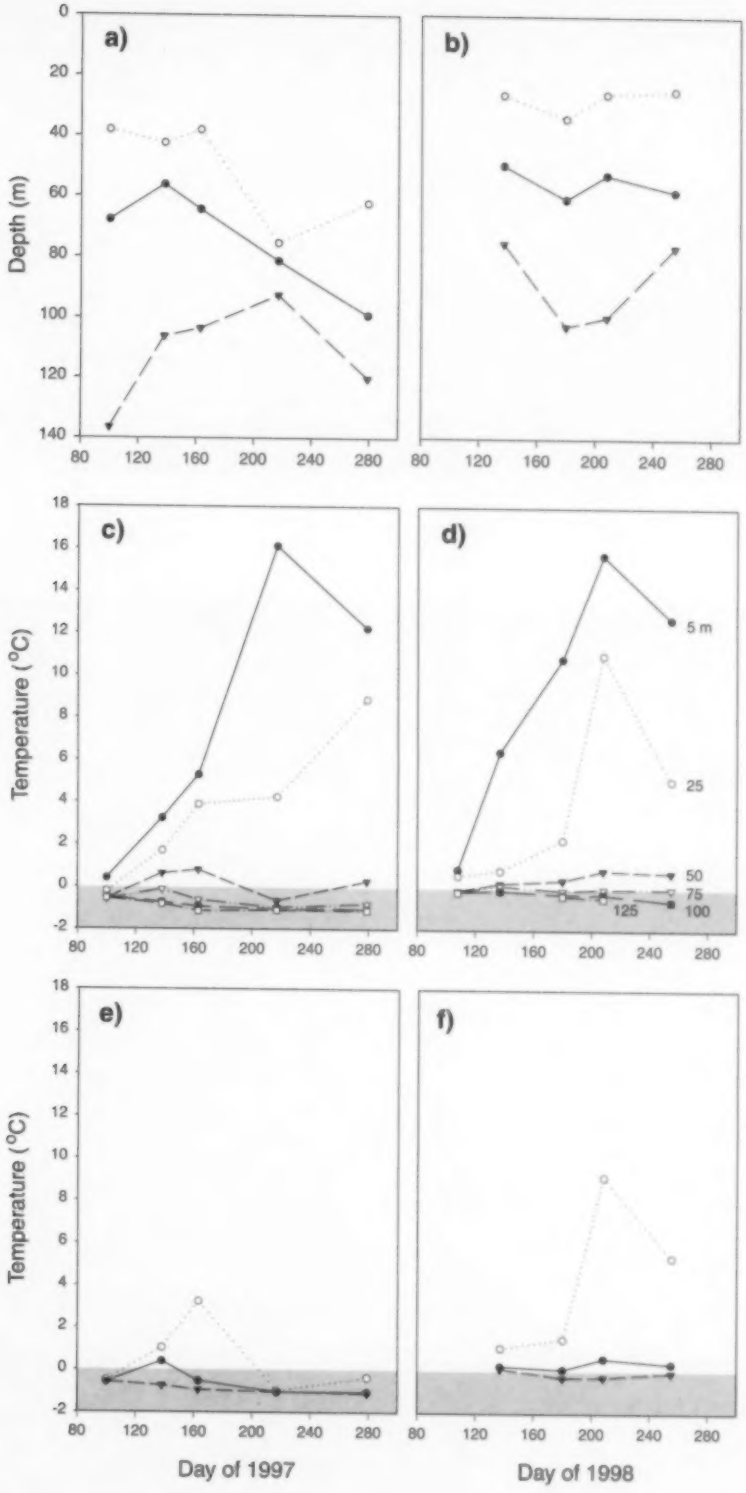

© 2000 NRC Canada

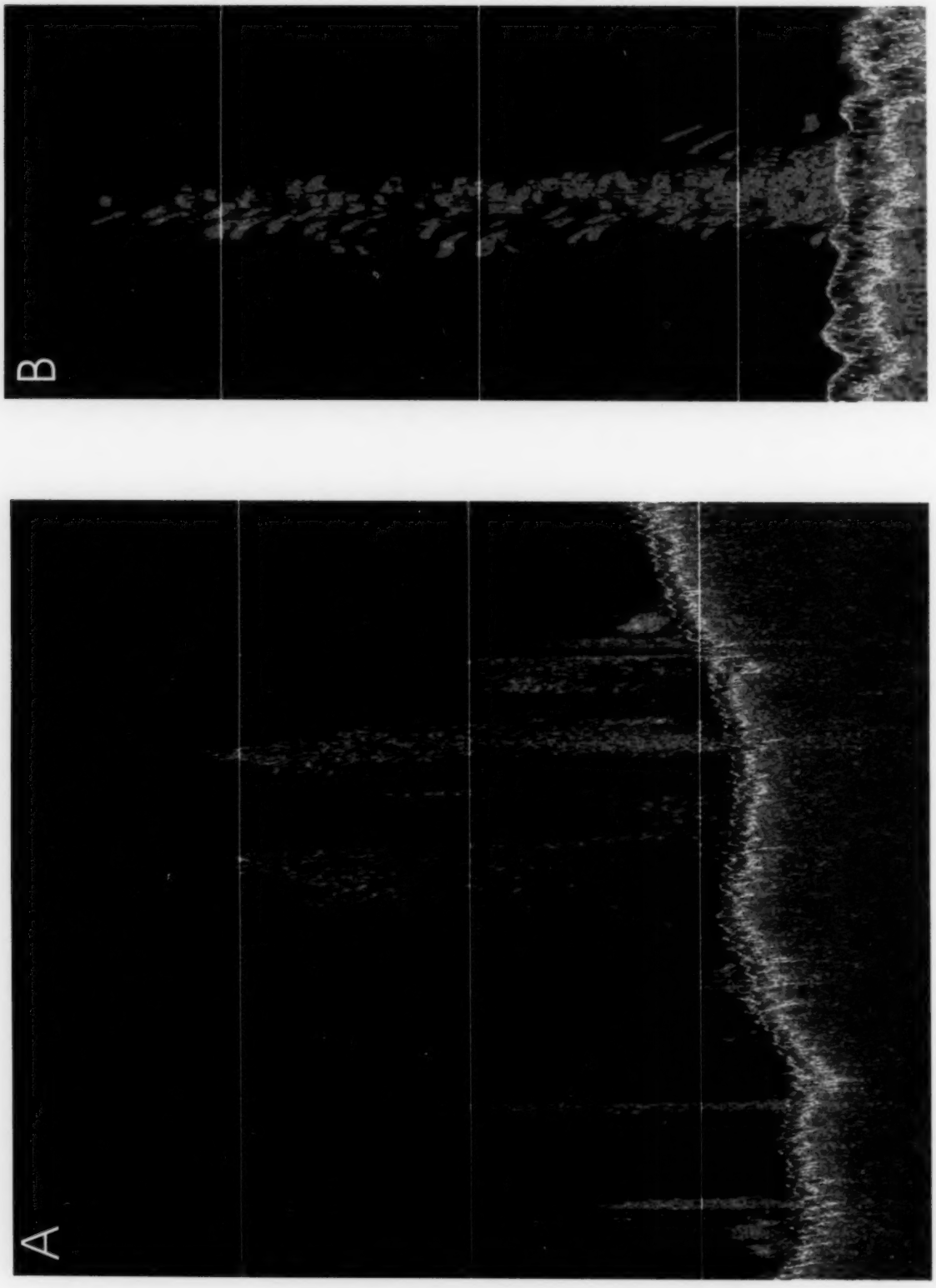

© 2000 NRC Canada

Fig. 5. (A) Echogram showing spawning columns at Cape St. Mary's in May 1997. The echogram spans 2.5 km. Bottom depth is 50–55 m. Horizontal grids are 12.5 m. Echo intensity is indicated by different colours (red > yellow > green > blue > purple). Open water appears black. (B) Enlarged view of the column second from the left (horizontal grids 6 m) showing individual cod within the column as distinct boomerang- or squiggle-shaped traces.

Fig. 6. Estimates of spawning female density at the Bar Haven grounds in 1997 (solid circles) and 1998 (open circles). Error bars show 95% confidence intervals (sampling error only).

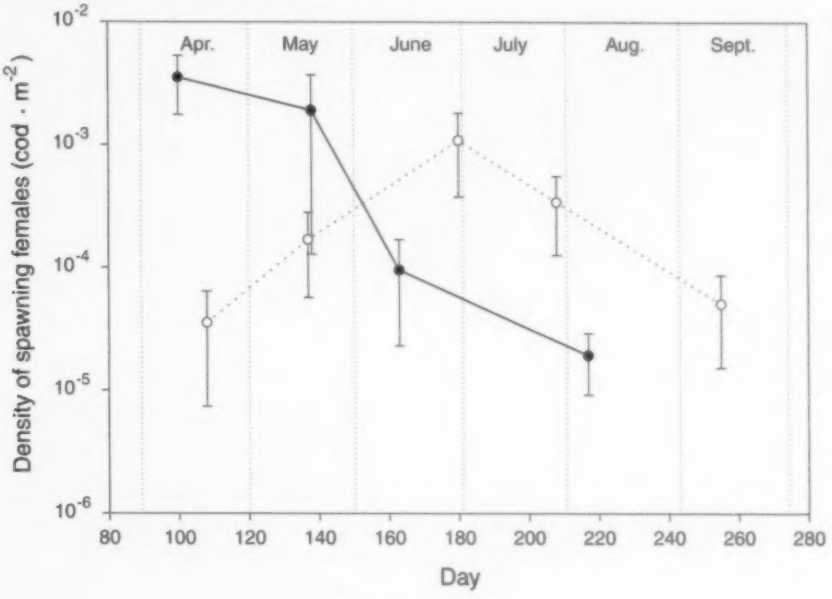

Table 2. Mean length and age (SE in parentheses) of mature female cod sampled at the Bar Haven spawning ground for each survey period of 1997 and 1998.

	1997		1998	
Survey month	Length (cm)	Age (years)	Length (cm)	Age (years)
April	61.0 (1.5) *b*	7.1 (0.24) *a*	60.8 (1.3) *b*	6.3 (0.23) *c*
May	66.8 (1.4) *a*	7.8 (0.21) *a*	67.8 (2.3) *a*	8.1 (0.48) *a*
June	60.0 (3.6) *b*	6.3 (0.52) *b*	70.2 (2.2) *a*	7.9 (0.34) *a*
July–August	61.2 (1.3) *b*	6.8 (0.22) *b*	62.3 (2.1) *b*	6.9 (0.30) *b*
September	55.2 (1.2) *c*	5.7 (0.24) *c*	62.4 (3.2) *b*	6.2 (0.28) *c*

Note: Lengths and ages are for all mature females and not for only those in spawning condition. Within columns, common letters indicate survey months where means did not differ (Duncan's multiple range test, $p > 0.05$).

Table 3. Probit analysis coefficients (SE in parentheses) for the effects of female cod age, survey date, and survey year on the proportions of females in spawning versus ripening state and females in spent versus spawning or ripening condition.

Effect	Spawning vs. ripening	Spent vs. nonspent
Female age	0.299 (0.073)***	–0.384 (0.109)***
Survey date	0.020 (0.006)**	0.004 (0.004) ns
Survey year	0.966 (0.485)*	–1.813 (0.661)**
Year × date interaction	0.014 (0.007)*	–0.023 (0.007)**

Note: * $0.05 < p < 0.01$; ** $0.01 < p < 0.001$; *** $0.001 < p < 0.0001$; ns, nonsignificant.

opment rates. Differences between age-specific overwintering patterns could account for differing spawning timing in relation to age both within and between stocks. A limitation of the above studies (including ours) is that the temperatures experienced by the fish over the full year prior to spawning are poorly known, especially during the fall and winter when gonad development peaks.

Spawning aggregations on the Bar Haven ground exhib-

© 2000 NRC Canada

Fig. 7. At Bar Haven, (*a*) sex ratio (females to males) of cod sampled during each spawning ground survey in 1997 (solid circles) and 1998 (open circles) and (*b*) the percentage of cod sampled that were immature.

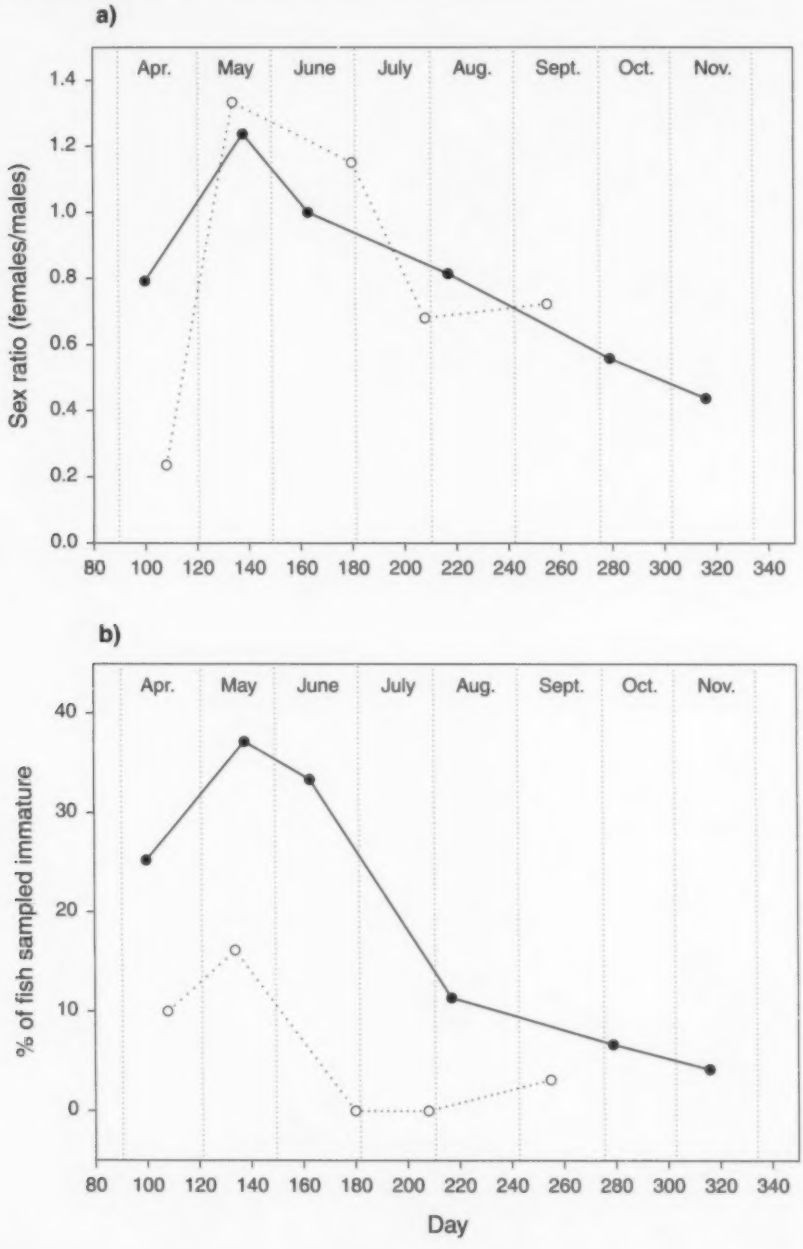

ited gender-based spatial and temporal patterns in both 1997 and 1998. Aggregations were dominated by males early and late in the spawning season. Females were more numerous in midseason and appear to move in to spawn, accompanied by prespawning older juveniles, after males have established the grounds. These observations are consistent with several earlier reports of males being more numerous early in the spawning season (McKenzie 1940; Morgan and Trippel 1996; Nordeide 1998), although no previous studies have shown the within-season progression in sex ratio documented here. Our data also indicate that older females are initially present in higher proportions and that younger females arrive in greater numbers later in the season. Hutchings et al. (1999) hypothesized that the mating system of cod is lek-like, based on laboratory observations of individual behaviour. Our data cannot resolve individual behaviour but with field observations add support to this hypothesis, to the extent that males appear to establish the

© 2000 NRC Canada

spawning grounds. In contrast with these findings, cod sex ratios in Iceland (Jónsson 1982) and the Barents Sea (summarized in Bergstad et al. 1987) have been reported to favour females early in the spawning season. Unfortunately, it is not possible to determine from these studies whether a higher proportion of males were present prior to the observation period. It is also possible that fundamental differences in behaviour exist among stocks.

The location and timing of spawning in cod populations are often determined from the proportion of fish in spawning condition in trawl or other catches (e.g., Jónsson 1982; Hutchings et al. 1993; Smedbol and Wroblewski 1997). However, the location and timing of spawning (i.e., egg production) also depend on abundance, age structure, sex ratio, and fecundity (e.g., Marshall et al. 1998). In the present study, the highest proportions of females spawning did not necessarily coincide with peaks in abundance and density of female spawners. Many areas in the bay had a high percentage of spawning females but very low densities of fish and no concentrations of eggs (Bradbury et al. 1999). We conclude that female condition data are an inadequate diagnostic of spawning location and timing without consideration of the relative abundance of the stock across the range.

In conclusion, we suggest that the bulk of spawning in coastal Newfoundland cod, and perhaps in all stocks, occurs in relatively large aggregations at specific, although not always utilized, grounds. The trawl data reported by Hutchings et al. (1993) suggest that cod spawning is more widespread at densities much lower than observed in this study on the grounds in Placentia Bay. Our acoustic data support the notion that spawning is widespread at low densities but differ in that they suggest that the majority of spawning occurs at well-defined grounds and high density (e.g., Kulka et al. 1995), as in other major cod stocks in the North Atlantic (e.g., Icelandic cod, Jónsson 1982; Arcto-Norwegian cod, Bergstad et al. 1987; Faroese cod, Jakupsstovu and Reinert 1994).

Acknowledgements

Funding was provided by the NSERC Industrial Chair in Fisheries Conservation. G.L.L. was supported by an NSERC postgraduate scholarship. We thank the crews of the RV *Innovation*, RV *Mares*, CCGS *Shamook*, and CCGS *Teleost*, the Fisheries Conservation Chair personnel for help with data collection, R. O'Driscoll for assistance with acoustic analyses, Y. Chen for statistical advice, and M. Burton, P.V.R. Snelgrove, and anonymous reviewers for helpful comments on an earlier draft of the manuscript.

References

Anonymous. 1999. DFO science stock status report for 3Ps cod. Department of Fisheries and Oceans, Science Branch, St. John's, Nfld.

Bergstad, O.A., Jørgensen, T., and Dragesund, O. 1987. Life history and ecology of the gadoid resources of the Barents Sea. Fish. Res. **5**: 119–161.

Bradbury, I.R., Snelgrove, P.V.R., and Fraser, S. 1999. Transport and development of cod eggs and larvae in Placentia Bay (3Ps) Newfoundland 1997–1998. CSAS Res. Doc. 99/71.

Brander, K.M. 1994. Spawning and life history information for North Atlantic cod stocks. ICES Coop. Res. Rep. No. 205.

Brawn, V.M. 1961. Reproductive behaviour of the cod (*Gadus callarias* L.). Behaviour, **18**: 177–198.

Burton, M.P.M., Penney, R.M., and Biddiscombe, S. 1997. Time course of gametogenesis in Northwest Atlantic cod (*Gadus morhua*). Can. J. Fish. Aquat. Sci. **54**: 122–131.

Colbourne, E. 1999. Oceanographic conditions in NAFO subdivisions 3Pn and 3Ps during 1997 and 1998 with comparisons to the long-term (1961–1990) average. CSAS Res. Doc. 99/39.

deYoung, B., and Rose, G.A. 1993. On recruitment and distribution of Atlantic cod (*Gadus morhua*) off Newfoundland. Can. J. Fish. Aquat. Sci. **50**: 2729–2741.

Foote, K.G., Knudsen, H.P., Vestnes, G., MacLennan, D.N., and Simmonds, E.J. 1987. Calibration of acoustic instruments for fish density estimation: a practical guide. ICES Coop. Res. Rep. No. 144.

Godo, O.-R. 1989. The use of tagging studies to determine the optimal time for estimating acoustic abundance of spawning cod. Fish. Res. **8**: 129–140.

Hutchings, J.A., and Myers, R.A. 1993. Effect of age on the seasonality of maturation and spawning of Atlantic cod, *Gadus morhua*, in the Northwest Atlantic. Can. J. Fish. Aquat. Sci. **50**: 2468–2474.

Hutchings, J.A., and Myers, R.A. 1994. Timing of cod reproduction: interannual variability and the influence of temperature. Mar. Ecol. Prog. Ser. **108**: 21–31.

Hutchings, J.A., Myers, R.A., and Lilly, G.R. 1993. Geographic variation in the spawning of Atlantic cod, *Gadus morhua*, in the Northwest Atlantic. Can. J. Fish. Aquat. Sci. **50**: 2457–2467.

Hutchings, J.A., Bishop, T.D., and McGregor-Shaw, C.R. 1999. Spawning behaviour of Atlantic cod, *Gadus morhua*: evidence of mate competition and mate choice in a broadcast spawner. Can. J. Fish. Aquat. Sci. **56**: 97–104.

Jakupsstovu, S.H., and Reinert, J. 1994. Fluctuations in the Faroe Plateau cod stock. ICES Mar. Sci. Symp. **198**: 194–211.

Jónsson, E. 1982. A survey of spawning and reproduction of the Icelandic cod. Rit Fiskideildar **6**(2).

Kjesbu, O.S. 1994. Time of start of spawning in Atlantic cod (*Gadus morhua*) females in relation to vitellogenic oocyte diameter, temperature, fish length and condition. J. Fish Biol. **45**: 719–735.

Kulka, D.W., Wroblewski, J.S., and Narayanan, S. 1995. Recent changes in the winter distribution and movements of northern Atlantic cod (*Gadus morhua* Linnaeus, 1758) on the Newfoundland–Labrador Shelf. ICES J. Mar. Sci. **52**: 889–902.

Lawson, G.L., and Rose, G.A. 1999. The importance of detectability to acoustic surveys of semi-demersal fish. ICES J. Mar. Sci. **56**: 370–380.

Lawson, G.L., and Rose, G.A. 2000. Seasonal distribution and movements of coastal cod (*Gadus morhua* L.) in Placentia Bay, Newfoundland. Fish. Res. In press.

LeFeuvre, P., Rose, G.A., Gosine, R., Hale, R., Pearson, W., and Khan, R. 2000. Acoustic species identification in the Northwest Atlantic using digital image processing. Fish. Res. In press.

Marshall, C.T., Kjesbu, O.S., Yaragina, N.A., Solemdal, P., and Ulltang, Ø. 1998. Is spawner biomass a sensitive measure of the reproductive and recruitment potential of Northeast Arctic cod? Can. J. Fish. Aquat. Sci. **55**: 1766–1783.

Marteinsdottir, G., and Petursdottir, G. 1995. Spatial and temporal variation in reproduction in Icelandic cod at Selvogsbanki and nearby coastal areas. ICES CM 1995/G:15.

McKenzie, R.A. 1940. Nova Scotian autumn cod spawning. J. Fish. Res. Board Can. **5**: 105–120.

Morgan, M.J., and Trippel, E.A. 1996. Skewed sex ratios in spawn-

© 2000 NRC Canada

ing shoals of Atlantic cod (*Gadus morhua*). ICES J. Mar. Sci. **53**: 820–826.

Morrison, C.M. 1990. Histology of the Atlantic cod, *Gadus morhua*: an atlas. Part 3. Reproductive tract. Can. Spec. Publ. Fish. Aquat. Sci. No. 110.

Myers, R.A., Mertz, G., and Bishop, C.A. 1993. Cod spawning in relation to physical and biological cycles of the northern Northwest Atlantic. Fish. Oceanogr. **2**: 154–165.

Neis, B., Schneider, D.C., Felt, L., Haedrich, R.L., Fischer, J., and Hutchings, J.A. 1999. Fisheries assessment: what can be learned from interviewing resource users? Can. J. Fish. Aquat. Sci. **56**: 1949–1963.

Nordeide, J.T. 1998. Coastal cod and north-east Arctic cod — do they mingle at the spawning grounds in Lofoten? Sarsia, **83**: 373–379.

Ouellet, P., Lambert, Y., and Castonguay, M. 1997. Spawning of Atlantic cod (*Gadus morhua*) in the northern Gulf of St. Lawrence: a study of adult and egg distributions and characteristics. Can. J. Fish. Aquat. Sci. **54**: 198–210.

Rose, G.A. 1993. Cod spawning on a migration highway in the north-west Atlantic. Nature (Lond.), **366**: 458–461.

Rose, G.A., and Kulka, D.W. 1999. Hyperaggregation of fish and fisheries: how catch-per-unit-effort increased as the northern cod (*Gadus morhua*) declined. Can. J. Fish. Aquat. Sci. **56**(Suppl. 1): 118–127.

Rose, G.A., and Lawson, G.L. 1999. Acoustic surveys in Placentia Bay and 3Ps, June 1996–1998. CSAS Res. Doc. 99/41.

Rose, G.A., and Porter, D.R. 1996. Target-strength studies on Atlantic cod (*Gadus morhua*) in Newfoundland waters. ICES J. Mar. Sci. **53**: 259–265.

Rose, G.A., deYoung, B., Kulka, D.W., Goddard, S.V., and Fletcher, G.L. 2000. Distribution shifts and overfishing the northern cod (*Godus morhua*): a view from the ocean. Can. J. Fish. Aquat. Sci. **57**: 644–663.

Serebryakov, V.P. 1965. Some results of Soviet research work on ichthyoplankton in the northwest Atlantic: eggs and larvae of cod. ICNAF Spec. Publ. **6**: 425–433.

Sinclair, M. 1988. Marine Populations: an essay on population regulation and speciation. Washington Sea Grant Program, Seattle, Wash.

Smedbol, R.K., and Wroblewski, J.S. 1997. Evidence for inshore spawning of northern Atlantic cod (*Gadus morhua*) in Trinity Bay, Newfoundland, 1991–1993. Can. J. Fish. Aquat. Sci. **54**(Suppl. 1): 177–186.

Sund, O. 1935. Echosounding in fishery research. Nature (Lond.), **135**: 953.

Taggart, C.T., Anderson, J., Bishop, C., Colbourne, E., Hutchings, J., Lilly, G., Morgan, J., Murphy, E., Myers, R., Rose, G., and Shelton, P. 1994. Overview of cod stocks, biology, and environment in the Northwest Atlantic region of Newfoundland, with emphasis on northern cod. ICES Mar. Sci. Symp. **198**: 140–157.

Templeman, W. 1958. How cod spawn — Nielsen's observations. Prog. Rep. Atl. Coastal Stn. **68**: 15–16.

Templeman, W. 1979. Migration and intermingling of stocks of Atlantic cod, *Gadus morhua*, of the Newfoundland and adjacent areas from tagging in 1962–66. ICNAF Res. Bull. **14**: 5–48.

Thompson, H. 1943. A biological and economic study of cod (*Gadus callarius* L.). Res. Bull. No. 14, Department of Natural Resources (Newfoundland Government), St. John's, Nfld.

© 2000 NRC Canada

A new approach toward evaluation of fish bioenergetics models[1]

Charles P. Madenjian, Daniel V. O'Connor, and David A. Nortrup

Abstract: A new approach was used to evaluate the Wisconsin bioenergetics model for lake trout (*Salvelinus namaycush*). Lake trout in laboratory tanks were fed alewife (*Alosa pseudoharengus*) and rainbow smelt (*Osmerus mordax*), prey typical of lake trout in Lake Michigan. Food consumption and growth by lake trout during the experiment were measured. Polychlorinated biphenyl (PCB) concentrations of the alewife and rainbow smelt, as well as of the lake trout at the beginning and end of the experiment, were determined. From these data, we calculated that lake trout retained 81% of the PCBs contained within their food. In an earlier study, application of the Wisconsin lake trout bioenergetics model to growth and diet data for lake trout in Lake Michigan, in conjunction with PCB data for lake trout and prey fish from Lake Michigan, yielded an estimate of PCB assimilation efficiency from food of 81%. This close agreement in the estimates of efficiency with which lake trout retain PCBs from their food indicated that the bioenergetics model was furnishing accurate predictions of food consumption by lake trout in Lake Michigan.

Résumé : On a utilisé une nouvelle approche pour évaluer le modèle bioénergétique Wisconsin pour le touladi (*Salvelinus namaycush*). Dans des bassins de laboratoire, on a nourri des touladis avec des gaspareaux (*Alosa pseudoharengus*) et des éperlans arc-en-ciel (*Osmerus mordax*), proies typiques des touladis dans le lac Michigan. On a mesuré la consommation alimentaire et la croissance des touladis durant l'expérience. On a déterminé les concentrations de polychlorobiphényles (PCB) chez les gaspareaux et les éperlans, de même que chez les touladis au début et à la fin de l'expérience. À partir de ces données, on a établi que les touladis conservaient 81% des PCB présents dans leurs proies. Dans une étude antérieure, en appliquant le modèle bioénergétique Wisconsin pour le touladi à des données de croissance et de consommation alimentaire recueillies chez des touladis du lac Michigan, ainsi qu'à des données sur les PCB présents chez les touladis et ses proies dans le lac Michigan, on a estimé à 81% le taux d'assimilation des PCB présents dans les proies par les touladis. Ces résultats convergents quant à l'assimilation des PCB présents dans les proies montrent que le modèle bioénergétique susmentionné a prévu avec précision la consommation alimentaire du touladi dans le lac Michigan.

[Traduit par la Rédaction]

Introduction

Bioenergetics modeling has proven useful in estimating consumption of prey fish by populations of piscivorous fish (Stewart et al. 1983; Hartman and Margraf 1992), modeling contaminant accumulation in fish (Weininger 1978; Madenjian et al. 1993), modeling nutrient cycling within aquatic food webs (Kraft 1992; He et al. 1993), and predicting the effects of global climate warming on fish growth (Hill and Magnuson 1990). Furthermore, estimation of consumption of prey fish by salmonines in Lake Michigan has been used as a management tool to arrive at salmonine stocking rates for the lake (Hansen et al. 1993). The status of fish bioenergetics models as well as directions for future research have been outlined by Hansen et al. (1993) and Ney (1993). These investigators agreed that further testing and evaluation of fish bioenergetics models is needed.

Traditionally, two approaches have been used to evaluate fish bioenergetics models (Ney 1993). One approach has been to estimate field ration and then compare the estimate of field ration with the prediction of consumption from the bioenergetics model. Field ration is typically estimated by capturing fish in the field, examining and weighing the stomach contents, and then applying knowledge of digestion rates to estimate daily food ration. A second approach has been to measure food consumption and growth of fish in laboratory tanks and then compare observed consumption with that predicted from the bioenergetics model. There are advantages and disadvantages associated with either approach (Hansen et al. 1993). Estimation of field ration represents an attempt to measure food consumption rate in the field, and therefore, this technique alleviates the problem of extrapolating laboratory results to the field. However, consumption is not directly measured in the field; rather, an estimate of daily ration is generated based on the stomach contents and application of some model for gastric evacuation rates. The model for gastric evacuation rates has its own assumptions (Whitledge and Hayward 1997). Food consumption by fish can be measured directly in laboratory tanks. However,

Received May 10, 1999. Accepted November 18, 1999.
J15132

C.P. Madenjian,[2] D.V. O'Connor, and D.A. Nortrup.[3]
U.S. Geological Survey, Great Lakes Science Center, 1451 Green Road, Ann Arbor, MI 48105, U.S.A.

[1]This article is Contribution 1097 of the U.S. Geological Survey Great Lakes Science Center.

[2]Author to whom all correspondence should be addressed. e-mail: chuck_madenjian@usgs.gov

[3]Present address: U.S. Food and Drug Administration, Center for Food Safety and Applied Nutrition, 200 C Street SW, Washington, DC 20204, U.S.A.

© 2000 NRC Canada

swimming activity in tanks is typically confined. So, a laboratory evaluation may indicate satisfactory model performance, but there still may be some question about accuracy of the model predictions in the field, where swimming activity is unconfined. Boisclair and Leggett (1989) suggested that energy costs related to swimming activity may represent one of the most important determinants of fish growth.

The intent of this paper is to introduce a new approach for evaluating fish bioenergetics models. We propose that a comparison of the efficiency with which fish assimilate polychlorinated biphenyls (PCBs), as measured in the laboratory, with that estimated using field data can serve as a vehicle to evaluate fish bioenergetics models. Although this new approach circumvents the problems associated with the other two methods, there are a few disadvantages in applying this new technique. Consequently, we do not offer this new approach as a replacement for the two previous methods. Rather, two or three methods could be used in combination to thoroughly evaluate fish bioenergetics models.

The efficiency with which fish assimilate PCBs from their food can be estimated from field data via application of bioenergetics modeling (Jackson and Schindler 1996; Madenjian et al. 1998*a*, 1998*b*). The Lake Michigan Mass Balance project, sponsored by the Great Lakes National Program of the U.S. Environmental Protection Agency, was conducted during 1994–1995, with the ultimate aim of developing a model for flow of contaminants within the Lake Michigan ecosystem. Lake trout (*Salvelinus namaycush*) and prey fish from Lake Michigan were caught, and the PCB concentrations of these fish were determined. Additionally, sizes of lake trout were measured, ages of lake trout were determined, and the stomach contents of the lake trout were analyzed. Using these data and applying the lake trout bioenergetics model developed by Stewart et al. (1983), Madenjian et al. (1998*a*) estimated that adult lake trout in Lake Michigan retain 81% of the PCBs contained in their food. The Stewart et al. (1983) model for lake trout is one of a suite of "Wisconsin" bioenergetics models; the metabolic components of these models are typically described as a function of water temperature and fish weight, and the model is fitted to observed growth to estimate consumption.

The efficiency with which fish retain PCBs from their food can also be measured in the laboratory (O'Connor 1984; Burreau et al. 1997; Gobas et al. 1999). Fish in laboratory tanks are fed food containing PCBs, and growth and consumption of the fish are measured. Additionally, the PCB concentrations in the fish are determined at the start and end of the experiment, and the PCB concentration in the food is also determined. From these measurements, the efficiency with which the fish retained the PCBs in their food can be calculated. The efficiency of PCB retention from food by lake trout has yet to be measured in the laboratory.

Because the accuracy of the estimate of PCB assimilation efficiency from the field data is dependent on the accuracy of the bioenergetics model, comparison of the estimate of PCB assimilation efficiency from field data with that derived from a laboratory experiment provides an evaluation of the accuracy of the bioenergetics model. This is the rationale for our new approach for evaluation of fish bioenergetics models. We conducted a laboratory experiment to measure the efficiency with which lake trout retained PCBs from their food, and we then compared the laboratory estimate with the estimate by Madenjian et al. (1998*a*) for lake trout in Lake Michigan.

Methods

Laboratory experiment

Our experiment to estimate the efficiency with which lake trout retain PCBs from their food was performed simultaneously with a lake trout feeding and growth study, which ran from fall 1980 through fall 1981. Refer to Madenjian and O'Connor (1999) for more details on the feeding and growth study.

The U.S. Fish and Wildlife Service Jordan River National Fish Hatchery supplied lake trout (Marquette strain) of the 1974 year-class during spring 1980; the Allegheny National Fish Hatchery provided lake trout (Marquette strain) of the 1977 year-class in October 1980. Both groups of fish were raised on a pelletized commercial trout food diet while at the hatchery but were then acclimated to a diet of alewife (*Alosa pseudoharengus*) and rainbow smelt (*Osmerus mordax*) in our laboratory at the Great Lakes Science Center (formerly known as the Great Lakes Fishery Laboratory) for several months before the start of our experiment. Lake trout ≥ 400 mm (total length) in nearshore Lake Michigan have fed chiefly on alewife and rainbow smelt from the 1970s to the present time (Madenjian et al. 1998*c*). All of the 1974 year-class lake trout supplied by the Jordan River National Fish Hatchery were mature males, whereas all of the 1977 year-class lake trout provided by the Allegheny National Fish Hatchery were immature.

Each of the two year-classes of lake trout were split into six lots (three different rations, two replicate tanks for each ration), with 15 fish per tank for each of the 1977 year-class tanks and 12 fish per tank for each of the 1974 year-class tanks. Lake trout were kept in 2380-L (1974 year-class) and 870-L (1977 year-class) circular fiberglass tanks with water exchange rates of 15 and 5 $L \cdot min^{-1}$. Each lake trout was weighed to the nearest gram at the start and end of the experiment. Lake trout were fed thawed alewife and rainbow smelt that had been caught in Lakes Michigan and Huron, frozen, and stored at –30°C. The three different feeding rates included ad libitum and 0.25 and 0.50% of their wet body weight per day. The 0.25 and 0.50% rations for each tank during a test period were based on the average weight of the fish in that tank at the end of the previous test period. Lake trout fed ad libitum were fed to satiation once a day, lake trout fed the 0.50% ration were fed every other day, and lake trout fed the 0.25% ration were fed every fourth day. All uneaten food was removed, air dried for 20 min, and weighed to the nearest 0.1 g. On the average, the 1974 and 1977 year-classes of lake trout fed ad libitum consumed 0.9 and 1.4% of their body weight per day. The three different rations represented a broad range in feeding rates. The 0.25% ration was nearly a maintenance feeding level, allowing for only minimal growth by lake trout. All lake trout in our laboratory tanks were subjected to an annual temperature regime similar to that experienced by Lake Michigan lake trout (Madenjian and O'Connor 1999).

At the start of the experiment, two lake trout were sacrificed from each of the large tanks, and five lake trout were sacrificed from each of the small tanks. The sacrificed fish were stored in plastic bags at –30°C until time of analysis. All 10 of the remaining fish in each tank at the conclusion of the experiment were frozen at –30°C until time of analysis. For 1974 year-class lake trout, the experiment ran from 3 December 1980 through 3 November 1981. For 1977 year-class lake trout, the experiment ran from 14 January 1981 through 3 November 1981. Additionally, subsamples (10–30 fish) of both alewife and rainbow smelt were stored at –30°C for later analysis. The prey fish used to feed the lake trout were caught at several locations in both Lakes Huron and

© 2000 NRC Canada

Michigan. A subsample was taken for each combination of location of capture and prey fish species (alewife or rainbow smelt).

PCB determinations

Frozen lake trout were thawed and grouped by tank and stage of experiment (start or end). Each grouping of fish was then homogenized in an industrial-strength mixer. Frozen prey fish were thawed and grouped by location of capture and species (alewife or rainbow smelt). Each group of prey fish was then homogenized in a food processor.

The procedure outlined by DeVault et al. (1986) was followed to determine total PCB concentrations in the lake trout and prey fish. The detection limit for PCB concentration using this technique was 0.05 $\mu g \cdot g^{-1}$. Appropriate quality control samples (blanks, matrix spikes, and duplicates) were used to ensure the accuracy and precision of the samples. All PCB determinations were completed within 1 year after termination of the laboratory experiment in November 1981.

Calculation of net trophic transfer efficiency of PCBs

Two fish per tank containing 1974 year-class lake trout were sacrificed at the start of the experiment, whereas five fish per tank containing 1977 year-class lake trout were initially sacrificed. These subsamples were taken to estimate the average PCB concentration of lake trout at the start of the experiment in each of the 12 tanks; however, a subsample of just two fish may lead to an inaccurate estimate of initial average PCB concentration. To reduce the potential for inaccuracy in the estimate of initial PCB concentration of lake trout in each of the 1974 year-class tanks, we averaged initial PCB concentrations across replicate tanks. Thus, the estimate of initial PCB concentration of lake trout in any of the 1974 year-class tanks was based on four fish rather than just two fish. To estimate the initial PCB concentration of lake trout in a 1977 year-class tank, we simply used the PCB determination from the five-fish composite specific to that tank.

The efficiency with which lake trout retained PCBs in their food, γ, was calculated as

$$(1) \qquad \gamma = \frac{\Delta\text{PCB body burden}}{\text{amount of PCBs ingested}}$$

where ΔPCB body burden is the average increase in the PCB body burden of lake trout in the tank during the course of the experiment (in micrograms of PCB) and amount of PCBs ingested is the average weight of PCBs in the food eaten by lake trout in the tank during the course of the experiment (in micrograms of PCB). We shall also refer to γ as the net trophic transfer efficiency of PCBs to lake trout from their food. Increase in PCB body burden was calculated as

$$(2) \qquad \Delta\text{PCB body burden} = ([\text{PCB}_f]W_f) - ([\text{PCB}_i]W_i)$$

where $[PCB_f]$ is the average PCB concentration of lake trout in the tank at the end of the experiment (in micrograms per gram wet weight), W_f is the average weight of lake trout in the tank at the end of the experiment (in grams wet weight), $[PCB_i]$ is the average PCB concentration of lake trout in the tank at the start of the experiment (in micrograms per gram wet weight), and W_i is the average weight of lake trout in the tank at the start of the experiment (in grams wet weight). The amount of PCBs ingested was calculated by summing the products of PCB concentration of a particular food type and the corresponding cumulative amount of that food type eaten by an average lake trout in the tank during the course of the experiment, across all food types. A food type was uniquely defined by prey fish species (alewife or rainbow smelt) and location of capture.

Statistical analysis of laboratory estimates of net trophic transfer efficiency

To investigate the significance of ration and lake trout year-class effects on the efficiency with which lake trout retain PCBs from their food, a two-way analysis of variance (ANOVA) with main effects of ration and year-class, and including the interaction between these two main effects, was applied to the estimates of γ.

Field estimate of net trophic transfer efficiency of PCBs

As formulated by Jackson and Schindler (1996), the estimator for γ, using field data, is

$$(3) \qquad \gamma = \frac{[\text{PCB}_{LT}]\alpha}{[\text{PCB}_{PREY}]}$$

where $[PCB_{LT}]$ is the PCB concentration in lake trout (in micrograms per gram wet weight), $[PCB_{PREY}]$ is the PCB concentration in the food of the lake trout (in micrograms per gram wet weight), and α is the gross growth efficiency of the lake trout. Gross growth efficiency is equal to the amount of lake trout growth (in grams wet weight) divided by the amount of food eaten by the lake trout (in grams wet weight). Amount of food eaten by the fish is estimated using a fish bioenergetics model applied to a population of fish in the field. The amount of growth can be estimated using size-at-age data for the fish population in the field (Madenjian et al. 1998*a*). Refer to Madenjian et al. (1998*a*, 1998*c*) for more details on diet and growth, as well as food consumption rates estimated via application of the Stewart et al. (1983) bioenergetics model, of lake trout in Lake Michigan. In their bioenergetics model for lake trout in Lake Michigan, Stewart et al. (1983) modeled lake trout swimming speed as a function of water temperature and lake trout weight. In estimating γ for Lake Michigan lake trout from field data, Madenjian et al. (1998*a*) used the same bioenergetics model developed by Stewart et al. (1983).

Estimates of γ were calculated for Lake Michigan lake trout of ages 2–10 (Madenjian et al. 1998*a*). The estimates of γ for ages 5–10 showed neither a decreasing nor an increasing trend with increasing age, and these estimates averaged 0.81; the corresponding 95% confidence interval ranged from 0.74 to 0.88 (Madenjian et al. 1998*a*). The estimates of γ for ages 5, 6, 7, 8, 9, and 10 were 0.73, 0.89, 0.86, 0.74, 0.79, and 0.87 (Madenjian et al. 1998*a*). The estimates of γ for ages 2, 3, and 4 were 0.62, 0.61, and 0.64. Madenjian et al. (1998*a*) suspected that γ was underestimated for ages 2–4 because PCB concentration in lake trout prey was likely overestimated. A substantial portion of the diet of lake trout <4 years old in Lake Michigan was composed of alewife <60 mm in total length. The regression line for alewife PCB concentration as a function of total length (refer to fig. 2 in Madenjian et al. 1998*a*) was based on alewife lengths between 68 and 185 mm, and therefore, the line had to be extrapolated to estimate PCB concentrations in alewife <60 mm in length. Extrapolation of the line probably resulted in overestimation of the PCB concentration in alewife <60 mm in length (Madenjian et al. 1998*a*). Consequently, Madenjian et al. (1998*a*) concluded that Lake Michigan lake trout retained about 80% of the PCBs contained within their food. Likewise, we considered 0.81 as the most reliable estimate of γ from the Lake Michigan field data. Therefore, we used field estimates corresponding to ages 5–10 for purposes of comparing field and laboratory estimates of γ.

Comparison of laboratory and field estimates of net trophic transfer efficiency

Comparison of the laboratory estimate of γ with the field estimate of γ serves as a direct evaluation of the accuracy of the bioenergetics model estimate of consumption in the field. Because γ is directly proportional to gross growth efficiency (eq. 3), and be-

© 2000 NRC Canada

cause gross growth efficiency is equal to growth divided by consumption, γ is inversely proportional to consumption. Therefore, an error in the estimate of consumption in the field is translated into an error in the field estimate of γ. For example, if consumption was underestimated by 10%, then net trophic transfer efficiency would be overestimated by 11%. If consumption was overestimated by 10%, then γ would be underestimated by 9%. Underestimation or overestimation of consumption by 20% would lead to overestimation of γ by 25% or underestimation of γ by 17%. Thus, a field estimate of γ that was 11% higher than the laboratory estimate of γ would imply that consumption in the field had been underestimated by 10%. A field estimate of γ equal to the laboratory estimate of γ would imply that the bioenergetics model was furnishing accurate predictions of consumption in the field. The above argument is based on two assumptions. First, the efficiency with which a fish retains PCBs from its food does not depend on whether the fish is situated in a laboratory tank or is located within a natural aquatic system. This assumption appears to be reasonable because we know of no studies that provide evidence to suggest otherwise, and there is no reason to expect that absorption of the PCBs through the gut wall of the fish depends on whether the fish is situated in a laboratory tank or in a natural system. Second, on the average, an error in the field estimate of γ solely reflects an error in estimation of consumption by the bioenergetics model. This also appears to be a reasonable assumption because fish growth and PCB concentrations in the predator and the prey are directly measured from field samples, but consumption in the field is not directly measured. Rather, consumption is estimated using the bioenergetics model. By averaging field estimates of γ across several ages, any small errors in measuring growth and PCB concentrations in predator and prey are minimized, leaving the error in estimating consumption as the predominant source of error in the average field estimate of γ. In sum, the comparison of field and laboratory estimates of γ is the crux of our new approach toward evaluation of fish bioenergetics models.

To compare the laboratory estimate of γ with the estimate of γ derived from Lake Michigan field data, we averaged the estimates of γ from all of the tanks containing lake trout fed the medium (0.5% of body weight per day) and high (ad libitum) rations. Rottiers and Tucker (1982) showed that caloric density of lake trout in Lake Michigan continued to increase with age and size. Similarly, the lake trout fed medium and high rations in our laboratory tanks increased in caloric density during the course of our experiment. In contrast, lake trout fed a low ration in our tanks actually decreased in caloric density during the course of the experiment (Madenjian and O'Connor 1999). Therefore, the feeding regime imposed on the low-ration lake trout in our laboratory tanks was definitely not applicable to lake trout in Lake Michigan. Consequently, an average of the estimates of γ from the medium-ration and high-ration tanks was the most appropriate statistic to compare with γ estimated by Madenjian et al. (1998*a*) using field data from Lake Michigan. To determine whether the mean estimate of γ from the medium-ration and high-ration tanks was significantly different from the mean estimate of γ using field data from Lake Michigan, we performed a t test.

Results

Initial PCB concentrations of lake trout composites ranged from 0.35 to 1.04 $\mu g \cdot g^{-1}$ (Table 1). Final PCB concentrations of lake trout composites ranged from 0.69 to 1.75 $\mu g \cdot g^{-1}$. In general, final PCB concentrations were higher for the 1974 year-class compared with the 1977 year-class (Table 1). Final PCB concentrations were highest for the 1974 year-class lake trout fed a medium-level ration. The 1974 year-class lake trout fed ad libitum attained the greatest weight by the end of the experiment, whereas 1977 year-class lake trout maintained on a low ration (0.25% of their body weight per day) exhibited the smallest weight at the end of the experiment (Table 1). Similarly, the amount of PCBs ingested was greatest for the 1974 year-class lake trout fed ad libitum and lowest for the 1977 year-class lake trout fed a low ration (Table 1).

The average PCB concentration of the alewife that were fed to the lake trout was 1.29 $\mu g \cdot g^{-1}$ with a standard error of the mean equal to 0.11 $\mu g \cdot g^{-1}$. The mean PCB concentration for alewife was based on nine different locations of capture. The alewife PCB concentrations ranged from 0.75 to 1.93 $\mu g \cdot g^{-1}$. Rainbow smelt PCB concentrations were considerably lower, averaging 0.42 $\mu g \cdot g^{-1}$ with a standard error of 0.04 $\mu g \cdot g^{-1}$. The mean PCB concentration for rainbow smelt was based on 17 different locations of capture. Rainbow smelt PCB concentrations ranged from 0.20 to 0.85 $\mu g \cdot g^{-1}$.

Net trophic transfer efficiencies of PCBs to lake trout from their food averaged 0.87, 0.91, and 0.71 for lake trout fed low, medium, and high rations (Table 1; Fig. 1). However, the effect of ration on γ was insignificant (two-way ANOVA: $F = 1.10$, df = 2,6, $P = 0.3913$). The average estimate of γ for the 1974 year-class, 0.86, was just slightly higher than average γ of 0.80 for the 1977 year-class. Correspondingly, the effect of year-class on γ was insignificant (two-way ANOVA: $F = 0.30$, df = 1,6, $P = 0.6038$). The response of γ to increasing ration was very similar between the two year-classes, as the interaction was not significant (two-way ANOVA: $F = 0.09$, df = 2,6, $P = 0.9139$). Mean estimates of γ for the low-, medium-, and high-ration lake trout from the 1974 year-class were 0.93, 0.91, and 0.75. Similarly, mean estimates of γ for the low-, medium-, and high-ration lake trout from the 1977 year-class were 0.81, 091, and 0.68. Variability among the replicate estimates of γ for the 1974 year-class tanks was substantially greater than that for the 1977 year-class tanks for lake trout fed medium and high rations (Fig. 1).

Averaging the estimates of γ from the medium- and high-ration tanks yielded an estimate of 0.81 for net trophic transfer efficiency of PCBs to lake trout from their food. The 95% confidence interval about this mean value ranged from 0.64 to 0.98. The mean value of γ from Lake Michigan field data was also 0.81. The mean value of γ from the medium- and high-ration tanks was not significantly different from the mean value of γ from the Lake Michigan field data (t test: $t = 0.0204$, df = 12, $P = 0.9840$).

The difference between the mean field and the mean laboratory estimates of γ was practically negligible. Presenting these estimates to the nearest one thousandth, the field estimate was 0.811, whereas the laboratory estimate was 0.813. Based on the reasoning outlined earlier in this paper, this difference indicated that food consumption by lake trout in Lake Michigan was very slightly overestimated by the Stewart et al. (1983) bioenergetics model. However, the degree of overestimation was practically negligible at 0.2%.

Discussion

The close agreement between the estimate of the efficiency with which lake trout retain PCBs contained in their

© 2000 NRC Canada

Table 1. Estimation of γ, the efficiency with which lake trout retain PCBs from their food, from a laboratory experiment.

Tank No.	Lake trout year-class	Ration level	Average initial weight of lake trout (g)	Average final weight of lake trout (g)	Average initial [PCB] of lake trout ($\mu g \cdot g^{-1}$)	Average final [PCB] of lake trout ($\mu g \cdot g^{-1}$)	Consumption (g)	Amount of PCBs ingested (μg)	γ
26	1977	Low	711	724	0.417	0.691	540	290	0.705
28	1977	Low	727	753	0.368	0.725	559	302	0.924
21	1974	Low	1899	1940	0.830	1.277	1635	1014	0.889
22	1974	Low	2121	2155	0.830	1.289	1763	1045	0.975
25	1977	Medium	718	854	0.473	1.009	1136	606	0.862
27	1977	Medium	766	914	0.347	0.965	1197	640	0.963
11	1974	Medium	1943	2372	0.876	1.332	3603	2189	0.666
12	1974	Medium	2212	2588	0.876	1.752	3785	2244	1.156
13	1977	High	795	1458	0.608	1.090	4042	1547	0.715
15	1977	High	794	1455	0.684	1.090	4159	1617	0.641
23	1974	High	2245	3153	1.043	1.253	7037	2938	0.548
24	1974	High	2406	3240	1.043	1.517	6729	2526	0.954

Note: The experiment ran 335 days for the 1974 year-class and 293 days for the 1977 year-class. Lake trout were fed alewife and rainbow smelt at three different rations: low (0.25% of their body weight per day), medium (0.5% of their body weight per day), and high (ad libitum). Consumption was equal to the total amount of food eaten by all of the lake trout in a tank divided by the number of lake trout in the tank. Amount of PCBs ingested was equal to the total amount of PCBs ingested by all of the lake trout in a tank divided by the number of lake trout in the tank. Refer to eqs. 1 and 2 for more details on the calculation of γ.

Fig. 1. Estimates of γ, the net trophic transfer efficiency of PCBs to lake trout from their food, derived from a laboratory experiment. The experiment ran 335 days for the 1974 year-class and 293 days for the 1977 year-class. Solid circles represent the 1974 year-class and open circles represent the 1977 year-class. Lake trout were fed alewife and rainbow smelt at three different rations: low (0.25% of their body weight per day), medium (0.5% of their body weight per day), and high (ad libitum). Refer to eqs. 1 and 2 for more details on the calculation of γ. The dashed line represents the estimate of γ from field data for Lake Michigan lake trout (Madenjian et al. 1998*a*).

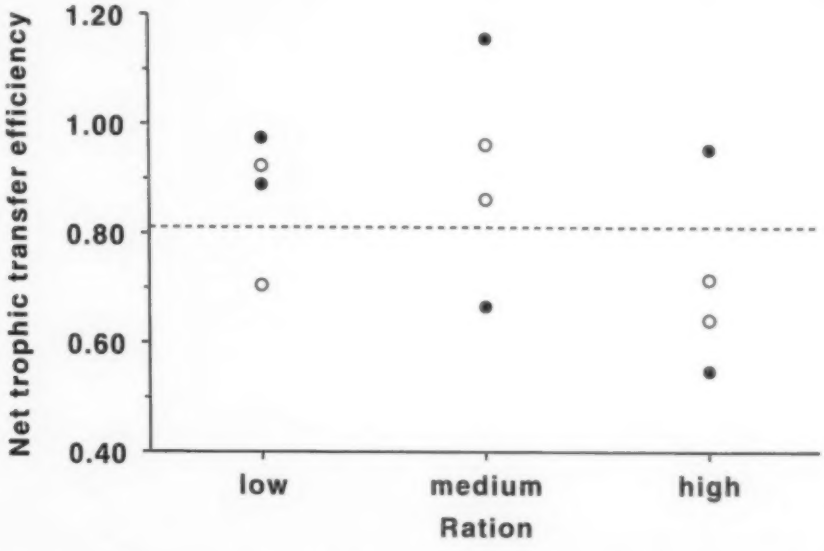

food, γ, from our laboratory experiment and the estimate of γ from the Lake Michigan field data implied that the model developed by Stewart et al. (1983) was accurately estimating food consumption by lake trout in Lake Michigan. Both estimates showed that lake trout were retaining 81% of the PCBs in their food. In an earlier study, the lake trout bioenergetics model predicted annual consumption of lake trout fed a medium ration in laboratory tanks to within 5% of observed annual consumption (Madenjian and O'Connor 1999). Thus, results from the traditional laboratory approach for evaluating fish bioenergetics models corroborated the results from the new evaluation approach of comparing the laboratory estimate of γ with the estimate of γ derived from field data. This corroboration further strengthened the conclusion that use of the Wisconsin bioenergetics model to estimate annual consumption of prey fish by lake trout in Lake Michigan is appropriate.

Additionally, findings from our laboratory study supported

© 2000 NRC Canada

the use of the value of 80% as the efficiency with which lake trout assimilate PCBs from their food for future modeling efforts. Both Thomann and Connolly (1984) and Madenjian et al. (1993) developed simulation models for PCB accumulation in Lake Michigan lake trout. The Thomann and Connolly (1984) model was based on field data from the early 1970s, whereas the Madenjian et al. (1993) model was based on field data from the late 1970s and early 1980s. In both cases, 80% was the value used for PCB assimilation efficiency from food. However, this parameter value had not been corroborated by laboratory measurement. Our study provided the first laboratory measurement of trophic transfer efficiency of PCBs to lake trout from their food, and our study provided further justification for the continued use of an 80% PCB assimilation efficiency in simulation models for PCB accumulation in lake trout.

Forseth et al. (1992) used a radioisotope method to estimate food consumption by brown trout (*Salmo trutta*) in a Norwegian lake. Although these researchers did not test a formal bioenergetics model for growth of brown trout, the concept underlying their radioisotope method is similar to the concept underlying our use of PCB accumulation to evaluate fish bioenergetics models. In both cases, the chemical (either radiocesium or PCBs) was used as a tracer for energy flow from the prey to the predator. Forseth et al. (1992) reported a close match between the field estimates of food consumption from a gut evacuation model and the field estimate of consumption from the radiocesium measurements. Rowan and Rasmussen (1996) employed a radioisotope approach to estimate the energy cost of fish activity in several freshwater systems. Although these researchers did not directly evaluate previously developed fish bioenergetics models, they concluded, based on radiocesium data for Lake Michigan lake trout and prey fish, that Stewart et al. (1983) had underestimated activity of mature lake trout in Lake Michigan by 50%. However, Rowan and Rasmussen (1996) based their estimates of consumption by lake trout on only one radiocesium determination for Lake Michigan lake trout (an age-4 immature fish). In contrast, the field estimate of net trophic transfer efficiency of PCBs to Lake Michigan lake trout from their prey was based on 70 lake trout PCB determinations, with the mean total length of the lake trout composites ranging from about 200 to 900 mm (Madenjian et al. 1998*a*).

Estimates of γ for lake trout fed ad libitum were lower than estimates of γ for lake trout fed at a medium or low ration, although the two-way ANOVA was not sufficiently powerful to detect a significant difference. The inability to detect a difference was undoubtedly due to the relatively high degree of variability in the estimates of γ for the 1974 year-class tanks (Fig. 1). Nevertheless, there was a suggestion from our data that the efficiency with which lake trout retained PCBs from their food was mediated by either ration or frequency of feeding. The fish fed ad libitum were fed every day, whereas the medium-ration fish were fed every other day, and the low-ration fish were fed every fourth day. Burreau et al. (1997) have suggested that PCB transport across the gut wall is not due to passive diffusion alone and that some PCBs may be actively transported across the gut wall. Perhaps the physiological mechanisms for transport across the gut wall can become saturated by frequent feeding or by a large amount of food within the gut, and consequently, the efficiency of PCB uptake is somewhat reduced.

We recommend that the comparison of the field and laboratory estimates of γ be used as an index of the reliability of the bioenergetics model estimates of food consumption by fish in the field. The researcher can judge whether the bioenergetics model estimates of food consumption by fish in the field are sufficiently accurate for purposes of the proposed research study. If the degree of underestimation or overestimation of consumption by the bioenergetics model is unacceptable, the model may have to be revised. A two-sample t test to compare the field and laboratory estimates of γ can supply guidance, but the ultimate decision for adequacy of the bioenergetics model estimates of consumption depends on the needs of the researcher.

Our new approach for evaluation of fish bioenergetics models has both advantages and disadvantages. One advantage of our approach is that it allows for evaluation of model predictions of consumption in the field. However, this new technique has several disadvantages. PCB determinations are costly, and this approach requires PCB determinations of both the predator and the prey. Second, the precision in the estimate of mean γ is sensitive to the accuracy of the estimate of the initial PCB concentration of the fish at the start of the laboratory experiment. Only two of 12 fish were initially subsampled in each of the 1974 year-class tanks, and these small subsamples could have led to inaccurate estimates of the average initial PCB concentration of lake trout in the tank. Estimates of γ from the 1974 year-class tanks exhibited relatively high variability compared with estimates from the 1977 year-class tanks, in which five of 15 fish were initially subsampled. Thus, the problem of low precision in the estimate of mean γ can be overcome by subsampling a sufficiently large number of fish at the start of the experiment. Third, our results suggested that the efficiency with which fish retain PCBs from their food is mediated by feeding rate. Therefore, we recommend that fish be fed at various rates in the laboratory tanks. At the very least, some fish should be fed at a relatively low rate and other fish should be fed at a relatively high rate (e.g., ad libitum). For most applications, the low feeding rate should be higher than a maintenance ration level because fish continue to grow (albeit slowly in some systems) throughout their lifetimes in most aquatic systems (Diana 1995). To evaluate the model, the average of the laboratory estimates of γ can then be compared with the average field estimate. The fish in laboratory tanks should be fed the same foods that fish eat in the field, as was the case for our study, because net trophic transfer efficiency of PCBs can be influenced by the food matrix (Madenjian et al. 1994; Gobas et al. 1999).

One strategy to consider in evaluating a fish bioenergetics model is to run the laboratory evaluation of the model simultaneously with the laboratory estimation of γ, as we have done for the lake trout bioenergetics model. To evaluate the bioenergetics model, growth and consumption of food by fish in laboratory tanks is measured, and then observed consumption and growth are compared with consumption and growth predicted by the bioenergetics model. For the additional cost of determining PCB concentrations in the fish

© 2000 NRC Canada

and its food, a laboratory estimate of γ can be obtained. To apply a fish bioenergetics model to a particular fish population in the field, data on diet and growth are necessary. For the additional cost of determining PCB concentrations in the fish and its prey in the field, a field estimate of γ can be generated. Thus, to apply our new technique for evaluation of fish bioenergetics models, standard sampling procedures for evaluation and application of bioenergetics models can be modified to include supplementary sampling for PCB determinations.

Modeling and laboratory studies have indicated that direct uptake of PCBs from water to lake trout in Lake Michigan accounts for a very small fraction of the PCBs found in Lake Michigan lake trout (Weininger 1978; Thomann and Connolly 1984; Madenjian et al. 1993). Madenjian et al. (1993) estimated that <1% of the PCBs found in large (≥600 mm total length) lake trout from Lake Michigan entered the fish's body by direct uptake from water; practically all of the PCBs found in large lake trout were from diet. Direct uptake in our laboratory tanks was also expected to be very low because the well water supplied to the tanks was not open to atmospheric contamination and therefore was probably as low or even lower in PCB concentration than lake water. Our evaluation approach should be valid regardless of the fish's ability to excrete PCBs, provided that the excretion rate (also referred to as long-term elimination rates by Weininger 1978) in the laboratory is similar to that in the field. Nevertheless, PCB excretion rate in salmonines is so low that it has not been detected in four of five experiments designed to measure it, even though a decrease in PCB body burden as low as 0.0001%·day^{-1} was within the detection limit (Madenjian et al. 1998*a*). Thus, as in the case of direct uptake of PCBs from water, excretion of PCBs plays a very minor role in regulating PCB accumulation in Lake Michigan lake trout.

Our new approach should be applicable to a wide variety of fish species. Interestingly, the available estimates of γ reveal that not all fishes retain as much as 80% of the PCBs contained within their food. Net trophic transfer efficiency, based on field data, of PCBs to Lake Michigan rainbow trout (*Oncorhynchus mykiss*) and coho salmon (*Oncorhynchus kisutch*) from their prey has been estimated at 50% (Madenjian et al. 1994, 1998*b*). Feeding experiments in laboratory tanks indicated fairly close agreement between the field estimates of γ and measurements of γ from the laboratory (Gruger et al. 1975; Gobas et al. 1999), which would suggest that the bioenergetics models developed for rainbow trout (Rand et al. 1993) and coho salmon (Stewart et al. 1981) are furnishing fairly accurate estimates of food consumption by these fishes in Lake Michigan. The laboratory experiments by Gruger et al. (1975) and Gobas et al. (1999) yielded estimates of γ ranging from 30 to 60%, with a mean of about 50%. The rainbow trout and coho salmon fed in the laboratory tanks were not fed natural foods; rather, these fish were fed commercial trout chow impregnated with a known amount of PCB congeners. Additionally, feeding rates were not varied among tanks, and therefore, the effect of feeding rate on γ was not investigated. Thus, additional experimental work should be completed, by maintaining the fish on natural foods, to fully evaluate the bioenergetics models for rainbow trout and coho salmon from the perspective of our new approach. Even so, preliminary results suggested that the bioenergetics models are providing accurate predictions of food consumption by rainbow trout and coho salmon in Lake Michigan. Moreover, these two other examples further demonstrate the utility of this new approach.

We offer this new approach for evaluation of fish bioenergetics models as another check on the accuracy of the model predictions. There are advantages and disadvantages associated with each approach toward evaluation of fish bioenergetics models, but as more approaches are applied to a particular fish bioenergetics model, more insight on model performance and reliability is gained. Additionally, some of the pitfalls associated with a particular approach may become exposed. The bioenergetics model for largemouth bass (*Micropterus salmoides*) developed by Rice (1981) has now been tested using two different approaches. Rice and Cochran (1984) showed that estimates of field ration for largemouth bass were similar to the model predictions of food consumption; Whitledge and Hayward (1997) evaluated the model in the laboratory to show that the model performed adequately when largemouth bass were fed restricted rations. Thus, it appears that application of the largemouth bass bioenergetics model to field populations is appropriate. Similarly, we can conclude that application of the lake trout bioenergetics model developed by Stewart et al. (1983) to populations in the field is appropriate. Including the present study, the adequacy of the lake trout bioenergetics model has now been investigated using two different approaches. Madenjian and O'Connor (1999) found that the model generated unbiased predictions of food consumption by lake trout fed a medium ration in the laboratory. The present study showed that the field estimate of the efficiency with which lake trout retain PCBs from their food is nearly identical to the laboratory estimate. Hence, repeated testing using multiple approaches can allow for a reasonably thorough evaluation of fish bioenergetics models.

Acknowledgments

J. Adams conducted some of the statistical analyses and managed the database. We also thank M. Bevelhimer, J. Breck, T. Edsall, G. Fleischer, C. Kraft, P. Landrum, J. Savino, and an anonymous reviewer for reviewing the manuscript and making helpful suggestions for its improvement.

References

Boisclair, D., and Leggett, W.C. 1989. The importance of activity in bioenergetics models applied to actively foraging fishes. Can. J. Fish. Aquat. Sci. **46**: 1859–1867.

Burreau, S., Axelman, J., Broman, D., and Jakobsson, E. 1997. Dietary uptake in pike (*Esox lucius*) of some polychlorinated biphenyls, polychlorinated naphthalenes and polybrominated diphenyl ethers administered in natural diet. Environ. Toxicol. Chem. **16**: 2508–2513.

DeVault, D.S., Willford, W.A., Hesselberg, R.J., Nortrup, D.A., Rundberg, E.G.S., Alwan, A.K., and Bautista, C. 1986. Contaminant trends in lake trout (*Salvelinus namaycush*) from the upper Great Lakes. Arch. Environ. Contam. Toxicol. **15**: 349–356.

Diana, J.S. 1995. Biology and ecology of fishes. Biological Sciences Press, Carmel, Ind.

© 2000 NRC Canada

Forseth, T., Jonsson, B., Næumann, R., and Ugedal, O. 1992. Radioisotope method for estimating food consumption by brown trout (*Salmo trutta*). Can. J. Fish. Aquat. Sci. **49**: 1328–1335.

Gobas, F.A.P.C., Wilcockson, J.B., Russell, R.W., and Haffner, G.D. 1999. Mechanism of biomagnification in fish under laboratory and field conditions. Environ. Sci. Technol. **33**: 133–141.

Gruger, E.H., Jr., Karrick, N.L., Davidson, A.I., and Hruby, T. 1975. Accumulation of 3,4,3′,4′-tetrachlorobiphenyl and 2,4,5,2′,4′,5′- and 2,4,6,2′,4′,6′-hexachlorobiphenyl in juvenile coho salmon. Environ. Sci. Technol. **9**: 121–127.

Hansen, M.J., Boisclair, D., Brandt, S.B., Hewett, S.W., Kitchell, J.F., Lucas, M.C., and Ney, J.J. 1993. Applications of bioenergetics models to fish ecology and management: where do we go from here? Trans. Am. Fish. Soc. **122**: 1019–1030.

Hartman, K.J., and Margraf, F.J. 1992. Effects of prey and predator abundances on prey consumption and growth of walleyes in western Lake Erie. Trans. Am. Fish. Soc. **121**: 245–260.

He, X., Kitchell, J.F., Carpenter, S.R., Hodgson, J.R., Schindler, D.E., and Cottingham, K.L. 1993. Food web structure and long-term phosphorus recycling: a simulation model evaluation. Trans. Am. Fish. Soc. **122**: 773–783.

Hill, D.K., and Magnuson, J.J. 1990. Potential effect of global climate warming on the growth and prey consumption of Great Lakes fish. Trans. Am. Fish. Soc. **119**: 265–275.

Jackson, L.J., and Schindler, D.E. 1996. Field estimates of net trophic transfer of PCBs from prey fishes to Lake Michigan salmonids. Environ. Sci. Technol. **30**: 1861–1865.

Kraft, C.E. 1992. Estimates of phosphorus and nitrogen cycling by fish using a bioenergetics approach. Can. J. Fish. Aquat. Sci. **49**: 2596–2604.

Madenjian, C.P., and O'Connor, D.V. 1999. Laboratory evaluation of a lake trout bioenergetics model. Trans. Am. Fish. Soc. **128**: 802–814.

Madenjian, C.P., Carpenter, S.R., Eck, G.W., and Miller, M.A. 1993. Accumulation of PCBs by lake trout (*Salvelinus namaycush*): an individual-based model approach. Can. J. Fish. Aquat. Sci. **50**: 97–109.

Madenjian, C.P., Carpenter, S.R., and Rand, P.S. 1994. Why are the PCB concentrations of salmonine individuals from the same lake so highly variable? Can. J. Fish. Aquat. Sci. **51**: 800–807.

Madenjian, C.P., Hesselberg, R.J., DeSorcie, T.J., Schmidt, L.J., Stedman, R.M., Quintal, R.T., Begnoche, L.J., and Passino-Reader, D.R. 1998*a*. Estimate of net trophic transfer efficiency of PCBs to Lake Michigan lake trout from their prey. Environ. Sci. Technol. **32**: 886–891.

Madenjian, C.P., Elliott, R.F., Schmidt, L.J., DeSorcie, T.J., Hesselberg, R.J., Quintal, R.T., Begnoche, L.J., Bouchard, P.M., and Holey, M.E. 1998*b*. Net trophic transfer efficiency of PCBs to Lake Michigan coho salmon from their prey. Environ. Sci. Technol. **32**: 3063–3067.

Madenjian, C.P., DeSorcie, T.J., and Stedman, R.M. 1998*c*. Ontogenic and spatial patterns in diet and growth of lake trout in Lake Michigan. Trans. Am. Fish. Soc. **127**: 236–252.

Ney, J.J. 1993. Bioenergetics modeling today: growing pains on the cutting edge. Trans. Am. Fish. Soc. **122**: 736–748.

O'Connor, J.M. 1984. Polychlorinated biphenyl transport in coastal marine foodwebs. U.S. Environmental Protection Agency Rep. No. EPA-600/3-84-083.

Rand, P.S., Stewart, D.J., Seelbach, P.W., Jones, M.L., and Wedge, L.R. 1993. Modeling steelhead population energetics in Lakes Michigan and Ontario. Trans. Am. Fish. Soc. **122**: 977–1001.

Rice, J.A. 1981. Derivation and application of a bioenergetics model for largemouth bass (*Micropterus salmoides*). M.S. thesis, University of Wisconsin, Madison, Wis.

Rice, J.A., and Cochran, P.A. 1984. Independent evaluation of a bioenergetics model for largemouth bass. Ecology, **65**: 732–739.

Rottiers, D.V., and Tucker, R.M. 1982. Proximate composition and caloric content of eight Lake Michigan fishes. U.S. Fish Wildl. Serv. Tech. Pap. 108.

Rowan, D.J., and Rasmussen, J.B. 1996. Measuring the bioenergetic cost of fish activity in situ using a globally dispersed radiotracer (^{137}Cs). Can. J. Fish. Aquat. Sci. **53**: 734–745.

Stewart, D.J., Kitchell, J.F., and Crowder, L.B. 1981. Forage fishes and their salmonid predators in Lake Michigan. Trans. Am. Fish. Soc. **110**: 751–763.

Stewart, D.J., Weininger, D., Rottiers, D.V., and Edsall, T.A. 1983. An energetics model for lake trout, *Salvelinus namaycush*: application to the Lake Michigan population. Can. J. Fish. Aquat. Sci. **40**: 681–698.

Thomann, R.V., and Connolly, J.P. 1984. Model of PCB in the Lake Michigan lake trout food chain. Environ. Sci. Technol. **18**: 65–71.

Weininger, D. 1978. Accumulation of PCBs by lake trout in Lake Michigan. Ph.D. thesis, University of Wisconsin, Madison, Wis.

Whitledge, G.A., and Hayward, R.S. 1997. Laboratory evaluation of a bioenergetics model for largemouth bass at two temperatures and feeding levels. Trans. Am. Fish. Soc. **126**: 1030–1035.

© 2000 NRC Canada

Seasonality in phosphorus release rates from the sediments of a hypereutrophic lake under a matrix of pH and redox conditions

Michael R. Penn, Martin T. Auer, Susan M. Doerr, Charles T. Driscoll, Carol M. Brooks, and Steven W. Effler

Abstract: Phosphorus release rates were measured on intact sediment cores collected from the major depositional basin of Onondaga Lake, a dimictic, calcareous, hypereutrophic system in Syracuse, N.Y., U.S.A. Release experiments were conducted under a matrix of redox and pH conditions to investigate the importance of Ca- and Fe-related physicochemistry on sediment cores collected seasonally, i.e., during the spring, summer, fall, and winter periods. Strong seasonal variation in P release was observed, with rates ranging from ~3 to 38 mg $P \cdot m^{-2} \cdot day^{-1}$. This variation is attributed to changes in redox status and P concentration gradients at the sediment–water interface. An oxidized microlayer at the sediment–water interface partially inhibits sediment P release under isothermal, well-mixed conditions in the spring and fall. Phosphorus trapped in the oxic microlayer (sorption) is freed when the microlayer is chemically reduced at the onset of anoxia and high P release rates are observed. The oxidized microlayer serves to regulate seasonality in rates of sediment P release but does not influence long-term sediment–water exchange. It is proposed that the long-term P release process is best represented by a time-weighted annual average rate, calculated here to be ~10 mg $P \cdot m^{-2} \cdot day^{-1}$.

Résumé : On a mesuré les taux de libération du P présent dans des carottes de sédiments intactes recueillies dans l'important bassin de dépôt du lac Onondaga, un système dimictique calcaire hypereutrophe à Syracuse, dans l'État de New York (É.-U.). On a effectué les expériences de libération sous diverses combinaisons de conditions d'oxydo-réduction et de pH pour examiner l'effet des processus physicochimiques liés au Ca et au Fe sur les carottes de sédiments recueillies dans les quatre saisons. On a observé une forte variation saisonnière des taux de libération du P (environ 3 à 38 mg $P \cdot m^{-2} \cdot jour^{-1}$). Cette variation est due aux changements dans les conditions d'oxydo-réduction et dans les gradients de concentration du P à l'interface entre les sédiments et l'eau. La présence d'une microcouche oxydée à cette interface inhibe partiellement la libération du P des sédiments sous des conditions d'isothermie et de fort mélange au printemps et à l'automne. Le P piégé dans la microcouche oxydée (sorption) est libéré quand la microcouche est chimiquement réduite au moment où s'installent les conditions d'anoxie; on observe alors des taux élevés de libération du P. La microcouche oxydée régule les variations saisonnières des taux de libération du P présent dans les sédiments, mais n'influe pas sur l'échange à long terme entre les sédiments et l'eau. On pense que le calcul d'un taux de libération annuel moyen pondéré en fonction du temps, qu'on a établi ici à environ 10 mg $P \cdot m^{-2} \cdot jour^{-1}$, est la meilleure façon de rendre compte du processus de libération du P à long terme.

[Traduit par la Rédaction]

Introduction

Efforts to restore surface water quality in eutrophied systems have typically focused on reduction of P loadings, particularly external P loadings (e.g., wastewater treatment plant effluent, agricultural runoff). However, internal loading resulting from sediment P release may contribute up to 80% of the total P input to some lakes (Larsen et al. 1981). These inputs may persist for extended periods following reductions in external loadings, serving to retard recovery of lake water quality (Larsen et al. 1981; Welch et al. 1986; Rossi and Premazzi 1991).

Boström et al. (1988) reviewed the conditions regulating sediment P release, noting that redox potential, pH, and temperature are the most important environmental factors. Einsele (1936) first suggested that increased hypolimnetic P levels may be associated with the depletion of oxygen and an increase in ferrous iron concentration. Ohle (1937) pro-

Received August 28, 1998. Accepted November 18, 1999.
J14778

M.R. Penn[1] **and M.T. Auer.** Department of Civil and Environmental Engineering, Michigan Technological University, Houghton, MI 49931, U.S.A.
S.M. Doerr, C.M. Brooks, and S.W. Effler. Upstate Freshwater Institute, P.O. Box 506, Syracuse, NY 13214, U.S.A.
C.T. Driscoll. Department of Civil and Environmental Engineering, Syracuse University, Syracuse, NY 13244, U.S.A.

[1]Author to whom all correspondence should be sent at the following address: Department of Civil and Environmental Engineering, University of Wisconsin–Platteville, Platteville, WI 53818, U.S.A. e-mail: mrpenn@uwplatt.edu

© 2000 NRC Canada

posed that the Fe–P association in oxic sediments was due to the adsorption of P to ferric iron (hydr)oxides. In his classical studies, Mortimer (1941, 1942) proposed the existence of an oxic microzone at the sediment–water interface and described the role of redox potential in the formation and dissolution of this layer. The release of sorbed P, under conditions of decreased redox potential, was observed experimentally and in situ in Lake Windemere, England. This concept has widely been accepted as the major factor controlling sediment P release. Several investigators have reported substantial P release from anoxic sediments and negligible or negative P release (removal from overlying water) by oxic sediments (Kamp-Nielsen 1974; Boström and Pettersson 1982; Eckert et al. 1997). However, Williams and Mayer (1972) questioned whether this barrier is effective in trapping P diffusing upward from deeper sediments if the surficial sediments are unconsolidated and contain a high water content. Phosphorus release from sediments under oxic conditions has been reported in several studies (e.g., Kamp-Nielsen 1975*a*; Löfgren and Boström 1989; Jensen and Andersen 1992). However, the widely varied nature of the lakes and experimental designs used in these studies makes cross-system comparison difficult. Only Kamp-Nielsen (1974, 1975*a*) and Eckert et al. (1997) measured rates on intact cores from dimictic, eutrophic lakes.

The influence of pH on sediment P release has also been shown to be potentially significant (Boers 1991; Jensen and Andersen 1992). Within the typical range of pH values for lakes, an increase in pH reduces the P sorption capacity of ferric iron (hydr)oxides (Lijklema 1980), thereby increasing the potential for sediment P release. However, P release may be controlled by interactions with Ca compounds which are also pH sensitive. Increased sorption of P to $CaCO_3$, coprecipitation of P with $CaCO_3$, and hydroxyapatite ($Ca_5(PO_4)_3OH$) formation are all favored at increased pH values. These Ca–P phenomena may result in reduced rates of sediment P release at increased pH values, contrary to the increased rates of P release expected under similar pH conditions from ferric iron P sorption as noted above.

Kamp-Nielsen (1975*b*) measured P release from undisturbed cores under both oxic and anoxic conditions over a range of temperatures (5–25°C), noting an exponential increase in release rate with increased temperature. Similar observations were reported by Jensen and Andersen (1992). Increased diffusion of porewater P and increased microbial activity were thought to explain these observations. However, temperature effects are difficult to isolate phenomenologically, as other sediment characteristics (e.g., organic matter content, redox potential, and pH) may vary independently of temperature (cf. Jensen and Andersen 1992).

A knowledge of the magnitude of and seasonal variability in sediment P release rates is fundamental to the development of mass balance models used in lake management. Kamp-Nielsen (1975*a*) presented release rates over a 1-year period measured on undisturbed cores collected at monthly intervals. Other researchers have reported on similar seasonal studies for a variety of lakes (Jensen and Andersen 1992; Eckert et al. 1997). This study documents seasonality in rates of sediment P release in a hypereutrophic, calcareous lake under a matrix of pH and redox conditions. The study's focus on pH and redox phenomena seeks to clarify the importance of Ca- and Fe-related P physicochemistry in regulating sediment P release.

Materials and methods

Study system

Onondaga Lake is a dimictic, hardwater lake with a surface area of 11.7 km^2 and a mean depth of 12 m (Fig. 1). Located in metropolitan Syracuse, N.Y., U.S.A., the lake has received treated and untreated domestic wastewater and industrial effluents for more than 100 years (Effler et al. 1981). Phosphorus discharges to the lake, originating primarily from the Metropolitan Syracuse Treatment Plant (METRO; Fig. 1), are several times in excess of the "acceptable" loading rate defined by Vollenweider (1975) and have resulted in hypereutrophy (Effler et al. 1981). Heidtke and Auer (1992) estimated that ~70% of the 320 kg $P \cdot day^{-1}$ external P loading to the lake originates from the METRO. Hypolimnetic P concentrations in Onondaga Lake can exceed 1000 $\mu g\ P \cdot L^{-1}$ during late summer (Fig. 2), largely due to anoxic summer sediment release rates averaging ~13 mg $P \cdot m^{-2} \cdot day^{-1}$ across the profundal plain (Auer et al. 1993). Water quality problems associated with the lake's hypereutrophic state (high algal standing crop and low transparency, oxygen depletion, hypolimnetic accumulations of ammonia and hydrogen sulfide) can be linked to excessive P loading. In addition to nutrient loadings, the lake has received ionic wastes (primarily Ca^{2+}, Na^+, and Cl^-) from a soda ash manufacturing facility. Operations at this plant were discontinued in 1986; however, leachate from chemical wastebeds that line the west shore of the lake and adjacent Ninemile Creek continue to contribute substantial loads of Ca^{2+}, Na^+, and Cl^- to the lake (Effler et al. 1991). The geochemical nature of the drainage basin, rich in limestone, combined with the Ca-rich wastes contributed by the soda ash facility, leads to an almost continuous condition of oversaturation with respect to calcite (Driscoll et al. 1993), resulting in extremely high $CaCO_3$ deposition rates.

Auer et al. (1996) have described the character and distribution of surficial sediments in the lake. The profundal sediments occupy ~65% of the bottom area and are enriched in organic C, N, and P; however, concentrations are atypically low for a hypereutrophic lake due to dilution by excessive $CaCO_3$ deposition (sediments are >50% of dry weight as $CaCO_3$). Table 1, included here to facilitate comparison with other systems, summarizes the surficial sediment characteristics of the profundal sediments of Onondaga Lake.

Core collection and experimental procedures

Release measurements were conducted on intact sediment cores collected at a deepwater (20 m) sampling station located centrally in the southern basin of Onondaga Lake (Fig. 1). An intensive surficial sediment survey (Auer et al. 1996) demonstrated that this site is representative of the physical and chemical composition over the entire profundal region of the lake. Auer et al. (1993) measured P release rates on replicate cores collected at three locations (north basin, midlake, and south basin) along the broad profundal plain of the lake. While the coefficient of variation in the release rates from the sites varied from 13 to 32%, no statistically significant variation in P release rates was noted with location. Undoubtedly, there will be some variability in P release rates from sediments at different locations. The rates reported from the deepwater station are likely to be maximum rates that would be observed from the profundal plain. For the study reported here, cores were collected periodically from May through November 1992 and in February 1994 (unsafe ice conditions due to a mild winter in 1993 prohibited core collection). Sediment cores containing ~0.7 L of overlying water and a similar volume of sediment (~25 cm depth) were obtained with a Jenkins corer (6.2-cm-diameter by

© 2000 NRC Canada

Fig. 1. Bathymetric map of Onondaga Lake, Syracuse, N.Y., and coring location (latitude 43°06′54″, longitude 76°14′34″).

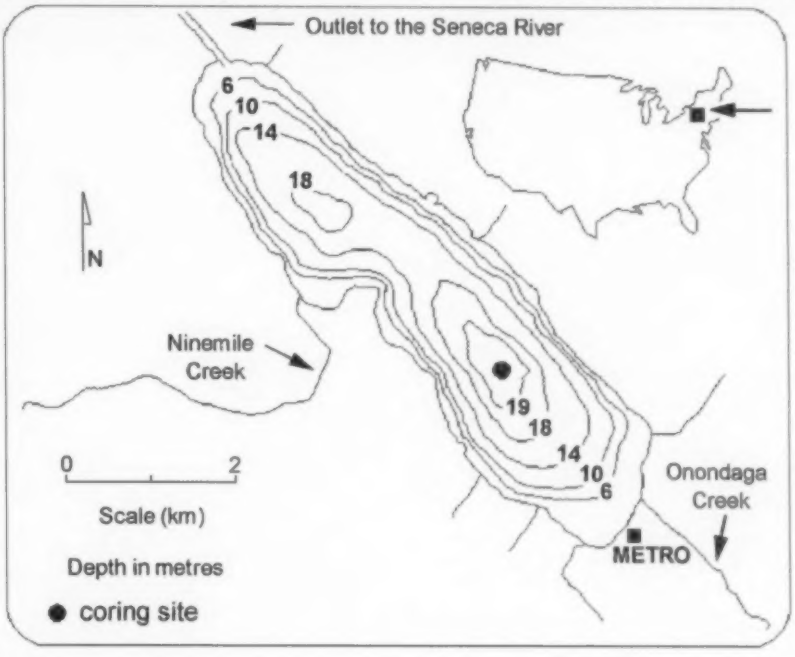

Fig. 2. SRP concentration at 19 m water depth (1 m above sediments) at the coring location in the south basin of Onondaga Lake.

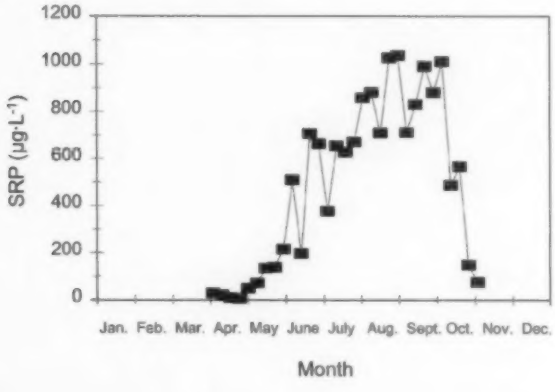

50-cm-long core tubes); attention was given to maintaining an undisturbed sediment–water interface. Table 2 summarizes data on pH and levels of soluble reactive phosphorus (SRP) and dissolved oxygen (DO) in the water overlying the sediment at 19 m depth (~1 m above the sediment–water interface) in the lake at the time of sampling. Cores were stored in the dark at 4°C and experiments were begun within 1 week of core collection.

Experiments were conducted in the spirit of those described by Kamp-Nielsen (1974) in which sediment P release was measured under oxic and anoxic conditions and at pH values that approximate the range observed in the hypolimnion and surficial sediments of Onondaga Lake. DO and pH levels were controlled by the constant bubbling of gas mixtures (air or N_2 for redox, CO_2 for pH) through the water overlying the sediment at a position ~10 cm above the sediment–water interface. The bubbles provided the mixing necessary to destroy concentration gradients in the overlying water without physically disturbing the sediment–water interface.

Replicate cores were examined under four conditions of pH and redox potential (oxic or anoxic, pH 6.5 or 7.5) yielding a total of

Table 1. Surficial (0–5 cm depth mean values) sediment characteristics in the south depositional basin of Onondaga Lake.

Parameter	Mean value
Moisture content[a]	85%
$CaCO_3$[a]	49% of dry weight
Volatile solids[a]	12% of dry weight
Clastics[a]	39% of dry weight
Total organic C[b]	4% of dry weight
Total N[b]	0.4% of dry weight
Total Fe[c]	1.7% of dry weight
Total P[a]	0.18% of dry weight
P fraction[a,d]	
NH_4Cl-SRP	18% of total P
NaOH-SRP	16% of total P
NaOH-NRP	12% of total P
HCl-SRP	35% of total P
Residual	19% of total P
Porewater P[e]	3–7 mg P·L^{-1}

[a]Penn et al. (1995).
[b]Auer et al. (1996).
[c]Rowell (1992).
[d]P fractions as a percentage of total P determined by the sequential extraction (fractionation) method of Hieltjes and Lijklema (1980) on bulk sediment. See Penn et al. (1995) for descriptions of each P fraction.
[e]Van Orman (1993).

© 2000 NRC Canada

Table 2. Chemical conditions in Onondaga Lake at 1 m above the sediment–water interface (19 m depth) at the time of core collections.

Stratification status	Sampling date	SRP ($\mu g\ P \cdot L^{-1}$)	DO ($mg \cdot L^{-1}$)	pH
Prestratification[a]	1 May 1992	50	10	8.0
Stratified	23 June 1992	660	0	7.7
Stratified	6 August 1992	880	0	7.5
Postturnover[b]	9 November 1992	150	8	7.9
Winter stratified[b]	10 February 1994	165	4	7.5

[a]Cores had an oxidized microlayer ~1 mm thick at the sediment–water interface.
[b]Cores had a microaerophilic bacterial mat (*Beggiatoa* spp.) at the sediment–water interface but no oxidized microlayer.

47 cores over the annual cycle. The cores were incubated in the dark at temperatures representative of the hypolimnion at the time of collection: 8°C in the May–November period and 4°C in February. Gases were introduced into the original overlying water and initial conditions were determined after 1 day of mixing. Aliquots of overlying water were removed daily or on alternate days using a syringe and analyzed for pH and SRP. Overlying water removed for chemical analysis was replaced with synthetic P-free Onondaga Lake water except in the February experiments where distilled, deionized water was used. The pH was determined using a Corning 130 pH meter and electrode. SRP concentrations were measured on filtered water samples (0.45-μm cellulose acetate membrane) using the ascorbic acid technique (American Public Health Association 1985). SRP accounts for more than 94% of the total dissolved P released from Onondaga Lake sediments (Auer et al. 1993) and 90–97% of the total dissolved P of the sediment porewater. Phosphorus analyses were performed immediately except in February where samples were filtered, acidified, and frozen. The release of Ca^{2+} was measured during experiments conducted in May with analysis by atomic adsorption spectrophotometry (American Public Health Association 1985).

Cores were collected from the sampling site on 14 September 1992 and 23 November 1993 for sediment pH analysis. The pH of the September cores was determined by inserting a Hach One flat-end pH electrode in the sediments, allowing 5 min for stabilization before reading. The core was then extruded and the electrode rinsed and reinserted at the next depth. The pH of the November core was determined on sediment porewater with an Orion/Ross combination pH electrode. Porewater was collected at depth intervals by extruding the sediment core in a nitrogen box, slicing, centrifuging at 2800 rpm (1500 × *g*) for 30 min, and filtering through glass fiber filters (Whatman 934AH).

Determination of release rates

The experiments were typically performed for a period of 2 weeks. Release rates were calculated as the time rate of accumulation of P in the overlying water divided by the sediment surface area of the core (Auer et al. 1993). Representative results of P release experiments conducted under anoxic and oxic experimental conditions are presented in Fig. 3. Release rates in anoxic cores were essentially constant over the first ~7 days of the experiment, decreasing thereafter (Fig. 3*a*), the two-phase pattern of release reported by Auer et al. (1993). Initial rates are reported here for anoxic cores (shown as the regression fit in Fig. 3*a*). Auer et al. (1993) speculated that the two-phase pattern occurs because laboratory cores receive no input of fresh, easily degradable particulate P, which constitutes ~20% of total seston P in Onondaga Lake (Penn and Auer 1997). Imposition of oxic conditions to cores collected under in situ anoxic conditions leads to the formation of a visible reddish brown oxic surface microlayer over a period of 2–5 days. During this period of transient dynamics, release rates were typically negative (P was removed from the overlying water; Fig. 3*b*), attributed to the adsorption of P by ferric iron (hydr)oxides. After this equilibration period, release rates became positive and remained constant for the duration of the experiments. The positive final rates are considered representative of release under oxic conditions and are those reported here (shown as the regression fit in Fig. 3*b*).

Fig. 3. Typical P release patterns in replicate sediment cores during incubation under (*a*) anoxic and (*b*) oxic conditions. Regression lines show the time period used for calculation of release rates.

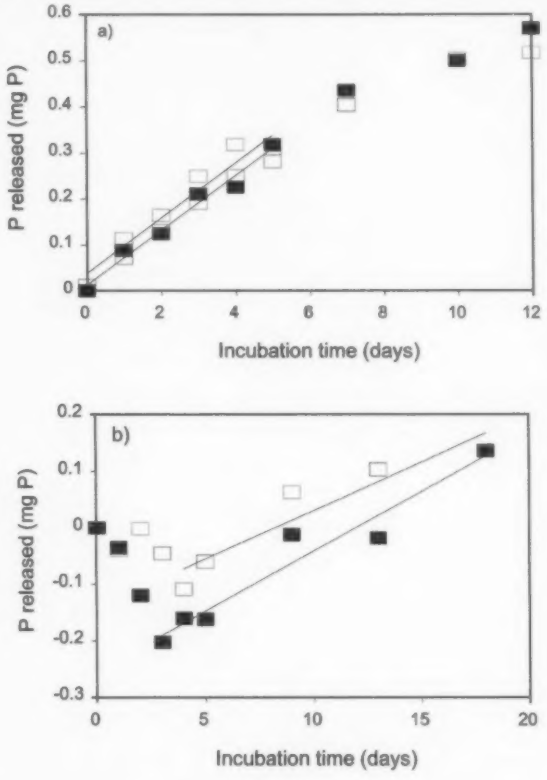

Results

Results of sediment P release experiments are summarized in Table 3 and Fig. 4. A three-way analysis of variance (ANOVA) was performed on the data using measured P release rates as the response variable and three experimental treatments including month (season) of core retrieval, pH, and redox (oxic–anoxic) of the incubated cores. Hypothesis testing was conducted to determine whether the mean P release rate was significantly different for these three experimental treatments. Results of the ANOVA, using Type III sum of squares analysis, are presented in Table 4. Month (season) and redox status were found to be highly significant ($p \leq 0.0001$). The pH of incubation indicated moderate significance ($p \leq 0.0383$). All main effects and interactions, with the exception of the two-way interaction of month × pH, were significant at $p < 0.05$.

© 2000 NRC Canada

Table 3. Sediment P release rate summary and statistics.

	May	June	August	November	February
Oxic, pH 6.5					
Mean ± SD	–0.8±0.5	5.6	6.4	12.9	na
Minimum	–1.4	4.8	5.7	10.4	
Maximum	–0.2	6.4	7	15.3	
n	3	2	2	2	
r^2 minimum	0.01	0.61	0.88	0.88	
r^2 maximum	0.9	0.81	0.94	0.97	
Oxic, pH 7.5					
Mean ± SD	3.4±1.5	7.0±0.8	4.8	10.3	1.3±1.0
Minimum	1.9	6.3	3.5	9.4	0.4
Maximum	5.5	8.2	6.2	11.3	2.7
n	3	3	2	2	4
r^2 minimum	0.84	0.83	0.92	0.90	0.04
r^2 maximum	0.99	0.92	0.99	0.90	0.8
Anoxic, pH 6.5					
Mean ± SD	44.2±3.2	13.0±0.6	10.5	19.8	na
Minimum	39.7	12.3	9.7	19.8	
Maximum	47	13.8	11.2	19.9	
n	3	3	2	2	
r^2 minimum	0.99	0.9	0.94	0.89	
r^2 maximum	1	0.95	0.95	0.98	
Anoxic, pH 7.5					
Mean ± SD	38.1±1.4	12.7±0.3	8	18	12.2±1.2
Minimum	36.6	12.3	7.6	17.9	10.9
Maximum	39.9	12.9	8.3	18	14
n	3	3	2	2	4
r^2 minimum	0.99	0.93	0.93	0.91	0.99
r^2 maximum	1	0.96	0.96	0.93	1

Note: Rates (mean, minimum, and maximum) are expressed as mg $P \cdot m^{-2} \cdot day^{-1}$. Anoxic rates are based on the initial phase release. Oxic rates are based on the period of positive P release after full development of the oxic microlayer at the sediment–water interface during incubation. Coefficients of determination (r^2) are based on a linear regression of mass of P released versus the duration in days for each of the cores.

Data from selected experiments are examined here to explore the relative importance of Ca and Fe in mediating P release and to illustrate seasonality in P release rates.

Discussion

Effects of pH

Calcium–phosphorus interactions

Higher release rates at low pH may be expected as a result of dissolution of $CaCO_3$ (with attendant release of adsorbed or coprecipitated P) and (or) Ca–P minerals (Driscoll et al. 1993). This was observed for sediment P release measured under anoxic conditions at pH 6.5 where rates were ~15% greater (range 2–24%) than at pH 7.5. The rate of Ca^{2+} release (measured in the May cores) more than doubled at the lower pH (561 versus 196 mg $Ca \cdot m^{-2} \cdot day^{-1}$). Kamp-Nielsen (1974) reported similar increases in P and Ca^{2+} release over the same range of pH values in cores from eutrophic, calcareous Lake Furesø, Denmark. This relationship between pH, Ca, and P is further supported by examination of sediment P profiles where ~25% of the P in the surficial sediments is associated with $CaCO_3$ (Penn et al. 1995). Concentrations of $CaCO_3$-associated P (extracted with NH_4Cl) decrease with depth in the upper 10 cm of sediments, as do pH levels (Fig. 5).

Iron–phosphorus interactions

Lower release rates at low pH may be expected as a result of the greater sorptive capacity of ferric iron (hydr)oxides for phosphate as pH decreases (Lijklema 1980). This was observed for sediment P release measured under oxic conditions in May and June (Table 3) where rates at pH 6.5 were lower than at pH 7.5. However, in August and November experiments under oxic conditions (Table 3), release rates were greater at pH 6.5. This difference may be attributed to the thickness of the oxic microlayer (<1 mm in August and November and 1–5 mm in May and June experiments). Variability in the thickness of the oxic microlayer may occur as a result of depletion of Fe levels in the sediment porewater over the course of the stratified anoxic period and (or) increased sediment oxygen demand from deposited organics over the course of the summer.

Role of pH

The findings reported here suggest that both Fe (redox effect) and Ca (pH effect) act to mediate sediment P release. It is important to note that the two processes are spatially separated. Iron and redox phenomena are important in the oxic

© 2000 NRC Canada

Fig. 4. Mean values for sediment P release rates determined under (*a*) anoxic and (*b*) oxic conditions from sediment cores collected seasonally. Solid bars indicate experiments at pH = 7.5 and open bars indicate pH = 6.5. Note the change of scale on the *y*-axes.

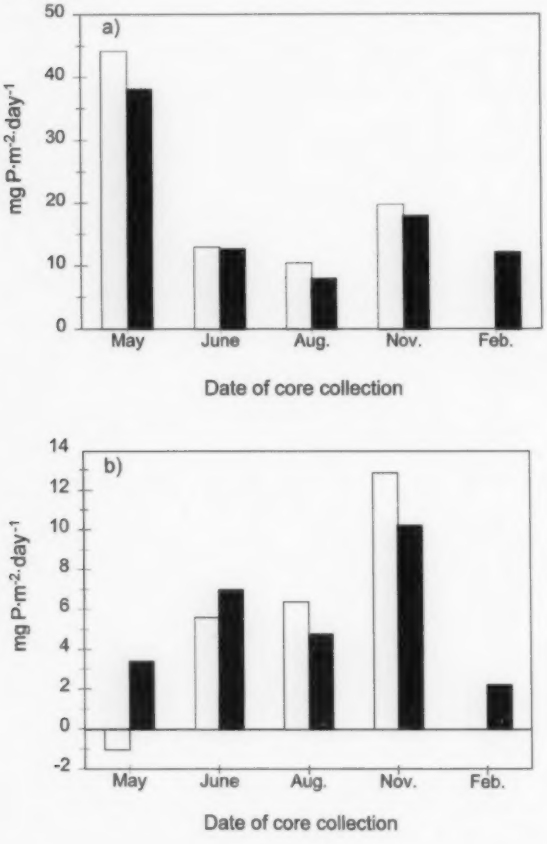

microzone mediating the movement of P across the sediment–water interface. Here, the trapping effect (Fe–pH interactions) masks the dissolution effect (Ca–pH interactions). Calcium–pH phenomena are thought to be significant in the deeper, anoxic sediments where dissolution and desorption phenomena ($CaCO_3$) and the mineralization of organics act to produce porewater P.

Our data suggest that pH plays a measurable role in sediment P release in Onondaga Lake, continuously in the deep sediments (Ca–pH interactions) and seasonally at the interface when an oxidized microlayer is present (Fe–pH interactions). However, as will be shown below, redox effects are more dramatic than pH effects and play a larger overall role in mediating seasonal P release.

Effects of redox conditions

Sustained oxic conditions

Oxic conditions are sustained at the sediment–water interface during spring and fall turnover and for a period of time following the onset of winter stratification. Cores collected in May had been exposed to sustained oxic conditions in

Table 4. Three-way ANOVA results for P release rates using month of core retrieval, pH, and redox (oxic/anoxic) conditions during incubation as experimental treatments.

Effect/interaction	df	MS	*F*	*p*
Month	4	358.4474	133.38	0.0001
Redox	1	2161.4755	804.30	0.0001
pH	1	12.6571	4.71	0.0383
Month × redox	4	605.6571	225.37	0.0001
Month × pH	1	22.3807	8.33	0.2679
Redox × pH	3	3.7145	1.38	0.0073
Month × redox × pH	3	15.8262	5.89	0.0029

Note: df, degrees of freedom; MS, mean square; *F*, likelihood ratio; *p*, probability.

Fig. 5. Profiles of pH (solid squares)and the $CaCO_3$-associated P fraction as a percentage of total P (open squares) in Onondaga Lake surficial sediments in relation to depth below the sediment–water interface. $CaCO_3$-P determined from NH_4Cl extractions (Penn et al. 1995).

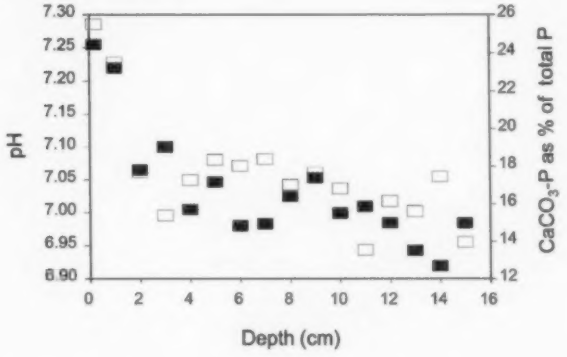

situ, probably since the onset of isothermal conditions in late winter – early spring. These sediments were capped by a 1-mm-thick reddish brown layer thought to consist of ferric iron (hydr)oxides. This assumption is supported by the results of sequential extraction (fractionation) measurements that suggest that this oxic surface layer is highly enriched in P sorbed to ferric iron compounds (SRP measured on NaOH extracts, unpublished data). Cores were incubated under oxic conditions to simulate this environment. Maintained in the laboratory at pH 7.5, release rates for these cores were the lowest measured (~3 mg $P \cdot m^{-2} \cdot day^{-1}$), demonstrating the importance of a well-developed oxic microlayer in mediating P release. Note, however, that these rates are higher than the negligible rates reported for other lakes under sustained oxic conditions (Kamp-Nielsen 1974). In fact, these oxic rates fall within the lower range of anoxic release rates for eutrophic lakes (Nürnberg 1988). It is concluded that the oxic microlayer is not able to completely suppress P release in Onondaga Lake under sustained oxic conditions. This may occur due to (*i*) low levels of Fe in the sediment (17 mg Fe·g dry $weight^{-1}$ in Onondaga Lake (Table 1); mean of 46 mg Fe·g dry $weight^{-1}$ for 19 eutrophic North American and European lakes (Boström and Pettersson 1982; Ostrofsky 1987)), (*ii*) high concentrations of SRP in the porewater (7 mg $P \cdot L^{-1}$ in Onondaga Lake (Table 1); mean

© 2000 NRC Canada

maximum value of 4.7 mg $P \cdot L^{-1}$ for 14 eutrophic and hypereutrophic lakes (Enell and Löfgren 1988)), (*iii*) a limited depth of oxygen penetration because of high sediment oxygen demand, and (*iv*) incomplete trapping of P diffusing through the layer due the unconsolidated nature of the sediments at the interface with a very high water content.

Exposure to anoxic conditions

Anoxic conditions occur at the sediment–water interface during the later stages of winter stratification and with the onset of summer stratification. The onset of anoxia represents a marked change in conditions at the sediment–water interface. Cores collected in May had been exposed to oxic conditions in situ and were incubated in an anoxic environment to simulate the onset of anoxia. These cores displayed the highest rates of sediment P release. This is attributed to the release of Fe-bound (sorbed) P during dissolution of the oxic microlayer (the reddish brown surface layer disappeared within 1 day of anoxic incubation) and to the presence of high porewater P concentrations. The rates measured under these conditions (~38 mg $P \cdot m^{-2} \cdot day^{-1}$) are considered representative of the late spring – early summer period in Onondaga Lake, when the onset of anoxia destroys the oxic microlayer, resulting in a "burst" of sediment P release. These spring P release rates likely decrease after an anoxic sediment–water interface becomes established: "second-phase" release following breakdown of the oxic microlayer in May cores at pH 7.5 was 22 mg $P \cdot m^{-2} \cdot day^{-1}$. Later in summer, diffusion and diagenesis establish a new equilibrium release rate.

Sustained anoxic conditions

Anoxic conditions may be sustained at the sediment–water interface during summer and winter stratification. Cores collected in June and August had been exposed to anoxic conditions since the last week of May. Release rates measured on these cores under anoxic conditions (8–13 mg $P \cdot m^{-2} \cdot day^{-1}$) were intermediate to the low rates observed under sustained oxic conditions (3 mg $P \cdot m^{-2} \cdot day^{-1}$) and those observed under imposed conditions of anoxia (38 mg $P \cdot m^{-2} \cdot day^{-1}$). The results of these experiments are considered representative of the summer period in Onondaga Lake when anoxic conditions persist. The rates measured here compare favorably with summer anoxic release rates measured previously in the lake (Auer et al. 1993).

During core collection in February, DO in the lake water 1–2 m above the sediment–water interface was 4 mg $\cdot L^{-1}$ (~30% of DO saturation, indicative of hypolimnetic oxygen depletion). February cores were considered anoxic, however, since no oxic microlayer was present at the interface at the time of collection. The water immediately overlying the sediment had insufficient DO for ferrous iron oxidation. This illustrates the strong redox gradient that exists across the sediment–water interface due to the high sediment oxygen demand. Rates measured on February cores under anoxic conditions (12 mg $P \cdot m^{-2} \cdot day^{-1}$; Table 3) were similar to those measured during summer (June and August). Anoxic rates measured on February cores are thought to represent sediment P release in late winter and early spring when hypolimnetic oxygen depletion has destroyed the oxic microlayer. Release rates measured under conditions of sustained anoxia may reflect a steady-state condition where diagenetic production of porewater P is balanced by loss through diffusion to the overlying water with no redox-mediated (ferric iron) inhibition at the interface.

Exposure to oxic conditions

Sediments are exposed to oxic conditions at fall and spring overturn. Cores were collected in early November, shortly after turnover. We treat these cores differently than those of sustained oxic conditions (e.g., May cores, collected ~2 months after turnover) because November is a period during which the oxic microlayer actually develops. As observed in February, even though oxygen was present in the water column at the time of core collection (8 mg $\cdot L^{-1}$ at 19 m depth; Table 2), the oxic microlayer was not present in the November cores. This suggests that formation of the oxic microlayer is a progressive process and that a transition period of unknown duration exists between fall turnover and fully oxic conditions at the sediment–water interface (the oxic microlayer was observed in cores collected in late November 1991). The duration of this transition period is likely a function of the depletion of reduced species gradients (particularly sulfides) in the porewater. The microaerophilic, sulfide-oxidizing bacterium *Beggiatoa* spp. was observed as a mat at the sediment–water interface at the time of core collection. *Beggiatoa* inhabits the interface between oxic and anoxic environments where both sulfide and oxygen are present (Jørgensen 1977). While oxygen was present in the overlying water, levels were insufficient at the sediment–water interface to support the development of an oxidized microlayer (i.e., no reddish brown ferric layer was present) but were sufficient to support *Beggiatoa* (which was not observed in February). Thus, it is appropriate to measure release rates for this period under anoxic conditions. Cores incubated under anoxic conditions had high rates of sediment P release (18 mg $P \cdot m^{-2} \cdot day^{-1}$). These rates are higher than those observed under sustained anoxic conditions (summer). Kamp-Nielsen (1975*a*) observed similar increases in sediment P release during fall turnover. At turnover (late October – early November), the sediment porewater – lake water P gradient increases as the SRP concentration in the lake water overlying the sediments decreases by an order of magnitude as a result of complete mixing (Fig. 1), leading to increased upward diffusion of porewater P. In addition, P-rich particles are deposited (P sorbed on ferric iron precipitates that form when reduced iron (Fe^{2+}) that had accumulated in the hypolimnion is oxidized during turnover; Penn and Auer 1997), which may contribute to the higher release rate when the Fe is reduced/solubilized with attendant P release. Later, sediment oxygen demand presumably decreases in early winter as less autochthonous deposition of organic C occurs. As a result, oxygen penetrates the sediment surface and an oxic microlayer develops (field observations, May 1992 and November 1991). The *Beggiatoa* mat is then found as a white layer immediately below the surface reddish brown oxic layer and above the remaining black, sulfide-rich anoxic sediments. Here, conditions are appropriately represented by rates measured under oxic conditions (10 mg $P \cdot m^{-2} \cdot day^{-1}$). It is suspected that oxic rates would decrease with increases in the thickness of the oxic microlayer, ultimately approaching those achieved under sustained oxic conditions.

© 2000 NRC Canada

Seasonal cycle of P release

Release rate measurements conducted on intact cores have demonstrated the importance of redox conditions (the oxic microlayer) in mediating seasonality in sediment P release. Figure 6 presents a chronology of release rate measurements. During spring turnover, oxic conditions are sustained and the P release rate is 3 mg $P \cdot m^{-2} \cdot day^{-1}$. Later in spring, with the onset of anoxia, a peak in release (38 mg $P \cdot m^{-2} \cdot day^{-1}$) is noted, followed by the second-phase rate of 22 mg $P \cdot m^{-2} \cdot day^{-1}$. Summer release rates, characteristic of a period of sustained anoxia, decrease to levels of 8–13 mg $P \cdot m^{-2} \cdot day^{-1}$. At fall turnover, anoxic sediments yield relatively high release rates (18 mg $P \cdot m^{-2} \cdot day^{-1}$). Lower rates (10 mg $P \cdot m^{-2} \cdot day^{-1}$) are characteristic of late fall as exposure to oxic conditions facilitates development of the oxic microlayer. With further development of the oxic microlayer in early winter, rates decrease, reaching levels characteristic of sediment exposed to sustained oxic conditions (3 mg $P \cdot m^{-2} \cdot day^{-1}$). Oxygen depletion in winter exposes sediments to anoxic conditions (rates of 12 mg $P \cdot m^{-2} \cdot day^{-1}$) and may also yield a burst of release (38 mg $P \cdot m^{-2} \cdot day^{-1}$), although this feature has not been experimentally confirmed. This seasonal pattern is similar to that reported by Kamp-Nielsen (1975*a*) for eutrophic Lake Esrom, Denmark. Notable exceptions for Onondaga Lake include considerably higher rates of sediment P release under oxic conditions and extremely high release rates at the onset of anoxia in spring.

Average annual rates of sediment P release are of value in developing mass balance P models. It would be inappropriate to estimate the annual average P release rate as the mean of the discrete measurements made here, as no consideration would be given to the duration ascribed to each rate of release. Two options, illustrated in Fig. 6, were considered in calculating a time-weighted annual average release rate.

Case 1: A step function is assumed with measured release rates held constant over the period between successive core collections. The pattern of release is a outlined above. The annual average P release rate for this case is 8.7 mg $P \cdot m^{-2} \cdot day^{-1}$.

Case 2: As for case 1, but a burst in P release is added during the period in winter when anoxic cores were noted. The shape and duration of that burst were made equal to those observed with exposure to anoxic conditions in spring. The annual average P release rate for this case is 9.7 mg $P \cdot m^{-2} \cdot day^{-1}$.

The annual average release rate for case 2 is thought to be most representative of actual conditions, as winter oxygen depletion is a regular feature of seasonal dynamics in Onondaga Lake. Note that the onset of anoxia is likely to vary spatially as the lake stratifies (occurring first in the deepest waters and then progressing to shallower water). However, this progression proceeds rapidly in Onondaga Lake due to the high sediment oxygen demand.

Long-term and seasonal release

The calculated annual rate of 9.7 mg $P \cdot m^{-2} \cdot day^{-1}$ is quite similar to the mean anoxic summer release rate of 10.4 mg $P \cdot m^{-2} \cdot day^{-1}$. This suggests that summer rates, free from the "trapping" influence of the oxic microlayer and the burst associated with exposure to anoxia, may best reflect steady-state conditions of sediment P release. Suppression of P release under oxic conditions is balanced by elevated release at the subsequent onset of anoxia. Thus, although redox conditions at the sediment–water interface can have a significant effect on the short-term (seasonal) dynamics of sediment P release, long-term (annual average) release rates are apparently uncoupled from the phenomena because the P that is trapped at the interface is ultimately released. Only under continual oxic conditions at the sediment–water interface (with no seasonal anoxia and the attendant P release) might the annual average release rate be significantly reduced. However, there is a likelihood of complete saturation of the oxic microzone (with respect to surface sites for P adsorption), which would ultimately result in uninhibited P diffusion from underlying anoxic sediments (cf. Gächter 1987). In such a case, oxic P release rates might approach the magnitude of those observed under anoxic conditions. These concepts may be of value in evaluating water quality management options such as hypolimnetic aeration.

Fig. 6. Chronology of measured sediment P release rates (R) and estimates of the seasonal variation of P release rates over an annual cycle. The bold line segments along the x-axis denote periods of winter and summer anoxia at the sediment–water interface. Solid squares indicate experimentally determined release rate values. The solid line denotes case 1: estimated annual average P release rate of 8.7 mg $P \cdot m^{-2} \cdot day^{-1}$. The broken line denotes modification for case 2: estimated annual average release rate of 9.7 mg $P \cdot m^{-2} \cdot day^{-1}$.

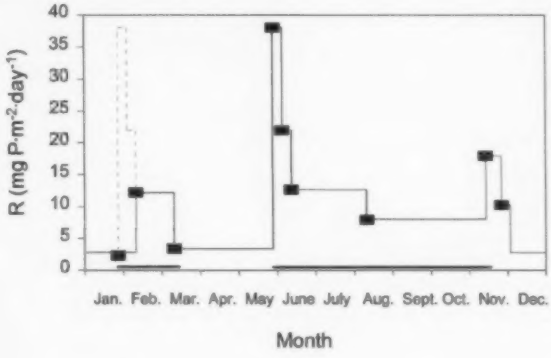

For Onondaga Lake, the calculated annual average P release rate occurring over the entire profundal plain results in an internal loading estimate of 73 kg $P \cdot day^{-1}$. Note that this is an upper-bound estimate based on P release rates from the sediments of the deepwater station. When added to the external loading of 320 kg $P \cdot day^{-1}$, a total P loading estimate of 393 kg $P \cdot day^{-1}$ is obtained for the lake, of which ~20% is due to sediment P release.

Acknowledgements

This research was funded under a cooperative agreement between the United States Environmental Protection Agency, Environmental Research Laboratory, Duluth, Minn., and Michigan Technological University (No. CR818513-01-0; Project Officer: E. Leonard). We thank B. Wagner, E. Haslam, J. Pauer, and R. Gelda for field and laboratory assistance and R. Schmitt for statistical analysis. We also thank

© 2000 NRC Canada

the reviewers and the editors for their contributions. This is contribution No. 159 of the Upstate Freshwater Institute.

References

American Public Health Association. 1985. Standard methods for the examination of water and wastewater. 16th ed. American Public Health Association, American Water Works Association, and Water Pollution Control Federation, Washington, D.C.

Auer, M.T., Johnson, N.A., Penn, M.R., and Effler, S.W. 1993. Measurement and verification of rates of sediment phosphorus release for a hypereutrophic urban lake. Hydrobiologia, **253**: 301–309.

Auer, M.T., Johnson, N.A., Penn, M.R., and Effler, S.W. 1996. Pollutant sources, depositional environment, and the surficial sediments of Onondaga Lake, New York. J. Environ. Qual. **25**: 46–55.

Boers, P.C.M. 1991. The influence of pH on phosphate release from lake sediments. Water Res. **25**: 309–311.

Boström, B., and Pettersson, K. 1982. Different patterns of phosphorus release from lake sediments in laboratory experiments. Hydrobiologia, **92**: 415–429.

Boström, B., Andersen, J.M., Fleischer, S., and Jansson, M. 1988. Exchange of phosphorus across the sediment–water interface. Hydrobiologia, **170**: 229–244.

Driscoll, C.T., Effler, S.W., Auer, M.T., Doerr, S.M., and Penn, M.R. 1993. Supply of phosphorus to the water column of a productive hardwater lake: controlling mechanisms and management considerations. Hydrobiologia, **253**: 61–72.

Eckert, W., Nishri, A., and Parparova, R. 1997. Factors regulating the flux of phosphate at the sediment–water interface of a subtropical calcareous lake: a simulation study with intact sediment cores. Water Air Soil Pollut. **99**: 401–409.

Effler, S.W., Field, S.D., Meyer, M.A., and Sze, P. 1981. Response of Onondaga Lake to restoration efforts. J. Environ. Eng. Div., ASCE, **107**: 191–210.

Effler, S.W., Brooks, C.M., Addess, J.M., Doerr, S.M., Storey, M.L., and Wagner, B. 1991. Pollutant loadings from Solvay wastebeds to lower Nine Mile Creek, New York. Water Air Soil Pollut. **55**: 427–444.

Einsele, W. 1936. Uber die Beziehungen des Eisenkreislaufs zum Phosphatkreislauf im eutrophen see. Arch. Hydrobiol. **29**: 664–686.

Enell, M., and Löfgren, S. 1988. Phosphorus in interstitial water: methods and dynamics. Hydrobiologia, **170**: 103–132.

Gächter, R. 1987. Lake restoration: why oxygenation and artificial mixing cannot substitute for a decrease in the external phosphorus loading. Schweiz. Z. Hydrol. **49**: 170–185.

Heidtke, T.M., and Auer, M.T. 1992. Partitioning phosphorus loads: implications for lake restoration. J. Water Resour. Planning Manage. Div., ASCE, **118**: 562–579.

Hieltjes, A.H.M., and Lijklema, L. 1980. Fractionation of inorganic phosphorus in calcareous sediments. J. Environ. Qual. **8**: 130–132.

Jensen, H., and Andersen, F. 1992. Importance of temperature, nitrate, and pH for phosphate release from aerobic sediments of four shallow, eutrophic lakes. Limnol. Oceanogr. **37**: 577–589.

Jørgensen, B.B. 1977. Distribution of colorless sulfur bacteria (*Beggiatoa* spp.) in a coastal marine sediment. Mar. Biol. **41**: 19–28.

Kamp-Nielsen, L. 1974. Mud–water exchange of phosphate and other ions in undisturbed sediment cores and factors affecting the exchange rates. Arch. Hydrobiol. **73**: 218–237.

Kamp-Nielsen, L. 1975*a*. Seasonal variation in sediment–water exchange of nutrient ions in Lake Esrom. Verh. Int. Ver. Limnol. **19**: 1057–1065.

Kamp-Nielsen, L. 1975*b*. A kinetic approach to the aerobic sediment–water exchange of phosphorus in Lake Esrom. Ecol. Model. **1**: 153–160.

Larsen, D.P., Schults, D.W., and Malereg, K.W. 1981. Summer internal phosphorus supplies in Shagawa Lake, Minnesota. Limnol. Oceanogr. **26**: 740–753.

Lijklema, L. 1980. Interaction of orthophosphate with iron(III) and aluminum hydroxides. Environ. Sci. Technol. **14**: 537–541.

Löfgren, S., and Boström, B. 1989. Interstitial water concentrations of phosphorus, iron and manganese in a shallow, eutrophic Swedish lake — implications for phosphorus cycling. Water Res. **23**: 1115–1125.

Mortimer, C.H. 1941. The exchange of dissolved substances between mud and water in lakes. Parts I and II. J. Ecol. **29**: 280–329.

Mortimer, C.H. 1942. The exchange of dissolved substances between mud and water in lakes. Parts III and IV. J. Ecol. **30**: 147–201.

Nürnberg, G.K. 1988. Prediction of phosphorus release rates from total and reductant soluble phosphorus in anoxic lake sediments. Can. J. Fish. Aquat. Sci. **45**: 453–462.

Ohle, W. 1937. Kolloidgele als Nahrstroffregulanten der Gewasser. Naturwissenschaften, **25**: 471–474.

Ostrofsky, M.L. 1987. Phosphorus species in the surficial sediments of lakes of eastern North America. Can. J. Fish. Aquat. Sci. **44**: 960–966.

Penn, M.R., and Auer, M.T. 1997. Seasonal variability in phosphorus speciation and deposition in a calcareous, eutrophic lake. Mar. Geol. **139**: 47–59.

Penn, M.R., Auer, M.T., Van Orman, E.L., and Korienek, J.J. 1995. Phosphorus diagenesis in lake sediments: investigations using fractionation techniques. Mar. Freshwater Res. **46**: 89–99.

Rossi, G., and Premazzi, G. 1991. Delay in lake recovery caused by internal loading. Water Res. **25**: 567–575.

Rowell, H.C. 1992. Paleolimnological indications of water quality in Onondaga Lake, New York. Ph.D. dissertation, College of Environmental Science and Forestry, State University of New York, Syracuse, N.Y.

Van Orman, E.L. 1993. Modeling sediment phosphorus release through analysis of sediment phosphorus profiles. M.S. thesis, Department of Civil and Environmental Engineering, Michigan Technological University, Houghton, Mich.

Vollenweider, R.A. 1975. Input–output models, with special reference to the phosphorus loading concept in limnology. Schweiz. Z. Hydrol. **37**: 53–84.

Welch, E.B., Spyridakis, D.E., Shuster, J.I., and Horner, R.R. 1986. Declining lake sediment phosphorus release and oxygen deficit following wastewater diversion. J. Water Pollut. Control Fed. **58**: 92–96.

Williams, J.D.H., and Mayer, T. 1972. Effects of sediment diagenesis and regeneration of phosphorus with special reference to Lakes Erie and Ontario. *In* Nutrients in natural waters. *Edited by* H.E. Allen and J.R. Kramer. Wiley Interscience, New York. pp. 281–315.

© 2000 NRC Canada

Patterns in fish species composition across the interface between streams and lakes

Theodore V. Willis and John J. Magnuson

Abstract: We compared fish species compositions among four site types (lake, lake mouth, stream mouth, stream) along the gradient from stream to lake for 12 tributary mouths. Comparison of species richness, rarefaction species diversity, and species density all supported the same pattern: stream-mouth sites contained the highest number of species, followed by stream sites, lake-mouth sites, and lake sites, even though lake and lake-mouth sites yielded more individuals and were larger in area and volume. Principal components analysis formed three clusters of mixed sites based on similarities in dominant fish species rather than designations of lake, lake mouth, etc. Rank order assemblage tests revealed that species composition of tributary-mouth sites was similar in only one quarter of the systems sampled; other systems showed a transition from "lake" to "stream" species compositions at or near the tributary mouth. Species assemblage comparisons within site types between systems revealed low consistency in the composition of stream-mouth sites and high consistency for the other site types. We concluded that the tributary mouth fits the definition of an ecotone and speculate that the difference in hydrologic and geomorphic properties of streams and lakes played a role in the patterns that we saw on either side of the tributary mouth.

Résumé : Nous avons comparé la composition spécifique des poissons entre quatre types de sites (lac, embouchure de lac, embouchure de cours d'eau, cours d'eau) le long d'un gradient allant du cours d'eau au lac pour 12 embouchures. La comparaison de la richesse spécifique, de la diminution de la diversité spécifique et de la densité des espèces ont révélé le même schéma : les embouchures de cours d'eau abritaient le plus grand nombre d'espèces, suivies par les cours d'eau, les embouchures de lac et les lacs, alors que les sites des lacs et des embouchures de lac présentaient un plus grand nombre d'individus et étaient supérieurs en superficie et en volume. L'analyse des composantes principales a fait ressortir trois grappes de sites mixtes en fonction des similarités dans les espèces dominantes plutôt qu'en fonction des types de site. Les tests d'assemblage ordinal ont révélé que la composition spécifique aux sites des embouchures était semblable dans seulement un quart des systèmes échantillonnés; les autres systèmes présentaient une transition des compositions spécifiques allant du « site de lac » au « site de cours d'eau » à l'embouchure ou à proximité. Les comparaisons des assemblages spécifiques du même type de site entre les systèmes ont révélé une faible cohérence dans la composition aux sites d'embouchure de cours d'eau, et une forte cohérence pour les autres types de site. Nous concluons que l'embouchure correspond à la définition de l'écotone, et posons que les différences dans les propriétés hydrologiques et géomorphologiques des cours d'eau et des lacs ont joué un rôle dans les schémas que nous avons observés de côté et d'autre de l'embouchure.

[Traduit par la Rédaction]

Introduction

Transitions in aquatic assemblages are pronounced where the convergence of two systems creates a definable boundary. Estuaries and oceanfronts where physically and chemically different water masses meet are well-documented examples (e.g., Brandt and Wadley 1981; Thiel et al. 1995). A less frequently studied transition zone, that which occurs between stream and lake, may also constitute an ecotone. Parameters measured at ecotones can be highly variable because ecotones are transitional regions between what are generally more homogenous habitats (Naiman 1988). Fluctuations in the extent and characteristics of an ecotone may change assemblage structure by facilitating the expansion of species into previously inaccessible or uninhabitable areas (e.g., Wiens et al. 1985; Risser 1995).

The tributary-mouth habitats that we studied share a number of parallels with riverine estuary systems. The mixing of water masses with different physical and chemical properties occurs in both systems and leads to deposition of organic matter and a gradient of mixing conditions (Leveau et al. 1990). In riverine estuary systems, fish species distribute along this gradient based on physical and chemical habitat features and feeding opportunities but tend to concentrate in abundance and diversity around the turbidity maxim (Grimes and Finucane 1991) where fresh and salt waters meet. Although differences in water between streams and lakes may be small, there are enough physical and chemical differences between the two for plumes to develop (T.V. Willis, personal observation). As in estuary systems, one might also expect species richness to be highest at the tributary mouth where lotic and lentic waters meet.

The diversity of fish species and their abundance in a hab-

Received May 20, 1999. Accepted January 4, 2000.
J15150

T.V. Willis[1] and J.J. Magnuson. Center for Limnology, University of Wisconsin–Madison, 680 North Park Street, Madison, WI 53706, U.S.A.

[1]Author to whom all correspondence should be addressed.
e-mail: tvwillis@students.wisc.edu

© 2000 NRC Canada

Fig. 1. Location of study lakes and streams in Vilas County, Wisconsin, U.S.A.

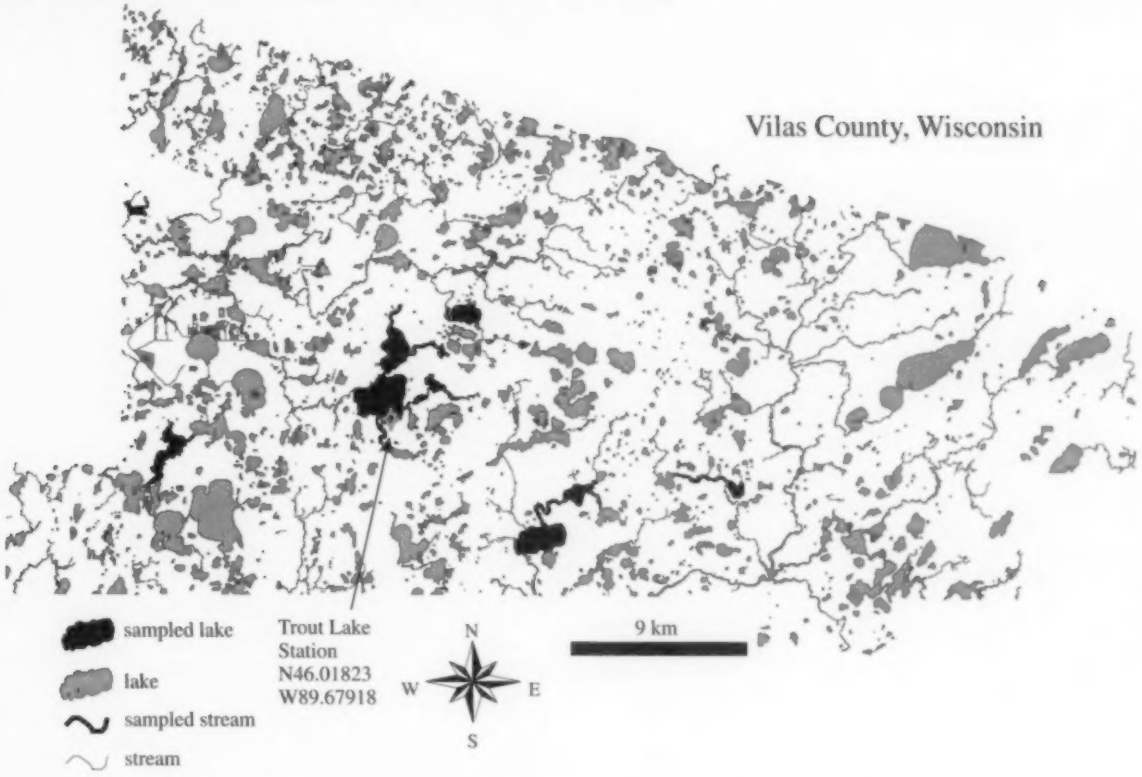

itat patch can be strongly influenced by neighboring habitats and the difficulties involved in crossing boundaries between habitats (e.g., Wiens et al. 1985; Schlosser 1995). The composition of the fish assemblage at the turbidity maxim in estuaries reflects the composition of the saltwater and freshwater assemblages that it separates, having more in common with either of those assemblages than with each other (Thiel et al. 1995). Similarly, we expect that species composition, the type and proportion of species, for the lake and stream samples would be more similar to the species composition of the intermediate tributary-mouth habitat than to each other.

The transition from stream to lake also parallels the transition from riffle to pool, from a relatively shallow, fast-flowing habitat to a relatively deep, slow-flowing habitat, i.e., from a more lotic to a more lentic habitat. In streams, pools tend to be occupied by more large-bodied fishes, including piscivores, whereas smaller fishes, such as darters and juveniles of many species, tend to occupy more shallow, less pool-like habitats. In the absence of large piscivores, cyprinids and other small-bodied fishes tend to be more abundant (Aadland 1993). Similar patterns could occur at the tributary mouth.

Physical constraints on what an individual fish can eat, including gape limitation and swimming ability, change over a species' life cycle. What a fish eats, along with how and where it captures those food items, are criteria for establishing foraging guilds. Because guilds integrate across species, they can be useful as analytical tools to include ontogenetic shifts in prey preference (Severinghaus 1981). These reorganizations can reveal clearer patterns in data than between-species comparisons of habitat use alone.

To review, we predicted that for a tributary mouth: (*i*) species richness, i.e., the median number of species, would be highest at the tributary mouth, (*ii*) some species would change their distribution along the stream–lake gradient, (*iii*) species composition of lake and stream sites would be more similar to the tributary-mouth species composition than to each other, and (*iv*) species distributions along the stream lake gradient would be clearer in the context of foraging guild distribution.

Materials and methods

Sample area

All sites were located in Vilas County, Wisconsin, U.S.A., in the Northern Highland Lake District. The district is an area of glacial till with over 1300 lakes. We sampled fish communities of 12 tributary-mouth systems, all of which were less than 20 m wide and 1 m or less in depth (Fig. 1). Lakes ranged from 90 to 1544 ha, and streams ranged from 1.6 to 9.4 km in length.

The tributary systems were Allequash, Found, Allequash Spring, North, Stevenson, White Sand, Big St. Germain, Boot, Circle Lilly, Lost, Mann, and Pokegema. Each tributary system consisted of four site types: a lake site, a lake-mouth site, a stream-mouth site, and a stream site (Fig. 2). The tributary mouth consisted of the lake-mouth and stream-mouth sites separated by an imaginary line

© 2000 NRC Canada

Fig. 2. Tributary system schematic with site locations relative to the tributary mouth along with mean distances to the lake and stream sites.

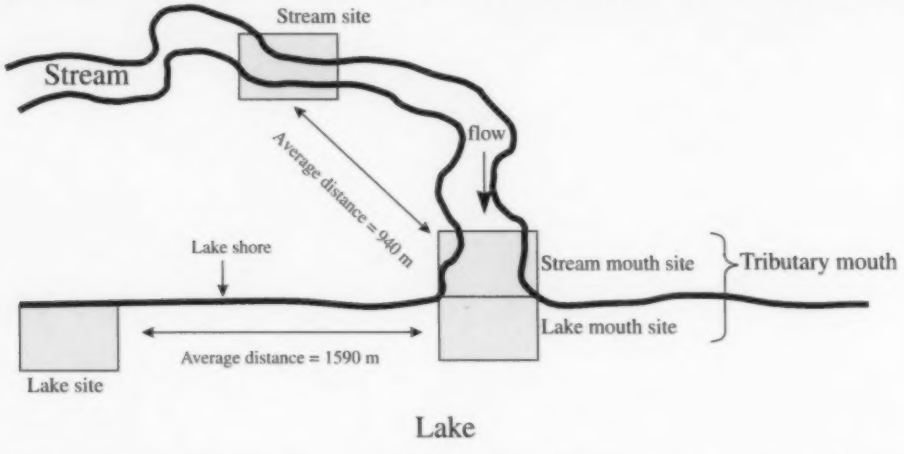

corresponding to the continuance of lake shoreline across the stream mouth. Lake and lake-mouth and stream and stream-mouth sites were chosen to be similar in water depth, substrate, vegetation type, and vegetation density. The lake and lake-mouth sites were 20 m on a side and averaged 404 and 441 m^2, respectively. The stream and stream-mouth sites were 20 m long by the wetted stream width and had an average area of 160 and 154 m^2, respectively.

We chose the size of our sample areas based on the extent of our focal sample sites, the lake mouth and stream mouth. The design of the lake-mouth site was to encircle the stream plume, excluding littoral zone not obviously affected by the plume. Lake sites were established to match lake-mouth sites in area. The 400-m^2 sample areas were designed to limit flight from the center of our sample area by increasing the ratio of sampled volume to edge. Dimensions of the stream-mouth sites were designed to sample the stream where it most directly contacted the lake. The 20-m length of both the stream and stream-mouth sites matched the length of the lake and lake-mouth sites.

Sampling methods

Sampling occurred between June 23 and August 23, 1997. Block nets (4-mm mesh) were employed at all sites to prevent fish from leaving the discrete sample areas. Lake and lake-mouth sites were block-netted from shore; stream and stream-mouth sites were block-netted at the upstream and downstream edges of the sites. Block nets were successful in containing fish once sampling commenced, although they were not 100% effective. We electrofished the 12 inlet tributary systems with a Smith-Root GPP 2.5 electrofishing unit or a Smith-Root dry cell backpack electrofisher. Electrofishing continued until the catch rate dropped appreciably. Captured fish were identified to species, measured for total length, and then returned to the site where they were caught.

Habitat data were collected on water speed, substrate complexity (dominant substrate type, number of substrate types, and substrate percent composition), percent vegetative cover, pH, and conductivity. We collected additional data in July 1998 on stream cross section at the top and bottom of stream and stream-mouth sites, depth at 5-m intervals in lake and lake-mouth sites, and distance between sites in the same system. See Willis (1999) for the complete data set.

One flow measurement was taken in the center of the stream and stream-mouth sites using the procedures outlined in Schlosser (1982). Three timed trials of a float moving a distance of 2 m in the plume were averaged for water speed in lake-mouth sites. A General Oceanic, OceanTech model 2031HR6 flowmeter with low-velocity impeller was used to calibrate flow measurements from the sampled sites. Littoral zone currents were not measured and were assigned a water speed of zero.

Three random tosses of a 0.5 × 0.5 m quadrat were used to characterize the substrate in a site. Substrate inside the quadrat was recorded as the percentage of silt, sand, gravel, rock, and boulder using the size categories in Schlosser (1982). Vegetative cover was determined as the mean percentage of the quadrat covered by vegetation. Water samples for conductivity and pH were collected also.

Analyses

We used four techniques to evaluate patterns in the number of species and species density along the stream–lake gradient. The first was a comparison of the median number of species. The second was a rarefaction technique using the Ecosim species diversity module (e.g., Gotelli and Graves 1996; Gotelli and Entsminger 1999). To facilitate direct comparison between lake and stream sites, we converted raw catch numbers to measures of species density using sample area (third method) and volume conversion (fourth method). The volumetric correction accounted for distinctions between lotic and lentic habitat and differences in individual habitat character from site to site. Volumetric, areal, and uncorrected values were $\log(x + 1)$ transformed to obtain normal distributions for some analyses.

Analyses using absolute abundance, rank order abundance, and presence–absence data are all affected differently by extensive zeros in the data set (Rahel 1984). Ordination analyses are also sensitive to zeros (Sharma 1996). We created a "common" species list to eliminate "rare" species, defining rare as species that either appeared in a low proportion of sites or were isolated individuals found in a number of sites. The common species list consisted of a homogenized species list from all four site types in which 90% of the total numerical catch per site type was included, starting with the most abundant species (Willis 1999). This list was used for rank order and principal components analyses.

We used foraging guilds to analyze the full data set, which included rare taxa, and accounted for ontogenetic shifts in forage preference. Assignments to foraging guilds were based on Becker (1983) and Schlosser (1982) and length data collected in the field. The five guilds were benthic insectivore, drift insectivore, piscivore, herbivore, and zooplanktivore. Given the variable feeding habits of most fish, these guilds are intended as an approximation of preferred prey.

All analyses were performed using SYSTAT (Wilkinson 1997). Tukey's post hoc test (Sokal and Rohlf 1995) was used to test for

© 2000 NRC Canada

Table 1. Total species list.

	Lake	Lake mouth	Stream mouth	Stream
Common species				
Finescale dace (*Phoxinus neogaeus*)			×	×
Central mudminnow (*Umbra limi*)			×	×
Brook stickleback (*Culaea inconstans*)			×	×
Blacknose dace (*Rhinichthys atratulus*)		×	×	×
Blacknose shiner (*Notropis heterolepis*)		×	×	×
Hornyhead chub (*Nocomis biguttatus*)		×	×	×
Northern redbelly dace (*Phoxinus eos*)		×	×	×
Rosyface shiner (*Notropis rubellus*)		×	×	×
Bluegill (*Lepomis macrochirus*)	×	×	×	×
Bluntnose minnow (*Pimephales notatus*)	×	×	×	×
Common shiner (*Luxilus cornutus*)	×	×	×	×
Creek chub (*Semotilus atromaculatus*)	×	×	×	×
Iowa darter (*Etheostoma exile*)	×	×	×	×
Johnny darter (*Etheostoma nigrum*)	×	×	×	×
Largemouth bass (*Micropterus salmoides*)	×	×	×	×
Rock bass (*Ambloplites rupestris*)	×	×	×	×
Mottled sculpin (*Cottus bairdi*)	×	×	×	×
White sucker (*Catostomus commersoni*)	×	×	×	×
Yellow perch (*Perca flavescens*)	×	×	×	×
Fantail darter (*Etheostoma flabellare*)	×	×	×	
Golden shiner (*Notemigonus crysoleucas*)	×	×	×	
Mimic shiner (*Notropis volucellus*)	×	×	×	
Smallmouth bass (*Micropterus dolomieu*)	×	×	×	
Rare species				
Pearl dace (*Semotilus margarita*)				×
Brook trout (*Salvelinus fontinalis*)				×
Black bullhead (*Ameiurus melas*)			×	
Blackchin shiner (*Notropis heterodon*)			×	
Burbot (*Lota lota*)	×		×	
Esox sp.	×	×	×	×
Logperch (*Percina caprodes*)	×	×	×	×
Pumpkinseed (*Lepomis gibbosus*)	×	×	×	×
Walleye (*Stizostedion vitreum*)		×	×	
Yellow bullhead (*Ameiurus natalis*)			×	×
Black crappie (*Pomoxis nigromaculatus*)	×			×
Muskellunge (*Esox masquinongy*)	×			

Note: Species are categorized as "common" (see text) and "rare" (excluded from the analyses described in the text).

significant differences between means. Stepwise linear regression was used as a data reduction technique, along with a test of the most robust general linear model, the model that explained the most variance with the fewest variables, following Draper and Smith (1981). Kendall's tau rank order coefficient (Sokal and Rohlf 1995) was used to evaluate similarity between any two assemblages, and Kendall's coefficient of concordance was used to evaluate similarity between more than two assemblages. Principal components analysis (Sharma 1996) was used to organize individual sites by commonalties in their assemblages.

Results

Species richness and density

A total of 35 species were caught, 23 of which were included in the analyses (Table 1). Median species richness (Fig. 3*a*) in the lake was significantly lower than in the stream mouth (Tukey's post hoc: $p < 0.05$, $n = 12$). Analysis of species diversity using rarefaction revealed that the relationships between site types, lake < lake mouth < stream << stream mouth, were consistent over 100 random sampling simulations of 1–400 individuals (Fig. 3*b*). Lake sites had the fewest total number of species, and stream-mouth sites had the highest total number of species; these were significant relationships given 95% confidence interval curves bracketing the rarefaction curves. Stepwise linear regression of species richness against habitat variables identified site type and sample area (square metres) as weak predictors of log species richness ($r^2 = 0.23$, $p < 0.05$, $n = 48$). The most robust linear model consisted only of site type ($r^2 = 0.19$, $p < 0.05$, $n = 48$). Species density (log x·100 m^{-2}), like species richness, was highest in the stream mouth (Fig. 3*c*). Species density in the lake and lake mouth was lower than in the stream and stream mouth (Tukey's post hoc: $p < 0.001$, $n = 12$). Site type was the best explanatory variable of log species density ($r^2 = 0.72$, $p < 0.001$, $n = 48$).

Correcting species richness for the volume of sampled

© 2000 NRC Canada

Fig. 3. Patterns in the diversity of species (common plus rare) compared between site types. (*a*) Number of species; (*b*) rarefaction species diversity curves generated from Ecosim modeling results; broken lines correspond to 95% confidence intervals; (*c*) log areal species density; (*d*) log volumetric species density. Lines within box plots represent the median, boxes represents the 25th and 75th percentiles, whiskers represent the 10th and 90th percentiles, and points are outliers.

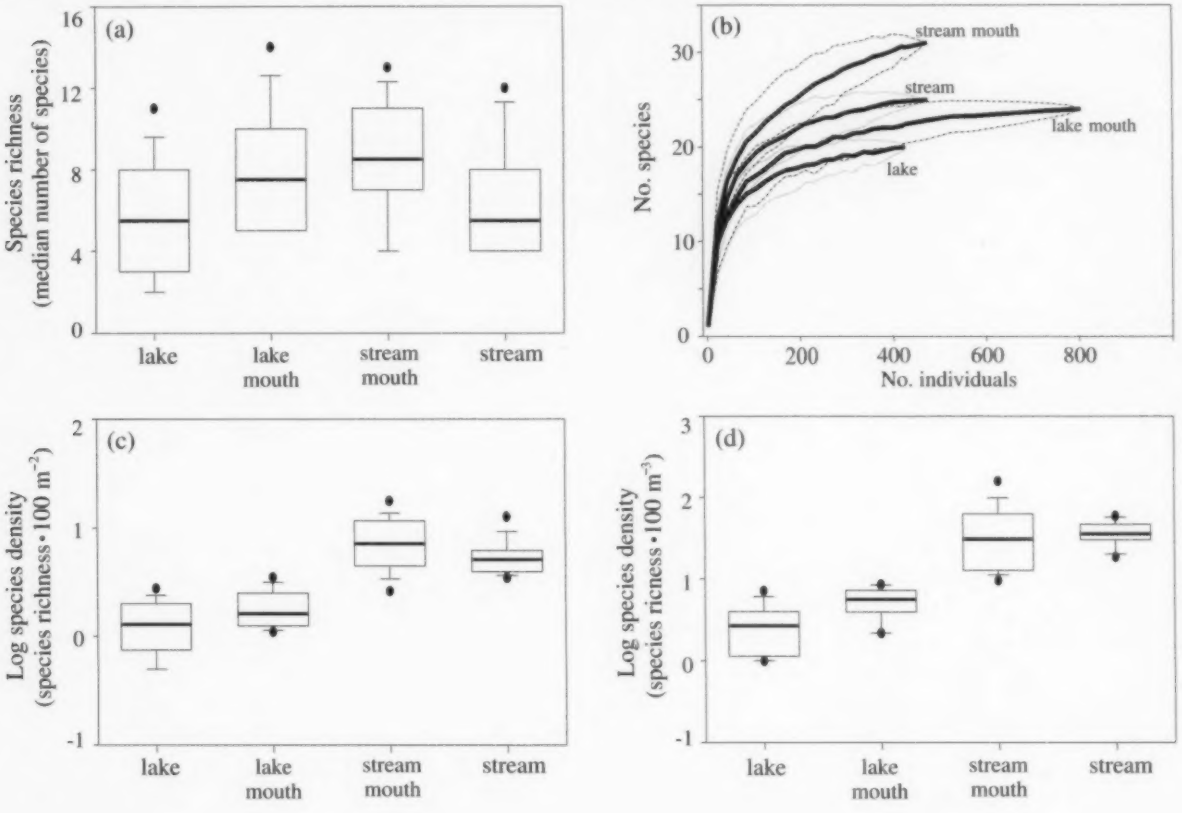

habitats revealed an increase in species density from lake to stream (Fig. 3*d*). Mean differences in species density were significant between lake and lake mouth (Tukey's post hoc: $p < 0.05$, $n = 12$) and between lake mouth and stream mouth (Tukey's post hoc: $p < 0.001$, $n = 12$). Site type was still the best explanatory variable of species density ($r^2 = 0.76$, $p < 0.001$, $n = 48$).

Species composition

The seven species in Fig. 4*a* are a compilation of the three most abundant species from each site type. Densities of some species decreased (mimic shiner and yellow perch) (see Table 1 for scientific names) with distance from the lake end of the gradient, whereas the density of other species increased (creek chub). Only creek chub showed a statistically significant increase in relative density along the gradient from lake to stream (Tukey's post hoc: $p < 0.01$, $n = 12$).

We used stepwise linear regression to identify mechanisms that might explain the uneven distribution of species across sites. Site type was included in the first step model and excluded from the second (Table 2) to isolate habitat effects from position in the gradient. Site type and water speed explained 42% of the variation in creek chub distribution. No other model explained more than 25% of the variation in species distribution.

The percent contribution of foraging guilds was not uniform along the stream–lake gradient. Drift insectivores were less abundant in the lake and lake-mouth sites than they were in the stream and stream-mouth sites (Fig. 4*b*). Conversely, zooplanktivores were more abundant in the lake and lake-mouth sites than in the other sites. Benthic insectivore contribution to the catch of all four site types was relatively uniform. Drift insectivore, zooplanktivore, and benthic insectivore abundances were similar to each other in the stream mouth. Piscivore and herbivore catches were low, but their abundances were highest in the stream site.

Three of four across-system comparisons of species composition in sites resulted in statistically significant Kendall's coefficient of concordance for assemblage similarity. Lake-mouth sites among the different lakes had the highest coefficient of concordance and thus the most similar assemblages (44.3) ($p < 0.005$). Stream-mouth sites did not have a statistically significant coefficient of concordance, so the 12 assemblages varied in their most dominant species or overall

© 2000 NRC Canada

Fig. 4. Contribution of the seven most abundant species and foraging guilds shown as a proportion of the total catch for site types and principal components clusters. The *x*-axis species and guild categories are oriented from left to right on a gradient from lake to stream. Plots correspond to proportional fish density of (*a*) species by site type, (*b*) guild by site type, (*c*) species by cluster, and (*d*) guild by cluster. Figures 4*a* and 4*b*: solid, lake sites; cross-hatched, lake-mouth sites; shaded, stream-mouth sites; open, stream sites. Figures 4*c* and 4*d*: solid, mimic cluster; cross-hatched, percid cluster; shaded, chub cluster. MS, mimic shiner; YP, yellow perch; JD, johnny darter; BM, bluntnose minnow; LB, largemouth bass; WS, white sucker; CC, creek chub; Zoop, zooplanktivore; Pisc, piscivore; Herb, herbivore; D.I., drift insectivore; B.I., benthic insectivore.

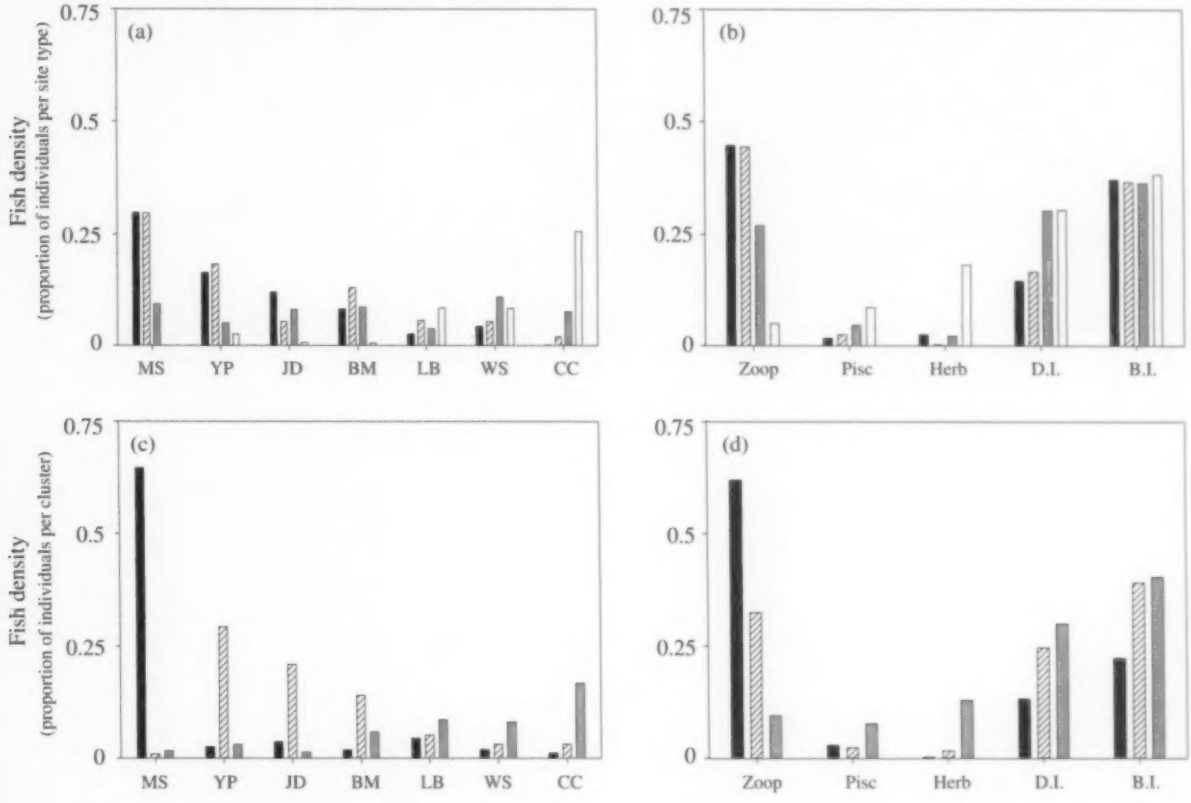

Table 2. Statistically significant stepwise linear regression results for the seven most abundant species (log number of individuals per 100 m^3 regressed against habitat variables).

	With site type		Without site type	
Bluntnose minnow	Temperature	$p > 0.005$	Temperature	$p > 0.005$
	Water speed	$r^2 = 0.25$	Water speed	$r^2 = 0.25$
Creek chub	Site type	$p > 0.001$	pH	$p > 0.005$
	Water speed	$r^2 = 0.42$		$r^2 = 0.17$
Johnny darter	Temperature	$p > 0.05$	Temperature	$p > 0.05$
		$r^2 = 0.2$		$r^2 = 0.2$
Largemouth bass	None		None	
Mimic shiner	Substrate	$p > 0.002$	Substrate	$p > 0.002$
		$r^2 = 0.2$		$r^2 = 0.2$
White sucker	Site type	$p > 0.005$	pH	$p > 0.05$
		$r^2 = 0.17$		$r^2 = 0.1$
Yellow perch	Substrate	$p > 0.02$	Substrate	$p > 0.02$
		$r^2 = 0.12$		$r^2 = 0.12$

Note: Analyses conducted with and without site type in the regression model; $n = 48$.

© 2000 NRC Canada

Table 3. Similarity coefficients of species composition between pairings of site types using Kendall's tau rank order coefficient.

		Lake – lake mouth	Lake mouth – stream mouth	Stream mouth – stream	Lake–stream
a	Allequash	0.38	0.79	0.06	–0.17
	Big St. Germain	0.57	0.62	0.28	0.17
	Boot	0.63	0.52	–0.01	0.01
	Found	0.35	0.43	0.10	0.30
b	Lost	0.60	0.03	0.32	0.01
	North	0.39	0.05	0.70	–0.17
	Stevenson	0.41	–0.21	0.35	–0.28
	White Sand	0.46	–0.01	0.31	0.19
c	Allequash Spring	–0.15	0.15	0.42	–0.09
d	Circle Lilly	0.61	0.17	0.20	0.03
	Mann	0.40	0.18	0.03	–0.25
	Pokegema	0.51	0.18	0.05	–0.10

Note: A significant correlation coefficient ($p < 0.05 = 0.3$, $p < 0.01 = 0.4$, $n = 23$) was interpreted as paired species compositions having more species in common than expected by chance alone. Shaded cells correspond to statistically similar paired species compositions. Letters correspond to the diagrams in Fig. 5. Rare taxa were not included in this analysis.

Fig. 5. Five main patterns in species composition for tributary-mouth systems based on Kendall's tau rank order coefficients (Table 3). Transitions in species composition between sites are represented by changes in shading and correspond to assemblages in adjacent sites not sharing a significant number of species. Patterns included one transition in species composition either (*a*) upstream of the tributary mouth or (*b*) between the stream and stream mouth; two transitions in species composition (*c*) downstream of the stream mouth or (*d*) upstream of the lake mouth. See Table 3 for specific systems that exhibit the described patterns.

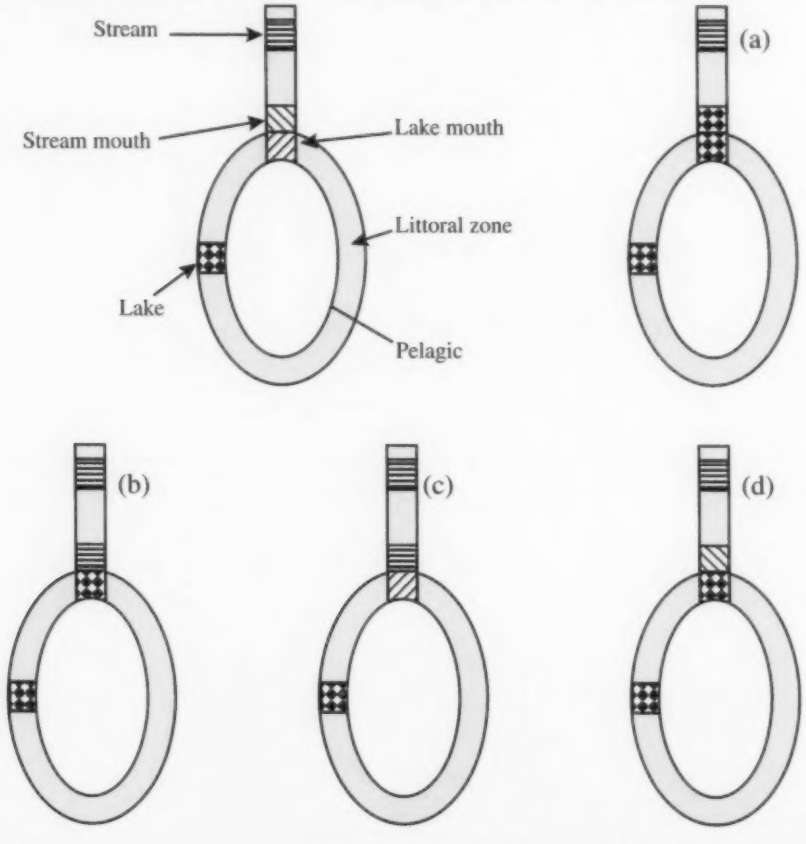

species composition. Stream and lake sites were intermediate in assemblage similarity, with coefficients of 34.6 ($p < 0.05$) and 40.4 ($p < 0.025$), respectively.

Our sampling sites represented discrete areas along the stream–lake gradient. We compared the species composition in adjacent sites, labeling dissimilarities as transitions from a more "stream-like" to a more "lake-like" assemblage, or vice versa. A transition in species composition corresponded

© 2000 NRC Canada

Fig. 6. Principal components ordination of individual sites based on species abundance. Component 1 accounted for 27.8% of the variation in the data and component 2 for an additional 16.1%. Rare taxa were removed prior to analysis. ●, lake sites; ○, lake-mouth sites; ▼, stream mouth sites; ▽, stream sites; $n = 48$.

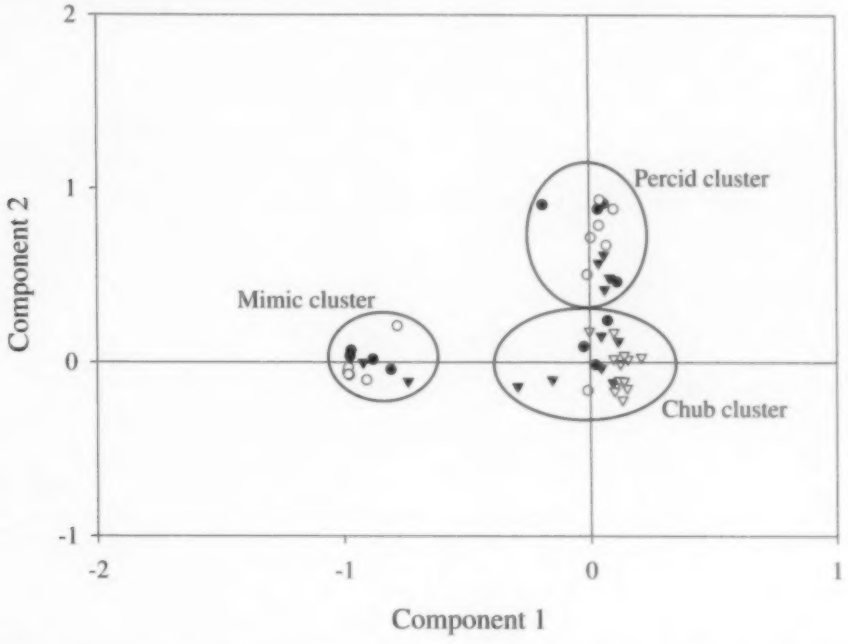

to adjacent sites within a system not sharing a significant number of species according to Kendall's tau rank order test. Stream sites were compared with stream-mouth sites, stream-mouth sites with stream and lake-mouth sites, lake-mouth sites with stream-mouth and lake sites, and lake sites with lake-mouth sites. Only four of the 12 assemblages shared similar assemblages between the stream mouth and lake mouth (Table 3). We found a single assemblage transition between stream and stream-mouth in three systems (Allequash, Big St. Germain, and Found) (Fig. 5*a*). There was a single assemblage transition between stream mouth and lake mouth in four systems (Lost, North, Stevenson, and White Sand) (Fig. 5*b*). We found assemblage transitions in Allequash Spring between the stream mouth and lake mouth and between the lake mouth and lake (Fig. 5*c*). Three systems (Circle Lilly, Pokegema, and Mann) had assemblage transitions between stream and stream mouth and stream mouth and lake mouth (Fig. 5*d*).

Site classification

Principal components analysis of a species' density by site matrix ordinated samples along 12 axes. Of these axes, the first two accounted for a cumulative 38% of the variation in the data and produced three clusters (Fig. 6). The data did not cluster according to site type, but rather the four dominant species. The clusters also corresponded roughly to foraging guilds (Fig. 4*c*). The mimic cluster corresponded generally to the lake and lake-mouth samples and was dominated by zooplanktivorous fishes, especially mimic shiner. The percid cluster corresponded generally to the lake-mouth and stream-mouth samples and had a high percentage of benthic insectivores, including yellow perch and johnny darter. The chub cluster generally corresponded to the stream samples and was dominated by drift and benthic insectivores, with a high percentage of creek chub. Reorganizing the data to match the clusters from the principal components analysis reveals a reciprocal pattern in abundance between zooplanktivores and drift and benthic insectivores (Fig. 4*d*); drift and benthic insectivores are more abundant in sites where zooplanktivores are less abundant.

Discussion

Species richness and density

Habitats that fit the definition of "ecotone" most often occur as the transitional region between two dissimilar ecological systems (Kolasa and Zalewski 1995). This boundary region needs to exhibit a change in diversity and alteration of physical and biological processes to qualify under the generally accepted definition of an ecotone (di Castri et al. 1988). Given the findings of this study, we believe that tributary-mouth systems exhibit these qualities.

We found a consistent pattern in both the numbers of species and species densities between our sites along the stream–lake gradient. For all four methods, median number of species, rarefaction simulation analysis, aerial species density, and volumetric species density, the stream mouth had the highest values, followed by the stream, lake mouth, and lake. We did not see an increase in species with an increase in stream habitat volume, as documented by Mendelson (1975). Median species diversity was highest at the stream mouth. The number of individuals caught did not appear to affect the species patterns along the stream–lake gradient, especially for the lake mouth. Adjusting the me-

© 2000 NRC Canada

dian species diversity by habitat area and volume strengthened the pattern seen along the stream–lake gradient.

Foraging potential in the stream and stream-mouth sites may be sufficient to support more biomass and diversity than the other sites. Lotic systems have higher per unit area production than lakes and should be capable of supporting a greater relative density of the same organisms (Minns 1995). In lotic systems, benthic production is further augmented by the delivery of food and nutrients from upstream reaches (Schlosser 1998). Drift expands the productivity that stream fish can exploit beyond their immediate surroundings. Without the downstream transport of terrestrial and aquatic prey, lake fish may find it necessary to cover larger areas to achieve the same potential food intake.

Streams and lakes influence each other's species density by providing secondary habitat for some species. Secondary habitat provides a refuge when conditions in the primary habitat are less than optimal (Schlosser 1995). Exposed shorelines disturbed by wave action and stream edges that experience significant reductions in flow can foster the establishment of overlap communities, where traditional lake and stream species coexist (Samways and Stewart 1997).

Species composition

Both assemblage and abundance changed dramatically in the 40 m that we designated as the tributary mouth. Most of the systems sampled exhibited more commonality in assemblage between the lake and lake-mouth sites, which were separated by 500 m or more of littoral zone habitat, than the adjacent lake-mouth and stream-mouth sites.

Species composition varied not only between tributary-mouth sites in a single system, but also between stream-mouth sites across all sampled systems. Opportunistic colonization and recolonization may dictate species composition in the lake mouth and stream mouth. In systems where alternating harsh and benign conditions are frequent, species composition may shift continually as opportunists immigrate and emigrate with ambient conditions (Angermeier and Schlosser 1989). Something as chaotic as day-to-day weather conditions may affect the tributary-mouth assemblage by altering the character of the tributary mouth to something more stream-like or lake-like. The corridor function of the tributary mouth, especially during the spawning season, may also mask any predictable site-to-site species composition.

Habitat complexity in streams (Gorman and Karr 1978) and lakes (Weaver et al. 1997) influences fish species composition. At the ecotone between stream and lake, drift insectivore and zooplanktivore feeding strategies are more reliant on favorable hydraulic conditions than are benthic insectivore feeding strategies. Fish that forage primarily on benthic invertebrates should be able to find a wide variety of prey, regardless of flow. Zooplanktivores depend on low-flow conditions because zooplankton are vulnerable to advection in habitats with more lotic characteristics (Pace et al. 1992). These conditions characterize lake and, to a lesser extent, lake-mouth habitats. Conversely, drift insectivores rely on moving water in stream and stream-mouth habitats to deliver their invertebrate and fish prey. Nearly equal percentages of benthic insectivores, drift insectivores, and zooplanktivores in the stream-mouth sites suggest that conditions suitable, if not favorable, for all three foraging types exist in this heterogeneous habitat.

The interaction of abiotic and biotic habitat elements may play a role in determining species composition at and around the tributary mouth. Patterns like those seen in Fig. 5 may be the result of fish biology interacting with varying physical templates. Emigration of certain species from habitats where they are at risk is documented in both lakes (He and Kitchell 1990) and streams (Snodgrass and Meffe 1998). Larger bodied fishes are more vulnerable to predation by avian (Power 1984) and terrestrial predators (Schlosser 1987) and may not be as mobile in shallow or high-flow habitats. Transitions from deep to shallow habitats may prevent some species, like large piscivores, from crossing the ecotone between stream and lake, creating a refuge for other species. Emigration and immigration into the stream mouth as a response to physical conditions (weather patterns, differences in water temperature, etc.), predation, and (or) prey may explain the high variation in stream-mouth species composition.

Site classification

Ordination by species revealed an organization that corresponded loosely to forage guilds rather than site type. Our designation of site types based on physical criteria may not have corresponded to criteria that our biotic indicators (captured fish) used in their habitat choice. The foraging strategy most represented in a sample site could be a better descriptor of lotic or lentic for that site. Microhabitat use and fish morphology are correlated (Wood and Bain 1995). Certain morphological features correspond to the autecology of species, like subterminal mouths for species that feed on the benthos. The best approach to classifying sites, and thus the likely species composition, may be to determine the foraging strategy that would most benefit from the hydrologic and geomorphic conditions there at the time of sampling.

The mimic cluster consisted mostly of lake and lake-mouth sites where water speeds and wave action tended to be low enough for small planktonic organisms to persist in the littoral zone and on the margins of the plume emerging from the stream. This cluster aggregated sites where zooplanktivores, like mimic shiners (e.g., Schlosser 1982; Becker 1983), were abundant and zooplanktivory was likely to be a successful foraging strategy.

Sites in the percid cluster appealed almost equally to drift insectivores, benthic insectivores, and zooplanktivores in similar abundances and appeared to support a generalist approach to foraging. Most sites in this cluster were tributary-mouth sites with a mixture of conditions and foraging opportunities in a small area. The sites in this cluster differ from those found in the mimic and chub clusters based on a more diverse species assemblage. Slowing water speed along the plume edge, wind-induced backups of water into the stream mouth, and wave action would result in different deposition rates of organic material in the tributary mouth. A bottom-up trophic interaction related to the deposition of organic material around the plume would enhance the number and diversity of aquatic invertebrates in the tributary mouth and benefit fishes that feed on these organisms. Johnny darter and 1+-year-old yellow perch, the major taxa in this group, tend to feed on benthic insects (e.g., Schlosser 1982; Becker 1983), but young-of-the-year yellow perch are zoo-

© 2000 NRC Canada

planktivorous. Fish like bluntnose minnow, which were also prevalent in this group, feed on both benthic insects and zooplankton.

The chub cluster of sites, mostly stream sites, provided the least foraging potential for zooplanktivorous fishes but the most foraging potential for drift insectivores. The benefits from feeding on invertebrate drift increase upstream from standing water (Schlosser 1998). Stream reaches concentrate drift more than the lake mouth, and small pools in the stream provide areas where consumption of drift can be maximized and predation risk minimized. Creek chub are general insectivores that eat benthic insects but also take advantage of stream drift fauna (e.g., Schlosser 1982; Becker 1983). They are soft-rayed fish that would probably be at risk in large-volume habitats with large piscivores.

In conclusion, our analysis revealed a strong pattern in the diversity of fish species and their assemblage structure across the ecotone between stream and lake. Although this study represents conditions from single summer samplings, or "snapshots," and does not capture the seasonal dynamics of fish in aquatic systems, we still discovered a consistent pattern. Species number and density were greatest at the stream mouth and decreased in order from stream to lake mouth to lake. Although our sample sites were too small to estimate diversity for an entire reach or lake, they did give us a basis for comparison between habitat patches. We saw patterns in foraging guild and assemblage distribution along the gradient from stream to lake, with a mixture of fish at the ecotone representing zooplanktivores, drift insectivores, and benthic insectivores. The nature of productivity and food availability between streams and lakes may explain the increase in species density that we saw across the tributary mouth and the diversity of feeding strategies at the ecotone. An indicator of a more dominant lotic or lentic character to the tributary mouth may be the mix of taxa found there and the foraging strategy that those fish generally favor.

Acknowledgements

We thank the students at the Center for Limnology, University of Wisconsin-Madison, for their suggestions on project design and various versions of this manuscript. We thank the staff at the Center for Limnology and the Trout Lake Biological Station for providing logistical support and access to equipment and field sites, along with Jim Kitchell and Carl Bowser for their help at various stages of this project. We also thank Jurek Kolasa and Ike Schlosser for their suggestions towards improving this manuscript in the review process. This study was supported by monies from a Graduate Research Traineeship grant (NSF GER9454162), a Long Term Ecological Research grant (NSF DEB9632853), a University of Wisconsin Advanced Opportunity Fellowship, and the Anna Grant Birge Memorial Fund. This work was completed as a part of the requirements for the degree Master of Science at the Center for Limnology.

References

Aadland, L.P. 1993. Stream habitat types: their fish assemblages and relationship to flow. N. Am. J. Fish. Manage. **13**: 790–806.

Angermeier, P.L., and Schlosser, I.J. 1989. Species–area relationships for stream fishes. Ecology, **70**: 1450–1462.

Becker, G.C. 1983. Fishes of Wisconsin. University of Wisconsin Press, Madison, Wis.

Brandt, S.B., and Wadley, V.A. 981. Thermal fronts as ecotones and zoogeographic barriers in marine and freshwater systems. Proc. Ecol. Soc. Aust. **11**: 13–26.

di Castri, F., Hansen, A.J., and Holland, M.M. (*Editors*). 1988. A new look at ecotones: emerging international projects on landscape boundaries. Biol. Int. Spec. Issue, **17**.

Draper, N.R., and Smith, H. 1981. Applied regression analysis. 2nd ed. John Wiley & Sons, Inc., New York.

Gorman, O.T., and Karr, J.R. 1978. Habitat structure and stream fish communities. Ecology, **59**: 507–515.

Gotelli, N.J., and Entsminger, G.L. 1999. EcoSim: null models software for ecology. Version 4.0. Acquired Intelligence Inc., and Kesey-Bear (http://homepages.together.net/~gentsmin/ecosim.htm).

Gotelli, N.J., and Graves, G.R. 1996. Null models in ecology. Smithsonian Institution Press, Washington, D.C.

Grimes, C.B., and Finucane, J.H. 1991. Spatial distribution and abundance of larval and juvenile fish, chlorophyll and macrozooplankton around the Mississippi River discharge plume, and the role of the plume in fish recruitment. Mar. Ecol. Prog. Ser. **75**: 109–119.

He, X., and Kitchell, J.F. 1990. Direct and indirect effects of predation on a fish community: a whole-lake experiment. Trans. Am. Fish. Soc. **119**: 825–835.

Kolasa, J., and Zalewski, M. 1995. Notes on ecotone attributes and functions. Hydrobiologia, **303**: 1–7.

Leveau, M., Lochet, F., Goutx, M., and Blanc, F. 1990. Effects of a plume front on the distribution of inorganic and organic matter off the Rhone River. Hydrobiologia, **207**: 87–93.

Mendelson, J. 1975. Feeding relationships among species of *Notropis* (Pisces: Cyprinidae) in a Wisconsin stream. Ecol. Monogr. **45**: 199–230.

Minns, C.K 1995. Allometry of home range size in lake and river fishes. Can. J. Fish. Aquat. Sci. **52**: 1499–1508.

Naiman, R.J. 1988. The potential importance of boundaries to fluvial ecosystems. J. North Am. Benthol. Soc. **7**: 289–306.

Pace, M.L., Findlay, S.E.G., and Lints, D. 1992. Zooplankton in advective environments: the Hudson River community and a comparative analysis. Can. J. Fish. Aquat. Sci. **49**: 1060–1069.

Power, M.E. 1984. Depth distribution of armored catfish: predator induced resource avoidance? Ecology, **65**: 523–528.

Rahel, F.J. 1984. Factors structuring fish assemblages along a bog lake successional gradient. Ecology, **65**: 1276–1289.

Risser, P.G. 1995. The status of the science of examining ecotones. BioScience, **45**: 318–352.

Samways, M.J., and Stewart, D.A.B. 1997. An aquatic ecotone and its significance in conservation. Biodivers. Conserv. **6**: 1429–1444.

Schlosser, I.J. 1982. Fish community structure and function along two habitat gradients in a headwater stream. Ecol. Monogr. **52**: 395–414.

Schlosser, I.J. 1987. The role of predation in age- and size-related habitat use by stream fishes. Ecology, **68**: 651–659.

Schlosser, I.J. 1995. Critical landscape attributes that influence fish population dynamics in headwater streams. Hydrobiologia, **303**: 71–81.

Schlosser, I.J. 1998. Fish recruitment, dispersal, and trophic interactions in a heterogeneous lotic environment. Oecologia, **113**: 260–268.

Severinghaus, W.D. 1981. Guild theory development as a mechanism for assessing environmental impact. Environ. Manage. **5**: 187–190.

© 2000 NRC Canada

Sharma, S. 1996. Applied multivariate techniques. 1st ed. John Wiley & Sons, Inc., New York.

Snodgrass, J.W., and Meffe, G.K. 1998. Influence of beavers on stream fish assemblages: effects of pond age and watershed position. Ecology, **79**: 928–942.

Sokal, R.R., and Rohlf, F.J. 1995. Biometry. 3rd ed. W.H. Freeman and Co., New York.

Thiel, R., Sepulveda, A., Kafeman, R., and Nellen, W. 1995. Environmental factors as forces structuring the fish community of the Elbe Estuary. J. Fish Biol. **46**: 47–69.

Weaver, M.J., Magnuson, J.J., and Murray, K.C. 1997. Distribution of littoral fishes in structurally complex macrophytes. Can. J. Fish. Aquat. Sci. **54**: 2277–2289.

Wiens, J.A., Crawford, C.S., and Gosz, J.R. 1985. Boundary dynamics: a conceptual framework for studying landscape ecosystems. Oikos, **45**: 421–427.

Wilkinson, L. 1997. SYSTAT for Windows: statistics, version 7 edition. SYSTAT, Inc., Evanston, Ill.

Willis, T.V. 1999. Patterns in species composition across the interface between streams and lakes. M.S. thesis, Memorial Library, University of Wisconsin, Madison, Wis.

Wood, B.M., and Bain, M.B. 1995. Morphology and microhabitat use in stream fish. Can. J. Fish. Aquat. Sci. **52**: 1487–1498.

© 2000 NRC Canada

Mercury in the Sudbury River (Massachusetts, U.S.A.): pollution history and a synthesis of recent research

James G. Wiener and Pamela J. Shields

Abstract: We review the transport, fate, and bioavailability of mercury in the Sudbury River, topics addressed in the following five papers. Mercury entered the river from an industrial complex (site) that operated from 1917 to 1978. Rates of mercury accumulation in sediment cores from two reservoirs just downstream from the site decreased soon after industrial operations ended and have decreased further since capping of contaminated soils at the site in 1991. The reservoirs contained the most contaminated sediments (some exceeding 50 μg Hg·g dry weight^{-1}) and were depositional sinks for total mercury. Methyl mercury concentrations in biota did not parallel concentrations of total mercury in the sediments to which organisms were exposed, experimentally or as residents. Contaminated wetlands within the floodplain about 25 km downstream from the site produced and exported methyl mercury from inorganic mercury that had originated from the site. Natural burial processes have gradually decreased the quantity of sedimentary mercury available for methylation within the reservoirs, whereas mercury in the lesser contaminated wetlands farther downstream has remained more available for transport, methylation, and entry into food webs.

Résumé : Nous examinons le transport, le devenir et la biodisponibilité du mercure dans la rivière Sudbury, sujets qui sont traités dans les cinq articles qui suivent. Le mercure a pénétré dans la rivière pendant l'exploitation d'un complexe industriel (site) en service de 1917 à 1978. L'accumulation de mercure dans les carottes de sédiments de deux réservoirs situés juste en aval du site a diminué peu après la cessation des activités industrielles et, depuis 1991, continue de diminuer depuis le recouvrement des sols contaminés de ce complexe. C'est dans les réservoirs que les sédiments étaient les plus contaminés (certains dépassant 50 μg Hg·g poids sec^{-1}) et constituaient des puits pour le mercure total. Les concentrations de méthyl mercure dans le biote ne correspondaient pas aux concentrations de mercure total dans les sédiments auxquels les organismes ont été exposés, de façon naturelle et expérimentale. Les milieux humides contaminés de la plaine d'inondation, situés à environ 25 km en aval du site, produisaient et exportaient du méthyl mercure issu du mercure inorganique provenant du site. Les processus naturels d'enfouissement ont fait diminuer progressivement la quantité de mercure sédimentaire libre pour la méthylation dans les réservoirs, tandis que le mercure présent dans les milieux humides moins contaminés situés en aval était plus disponible pour le transport, la méthylation et l'entrée dans les réseaux trophiques.

[Traduit par la Rédaction]

Introduction

Concerns about mercury pollution of aquatic ecosystems stem primarily from the high neurotoxicity of methyl mercury (Clarkson 1992), an organic form that readily accumulates in aquatic organisms and biomagnifies in food webs (Francesconi and Lenanton 1992; Watras and Bloom 1992). Wildlife near the top of aquatic food webs can be exposed to harmful doses of methyl mercury in ecosystems with contaminated fish (Meyer et al. 1998; Scheuhammer et al. 1998). Likewise, human exposure to methyl mercury is now almost totally due to consumption of contaminated fish (Clarkson 1992).

In recent decades, recognition of the serious consequences of methyl mercury contamination of aquatic food webs has prompted widespread reductions in direct discharges of mercury into surface waters in many industrialized countries. Much of the mercury formerly released into surface waters now resides in the bottom sediments (Kudo 1989), yet the extent to which sediments serve as a continuing internal source of methyl mercury in aquatic ecosystems is poorly understood (Gilmour and Henry 1991; Rudd 1995). Sediments can function as a sink for mercury in aquatic ecosystems, largely removing the mercury from active biogeochemical cycling (Henry et al. 1995). Conversely, the sediments can serve as a source of methyl mercury if some of the inorganic mercury in the sediment is methylated (Gilmour and Henry 1991; Ramlal et al. 1993) and becomes available to biota. Methyl mercury is formed largely by the microbial methylation of inorganic Hg(II) in the environment, a key process affecting the methyl mercury content of aquatic organisms (Gilmour and Henry 1991; Bodaly et al. 1993; Kelly et al. 1997). Information on the biological avail-

Received December 11, 1997. Accepted December 7, 1999. J14339

J.G. Wiener.[1] U.S. Geological Survey, Biological Resources Division, Upper Midwest Environmental Sciences Center, 2630 Fanta Reed Road, La Crosse, WI 54603, U.S.A.
P.J. Shields. U.S. Environmental Protection Agency, Region I, John F. Kennedy Federal Building, Mail Code CHW, Boston, MA 02203-2211, U.S.A.

[1]Author to whom all correspondence should be addressed. e-mail: james_wiener@usgs.gov

© 2000 NRC Canada

ability of sediment-associated mercury is necessary to define appropriate management practices for contaminated habitats and sediments.

The Sudbury River in eastern Massachusetts (U.S.A.) was contaminated with mercury from the Nyanza chemical waste dump site (Nyanza site), an industrial complex that operated from 1917 to 1978. Initial surveys revealed high mercury concentrations in sediment and fish in downstream reaches of the river, which included fluvial habitat, impoundments, extensive palustrine wetlands, and a riverine lake (NUS Corporation 1992; National Park Service 1996). These findings prompted the U.S. Environmental Protection Agency Superfund Program to initiate detailed, multidisciplinary studies to assess the transport, distribution, bioavailability, bioaccumulation, and ecological risk of mercury in the river.

We briefly describe the Sudbury River, the history of mercury contamination, and remedial measures applied at the Nyanza site. We follow with a concise synthesis of recent findings on the transport, environmental fate, and bioavailability of mercury in the Sudbury River ecosystem as an introduction to the five original research papers that follow.

Study area

From its headwaters at Cedar Swamp Pond in Westborough, Massachusetts, the Sudbury River flows about 13 km eastward and then about 40 km northward until it joins the Assabet River to form the Concord River (McAdow 1990; NUS Corporation 1992). Impoundments on the river include Reservoir 2, Reservoir 1, and the Saxonville Impoundment (Fig. 1). The floodplain along about 10 km of the northern reach of the river lies within the 12-km^2 Great Meadows National Wildlife Refuge (Fig. 1), which contains extensive wetlands that are generally classified as palustrine wetlands with scrub-shrub and persistent, emergent herbaceous plants (Harris 1996). The northern reach of the river also contains a natural riverine lake, Fairhaven Bay.

The elevation of the river drops 47 m from its headwaters to the confluence with the Assabet River, with an average gradient of 90–100 $cm \cdot km^{-1}$. The gradient of the downstream reach of the river is considerably less, however, averaging only 1.5 $cm \cdot km^{-1}$ (National Park Service 1996). Most of the contaminated reach is characterized by slow current velocity and depositional environments, with velocities approaching 0 $cm \cdot s^{-1}$ during summer months in the downstream reach of the river. Water samples taken during two water years, 1994 (1 October 1993 to 30 September 1994) and 1995 (1 October 1994 to 30 September 1995), had annual mean (values for one or both years) pH of 6.9–7.0, alkalinity of 18 $mg \cdot L^{-1}$ (as $CaCO_3$), hardness of 38 $mg \cdot L^{-1}$ (as $CaCO_3$), total suspended solids of 10.5 $mg \cdot L^{-1}$ in 1994 and 5.5 $mg \cdot L^{-1}$ in 1995, dissolved organic carbon of 5–6 $mg \cdot L^{-1}$, sulfate of 10.7 $mg \cdot L^{-1}$ (as SO_4^{2-}), and specific conductance of about 290 $\mu S \cdot cm^{-1}$ (J.A. Colman, U.S. Geological Survey, Northborough, Mass., personal communication).

The river receives flow from a number of tributaries draining its 425-km^2 basin. At Reservoir 1, flow enters from the Sudbury Reservoir and Reservoir 3. The river also receives water from the Whitehall, Hopkinton, and Ashland reservoirs (Fig. 1). The estimated average annual discharge is 8.44 $m^3 \cdot s^{-1}$ at the mouth of the Sudbury River, where it meets the Assabet River (Socolow et al. 1995). The primary land use in the watershed is suburban residential, and the terrain is rolling and hilly (NUS Corporation 1992).

The Sudbury River provides habitat for many warmwater fishes, including largemouth bass (*Micropterus salmoides*), bluegill (*Lepomis macrochirus*), pumpkinseed (*Lepomis gibbosus*), white perch (*Morone americana*), yellow perch (*Perca flavescens*), and bullheads (*Ameiurus* spp.) (NUS Corporation 1992; National Park Service 1996). The river and adjoining areas also provide habitat for a number of aquatic mammals, including raccoon (*Procyon lotor*), muskrat (*Ondatra zibethicus*), and river otter (*Lutra canadensis*). Nesting birds include osprey (*Pandion haliaetus*), great blue heron (*Ardea herodias*), mallard (*Anas platyrhynchos*), and other waterfowl (McAdow 1990).

Sudbury River contamination

Mercury pollution of the river was discovered in 1970 during a survey of mercury in fish and sediment. A subsequent study in 1972 identified the Nyanza site in the town of Ashland as a probable major source of the mercury entering the river (JBF Scientific Corporation 1973). The 14-ha Nyanza site was occupied by a series of companies involved in the manufacture of various products, primarily textile dyes and dye intermediates. These companies operated and disposed of their waste products at the Nyanza site from 1917 until 1978. These chemical wastes, which included large quantities of mercury, were transported from the Nyanza site via overland flow into adjacent wetlands and eventually reached the Sudbury River channel, about 300 m north of the Nyanza site.

In 1983, the Nyanza site was included on the U.S. Environmental Protection Agency's national priority list of Superfund sites. Subsequent state and federal responses to this mercury problem have included provision of advice warning against consumption of contaminated sport fish, remedial actions to reduce the migration of mercury from the Nyanza site into the river, and scientific investigations of mercury in the ecosystem. On-site studies showed high concentrations of mercury and other heavy metals in soils, prompting the U.S. Environmental Protection Agency to excavate and cap highly contaminated soils at the Nyanza site. These remedial actions, completed in 1991, have reduced the influx of mercury to the Sudbury River (Frazier et al. 2000).

Further sampling and analysis of sediment and biota during 1989–1991 better defined the nature and extent of contamination of the river. Mercury concentrations in sediments were typically greatest in impoundments and slow-flowing reaches, with peak values exceeding 50 $\mu g \cdot g$ dry $weight^{-1}$ in Reservoir 2, an impoundment beginning just 1.2 km downstream from the Nyanza site. Concentrations generally decreased with increasing distance from the Nyanza site, yet sediments were notably contaminated as far downstream as Fairhaven Bay, more than 30 km downstream. Fish from Reservoir 2 generally had the greatest mercury concentrations, with a maximum of 7.6 $\mu g \cdot g$ wet $weight^{-1}$ in a fillet of largemouth bass from the reservoir (NUS Corporation 1992). Sediments and fish from reference locations con-

© 2000 NRC Canada

Fig. 1. Map of the Sudbury River basin in eastern Massachusetts (U.S.A.) showing the study areas in relation to the Nyanza chemical waste dump site (Nyanza site), the principal source of mercury for the river during industrial operations there.

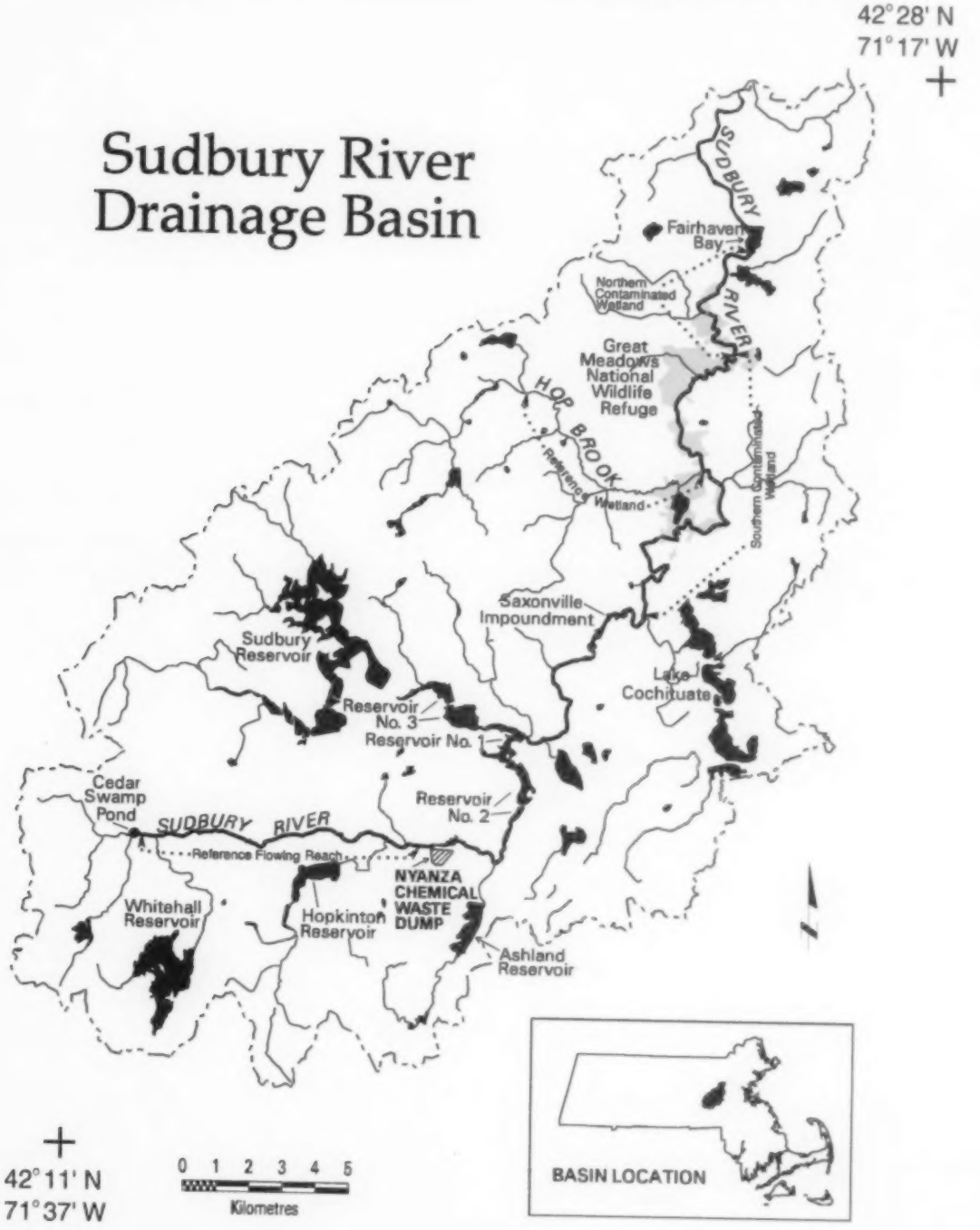

© 2000 NRC Canada

tained comparatively small concentrations of mercury (NUS Corporation 1992). Based on site-specific risk assessments, the health and ecological risks associated with elevated mercury levels in fish were judged to be unacceptably high for humans and fish-eating wildlife (NUS Corporation 1992).

Information gaps and multidisciplinary investigations

The identification of remedial options for the Sudbury River was precluded by a number of key information gaps that are often applicable to aquatic sites contaminated with toxic substances (Kamrin et al. 1994), particularly mercury. A central information gap concerned the biological availability of sedimentary mercury in the ecosystem. Stated more specifically, it was important to know the extent to which methyl mercury, the highly toxic form accumulated in fish and biomagnified in aquatic food webs, was being actively produced within the surficial sediments and subsequently accumulated by benthic organisms or released to the water column.

The cost of conventional remedial methods, such as the dredging or capping (Palermo 1998) of contaminated sediments, constrains their large-scale application throughout such a large reach of contaminated river. It was therefore desirable to identify habitats or reaches of the river having the greatest potential for entry of methyl mercury into the water column or food web so that management efforts could be focused spatially. A related question was to determine the relationship, if any, between the production of methyl mercury and the total mercury concentration in sediment within specific reaches or habitats of the river. Other questions concerned the historic deposition and distribution of mercury in sediments and the potential transport of the most contaminated sediments.

These information gaps led to the multidisciplinary investigations reported here, which critically examined the environmental fate, physical transport, bioavailability, and bioaccumulation of mercury in the Sudbury River system. These investigations encompassed contaminated and reference impoundments, flowing reaches, and palustrine wetlands in the river floodplain and employed both mensurative studies and manipulative experiments.

Temporal and spatial patterns in mercury contamination

Patterns in mercury contamination of sediment and river water confirmed the Nyanza site as the primary historic source of mercury in the Sudbury River. Analyses of dated sediment cores taken in 1994 (Frazier et al. 2000) showed that the chronology of mercury pollution of the river strongly coincided with industrial operations at the Nyanza site. Mercury accumulation in cores from Reservoirs 1 and 2 increased greatly within one or two decades after industrial operations began. Rates of sedimentary mercury accumulation in these cores were greatest in the late 1970s through 1982, decreasing a few years after industrial operation ceased in 1978, and decreasing further after the excavation and capping of contaminated soils at the Nyanza site was completed in 1991.

The natural abundance (preindustrial background concentration) of total mercury in fine-grained sediments from the Sudbury River basin, based on concentrations in the deepest strata of sediment cores, averaged 44 ng·g dry weight^{-1} (Frazier et al. 2000). The maximum concentration of total mercury in a sediment core from Reservoir 2 exceeded the natural abundance by almost 1000-fold (Frazier et al. 2000). During the period of most intense pollution, an estimated 98% of the anthropogenic mercury accumulating in the sediments of Reservoirs 2 and 1 was from the Nyanza site (Frazier et al. 2000).

Concentrations of total mercury in surficial sediments, as well as recent rates of mercury accumulation in depositional sediments, generally decreased with increasing distance downstream from the Nyanza site (Fig. 2). Concentrations of total mercury in river water decreased after passage through Reservoir 2, Reservoir 1, and the Saxonville Impoundment, partly because of the sedimentation of particulate mercury (Waldron et al. 2000). Although the most contaminated sediments in the reservoirs have been buried, the surficial sediments remain substantially contaminated in the reservoirs, flowing reaches, palustrine wetlands, and riverine lake downstream from the Nyanza site (Colman et al. 1999; Frazier et al. 2000; Naimo et al. 2000).

The continuing contamination of surficial sediments indicates that some mercury is still entering or being recycled within the ecosystem. During our investigations, the Nyanza site continued to be the major source of mercury for the reach just downstream, including Reservoirs 2 and 1 (Waldron et al. 2000). Frazier et al. (2000) estimated that more than 90% of the anthropogenic mercury in the uppermost 1-cm stratum in sediment cores from Reservoirs 2 and 1 was from the Nyanza site. During the 1995 water year, the mean load of total mercury transported in river water increased sixfold where the river flowed past the Nyanza site (Waldron et al. 2000). Downstream from the Saxonville Impoundment (15 km downstream from the Nyanza site), however, little of the mercury transported in river water or accumulating in surficial sediments during these investigations could be attributed to contemporary inputs from the Nyanza site (Frazier et al. 2000; Waldron et al. 2000). Loads and concentrations of total mercury in the river increased substantially where it flowed through palustrine wetlands on the floodplain (Fig. 2), suggesting that mercury was entering from the wetlands, from contaminated bed sediments in the channel, or from other, unidentified local sources (Waldron et al. 2000).

Methyl mercury and total mercury in ecosystem components

Patterns in the concentrations and loads of methyl mercury in water differed markedly from those for total mercury. In 1995, the Nyanza site did not notably contribute methyl mercury to the Sudbury River; rather, the mass balance of methyl mercury in water showed that the production of methyl mercury varied considerably among the studied reaches (Waldron et al. 2000). In the sediment, the concentrations of methyl mercury were usually greatest near the sediment surface and were independent of the total mercury concentration in the surficial sediments (Colman et al.

© 2000 NRC Canada

Fig. 2. Longitudinal patterns in mercury concentrations in physical components, selected resident biota, test organisms, and test water (exposed experimentally to water and (or) sediment from the Sudbury River basin), with study areas arranged left to right from upstream to downstream. The Nyanza site (not shown) is located between the reference flowing reach and Reservoir 2. The three reference areas (Whitehall Reservoir, reference flowing reach, and reference wetland, areas not measurably contaminated with mercury from the Nyanza site) are denoted by open bars. Shown are means and standard errors for (A) total mercury in surficial bed sediment (note the discontinuous scale), (B) methyl mercury (MeHg, bars) and total mercury (means denoted by horizontal lines offset to the right) in unfiltered surface water, (C) MeHg in resident largemouth bass (adjusted means for whole 0.64-kg fish), (D) MeHg in resident whole larval dragonflies, (E) MeHg in mayfly nymphs (*Hexagenia*, bars) and test water (means denoted by horizontal lines offset to the right) exposed in laboratory experiments to surficial sediments from the basin, and (F) MeHg in freshwater mussels (*E. complanata* transplanted and exposed in situ). Data were compiled from Waldron et al. (2000), Frazier et al. (2000), Colman et al. (1999), T.A. Haines (U.S. Geological Survey, Leetown Science Center, Field Station, Orono, Me., unpublished data), Naimo et al. (2000), and Beckvar et al. (2000).

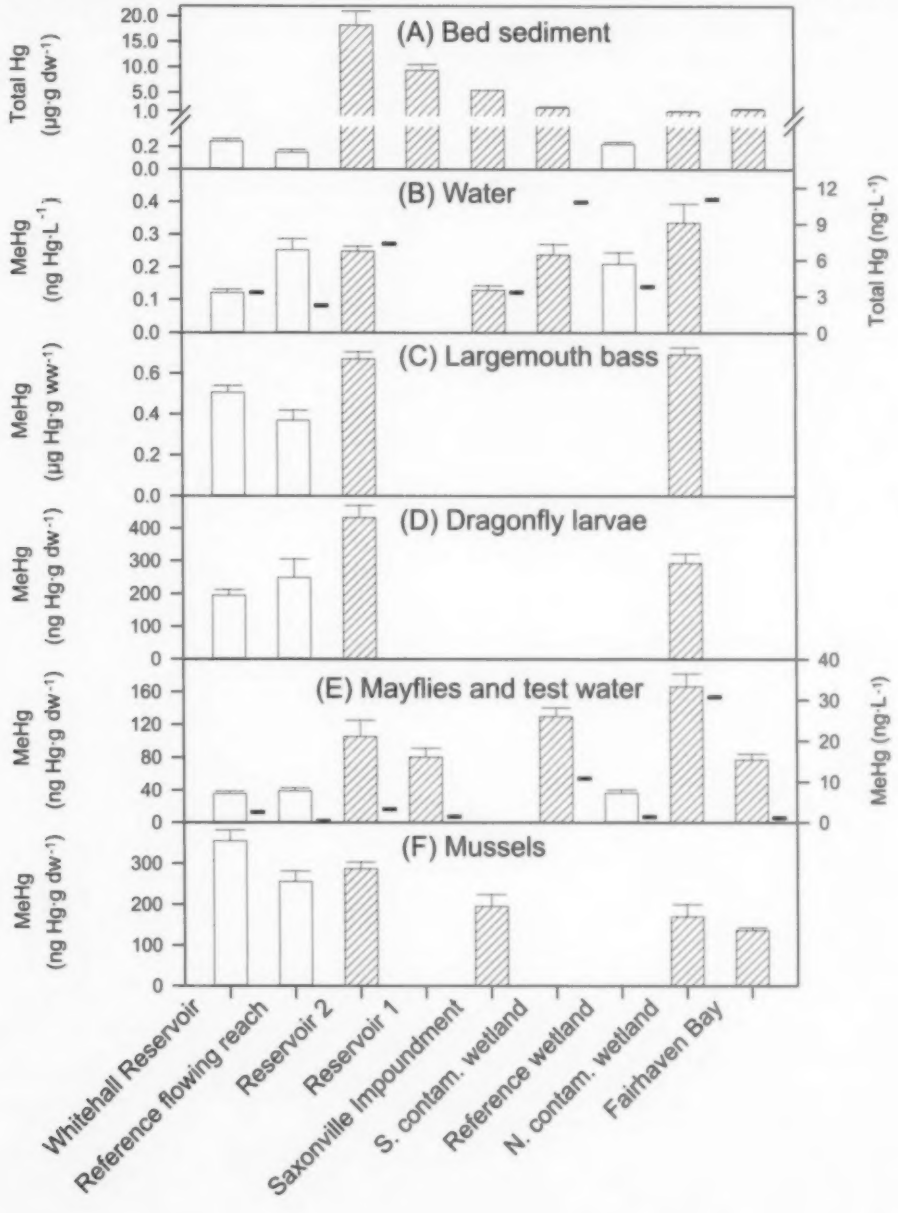

© 2000 NRC Canada

1999). Naimo et al. (2000), who experimentally exposed burrowing nymphs of *Hexagenia* mayflies (Insecta: Ephemeroptera) to contaminated sediments from the basin in 21-day laboratory tests, found that concentrations of total (mostly inorganic) mercury in mayflies were correlated with the total mercury concentration in test sediments. In contrast, the mean final concentrations of methyl mercury in mayfly nymphs were not correlated with total mercury concentration in the test sediments.

The in situ bioaccumulation of total mercury and methyl mercury was examined by Beckvar et al. (2000), who emplaced caged freshwater mussels (*Elliptio complanata*, a native filter-feeding bivalve) at eight locations (six contaminated with mercury from the Nyanza site and two reference areas). Patterns in mercury accumulation in the caged mussels during the 12-week exposure can best be evaluated by examining changes in tissue burdens of methyl mercury, which increased significantly at all six contaminated locations and at one of the two reference areas, Whitehall Reservoir (Beckvar et al. 2000). Accumulation of methyl mercury was greatest in mussels encaged within Reservoir 2; burdens also increased in mussels encaged at the Reservoir 2 inlet, the Saxonville Impoundment, Fairhaven Bay, and a Concord River location 39 km downstream from the Nyanza site. In contrast, mean burdens of total mercury in caged mussels did not change significantly during the 12-week exposure (Beckvar et al. 2000).

Concentrations of methyl mercury in resident fishes and larval dragonflies (Insecta: Odonata) were typically greater in the contaminated reaches than in reference areas; however, concentrations of methyl mercury in these biota were not *proportional* to concentrations of total mercury in sediment (T.A. Haines, U.S. Geological Survey, Leetown Science Center, Field Station, Orono, Me., unpublished data). In largemouth bass, for example, mean (size-adjusted) concentrations of mercury in whole fish from Reservoir 2 (0.67 μg·g wet weight^{-1}) were similar to values in those from the much lesser contaminated wetland reach (0.69 μg·g wet weight^{-1}). Moreover, the size-adjusted means for these two contaminated reaches exceeded that for largemouth bass from the Whitehall Reservoir, a reference area unaffected by the Nyanza site, by less than 0.2 μg·g wet weight^{-1} (T.A. Haines, U.S. Geological Survey, Leetown Science Center, Field Station, Orono, Me., unpublished data). The mean concentrations in largemouth bass from the Sudbury River and the Whitehall Reservoir did not differ greatly from the mean (0.56 μg·g wet weight^{-1}) reported for largemouth bass from Maine lakes (Stafford and Haines 1997). Interestingly, such a pattern would be expected if atmospheric deposition were the primary source of the mercury accumulating in fish inhabiting the region's lakes.

Wetlands as sites of methyl mercury production

Mass-balance studies (Colman and Breault 2000; Waldron et al. 2000) and bioaccumulation experiments with *Hexagenia* mayflies (Naimo et al. 2000) showed that methyl mercury was actively produced in the contaminated palustrine wetlands adjoining the Sudbury River, which had total concentrations of sedimentary mercury considerably less than those in Reservoirs 1 and 2 (Fig. 2). Concentrations and loads of methyl mercury increased in the reach of river flowing through the adjoining palustrine wetlands (Waldron et al. 2000). Furthermore, the contaminated overbank sediments in the wetlands on the floodplain seem to be a site of active methylation, based on analyses of methyl mercury in sediment cores (Colman et al. 1999) and on the bioaccumulation of methyl mercury in mayflies exposed experimentally to wetland sediments (Naimo et al. 2000). The export of methyl mercury from the contaminated palustrine wetlands clearly exceeded that from the contaminated reservoirs upstream, which had surficial sediments with much greater mercury concentrations. These findings agree with recent reports showing that wetlands are sites of active methyl mercury production (Hurley et al. 1995; Krabbenhoft et al. 1995; St. Louis et al. 1996).

Even lightly contaminated wetlands can produce significant amounts of methyl mercury (St. Louis et al. 1996; Kelly et al. 1997; Gilmour et al. 1998). Thus, it would be reasonable to question whether the methyl mercury exported by the contaminated wetlands was derived from mercury in atmospheric deposition to the wetlands rather than from the mercury-contaminated wetland sediments. The laboratory experiments of Naimo et al. (2000) show that most of the methyl mercury produced in the contaminated wetlands can be attributed to methylation of sedimentary mercury derived mostly from the Nyanza site; the final concentrations of methyl mercury in test water and mayflies exposed to contaminated wetland sediments far exceeded those in treatments with sediments from a nearby reference wetland in the river basin (Fig. 3). Given their close proximity, the reference and contaminated wetland areas presumably received similar historical atmospheric inputs of mercury. These findings indicate that the methyl mercury exported from the contaminated wetlands adjoining the Sudbury River was derived largely from methylation of anthropogenic, inorganic mercury that had originated largely from the Nyanza site.

Similarly, concentrations of methyl mercury in test water and burrowing mayfly nymphs, both exposed for 21 days to surficial sediments from the basin, were greater in treatments with contaminated wetland sediments than in treatments with the highly contaminated reservoir sediments (Naimo et al. 2000). Mean sedimentary concentrations of total mercury in treatments with contaminated wetland sediment ranged from 1.2 to 2.6 μg·g dry weight^{-1}, considerably less than mean concentrations in treatments with reservoir sediments (range 7.5–22 μg·g dry weight^{-1}). Yet, concentrations of waterborne methyl mercury ranged from 8 to 47 ng Hg·L^{-1} in treatments with contaminated wetland sediments, far exceeding the concentrations of 1–3 ng Hg·L^{-1} in treatments with sediments from Reservoirs 2 and 1. In mayflies, final mean concentrations of methyl mercury were greater in treatments with contaminated wetland sediments than in treatments with contaminated sediments from Reservoir 2, Reservoir 1, flowing reaches, and Fairhaven Bay (Naimo et al. 2000).

Studies of the Sudbury River ecosystem add to a growing body of evidence indicating that wetlands are mercury-sensitive environments. Methyl mercury production in wetland habitats greatly exceeds that in other aquatic and terrestrial habitats (Hurley et al. 1995; St. Louis et al. 1996).

© 2000 NRC Canada

Fig. 3. Mean concentrations (±1 SE) of (A) total mercury in test sediment and final mean concentrations (±1 SE) of methyl mercury (MeHg) in (B) test water and (C) *Hexagenia* mayfly nymphs exposed in the laboratory to surficial sediments sampled in May and September 1995 from three wetland areas in the Sudbury River basin in two 21-day bioaccumulation tests (data from Naimo et al. 2000). The two contaminated wetlands (southern and northern) received mercury originating from the Nyanza site, whereas the nearby reference wetland (bordering Hop Brook; Fig. 1) was not measurably contaminated with mercury from the Nyanza site.

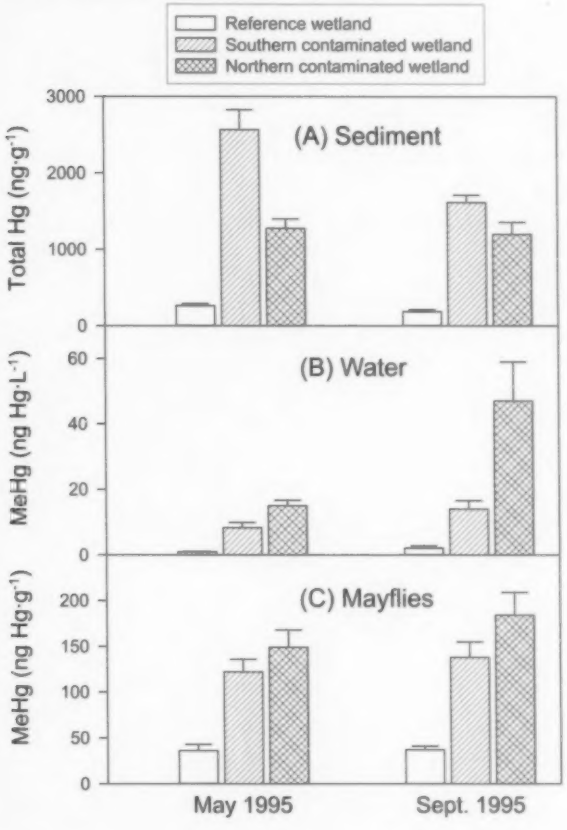

Moreover, the production of methyl mercury in wetlands increases during flooding (Kelly et al. 1997), a frequent event in the wetlands adjoining the Sudbury River. The findings summarized here suggest that sedimentary mercury in these palustrine wetlands could remain available for mobilization, biogeochemical cycling, and entry into food webs for decades.

Biological effects of mercury exposure

The concentrations of total mercury and methyl mercury in Sudbury River water measured by Waldron et al. (2000) were far below concentrations known to be directly toxic to freshwater invertebrates and fish (Wren and Stephenson 1991; Wiener and Spry 1996). Yet burrowing organisms inhabiting soft sediments are also exposed to sediment-associated inorganic mercury and methyl mercury. Nymphal *Hexagenia* exposed experimentally to contaminated sediments from the Sudbury River basin accumulated mercury but showed no adverse effects attributable to mercury exposure (Naimo et al. 2000). The survival of mayflies exposed for 21 days to contaminated and reference sediments exceeded 90% in all tests and did not vary among sediment treatments. The growth of nymphs varied among treatments but was unrelated to exposure of nymphs to either total mercury or methyl mercury (Naimo et al. 2000). The survival of caged *Elliptio* mussels in the river was also unrelated to mercury exposure (Beckvar et al. 2000). Although the growth of caged mussels was inversely correlated with mercury concentrations in mussel tissue, a causal relationship between mercury exposure and growth rate cannot be inferred (Beckvar et al. 2000). The growth of mussels held at Nyanza-contaminated locations generally increased with increasing distance downstream from the Nyanza site; however, longitudinal variation in other environmental factors, such as water temperature or food resources, may have caused the observed longitudinal pattern in mussel growth.

The health of adult riverine fishes was presumably not adversely affected by exposure to mercury in the Sudbury River system. The recent concentrations of mercury in resident prey fishes and largemouth bass, measured by T.A. Haines (U.S. Geological Survey, Leetown Science Center, Field Station, Orono, Me., unpublished data), were considerably less than tissue residues associated with overt toxicity in adult freshwater fish (Wiener and Spry 1996).

Methyl mercury contamination of aquatic food webs can adversely affect organisms in upper trophic levels, such as fish-eating birds and mammals. The mercury present in fish is mostly methyl mercury (Bloom 1992; Hammerschmidt et al. 1999). Methyl mercury damages the central nervous system, and early life stages are far more sensitive than juveniles or adults to methyl mercury (Scheuhammer 1991; Clarkson 1992). In birds, for example, the effects of methyl mercury are most severe in embryos and chicks, and low-level dietary exposures that cause no measurable effect in adults can significantly impair egg fertility, hatchling survival, and overall reproductive success (Scheuhammer 1991).

Certain prey fish in contaminated reaches of the Sudbury River may have contained toxicologically significant quantities of methyl mercury for certain species of fish-eating wildlife. In common loons (*Gavia immer*), for example, a mercury concentration of 0.3 μg·g wet weight^{-1} in prey fish is the estimated dietary threshold associated with reproductive impairment (Scheuhammer 1991). For comparison, the size-adjusted mean concentration of mercury in whole yellow perch, the preferred prey of common loons (Barr 1996), was 0.41 μg·g wet weight^{-1} in Reservoir 2 (T.A. Haines, U.S. Geological Survey, Leetown Science Center, Field Station, Orono, Me., unpublished data).

Trends, predictions, and uncertainties

Reductions in discharges of mercury to surface waters are typically followed by gradual declines in mercury levels in resident fishes, although concentrations in fish can remain elevated for many years (Parks and Hamilton 1987; Francesconi et al. 1997). Although trend data on mercury in fish are not presently available, it seems probable that the

© 2000 NRC Canada

sedimentary mercury in the contaminated wetlands will be much more available than that in the reservoirs for physical transport, conversion to methyl mercury, and entry into food webs.

The most contaminated sediments in Reservoir 2, Reservoir 1, and Fairhaven Bay now lie below the vertical sedimentary zone of greatest mercury methylation. The microbial production of methyl mercury from inorganic Hg(II) is most rapid near the sediment–water interface; moreover, investigations of other freshwater systems have consistently shown that the rate of mercury methylation is greatest in the uppermost 5 cm of the sediment profile and that little methyl mercury is produced in deeper sediments (Rudd et al. 1983; Gilmour et al. 1998; Bloom et al. 1999). In cores from Reservoirs 2 and 1, the most contaminated sediments were 6–12 cm or more deep (Colman et al. 1999; Frazier et al. 2000). We believe that the gradual burial of the most contaminated sediments is decreasing the amount of inorganic mercury available for microbial methylation in the reservoirs, whereas the sedimentary mercury in the contaminated wetlands is more readily available for physical transport, biogeochemical cycling, and entry into food webs (Branfireun et al. 1996; Naimo et al. 2000; Waldron et al. 2000).

Remedial investigations at contaminated sites commonly focus on environmental contamination and adverse effects near the source area(s). Results of the Sudbury River investigations show that mercury transported to palustrine wetlands located 25 km or farther downstream from a source area can be more problematic than the greater mercury levels near the Nyanza site. These observations emphasize the importance of investigating impacts to mercury-sensitive receptor areas located a significant distance from the source of contamination.

The probability of substantial hydrologic resuspension and transport of bottom sediments in the most contaminated reservoirs seems to be small under prevailing conditions. Sediment transport modeling of Reservoirs 2 and 1 (D. Abraham and G. Nail, U.S. Army Corps of Engineers, Waterways Experiment Station, Vicksburg, Miss., unpublished data) showed that scouring and transport of soft bottom sediments would be minimal and limited to small areas of the reservoirs, even during a 100-year flood. The predictions from the sediment transport modeling are supported by results from ^{210}Pb dating of sediment cores from the reservoirs, which indicated intact sediment profiles with little evidence of past physical disturbance, even though a 100-year flood occurred in 1955 (Frazier et al. 2000). Similarly, mass-balance studies by Waldron et al. (2000) showed that the reservoirs were sinks for total mercury.

In closing, we caution that ongoing or future environmental changes originating outside the Sudbury River basin could significantly alter the biogeochemical cycling, partitioning, and bioavailability of mercury in this ecosystem. Projected annual temperature increases of 3–5°C linked to climate change and global warming (Moore et al. 1997), for example, could stimulate greater microbial production of methyl mercury in these contaminated riverine and wetland environments (Ramlal et al. 1993). This could notably increase the concentrations of methyl mercury in fish and other aquatic biota (Bodaly et al. 1993; Schindler 1997). Such external factors add uncertainty to predictions based on site-specific information for this or any other mercury-contaminated ecosystem.

Acknowledgments

Preparation of this paper was facilitated by the following investigators, who graciously allowed access to their data on the Sudbury River: David Abraham, Nancy Beckvar, Robert Breault, John Colman, Kenneth Finkelstein, Bradley Frazier, Terry Haines, Gary Morin, Gregory Nail, Teresa Naimo, Michael Salazar, Sandra Salazar, and Marcus Waldron. We thank David Abraham, Nancy Beckvar, Drew Bodaly, Mary Garren, Douglas Knauer, Teresa Naimo, Ronald Rada, Susan Svirsky, and an anonymous referee for helpful comments on earlier drafts of the manuscript. Bradley Frazier and Amy Hoyt prepared the figures.

References

Barr, J.F. 1996. Aspects of common loon (*Gavia immer*) feeding biology on its breeding ground. Hydrobiologia, **321**: 119–144.

Beckvar, N., Salazar, S., Salazar, M., and Finkelstein, K. 2000. An in situ assessment of mercury contamination in the Sudbury River, Massachusetts, using transplanted freshwater mussels (*Elliptio complanata*). Can. J. Fish. Aquat. Sci. **57**: 1103–1112.

Bloom, N.S. 1992. On the chemical form of mercury in edible fish and marine invertebrate tissue. Can. J. Fish. Aquat. Sci. **49**: 1010–1017.

Bloom, N.S., Gill, G.A., Cappellino, S., Dobbs, C., McShea, L., Driscoll, C., Mason, R., and Rudd, J. 1999. Speciation and cycling of mercury in Lavaca Bay, Texas, sediments. Environ. Sci. Technol. **33**: 7–13.

Bodaly, R.A., Rudd, J.W.M., Fudge, R.J.P., and Kelly, C.A. 1993. Mercury concentrations in fish related to size of remote Canadian Shield lakes. Can. J. Fish. Aquat. Sci. **50**: 980–987.

Branfireun, B.A., Heyes, A., and Roulet, N.T. 1996. The hydrology and methylmercury dynamics of a Precambrian Shield headwater peatland. Water Resour. Res. **32**: 1785–1794.

Clarkson, T.W. 1992. Mercury: major issues in environmental health. Environ. Health Perspect. **100**: 31–38.

Colman, J.A., and Breault, R.F. 2000. Sampling for mercury at subnanogram per litre concentrations for load estimation in rivers. Can. J. Fish. Aquat. Sci. **57**: 1073–1079.

Colman, J.A., Waldron, M.C., Breault, R.F., and Lent, R.M. 1999. Distribution and transport of total mercury and methylmercury in mercury-contaminated sediments in reservoirs and wetlands of the Sudbury River, east-central Massachusetts. U.S. Geol. Surv. Water-Resour. Invest. Rep. 99-4060.

Francesconi, K.A., and Lenanton, R.C.J. 1992. Mercury contamination in a semi-enclosed marine embayment: organic and inorganic mercury content of biota, and factors influencing mercury levels in fish. Mar. Environ. Res. **33**: 189–212.

Francesconi, K.A., Lenanton, R.C.J., Caputi, N., and Jones, S. 1997. Long-term study of mercury concentrations in fish following cessation of a mercury-containing discharge. Mar. Environ. Res. **43**: 27–40.

Frazier, B.E., Wiener, J.G., Rada, R.G., and Engstrom, D.R. 2000. Stratigraphy and historic accumulation of mercury in recent depositional sediments in the Sudbury River, Massachusetts, U.S.A. Can. J. Fish. Aquat. Sci. **57**: 1062–1072.

Gilmour, C.C., and Henry, E.A. 1991. Mercury methylation in aquatic systems affected by acid deposition. Environ. Pollut. **71**: 131–169.

© 2000 NRC Canada

Gilmour, C.C., Riedel, G.S., Ederington, M.C., Bell, J.T., Benoit, J.M., Gill, G.A., and Stordal, M.C. 1998. Methylmercury concentrations and production rates across a trophic gradient in the northern Everglades. Biogeochemistry, **40**: 327–345.

Hammerschmidt, C.R., Wiener, J.G., Frazier, B.E., and Rada, R.G. 1999. Methylmercury content of eggs in yellow perch related to maternal exposure in four Wisconsin lakes. Environ. Sci. Technol. **33**: 999–1003.

Harris, S.L. 1996. Massachusetts wetland resources. *In* National water summary on wetland resources. U.S. Geol. Surv. Water-Supply Pap. 2425.

Henry, E.A., Dodge-Murphy, L.J., Bigham, G.N., Klein, S.M., and Gilmour, C.C. 1995. Total mercury and methylmercury mass balance in an alkaline, hypereutrophic urban lake (Onondaga Lake, NY). Water Air Soil Pollut. **80**: 509–518.

Hurley, J.P., Benoit, J.M., Babiarz, C.L., Shafer, M.M., Andren, A.W., Sullivan, J.R., Hammond, R., and Webb, D.A. 1995. Influences of watershed characteristics on mercury levels in Wisconsin rivers. Environ. Sci. Technol. **29**: 1867–1875.

JBF Scientific Corporation. 1973. An investigation of mercury problems in Massachusetts. JBF Scientific Corporation, Burlington, Mass.

Kamrin, M.A., Fischer, L.J., Suk, W.A., Fouts, J.R., Pellizzari, E., and Thornton, K. 1994. Assessment of human exposure to chemicals from Superfund sites. Environ. Health Perspect. **102**(Suppl. 1): 221–228.

Kelly, C.A., Rudd, J.W.M., Bodaly, R.A., Roulet, N.P., St. Louis, V.L., Heyes, A., Moore, T.R., Schiff, S., Aravena, R., Scott, K.J., Dyck, B., Harris, R., Warner, B., and Edwards, G. 1997. Increases in fluxes of greenhouse gases and methyl mercury following flooding of an experimental reservoir. Environ. Sci. Technol. **31**: 1334–1344.

Krabbenhoft, D.P., Benoit, J.M., Babiarz, C.L., Hurley, J.P., and Andren, A.W. 1995. Mercury cycling in the Allequash Creek watershed, northern Wisconsin. Water Air Soil Pollut. **80**: 425–433.

Kudo, A. 1989. Mercury in the Ottawa River (Canada). *In* Aquatic ecotoxicology: fundamental concepts and methodologies. Vol. 1. *Edited by* A. Boudou and F. Ribeyre. CRC Press, Boca Raton, Fla. pp. 201–217.

McAdow, R. 1990. The Concord, Sudbury, and Assabet rivers. Bliss Publishing Co., Marlborough, Mass.

Meyer, M.W., Evers, D.C., Hartigan, J.J., and Rasmussen, P.S. 1998. Patterns of common loon (*Gavia immer*) mercury exposure, reproduction, and survival in Wisconsin, USA. Environ. Toxicol. Chem. **17**: 184–190.

Moore, M.V., Pace, M.L., Mather, J.R., Murdoch, P.S., Howarth, R.W., Folt, C.L., Chen, C.Y., Hemond, H.F., Flebbe, P.A., and Driscoll, C.T. 1997. Potential effects of climate change on freshwater ecosystems of the New England/Mid-Atlantic region. Hydrol. Processes, **11**: 925–947.

Naimo, T.J., Wiener, J.G., Cope, W.G., and Bloom, N.S. 2000. Bioavailability of sediment-associated mercury to *Hexagenia* mayflies in a contaminated floodplain river. Can. J. Fish. Aquat. Sci. **57**: 1092–1102.

National Park Service. 1996. Sudbury, Assabet and Concord: wild and scenic rivers study. Report, National Park Service, Boston, Mass.

NUS Corporation. 1992. Final remedial investigation report. Nyanza Operable Unit III, Sudbury River Study, Middlesex County, Massachusetts. Vol. 1. NUS Rep. W92194F. NUS Corporation, Wilmington, Mass.

Palermo, M.R. 1998. Design considerations for in-situ capping of contaminated sediments. Water Sci. Technol. **37**: 315–321.

Parks, J.W., and Hamilton, A.L. 1987. Accelerating recovery of the mercury-contaminated Wabigoon/English River system. Hydrobiologia, **149**: 159–188.

Ramlal, P.S., Kelly, C.A., Rudd, J.W.M., and Furutani, A. 1993. Sites of methyl mercury production in remote Canadian Shield lakes. Can. J. Fish. Aquat. Sci. **50**: 972–979.

Rudd, J.W.M. 1995. Sources of methyl mercury to freshwater ecosystems: a review. Water Air Soil Pollut. **80**: 697–713.

Rudd, J.W., Turner, M.A., Furutani, A., Swick, A.L., and Townsend, B.E. 1983. The English–Wabigoon River system: I. A synthesis of recent research with a view towards mercury amelioration. Can. J. Fish. Aquat. Sci. **40**: 2206–2217.

Scheuhammer, A.M. 1991. Effects of acidification on the availability of toxic metals and calcium to wild birds and mammals. Environ. Pollut. **71**: 329–375.

Scheuhammer, A.M., Atchison, C.M., Wong, A.H.K., and Evers, D.C. 1998. Mercury exposure in breeding common loons (*Gavia immer*) in central Ontario, Canada. Environ. Toxicol. Chem. **17**: 191–196.

Schindler, D.W. 1997. Widespread effects of climatic warming on freshwater ecosystems in North America. Hydrol. Processes, **11**: 1043–1067.

Socolow, R.S., Comeau, L.Y., Casey, R.G., and Ramsbey, L.R. 1995. Water resources data, Massachusetts and Rhode Island, water year 1995. U.S. Geol. Surv. Water-Data Rep. MA-RI-95-1.

Stafford, C.P., and Haines, T.A. 1997. Mercury concentrations in Maine sport fishes. Trans. Am. Fish. Soc. **126**: 144–152.

St. Louis, V.L., Rudd, J.W.M., Kelly, C.A., Beaty, K.G., Flett, R.J., and Roulet, N.T. 1996. Production and loss of methylmercury and loss of total mercury from boreal forest catchments containing different types of wetlands. Environ. Sci. Technol. **30**: 2719–2729.

Waldron, M.C., Colman, J.A., and Breault, R.F. 2000. Distribution, hydrologic transport, and cycling of total mercury and methyl mercury in a contaminated river–reservoir–wetland system (Sudbury River, eastern Massachusetts). Can. J. Fish. Aquat. Sci. **57**: 1080–1091.

Watras, C.J., and Bloom, N.S. 1992. Mercury and methylmercury in individual zooplankton: implications for bioaccumulation. Limnol. Oceanogr. **37**: 1313–1318.

Wiener, J.G., and Spry, D.J. 1996. Toxicological significance of mercury in freshwater fish. *In* Environmental contaminants in wildlife: interpreting tissue concentrations. *Edited by* W.N. Beyer, G.H. Heinz, and A.W. Redmon-Norwood. Spec. Publ. Soc. Environ. Toxicol. Chem. Lewis Publishers, Boca Raton, Fla. pp. 297–339.

Wren, C.D., and Stephenson, G.L. 1991. The effect of acidification on the accumulation and toxicity of metals to freshwater invertebrates. Environ. Pollut. **71**: 205–241.

© 2000 NRC Canada

Stratigraphy and historic accumulation of mercury in recent depositional sediments in the Sudbury River, Massachusetts, U.S.A.

Bradley E. Frazier, James G. Wiener, Ronald G. Rada, and Daniel R. Engstrom

Abstract: The distribution and deposition of sedimentary mercury in the Sudbury River were linked to an industrial complex (Nyanza site) that operated from 1917 through 1978. In two reservoirs just downstream from the Nyanza site, estimated rates of mercury accumulation increased markedly in the 1920s and 1930s, were greatest during 1976–1982, decreased within 5 years after industrial operations ceased, and have decreased further since capping of contaminated soil at the Nyanza site was completed in 1991. The most contaminated sediments were typically buried, yet the 0- to 1-cm stratum remained substantially contaminated in all cores. Mercury accumulating in the surficial, reservoir sediments was probably from continuing, albeit much lesser, inputs from the Nyanza site, whereas recent inputs to downstream wetland areas were attributed to recycling of sedimentary mercury or to mercury from unidentified local sources. In the reservoirs, burial of highly contaminated sediments is gradually decreasing the amount of sedimentary mercury available for methylation. In downstream wetlands, however, sedimentary mercury seemed to be more available than that in the reservoirs for physical transport and biogeochemical cycling.

Résumé : Le dépôt et la distribution de mercure sédimentaire dans la rivière Sudbury étaient associés à un complexe industriel (site Nyanza) exploité de 1917 à 1978. Dans deux réservoirs situés immédiatement en aval du site Nyanza, les taux estimés de l'accumulation de mercure ont augmenté nettement dans les années 20 et 30, étaient très élevés entre 1976 et 1982, puis ont diminué dans les cinq années qui ont suivi la cessation des activités industrielles et continuent de diminuer depuis la fin des travaux de recouvrement du sol contaminé de ce site en 1991. En général, les sédiments les plus contaminés ont été enfouis, mais la contamination de la strate de 0 à 1 cm est assez marquée dans toutes les carottes prélevées. L'accumulation de mercure dans les sédiments de surface du réservoir était probablement due aux apports continus, bien que beaucoup moindres, du site Nyanza, tandis que les apports récents dans les milieux humides situés en aval étaient attribuables à la remise en circulation du mercure sédimentaire ou au mercure provenant de sources locales non identifiées. Dans les réservoirs, l'enfouissement de sédiments fortement contaminés diminue progressivement la quantité de mercure sédimentaire disponible pour la méthylation. Toutefois, la disponibilité du mercure sédimentaire pour le transport physique et la remise en circulation dans le cycle biogéochimique semblait être plus grande dans les milieux humides situés en aval que dans les réservoirs.

[Traduit par la Rédaction]

Introduction

The Sudbury River in eastern Massachusetts was contaminated by mercury from the Nyanza chemical waste dump site (Nyanza site), a former industrial complex that operated from 1917 to 1978 in the town of Ashland (Wiener and Shields 2000). Fine-grained sediment in downstream areas of the Sudbury River contain substantial mercury, posing potential risks to biota in the river and adjoining wetlands, including the Great Meadows National Wildlife Refuge (Fig. 1). Fish in contaminated reaches of the Sudbury River contained elevated concentrations of mercury, prompting advisories warning against consumption of sport fish from the River (NUS Corporation 1992; Wiener and Shields 2000). To decrease further influx of mercury into the River, the U.S. Environmental Protection Agency excavated and capped highly contaminated soils at the Nyanza site, a remedial action completed in 1991.

The vast majority of mercury retained in freshwater ecosystems eventually becomes associated with bottom sediments (Kudo 1989; Rada et al. 1993). Sediment can function as a sink for mercury in aquatic ecosystems if sediment-associated mercury is isolated from active biogeochemical cycling (Henry et al. 1995). Conversely, the sediments can serve as a source of potentially available mercury, given that some of the inorganic mercury in the sediment can be meth-

Received August 29, 1997. Accepted June 8, 1999.
J14190

B.E. Frazier[1] **and R.G. Rada.** River Studies Center, University of Wisconsin-La Crosse, La Crosse, WI 54601, U.S.A.
J.G. Wiener.[2] U.S. Geological Survey, Biological Resources Division, Upper Midwest Environmental Sciences Center, 2630 Fanta Reed Road, La Crosse, WI 54603, U.S.A.
D.R. Engstrom. St. Croix Watershed Research Station, Science Museum of Minnesota, Marine on St. Croix, MN 55047, U.S.A.

[1]Current address: U.S. Fish and Wildlife Service, 11103 E Montgomery Dr., Spokane, WA 99206, U.S.A.
[2]Author to whom all correspondence should be addressed. e-mail: james_wiener@usgs.gov

© 2000 NRC Canada

Fig. 1. Map of the Sudbury River basin showing the four contaminated areas downstream from the Nyanza site (Reservoir 2, Reservoir 1, the wetland coring sites within the Great Meadows National Wildlife Refuge, and Fairhaven Bay) and the reference area (Whitehall Reservoir) from which sediment cores were taken. The river flows in a northeasterly direction. The black bars represent dams on the Sudbury River system.

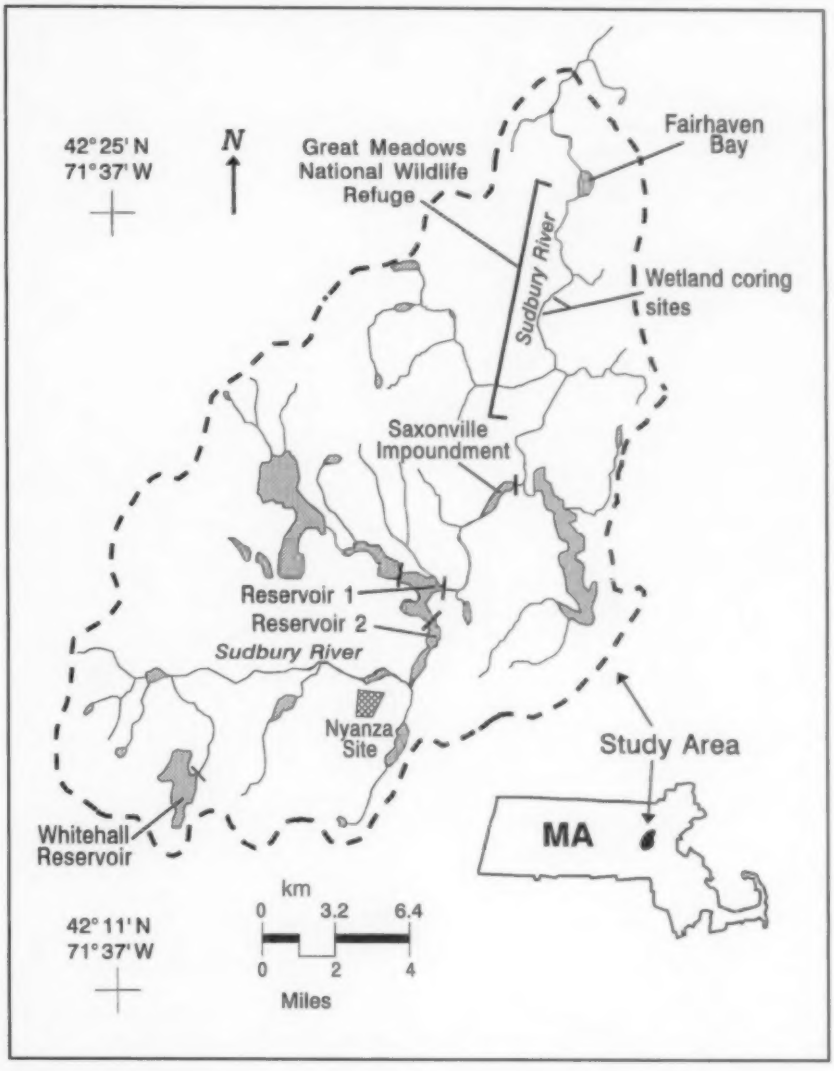

ylated (Winfrey and Rudd 1990; Ramlal et al. 1993; Gilmour et al. 1998).

The present study assessed the vertical distribution (stratigraphy) and historic accumulation of mercury in recent depositional sediments in the Sudbury River, focusing on depositional areas and palustrine wetlands in the river basin. Burial in sediments often creates a stratigraphic record that reflects the time of deposition and relative environmental concentrations of mercury. Inorganic mercury binds tightly to organic particles and shows little tendency to diffuse within the sediment profile once buried (Fitzgerald et al. 1998; Bloom et al. 1999). Thus, long-term temporal trends in influxes of mercury to surface waters can be estimated or reconstructed by detailed analyses of sediment cores (Swain et al. 1992; Engstrom and Swain 1997). Our objectives were to (*i*) determine the vertical distribution of mercury in sediments from the river basin and (*ii*) estimate the recent accumulation of mercury in depositional sediments.

Methods

Study area

We studied five areas in the Sudbury River basin. Four of these areas (Reservoir 2, Reservoir 1, a wetland area within the Great Meadows National Wildlife Refuge, and Fairhaven Bay) spanned a spatial gradient in the intensity of mercury pollution attributed to the upstream Nyanza site (Fig. 1). Reservoirs 2 and 1 were small reservoirs constructed in the 1870s to provide water to Boston,

© 2000 NRC Canada

Massachusetts. Reservoir 2 was filled in August 1879, and Reservoir 1 was filled in December 1879 (Boston Water Works 1882). The fifth study area, Whitehall Reservoir, was a reference area that had not been directly contaminated by wastes from the Nyanza site. The inundation of Whitehall Reservoir in 1900 flooded what was formerly called Whitehall Pond.

Field procedures

Sediment cores were taken during 14–18 May 1994 with an 88-mm inside diameter piston corer (ASTM 1989). This device recovers the watery uncompacted sediment surface as well as deeper strata without disturbance, displacement, or core shortening (Wright 1991). In Reservoirs 2 and 1, cores were taken within the zones of maximum water depth and sediment thickness, based on a survey by Izbicki and Parker (1991). In Fairhaven Bay and Whitehall Reservoir, cores were taken near the center of the zone of maximum water depth. The core from Whitehall Reservoir was taken within the boundary of the original Whitehall Pond (Boston Water Works 1882).

Two cores were taken within the contaminated wetland area, one near the main channel of the river (wetland near-channel core) and one in a vegetated palustrine wetland about 100 m from the channel (wetland off-channel core). Sampling sites were identified by latitude and longitude with a global positioning system (Magellan® Nav 1000 Pro). Sampling coordinates, water depths, and lengths of cores are given in Table 1.

All cores were maintained in vertical position and sectioned on site with stainless steel implements that were rinsed with surface water to prevent cross-contamination between strata. The uppermost 6 cm of each core was sectioned into 1-cm strata. Sediments at core depths of 6–20 cm were sectioned into 2-cm strata, sediments at 20–50 cm into 3-cm strata, and sediments deeper than 50 cm into 5-cm strata.

The sediment from each stratum was placed into a labeled Zip-Loc® freezer bag, which was sealed and stored on ice in a cooler while in the field. For ^{210}Pb dating, we subsampled each stratum from the cores and placed each subsample into a 20-mL scintillation vial. Within 8 h after collection, the samples were transferred to a conventional freezer (–20°C). Frozen sediment samples were transported to the laboratory and held at –20°C until analysis. Chain-of-custody procedures were followed during the transport and storage of samples (APHA et al. 1992).

Laboratory procedures

After thawing for 1–2 h at room temperature (20 ± 3°C), the bags with samples were massaged by hand to homogenize the sediments. Water and volatile solids content were determined on a 2- to 5-g wet weight subsample from each stratum (APHA et al. 1992). Density of sediment was calculated from the water and volatile solids content with equations from Häkanson and Jansson (1983).

The remaining sediment from each stratum was air-dried at 20 ± 3°C, ground with a porcelain mortar and pestle, passed through a 2-mm sieve, and homogenized (Rada et al. 1993). Total mercury was determined for subsamples (0.2–0.5 g) of air-dried sediment from each stratum, which were digested and analyzed by cold-vapor atomic absorption spectrophotometry following the methods in Rada et al. (1993). Concentrations of total mercury are reported as micrograms per gram dry weight. We determined aluminum as a reference element to assess differences in grain size of the sediment among strata (Rada et al. 1986; Hanson et al. 1993). Total acid-extractable aluminum was determined for 1-g subsamples of the dried sediment. Samples were digested with 20 mL of a 2:1:1 (v/v/v) solution of 16 M HNO_3, 12 M HCl, and deionized water in ignition tubes heated for 1 h at 50°C and then for 12 h at 120°C in aluminum blocks. Samples were analyzed by flame atomic absorption spectrophotometry (APHA et al. 1992).

Sediment cores from the Sudbury River basin were analyzed for excess ^{210}Pb activity to determine age and sediment accumulation rates for the past 100–150 years. ^{210}Pb was measured in 15 to 20 strata for each core through its granddaughter product ^{210}Po, with ^{208}Po added as an internal yield tracer. The polonium isotopes were distilled from 0.5–2.0 g of dry sediment at 550°C following pretreatment with concentrated HCl and plated directly onto silver planchets from a 0.5 N HCl solution (modified from Eakins and Morrison 1978). Activity was measured for 1×10^5 to 6×10^5 s with ion-implanted or silicon-depleted surface barrier detectors and an Ortec alpha spectroscopy system. Unsupported ^{210}Pb was calculated by subtracting supported activity from the total activity measured at each level; supported ^{210}Pb was estimated from the asymptotic activity at depth (the mean of the lowermost samples in a core). Dates and sediment accumulation rates were determined according to the constant rate of supply (CRS) model (Appleby and Oldfield 1978), with confidence intervals calculated by first-order error analysis of counting uncertainty (Binford 1990). The CRS model, which assumes a constant flux of ^{210}Pb to the core site, is the preferred model for systems with variable rates of sediment accumulation (Appleby and Oldfield 1983; Oldfield and Appleby 1984). However, the assumption of a constant ^{210}Pb flux may not be strictly met in the Sudbury River where sedimentation patterns might have shifted with flow or, more specifically, impoundment. This dating uncertainty is greatest for older strata, especially in the cores from the two reservoirs. Nonetheless, the agreement between basal dates from the reservoir cores and the dates of impoundment provides empirical evidence that assumptions of the CRS model have not been seriously violated, and thus, our estimates of the rate of sediment accumulation and mercury accumulation at the coring sites are reasonably accurate.

The mercury accumulation rate for each dated stratum was calculated as the product of the sediment accumulation rate (kilograms per square metre per year) and the total mercury concentration (micrograms per gram dry weight) in the stratum. Sediment enrichment factors (SEF) and mercury flux ratios were estimated for surface and peak strata in each core. The SEF was calculated with the equation

$$(1) \qquad \mathrm{SEF} = (C_s - C_b)/C_b$$

where C_s is the concentration of mercury in the surface or peak stratum and C_b is the estimated natural abundance of mercury (defined as the concentration of mercury in fine-grained sediments attributed to natural mercury cycling processes and native soils of watersheds, before industrial influences in the basin). In each of the cores from the wetland near-channel area, Fairhaven Bay, and Whitehall Reservoir, C_b was calculated as the mean concentration of the six deepest strata. The grand mean of the estimated natural abundance for these three cores was used as the estimate of C_b for the cores from Reservoir 2, Reservoir 1, and the wetland off-channel coring sites; mercury concentrations in the deepest strata of these latter three cores exceeded our estimate of its natural abundance.

To assess the impact of the Nyanza site on recent and maximal mercury enrichment in the sediments from Reservoirs 2 and 1, we estimated what we termed the "source-specific" SEF (S'SEF) for the coring sites in Reservoirs 2 and 1 with the equation

$$(2) \qquad \mathrm{S'SEF} = (C_s - C_{\text{pre-Nyanza}})/C_b$$

where $C_{\text{pre-Nyanza}}$ is the concentration of mercury in the last stratum deposited before 1917. The S'SEF is similar to the SEF, but the numerator was adjusted by subtracting the pre-Nyanza site concentration of mercury in the last stratum deposited before 1917, the year when industrial operations began at the Nyanza site. In calculating the S'SEF, it was assumed that mercury inputs (into Reservoirs 2

© 2000 NRC Canada

Table 1. Information on study areas, coring locations, and sediment cores taken from the Sudbury River basin in May 1994.

Study area	Surface area (ha)	Coring location		Water depth (m)	Core length (cm)	Oldest datable stratum	
		Latitude	Longitude			Depth (cm)	Date[d]
Reservoir 2	47[a]	42°16′42″	71°26′30″	4.4	55	23–26	1894
Reservoir 1	49[a]	42°17′29″	71°26′37″	3.9	38	35–38	1888
Wetland (off-channel)	na	42°23′04″	71°22′59″	1.2	60	32–35	1851
Wetland (near-channel)	na	42°23′15″	71°22′29″	1.0	80	23–26	1846
Fairhaven Bay	27[b]	42°25′28″	71°21′12″	3.4	110	35–38	1838
Whitehall Reservoir	233[c]	42°13′03″	71°34′44″	8.3	125	60–65	1831

Note: Sites in the Sudbury River are listed in order from nearest to furthest downstream from the Nyanza site. Whitehall Reservoir is a reference area in the basin. na, not applicable.

[a]Izbicki and Parker (1991).

[b]U.S. Geological Survey, Maynard, Mass., topographical map 42071-D3-TM-025.

[c]Massachusetts Division of Fisheries and Wildlife, Westboro, Mass, map of Whitehall Reservoir.

[d]Estimated date of sediment deposition at the bottom of the stratum based on ^{210}Pb dating.

and 1) attributable to sources other than the Nyanza site remained constant since the last stratum before 1917 was deposited.

The Hg flux ratio is analogous to the SEF but uses the rate of mercury accumulation rather than concentration, as follows:

$$\text{Hg flux ratio} = (A_s - A_b)/A_b \quad (3)$$

where A_s is the rate of mercury accumulation in the surface or peak stratum and A_b is the background rate of mercury accumulation. The A_b for the wetland near-channel, wetland off-channel, Fairhaven Bay, and Whitehall Reservoir cores was estimated from the deepest datable stratum in each core. For the Reservoir 2 and 1 cores, A_b was estimated as the product of the sediment accumulation rate (in the oldest datable stratum) and the estimated grand mean of the natural abundance of mercury. The mercury flux ratio for the Reservoir 2 and 1 coring sites, therefore, is a theoretical flux ratio based on presumed conditions in the reservoirs had they existed in preindustrial times.

Quality assurance

To estimate the accuracy of our mercury determinations, we digested and analyzed the following quality assurance samples with each analytical batch of samples: procedural blanks, procedural calibration standards, procedurally (matrix) spiked samples, National Institute of Standards and Technology standard reference materials (NIST river sediment, Buffalo River sediment, and Montana soil), and a National Research Council of Canada certified reference material (NRCC PACS-1 sediment). Our mean measured concentrations of total mercury were within the certified ranges for three reference materials and within 6% of the lower limit of the certified range for the fourth material, NIST Montana soil. Recovery of mercury from analyses of 70 procedurally spiked sediment samples averaged 97 ± 2% (95% confidence interval). Our method precision (relative standard deviation), estimated from analyses of 26 sets of triplicate subsamples, averaged 9% and ranged from less than 1 to 24%. Mercury concentrations in all core strata analyzed exceeded our method detection limit (0.7 ng·g dry weight^{-1}) and our limit of quantitation (1.8 ng·g^{-1}), both calculated according to APHA et al. (1992).

The error (±1 SD) of estimating the age of sediment strata was less than 2 years for strata up to the following ages: 65 years in the Reservoir 2 core, 30 years in the Reservoir 1 core, 48 years in the wetland off-channel core, 40 years in the wetland near-channel core, and 67 years in the Fairhaven Bay core. For the Whitehall Reservoir core, the error ranged from about 3 to 4 years in strata dated up to 76 years old.

Results

Variation in mercury concentration in cores taken downstream of the Nyanza site was not caused by variation in either the grain size or the volatile solids content of sediment. The stratigraphic profile for the ratio of mercury to aluminum in each core, for example, closely paralleled the profile for mercury concentration. Consequently, we do not present data on aluminum concentrations or volatile solids in the cores.

Dating and sediment accumulation

The ^{210}Pb dating of the cores provided fairly robust chronologies that dated back to the mid- to late 1800s. In all cases, rates of sediment accumulation appeared conformable, with little evidence of depositional hiatuses, slumping, or substantial bioturbation.

All cores showed declining levels of unsupported ^{210}Pb to a depth of 30–60 cm. Supported (background) activity, indicated where ^{210}Pb becomes constant, was reached in the deeper sections of cores from Fairhaven Bay (0.65 pCi·g^{-1}) (1 pCi = 37 mBq), Whitehall Reservoir (0.56 pCi·g^{-1}), and the two wetland areas (0.29 and 0.68 pCi·g^{-1}) (Fig. 2). Both Fairhaven Bay and Whitehall Reservoir were lake basins before impoundment of the Sudbury River (Fairhaven Bay was never dammed); therefore, the older sediments in these cores can be used to estimate supported ^{210}Pb for Reservoirs 1 and 2, which lack lacustrine sediments older than 1879. The core from Reservoir 1, which terminated on hard clay at 39.5 cm, showed a continuous decline in total ^{210}Pb to a minimum of 1.08 pCi·g^{-1}, indicating that supported ^{210}Pb values were not reached at this site. The core from Reservoir 2 showed a sharp transition from lacustrine sediments to peat below 26 cm. ^{210}Pb activity continued to decline below this transition to values approaching 0.39 pCi·g^{-1}. Because peat probably contains less supported ^{210}Pb than lake sediment (as shown by the wetland off-channel core), the ^{210}Pb activities in the peat cannot be used to estimate supported activity for the overlying deposits. Instead, supported ^{210}Pb for Reservoirs 1 and 2 was estimated from values from the Fairhaven Bay core. In both cases, the missing inventory of unsupported ^{210}Pb, estimated by extrapolation, was less than 5% of the total inventory for the core, indicating that dating should be reliable except for the oldest strata.

In all six cores, the decline in unsupported ^{210}Pb activity with depth was nonexponential, indicating changes in sedi-

© 2000 NRC Canada

Fig. 2. Stratigraphic profiles for total ^{210}Pb in sediment cores from the Sudbury River basin. Supported ^{210}Pb for Reservoirs 1 and 2 was estimated from the Fairhaven Bay core (see text). Error bars represent ±1 SD based on counting statistics.

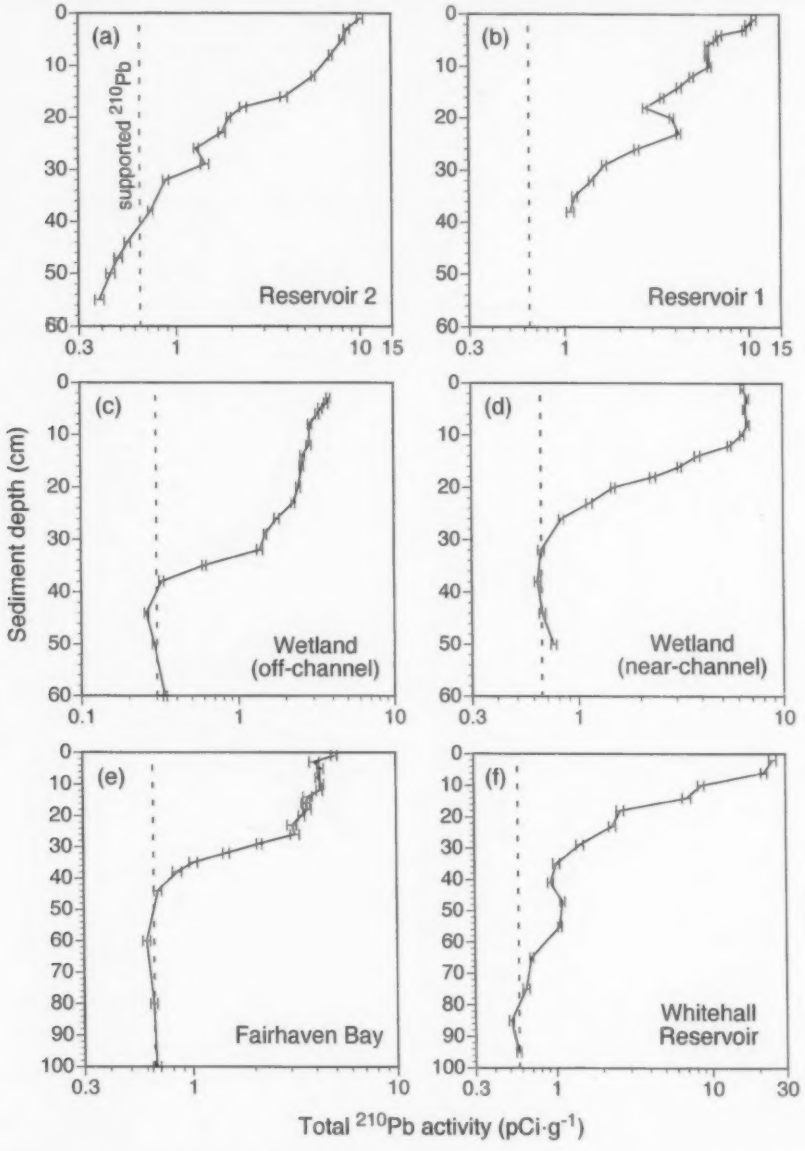

ment accumulation according to the CRS dating model (Fig. 2). In the wetland near-channel core, ^{210}Pb was nearly constant in the uppermost 10 cm of sediment. Although it is possible that this zone of uniform ^{210}Pb indicates sediment mixing (bioturbation), addition of a mixing term to the CRS model changed the resulting dates only slightly because the putative mixed zone was less than 15% of the length (density corrected) of the ^{210}Pb profile (Oldfield and Appleby 1984).

The oldest date from Reservoir 1 was 1887 at 38 cm. This value is quite reasonable given that the impoundment was created in 1879 and an additional centimetre or so of sediments lied beneath the deepest dated stratum. In Reservoir 2, the shift from lake sediment to preimpoundment peat (26 cm) was dated at 1894. Although this date was 15 years later than the date of impoundment (also 1879), the sediment increment at 26–29 cm was intermediate in volatile solids content, compared with shallower and deeper strata, and may represent a transition layer corresponding more closely to the time of reservoir inundation. The ^{210}Pb chronologies from Whitehall Reservoir, Fairhaven Bay, and the two wetland cores were reasonable, and the modeling of these data was straightforward.

Plots of sediment accumulation rate versus ^{210}Pb dates showed distinctly different trends among the six cores (Fig. 3). Reservoir 2 showed a doubling in sediment flux

© 2000 NRC Canada

Fig. 3. Sediment accumulation rates versus ^{210}Pb dates for sediment cores from the Sudbury River basin. Error bars represent ±1 SD based on first-order propagation of counting uncertainty.

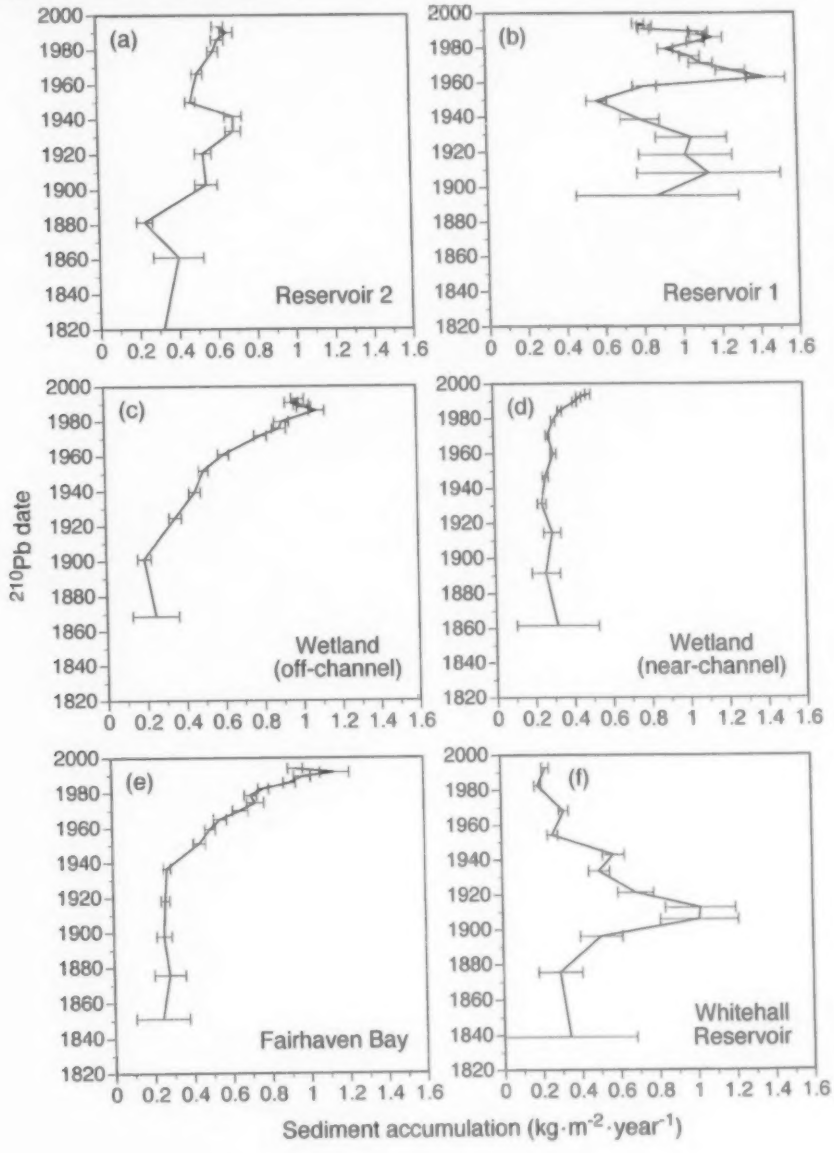

from about 0.3 to 0.6 kg·m^{-2}·year^{-1} at the transition from peat to lacustrine sediment after 1880, which was close to the time of impoundment. Increased sediment accumulation rate might be expected under conditions where a preexisting wetland was permanently inundated by a larger drainage system. Likewise, Whitehall Reservoir (formerly Whitehall Pond) showed a major increase in the rate of sediment accumulation after impoundment in 1900 but declined sharply after 1910. The rate of sediment accumulation varied little at the Reservoir 2 coring site between the time of impoundment and 1994, the year of sampling. In Reservoir 1, sediment accumulation rate fluctuated around a mean of 1 kg·m^{-2}·year^{-1} but was asynchronous with Reservoir 2 and the other coring sites. Patterns of sediment accumulation were similar in the wetland off-channel site and Fairhaven Bay, with sediment flux remaining relatively steady at 0.2–0.4 kg·m^{-2}·year^{-1} until about 1940 and increasing sharply thereafter. At the wetland near-channel coring site, sediment accumulation rates remained constant at 0.3 kg·m^{-2}·year^{-1} until about 1980. The increase in the rate of sediment accumulation at this wetland site after 1980 may have been real or an artifact of bioturbation; in either case, the increase only slightly influenced the profile of mercury accumulation for this location.

© 2000 NRC Canada

Mercury concentrations and SEFs

The natural abundance of mercury, estimated from concentrations in the six deepest strata, was 0.049 μg·g dry weight^{-1} in the wetland near-channel core, 0.038 μg·g^{-1} in Fairhaven Bay, and 0.046 μg·g^{-1} in Whitehall Reservoir. The grand mean of these three cores was 0.044 μg·g^{-1}; this value is a reasonable estimate of the preindustrial background concentration of mercury in fine-grained sediments in the Sudbury River basin.

SEFs in contaminated sediments at coring sites downstream from the Nyanza site ranged from 20 to nearly 1000 (Table 2). Concentrations of mercury and SEFs for the uppermost 1 cm of the cores from Reservoir 2, Reservoir 1, the wetland (near-channel core), and Fairhaven Bay were roughly one fourth to one half of those in the deeper, most-contaminated strata (Fig. 4; Table 2). In the Reservoir 2 core, taken about 4.3 km downstream from the Nyanza site, concentrations of mercury were 18 μg·g^{-1} in the 0- to 1-cm stratum, 41–44 μg·g^{-1} in the 6- to 12-cm stratum, and 0.09–0.14 μg·g^{-1} in strata deeper than 32 cm, which were probably preimpoundment soils (Fig. 4). In the Reservoir 1 core, taken 6.5 km downstream from the Nyanza site, the most contaminated sediments (20–32 μg·g^{-1}) were also 6–12 cm deep, with concentrations declining from 13.5 μg·g^{-1} at 5–6 cm to 7.2 μg·g^{-1} at the sediment surface (Fig. 4).

In the wetland off-channel core, concentrations of mercury ranged from 0.07 to 0.09 μg·g^{-1} below 35 cm; moving upward through the core, concentrations increased about 10-fold, ranging from 0.86 to 1.20 μg·g^{-1} in the uppermost 32 cm (Fig. 4). At this location, the surface SEF was about 77% of the peak SEF (Table 2). Mercury concentration in the wetland near-channel core ranged from 1.1 to 1.7 μg·g^{-1} in the upper 10 cm, was about 6 μg·g^{-1} at 12–16 cm deep, and ranged from 0.03 to 0.07 μg·g^{-1} below 29 cm (Fig. 4). The sharp peak in mercury concentration at 12–16 cm in this core would not have been preserved if sediments had been substantially mixed, indicating that bioturbation had little impact on core stratigraphy. In the Fairhaven Bay core, taken about 36 km downstream from the Nyanza site, concentrations were about 2 μg·g^{-1} in the uppermost 12 cm and ranged from 3.4 to 3.7 μg·g^{-1} in strata between 14 and 26 cm and from 0.03 to 0.05 μg·g^{-1} below 47 cm.

Concentrations of mercury in the core from the reference area, Whitehall Reservoir, ranged from 0.04 to 0.06 μg·g^{-1} in strata below 70 cm. Concentrations gradually increased upward through the core and were greatest in the uppermost 10 cm, ranging from 0.32 to 0.38 μg·g^{-1} (Fig. 4). The surface and peak SEFs in this core were 6.9 and 7.2, respectively (Table 2).

The S′SEFs for the Reservoir 2 coring site were 376 for the surface stratum and 971 for the most contaminated stratum. For the Reservoir 1 core, the surface S′SEF value was 149 and the maximum value was 703. Comparison of these S′SEF values with the calculated SEFs (Table 2) indicated that 91–94% of the most recent (i.e., surficial) anthropogenic mercury was from the Nyanza site. When the most contaminated sediments were deposited, an estimated 97–98% of the anthropogenic mercury was from the Nyanza site.

Mercury accumulation rates and flux ratios

The estimated annual rates of mercury accumulation were greatest during the late 1970s to early 1980s at the Reservoir 2 and 1 coring sites and during the mid-1950s to the mid-1960s at the wetland near-channel coring site but have since decreased at these sites (Fig. 5). The most recent estimated mercury accumulation rates and Hg flux ratios were 18–42% of the earlier maximal values at these three sites (Fig. 5; Table 2). The estimated rate of mercury accumulation at the Reservoir 1 coring site, for example, was less than 1.0 mg·m^{-2}·year^{-1} from the time of inundation through the 1920s, increased greatly to a maximum of 29 mg·m^{-2}·year^{-1} during the late 1970s to early 1980s, and thereafter declined to 5.7 mg·m^{-2}·year^{-1} in the 0- to 1-cm stratum (Fig. 5). In contrast, the estimated annual rate of mercury accumulation has not changed notably at the Fairhaven Bay site since the mid-1940s or at the wetland off-channel site since the 1960s (Fig. 5). The surface (most recent) mercury flux ratios were still estimated to be more than 75% of the peak mercury flux ratios at the Fairhaven Bay and wetland off-channel coring sites. At the wetland off-channel coring site, the estimated rates of mercury accumulation were less than 0.5 mg·m^{-2}·year^{-1} before the 1930s; thereafter, the rate gradually increased and has varied little (0.86–1.08 mg·m^{-2}·year^{-1}) since about 1969. In contrast, the estimated rate of mercury accumulation at the wetland near-channel coring site has varied greatly over the past 150 years; rates of mercury accumulation were less than 0.10 mg·m^{-2}·year^{-1} until the early 1900s, increased to nearly 2.0 mg·m^{-2}·year^{-1} in the 1950s, and decreased to 0.7 mg·m^{-2}·year^{-1} in the 1990s. At the Fairhaven Bay coring site, estimated rates of mercury accumulation increased in the early 1900s but varied little between 1946 and 1994 (1.6–2.4 mg·m^{-2}·year^{-1}) (Fig. 5). The estimated rate of mercury accumulation in the uppermost stratum (1.8 mg·m^{-2}·year^{-1}) was similar to rates during about 1930–1970, when the most contaminated strata were deposited.

The estimated rates of mercury accumulation in the most recently deposited sediments generally decreased with increasing distance downstream from the Nyanza site (Fig. 5). Recent accumulation rates were 11, 5.7, 0.9, 0.7, and 1.8 mg·m^{-2}·year^{-1} at coring sites in Reservoir 2, Reservoir 1, wetland off-channel, wetland near-channel, and Fairhaven Bay, respectively. Maximal estimated rates of mercury accumulation were similar in the Reservoir 2 and 1 coring sites but were much less at the downstream wetland and Fairhaven Bay coring sites.

Estimated mercury accumulation rates and mercury flux ratios at the coring site in Whitehall Reservoir, the reference area, were very low compared with those in contaminated reaches of the Sudbury River (Fig. 5). In the mid-1800s, the estimated rate of mercury accumulation was about 0.02 mg·m^{-2}·year^{-1}, and the rate of sediment accumulation was about 0.3 kg·m^{-2}·year^{-1} (Figs. 3 and 5). Estimated rates of both mercury and sediment accumulation began to increase in the late 1800s. After impoundment in 1900, the rate of sediment accumulation increased to just over 1.0 kg·m^{-2}·year^{-1}, and the estimated rate of mercury accumulation increased to about 0.09 mg·m^{-2}·year^{-1}. From the late 1910s to about 1940, the rate of sediment accumulation decreased to 0.50 kg·m^{-2}·year^{-1}, but the estimated rate of mercury accumulation remained at about 0.09 mg·m^{-2}·year^{-1}. The estimated rate of mercury accumulation was greatest in the 1940s (0.12 mg·m^{-2}·year^{-1}) and corresponded to a slight

© 2000 NRC Canada

Table 2. Sediment enrichment factors (SEF) and mercury flux ratios in the most-recent (surface) sediment strata and in the most-contaminated (peak) strata of cores from the Sudbury River basin.

	Surface[a]		Peak[b]	
Study area	SEF	Hg flux ratio	SEF	Hg flux ratio
Reservoir 2	401	456	997 (6–8)	1084 (6–8)
Reservoir 1	163	146	717 (8–10)	754 (8–10)
Wetland (off-channel)	20	8.9	26 (18–20)	11 (6–8)
Wetland (near-channel)	28	18	130 (12–14)	53 (12–14)
Fairhaven Bay	51	31	97 (18–20)	41 (2–3)
Whitehall Reservoir	6.9	2.4	7.2 (2–3)	4.1 (16–18)

Note: The sediment depth (cm) for the most-contaminated stratum is given in parentheses.

[a]The surface SEF pertains to the uppermost 1 cm of a core; the surface mercury flux ratio pertains to the uppermost 1 cm of a core, except the core from the wetland off-channel site (uppermost 3 cm) and the Whitehall Reservoir (uppermost 2 cm).

[b]The peak SEF pertains to the stratum with the greatest concentration of mercury, whereas the peak flux ratio pertains to the stratum with the greatest rate of mercury accumulation.

Fig. 4. Mercury in sediment cores from the Sudbury River basin. Arrows denote the bottom of each sediment core. The estimated year of deposition is given for the bottom of the stratum with the greatest mercury concentration, delineated in solid black for each core. The triangle denotes the last stratum deposited before 1917, the year that industrial operations began at the Nyanza site.

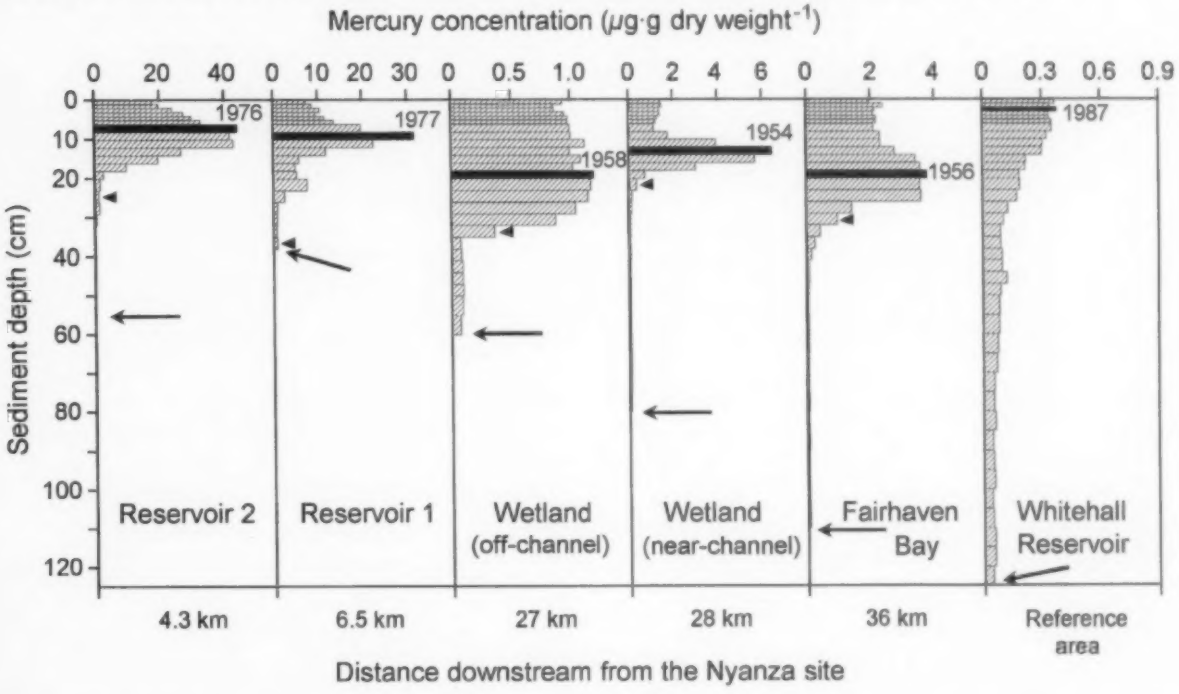

increase in the rate of sediment accumulation (0.58 kg·m^{-2}·year^{-1}). Since the early 1950s, the estimated rate of mercury accumulation has ranged from 0.06 to 0.10 mg·m^{-2}·year^{-1}, correlating with the rate of sediment accumulation (0.19–0.32 kg·m^{-2}·year^{-1}).

Discussion

Temporal and spatial patterns in mercury contamination of sediments and analysis of SEFs confirm the Nyanza site as a primary source of the mercury in the Sudbury River ecosystem. The timing of mercury accumulation in Reservoirs 2 and 1, the two coring areas nearest the Nyanza site, coincided with industrial operations there. The estimated rate of mercury accumulation at the reservoir coring sites increased markedly in the 1920s and 1930s, soon after the industrial complex opened in 1917, and were greatest during the late 1970s to early 1980s. Estimated rates of mercury accumulation at the two reservoir coring sites decreased a few years after industrial operations ended in 1978 and have decreased further since excavation and capping of contaminated soil at the Nyanza site was completed in 1991.

Concentrations and accumulation rates of mercury in recent sediment deposits generally decreased with increasing

© 2000 NRC Canada

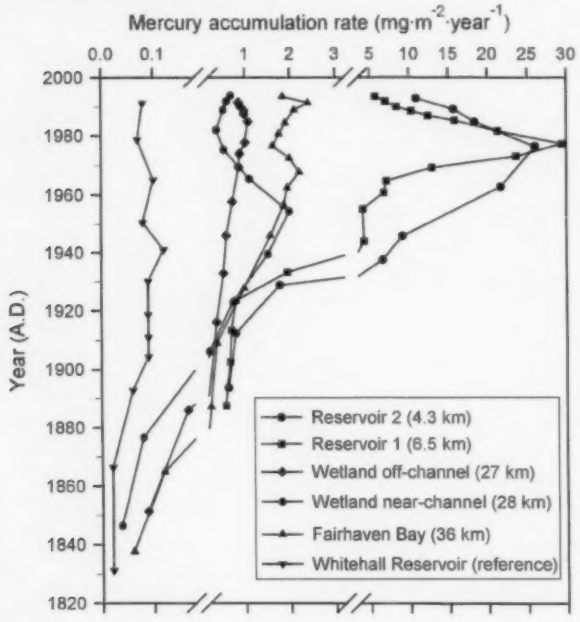

Fig. 5. Estimated annual rates of mercury accumulation in sediment cores from the Sudbury River basin. Note the two changes in scale on the horizontal axis.

distance downstream from the Nyanza site. This pattern in sedimentary mercury concentration was also found by Colman et al. (1999) and Naimo et al. (2000). In our study, the concentration of mercury in sediments was greatest (44 μg·g dry weight^{-1}) in Reservoir 2, the first reservoir downstream from the Nyanza site.

Our estimates of the natural abundance of mercury in cores from the Sudbury River basin (0.038–0.049 μg·g^{-1}) were similar to estimates for fine-grained sediments from midcontinental lakes and rivers in North America. Rada et al. (1989), for example, reported natural mercury concentrations of 0.04–0.07 μg·g^{-1} in cores from 11 northern Wisconsin lakes. Balogh et al. (1997) estimated a value of 0.044 μg·g^{-1} for soils in the Minnesota River basin, and J.G. Wiener (U.S. Geological Survey, La Crosse, Wis., unpublished data) estimated a natural abundance of 0.041 μg·g^{-1} in a core from Lake Pepin on the Upper Mississippi River.

Concentrations of mercury in the most recently deposited sediments (uppermost 1 cm) ranged from 0.93 to 17.7 μg·g^{-1} in our cores taken downstream from the Nyanza site, far exceeding the natural abundance of mercury in fine-grained sediments from the river basin. The high concentrations in surficial sediments were presumably not derived from the upward movement of mercury within the core profiles. Upward diffusion of mercury from the deeper, more contaminated strata seems improbable, given the high organic content of these sediments (Gobeil and Cossa 1993; Hurley et al. 1994). Substantial vertical mixing of sediments was not evident from the ^{210}Pb profiles. Rather, the high concentrations in surficial sediments indicate that some mercury is still entering or recycling within the ecosystem. The continuing recent accumulation of mercury in Reservoirs 2 and 1 was probably from the continuing, albeit much lesser, inputs of mercury from the Nyanza site, based on our findings and the mass-balance analysis of Waldron et al. (2000).

Further downstream, at the wetland off-channel and Fairhaven Bay locations, estimated rates of mercury accumulation and mercury flux ratios in the surficial sediments were more than three fourths of the historic maximal values. This temporal pattern is in contrast with the recent substantive decreases in mercury accumulation rates at the coring sites in Reservoirs 2 and 1. The continued high rates of mercury accumulation at the wetland off-channel and Fairhaven Bay sites are attributable partly to the increased rates of sedimentation at these sites during recent decades. Moreover, some of the mercury accumulating in surficial sediments at the wetland off-channel and Fairhaven Bay sites may have originated from other, unidentified point sources downstream of the Nyanza site (NUS Corporation 1992; Waldron et al. 2000).

Mercury in surficial sediments at these downstream sites cannot be logically attributed to contemporary inputs of mercury from the Nyanza site or to mobilization of contaminated sediments from the reservoirs upstream (Reservoir 2, Reservoir 1, and the Saxonville Impoundment). In 1995, only 32% of the mercury load transported in the river downstream of the Saxonville Impoundment (15 km downstream) was attributable to contemporary inputs from the Nyanza site (Waldron et al. 2000). Under normal flow conditions, the upstream impoundments export considerably less total mercury than they import (Waldron et al. 2000). Results of sediment transport modeling similarly indicate that very little contaminated bed sediment is mobilized and transported from Reservoirs 2 and 1 to downstream areas, even during record floods (D. Abraham, U.S. Army Corps of Engineers, Waterways Experiment Station, Vicksburg, Miss., unpublished data).

A possible source of the continuing sedimentary mercury accumulations at the wetland off-channel and Fairhaven Bay sites is remobilization and recycling of contaminated sediments from wetland areas or the river channel upstream. Waldron et al. (2000) found that during July 1995, concentrations of total mercury in the river increased from about 5 to 25 ng·L^{-1} after flowing through 5 km of palustrine wetlands downstream from the Saxonville Impoundment. This suggests that mercury was being transported laterally from the adjoining wetlands, presumably in association with suspended sediment or organic particles (Balogh et al. 1997; Waldron et al. 2000).

The pattern of mercury deposition at our wetland near-channel coring site (taken about 5 m beyond the river bank) was similar to that in a core taken within the river channel at a point about 6 km upstream by Colman et al. (1999). These two cores had low mercury concentrations at depths greater than 25 cm, maximum concentrations between 5 and 15 cm, and decreasing concentrations toward the surface of the sediment. At our near-channel coring site, the estimated mercury accumulation rate declined sharply in recent decades, as it did in the two upstream reservoir sites, but the decrease preceded the closure of the Nyanza site by about 20 years. The estimated maximum rate of mercury accumulation at the wetland near-channel location occurred during the mid-1950s to the mid-1960s, whereas the largest recorded flood

© 2000 NRC Canada

in the river occurred in 1955. Maximum flow during this flood at the Reservoir 1 dam was 137 $m^3 \cdot s^{-1}$. For comparison, the 110-year average flow at the dam was 3.3 $m^3 \cdot s^{-1}$ (U.S. Geological Survey 1987). The 1955 flood, which is considered a 100-year flood, could have moved substantial amounts of mercury from the Nyanza site to the wetland areas downstream. Concentrations of total mercury, for example, reached 92 $ng \cdot L^{-1}$ at a location just downstream from the Nyanza site during peak flow after a brief storm in July 1995 (Waldron et al. 2000). Similarly, in the Minnesota River, concentrations of total mercury ranged from less than 1.0 $ng \cdot L^{-1}$ in winter (low-flow months) to greater than 35 $ng \cdot L^{-1}$ following a spring precipitation event (Balogh et al. 1997). The decrease in mercury concentration and mercury accumulation rate toward the surface of the wetland near-channel core could reflect remobilization or dilution of highly contaminated sediments deposited during the 1955 flood.

As expected, sedimentary concentrations and estimated recent accumulation rates of mercury in contaminated reaches of the Sudbury River vastly exceeded those in cores from the Whitehall Reservoir as well as several mid-continental North American lakes that received mercury largely via atmospheric deposition (Rada et al. 1989; Engstrom and Swain 1997). Surficial sediments in the core from the Whitehall Reservoir were enriched with mercury, and the maximum SEF of 7.2 in the Whitehall Reservoir core was much greater than the maximum SEFs (0.8–2.8) reported for 11 northern Wisconsin seepage lakes lacking on-site anthropogenic sources of mercury (Rada et al. 1989). The enrichment of surficial lacustrine sediments in North America is a widespread phenomenon, often attributed to atmospheric deposition of mercury from anthropogenic sources (Rada et al. 1989; Swain et al. 1992; Engstrom and Swain 1997).

The cores from Reservoir 2, Reservoir 1, the wetland near-channel site, and Fairhaven Bay had subsurface peaks in total mercury concentration, a stratigraphic pattern observed in other aquatic systems where mercury loadings from industrial point sources have decreased (Rada et al. 1986; Parks and Hamilton 1987; Lodenius 1991; Klein and Jacobs 1995). The gradual burial of the most contaminated sediments is probably decreasing the amount of inorganic mercury available for microbial methylation within the reservoirs and Fairhaven Bay, given that the net rate of methylation is consistently greatest in the uppermost 5 cm of the sediment profile and that little methyl mercury is produced in deeper sediments (Rudd et al. 1983; Korthals and Winfrey 1987; Gilmour et al. 1998). Disturbance of the contaminated sediments in the Sudbury River could, however, substantively increase the exposure of resident biota to mercury. Contaminated bottom sediments can be resuspended into the water column by human disturbance or by natural processes, such as bioturbation and wind-induced turbulence (Kristensen et al. 1992; Evans 1994). Results from ^{210}Pb dating of our sediment cores, however, indicated intact sediment profiles showing little evidence of bioturbation or past physical disturbance. The profiles for mercury in the cores from Reservoirs 1 and 2 also showed no evidence of bioturbation or physical disturbance. These cores displayed fine-scale trends of decreasing contamination from the most contaminated strata to the sediment–water interface, a pattern evident across 1-cm strata in each of the cores. Similarly, sediment-transport modeling of Reservoirs 2 and 1 (D. Abraham, U.S. Army Corps of Engineers, Waterways Experiment Station, Vicksburg, Miss., unpublished data) showed that scouring and movement of sediments would be minimal and occur only in small, localized areas of the reservoirs, even during extreme floods. Barring human disturbance or dam failure, the probability of substantial resuspension or transport of the contaminated sediments in the reservoirs would seem to be small.

Acknowledgments

This work was funded by the U.S. Environmental Protection Agency (Region I) through an interagency agreement with the U.S. Fish and Wildlife Service (Region 5). We thank Pamela Shields, Susan Svirsky, and Steven Mierzykowski for assistance during the initial planning of this study. We are grateful to personnel at the Great Meadows National Wildlife Refuge for allowing the use of their facility during sampling trips. Teresa Naimo and Elizabeth Allen assisted with the sampling. Elizabeth Allen, Lorrine Rabuck, Chad Hammerschmidt, and Kristi Jackson provided technical assistance in the laboratory. We thank Clare Kirk and Thomas Patriarca of the Massachusetts Water Resource Authority for providing access to archived historical records on the reservoirs. We are grateful to Teresa Naimo, William Orem, David Powell, Edward Swain, Marcus Waldron, two anonymous referees, and an Associate Editor for constructive reviews of an earlier draft of the manuscript.

References

APHA et al. (American Public Health Association, American Water Works Association, and Water Environment Federation). 1992. Standard methods for the examination of water and wastewater. 18th ed. APHA, Washington, D.C.

Appleby, P.G., and Oldfield, F. 1978. The calculation of lead-210 dates assuming a constant rate of supply of unsupported ^{210}Pb to the sediment. Catena, **5**: 1–8.

Appleby, P.G., and Oldfield, F. 1983. The assessment of ^{210}Pb data from sites with varying sediment accumulation rates. Hydrobiologia, **103**: 29–35.

ASTM (American Society of Testing and Materials). 1989. Standard guide for core sampling submerged, unconsolidated sediments. *In* 1989 Annual book of ASTM standards: water and environmental technology. Vol. 11.02. Water (II). ASTM, Philadelphia, Pa. pp. 585–597.

Balogh, S.J., Meyer, M.L., and Johnson, D.K. 1997. Mercury and suspended sediment loadings in the lower Minnesota River. Environ. Sci. Technol. **31**: 198–202.

Binford, M.W. 1990. Calculation and uncertainty analysis of ^{210}Pb dates for PIRLA Project lake sediment cores. J. Paleolimnol. **3**: 253–267.

Bloom, N.S., Gill, G.A., Camppellino, S., Dobbs, C., McShea, L., Driscoll, C., Mason, R., and Rudd, J. 1999. Speciation and cycling of mercury in Lavaca Bay, Texas, sediments. Environ. Sci. Technol. **33**: 7–13.

Boston Water Works. 1882. Additional supply from Sudbury River. Rockwell and Churchill, Boston, Mass.

© 2000 NRC Canada

Colman, J.A., Waldron, M.C., Breault, R.F., and Lent R.M. 1999. Distribution and transport of total mercury and methylmercury in mercury-contaminated sediments in reservoirs and wetlands of the Sudbury River, east-central Massachusetts. U.S. Geol. Surv. Water-Resour. Invest. Rep. 99-4060.

Eakins, J.D., and Morrison, R.T. 1978. A new procedure for the determination of lead-210 in lake and marine sediments. Int. J. Appl. Radiat. Isot. **29**: 531–536.

Engstrom, D.R., and Swain, E.B. 1997. Recent declines in atmospheric mercury deposition in the Upper Midwest. Environ. Sci. Technol. **31**: 960–967.

Evans, R.D. 1994. Empirical evidence of the importance of sediment resuspension in lakes. Hydrobiologia, **284**: 5–12.

Fitzgerald, W.F., Engstrom, D.R., Mason, R.P., and Nater, E.A. 1998. The case for atmospheric mercury contamination in remote areas. Environ. Sci. Technol. **32**: 1–7.

Gilmour, C.C., Riedel, G.S., Ederington, M.C., Bell, J.T., Benoit, J.M., Gill, G.A., and Stordal, M.C. 1998. Methylmercury concentrations and production rates across a trophic gradient in the northern Everglades. Biogeochemistry, **40**: 327–345.

Gobeil, C., and Cossa, D. 1993. Mercury in sediments and sediment pore water in the Laurentian Trough. Can. J. Fish. Aquat. Sci. **50**: 1794–1800.

Häkanson, L., and Jansson, M. 1983. Principles of lake sedimentology. Springer-Verlag, Berlin.

Hanson, P.J., Evans, D.W., Colby, D.R., and Zdanowicz, V.S. 1993. Assessment of elemental contamination in estuarine and coastal environments based on geochemical and statistical modeling of sediments. Mar. Environ. Res. **36**: 237–266.

Henry, E.A., Dodge-Murphy, L.J., Bigham, G.N., Klein, S.M., and Gilmour, C.C. 1995. Total mercury and methylmercury mass balance in an alkaline, hypereutrophic urban lake (Onondaga Lake, N.Y.). Water Air Soil Pollut. **80**: 509–518.

Hurley, J.P., Krabbenhoft, D.P., Babiarz, C.L., and Andren, A.W. 1994. Cycling processes of mercury across sediment/water interfaces in seepage lakes. *In* Environmental chemistry of lakes and reservoirs. *Edited by* L.A. Baker. American Chemical Society, Washington, D.C. pp. 425–449.

Izbicki, J.A., and Parker, G.W. 1991. Water depth and thickness of sediment in Reservoirs 1 and 2, Framingham and Ashland, Massachusetts. U.S. Geol. Surv. Open-File Rep. 91-508.

Klein, S.M., and Jacobs, L.A. 1995. Distribution of mercury in the sediments of Onondaga Lake, N.Y. Water Air Soil Pollut. **80**: 1035–1038.

Korthals, E.T., and Winfrey, M.R. 1987. Seasonal and spatial variations in mercury methylation and demethylation in an oligotrophic lake. Appl. Environ. Microbiol. **53**: 2397–2404.

Kristensen, P., Sondergaard, M., and Jeppesen, E. 1992. Resuspension in a shallow eutrophic lake. Hydrobiologia, **228**: 101–109.

Kudo, A. 1989. Mercury in the Ottawa River (Canada). *In* Aquatic ecotoxicology: fundamental concepts and methodologies. Vol. 1. *Edited by* A. Boudou and F. Ribeyre. CRC Press, Boca Raton, Fla. pp. 201–217.

Lodenius, M. 1991. Mercury concentrations in an aquatic ecosystem during twenty years following abatement of the pollution source. Water Air Soil Pollut. **56**: 323–332.

Naimo, T.J., Wiener, J.G., Cope, W.G., and Bloom, N.S. 2000. Bioavailability of sediment-associated mercury to *Hexagenia* mayflies in a contaminated floodplain river. Can. J. Fish. Aquat. Sci. **57**: 1092–1102.

NUS Corporation. 1992. Final remedial investigation report. Nyanza Operable Unit III, Sudbury River study, Middlesex County, Massachusetts. Vol. 1. NUS Rep. W92194F. NUS Corporation, Wilmington, Mass.

Oldfield, F., and Appleby, P.G. 1984. Empirical testing of ^{210}Pb-dating models for lake sediments. *In* Lake sediments and environmental history. *Edited by* E.Y. Haworth and J.W.G. Lund. University of Minnesota Press, Minneapolis, Minn. pp. 93–124.

Parks, J.W., and Hamilton, A.L. 1987. Accelerating recovery of the mercury-contaminated Wabigoon/English River system. Hydrobiologia, **149**: 159–188.

Rada, R.G., Findley, J.E., and Wiener, J.G. 1986. Environmental fate of mercury discharged into the upper Wisconsin River. Water Air Soil Pollut. **29**: 57–76.

Rada, R.G., Wiener, J.G., Winfrey, M.R., and Powell, D.E. 1989. Recent increases in atmospheric deposition of mercury to north-central Wisconsin lakes inferred from sediment analyses. Arch. Environ. Contam. Toxicol. **18**: 175–181.

Rada, R.G., Powell, D.E., and Wiener, J.G. 1993. Whole-lake burdens and spatial distribution of mercury in surficial sediments in Wisconsin seepage lakes. Can. J. Fish. Aquat. Sci. **50**: 865–873.

Ramlal, P.S., Kelly, C.A., Rudd, J.W.M., and Furutani, A. 1993. Sites of methyl mercury production in remote Canadian Shield lakes. Can. J. Fish. Aquat. Sci. **50**: 972–979.

Rudd, J.W., Turner, M.A., Furutani, A., Swick, A.L., and Townsend, B.E. 1983. The English–Wabigoon River system: I. A synthesis of recent research with a view towards mercury amelioration. Can. J. Fish. Aquat. Sci. **40**: 2206–2217.

Swain, E.B., Engstrom, D.R., Brigham, M.E., Henning, T.A., and Brezonik, P.L. 1992. Increasing rates of atmospheric mercury deposition in midcontinental North America. Science (Washington, D.C.), **257**: 784–787.

U.S. Geological Survey. 1987. Water resources data for Massachusetts and Rhode Island, water year 1985. U.S. Geol. Surv. Water-Data Rep. MA-RI-85-1.

Waldron, M.C., Colman, J.A., and Breault, R.F. 2000. Distribution, hydrologic transport, and cycling of total mercury and methyl mercury in a contaminated river–reservoir–wetland system (Sudbury River, eastern Massachusetts). Can. J. Fish. Aquat. Sci. **57**: 1080–1091.

Wiener, J.G., and Shields, P.J. 2000. Mercury in the Sudbury River (Massachusetts, U.S.A.): pollution history and a synthesis of recent research. Can. J. Fish. Aquat. Sci. **57**: 1053–1061.

Winfrey, M.R., and Rudd, J.W.M. 1990. Environmental factors affecting the formation of methylmercury in low pH lakes. Environ. Toxicol. Chem. **9**: 853–869.

Wright, H.E., Jr. 1991. Coring tips. J. Paleolimnol. **6**: 37–49.

© 2000 NRC Canada

Sampling for mercury at subnanogram per litre concentrations for load estimation in rivers

John A. Colman and Robert F. Breault

Abstract: Estimation of constituent loads in streams requires collection of stream samples that are representative of constituent concentrations, that is, composites of isokinetic multiple verticals collected along a stream transect. An all-Teflon isokinetic sampler (DH-81) cleaned in 75°C, 4 N HCl was tested using blank, split, and replicate samples to assess systematic and random sample contamination by mercury species. Mean mercury concentrations in field-equipment blanks were low: 0.135 ng·L^{-1} for total mercury (ΣHg) and 0.0086 ng·L^{-1} for monomethyl mercury (MeHg). Mean square errors (MSE) for ΣHg and MeHg duplicate samples collected at eight sampling stations were not statistically different from MSE of samples split in the laboratory, which represent the analytical and splitting error. Low field-blank concentrations and statistically equal duplicate- and split-sample MSE values indicate that no measurable contamination was occurring during sampling. Standard deviations associated with example mercury load estimations were four to five times larger, on a relative basis, than standard deviations calculated from duplicate samples, indicating that error of the load determination was primarily a function of the loading model used, not of sampling or analytical methods.

Résumé : Pour estimer la charge des constituants dans les cours d'eau, il faut prélever des échantillons d'eau représentatifs des concentrations des constituants, c'est-à-dire des échantillons composites de prélèvements verticaux multiples isocinétiques recueillis le long d'un transect. Un échantillonneur isocinétique fait entièrement de Teflon (DH-81), nettoyé à l'aide d'une solution de HCl 4 N, à 75°C, a été mis à l'essai, au moyen d'échantillons à blanc, d'échantillons fractionnés et d'échantillons répétés, pour évaluer la contamination systématique et au hasard des échantillons par des espèces de mercure. Les concentrations moyennes de mercure dans les échantillons à blanc mesurés sur le terrain étaient faibles : 0,135 ng·L^{-1} pour le mercure total (ΣHg) et 0,0086 ng·L^{-1} pour le méthyl mercure (MeHg). Les erreurs quadratiques moyennes pour le mercure total (ΣHg) et le MeHg des échantillons répétés prélevés à huit stations d'échantillonnage n'étaient pas statistiquement différentes des erreurs quadratiques moyennes des échantillons fractionnés en laboratoire, qui représentent l'erreur analytique et de fractionnement. Les concentrations mesurées sur le terrain dans les échantillons à blanc étaient peu élevées, et les erreurs quadratiques moyennes des échantillons répétés et fractionnés étaient statistiquement égales, ce qui indique qu'aucune contamination mesurable ne s'est produite pendant l'échantillonnage. Les écarts-types associés à des estimations modèles de la charge de mercure étaient quatre à cinq fois plus importants, sur une base relative, que les écarts-types standard calculés à partir d'échantillons répétés, ce qui indique que l'erreur de la mesure de la charge était principalement une fonction du modèle de charge utilisé, et non des méthodes d'échantillonnage ou d'analyse.

[Traduit par la Rédaction]

Introduction

Ultraclean sampling procedures for stream water recently have been published for trace metals that occur at concentrations of 1 ng·L^{-1} or less (Windom et al. 1991; Bloom 1995; Hurley et al. 1995). The use of new sampling methods, which avoid previously encountered problems with sample contamination, has resulted in new estimates of trace metal concentrations in many rivers (Shiller and Boyle 1987; Windom et al. 1991; Taylor and Shiller 1995) and oceans (Bruland 1983; Chester 1990) that are, for some metals, orders of magnitude lower than previous estimates.

Received April 2, 1998. Accepted May 13, 1999.
J14524

J.A. Colman[1] and R.F. Breault. U.S. Geological Survey, Water Resources Division, 10 Bearfoot Road, Northborough, MA 01532, U.S.A.

[1]Author to whom all correspondence should be addressed.
e-mail: jacolman@usgs.gov

The new sampling methods are appropriate for determining metal concentrations in discrete samples but do not provide a means for obtaining channel-integrated, flow-weighted, isokinetic samples, which are representative of a stream cross section, as is required for constituent load estimation (Guy 1970; Martin et al. 1992). Load estimations (mass transported per time) in turn are required for many biogeochemical investigations of lakes and rivers.

Integrated sampling is necessary because stream cross sections commonly are not well mixed, a result of sediment settling, riparian introduction of constituents, such as that from outfall pipes or groundwater, or proximity to the confluence of streams (Meade and Stevens 1990). Compositing of multiple, flow-weighted samples is used to obtain representative samples of streams that are not well mixed across a cross section. The individual samples are obtained from a sampler that collects water through a nozzle during transit through vertical profiles of the stream. Samplers with nozzles may bias collection of suspended sediment and chemical constituents attached to suspended sediment because of water acceleration at the sampler nozzle intake (Guy 1970;

© 2000 NRC Canada

Martin et al. 1992). Isokinetic samplers are required, which avoid sampling bias by collecting water through the sampling nozzle at the same velocity that the water is flowing past the sampler. A sample collected isokinetically also is a flow-weighted average sample of the water through which the sampler was moved in a constant (sampler) velocity vertical profile.

Field compositing procedures from multiple sampler deployments in the stream cross section may introduce contamination from airborne particles or resuspended sediment, disturbed during vertical profiling. Contamination introduced during representative sampling of a stream cross section has not yet been assessed.

This paper describes new sampling methods for collecting very low concentration samples intended for use in load estimation. Sampling design and analytical quality assurance results are reported that assess the degree of contamination that occurs during load estimation sampling for total mercury (ΣHg) and monomethyl mercury (MeHg) concentrations that range from 0.01 to 130 ng·L^{-1}. Mercury is the only metal investigated, but methods used are appropriate for other metals that occur at low concentrations. An example load estimate based on data from integrated sampling is also reported. The results are part of an investigation of mercury upstream and downstream from a U.S. Environmental Protection Agency Superfund site on the Sudbury River in east-central Massachusetts (Fig. 1).

Materials and methods

Integrating samplers

Integrating, isokinetic sampling equipment is available that can be deployed in all sizes of streams and hydrologic conditions, including flood flows (Guy and Norman 1970; Edwards and Glysson 1988). However, much of the equipment designed for integrated sampling of streams is inappropriate or untested for sampling of ultralow concentrations of constituents because it was intended primarily for sampling bulk suspended sediment. Isokinetic samplers typically are made of metal, glass, silicone rubber, and plastic. However, an all-Teflon,[2] 3-L isokinetic sampler, DH-81 (Fig. 2), is available, described by Edwards and Glysson (1988). Associated equipment for the DH-81 was modified by substituting the stainless steel wading rod with a 1.2-m solid PVC rod that was threaded into a nylon, rather than metal, fixture in the plastic collar on the sampler. The modified Teflon sampler can be rigorously cleaned by hot concentrated acid, a requirement for samplers of constituents present at concentrations less than 1 ng·L^{-1}.

Sample blanks

Blank procedures used low-mercury water, prepared at the Frontier Geosciences, Inc., laboratory (Seattle, Wash.), and were conducted at sampling stations in the open air to mimic field conditions and to avoid exposure to mercury that is associated with indoor atmospheres. Teflon bottle and Teflon sampling equipment blanks were generated after three rinses of shaking low-mercury water (0.1 ± 0.1 ng·L^{-1}) in the sampler or bottle. Then bottles were filled again and capped; samplers were filled and poured into a rinsed bottle.

Fig. 1. Location of the Sudbury River basin and surface water stations used for duplicate sampling.

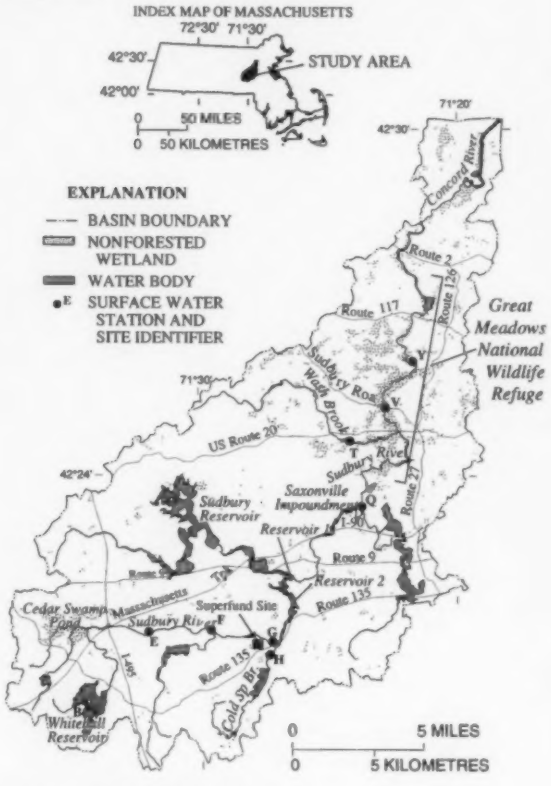

Base from U.S. Geological Survey
Digital Line Graphs, 1:100,000, 1988
Universal Transverse Mercator projection

Sampling and duplicates

Sampling stations were in flowing stream and riparian wetland reaches of the Sudbury River and its tributaries upstream and downstream from the Superfund site (Fig. 1; Table 1). Samples were collected during May 1994 – September 1995.

Teflon DH-81samplers were disassembled and acid cleaned between each sampling round by rigorous methods established for Teflon sample bottles in investigations of mercury at ultratrace concentrations (Bloom et al. 1995). The procedure includes sequential 48-h, 75°C soaks in low-mercury, 4 N HCl and in 1% HCl, with subsequent drying and double plastic bagging in a mercury-free, class 100, clean-air station (Bloom et al. 1995). The double plastic bagged equipment was transported to the field and assembled in the open air using clean hands – dirty hands protocol as described by Bloom (1995).

All sampling and sample processing steps were conducted by personnel wearing Tyvek coveralls and shoulder-length plastic gloves using clean protocol. Integrated samples of the cross section were collected using standard U.S. Geological Survey methods (Edwards and Glysson 1988) with the DH-81 sampler by wading at sampling stations or from the bow of a fiberglass boat equipped with an electric motor and pointed upstream. Vertical profiles were collected by moving the sampler at constant vertical velocity from

[2] The use of trade names in this paper is for identification purposes only and does not constitute endorsement by the U.S. Geological Survey.

© 2000 NRC Canada

Fig. 2. Teflon DH-81 isokinetic sampler. (A) Vertical PVC rod attached to a plastic collar, and from left to right, the Teflon bottle, adapter, cap, and nozzle, which screws into the cap; (B) sampler deployment in a stream.

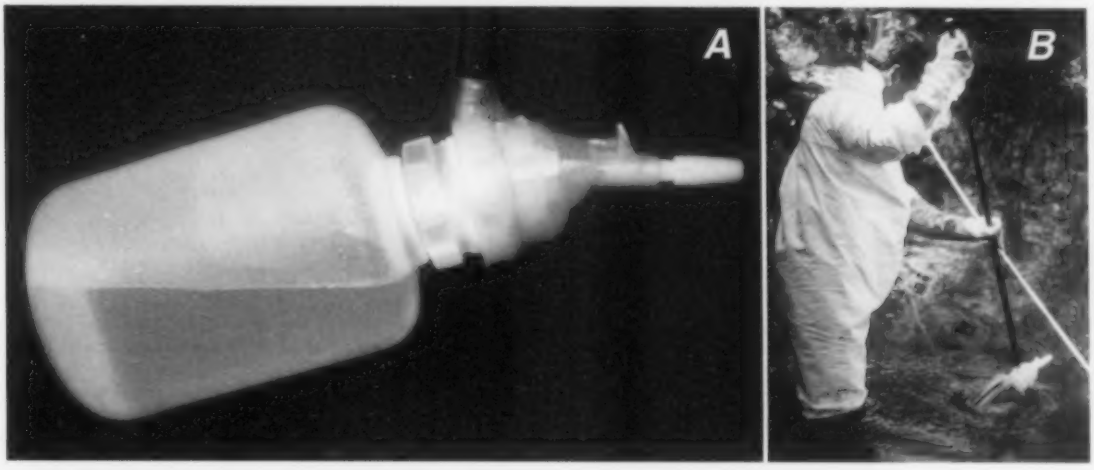

Table 1. Station names and map letters (see Fig. 1) for duplicate sampling.

Station name	Map letter	U.S. Geological Survey station No.
Sudbury River at Cedar Street at Southville, Mass.	E	01097462
Sudbury River at Howe Street near Ashland, Mass.	F	01097466
Sudbury River at Ashland, Mass. (Front Street)	G	01097480
Cold Spring Brook at Main Street at Ashland, Mass.	H	01097481
Sudbury River at Saxonville, Mass.	Q	01098530
Wash Brook near Sudbury, Mass.	T	01098795
Sudbury River at Route 27 bridge near Wayland, Mass.	V	01098805
Sudbury River at Sherman Bridge near Wayland, Mass.	Y	01098815

the surface to the streambed at 10 or more equally spaced intervals determined by a metered tag line stretched across the stream. The 3-L bottle was large enough to contain all profile samples so that a separate compositing step was not necessary. After sample collection, the sampler was shaken to suspend particulates and a sample poured into a cleaned Teflon sample bottle. Dip samples at 20 cm depth were also obtained by wading (or boating) upstream and submersing a hand-held sample bottle. The DH-81 sampler and sample bottles were rinsed three times with stream water before filling.

Samples used in this investigation were taken in duplicate pairs. The two members of duplicate samples were not obtained by the same procedure. Each duplicate pair consisted of one representative composite and one dipped sample taken within a 20-min period.

Analysis and sample splits

Samples were sent the same day as collection by overnight delivery for analysis at Frontier Geosciences, Inc., where they were acidified on the day of receipt to 0.5% (v/v) with preanalyzed HCl. Samples were analyzed for ΣHg by digesting samples in acid BrCl (Bloom and Crecelius 1983), reduction of mercury by $SnCl_2$, and detection by cold-vapor atomic fluorescence spectrometry (Bloom and Fitzgerald 1988). The MeHg analysis used distillation separation from sample matrix (Horvat et al. 1993), aqueous-phase ethylation, gas chromatographic separation of the ethyl analogues, and detection by cold-vapor atomic fluorescence spectrometry (Bloom and Fitzgerald 1988; Bloom 1989). About 10% of the samples were split at the laboratory and analyzed in duplicate. The results of split analyses were used to assess analytical error.

Assessment of contamination during sampling

Duplicate sampling and equipment and bottle blanks of deionized water were used to assess contamination during sampling and sample processing under field conditions. Sample blanks can determine if systemic contamination (leaching from inappropriate or unclean sampling materials) is a problem, but blanks are not so useful as indicators of certain more random kinds of contamination that can occur during the sampling. For instance, blanks cannot be used to assess contamination from inadvertently stirred up bed sediments that might occur while the sampler is submerged and filling. Duplicates, by contrast, are exposed to all conditions involved in sampling. Because of the random occurrence of field contamination sources such as airborne particles or inadvertently stirred up bed sediment, duplicates are unlikely to be equally affected by these contamination sources. Consequently, equal or nearly equal results in duplicate samples can be used to indicate that random contamination sources are not a problem.

Equality was assessed by statistical comparison of the mean square error (MSE) associated with duplicate samples and MSE of samples split in the laboratory, the analytical error. In this investigation, members of duplicate samples were not obtained by the same procedure; composite and dip sampling was used. Therefore, equality in sample pairs would indicate that both random contamination and differences in sampling technique were not affecting concentration.

Results

Sample blanks

Blank values, pooled for the Teflon sampling equipment and sample bottles, are summarized in Table 2. All ΣHg blanks were above the detection limit; six MeHg blanks were below the detection limit (<0.008 $ng \cdot L^{-1}$) and were assigned half the detection limit to compute the mean. The

© 2000 NRC Canada

mean blank values are low and represent 3 and 4% of the mean sample concentrations at the sampling stations for ΣHg and MeHg, respectively. The source of mercury in the blanks could have been contamination during processing, leaching from equipment, or the source blank water.

Duplicates and splits

Duplicate- and split-sample concentrations of ΣHg and MeHg are plotted in Fig. 3. Segregation of duplicate ΣHg concentrations by sampling station (Fig. 3A) reflects the high concentrations of ΣHg adjacent to the Superfund site and progressively lower concentrations in the downstream direction. Duplicate MeHg concentrations (Fig. 3C) were not greater downstream from the Superfund site compared with upstream and are not as segregated by station. Most of the duplicate- and split-sample pairs for ΣHg and MeHg are on or near the lines of equivalence, indicating that the dipped sample concentration often approximately equals the representative composite concentration and that the sample concentrations produced by splitting are approximately equal.

Mean square error analysis

The evaluation of random field contamination was based on statistical comparison of the degree of sample pair equality in the duplicate- and split-sample sets. Variation between sample pairs was determined for each data set (duplicate and split) by computing the MSE of the sample pair differences: the sum of the squares of the differences of the sample pairs divided by the number of sample pairs (Table 3). The MSE in the split-sample sets is caused by analytical error and splitting error that occurs with whole-water samples. Because of propagation of error in measurements, MSE for duplicate sampling includes analytical error as well as error from contamination during sampling and sample processing, error from sampling differing parts of the cross section by integrated versus dipped sampling, and error from variation in river concentration during the 20 min that elapsed between sampling replicates.

The multiple sources of error for the duplicate-sample sets are reflected in comparison of MSE values for ΣHg duplicates and splits, 30.5 and 0.112, respectively. One sample from station G contributes most heavily to the MSE of the ΣHg duplicates (Fig. 3A). Station G is just 300 m downstream from an outfall creek that drains the Superfund site, and concentrations there probably were more variable in time or in the cross section than were concentrations at other stations farther away from the confluence. When the sample is removed from the data set, duplicate MSE decreases to 0.250. If all station G data are removed from the duplicate data, MSE decreases to 0.122, which is approximately equal to the MSE of the split samples.

Statistical equality of the 0.122 and 0.112 MSE values can be evaluated using an F test. The probability of Type I error associated with rejecting the hypothesis of equality between the two MSE values is 0.408, indicating that the hypothesis should not be rejected. Probabilities of Type I error for MSE comparisons are given in Table 4. Requirements that must be met for the compared difference statistics, normal distribution, zero mean, and constant variance, were established using the Shapiro–Wilk W test for normality (Shapiro and Francia 1972) and visual inspection of graphs.

Table 2. Summary statistics for mercury concentrations in field blanks.

Constituent	No. of samples	Mean ($ng \cdot L^{-1}$)	SD ($ng \cdot L^{-1}$)
ΣHg	8	0.135	0.113
MeHg	8	0.0086	0.003 03

The MSE values for MeHg actually were less for duplicate samples than for split samples, 0.000 903 and 0.0371, respectively (Table 3), despite the added sources of error for the duplicates. This is caused apparently by an increase in variance of the split data at high concentrations (Fig. 3D). If the split sample set is limited to concentrations less than 0.6 $ng \cdot L^{-1}$, the range represented in the duplicate data, then duplicate and split MSE are similar, 0.000 903 and 0.000 666, respectively. Outlier MeHg values occur for station G (Fig. 3C) probably for the same reasons that they did for ΣHg. If station G values are deleted, MSE is reduced to 0.000 202. The probability of Type I error associated with rejecting the hypothesis of equality of the latter MSE values, 0.000 202 and 0.000 666, is 0.989, indicating that the hypothesis should not be rejected. The complete split sample differences data did not pass the Shapiro–Wilk W test for normality, but the differences from data pairs less than 0.6 $ng \cdot L^{-1}$ did pass the test.

Discussion

Assessment of contamination

Blank values for ΣHg and MeHg were very low so that systemic contamination from sampling equipment did not appear to occur. The approximate equality of duplicate and split MSE values for ΣHg and MeHg exclusive of the station G data indicated that analytical error, which was included in both paired data sets, was responsible for MSE, and other sources of error including random contamination from sampling and sample processing were small. The more likely explanation for the increase in MSE at station G is variation in the stream ΣHg concentrations with time or in the cross section, rather than sample contamination, because sampling and processing procedures, the sources of contamination, were the same at all stations. All sources of sampling error, not just contamination, were small in comparison with analytical error. Thus, ΣHg and MeHg concentrations did not change significantly between the representative sampling and the dip sampling some 20 min later, and dip samples were not different from representative samples at the selected stations, except for station G, where mixing across the cross section may be incomplete.

Comparison of mercury concentrations from whole-water and filtered samples (Waldron et al. 2000) indicated that 30–90% of the ΣHg and 0–10% of the MeHg did not pass through a 0.45-μm pore size filter. The percentage not passing increased for ΣHg at higher ΣHg concentrations. Failure of the implied particulate transport of ΣHg to cause an increase in the representative sample compared with the dip sample may indicate that the particulate material is of small

© 2000 NRC Canada

Fig. 3. Mercury concentration comparisons. (A) ΣHg concentrations compared for integrated and dipped samples from stations in the Sudbury River basin; (B) ΣHg compared for samples split in the laboratory; (C) as for Fig. 3A, but for MeHg concentrations; (D) as for Fig. 3B, but for MeHg.

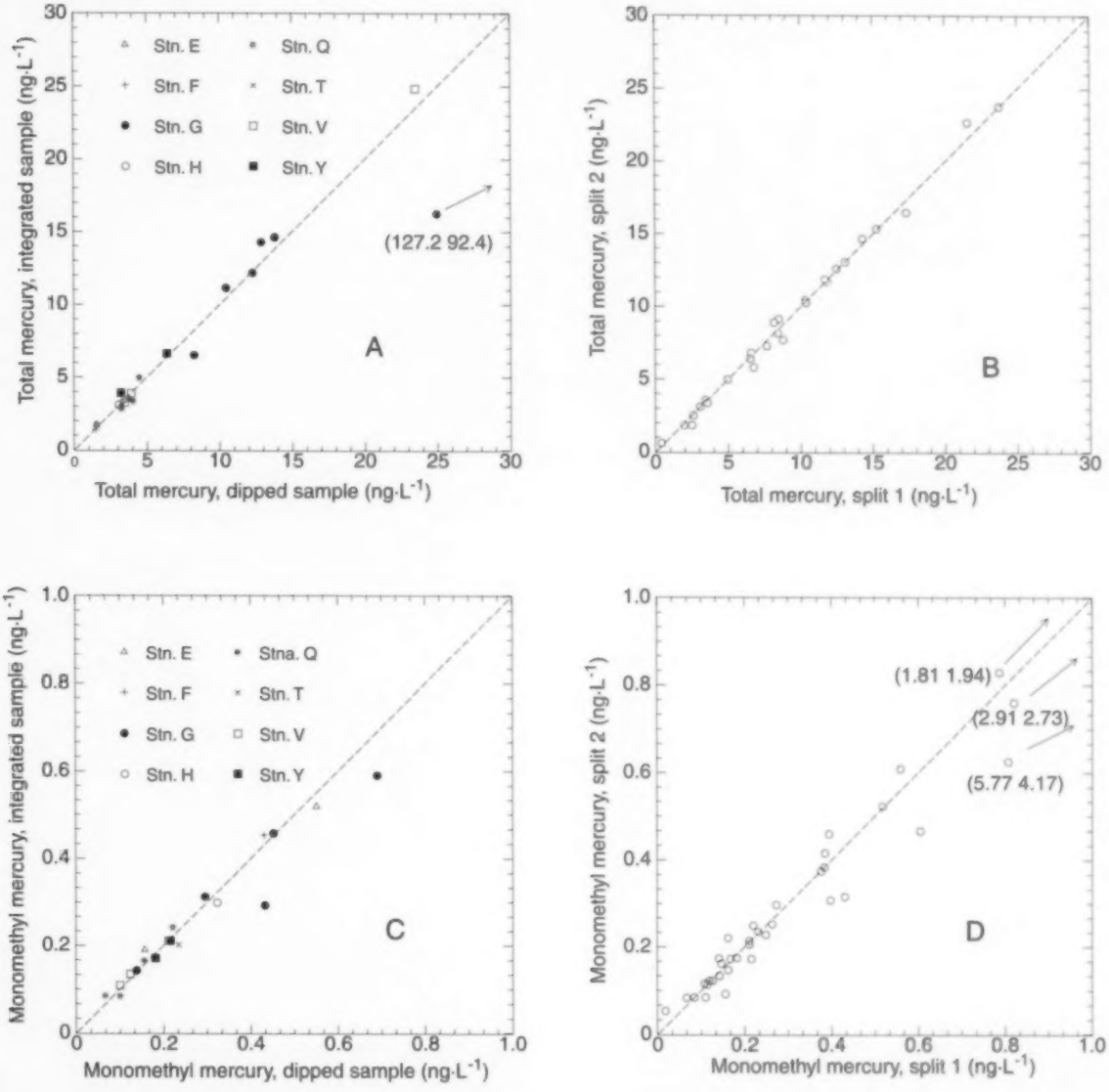

size and thus kept in a well-mixed suspension by turbulence. The concentration of suspended sediment in the Sudbury River system was low, 3–23 mg·L^{-1}. The association of mercury with particulates may be quite different in midwestern and western rivers, where mean suspended sediment concentrations can range to many thousands of milligrams per litre (Britton et al. 1983).

Besides being useful for assessment of contamination, replicate samples are useful as a direct measure of precision of a sampling procedure. The square root of duplicate MSE values divided by 2 is an estimate of standard deviation for a population of ΣHg concentrations from samples collected by representative techniques at one time and place, 0.246 and 0.0100 ng·L^{-1} for ΣHg and MeHg, respectively. Relative standard deviations computed from standard deviations and mean concentrations, 4.98 and 0.219 ng·L^{-1} for ΣHg and MeHg, respectively, were 4.9% for ΣHg and 4.6% for MeHg. These precise results were predicated on extreme precautions in equipment cleaning, transport, and deployment.

Mercury load computation

An example load computation can be used to compare errors associated with sampling with errors associated with an empirical model used to compute loads. Concentration and discharge data as a function of time, which are used to estimate mercury loads, are given in Fig. 4. The data are from

© 2000 NRC Canada

Table 3. Mean square error for duplicate and split sample sets.

	MSE for duplicate samples		MSE for split samples	
Sample selection	ΣHg	MeHg	ΣHg	MeHg
All samples	30.5 (20)	0.000 903 (20)	0.112 (27)	0.037 1 (36)
Less one outlier	0.250 (19)	0.000 682 (19)	—	—
Less all station G values	0.122 (14)	0.000 202 (14)	—	—
Samples less than 0.6 ng·L^{-1}	—	—	—	0.000 666 (31)

Note: Degrees of freedom are given in parentheses. A dash indicates that no value was calculated.

Table 4. Type I error test results of equal variance hypothesis.

MSE values tested	p value for Type I error	Conclusion
30.5 and 0.112	4.4×10^{-66}	Reject hypothesis that variances are equal
0.250 and 0.112	0.027	Reject hypothesis that variances are equal
0.122 and 0.112	0.408	Fail to reject hypothesis
0.000 903 and 0.000 666	0.218	Fail to reject hypothesis
0.000 202 and 0.000 666	0.989	Fail to reject hypothesis

Fig. 4. Discharge hydrograph, and ΣHg and MeHg concentrations, Sudbury River at Saxonville, U.S. Geological Survey station No. 01098530, map letter Q.

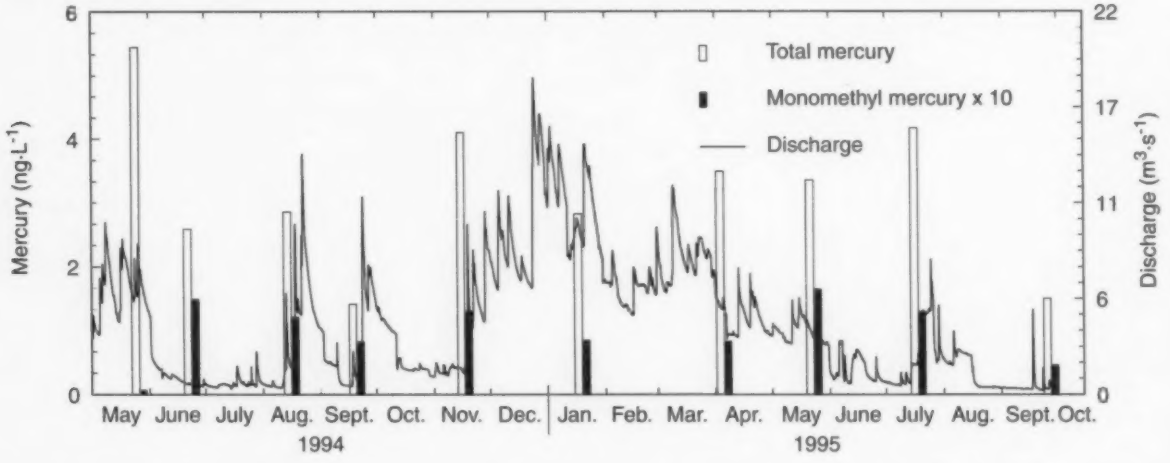

station Q, downstream from several reservoirs that regulate discharge. Loads and MSE of loads are computed for the mercury data using ESTIMATOR.93, a U.S. Geological Survey computer program that implements a minimum variance unbiased estimator (Cohn et al. 1989) of load based on a log-linear regression model. Because of the small data set, simple regressors were used, as described in Cohn et al. (1992). It was assumed that concentration, C, was related to discharge according to the following equation:

$$C = \exp(\beta_0 + \beta_1 \ln(Q) + \varepsilon)$$

where Q is discharge, β_0 and β_1 are parameters to be estimated, and ε is an independent random error. The corresponding instantaneous load, L, is given by

$$L = KQ\exp(\beta_0 + \beta_1 \ln(Q) + \varepsilon)$$
$$= \exp(\beta_0' + \{\beta_1 + 1\}\ln(Q) + \varepsilon)$$

where K is a conversion factor and $\beta_0' = \beta_0 + \ln(K)$.

Annual mean loads (arithmetic mean of the individual daily loads) computed by ESTIMATOR.93 for ΣHg and MeHg at station Q for the 1995 water year were 1.65 g·day^{-1} (standard deviation 0.249) and 0.0593 g·day^{-1} (standard deviation 0.0124), respectively. Standard deviation of loads are computed by comparison of the model regression equation prediction of load with the actual load in the calibration data set of concentration and discharge. Relative standard deviations of the load estimates were 15 and 21%, respectively. A greater precision in the load estimate is prevented by the lack of a strong relationship between concentration and the model regressor, discharge (Fig. 4). More precise load estimates would require collection of more data over a longer period of time so that more regressors, such as time or season, could be used in the model.

Acknowledgments

We are grateful to David Krabbenhoft for starting us in mercury sampling techniques, to Gregory Schwarz and Rob-

© 2000 NRC Canada

ert Lent for technical reviews of the manuscript, and to Robert Flett and Patrick Brezonik for peer reviews. We gratefully acknowledge support from the U.S. Environmental Protection Agency Region I Superfund program.

References

Bloom, N.S. 1989. Determination of picogram levels of methyl mercury by aqueous phase ethylation, followed by cryogenic gas chromatography with cold vapour atomic fluorescence detection. Can. J. Fish. Aquat. Sci. **46**: 1131–1140.

Bloom, N.S. 1995. Mercury as a case study of ultra-clean sample handling and storage in aquatic trace-metal research. Environ. Lab. March/April. pp. 20–25.

Bloom, N.S., and Crecelius, E.A. 1983. Determination of mercury in seawater at sub-nanogram per liter levels. Mar. Chem. **14**: 49–59.

Bloom, N.S., and Fitzgerald, W.F. 1988. Determination of volatile mercury species at the picogram level by low-temperature gas chromatography with cold-vapour atomic fluorescence detection. Anal. Chim. Acta, **208**: 151–161.

Bloom, N.S., Horvat, M., and Watras, C.J. 1995. Results of the international aqueous mercury speciation intercomparison exercise. *In* Mercury as a global pollutant. *Edited by* D.B. Porcella, J.W. Huckabee, and B. Sheatley. Kluwer Academic Publishers, Boston, Mass. pp. 1257–1268.

Britton, L.J., Goddard, K.E., and Briggs, J.C. 1983. Quality of rivers of the United States, 1976 water year — based on the national stream quality accounting network (NASQAN). U.S. Geol. Surv. Open-File Rep. 80-594.

Bruland, K.W. 1983. Trace elements in seawater. *In* Chemical oceanography. Vol. 8. *Edited by* J.P. Riley and R. Chesters. Academic Press, New York. pp. 157–220.

Chester, R. 1990. Marine geochemistry. Unwin Hyman, Boston, Mass.

Cohn, T.A., Delong, L.L., Gilroy, E.J., Hirsch, R.M., and Well, D. 1989. Estimating constituent loads. Water Resour. Res. **25**: 937–942.

Cohn, T.A., Caulder, D.L., Gilroy, E.J., Zunjuk, L.D., and Summers, R.M. 1992. The validity of a simple statistical model for estimating fluvial constituent loads: an empirical study involving nutrient loads entering Chesapeake Bay. Water Resour. Res. **25**: 2353–2363.

Edwards T.K., and Glysson, G.D. 1988. Field methods for measurement of fluvial sediment. U.S. Geol. Surv. Open-File Rep. 86-531.

Guy, H.P. 1970. Fluvial sediment concepts. U.S. Geol. Surv. Tech. Water Res. Invest., Book 3, Chap. C1.

Guy, H.P., and Norman, V.W. 1970. Field methods for measurements of fluvial sediment. U.S. Geol. Surv. Tech. Water Res. Invest., Book 3, Chap. C2.

Horvat, M., Liang, L., and Bloom, N.S. 1993. A comparison of distillation with other current preseparation methods for the determination of methylmercury in low level environmental samples. Part II. Anal. Chim. Acta, **82**: 153–168.

Hurley, J.P., Benoit, J.M., Babiarz, C.L., Shafer, M.M., Andren, A.W., Sullivan, J.R., Hammond, R., and Webb, D.A. 1995. Influences of watershed characteristics on mercury levels in Wisconsin rivers. Environ. Sci. Technol. **29**: 1867–1875.

Martin, G.R., Smoot, J.L., and White, K.D. 1992. A comparison of surface-grab and cross sectionally integrated stream-water-quality sampling methods. Water Environ. Res. **64**: 866–876.

Meade, R.H., and Stevens, H.H. 1990. Strategies and equipment for sampling suspended sediment and associated toxic chemicals in large rivers — with emphasis on the Mississippi River. Sci. Total Environ. **97/98**: 125–135.

Shapiro, S.S., and Francia, R.S. 1972. An approximate analysis of variance test for normality. J. Am. Stat. Assoc. **68**: 215–216.

Shiller, A.M., and Boyle, E.A. 1987. Variability of dissolved trace metals in the Mississippi River. Geochim. Cosmochim. Acta, **51**: 3273–3277.

Taylor, H.E., and Shiller, A.M. 1995. Mississippi River methods comparison study: implications for water quality monitoring of dissolved trace elements. Environ. Sci. Technol. **29**: 1313–1317.

Waldron, M.C., Colman, J.A., and Breault, R.F. 2000. Distribution, hydrologic transport, and cycling of total mercury and methyl mercury in a contaminated river–reservoir–wetland system (Sudbury River, eastern Massachusetts). Can. J. Fish. Aquat. Sci. **57**: 1080–1091.

Windom, H.L., Byrd, J.T., Smith, R.G., and Huan, F. 1991. Inadequacy of NASQAN data for assessing metal trends in the nation's rivers. Environ. Sci. Technol. **25**: 1137–1142.

© 2000 NRC Canada

Distribution, hydrologic transport, and cycling of total mercury and methyl mercury in a contaminated river–reservoir–wetland system (Sudbury River, eastern Massachusetts)

Marcus C. Waldron, John A. Colman, and Robert F. Breault

Abstract: Riparian wetlands contaminated with Hg from an industrial point source were found to be important sites of production and release of methyl mercury (MeHg) in a 40-km reach of the Sudbury River in eastern Massachusetts. Stream discharge and concentration measurements were used to calculate annual mean loads for total Hg (ΣHg) and MeHg in contaminated river reaches, a reservoir, and a riparian wetland downstream from the industrial source. Budgets based on these loads indicate that the annual mean ΣHg load increased sixfold in a reach receiving flow from the point source, but the annual mean MeHg load did not increase. About 23% of the ΣHg load was removed by sedimentation during flow through the reservoir. Net production of MeHg in the reservoir was similar to that reported elsewhere for lakes receiving Hg from atmospheric deposition only. ΣHg concentrations and loads increased significantly as the river passed through the riparian wetland reach. On the basis of flooded wetland area, net production of MeHg was 15 times greater in the wetland reach than in wetland-associated drainages described in other studies.

Résumé : Des terres humides riveraines contaminées par du Hg provenant d'une source industrielle ponctuelle se sont avérées être d'importants lieux de production et de libération de méthyl mercure (MeHg) dans un segment de 40 km de la rivière Sudbury, dans l'est du Massachusetts. Des mesures du rejet et de la concentration dans le cours d'eau ont servi au calcul de la charge annuelle moyenne de Hg total (ΣHg) et de MeHg dans des segments de la rivière, un réservoir et les terres humides riveraines contaminées situées en aval de la source industrielle. Les bilans établis à partir de cette charge montrent que la charge annuelle moyenne de ΣHg s'est accrue de six fois dans un segment recevant de l'eau en provenance de la source ponctuelle, mais que la charge annuelle moyenne de MeHg n'a pas augmenté. Environ 23% de la charge de ΣHg sont disparus par sédimentation pendant l'écoulement au travers du réservoir. La production nette de MeHg dans le réservoir était semblable à celle signalée ailleurs pour des lacs où l'apport de Hg se limitait aux apports atmosphériques. Les concentrations et les charges de ΣHg augmentaient de façon appréciable quand les eaux de la rivière traversaient le segment bordé de terres humides. L'utilisation de la superficie de terres humides inondées a permis de déterminer une production nette de MeHg de 15 fois supérieure dans le segment de terres humides comparativement aux bassins à terres humides décrits dans d'autres études.

[Traduit par la Rédaction]

Introduction

This investigation examined the distribution, transport, and biogeochemical cycling of Hg in the Sudbury River, a system of flowing reaches, impounded reaches, and riparian wetlands in eastern Massachusetts that was contaminated over a 60-year period with Hg from the Nyanza chemical waste dump site in the town of Ashland, Massachusetts (Wiener and Shields 2000). The purpose of the investigation was to determine the effects of high Hg concentrations on rates and amounts of Hg methylation in a complex aquatic system. Methyl mercury (MeHg) is bioconcentrated in aquatic food chains in a process that starts with MeHg uptake by algae (Bloom 1992; Rodgers 1994; Mason et al. 1995). Most Hg released to the environment is not in the methyl form (Parks et al. 1989; Fitzgerald et al. 1991; St. Louis et al. 1994) but may become methylated following deposition in bed sediments and wetland soils (Rudd 1995). Thus, factors controlling MeHg production and release in water may contribute to body burdens of Hg in fish. The extent to which increased concentrations of inorganic Hg result in increased exposure to MeHg is not known, but the answer is critical to assessing the environmental impact of nonpoint atmospheric Hg sources and of point sources such as the Nyanza site.

In this investigation, measurements of the total concentration of all Hg species (ΣHg) and of MeHg were used, together with streamflow data collected during a 17-month period, to compute loads of ΣHg and MeHg transported in the Sudbury River. Loads were used to determine watershed yields and input–output budgets for the first reservoir downstream from the Nyanza site and for four river reaches. The budgets indicate that ΣHg and MeHg transport were affected

Received April 2, 1998. Accepted July 17, 1999.
J14525

M.C. Waldron,[1] J.A. Colman, and R.F. Breault.
U.S. Geological Survey, Water Resources Division,
10 Bearfoot Road, Northborough, MA 01532, U.S.A.

[1]Author to whom all correspondence should be addressed.
e-mail: mwaldron@usgs.gov

© 2000 NRC Canada

by contamination from the Nyanza site and that riverine, reservoir, and riparian wetland environments affect Hg methylation, mobilization, and sedimentation.

Materials and methods

Study design and sampling sites

Nine primary sampling sites were used to assess Hg distribution and transport, seven on the Sudbury River mainstem and two on tributary streams (Fig. 1). Two of the mainstem sampling sites (B1 and B2) were upstream from the Nyanza site and presumably received only background levels of Hg contamination through atmospheric deposition. These upstream sites and the tributary sites constitute the reference sites. The tributary sites were on Cold Spring Brook (T1), which enters Reservoir 2 downstream from the Nyanza site outfall, and on Hop Brook (T2), which enters the Sudbury River about 24 km downstream from the Nyanza site. The remaining five primary sites were on the river mainstem (M1, M2, M5, and M6) and at the Reservoir 2 dam (R4) at locations ranging from 1.4 to 31 km downstream from the Nyanza site. Three additional sampling sites (R1, R2, and R3) were established in separate subbasins of Reservoir 2 and were used to estimate changes in Hg storage in the reservoir. In July 1995, concentrations of ΣHg and MeHg were measured synoptically (during a 4-day period) at seven mainstem sampling sites, including three primary sampling sites (M2, M5, and M6) and four additional sampling sites located 21 km (site M3), 24 km (site M4), 35 km (site M7), and 38 km (site M8) downstream from the Nyanza site.

Mercury sampling and analysis

Primary and reservoir sites were sampled every 6 weeks from May 1994 to September 1995. Water samples for ΣHg and MeHg analysis were collected at stream and reservoir sampling sites using clean-sampling protocols for low-concentration Hg (Bloom 1995; Colman and Breault 2000) for all aspects of sample collection, preservation, and transport. Samples were collected in a 3-L Teflon[2] isokinetic sampler (DH-81) attached to a PVC wading rod (Colman and Breault 2000). Discharge-weighted, representative samples were collected from multiple vertical profiles distributed at equal distances along a stream cross section (Guy 1970). Filterable fractions of ΣHg and MeHg were obtained by filtration through acid-cleaned, in-line Calyx filter capsules with 0.45-μm pore size filters.

Samples from reservoir sites were pumped through an all-Teflon, weighted tubing system with a peristaltic pump equipped with precleaned C-flex pumphead tubing. All water samples were pumped directly into Teflon sample bottles or prefiltered as described previously.

Samples for Hg analysis were delivered for analysis at Frontier Geosciences, Inc., Seattle, Wash., where samples were acidified immediately upon receipt (0.5% (v/v) preanalyzed HCl). Samples were analyzed for ΣHg by the techniques of Bloom and Crecelius (1983) and Bloom and Fitzgerald (1988). MeHg was analyzed by the technique of Horvat et al. (1993).

A detailed quality assurance analysis of the Hg concentration data is given in Colman and Breault (2000). Comparison of sample blanks, sample duplicates, and samples split in the laboratory indicate that no observable contamination occurred during collection, handling, or preparation. Results from the analysis also indicate that water column Hg concentrations did not change over the short (20 min) time intervals between duplicate samplings. Sample splitting and analytical variance dominated the total variance associated with duplicate sampling and sample analysis. Standard deviations determined from duplicate samples were 0.25 $ng \cdot L^{-1}$ for ΣHg and 0.010 $ng \cdot L^{-1}$ for MeHg (Colman and Breault 2000).

Stage and discharge measurements

Discharge was measured with current meters using standard U.S. Geological Survey procedures (Rantz et al. 1982). Two of the mainstem sampling sites (M1 and R4) were instrumented for continuous recording of stage during the investigation; a third site (M2) has been instrumented since 1979. Stage was converted to discharge using measured stage–discharge relationships (Kennedy 1984) or a dam rating. Staff gauges were installed at all of the six remaining sampling sites except U. Stage and discharge were determined simultaneously at intervals of about 6 weeks during the 17-month study period.

Discharge records at the three continuous-record sites were used to estimate mean daily discharge at the five sites with periodic discharge measurements (partial-record sites). Concurrent discharge measurements for partial-record and continuous-record sites were linearly related, so the maintenance of variance extension Type 1 technique (MOVE.1) (Hirsch 1982; Ries 1993) was used to generate continuous-discharge records for the five partial-record sites.

Loading calculations

Annual mean loads for ΣHg and MeHg were computed for water year 1995 (October 1, 1994 – September 30, 1995) at the seven mainstem transport sampling sites and at the Cold Spring Brook site using the U.S. Geological Survey program ESTIMATOR.93. Loads of constituents at stations were computed with periodic measurements of constituent concentrations and daily discharge values using a log–log regression model and the minimum variance unbiased estimator as described in Cohn et al. (1989). Recent studies have demonstrated the validity of using the minimum variance unbiased estimator for estimating constituent loads and the uncertainties associated with total load estimates (Cohn et al. 1992). In this study, two simple regressors, log(discharge) and a constant, were used to compute loads.

Results

All budget and transport calculations apply to Hg species measured in digested, unfiltered water samples. Results presented as ΣHg or MeHg concentrations or loads refer to the total amount of Hg species in an unfiltered sample. When results from filtered samples are discussed, they are presented as filtered ΣHg or filtered MeHg concentrations.

Total Hg distribution

Mean concentrations of ΣHg measured during the study period at the nine primary sampling sites ranged from about 2 $ng \cdot L^{-1}$ at reference sites to 16 $ng \cdot L^{-1}$ at the first sampling site (M1) downstream from the Nyanza site (Table 1). The increase in the mean ΣHg concentration in the river reach that passes the Nyanza site was likely a result of input from a tributary stream draining the Nyanza site. Water samples collected in June 1995 from two locations in the tributary had ΣHg concentrations (1200 and 1500 $ng \cdot L^{-1}$) more than 100 times greater than those in the Sudbury mainstem.

Mean concentrations of ΣHg decreased downstream from site M1 as the river passed through the three reservoirs and was diluted by inflow from the Sudbury Reservoir (Fig. 1). Concentrations reached a local minimum of about 3 $ng \cdot L^{-1}$ 15 km downstream from the Nyanza site at site M2. Mean

[2] Use of brand, firm, or trade names in this paper is for identification purposes and does not constitute endorsement by the U.S. Geological Survey.

© 2000 NRC Canada

Fig. 1. Study area and locations of sampling sites in the Sudbury River system, eastern Massachusetts.

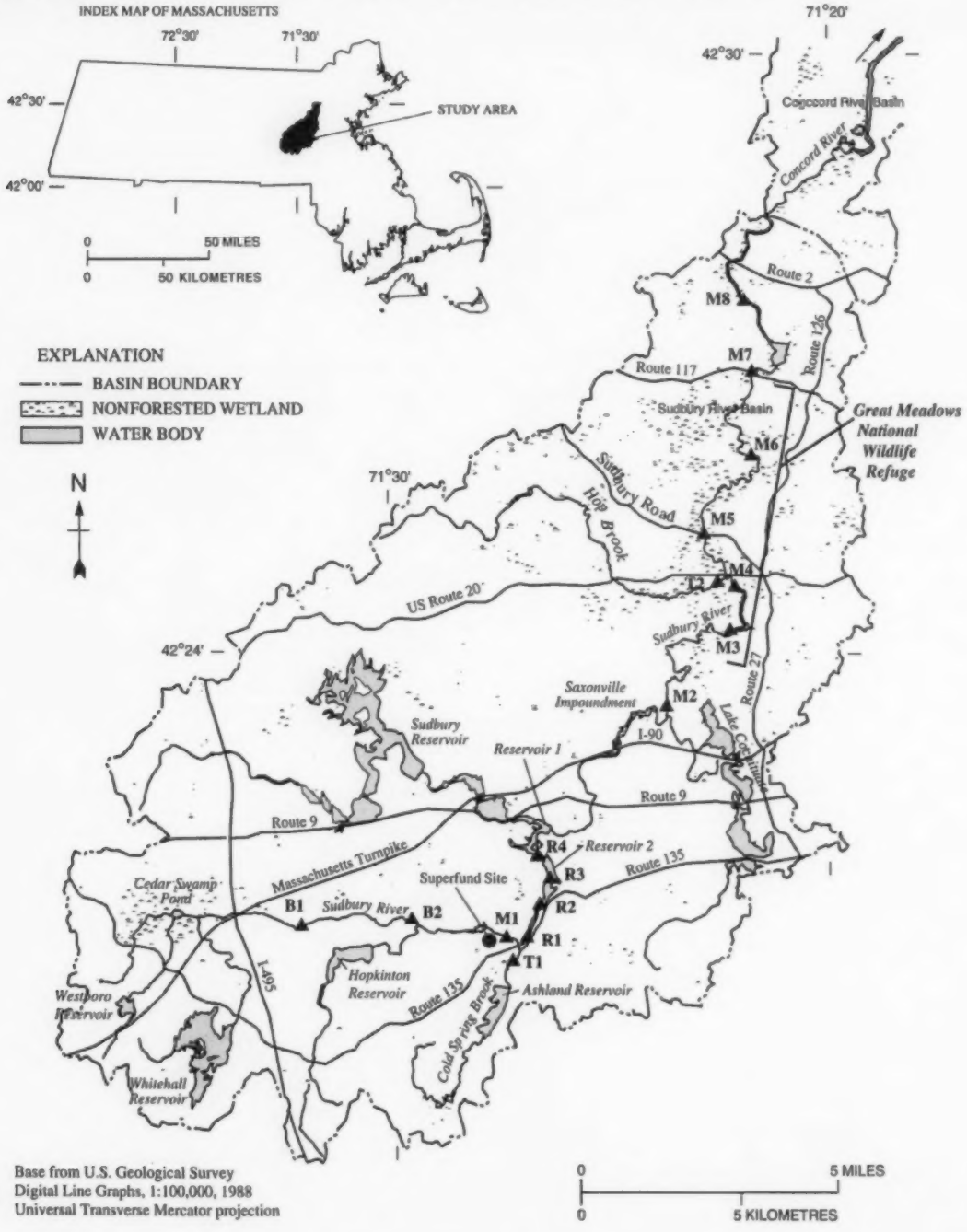

ΣHg concentrations increased fourfold farther downstream in the wetland-associated reach, approaching the value of the mean at site M1 (Table 1).

Mean concentrations of ΣHg measured at sampling sites downstream from the Nyanza site are generally higher (3.1–16 ng·L^{-1}) than those reported recently for riverine sites in Wisconsin and for several other North American rivers. Hurley et al. (1995) reported mean ΣHg concentrations of 3.5 ng·L^{-1} in autumn and 7.9 ng·L^{-1} in spring for 39 Wisconsin rivers chosen to reflect a range of basin types and Hg

© 2000 NRC Canada

Table 1. Means, medians, and ranges of ΣHg and MeHg concentration ($ng \cdot L^{-1}$) in unfiltered (total) and filtered (dissolved) water samples collected at six mainstem sites, one reservoir site, and two tributary sites on the Sudbury River, May 1994 – September 1995.

Hg species	*n*	Mean	Median	Minimum	Maximum
Site B1, Sudbury River at Cedar St. at Southville, Mass.; 01097462					
ΣHg (total)	9	2.1	2.2	0.80	3.3
ΣHg (dissolved)	3	3.2	2.2	1.9	5.4
MeHg (total)	9	0.27	0.26	0.057	0.61
MeHg (dissolved)	3	0.33	0.31	0.073	0.60
Site B2, Sudbury River at Howe St. near Ashland, Mass.; 01097466					
ΣHg (total)	9	2.3	2.2	0.99	3.6
ΣHg (dissolved)	3	1.5	1.3	0.85	2.2
MeHg (total)	9	0.21	0.22	0.23	0.45
MeHg (dissolved)	3	0.21	0.14	0.062	0.42
Site M1, Sudbury River at Ashland, Mass.; 01097480					
ΣHg (total)	18	16	12	5.2	92
ΣHg (dissolved)	14	4.9	5.1	3.2	7.4
MeHg (total)	18	0.23	0.17	0.087	0.59
MeHg (dissolved)	14	0.19	0.15	0.067	0.48
Site R4, Bracket Reservoir (Reservoir 2) at dam at Coburnville, Mass.; 01097484					
ΣHg (total)	11	7.5	7.7	3.6	13
ΣHg (dissolved)	11	4.8	5.0	3.0	6.3
MeHg (total)	11	0.23	0.27	0.11	0.30
MeHg (dissolved)	11	0.20	0.19	0.070	0.49
Site M2, Sudbury River at Saxonville, Mass.; 01098530					
ΣHg (total)	10	3.1	3.1	1.4	5.0
ΣHg (dissolved)	7	2.2	2.1	0.97	3.2
MeHg (total)	10	0.13	0.13	0.046	0.24
MeHg (dissolved)	7	0.11	0.11	0.047	0.22
Site M5, Sudbury River at Route 27 Bridge near Wayland, Mass.; 01098805					
ΣHg (total)	11	11	8.8	3.3	27
ΣHg (dissolved)	9	3.3	2.8	1.5	6.8
MeHg (total)	11	0.27	0.23	0.11	0.48
MeHg (dissolved)	9	0.20	0.12	0.063	0.42
Site M6, Sudbury River at Sherman Bridge near Wayland, Mass.; 01098815					
ΣHg (total)	10	12	9.7	3.9	24
MeHg (total)	10	0.37	0.22	0.15	0.75
Site T1, Cold Spring Brook at Main St. at Ashland, Mass.; 01097481					
ΣHg (total)	8	2.1	2.2	1.2	3.1
MeHg (total)	8	0.18	0.16	0.14	0.30
Site T2, Hop Brook near South Sudbury, Mass.; 01098797					
ΣHg (total)	11	3.8	2.5	1.4	11
ΣHg (dissolved)	3	1.9	1.4	1.3	2.9
MeHg (total)	11	0.22	0.23	0.030	0.42
MeHg (dissolved)	3	0.16	0.15	0.14	0.19

Note: Eight-digit numbers are U.S. Geological Survey station numbers.

sources. Similar values (3.1 $ng \cdot L^{-1}$ in autumn and 5.5 $ng \cdot L^{-1}$ in spring) were obtained by Babiarz and Andren (1995) for rivers in Wisconsin. Gill and Bruland (1990) reported a mean ΣHg concentration range of 0.14–2.8 $ng \cdot L^{-1}$ for large rivers in Washington, Oregon, and California. The maximum mainstem ΣHg concentration measured in this study (92 $ng \cdot L^{-1}$ at site M1, measured at the peak discharge during a 2-day storm in August 1994) was substantially higher than the maximum reported by Gill and Bruland (1990) for a California stream (Davis Creek) receiving Hg mine effluent (34 $ng \cdot L^{-1}$).

ΣHg concentrations varied because of season, discharge, and Hg source (Fig. 2). Variation was small at reference sites where mean ΣHg concentrations were small but was larger just downstream from the point source and in the wetland reach where the means were larger (Table 1).

ΣHg concentrations averaged slightly lower at site M1, just downstream from the Nyanza site, during the winter high-flow period than during the summer low-flow period but were strongly affected during low flow by precipitation (Fig. 2*a*). ΣHg concentrations at the wetland-associated sampling sites also were affected by summer precipitation. However, the increased July 1995 concentrations and discharge at site M6 were not the result of a storm but rather of upstream

© 2000 NRC Canada

Fig. 2. ΣHg and MeHg concentrations and study period hydrographs for four Sudbury River mainstem sampling sites: (*a*) site B2, Sudbury River at Howe St. near Ashland, Mass., (*b*) site M1, Sudbury River at Ashland, Mass., (*c*) site M2, Sudbury River at Saxonville, Mass., and (*d*) site M6, Sudbury River at Sherman Bridge near Wayland, Mass. Discharge at full scale is 18 $m^3 \cdot s^{-1}$.

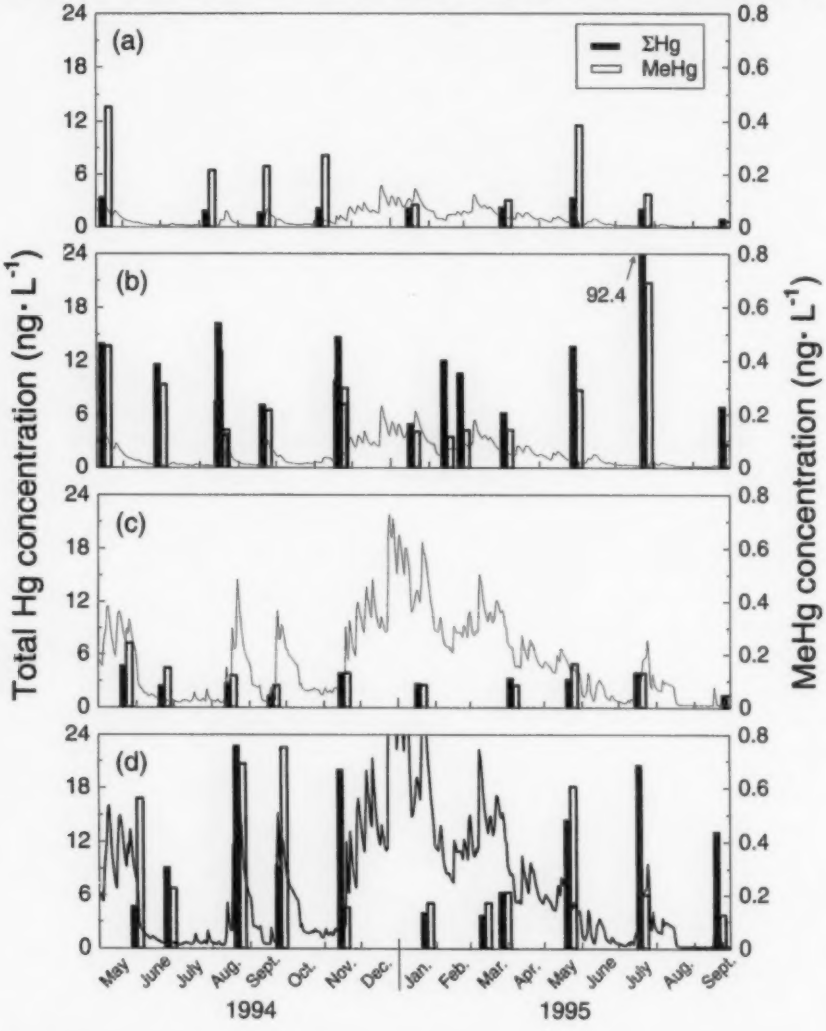

dam regulation (Fig. 2*d*). Hydrographs at sampling sites B2 and M1 (Fig. 2*b*) upstream from the three reservoirs did not show increased discharge during this period. Storm-related variability in ΣHg concentration was greater at sites with higher ΣHg concentrations than it was at those with lower ΣHg concentrations (Table 1). However, concentration was not simply related to discharge because high winter flows did not result in particularly high concentrations.

The effect of changes in stream discharge on ΣHg concentration at site M2 (Fig. 2*c*) was similar to that at site B2. Concentrations generally were low in the high-flow winter period and higher in the lower-flow summer period. Storm-related increases in stream discharge had little effect at these sampling sites. Comparison of unfiltered and filtered ΣHg concentrations (Table 1) indicated that the higher ΣHg concentrations at most sites were associated primarily with suspended particles.

MeHg distribution

MeHg concentrations did not appreciably change as the river flowed past the Nyanza site (Table 1). Mean MeHg concentrations actually were higher (0.27 $ng \cdot L^{-1}$) at reference sites upstream from the Nyanza site, which receive water from a large wetland drainage, than at site M1 just downstream from the Nyanza site (0.23 $ng \cdot L^{-1}$). MeHg concentrations measured in early June 1995 in the small tributary draining the Nyanza site were 20 times higher (4.8 and 5.8 $ng \cdot L^{-1}$) than the downstream Sudbury River concentration, compared with 100 times higher for ΣHg. A small amount (0.07–0.12 $ng \cdot L^{-1}$) of the apparent MeHg enrichment in the tributary may be attributable to methylation of inorganic Hg during the distillation step in the analytical procedure (Bloom et al. 1997).

MeHg concentrations continued unchanged with passage through Reservoir 2. The mean concentration was lowest

© 2000 NRC Canada

Fig. 3. Stream concentrations of ΣHg and MeHg along a longitudinal transect of the Sudbury River, sampled July 18–21, 1995.

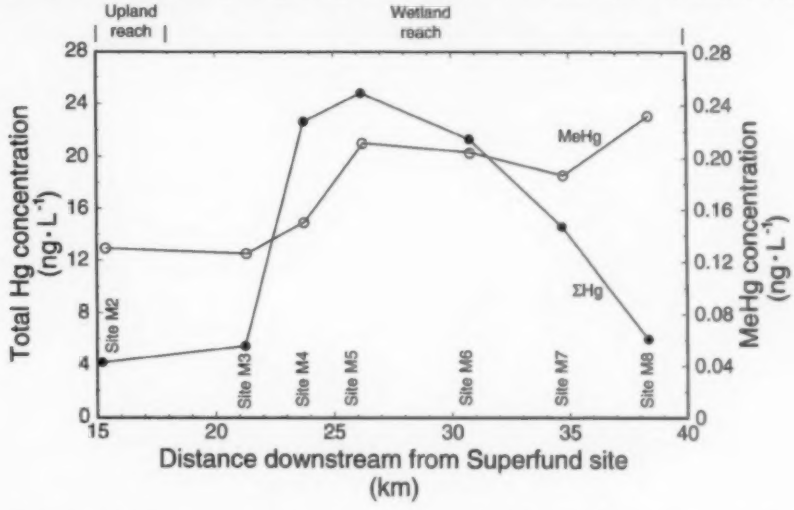

(0.13 ng·L^{-1}) at site M2, possibly because of dilution by flow from the Sudbury Reservoir. However, mean MeHg concentrations in the riparian wetland reaches downstream from site M2 increased to values similar to those in the upstream reference sites.

Seasonal variation in MeHg concentration was pronounced (Fig. 2). Concentrations were high during periods of decreased flow and warm temperatures (summer and early autumn) and were low during periods of increased flow and cold temperatures (winter and early spring). MeHg concentrations at site M1 appeared to be less affected by runoff than ΣHg concentrations and did not increase appreciably during the August 1994 storm (Fig. 2*b*). High summer MeHg concentrations were associated with storms at sites in the wetland reach (Fig. 2*d*), as was the case for ΣHg at that site. However, MeHg concentrations did not increase during the July 1995 increase in discharge that resulted from regulation of the upstream dam.

Filtered MeHg concentrations were generally a greater fraction of unfiltered MeHg concentrations than was the case for ΣHg. At high concentrations, nearly all the MeHg (80–100%) was dissolved.

Mercury distribution in wetland-associated reaches

In an attempt to identify the source of the measured wetland increases in ΣHg and MeHg concentrations, a synoptic survey of ΣHg and MeHg concentrations in the riparian wetland reach was conducted along a transect from sites M2 to M8, 15–38 km downstream from the Nyanza site. Seven sites were sampled during July 18–21, 1995. Stream discharge at site M2 increased from 2.04 to 4.51 m^3·s^{-1} during the sampling period (Fig. 2*c*) following a 23-day period when discharge was less than the 90% exceedence value (0.96 m^3·s^{-1}) for the site. The increased daily mean discharge was not associated with precipitation, but rather resulted from releases from upstream reservoirs.

Little change was noted in ΣHg from sites M2 to M3, 3 km into the wetland reach (Fig. 3). From sites M3 to M4, 2 km farther into the wetland reach, the ΣHg concentration increased from 5.4 to 25 ng·L^{-1}. Concentrations then decreased with further distance along the transect.

The increase in ΣHg concentration between sites M3 and M5 and the subsequent downstream decrease in concentration during a period of no rainfall are suggestive of point-source inputs, although there are no known point sources in this reach. An alternative explanation is that Hg previously deposited in wetland floodplain soils and streambed sediments was being mobilized. However, ΣHg concentrations were high despite increased discharge from regulated releases at the upstream dams. The increased stage associated with increased discharge would produce a hydraulic gradient away from the stream channel in the absence of runoff from a storm. ΣHg increases could be associated with scour from stream-channel bed sediment, which has a higher than background Hg concentration (Colman et al. 1999); however, channel velocities in the wetland-associated reach generally are too low for scour to result.

MeHg concentrations along the July 1995 transect increased moderately in the wetland-associated reach (Fig. 3). The large increase in ΣHg from sites M3 to M4 did not occur for MeHg. High concentrations of MeHg and ΣHg were found together at wetland-associated sampling sites during summer 1994, but those samplings followed storms. MeHg concentrations associated with summer precipitation were more than three times the peak concentration measured at sites on the transect during July 1995.

Mercury transport

Annual mean ΣHg and MeHg loads and standard errors of the loads for water year 1995 were calculated for each of the seven mainstem and reservoir sampling sites and one tributary site for use in watershed yield and stream reach budget calculations (Fig. 4, for mainstem and reservoir sites). Background loads were calculated by multiplying the annual mean streamflow at each sampling site by the annual mean ΣHg and MeHg concentrations at sampling site B2 in the upstream reference reach. Concentrations in the reference reach upstream from the Nyanza site were considered to be

© 2000 NRC Canada

Fig. 4. Calculated annual mean (water year 1995) loads of ΣHg and MeHg and estimated background loads for both species at Sudbury River sampling sites of varying distance from the Nyanza Superfund site. Error bars indicate ±1 SE.

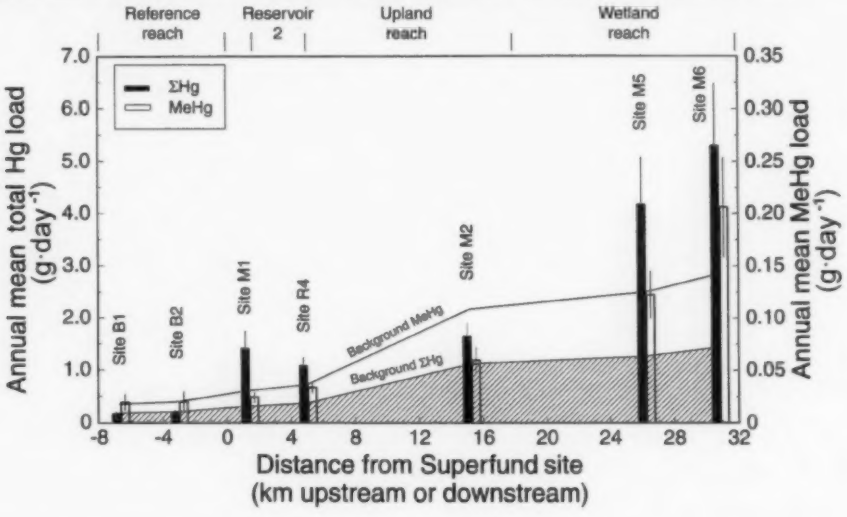

indicative of inputs from nonpoint sources in the drainage basin.

Concentration variation that cannot be explained by discharge contributes to error in load estimates when using discharge regression models. Error bars shown in Fig. 4 reflect variability in the concentration data and the inability of the log(flow) regressions used in ESTIMATOR.93 to explain all variability in concentration. Thus, errors of load estimation were least at the reference site where concentrations were nearly constant and greatest in the wetland sites where concentrations varied and were not simply related to flow.

As was the case with the ΣHg concentration data, the annual mean ΣHg load increased as the river flowed past the Nyanza site. The load increased from 0.17 ± 0.03 g·day^{-1} at site B1 to 1.4 ± 0.34 g·day^{-1} at site M1 and then decreased to 1.1 ± 0.16 g·day^{-1} at site R4. The decrease with passage through the reservoir probably was due to sedimentation of particle-bound Hg. Particle-bound Hg comprised 56% of the median ΣHg concentration at site M1 but was only 35% of the total at site R4. (Table 1).

Despite sedimentation, however, the annual mean ΣHg load was higher than background at all sampling sites downstream from the Nyanza site. In the wetland-associated reach (sites M5 and M6), the difference between ΣHg load and estimated background load was five times greater than it was at the Nyanza site (site M1). The calculated annual mean ΣHg load for the Cold Spring Brook tributary sampling site (site T1) was 0.06 ± 0.01 g·day^{-1}. Loads were not calculated for Hop Brook (site T2) because of the lack of a suitable discharge record for that site.

The annual mean MeHg load did not appreciably change relative to background as the river passed the Nyanza site and Reservoir 2 but was lower at site M2 (Fig. 4). As the river entered wetlands, the annual mean MeHg load returned to background at site M5 and exceeded the estimated background load at site M6 by 36%.

Watershed yield rates

Watershed yield rates (WY, milligrams per square kilometre per day) were computed for each of the primary Sudbury River sampling sites (except site T2) by dividing annual mean load by the total drainage area (square kilometres). The annual mean WY for ΣHg was about 3.2 mg·km^{-2}·day^{-1} at the two mainstem reference sampling sites (Table 2) and was similar (2.9 mg·km^{-2}·day^{-1}) at the Cold Spring Brook tributary sampling site (site T1). The WY for ΣHg increased nearly fivefold to 16 mg·km^{-2}·day^{-1} as the river flowed past the Nyanza site and then decreased in Reservoir 2 and reached a downstream minimum of 6.0 mg·km^{-2}·day^{-1} at site M2. The WY again increased farther downstream in the wetland-associated reach and was nearly as high at site M6 (14 mg·km^{-2}·day^{-1}) as it was adjacent to the Nyanza site.

WYs for ΣHg in the Sudbury River reference sites are similar to the low end of the range of measurements reported by Hultberg et al. (1994) and Linqvist et al. (1991) for forested Swedish watersheds (1.6–16 mg·km^{-2}·day^{-1}) and for Wisconsin streams investigated by Hurley et al. (1995). The latter investigation was based on two sets of measurements of discharge and Hg concentration, one made in the autumn at low flow and the other made in the spring at high flow at sites located in various watershed types. Values reported here for the Sudbury River system are based on annual means and would be expected to be intermediate between the seasonal extremes reported by Hurley et al. (1995).

The annual mean WY for MeHg varied by a factor of 3 across the sampling sites. WY generally was highest where the watershed contained large amounts of wetland acreage, at the upstream reference site, for example, and in the reaches that include part of the Great Meadows National Wildlife Refuge (Fig. 1). The highest WY for MeHg was about 0.6 mg·km^{-2}·day^{-1} at site M6. The lowest WY was 0.2 mg·km^{-2}·day^{-1} at the Cold Spring Brook sampling site

© 2000 NRC Canada

Table 2. Distances (upstream or downstream) from the Nyanza Superfund site, cumulative drainage areas, watershed yield rates for ΣHg and MeHg, and annual mean net production rates for MeHg at six mainstem sampling sites, one reservoir sampling site, and one tributary sampling site on the Sudbury River, May 1994 – September 1995.

Sampling site	Distance from Superfund site (km)	Drainage area (km^2)	Watershed yield rate ($mg \cdot km^{-2} \cdot day^{-1}$) ΣHg	Watershed yield rate ($mg \cdot km^{-2} \cdot day^{-1}$) MeHg	Annual mean net MeHg production rate ($mg \cdot km^{-2} \cdot day^{-1}$)[a]
B1	–6.7	53.3	3.2	0.36	0.11
B2	–3.1	62.3	3.3	0.32	0.071
M1	1.4	90.9	16	0.27	0.020
R4	5.0	116	9.6	0.29	0.040
M1	15.2	275	6.0	0.22	–0.032
M5	26.2	363	12	0.34	0.090
M6	30.8	376	14	0.55	0.30
T1	—	20.3	2.9	0.20	–0.045

Note: See text for locations and descriptions of sampling sites.
[a]Assuming an annual mean rate of atmospheric deposition of MeHg of 0.25 $mg \cdot km^{-2} \cdot day^{-1}$ (Fitzgerald et al. 1991).

(site T1), where the watershed contains more upland than wetland acreage. The range of yields was somewhat higher than those of mixed-drainage wetland and forest but lower than a wetland drainage in Wisconsin (Hurley et al. 1995).

Reach-specific Hg budgets

Mercury budgets were constructed to assess net rates of ΣHg sedimentation and MeHg production in impounded versus free-flowing reaches. The net rates were determined by calculating the difference between river input and output transport rates for a reach according to the following relationship:

$$Hg_{net\ production/sedimentation} = Hg_{in} - Hg_{out} + Hg_{at} - \Delta Hg_{storage}$$

where Hg_{in} is ΣHg or MeHg load in all reach inflows, Hg_{out} is ΣHg or MeHg load in the reach outflow, Hg_{at} is net atmospheric exchange, and $\Delta Hg_{storage}$ is the change in water column mass of ΣHg or MeHg.

Values for atmospheric deposition of ΣHg and MeHg and evasion of Hg^0 were estimated from data for northern Wisconsin lakes (Fitzgerald et al. 1991; Lamborg et al. 1995). The value used for deposition of ΣHg (10 $\mu g \cdot m^{-2} \cdot year^{-1}$) was similar to measured values for wet deposition in the Lake Champlain basin (9.26 $\mu g \cdot m^{-2} \cdot year^{-1}$, Burke et al. 1995) and the Great Lakes region (9.0 $\mu g \cdot m^{-2} \cdot year^{-1}$, Hoyer et al. 1995). Reported values for atmospheric deposition of MeHg vary widely from 0.04 $\mu g \cdot m^{-2} \cdot year^{-1}$ in remote parts of northwestern Ontario (St. Louis et al. 1994) to 0.4 $\mu g \cdot m^{-2} \cdot year^{-1}$ in southern Sweden (Hultberg et al. 1994). The value used in this study (0.1 $\mu g \cdot m^{-2} \cdot year^{-1}$) is intermediate between values for remote and industrialized areas but may be low if significant amounts of MeHg are entering through litterfall (Rudd 1995). Evasion of Hg^0 was estimated at 1 $\mu g \cdot m^{-2} \cdot year^{-1}$, based on the value reported for Little Rock Lake (0.7 $\mu g \cdot m^{-2} \cdot year^{-1}$, Watras et al. 1994), which also may be low given the high ΣHg concentrations measured in the Sudbury River.

For flowing reaches with no flooded surface area, there was little change in Hg storage in the water column or in net atmospheric Hg exchange, and budgets for these reaches depended entirely on streamflow input and output terms. In the budgets, ungauged flows in small tributaries and groundwater seepage were determined by outflow minus inflow and Hg concentrations were assumed equal to the annual average for the upstream reference site (site B2).

Results of these calculations for five reaches on the Sudbury River mainstem are presented in Table 3. Standard errors for annual mean load estimates used in the calculations ranged from 11.7% of the estimate at site T1 to 23.8% of the estimate at site M1. Although budget terms determined by difference are uncertain when the error bars for annual mean input and output overlap (as in sites M1 and R4, Fig. 4), budget results still can be examined quantitatively with the understanding that the values may not be exact.

In the 4-km reach between sites B1 and B2, there was very little net increase or loss of ΣHg or net production of MeHg. Between sites B2 and M1, there was a net increase in the ΣHg load because of input from the Nyanza site and a net decrease in the MeHg load that is probably the result of dilution by inflow from a tributary draining the Hopkinton Reservoir (Fig. 1).

The next reach in downstream order contains Reservoir 2. Because its hypolimnion becomes anoxic during summer low-flow periods, this impounded reach was expected to show substantial conversion of ΣHg to MeHg. On an annual basis, about 27% of the incoming ΣHg was deposited in the reservoir sediments, about 73% was transported downstream, and less than 0.001% was lost to the atmosphere (Table 3). Mercury originating from the Nyanza site probably increased the background ΣHg load entering the reservoir by about 75% (402 $g \cdot year^{-1}$). The annual mean concentration of ΣHg in the water column was 8.5 $ng \cdot L^{-1}$, and the outflow from the reservoir contributed a ΣHg load of 395 $g \cdot year^{-1}$.

Despite the high levels of Hg contamination in Reservoir 2 sediments, annual mean rates of MeHg production did not appear to be elevated. There was a net annual production of MeHg in Reservoir 2 of 3.8 $\mu g \cdot m^{-2} \cdot year^{-1}$ (Table 3), which is comparable with the maximum value estimated for Little Rock Lake (3.0 $\mu g \cdot m^{-2} \cdot year^{-1}$) using a similar mass-balance

© 2000 NRC Canada

Table 3. Measured and estimated annual mean loading, calculated net yield or retention rate, and estimated wetland areal yield of ΣHg and MeHg in selected reaches of the Sudbury River.

River reach		Hg load in measured inflow ($mg \cdot day^{-1}$)	Hg load in unmeasured inflow ($mg \cdot day^{-1}$)[a]	Estimated atmospheric Hg deposition rate ($mg \cdot day^{-1}$)[b]	Hg load in measured outflow ($mg \cdot day^{-1}$)	Calculated net Hg yield (+) or retention (–) rate ($mg \cdot day^{-1}$)	Estimated yield (+) or retention (–) rate per unit flooded surface area[b]	
							$\mu g \cdot m^{-2} \cdot year^{-1}$	$mg \cdot km^{-2} \cdot day^{-1}$
Site B1 to site B2	ΣHg	170	25	—	200	5.0	—	—
	MeHg	19	2.3	—	20	–1.3	—	—
Site B2 to site M1	ΣHg	200	110	—	1400	1090	—	—
	MeHg	20	11	—	24	–7.0	—	—
Site M1 to site R4	ΣHg	1500[c]	B	13	1100	–413	–323	–885
	MeHg	28[c]	B	0.13	33	4.9	3.8	11
Site M2 to site M5	ΣHg	1600	170	130	4200	2300	175	479
	MeHg	60	16	1.3	120	43	3.3	9.0
Site M5 to site M6	ΣHg	4200	180	90	5300	830	92	252
	MeHg	120	17	0.90	210	72	8.0	22

Note: See text for locations and descriptions of sampling sites and reaches.

[a]Measured outflow minus measured inflow for the reach × annual mean Hg concentration at site B2; "B" indicates that inflows and outflow are approximately equal.

[b]Atmospheric deposition and areal yield rates determined only for reaches where flooded surface area extends beyond stream channel; a dash indicates negligible flooded surface area.

[c]Includes measured Hg loads for Cold Spring Brook (site T1).

approach (Watras et al. 1994). In contrast, in a mass-balance study of a heavily contaminated system of rivers and impoundments in northwestern Ontario (the Wabigoon – English Lake system, Parks et al. 1989), the net rate of production of MeHg for Clay Lake during the ice-free period was 0.037 $\mu g \cdot m^{-2} \cdot day^{-1}$. The equivalent (ice-free period only) net production rate for Reservoir 2 is 0.010 $\mu g \cdot m^{-2} \cdot day^{-1}$. If the estimated rate of deposition of atmospheric MeHg is increased from 0.1 to 0.4 $\mu g \cdot m^{-2} \cdot year^{-1}$, the highest value reported for industrialized areas in southern Sweden (Hultberg et al. 1994), the net MeHg production decreases by about 8% to 3.5 $\mu g \cdot m^{-2} \cdot year^{-1}$.

Recently, Sellers et al. (1996) reported that MeHg can be decomposed by sunlight in surface waters at a rate that is first order with respect to the initial MeHg concentration and the intensity of solar radiation. The annual mean epilimnetic MeHg concentration in Reservoir 2 (0.26 $ng \cdot L^{-1}$) was 3.7 times that reported by Sellers et al. (1996) for Lake 240 in the Experimental Lakes Area in northwestern Ontario. This factor applied to the estimated photodegradation rate for Lake 240 (1.5 $\mu g \cdot m^{-2} \cdot year^{-1}$) and corrected for differences in surface area results in an estimated MeHg loss of 5.7 $\mu g \cdot m^{-2} \cdot year^{-1}$ due to photodegradation in Reservoir 2. This additional loss term, when added to the annual MeHg budget for Reservoir 2, increases the net MeHg production from 3.8 to 9.5 $\mu g \cdot m^{-2} \cdot year^{-1}$. The analysis does not account for differences in the amount of solar radiation entering the two lakes, but it does suggest a range for the actual rate of MeHg production in Reservoir 2.

The 10-km reach between sites R4 and M2 could not be budgeted because of a large inflow from the Sudbury Reservoir of unknown Hg concentration. Two contiguous wetland-associated reaches downstream from site M2 were budgeted: one from site M2 to site M5 that includes some upland drainage and a downstream reach from site M5 to site M6 that is entirely bordered by wetlands. Both reaches have relatively small amounts of unmeasured inflows, so net changes in Hg loads could appropriately be assigned to within-reach processes. In the wetland reaches, the budgets began in August 1994 and ended in July 1995. Storage changes may be ignored for annual budgets beginning and ending during summer low-flow periods, when the river is entirely within its banks, because net changes during those intervals are negligible. As with the other reaches, Hg fluxes in unmeasured inflows were estimated by subtracting measured inflows from measured outflows and multiplying the results by the annual mean Hg concentrations for the upstream reference site (site B2). The water-balance approach to determining ungauged flows was not adjusted for evapotranspiration from the riparian wetland surface (0.18 $m \cdot month^{-1}$ in July and 0.02 $m \cdot month^{-1}$ in December, Rykiel (1977)) or for rainfall because these contributions are opposite and nearly equal. Budget results (Table 3) indicate large wetland yield terms for ΣHg and MeHg in the upstream reach (site M2 to site M5) and a large yield of MeHg in the downstream reach (site M5 to site M6).

Areal Hg species yields were determined for the two reaches by dividing yield terms by the maximum flooded surface area during high-flow periods (4.8 km^2 for site M2 to site M5 and 3.3 km^2 for site M5 to site M6). These values are compared in Table 3 with areal net production and sedimentation rates for Reservoir 2. Although there was a net loss of ΣHg because of sedimentation in Reservoir 2, the flooded riparian wetland associated reaches appear to be a major source of ΣHg to the river. Expressed in terms of wetland yield rates, the flooded areal production of ΣHg in the site M2 to site M5 wetland reach (479 $mg \cdot km^{-2} \cdot day^{-1}$) was more than 60 times higher than the wetland-specific WY

© 2000 NRC Canada

(7.7 mg·km^{-2}·day^{-1}) reported by Krabbenhoft et al. (1995) for a small watershed in northern Wisconsin. The net yield of ΣHg decreased from 479 mg·km^{-2}·day^{-1} in the site M2 to site M5 reach to 252 mg·km^{-2}·day^{-1} in the reach comprising site M5 to site M6, farther downstream, which is consistent with the spatial distribution of Hg contamination in floodplain soils in those reaches of the river (Colman et al. 1999). The wetland reaches also were net sources of MeHg. The flooded WY for MeHg in the site M5 to site M6 reach (22 mg·km^{-2}·day^{-1}) was about 15 times higher than the maximum wetland-specific WY for MeHg reported by Krabbenhoft et al. (1995) for a northern Wisconsin watershed (0.6–1.5 mg·km^{-2}·day^{-1}) and by St. Louis et al. (1994) for catchments in northwestern Ontario (1.5 mg·km^{-2}·day^{-1}).

Discussion

Total Hg

Because MeHg is the form of Hg that bioaccumulates in aquatic food chains, the primary ecological significance of increased ΣHg exposure in aquatic systems may be increased MeHg production. Reservoir sediments and wetland soils are known locations of Hg methylation (Gilmour and Henry 1991; St. Louis et al. 1994). This investigation was designed to determine whether ΣHg has been and continues to be transported to Sudbury River environments that are locations of Hg methylation and whether such transport results in increased MeHg concentration.

During the 1995 water year budget period, concentration and load data indicated that the Nyanza site continued to be a significant ΣHg source to the upper Sudbury River, increasing transport by a factor of 4.5 relative to an upstream reference site. Investigation of downstream reservoir sediments (Frazier et al. 2000) confirms that recent Hg sedimentation rates are greater than background rates, measured at the bottom of cores, and sedimentation rates in the recent past were substantially greater than present day. Downstream from the Nyanza site, ΣHg transport was greater than the expected background rate. However, the amount greater than background decreased because of Hg sedimentation through site M2, about 15 km downstream from the Nyanza site. Mercury release from contaminated reservoir sediments is minimal and previously deposited Hg is unlikely to be resuspended, so that even in the first reservoir downstream from the Nyanza site, there is net sedimentation of ΣHg. It is likely that transport and sedimentation of ΣHg would decrease to background levels through site M2 if the continuing source at the Nyanza site were eliminated.

Processes other than sedimentation appear to control ΣHg concentrations and transport farther downstream in the riparian wetland reaches where substantial increases in ΣHg concentrations and loads were measured. Consistently low concentrations and loads at site M2, immediately upstream from the wetlands, indicate that these increases are not related to present-day Nyanza site releases or to mobilization of Hg from contaminated sediments in upstream reservoirs. The source for the ΣHg increases in the wetland-associated reach may be the Hg previously deposited on riparian wetland soils and streambed sediments (Colman et al. 1999). Transport from the wetland soils to the river channel would be driven by hydraulic gradient during late spring and early summer. Drainage also would occur during summer precipitation. If the source for the increased ΣHg is wetland soils, the release on an areal basis is very significant (60 times greater than published values (Krabbenhoft et al. 1995) for other wetland drainages). Another implication is that the mobility of Hg deposited in periodically flooded wetlands is much greater than that of Hg deposited in reservoir sediments.

Some features of the ΣHg increase in the riparian wetland reach are more compatible with a point source rather than wetland soils source. The July 1995 synoptic sampling (Fig. 3) indicated that Hg increase below site M2 occurred abruptly between sites M3 and M4, rather than progressively throughout the wetland reach. Also, increased concentrations measured during summer low flow were not all connected with precipitation. In the absence of precipitation, the mechanism for transport from the wetlands to the stream channel is unclear. A small tributary enters the Sudbury River between sites M3 and M4, but it was not monitored and there are no known point sources of Hg currently discharging to the river.

MeHg

MeHg stream reach budgets and WYs were computed for several flowing and lentic environments in the Sudbury River, where the effect of wetland and ΣHg presence on MeHg production could be observed. The importance of wetland drainage to MeHg concentration is even demonstrated in the budgeted reaches upstream from the reservoirs. Substantial concentrations and loads of MeHg (WY = 0.36 mg·km^{-2}·day^{-1}) were measured for the mixed wetland and forest drainage evaluated at site B1, which is well upstream from the Nyanza site. MeHg was conserved in the nonwetland reaches upstream from Reservoir 2. The MeHg load delivered to the reservoirs is about the same as that generated in the wetland–upland drainage upstream from site B1. The conservative transport occurred despite tributary input from the Nyanza site.

Although MeHg loading from the Nyanza site was not great enough to alter MeHg loading in the Sudbury River, the draining tributary did contain the highest concentration of MeHg measured in the investigation (5.8 ng·L^{-1}). This could be considered an example of increased ΣHg resulting in increased MeHg, although the ratio MeHg to ΣHg in the drainage was small (0.39%).

An effect of ΣHg on MeHg production was expected in Reservoir 2 because of the significant amounts of Hg in the anoxic bed sediments, a known location of MeHg production. However, net production of MeHg on an areal basis in Reservoir 2 for the 1995 water year was similar to that reported elsewhere for lakes receiving only atmospheric Hg contamination. In contrast, results from the budget of the downstream wetland, an environment also conducive to MeHg production, indicated production rates 15 times greater (areal basis) than those reported from other wetland investigations without point-source contamination. As discussed by Colman et al. (1999), ΣHg and MeHg concentrations are directly correlated in both reservoir and wetland bulk sediments from the Sudbury River. The apparent differential transport of MeHg to the water column from these two sediment environments may be a function of the hydraulic gradients that occur in the periodically flooded wetlands as

© 2000 NRC Canada

compared with diffusive processes controlling transport from the reservoir sediments.

Diluted by discharge from the Sudbury River, the MeHg export from the riparian wetland produced river concentrations averaging only 37% greater than concentrations from wetlands in the headwater drainage at site B1, but these averaged 185% greater than the average at site M2, immediately upstream. Thus, the wetland river MeHg concentrations were greater than expected at a downstream location in a mostly upland drainage and may contribute to greater concentrations of Hg in fish than would be the case if the contaminated wetlands were not present.

Whereas MeHg export from the riparian wetland to the Sudbury River increases the local MeHg concentration, the cause and rate of export may have a greater importance for the biogeochemical cycling of Hg. Previous correlations of ΣHg and MeHg in aquatic environments have been weak or nonexistent. Kelly et al. (1995) did not find a correlation between ΣHg and MeHg exported from wetland drainages. In this investigation, a15-fold increase in measured MeHg export from wetland soils, compared with other investigations, could indicate a relationship between the concentrations of ΣHg in wetland soils and the export of MeHg from the soils. Measuring the effect of increased Hg exposure in aquatic environments is a new concern. In future investigations, it will be important to verify whether concentrations of ΣHg in wetland soils correlate with MeHg export from the soils. Verification of such a relationship would be an important consideration in decisions regulating Hg in the environment.

Acknowledgments

The authors thank Mary Garren, Pamela Shields, and Susan Svirsky for help in planning and facilitating this study. We also thank David Abraham, Nicolas Bloom, Kenneth Finkelstein, Bradley Frazier, Terry Haines, Steven Mierzykowski, Gary Morin, Gregory Nail, Teresa Naimo, and James Wiener for sharing data and ideas related to the study. David Krabbenhoft, Robert Lent, and two anonymous reviewers read earlier versions of the manuscript and provided many helpful comments. The study was funded by the U.S. Environmental Protection Agency (Region I) through an interagency agreement with the U.S. Geological Survey.

References

Babiarz, C.L., and Andren, A.A. 1995. Total concentrations of mercury in Wisconsin (U.S.A.) lakes and rivers. Water Air Soil Pollut. **83**: 173–183.

Bloom, N.S. 1992. On the chemical form of mercury in edible fish and marine invertebrate tissue. Can. J. Fish. Aquat. Sci. **49**: 1010–1017.

Bloom, N.S. 1995. Mercury as a case study of ultra-clean sample handling and storage in aquatic trace-metal research. Environ. Lab. March/April. pp. 20–25.

Bloom, N.S., and Crecelius, E.A. 1983. Determination of mercury in seawater at sub-nanogram per liter levels. Mar. Chem. **14**: 49–59.

Bloom, N.S., and Fitzgerald, W.F. 1988. Determination of volatile mercury species at the picogram level by low-temperature gas chromatography with cold-vapour atomic fluorescence detection. Anal. Chim. Acta, **208**: 151–161.

Bloom, N.S., Colman, J.A., and Barber, L. 1997. Artifact formation of methyl mercury during aqueous distillation and alternative techniques for the extraction of methyl mercury from environmental samples. Fresenius J. Anal. Chem. **358**: 371–377.

Burke, J., Hoyer, M., Keeler, G., and Scherbatskoy, T. 1995. Wet deposition of mercury and ambient mercury concentrations at a site in the Lake Champlain Basin. Water Air Soil Pollut. **80**: 353–362.

Cohn, T.A., Delong, L.L., Gilroy, E.J., Hirsch, R.M., and Well, D. 1989. Estimating constituent loads. Water Resour. Res. **25**: 937–942.

Cohn, T.A., Caulder, D.L., Gilroy, E.J., Zynjuk, L.D., and Summers, R.M. 1992. The validity of a simple statistical model for estimating fluvial constituent loads: an empirical study involving nutrient loads entering Chesapeake Bay. Water Resour. Res. **28**: 2353–2363.

Colman, J.A., and Breault, R.F. 2000. Sampling for mercury at subnanogram per litre concentrations for load estimation in rivers. Can. J. Fish. Aquat. Sci. **57**: 1073–1079.

Colman, J.A., Waldron, M.C., Breault, R.F., and Lent, R.F. 1999. Distribution and transport of total mercury and methylmercury in mercury-contaminated sediments in reservoirs and wetlands of the Sudbury River, east-central Massachusetts. U.S. Geol. Surv. Water Resour. Invest. Rep. 99-4060.

Fitzgerald, W.F., Mason, R.P., and Vandal, G.M. 1991. Atmospheric cycling and air–water exchange of mercury over mid-continental lacustrine regions. Water Air Soil Pollut. **56**: 745–768.

Frazier, B.E., Wiener, J.G., Rada, R.G., and Engstrom, D.R. 2000. Stratigraphy and historic accumulation of mercury in recent depositional sediments in the Sudbury River, Massachusetts, U.S.A. Can. J. Fish. Aquat. Sci. **57**: 1062–1072.

Gill, G.A., and Bruland, K.W. 1990. Mercury speciation in surface freshwater systems in California and other areas. Environ. Sci. Technol. **24**: 1392–1400.

Gilmour, C.C., and Henry, E.A. 1991. Mercury methylation in aquatic systems affected by acid deposition. Environ. Pollut. **71**: 131–169.

Guy, H.P. 1970. Fluvial sediment concepts. U.S. Geol. Surv. Tech. Water Resour. Invest. Book 3, Chap. C1.

Hirsch, R.M. 1982. A comparison of four streamflow record extension techniques. Water Resour. Res. **18**: 1081–1088.

Horvat, M., Liang, L., and Bloom, N.S. 1993. A comparison of distillation with other current preparation methods for the determination of methylmercury in low level environmental samples. Part II. Anal. Chim. Acta, **282**: 153–168.

Hoyer, M.E., Burke, J.M., and Keeler, G.J. 1995. Atmospheric sources, transport, and deposition of mercury in Michigan: two years of event precipitation. Water Air Soil Pollut. **80**: 199–208.

Hultberg, H., Iverfeldt, A., and Lee, Y.-H. 1994. Methylmercury input/output and accumulation in forested catchments and critical loads for lakes in southwestern Sweden. *In* Mercury pollution: integration and synthesis. *Edited by* C.J. Watras and J.W. Huckabee. Lewis Publishers, Boca Raton, Fla. pp. 313–321.

Hurley, J.P., Benoit, J.M., Babiarz, C.L., Shafer, M.M., Andren, A.W., Sullivan, J.R., Hammond, R., and Webb, D.A. 1995. Influences of watershed characteristics on mercury levels in Wisconsin rivers. Environ. Sci. Technol. **29**: 1867–1875.

Kelly, C.A., Rudd, J.W.M., St. Louis, V.L., and Heyes, A. 1995. Is total mercury concentration a good predictor of methylmercury concentration in aquatic systems? Water Air Soil Pollut. **80**: 715–724.

Kennedy, E.J. 1984. Discharge ratings at gaging stations. U.S. Geol. Surv. Tech. Water Resour. Invest. Book 3, Chap. A10.

Krabbenhoft, D.P., Benoit, J.M., Babiarz, C.L., Hurley, J.P., and Andren, A.W. 1995. Mercury cycling in the Allequash Creek watershed, northern Wisconsin. Water Air Soil Pollut. **80**: 425–433.

© 2000 NRC Canada

Lamborg, C.H., Fitzgerald, W.F., Vandal, G.M., and Rolfhus, K.R. 1995. Atmospheric mercury in northern Wisconsin: sources and species. Water Air Soil Pollut. **80**: 189–198.

Lindqvist, O., Johansson, K., Aastrup, M., Andersson, A., Bringmark, L., Hovsenius, G., Håkanson, L., Iverfeldt, Å., Meili, M., and Timm, B. 1991. Mercury in the Swedish environment–Recent research on causes, consequences and corrective methods. Water Air Soil Pollut. **55**: 143–177.

Mason, R.P., Reinfelder, J.R., and Morel, F.M.M. 1995. Bioaccumulation of mercury and methylmercury. Water Air Soil Pollut. **80**: 915–921.

Parks, J.W., Lutz, A., Sutton, J.A., and Townsend, B.E. 1989. Water column methylmercury in the Wabigoon/English River Lake system: factors controlling concentrations, speciation, and net production. Can. J. Fish. Aquat. Sci. **46**: 2184–2202.

Rantz, S.E., et al. 1982. Measurement and computation of streamflow. Vol. 1. Measurement of stage and discharge; Vol. 2. Computation of discharge. U.S. Geol. Surv. Water-Supply Pap. 2175.

Ries, K.G., III. 1993. Estimation of low-flow duration discharges in Massachusetts. U.S. Geol. Surv. Open-File Rep. 93-38.

Rodgers, D.W. 1994. You are what you eat and a little bit more: bioenergetics-based models of methylmercury accumulation in fish revisited. *In* Mercury pollution: integration and synthesis. *Edited by* C.J. Watras and J.W. Huckabee. Lewis Publishers, Boca Raton, Fla. pp. 427–439.

Rudd, J.W.M. 1995. Sources of methyl mercury to freshwater ecosystems: a review. Water Air Soil Pollut. **80**: 697–713.

Rykiel, E.J., Jr. 1977. Toward simulation and systems analysis of nutrient cycling in the Okefenokee Swamp, Georgia. Tech. Completion Rep. USDI/OWRT Project No. A-060-GA, University of Georgia, Athens, Ga.

Sellers, P., Kelly, C.A., Rudd, J.W.M., and MacHutchon, A.R. 1996. Photodegradation of methylmercury in lakes. Nature (Lond.), **380**: 694–697.

St. Louis, V.L., Rudd, J.W.M., Kelly, C.A., Baety, K.G., Bloom, N.S., and Flett, R.J. 1994. Importance of wetlands as sources of methylmercury to boreal forest ecosystems. Can. J. Fish. Aquat. Sci. **51**: 1065–1076.

Watras, C.J., et al. 1994. Sources and fates of mercury and methylmercury in Wisconsin lakes. *In* Mercury pollution: integration and synthesis. *Edited by* C.J. Watras and J.W. Huckabee. Lewis Publishers, Boca Raton, Fla. pp. 153–177.

Wiener, J.G., and Shields, P.J. 2000. Mercury in the Sudbury River (Massachusetts, U.S.A.): pollution history and a synthesis of recent research. Can. J. Fish. Aquat. Sci. **57**: 1053–1061.

© 2000 NRC Canada

Bioavailability of sediment-associated mercury to *Hexagenia* mayflies in a contaminated floodplain river

Teresa J. Naimo, James G. Wiener, W. Gregory Cope, and Nicolas S. Bloom

Abstract: We examined the bioavailability of mercury in sediments from the contaminated Sudbury River (Massachusetts, U.S.A.). Mayfly nymphs (*Hexagenia*) were exposed in four 21-day bioaccumulation tests to contaminated and reference sediments (treatments) from reservoirs, flowing reaches, palustrine wetlands, and a riverine lake. Mean total mercury (ΣHg) ranged from 880 to 22 059 ng·g dry weight^{-1} in contaminated sediments and from 90 to 272 ng·g^{-1} in reference sediments. Mean final concentrations of methyl mercury (MeHg) in test water were greatest (8–47 ng Hg·L^{-1}) in treatments with contaminated wetland sediments, which had mean ΣHg ranging from 1200 to 2562 ng·g^{-1}. In mayflies, final mean concentrations of MeHg were highest in treatments with contaminated wetland sediments (122–183 ng Hg·g^{-1}), intermediate in treatments with contaminated sediments from reservoirs, flowing reaches, and a riverine lake (75–127 ng Hg·g^{-1}), and lowest in treatments with reference sediments (32–41 ng Hg·g^{-1}). We conclude that the potential entry of MeHg into the benthic food chain was greater in contaminated palustrine wetlands than in the contaminated reservoirs, which had the most contaminated sediments.

Résumé : Nous avons étudié la biodisponibilité du mercure dans les sédiments d'un cours d'eau pollué des États-Unis (rivière Sudbury, au Massachusetts). Des nymphes d'éphémères (*Hexagenia*) ont été exposées, dans le cadre de quatre épreuves de bioaccumulation de 21 jours, à des sédiments de référence et à des sédiments contaminés provenant de réservoirs, de tronçons d'eau vive, de milieux humides palustres et d'un lac fluvial. La quantité moyenne de mercure total (ΣHg) était comprise entre 880 et 22 059 ng·g poids sec^{-1} dans les sédiments contaminés et entre 90 et 272 ng·g^{-1} dans les sédiments de référence. La concentration moyenne finale de méthyl mercure (MeHg) dans l'eau étudiée était au plus haut (8–47 ng Hg·L^{-1}) dans les expériences sur des sédiments contaminés provenant de milieux humides, dont la ΣHg moyenne était comprise entre 1200 et 2562 ng·g^{-1}. Chez les éphémères, la concentration moyenne finale de MeHg était au plus haut dans les expériences sur des sédiments contaminés de milieux humides (122–183 ng Hg·g^{-1}), intermédiaire dans les expériences sur des sédiments contaminés provenant de réservoirs, de tronçons d'eau vive et d'un lac fluvial (75–127 ng Hg·g^{-1}) et au plus bas dans les expériences en présence de sédiments de référence (32–41 ng Hg·g^{-1}). Nous concluons que la possibilité d'entrée du MeHg dans la chaîne alimentaire benthique était plus grande dans les milieux humides palustres contaminés que dans les réservoirs contaminés, qui pourtant renfermaient les sédiments les plus contaminés.

[Traduit par la Rédaction]

Introduction

The Sudbury River in eastern Massachusetts (U.S.A.) has been contaminated by chemical wastes originating from the Nyanza chemical waste dump site (Nyanza site), a former industrial complex in the town of Ashland. Large quantities of mercury, a toxic metal with no known essential biological function, were released to the environment at the Nyanza site (NUS Corporation 1992; Wiener and Shields 2000). The fine-grained sediments in downstream reaches of the Sudbury River now contain a substantial quantity of inorganic mercury (Colman et al. 1999; Frazier et al. 2000), posing a potential hazard to biota in the river and its adjoining wetlands. High concentrations of mercury were found in fish taken downstream from the Nyanza site (NUS Corporation 1992), but it was not known whether the mercury accumulating in fish and other biota was derived from contaminated sediments or from other inputs to the river.

Information on the bioavailability of mercury in contaminated sediments in the Sudbury River and its floodplain was needed to assess the potential entry of methyl mercury (MeHg) into aquatic food chains supporting fish and higher trophic levels. Potential sources of MeHg to riverine biota include methylation of inorganic mercury in flowing reaches, reservoirs, riverine lakes, and adjoining wetlands (St. Louis et al. 1994; Hurley et al. 1995; Krabbenhoft et al. 1995; Rudd 1995). MeHg may also enter the river in atmospheric deposition (Rudd 1995).

In the present study, the bioavailability of mercury in fine-

Received June 20, 1997. Accepted May 6, 1999.
J14076

T.J. Naimo,[1] **J.G. Wiener, and W.G. Cope.**[2]
U.S. Geological Survey, Biological Resources Division, Upper Midwest Environmental Sciences Center, 2630 Fanta Reed Road, La Crosse, WI 54603, U.S.A.
N.S. Bloom. Frontier Geosciences, 414 Pontius Avenue North, Suite B, Seattle, WA 98109, U.S.A.

[1]Author to whom all correspondence should be addressed.
e-mail: teresa_naimo@usgs.gov
[2]Present address: Department of Toxicology, North Carolina State University, Box 7633, Raleigh, NC 27695-7633, U.S.A.

© 2000 NRC Canada

grained, surficial sediments from the Sudbury River was assessed in bioaccumulation tests with burrowing mayfly nymphs (*Hexagenia*) experimentally exposed to sediments from the river basin. *Hexagenia* is a benthic detritivore common in many North American rivers, including the Sudbury River. Burrowing mayflies and other benthic invertebrates are potentially important in the trophic transfer of MeHg because of their significance in the diets of fish and certain waterfowl. *Hexagenia* nymphs select substrates with high organic and silt content, an association that increases their exposure to sediment-associated contaminants. *Hexagenia* nymphs have been widely used as test organisms in laboratory tests, including bioaccumulation tests with inorganic mercury and MeHg (Saouter et al. 1991, 1993; Odin et al. 1994, 1995). Burrowing mayflies readily bioaccumulate MeHg associated with ingested sediment and detritus (Saouter et al. 1991, 1993; Odin et al. 1994, 1995). Bioaccumulation tests with *Hexagenia*, therefore, provide an indirect measure of the production of MeHg in mercury-contaminated surficial sediments and of the potential entry (flux) of MeHg into the benthic food chain.

Our objectives were (*i*) to determine if *Hexagenia* mayfly nymphs exposed to mercury-contaminated surficial sediment from the Sudbury River accumulate MeHg, (*ii*) to determine if the accumulation of MeHg in mayflies is related to total mercury (ΣHg) concentration in sediment, and (*iii*) to assess which contaminated areas on the Sudbury River have the greatest potential for MeHg transfer from sediments into the benthic food chain.

Methods

Experimental approach

Four 21-day bioaccumulation tests were conducted with nymphs of *Hexagenia* experimentally exposed in the laboratory to sediments from the river basin. In 1994, bioaccumulation tests were conducted with sediments sampled from impoundments, flowing reaches, and a riverine lake during July (test 1) and September (test 2). In 1995, the bioaccumulation tests focused on wetland areas within the river floodplain, with sediments obtained in May (test 3) and September (test 4).

Microbial methylating activity in aquatic sediments follows an annual cycle that is closely linked to temperature, with peak MeHg production occurring during the warmest months (Ramlal et al. 1993). Our sediment sampling was done in May, July, and September, months of active MeHg production (Ramlal et al. 1993). Each bioaccumulation test employed a randomized block experimental design; tests 1 and 2 included six replicates of six sediment treatments, whereas tests 3 and 4 had nine replicates of four sediment treatments.

Test sediments

Sediments for the four tests were obtained from a total of nine study areas, with sediments from a given study area representing a treatment in our tests. In tests 1 and 2, sediments were obtained from four depositional areas and two free-flowing reaches in the Sudbury River basin (Fig. 1). Three of the depositional areas (Reservoir 1 (49 ha), Reservoir 2 (47 ha), and Fairhaven Bay (27 ha)) were contaminated areas that spanned the mercury contamination gradient attributed to the Nyanza site (NUS Corporation 1992). The fourth depositional area, the Whitehall Reservoir (233 ha), was a reference area that had not been directly contaminated by wastes from the Nyanza site. The two free-flowing reaches included one contaminated site (within the Great Meadows National Wildlife Refuge) and one upstream reference site that had not been directly contaminated by wastes from the Nyanza site.

Test sediments for tests 3 and 4 were obtained from four study areas, including two contaminated wetlands (both containing mercury from the Nyanza site), one reference wetland (Hop Brook wetland, not measurably contaminated by mercury from the Nyanza site), and one contaminated depositional area (Fairhaven Bay) (Fig. 1). Sediments from Fairhaven Bay were included in all four tests to facilitate comparison of test results between years. About 8% of the 427-km^2 Sudbury River watershed is covered by nonforested wetlands (NUS Corporation 1992). In particular, the reach about 20–35 km downstream from the Nyanza site contains an extensive floodplain and associated palustrine wetlands, lying within the 12-km^2 Great Meadows National Wildlife Refuge. These wetlands have been classified as palustrine wetlands with scrub-shrub and persistent, emergent herbaceous plants (Harris 1996).

Within each area, sediment was obtained from randomly selected sampling sites, identified by latitude and longitude coordinates. The spatial randomization of sampling allowed extrapolation of test data from the sampled sites to the soft sediments within a defined study area. When sampling in wetland reaches, we first located the randomly selected position in the main channel of the stream and then randomly selected a sampling site in the adjoining floodplain within 10 m (in 1-m increments) of either the left or right stream bank.

Surficial sediments (uppermost 4–6 cm) for tests 1 and 2 were obtained with a Van Veen sampler, and sediments for test 3 were taken with an Ekman grab sampler (American Society for Testing and Materials 1992). During test 4, sediments in the three wetland areas were exposed due to drought-associated low water levels, and sampling of wetland sediments was done with a stainless steel spatula. In Fairhaven Bay, sediments for test 4 were taken with an Ekman sampler. Sediment for all tests was passed on site through a 2-mm Nalgene® sieve. Each sample was placed into a 1.9-L Nalgene® container with a screw top, held on ice in the field, and later stored at 10 ± 5°C for a maximum of 24 days before beginning a bioaccumulation test.

Test sediments were analyzed for texture (sieve-pipet method; Guy 1969; Plumb 1981) and for volatile matter content (loss on ignition at 550°C), a surrogate for organic matter content. Two textural groups were delineated, sand (62–2000 μm) and silt plus clay (<62 μm). During tests 1 and 2, the physical characteristics of test sediment varied significantly among treatments (Table 1). In particular, sediment from the Whitehall Reservoir had greater volatile matter content (about 60%) than sediment from the other treatments (range 14–25%). Sediments from five of the six study areas in tests 1 and 2 were primarily silt and clay (Table 1). The physical characteristics of sediments in tests 3 and 4 were less variable than those in tests 1 and 2 (Table 1). The mean textural composition of sediments from the Hop Brook wetland treatment differed from the that of other treatments in test 3 but not in test 4 (Table 1).

Bioaccumulation tests

The experimental unit in each 21-day bioaccumulation test was a 4-L glass beaker containing 725 mL of wet sediment from a given sampling site and 2900 mL of test water, providing a 4:1 (v/v) water to sediment ratio. During the allocation of test sediment to each beaker, a sample (>10 g wet weight) of the sediment added was placed into a 125-mL Nalgene® container. Samples of test sediment were stored in a freezer at –15°C or colder until analyzed for ΣHg.

Each beaker was covered with a 20-cm-diameter watch glass to reduce evaporation of test water. The 36 experimental units in each test were held within two 900-L water baths. A temperature of

© 2000 NRC Canada

Fig. 1. Map of the Sudbury River basin showing the areas from which test sediments were taken.

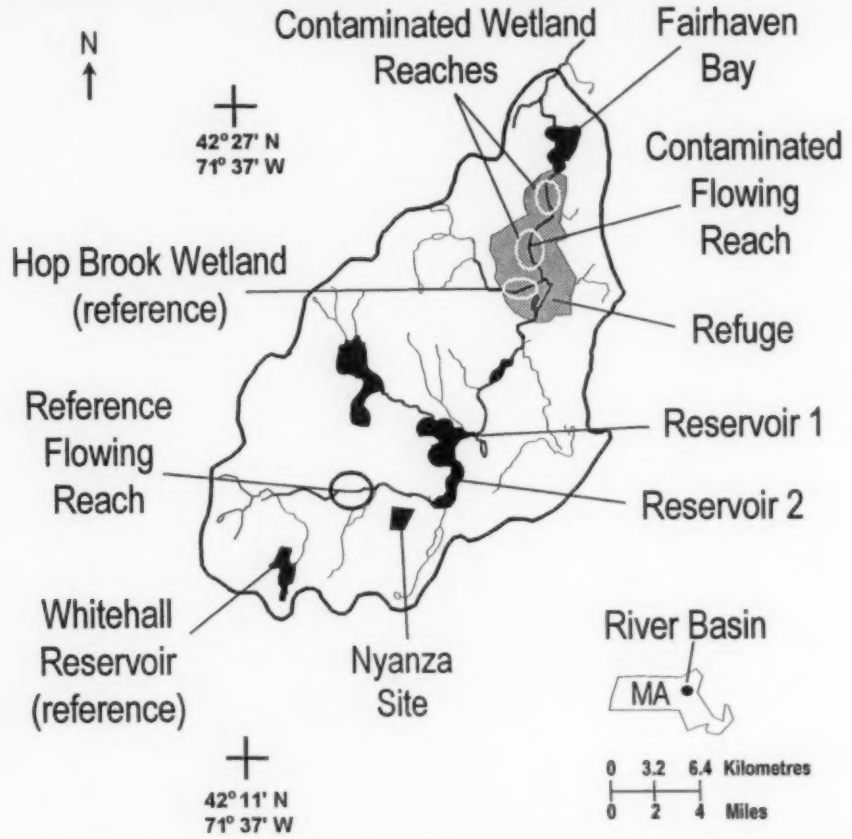

20 ± 2°C was maintained by a recirculation pump. Photoperiod was 16 h light : 8 h dark.

The overlying test water was soft, similar in hardness and pH to water from the Sudbury River. The test water was prepared by adding 36 mg $NaHCO_3 \cdot L^{-1}$, 7.5 mg $CaSO_4 \cdot L^{-1}$, 7.5 mg $MgSO_4 \cdot L^{-1}$, and 0.009 mL 36 N $H_2SO_4 \cdot L^{-1}$ to deionized water. During the four tests, the test water before sediment addition had a mean pH of 6.9, a mean conductivity of 234 $\mu S \cdot cm^{-1}$, a mean total alkalinity of 29.1 mg $CaCO_3 \cdot L^{-1}$, and a mean total hardness of 34.9 mg $CaCO_3 \cdot L^{-1}$. During each test, the overlying water in each beaker was gently aerated to maintain sufficient dissolved oxygen (>5 $mg \cdot L^{-1}$) for mayflies. Gaseous mercury (Hg^0) was removed from the air supply with two gold-coated quartz sand traps (Fitzgerald et al. 1991) placed in series in the air line delivering air to all beakers.

Hexagenia nymphs (almost entirely *Hexagenia bilineata*) were obtained with a Ponar dredge within 1 day before the start of each bioaccumulation test from Pool 8 of the Upper Mississippi River, an area with low ΣHg concentrations in both sediment and resident *Hexagenia* (Beauvais et al. 1995). The mean initial (day 0) concentrations (±1 SE) of ΣHg and MeHg were 81 ± 8 $ng \cdot g$ dry $weight^{-1}$ and 28 ± 10 ng $Hg \cdot g^{-1}$, respectively, based on analysis of three composite samples of 10 whole mayflies per bioaccumulation test.

Each mayfly was measured (total length) and transferred into a beaker with a spoon-shaped piece of Nitex® mesh attached to a glass rod. Fifteen nymphs, ranging from 10 to 19 mm in total length, were randomly allocated to each beaker 7–10 days after the test sediment and water had been placed into the beaker. Day 0 of a given test was defined as the day on which mayflies were introduced into the beakers.

On day 21 of each test, about 100 mL of overlying water, to be analyzed for MeHg, was taken from each beaker by immersion of a 125-mL Teflon®-coated bottle. Water samples were stored at −15°C or colder until analyzed. Mayflies in each beaker were separated from the test sediment by passing the sediment through a 2-mm Nalgene® sieve. Mayflies retained on the sieve were removed with forceps, counted, and measured. Ten nymphs from each beaker were placed into a single 125-mL Nalgene® container to yield one composite sample to be analyzed for ΣHg and MeHg; these samples were stored at −15°C or colder until analyzed. We were interested in the trophic transfer of MeHg from sediments into the benthic food chain; therefore, we did not allow mayflies to depurate their gut contents before analysis (Hare et al. 1989).

Test water

The temperature of the overlying water, measured daily in situ, ranged from 19.5 to 20.8°C and did not vary among treatments in any of the four tests. The mean concentrations of dissolved oxygen, measured daily in situ, did not vary among treatments in test 1 or 3 but varied slightly in test 2 (from 7.5 to 7.9 $mg \cdot L^{-1}$) and in test 4 (from 7.5 to 7.7 $mg \cdot L^{-1}$). Although the mean pH, measured daily in situ, in the overlying water varied significantly among treatments in all four tests (Table 1), the range in mean pH was 0.6 pH unit or less in all but test 4, in which mean pH ranged from 5.9 in the northern contaminated wetland treatment to 7.2 in the Fairhaven Bay treatment. On day 21 of each test, a water sample was

© 2000 NRC Canada

Table 1. Mean (±1 SE) values for selected characteristics of test sediment and test water to which *Hexagenia* mayflies were exposed in four bioaccumulation tests.

	Test sediment		Test water		
Treatment	Volatile matter (%)	Silt plus clay content (%)	pH	Conductivity ($\mu S \cdot cm^{-1}$)	Hardness (mg $CaCO_3 \cdot L^{-1}$)
Test 1 (July 1994 sediments)					
Whitehall Reservoir	58.0±1.5 *a*	79±3 *ab*	6.88 *a*	143 *a*	11.6 *a*
Reference flowing reach	16.8±3.0 *bc*	37±6 *c*	7.25 *b*	215 *b*	33.9 *b*
Reservoir 2	15.8±1.7 *c*	78±6 *ab*	7.16 *d*	237 *b*	33.5 *b*
Reservoir 1	13.6±1.6 *c*	76±6 *ab*	6.91 *a*	254 *b*	43.7 *b*
Contaminated flowing reach	17.7±2.5 *bc*	57±9 *bc*	7.37 *c*	230 *b*	42.6 *b*
Fairhaven Bay	24.7±1.2 *b*	84±4 *a*	7.24 *bd*	211 *b*	36.9 *b*
Test 2 (September 1994 sediments)					
Whitehall Reservoir	62.2±5.2 *a*	77±4 *a*	6.99 *a*	112 *a*	10.3 *a*
Reference flowing reach	15.7±3.8 *b*	50±4 *b*	7.21 *b*	195 *b*	37.2 *b*
Reservoir 2	16.6±1.2 *b*	86±5 *a*	6.91 *e*	197 *b*	28.6 *b*
Reservoir 1	14.9±1.5 *b*	83±5 *a*	7.07 *d*	197 *b*	30.3 *b*
Contaminated flowing reach	20.8±1.2 *b*	82±2 *a*	7.28 *c*	200 *b*	42.4 *b*
Fairhaven Bay	18.4±2.3 *b*	66±11 *ab*	7.15 *b*	180 *b*	34.9 *b*
Test 3 (May 1995 sediments)					
Hop Brook wetland (reference)	33.1±3.2 *a*	78±3 *a*	7.19 *a*	148 *ab*	26.4 *a*
Southern contaminated wetland	25.4±0.5 *b*	89±1 *b*	6.84 *d*	126 *c*	16.7 *b*
Northern contaminated wetland	27.2±1.6 *ab*	90±1 *b*	6.62 *c*	108 *c*	13.1 *b*
Fairhaven Bay	25.0±0.9 *b*	86±1 *b*	6.94 *b*	177 *b*	40.0 *a*
Test 4 (September 1995 sediments)					
Hop Brook wetland (reference)	36.1±3.5 *a*	80±5	6.83 *a*	329 *a*	78.5
Southern contaminated wetland	26.2±1.7 *ab*	90±1	6.50 *d*	214 *ac*	37.9
Northern contaminated wetland	27.2±2.4 *ab*	91±1	5.93 *c*	301 *ac*	41.0
Fairhaven Bay	21.7±3.5 *b*	63±10	7.18 *b*	201 *bc*	48.0

Note: Means for a given variable and test that are not accompanied by a common letter were significantly different (Tukey's HSD procedure, $\alpha = 0.05$). Treatments (sediment source) for each test are listed in longitudinal sequence from upstream to downstream.

taken from each beaker and analyzed for hardness, alkalinity, and conductivity. In tests 1 and 2, conductivity and hardness in the Whitehall Reservoir treatment were significantly lower than in the other five treatments, which did not differ. Conductivity also varied among treatments in tests 3 and 4 (Table 1). Mean alkalinity varied significantly among treatments in all four tests, with means for individual treatments ranging from 12 to 58 mg $CaCO_3 \cdot L^{-1}$. Total ammonia nitrogen and un-ionized ammonia nitrogen, determined in water from one randomly selected beaker from each treatment, ranged from 0.05 to 1.20 $mg \cdot L^{-1}$ and from 0.2 to 5.2 $\mu g \cdot L^{-1}$, respectively, in the tests.

Diet and ration

To supply organic carbon to support microbial activity, each beaker was provided with dried, finely ground leaves of submersed aquatic plants. In tests 1 and 2, we used wild celery (*Vallisneria americana*) from Lake Onalaska (Pool 7, Upper Mississippi River) as a source of organic carbon. Curly pondweed (*Potamogeton crispus*) was used in tests 3 and 4 because wild celery was not yet available when test 3 was initiated. Fresh leaves were dried at 104°C for 72 ± 12 h, ground to a fine homogenate with a mortar and pestle, and stored in Nalgene® bottles in a desiccator. Beginning 2–3 days before day 0 of a test, 193 ± 5 mg dry weight of curly pondweed or 228 ± 5 mg dry weight of wild celery was added to each beaker every third day. These rates of wild celery and curly pondweed addition equated to a mean daily loading rate of organic carbon of about 100 mmol per square metre of sediment surface in our beakers, a typical value for mesotrophic freshwater ecosystems (C.A. Kelly, Department of Microbiology, University of Manitoba, Winnipeg, MB R3T 2N2, Canada, and J.W.M. Rudd, Department of Fisheries and Oceans, Freshwater Institute, 501 University Crescent, Winnipeg, MB R3T 2N6, Canada, personal communication). Concentrations of MeHg in a subsample of the plant homogenate were 5.1, 1.1, 5.3, and 4.2 ng $Hg \cdot g$ dry $weight^{-1}$ in tests 1, 2, 3, and 4, respectively.

During test 3, we evaluated the potential effect of the change in plant species on test results by placing sediment from a given site into two separate beakers and adding pondweed to one beaker and wild celery to the other. This evaluation was done with sediments from one sampling site in each of two sediment treatments (a contaminated wetland and a riverine lake). Test results were not measurably affected by the difference in plant species used as a source of carbon. At the end of test 3, the MeHg concentration in overlying water from beakers with sediment from the contaminated wetland was 11.8 ng $Hg \cdot L^{-1}$ in the beaker provided wild celery and 13.8 ng $Hg \cdot L^{-1}$ in the beaker provided curly pondweed. The MeHg concentration in overlying water from beakers with sediment from the riverine lake was 0.7 ng $Hg \cdot L^{-1}$ in the beaker provided wild celery and 1.0 ng $Hg \cdot L^{-1}$ in the beaker provided curly pondweed.

Mercury determinations

For determinations of ΣHg, 1.0-g samples of sediment and 0.1-g aliquots of the mayfly composites were digested in refluxing 7:3 HNO_3–H_2SO_4 (Bloom and Crecelius 1987) and analyzed by $SnCl_2$ reduction, dual gold amalgamation, and atomic fluorescence detection (Bloom and Crecelius 1983; Bloom and Fitzgerald 1988). For determination of MeHg in mayflies, 0.1-g samples were digested in 25% KOH in methanol (Bloom 1989, 1992), and aliquots were analyzed by aqueous-phase ethylation (Bloom 1989), carbotrap collection, isothermal gas chromatographic separation (Liang et al.

© 2000 NRC Canada

1994), and atomic fluorescence detection. Water samples (35 mL) were pre-separated by distillation (Horvat et al. 1993; Bloom and Von Der Geest 1995) before analysis for MeHg by the ethylation technique.

An aliquot of each sample of sediment and mayflies was analyzed for percent dry solids. The dry fraction was determined gravimetrically after drying overnight in an oven at 105 ± 5°C. Mercury concentrations in sediment and mayflies were reported on a dry weight basis.

Quality assurance

All samples were handled according to chain-of-custody procedures. All glassware, plasticware, and tubing used in the bioaccumulation tests was acid washed (10% HNO_3 for 24 h) before use. Precision (relative standard deviation) during volatile matter and particle size determinations on sediment and during determinations of total alkalinity, total hardness, and conductivity in water (day 21) was estimated from triplicate analyses of 10% or more of the samples analyzed. Relative standard deviations were 0–15% for total alkalinity, 0–11% for total hardness, 0–3% for conductivity, 0.1–5% for volatile matter, 2–44% for percent sand, and 0.3–1% for percent silt plus clay (data from all four bioaccumulation tests combined).

During the determination of ΣHg and MeHg in mayflies, water, and sediment, we analyzed one method blank, appropriate certified reference materials, analytical duplicates, and blind duplicates per 20 samples analyzed. Concentrations of ΣHg and MeHg in certified reference materials (dogfish muscle (DORM-2) and marine sediment (PACS-1)) were within the certified ranges, whereas our mean concentration of 78.7 ± 2.9 ng·g dry weight^{-1} for ΣHg in estuarine sediment (NIST-1646) slightly exceeded the certified range of 63 ± 11 ng·g dry weight^{-1}. Estimated method detection limits were 0.053 ng Hg·L^{-1} for MeHg in water, 0.44 ng·g wet weight^{-1} for ΣHg in sediment, 3.5 ng Hg·g wet weight^{-1} for MeHg in mayflies, and 1.8 ng·g wet weight^{-1} for ΣHg in mayflies. Mean (±1 SD) matrix-spike percent recoveries were 97 ± 13 for MeHg in water, 105 ± 14 for ΣHg in sediment, 109 ± 15 for MeHg in mayflies, and 97 ± 11 for ΣHg in mayflies. The mean relative percent difference between duplicate samples ranged from 4 to 25%.

Statistical analyses

Mercury concentrations in sediment, water, and mayflies were tested for normality and homogeneity of variance. The data were not normally distributed and had inequality of variances; thus, all subsequent analyses were performed on rank-transformed data. For each bioaccumulation test, variation in mean concentrations of ΣHg or MeHg in sediment, mayflies, and water among treatments was compared by one-way analysis of variance. Tukey's HSD multiple range test was performed to compare treatment means when the analysis of variance was significant. The mean net MeHg accumulation (nanograms per mayfly) in each experimental unit was calculated as the mean final MeHg burden minus the mean initial burden. Estimates of mayfly dry weights used in this calculation were predicted from regression of total length (millimetres) and dry weight (milligrams) of *Hexagenia* mayflies sampled during 1994 and 1995 in the Upper Mississippi River (log dry weight = –2.666 + 2.849(log total length); $r^2 = 0.80$, $n = 633$). A Type I error of 0.05 was used to judge the significance of all statistical tests.

Results

Mercury in sediment, water, and mayflies

Mean concentrations of ΣHg in test sediments varied more than 100-fold among the six treatments in both test 1 and test 2 (Table 2). Mean concentrations in sediments ranged from 90 to 272 ng·g dry weight^{-1} in the reference areas, from 880 to 1920 ng·g^{-1} in the contaminated flowing reach and Fairhaven Bay, and from 7548 to 22 059 ng·g^{-1} in Reservoirs 1 and 2. In contrast, mean concentrations of MeHg in water at the end of tests 1 and 2 (all treatments) varied only 10-fold (Table 2). In general, concentrations of MeHg in test water were lowest in the reference flowing reach, intermediate in Fairhaven Bay, the contaminated flowing reach, and Reservoir 1, and highest in Reservoir 2.

Mayflies exposed to sediments from mercury-contaminated sites accumulated more MeHg than did mayflies exposed to reference sediments (Table 2). Concentrations of MeHg in mayflies exposed to sediments from the four contaminated areas were two (test 2) to three (test 1) times those in mayflies exposed to sediments from the two reference areas. In mayflies, the fraction of ΣHg present as MeHg ranged from 1.2 to 28.5%, with the highest percent MeHg occurring in mayflies exposed to sediment from the reference areas (Table 2).

In tests 3 and 4, mean concentrations of ΣHg in sediments varied about 10-fold among the four treatments, ranging from 186 to 261 ng·g^{-1} in the reference wetland and from 1200 to 2562 ng·g^{-1} in the two contaminated wetland areas and Fairhaven Bay (Table 2). MeHg concentrations in test water varied considerably among treatments at the end of tests 3 and 4 (Table 2). In both tests, waterborne concentrations of MeHg were much greater in treatments with contaminated wetland sediments (8–47 ng Hg·L^{-1}) than in the treatment with reference wetland sediments (0.9–2.1 ng Hg·L^{-1}).

Mean concentrations of MeHg in mayflies at the end of tests 3 and 4 ranged from 122 to 184 ng Hg·g^{-1} in treatments with contaminated wetland sediments, whereas concentrations in mayflies exposed to reference wetland sediments averaged about 36 ng Hg·g^{-1}. The fraction of ΣHg present as MeHg ranged from 11 to 41%; the highest percentage was in mayflies exposed to sediments from the reference wetland (Table 2). Net MeHg accumulation was significantly greater in mayflies exposed to mercury-contaminated wetland sediments than in mayflies exposed to reference wetland sediment (Table 2).

When data from all four bioaccumulation tests were combined, there was a significant, positive correlation between the concentration of ΣHg in mayflies and that in test sediment (Fig. 2). In general, concentrations of ΣHg in mayflies were less than those in sediments. However, the net amount of MeHg accumulated in mayflies was not correlated with the concentration of ΣHg in sediments (Spearman correlation, $r_s = 0.54$, $p = 0.32$).

Mayfly growth and survival

The survival of *Hexagenia* in the four bioaccumulation tests was unrelated to the concentration of ΣHg in test sediment. The overall survival of *Hexagenia* mayflies ranged from 90% in test 3 to 96% in test 2. The mean survival of nymphs did not vary among treatments in any test ($p \geq 0.38$ in all tests).

The growth of *Hexagenia* during tests 1 and 2 varied significantly among sediment treatments but was unrelated to the mercury concentration in test sediment (Table 2). The mean growth of mayflies in the Whitehall Reservoir (reference) treatment was significantly less than that in four of the other five treatments in test 1 and less than that in all other

© 2000 NRC Canada

Table 2. Mean growth of *Hexagenia* mayflies and mean (±1 SE) ΣHg in test sediment and mayflies, MeHg in test water and mayflies, percentage of ΣHg present as MeHg, and net MeHg accumulation in mayflies exposed to sediments from the Sudbury River basin in 21-day bioaccumulation tests.

Treatment	Growth of mayflies (mm)	ΣHg in sediment (ng·g dry weight^{-1})	ΣHg in mayflies (ng·g dry weight^{-1})	MeHg in water (ng Hg·L^{-1})	MeHg in mayflies (ng Hg·g dry weight^{-1})	MeHg as mean percentage of ΣHg	MeHg accumulation (ng Hg·mayfly^{-1})
Bioaccumulation test 1 (July 1994 sediments)							
Whitehall Reservoir	2.2 *a*	149±19 *a*	123±19 *a*	1.68±0.51 *a*	32.4±3.8 *a*	27.3±2.0 *a*	0.15±0.03 *a*
Reference flowing reach	6.2 *c*	90±19 *a*	149±13 *a*	0.30±0.05 *b*	41.0±5.8 *ab*	28.5±4.5 *a*	0.41±0.05 *ab*
Reservoir 2	5.9 *bc*	14 780±4843 *c*	6 360±1448 *c*	3.26±1.23 *a*	117.8±40.3 *c*	2.5±0.9 *c*	1.38±0.53 *c*
Reservoir 1	6.1 *bc*	7 548±694 *c*	5 182±1477 *c*	1.12±0.30 *ab*	84.1±19.4 *bc*	1.9±0.4 *c*	1.03±0.28 *bc*
Contaminated flowing reach	4.9 *ab*	880±105 *b*	759±194 *b*	1.85±0.47 *a*	105.4±40.7 *bc*	13.1±2.8 *b*	1.06±0.44 *bc*
Fairhaven Bay	5.3 *bc*	1 719±229 *b*	874±162 *b*	1.65±0.46 *a*	127.1±27.1 *c*	14.5±1.0 *b*	1.39±0.36 *c*
Bioaccumulation test 2 (September 1994 sediments)							
Whitehall Reservoir	2.3 *a*	272±39 *a*	171±16 *a*	3.46±1.07 *a*	39.0±4.1 *a*	23.5±2.4 *a*	0.14±0.03 *a*
Reference flowing reach	5.8 *b*	200±39 *a*	167±24 *a*	0.75±0.15 *b*	37.0±5.0 *a*	24.3±4.6 *a*	0.29±0.08 *a*
Reservoir 2	5.8 *b*	22 059±4077 *c*	10 819±2282 *c*	3.40±0.59 *a*	93.0±9.1 *b*	1.2±0.5 *c*	0.92±0.07 *b*
Reservoir 1	6.5 *b*	11 221±2279 *c*	4 147±814 *c*	2.00±0.58 *ab*	77.2±11.2 *b*	2.4±0.7 *c*	0.76±0.09 *b*
Contaminated flowing reach	6.3 *b*	1 920±216 *b*	762±105 *b*	1.21±0.38 *ab*	75.0±13.4 *b*	10.3±1.7 *b*	0.79±0.15 *b*
Fairhaven Bay	6.2 *b*	1 775±375 *b*	711±76 *b*	1.75±0.58 *ab*	82.5±3.9 *b*	12.3±1.4 *b*	0.89±0.07 *b*
Bioaccumulation test 3 (May 1995 sediments)							
Hop Brook wetland (reference)	6.4 *a*	261±27 *a*	113±5 *a*	0.93±0.08 *a*	36.3±6.9 *a*	33.0±7.0 *a*	0.30±0.11 *a*
Southern contaminated wetland	6.0 *ab*	2 562±263 *c*	1 161±183 *c*	8.34±1.62 *d*	122.1±13.7 *c*	11.2±0.9 *b*	1.25±0.18 *b*
Northern contaminated wetland	4.8 *b*	1 275±123 *b*	655±78 *b*	14.92±1.70 *c*	149.3±18.7 *c*	24.1±2.7 *a*	1.39±0.22 *b*
Fairhaven Bay	6.1 *ab*	1 791±308 *bc*	833±147 *bc*	0.58±0.07 *b*	63.7±3.1 *b*	12.5±4.3 *b*	0.62±0.07 *a*
Bioaccumulation test 4 (September 1995 sediments)							
Hop Brook wetland (reference)	4.0 *ab*	186±24 *a*	98±12 *a*	2.05±0.70 *a*	36.9±4.3 *a*	40.6±5.0 *a*	0.21±0.04 *a*
Southern contaminated wetland	2.8 *bc*	1 612±98 *b*	515±28 *b*	13.79±2.62 *b*	138.0±16.9 *b*	27.2±3.2 *a*	0.91±0.16 *b*
Northern contaminated wetland	1.5 *c*	1 200±157 *b*	539±70 *b*	47.05±11.51 *b*	183.7±25.0 *b*	37.1±4.9 *a*	0.91±0.16 *b*
Fairhaven Bay	5.7 *a*	1 429±339 *b*	492±64 *b*	0.96±0.12 *a*	54.6±5.0 *a*	12.2±1.4 *b*	0.46±0.06 *b*

Note: Means for a given variable and test that are not accompanied by a common letter were significantly different (Tukey's HSD procedure, $\alpha = 0.05$). Treatments (sediment source) for each test are listed in longitudinal sequence from upstream to downstream.

© 2000 NRC Canada

Fig. 2. Relationship between ΣHg concentration in *Hexagenia* mayflies and that in test sediments from all study sites in the Sudbury River basin (combined data from all four bioaccumulation tests).

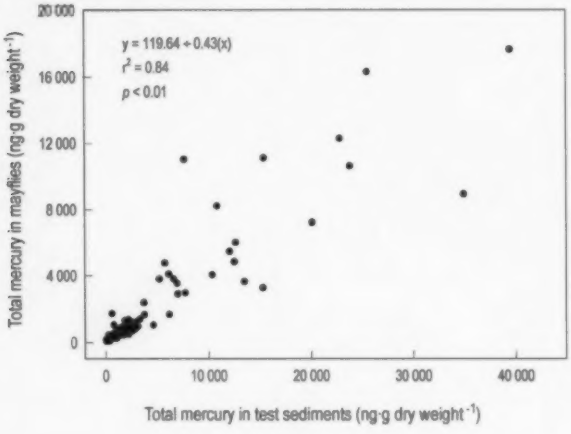

treatments in test 2 (Table 2). In tests 3 and 4, the growth of *Hexagenia* varied among treatments and between tests. In test 3, the mean growth of mayflies in the northern contaminated wetland treatment (4.8 mm) was significantly less than that in the reference wetland treatment (Table 2). In test 4, the growth of mayflies averaged 1.5 mm for the northern contaminated wetland, 2.8 mm for the southern contaminated wetland, 4.0 mm for the reference wetland, and 5.7 mm for Fairhaven Bay (Table 2). The overall mean growth of mayflies (all treatments combined) was greater in test 3 (5.8 mm) than in test 4 (3.5 mm). Variation in the growth of mayfly nymphs was seemingly unrelated to mercury exposure, given that growth did not diminish with increasing concentrations of MeHg in test water, ΣHg in sediment, ΣHg in mayflies, or MeHg in mayflies (Fig. 3).

Discussion

The concentrations of ΣHg in our test sediments far exceeded the estimated natural abundance of 40–50 ng·g dry weight^{-1} (Frazier et al. 2000), confirming substantial mercury contamination throughout the studied 34-km reach of the Sudbury River. Test sediments from the three reference areas had mercury concentrations ranging from two to five times the estimated natural abundance, indicating the presence of anthropogenic mercury throughout the basin. Concentrations of ΣHg in surficial sediments diminished, as expected, with increasing distance downstream from the Nyanza site (Fig. 4). The greatest concentrations of ΣHg in sediments in this study were in Reservoir 2, about 3 km downstream from the Nyanza site. In sediments taken 25–35 km downstream from the Nyanza site, the concentration of mercury was roughly 10-fold higher than concentrations in the reference flowing reach, upstream of the Nyanza site.

The growth of mayflies was unrelated to the ΣHg concentration in sediment. The slower growth of *Hexagenia* exposed to sediments from Whitehall Reservoir (tests 1 and 2) may have resulted from the physical characteristics of sediment, given that Whitehall Reservoir sediments contained more volatile matter than other sediments (Table 1). Mayflies exposed to wetland sediment grew less in test 4 than in test 3, probably because of differences in test conditions related to water levels in the wetlands when test sediments were obtained. Wetland sediments for test 3 were obtained from an inundated floodplain, whereas wetland sediments for test 4 were not inundated, due to severe drought conditions in the basin during the summer of 1995. Growth was slowest in mayflies exposed to sediments taken from the northern contaminated wetland in September 1995; this treatment had the highest MeHg concentration and the lowest pH (mean 5.9) in test water. This pH value is near the pH threshold of 5.2–5.5 suggested by McNicol et al. (1995) as the pH below which recolonization of lake sediments by acid-sensitive invertebrate taxa is unlikely. We suspect that the lower pH of our test waters in wetland treatments in test 4, relative to test 3, resulted from the release of hydrogen ion during oxidation of sulfide in the air-exposed wetland sediment (Yan et al. 1996; Anisfeld and Benoit 1997). In contrast with the wetland areas studied, sediments from Fairhaven Bay were inundated during sampling for tests 3 and 4, and the growth of mayflies in the Fairhaven Bay treatment did not differ between the two tests.

The concentration of ΣHg was not a reliable indicator of MeHg concentration in mayflies in our study. Neither the concentration nor the burden of MeHg accumulated by mayflies was correlated with the concentration of ΣHg in the sediment to which they were exposed. In addition, the fraction of ΣHg present as MeHg in exposed mayflies was highly variable, ranging from 1 to 41% in our tests. The MeHg to ΣHg ratio in mayflies was greatest in nymphs exposed to reference sediments and lowest in nymphs exposed to the most contaminated sediments. These observations reinforce the importance of measuring MeHg in benthic macroinvertebrates such as aquatic insects (Hall et al. 1998). In our study, no inferences on MeHg contamination of sediment-dwelling mayflies could be made from information on concentrations of ΣHg in either sediment or mayflies.

The whole-body content of metals in benthic insects can be influenced by ingested materials, such as sediment particles, in the gut (Hare et al. 1989; Cain et al. 1995). We estimated the potential contribution of gut contents to the whole-body burdens of ΣHg and MeHg accumulated by mayfly nymphs in our tests by assuming that the gut of a *Hexagenia* contained 1.2 mg dry weight of ingested sediment, a value derived for individual *Hexagenia rigida* by Odin et al. (1997). In mayflies exposed to sediments from contaminated reaches, we estimated that from 13 to 52% of the ΣHg in the whole mayfly was contributed by gut contents, with the remainder of the whole-body burden contributed by bioaccumulation and adsorption. In mayflies exposed to reference sediments, we estimate that from 6 to 28% of the ΣHg in the body was contributed by ingested sediment in the gut. To assess the potential contribution of ingested sediment to MeHg burdens in mayflies, we used data from Colman et al. (1999) on maximum concentrations of MeHg in surficial sediments from contaminated palustrine wetlands along the Sudbury River. The gut of an individual mayfly would have contained an estimated maximum of 0.02 ng of mercury present as MeHg. During our tests, individual mayflies exposed to contaminated wetland sediments

© 2000 NRC Canada

Fig. 3. Growth of *Hexagenia* mayfly nymphs during all four 21-day bioaccumulation tests with sediments from the Sudbury River basin, with the increase in total length plotted against (*a*) MeHg in test water, (*b*) ΣHg in test sediments, (*c*) ΣHg in mayflies, and (*d*) MeHg in mayflies.

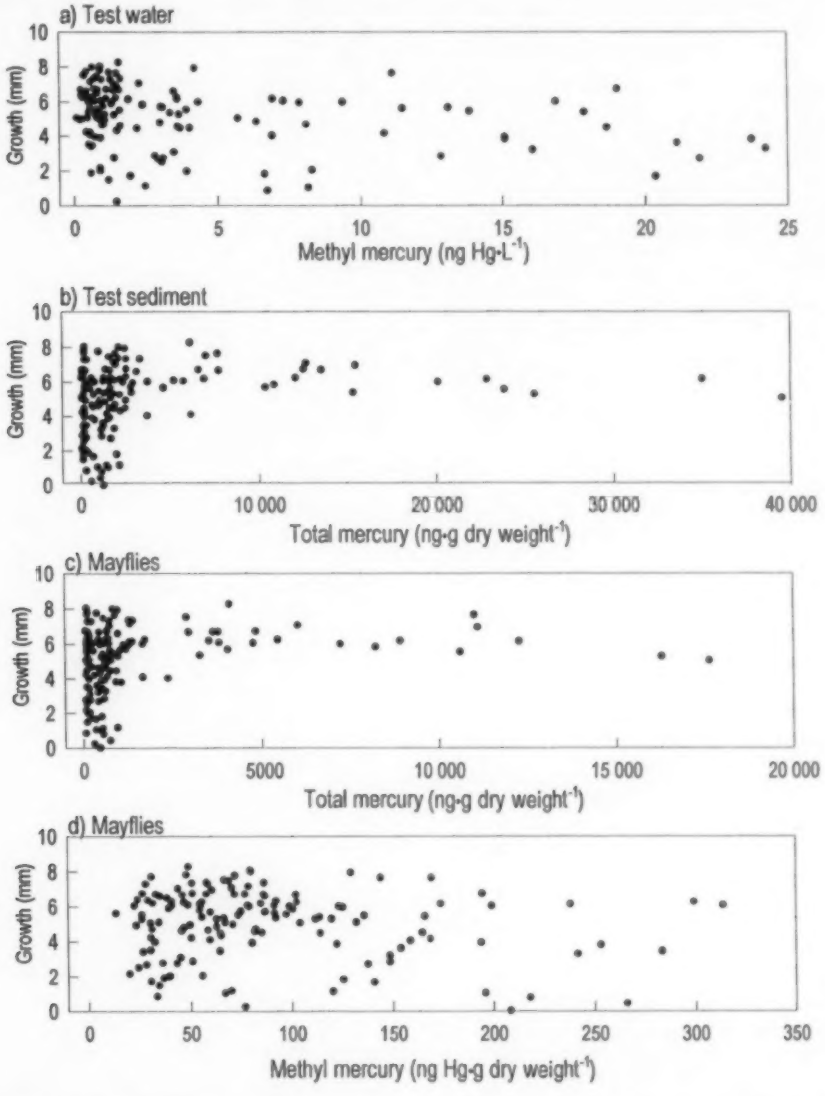

accumulated between 0.91 and 1.39 ng of mercury as MeHg. Our admittedly crude calculations indicate that very little, at most perhaps 2%, of the MeHg in the whole body was contributed by MeHg in ingested sediment present in the gut.

Comparison of MeHg in test water and mayflies with ΣHg in test sediments from the two highly contaminated reservoirs indicated that very little MeHg was produced from the large sedimentary inventories of inorganic mercury at these sites (Fig. 5). In contrast, our tests clearly showed that MeHg, the form readily accumulated in fish and biomagnified in aquatic food chains (Bloom 1992; Wiener and Spry 1996), was actively produced in surficial sediments from the lesser contaminated wetlands (Fig. 5). Moreover, this MeHg was available for uptake by detritus-feeding benthic organisms in the riverine food web. Colman et al. (1999), who analyzed sediment cores from wetlands on the Sudbury River floodplain, found that MeHg concentrations in both bulk sediment and pore water were greatest in the uppermost stratum of each core. Within this upper stratum, concentrations of MeHg ranged from about 6 to 22 ng Hg·g dry weight^{-1} in bulk sediments (six cores) and from about 4.5 to 7.1 ng Hg·L^{-1} in pore water (three cores). Moreover, MeHg was present in the wetland sediments throughout the summer, even when floodplain sediments were exposed to the atmosphere (Colman et al. 1999).

Our results showing the importance of wetland sediments as active sites of MeHg production agree with the results of Waldron et al. (2000), who examined spatial trends in the

© 2000 NRC Canada

Fig. 4. ΣHg in test sediments (solid circles) and MeHg in *Hexagenia* mayflies (open circles) as a function of distance downstream from the Nyanza site (combined data from all four bioaccumulation tests). Approximate downstream distances from the Nyanza site were as follows: Reservoir 2, 4 km; Reservoir 1, 6 km; contaminated flowing reach and contaminated wetland reaches, 25–31 km; Fairhaven Bay, 34 km. The three reference areas (Whitehall Reservoir, reference flowing reach, and Hop Brook wetland) were plotted as negative distance because all are upstream from or uninfluenced by the Nyanza site.

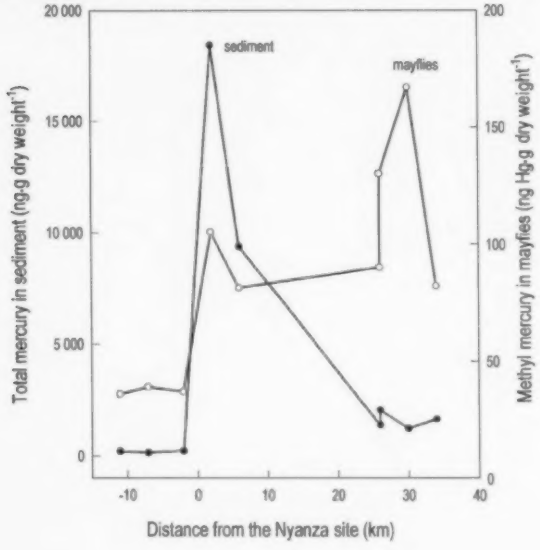
sediment
mayflies
Total mercury in sediment (ng·g dry weight⁻¹)
Methyl mercury in mayflies (ng Hg·g dry weight⁻¹)
Distance from the Nyanza site (km)

Fig. 5. Concentrations of MeHg in (*a*) test water (note the discontinuous scale on the vertical axis) and (*b*) *Hexagenia* mayflies, plotted against ΣHg in test sediments from habitats in the Sudbury River basin (combined data from all four bioaccumulation tests).

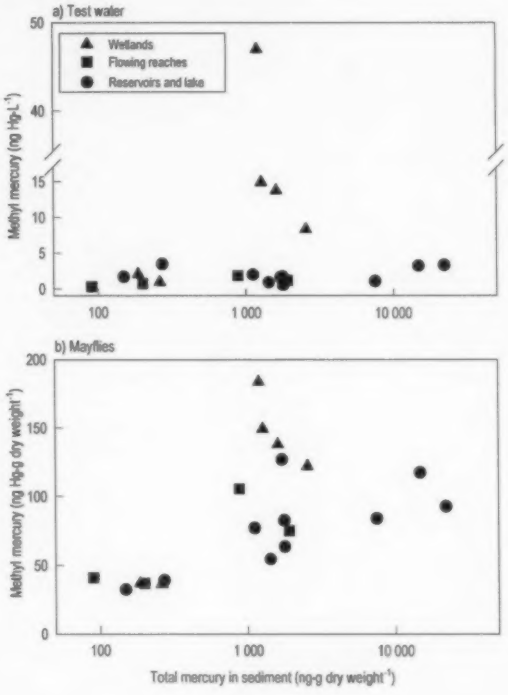

abundances of MeHg and ΣHg in water from the Sudbury River. MeHg production in wetlands has also been documented elsewhere, including boreal forest ecosystems in Canada (St. Louis et al. 1994, 1996; Kelly et al. 1997) and several watersheds in Wisconsin (Hurley et al. 1995; Krabbenhoft et al. 1995). St. Louis et al. (1994), for example, reported that MeHg yields from wetlands were 26–79 times greater than yields from purely upland catchment areas. In subsequent work, St. Louis et al. (1996) documented that different types of wetlands (i.e., headwater wetlands, riverine wetlands, valley-bottom wetlands) can function as sources or sinks of MeHg and ΣHg to downstream reaches, depending on the percent wetland in a given catchment and the annual water yield. Furthermore, yields of MeHg from wetland areas can greatly exceed the inputs of MeHg in atmospheric deposition (Krabbenhoft et al. 1995).

The net production of MeHg in our treatments with wetland sediments may have been enhanced partly by low pH. Several studies have shown that the net rate of microbial production of MeHg (i.e., methylation minus demethylation) in aquatic ecosystems increases in response to acidification or lowered pH (Xun et al. 1987; Gilmour et al. 1992). The northern contaminated wetland treatment had the lowest mean pH and the highest mean MeHg in water (15 ng $Hg \cdot L^{-1}$ at pH 6.6 in test 3 and 47 ng $Hg \cdot L^{-1}$ at pH 5.9 in test 4) measured in the present study. Moreover, mean concentrations of MeHg in water in the three treatments with wetland sediments were higher in test 4, which had lower pH in test water, than in test 3.

Viewed longitudinally, the patterns of MeHg in sediment-exposed mayflies and in river water (Waldron et al. 2000) clearly did not correspond to the spatial gradient in ΣHg concentration in the surficial sediments (Fig. 4). MeHg concentrations peaked about 3–5 km downstream from the Nyanza site, leveled off between 5 and 25 km downstream from the Nyanza site, and peaked again in the contaminated wetland reaches (Fig. 4). Moreover, the spatial trend in MeHg concentrations in mayflies paralleled the spatial trend in abundance of MeHg in water from the river (Waldron et al. 2000). In their field study, Waldron et al. (2000) found that MeHg concentrations in unfiltered river water were highest in the reach just downstream from the Nyanza site (0.19–0.29 ng $Hg \cdot L^{-1}$), substantially lower at sampling points between 5 and 25 km downstream from the Nyanza site (0.11–0.15 ng $Hg \cdot L^{-1}$), and higher in the wetland reaches (0.19–0.23 ng $Hg \cdot L^{-1}$).

Fish in natural waters obtain MeHg almost entirely through the diet (Rodgers 1994; Wiener and Spry 1996; Hall et al. 1997). Our estimates of net MeHg accumulation in individual mayfly nymphs consequently provide a relevant index of the potential transfer (flux) of MeHg from the sediments into aquatic food webs. Mayflies accumulated between 0.14 and 1.4 ng of mercury (as MeHg) per nymph during our 21-day bioaccumulation tests. Nymphs exposed

© 2000 NRC Canada

to mercury-contaminated sediments usually accumulated considerably more MeHg than those exposed to reference sediments. The potential significance of the mercury-contaminated wetland areas as sources of MeHg in this ecosystem is increased by the tendency of wetland habitats to export waterborne MeHg to adjoining surface waters (Hurley et al. 1995; St. Louis et al. 1996; Waldron et al. 2000).

In conclusion, mayfly nymphs accumulated significant quantities of MeHg during 21-day exposures to contaminated sediments from the Sudbury River. Mercury-contaminated, surficial sediments from impoundments, flowing reaches, and palustrine wetlands in the basin were not toxic to burrowing mayflies, and the growth of mayflies was unrelated to the concentration of ΣHg in sediments. Concentrations of MeHg were greatest in mayflies and test water exposed to sediment from contaminated wetland areas about 30 km or more downstream from the Nyanza site. The production of MeHg and its potential entry into the benthic food web in this ecosystem were greater in the contaminated floodplain wetlands than in the more heavily contaminated reservoirs nearer the Nyanza site.

Acknowledgments

This work was funded by the U.S. Environmental Protection Agency (Region I) through an interagency agreement with the U.S. Fish and Wildlife Service (Region V). We thank the staff of the Great Meadows National Wildlife Refuge for use of their facility during sampling trips. The assistance of Pamela Shields (U.S. Environmental Protection Agency), Susan Svirsky (U.S. Environmental Protection Agency), and Steven Mierzykowski (U.S. Fish and Wildlife Service) during planning of the study is gratefully acknowledged. Assistance in the field and (or) laboratory was provided by Lori Bliss, Erika Damschen, Martin Deters, Bradley Frazier, Michael Oetker, Peter Rust, and Kimberly Skroch. We thank John Besser, Britt Hall, James Hurley, Efrosini Tsalkitzis, and two anonymous reviewers for helpful comments on earlier drafts of the manuscript.

References

American Society for Testing and Materials. 1992. Annual book of ASTM standards. Vol. 11.04. Water and environmental technology. Standard Guide E 1391-90. Collection, storage, characterization, and manipulation of sediments for toxicological testing. American Society for Testing and Materials, Philadelphia, Pa.

Anisfeld, S.C., and Benoit, G. 1997. Impacts of flow restrictions on salt marshes: an instance of acidification. Environ. Sci. Technol. **31**: 1650–1657.

Beauvais, S.L., Wiener, J.G., and Atchison, G.J. 1995. Cadmium and mercury in sediment and burrowing mayfly nymphs (*Hexagenia*) in the Upper Mississippi River, U.S.A. Arch. Environ. Contam. Toxicol. **28**: 178–183.

Bloom, N.S. 1989. Determination of picogram levels of methylmercury by aqueous phase ethylation, followed by cryogenic gas chromatography with cold vapour atomic fluorescence detection. Can. J. Fish. Aquat. Sci. **46**: 1131–1140.

Bloom, N.S. 1992. On the chemical form of mercury in edible fish and marine invertebrate tissue. Can. J. Fish. Aquat. Sci. **49**: 1010–1017.

Bloom, N.S., and Crecelius, E.A. 1983. Determination of mercury in seawater at sub-nanogram per liter levels. Mar. Chem. **14**: 49–59.

Bloom, N.S., and Crecelius, E.A. 1987. Distribution of silver, mercury, lead, copper, and cadmium in central Puget Sound sediments. Mar. Chem. **21**: 377–390.

Bloom, N.S., and Fitzgerald, W.F. 1988. Determination of volatile mercury species at the picogram level by low temperature gas chromatography with cold vapor atomic fluorescence detection. Anal. Chim. Acta, **208**: 151–161.

Bloom, N.S., and Von Der Geest, E.J. 1995. Matrix modification to improve the recovery of MMHg from clear water using distillation. Water Air Soil Pollut. **80**: 1319–1323.

Cain, D.J., Luoma, S.N., and Axtmann, E.V. 1995. Influence of gut content in immature aquatic insects on assessments of environmental metal contamination. Can. J. Fish. Aquat. Sci. **52**: 2736–2746.

Colman, J.A., Waldron, M.C., Breault, R.F., and Lent, R.M. 1999. Distribution and transport of total mercury and methylmercury in mercury-contaminated sediments in reservoirs and wetlands of the Sudbury River, east-central Massachusetts. U.S. Geol. Surv. Water-Resour. Invest. Rep. 99-4060.

Fitzgerald, W.F., Mason, R.P., and Vandal, G.M. 1991. Atmospheric cycling and air–water exchange of mercury over mid-continental lacustrine regions. Water Air Soil Pollut. **56**: 745–767.

Frazier, B.E., Wiener, J.G., Rada, R.G., and Engstrom, D.R. 2000. Stratigraphy and historic accumulation of mercury in recent depositional sediments in the Sudbury River, Massachusetts, U.S.A. Can. J. Fish. Aquat. Sci. **57**: 1062–1072.

Gilmour, C.C., Henry, E.A., and Mitchell, R. 1992. Sulfate stimulation of mercury methylation in freshwater sediments. Environ. Sci. Technol. **26**: 2281–2287.

Guy, H.P. 1969. Laboratory theory and methods for sediment analysis. Techniques of water resources investigations. Book 5, Chap. C1. U.S. Geological Survey, Washington, D.C.

Hall, B.D., Bodaly, R.A., Fudge, R.J.P., Rudd, J.W.M., and Rosenberg, D.M. 1997. Food as the dominant pathway of methylmercury uptake by fish. Water Air Soil Pollut. **100**: 13–24.

Hall, B.D., Rosenberg, D.M., and Wiens, A.P. 1998. Methyl mercury in aquatic insects from an experimental reservoir. Can. J. Fish. Aquat. Sci. **55**: 2036–2047.

Hare, L., Campbell, P.G.C., Tessier, A., and Belzile, N. 1989. Gut sediments in a burrowing mayfly (Ephemeroptera, *Hexagenia limbata*): their contribution to animal trace element burdens, their removal, and the efficacy of a correction for their presence. Can. J. Fish. Aquat. Sci. **46**: 451–456.

Harris, S.L. 1996. Massachusetts wetland resources. *In* National water summary on wetland resources. U.S. Geol. Surv. Water-Supply Pap. 2425. pp. 225–230.

Horvat, M., Liang, L., and Bloom, N.S. 1993. Comparison of distillation with other current isolation methods for the determination of methyl mercury-compounds in low-level environmental samples. 2. Water. Anal. Chim. Acta, **282**: 153–168.

Hurley, J.P., Benoit, J.M., Babiarz, C.L., Shafer, M.M., Andren, A.W., Sullivan, J.R., Hammond, R., and Webb, D.A. 1995. Influences of watershed characteristics on mercury levels in Wisconsin rivers. Environ. Sci. Technol. **29**: 1867–1875.

Kelly, C.A., Rudd, J.W.M., Bodaly, R.A., Roulet, N.P., St. Louis, V.L., Heyes, A., Moore, T.R., Schiff, S., Aravena, R., Scott, K.J., Dyck, B., Harris, R., Warner, B., and Edwards, G. 1997. Increases in fluxes of greenhouse gases and methyl mercury following flooding of an experimental reservoir. Environ. Sci. Technol. **31**: 1334–1344.

Krabbenhoft, D.P., Benoit, J.M., Babiarz, C.L., Hurley, J.P., and Andren, A.W. 1995. Mercury cycling in the Allequash Creek watershed, northern Wisconsin. Water Air Soil Pollut. **80**: 425–433.

© 2000 NRC Canada

Liang, L., Bloom, N.S., and Horvat, M. 1994. Simultaneous determination of mercury speciation in biological materials by GC/CVAFS after ethylation and room temperature precollection. Clin. Chem. **40**: 602–607.

McNicol, D.K., Bendell, B.E., and Mallory, M.L. 1995. Evaluating macroinvertebrate responses to recovery from acidification in small lakes in Ontario, Canada. Water Air Soil Pollut. **85**: 451–456.

NUS Corporation. 1992. Final remedial investigation report. Nyanza Operable Unit III, Sudbury River study, Middlesex County, Massachusetts. Vol. 1. NUS Rep. W92194F. NUS Corporation, Wilmington, Mass.

Odin, M., Feurtet-Mazel, A., Ribeyre, F., and Boudou, A. 1994. Actions and interactions of temperature, pH, and photoperiod on mercury bioaccumulation by nymphs of the burrowing mayfly *Hexagenia rigida*, from the sediment contamination source. Environ. Toxicol. Chem. **13**: 1291–1302.

Odin, M., Ribeyre, F., and Boudou, A. 1995. Cadmium and methylmercury bioaccumulation by nymphs of the burrowing mayfly *Hexagenia rigida* from the water column and sediment. Environ. Sci. Pollut. Res. **2**: 145–152.

Odin, M., Ribeyre, F., and Boudou, A. 1997. Depuration processes after exposure of burrowing mayfly nymphs (*Hexagenia rigida*) to methylmercury and cadmium from water column or sediment: effects of temperature and pH. Aquat. Toxicol. **37**: 125–137.

Plumb, R.H., Jr. 1981. Procedures for handling and chemical analysis of sediment and water samples. Tech. Rep. EPA/CE-81-1. U.S. Environmental Protection Agency and U.S. Army Corps of Engineers, Technical Committee on Criteria for Dredged and Fill Material, Vicksburg, Miss.

Ramlal, P.S., Kelly, C.A., Rudd, J.W.M., and Furutani, A. 1993. Sites of methyl mercury production in remote Canadian Shield lakes. Can. J. Fish. Aquat. Sci. **50**: 972–979.

Rodgers, D.W. 1994. You are what you eat and a little bit more: bioenergetics-based models of methylmercury accumulation in fish revisited. *In* Mercury pollution: integration and synthesis. *Edited by* C.J. Watras and J.W. Huckabee. Lewis Publishers, Boca Raton, Fla. pp. 427–439.

Rudd, J.W.M. 1995. Sources of methyl mercury to freshwater ecosystems: a review. Water Air Soil Pollut. **80**: 697–713.

Saouter, E., Ribeyre, F., Boudou, A., and Maury-Brachet, R. 1991. *Hexagenia rigida* (Ephemeroptera) as a biological model in aquatic ecotoxicology: experimental studies on mercury transfers from sediment. Environ. Pollut. **69**: 51–67.

Saouter, E., Hare, L., Campbell, P.G.C., Boudou, A., and Ribeyre, F. 1993. Mercury accumulation in the burrowing mayfly *Hexagenia rigida* (Ephemeroptera) exposed to CH_3HgCl or $HgCl_2$ in water and sediment. Water Res. **27**: 1041–1048.

St. Louis, V.L., Rudd, J.W.M., Kelly, C.A., Beaty, K.G., Bloom, N.S., and Flett, R.J. 1994. Importance of wetlands as sources of methyl mercury to boreal forest ecosystems. Can. J. Fish. Aquat. Sci. **51**: 1065–1076.

St. Louis, V.L., Rudd, J.W.M., Kelly, C.A., Beaty, K.G., Flett, R.J., and Roulet, N.T. 1996. Production and loss of methylmercury and loss of total mercury from boreal forest catchments containing different types of wetlands. Environ. Sci. Technol. **30**: 2719–2729.

Waldron, M.C., Colman, J.A., and Breault, R.F. 2000. Distribution, hydrologic transport, and cycling of total mercury and methyl mercury in a contaminated river–reservoir–wetland system (Sudbury River, eastern Massachusetts). Can. J. Fish. Aquat. Sci. **57**: 1080–1091.

Wiener, J.G., and Shields, P.J. 2000. Mercury in the Sudbury River (Massachusetts, U.S.A.): pollution history and a synthesis of recent research. Can. J. Fish. Aquat. Sci. **57**: 1053–1061.

Wiener, J.G., and Spry, D.J. 1996. Toxicological significance of mercury in freshwater fish. *In* Environmental contaminants in wildlife: interpreting tissue concentrations. *Edited by* W.N. Beyer, G.H. Heinz, and A.W. Redmon-Norwood. Special Publication of the Society of Environmental Toxicology and Chemistry. Lewis Publishers, Boca Raton, Fla. pp. 297–339.

Xun, L., Campbell, N.E.R., and Rudd, J.W.M. 1987. Measurements of specific rates of net methyl mercury production in the water column and surface sediments of acidified and circumneutral lakes. Can. J. Fish. Aquat. Sci. **44**: 750–757.

Yan, N.D., Keller, W., Scully, N.M., Lean, D.R.S., and Dillon, P.J. 1996. Increased UV-B penetration in a lake owing to drought-induced acidification. Nature (Lond.), **381**: 141–143.

© 2000 NRC Canada

An in situ assessment of mercury contamination in the Sudbury River, Massachusetts, using transplanted freshwater mussels (*Elliptio complanata*)

Nancy Beckvar, Sandra Salazar, Michael Salazar, and Ken Finkelstein

Abstract: Freshwater mussels (*Elliptio complanata*) were transplanted into the Sudbury River, Massachusetts, to evaluate the bioavailability of total Hg and methyl mercury (MeHg) and the potential impacts to resident species. The principal Hg source is the Nyanza Superfund site, a former textile dye production facility. Mussels (initial tissue concentrations = 640 ng Hg·g dry weight^{-1} and 120 ng MeHg·g dry weight^{-1}) were transplanted to eight locations in the Sudbury River watershed for 12 weeks. Tissue total Hg concentration increased significantly in mussels at the station closest to the Nyanza site (950 ng Hg·g dry weight^{-1}). Mussel growth, which increased downstream with distance away from the site, was significantly negatively correlated with tissue concentrations of total Hg (r = –0.95) and positively correlated with average temperature (r = 0.85). Due to growth differences, uptake was best assessed by changes in content. Tissue total Hg and MeHg burdens were greatest in mussels at two stations closest to the Nyanza site, with less Hg accumulated in downstream mussels. However, the MeHg content in mussel tissue increased significantly at all Sudbury River stations, indicating that MeHg was bioavailable in all portions of the river evaluated.

Résumé : Des bivalves d'eau douce (*Elliptio complanata*) ont été transplantés dans la rivière Sudbury (Massachusetts) pour évaluer la biodisponibilité du Hg total et du méthyl mercure (MeHg) et les impacts potentiels chez les espèces résidantes. La principale source de Hg est le site Nyanza, une ancienne installation de production de colorant de textile, couvert par le Superfund pour la dépollution. Les bivalves (concentrations initiales dans les tissus = 640 ng Hg·g poids sec^{-1} et 120 ng MeHg·g poids sec^{-1}) ont été transplantés, pour une période de 12 semaines, à huit endroits dans le bassin hydrographique de la rivière Sudbury. La concentration de Hg total dans les tissus a augmenté significativement chez les bivalves de la station la plus proche du site Nyanza (950 ng Hg·g poids sec^{-1}). La croissance des bivalves, qui augmentait en aval à mesure que l'on s'éloignait du site, présentait une corrélation négative marquée avec les concentrations tissulaires de Hg total (r = –0,95) et une corrélation positive avec la température moyenne (r = 0,85). À cause des écarts de croissance, les modifications de la teneur ont permis une meilleure évaluation de l'absorption. Les charges de Hg total et de MeHg dans les tissus étaient plus importantes chez les bivalves de deux stations situées à proximité du site Nyanza, l'accumulation de Hg étant plus faible chez les bivalves des zones situées en aval. Toutefois, dans toutes les stations de la rivière Sudbury, on a noté une augmentation considérable de la teneur en MeHg dans les tissus des bivalves, ce qui est une indication de la biodisponibilité du MeHg dans toutes les parties de la rivière qui ont été évaluées.

[Traduit par la Rédaction]

Introduction

The Nyanza chemical waste dump site, declared a Superfund site in 1982, is the former location of several textile dye production companies near the Sudbury River in Ashland, Massachusetts (Fig. 1). Numerous studies have assessed contamination in the river from the release of 45 to 57 t of Hg, and other textile dye production wastes, from activities conducted at the Nyanza site from 1917 to 1978 (JBF Scientific Corporation 1973; U.S. Fish and Wildlife Service 1990; NUS Corporation 1992). Concentrations of total Hg as high as 55 mg·kg^{-1} and 8 mg·kg^{-1} have been measured in sediment and fish, respectively (NUS Corporation 1992). The Massachusetts Department of Environmental Protection and the U.S. Environmental Protection Agency have posted advisories against consumption of fish from the river because of the continued bioavailability of Hg within the Sudbury River system.

In 1994, the National Oceanic and Atmospheric Administration (NOAA) participated in an U.S. Environmental Protection Agency sponsored, multiagency study to define the extent and magnitude of Hg contamination in the Sudbury River. The U.S. Environmental Protection Agency will use the data generated from these studies to develop a scientifically defensible ecological risk assessment for the Sudbury

Received August 29, 1997. Accepted May 18, 1999.
J14191

N. Beckvar[1] **and K. Finkelstein.** National Oceanic and Atmospheric Administration, Office of Response and Restoration, 7600 Sand Point Way NE, Seattle, WA 98115-6349, U.S.A.
S. Salazar and M. Salazar. Applied Biomonitoring, 11648 72nd Place NE, Kirkland, WA 98034, U.S.A.

[1]Author to whom all correspondence should be addressed.
e-mail: beckvar@hazmat.noaa.gov

© 2000 NRC Canada

Fig. 1. Nyanza site and sampling locations in the Sudbury River drainage basin in Middlesex County, Massachusetts.

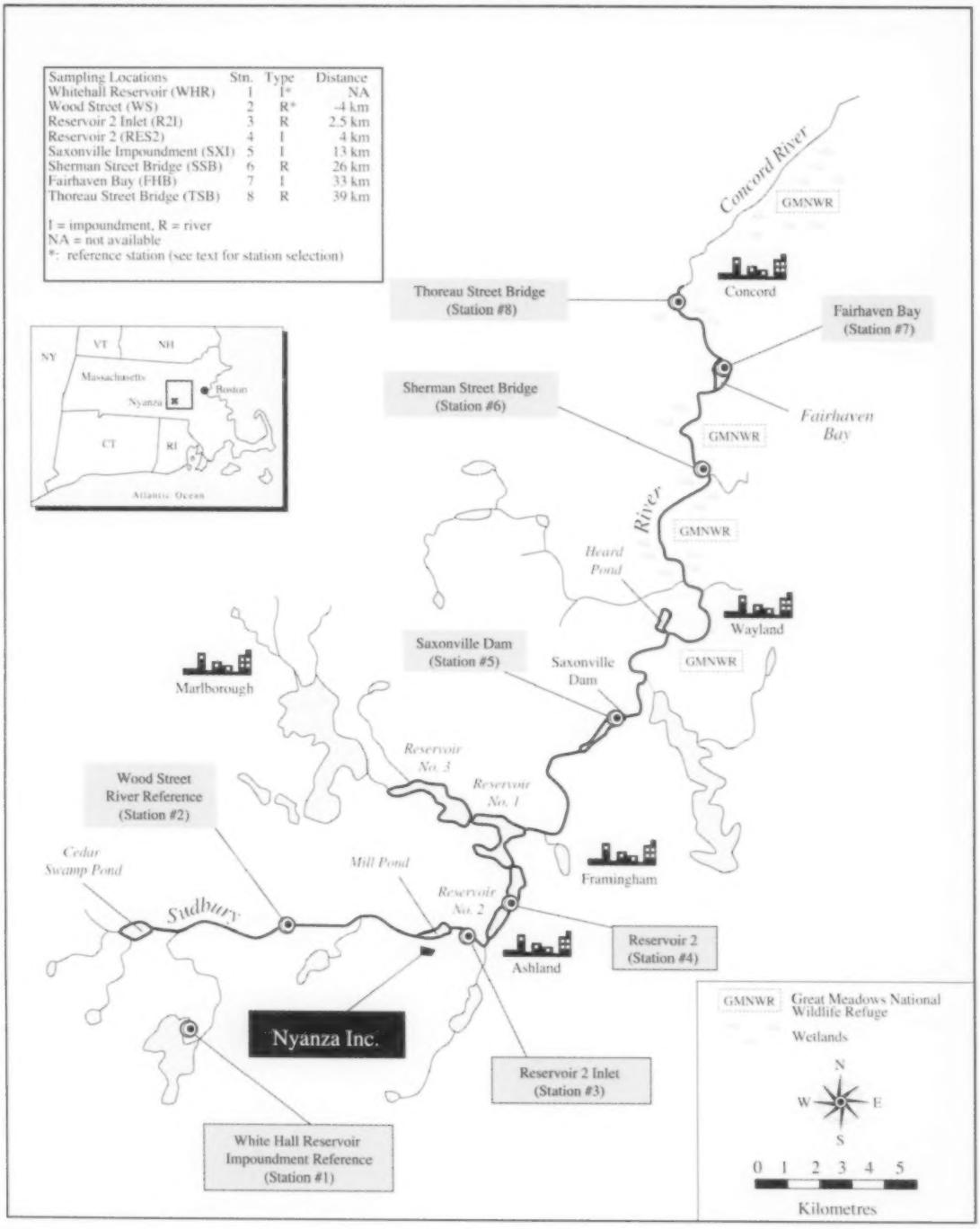

River. The NOAA will use the data to assess potential impacts to trustee natural resources with access to the downstream reaches of the river.

The NOAA conducted an in situ field study with caged freshwater mussels (*Elliptio complanata*) to evaluate Hg exposure and effects. *Elliptio complanata* is a long-lived, sedentary, filter-feeding bivalve that is widely distributed in the streams of northeastern North America, including the Sudbury River (Curry 1977; Heit et al. 1980). *Elliptio complanata* was selected for this biomonitoring study be-

© 2000 NRC Canada

Fig. 1. Nyanza site and sampling locations in the Sudbury River drainage basin in Middlesex County, Massachusetts.

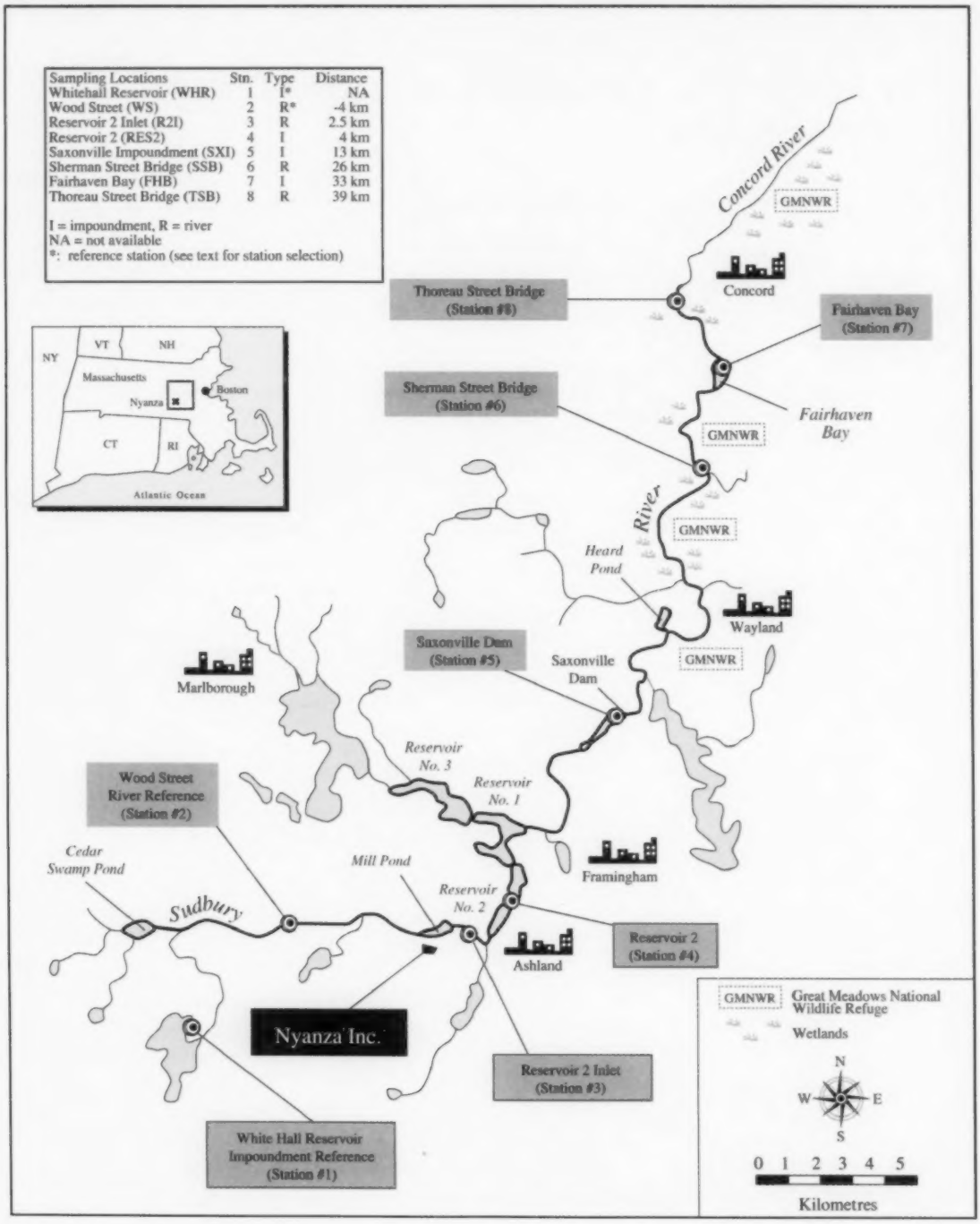

River. The NOAA will use the data to assess potential impacts to trustee natural resources with access to the downstream reaches of the river.

The NOAA conducted an in situ field study with caged freshwater mussels (*Elliptio complanata*) to evaluate Hg exposure and effects. *Elliptio complanata* is a long-lived, sedentary, filter-feeding bivalve that is widely distributed in the streams of northeastern North America, including the Sudbury River (Curry 1977; Heit et al. 1980). *Elliptio complanata* was selected for this biomonitoring study be-

© 2000 NRC Canada

cause it readily accumulates trace metals, including Hg, and organic contaminants (Kauss and Hamdy 1991; Metcalfe-Smith et al. 1992). *Elliptio complanata* has also been used in a number of contaminant monitoring studies with both resident populations (Tessier et al. 1984; Elder and Collins 1991; Metcalfe-Smith et al. 1992) and transplanted animals (Curry 1977; Kauss and Hamdy 1991; Langdon 1993). Metcalfe-Smith (1994) found that *E. complanata* demonstrated a broader response range to metal exposures (including Hg) than other species, suggesting that this species may be more sensitive to changes in pollution status.

The purpose of the NOAA study was to determine (*i*) whether *E. complanata* transplanted to the Sudbury River took up total Hg and methyl mercury (MeHg), (*ii*) how far downstream from the Nyanza site Hg was bioaccumulated, and (*iii*) whether the accumulated Hg affected mussel growth during the duration of the test.

Methods

Mussel collection, processing, and deployment

Elliptio complanata were collected from Lake Massesecum, Bradford, New Hampshire, on June 26, 1994, and deployed the next day. Mussels were collected by SCUBA divers from a large bed found in shallow water (0.5–3 m) overlying a predominantly sand substrate. Mussels from 57 to 63 mm shell length were used in this study because this was the minimum size range with a large number of mussels. Small mussels were needed because they were expected to grow fast enough to detect growth differences during the 12-week study. Deployed mussels were estimated to be 9 years old based on an average shell length of approximately 60 mm. Mussels of this age grow about 5 mm·year^{-1} and increase tissue weights by about 1 g wet weight·year^{-1} (McMahon 1991).

Mussel sorting and distribution followed the procedures outlined in Salazar and Salazar (1995). Mussels were measured for whole-animal wet weight (to the nearest 0.01 g) and length (to the nearest 0.1 mm) before placement in mesh bags (4-in. diameter, 0.5-in. mesh size). Each of three replicate cages per station consisted of a square frame (made from 0.75-in. PVC pipe) to which seven mesh bags were attached, each containing five mussels (total of 35 discrete mussels per cage and 105 mussels per station). Mussels were separated from each other within the mesh bags. An analysis of variance (ANOVA) was used to confirm no statistical difference ($\alpha = 0.05$) in the size distribution of both mussel length and weight among replicates and among stations. One continuously recording temperature monitor was attached to one replicate rack for each station. The racks were placed directly on top of the river sediments and anchored in place.

Mussels were transplanted to eight stations: six stations in the river downstream of the Nyanza site, one reference station upstream (river reference) of the facility, and one reference station in Whitehall Reservoir (reservoir reference, Fig. 1). Stations were located as far downstream as the Concord River, approximately 39 km from the site.

The stations were situated in both free-flowing (stations 2, 3, 6, and 8) and impounded (stations 1, 4, 5, and 7) areas of the river. Stations were selected to represent a gradient of Hg contamination associated with sediments. Highest sediment Hg concentrations were expected at station 3, approximately 2.5 km from the Nyanza site. Mussel deployment sites were situated near the shore (water depths 0.6–1.3 m) for easy access from the shoreline. Stations 6 and 8 were located within wetland areas of the river in an attempt to assess availability of Hg where MeHg production may be higher (St. Louis et al. 1994). Station descriptions and distances from the suspected Hg source are provided in Fig. 1. Mussels at station 6 were moved a few hundred metres upstream halfway through the study due to high mortality (>50%) at the original deployment location. Mortality was likely caused by low dissolved oxygen at the Sherman Street Bridge (station 6) (Goldman Environmental Consultants, Inc. 1994).

Using a hand-held ponar, three sediment grabs were collected from each station for chemical analysis. The top 5 cm of each sample was collected for analysis.

Water temperatures at each station were recorded at 24-min intervals over the 12-week period using one in situ computerized data logger per station (HoboTemp, Onset Instruments). Data were downloaded from the logging devices using the instruments' data recovery software.

The mussel racks were retrieved after 12 weeks. Mussels were transported to the laboratory work area in coolers lined with wet ice and moist packing. End-of-test measurements were whole-animal wet weights, shell lengths, shell widths, and shell heights. Tissues from all surviving mussels for each rack were pooled and frozen before chemical analysis. This procedure provided three replicates at all sites except station 6 where only two replicates were available due to high mortality. A minimum of eight mussels were used in the composites for station 6.

Sediment and tissue analyses

The 24 sediment samples (three replicates for each of eight stations) collected during mussel deployment were analyzed for selected metals (Sb, As, Cd, Cr, Pb, and Hg) and total solids, total organic C (Plumb 1981), and grain size. All metal analyses and grain size determinations were conducted according to Puget Sound Estuary Program (1989) protocols. Antimony, As, and Pb were analyzed by graphite furnace atomic absorption spectrophotometry, Cd and Cr by inductively coupled argon plasma spectroscopy, and Hg by cold-vapor atomic absorption.

Mussel tissues were analyzed for total Hg and MeHg concentrations according to the methods provided in Bloom (1989, 1992) and Bloom and Fitzgerald (1988). MeHg was analyzed in 50-µL aliquots of KOH digest by aqueous-phase ethylation, isothermal gas chromatograph separation, and cold-vapor atomic fluorescence detection (instrument detection limits of approximately 0.2 pg). Total Hg was analyzed in 50-µL aliquots of acid digest by $SnCl_2$ reduction, dual gold amalgamation, and cold-vapor atomic fluorescence detection. Detection limits for total Hg and MeHg were 0.5 and 0.2 ng·g dry weight^{-1}, respectively. The dry fraction material of the samples was determined by drying an aliquot (approximately 5 g) overnight at 105°C in aluminum drying pans.

Initial total Hg and MeHg concentrations in mussel tissues before deployment in the Sudbury River were estimated by measuring a subsample of 30 mussels (61.3–63.8 mm long, 10 mussels in each of three replicates) collected from Lake Massesecum. Inorganic Hg concentration was calculated as the difference between total Hg and MeHg. The total Hg and MeHg contents were determined for all tissue samples using the following equation:

$$(1) \quad \text{Content (ng)} = \text{Concentration (ng·g}^{-1}\text{)} \times \text{Tissue weight (g)}$$

Statistical analyses of growth parameters

We assessed the effects resulting from exposure to conditions in the Sudbury River by evaluating growth of individual transplanted mussels. Growth rates during the 12-week study were calculated from changes in whole-animal wet weight, shell length, shell weight, and soft tissue weight, which provide integrated measures of animal response. Changes in tissue weights were used as an estimate of mussel growth. Since determining tissue wet weights is a destructive process, the initial wet weight was estimated from the

© 2000 NRC Canada

Table 1. Results of selected trace element analyses and conventional parameters for sediments collected from Whitehall Reservoir and the Sudbury River.

	Station							
	1 (WHR)	2 (WS)	3 (R2I)	4 (RES2)	5 (SXI)	6 (SSB)	7 (FHB)	8 (TSB)
Trace element (mg·kg dry weight^{-1})[a]								
Total Hg	0.17	0.11	17.9	0.17	5.4	0.5	0.07	0.36
Cr	24.3	10.3	152.3	14	78	22.3	7.9	28
Pb	132.7	107	225	17.7	410	58.7	5.4	40
Sb	U (0.4)	U (0.3)	1.4	U (0.2)	1.1	U (0.5)	U (0.2)	U (0.2)
As	5.9	3.7	12.2	3	11.9	8.1	9.2	10.7
Cd	U (0.8)	0.6	3.3	0.4	10	3.6	0.3	1
Physical parameter (%)[b]								
Total organic C	5.93	3.45	11.7	3.37	7.7	10	1.62	4.58
Total solids	22.87	43.97	18.57	49.43	19.28	18.98	65.98	38.79
Grain size								
Sand	17	82	30	80	38	34	90	85
Silt	70	14	58	16	46	42	6	10
Clay	10	3	10	2	14	22	4	5

Note: Detection limits (mg·kg^{-1}): Hg = 0.05, Cr = 0.5, Pb = 0.1, Sb = 0.1, As = 0.1, and Cd = 0.2. U, undetected; concentration in parentheses equals the detection limit achieved for that sample.

[a]Concentrations were determined as the mean of three replicate samples.

[b]Measurements were made on one sample only at each station, except for grain size at station 6, determined as a mean of triplicate samples.

following regression equation generated for the subsample of 30 individuals measured at the start of the test:

(2) Initial tissue weight (g wet) =

0.21(initial whole-animal wet weight) + 0.66

All data sets were analyzed for homogeneity in variances (Zar 1974) before conducting ANOVAs and Duncan's multiple range test to determine differences among stations. If data did not meet the requirements for parametric analyses, the nonparametric equivalents were used (i.e., Kruskal–Wallis nonparametric ANOVA and Dunn's multiple comparison test). At no station was there a significant difference among the three replicate racks. This allowed pooling of the data for each station and analyses on a station-by-station basis. A correlation analysis was run between selected variables to help identify trends and potential relationships. All statistical analyses were run at the 95% confidence level.

Results

Sediment chemistry

Mean total Hg concentrations in sediments ranged from 0.07 mg·kg dry weight^{-1} at station 7 (Fairhaven Bay) to 17.9 mg·kg dry weight^{-1} at station 3 (reservoir 2 inlet) (Table 1). The second highest total Hg concentration, 5.4 mg·kg dry weight^{-1}, was measured in sediments from station 5 (Saxonville Impoundment). Total Hg concentrations in sediments collected from reservoir 2 (station 4) were low (0.17 mg·kg dry weight^{-1}) compared with a value of 18 mg·kg dry weight^{-1} measured by Frazier et al. (2000).

Elevated concentrations of Cr and Pb were also detected in sediments, with the highest concentrations at stations 3 (reservoir 2 inlet) and 5 (Saxonville Impoundment) (Table 1). Results of correlation analyses show a strong, significant association between Hg and Cr (r = 0.98). Mercury was not strongly associated with other metals. Both Hg and Cr concentrations were moderately associated with total organic C concentration (r = 0.72 and r = 0.76, respectively).

Sediment grain size varied among stations (Table 1). Although attempts were made to locate stations in similar substrate types, stations 2, 4, 7, and 8 were predominantly sand (>80% sand), while the remaining stations were predominantly fines (61–80% silt and clay). Total organic C concentrations ranged from 1.62 to 11.7% (Table 1).

Survival and condition

Mussel survival rates were high, ranging from 83 to 95% at all stations, except station 6 where survival was 36% (Table 2). Most of the surviving mussels at station 6 were in the larger size-classes. Although the data for station 6 are included for completeness, they were not included in statistical comparisons because of high mortality, low growth rates, and the station relocation halfway through the study.

Condition index (Davenport and Chen 1987) calculated on a subset of 30 mussels at the start of the test was 56 (Table 2). At the end of the study, condition indices ranged from 57 to 77. The highest indices were from mussels at stations 7 and 8, and the lowest were from mussels at reference station 2 and test station 3.

Tissue chemistry

Prior to deployment, mussel tissues had mean total Hg and MeHg concentrations of 640 and 140 ng·g dry weight^{-1}, respectively (Table 2). These concentrations were much higher than expected for mussels collected from a relatively pristine lake. After the 12-week deployment in the Sudbury River, the mean concentrations of total Hg, inorganic Hg, and MeHg in mussel tissues decreased downstream (with distance away) from Nyanza (Fig. 2). The total Hg concentrations were significantly higher for mussels deployed at stations 1, 2, and 3 at the end of the test than at the start, while total Hg concentrations at stations 7 and 8 were significantly lower. Mean tissue total Hg concentrations at the end of the test ranged from a high of 950 ng·g dry weight^{-1} at

© 2000 NRC Canada

Table 2. Initial condition index and tissue Hg concentrations and contents (±SD) in mussels collected from Lake Massesecum at the start of the test and survival, growth rate (whole-animal wet weight), condition index, and tissue Hg concentrations and contents by station for mussels after 12 weeks in the Sudbury River.

				Concentration (ng·g dry weight^{-1})			Content (ng)				
Station	Survival (%)	Growth rate (mg·week^{-1})	Condition index[a]	Total Hg	MeHg	Inorganic Hg	Total Hg	MeHg	Inorganic Hg	% inorganic Hg depurated	% MeHg
Initial	—	—	56	640 (103)	140 (9.29)	500	510 (125)	110 (18.2)	400		22
1 (WHR)	83	–21	63	890 (85.5)	360 (46.7)	530	440 (70.4)	180 (28.5)	260	35	40
2 (WS)	91	–38	57	850 (71.9)	260 (44.3)	600	440 (90.5)	130 (28.0)	310	23	30
3 (R2I)	93	23	60	950 (33.3)	320 (29.6)	640	550 (73.1)	180 (25.2)	370	8	33
4 (RES2)	95	185	67	690 (228)	260 (24.8)	430	570 (140)	220 (33.4)	350	13	38
5 (SXI)	87	198	62	520 (56)	200 (49.8)	320	390 (64.5)	150 (31.0)	240	40	38
6 (SSB)	36	46	+	590 (127)	170 (42.8)	420	450 (108)	150 (25.5)	350	13	33
7 (FHB)	88	270	70	400 (51.1)	140 (11.0)	260	430 (92.5)	150 (31.2)	280	30	34
8 (TSB)	87	303	77	340 (35.7)	130 (3.5)	210	430 (59.5)	170 (20.1)	260	35	39

Note: +, high mortality.
[a](Tissue wet weight/shell weight) × 100.

Fig. 2. Initial and end-of-test mussel concentrations (±SD) of (*a*) total Hg, (*b*) MeHg, and (*c*) inorganic Hg by station. Station 6 data are presented for comparative purposes only (open bar); they were not included in the statistical analyses. Asterisks indicate end-of-test tissue concentrations significantly different from the initial concentration.

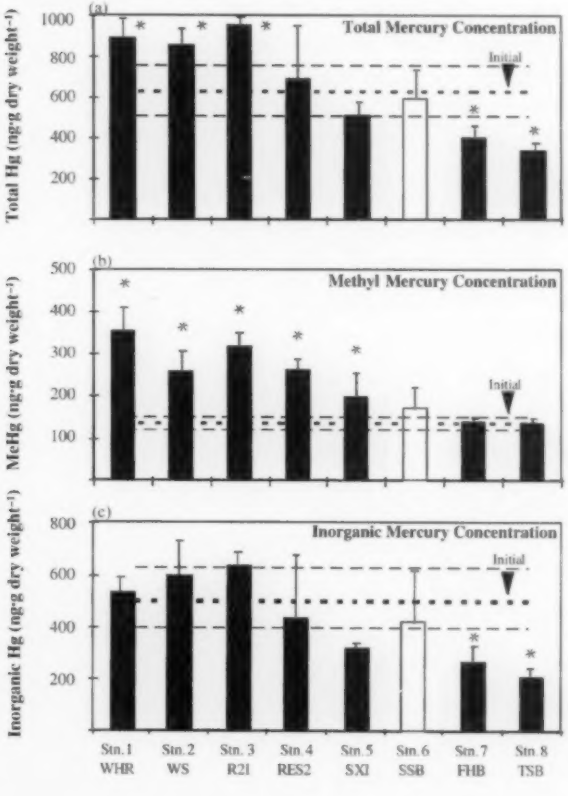

Fig. 3. Initial and end-of-test mussel content (±SD) of (*a*) total Hg, (*b*) MeHg, and (*c*) inorganic Hg by station. Station 6 data are presented for comparative purposes only (open bar); they were not included in the statistical analyses. Asterisks indicate end-of-test tissue concentrations significantly different from the initial concentration.

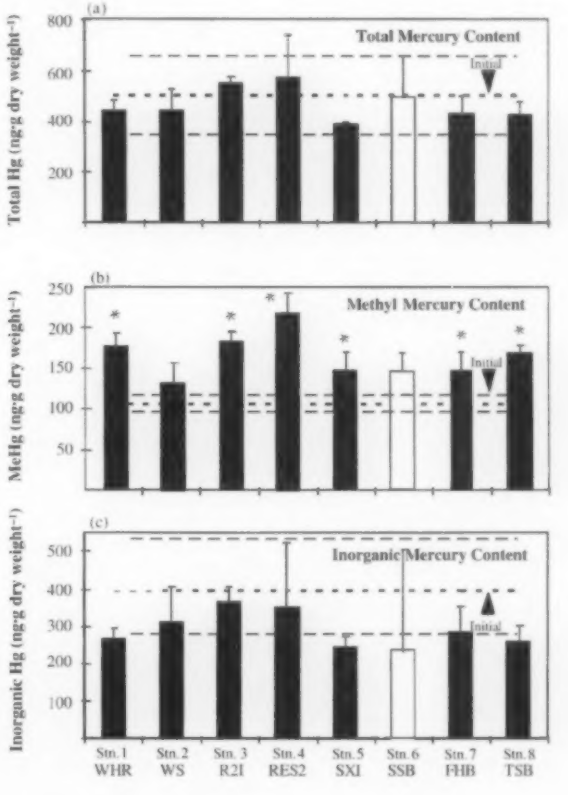

station 3 to a low of 340 ng·g dry weight^{-1} at station 8. Because total Hg concentrations in reference stations 1 and 2 were only slightly lower than those measured in mussels deployed at station 3, the station closest to Nyanza, the data suggest that mussels at stations 1 and 2 were exposed to bioavailable Hg and are not appropriate as reference animals.

© 2000 NRC Canada

Fig. 4. (*a*) Mussel growth rates (based on whole-animal wet weights) and changes in (*b*) tissue weight, (*c*) shell length, and (*d*) shell weight by station. Station 6 data are presented for comparative purposes only (open bar); they were not included in statistical analyses. Lines of asterisks indicate stations that form a statistically similar group (based on nonparametric ANOVA and Duncan's multiple range test).

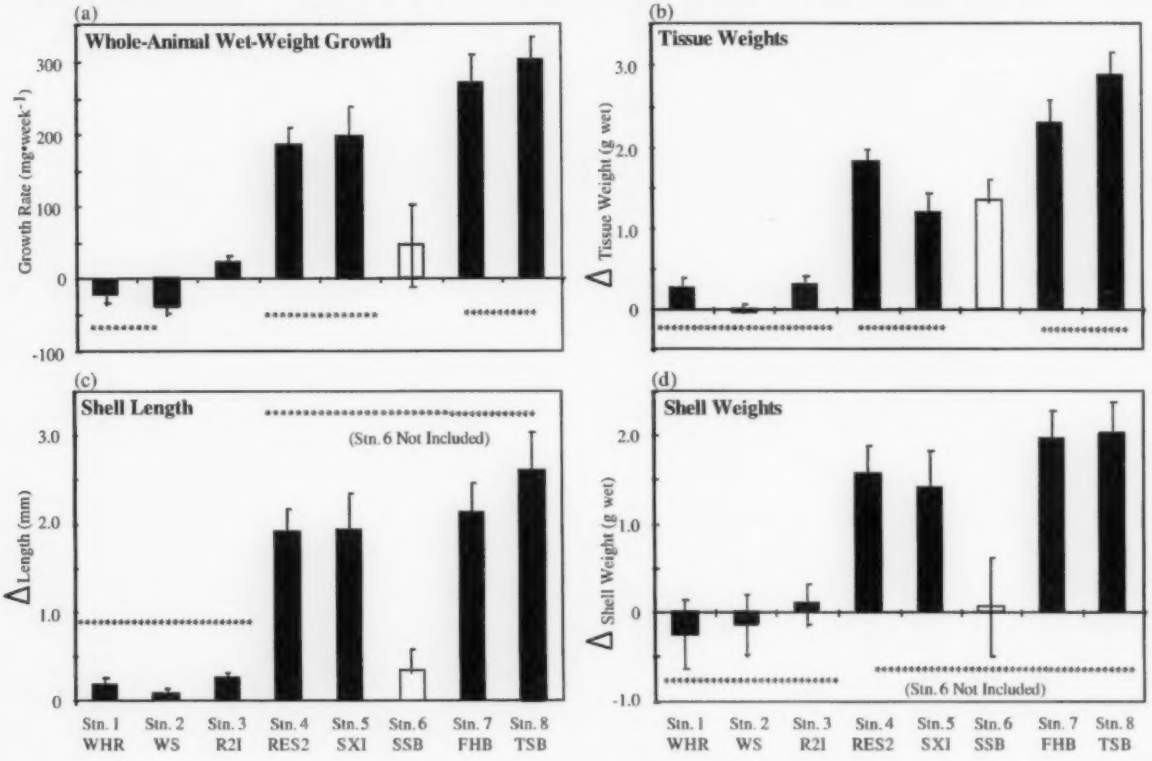

Fig. 5. Mercury in mussel tissue, mussel growth rates, and average temperature as a function of distance downstream from the Nyanza site.

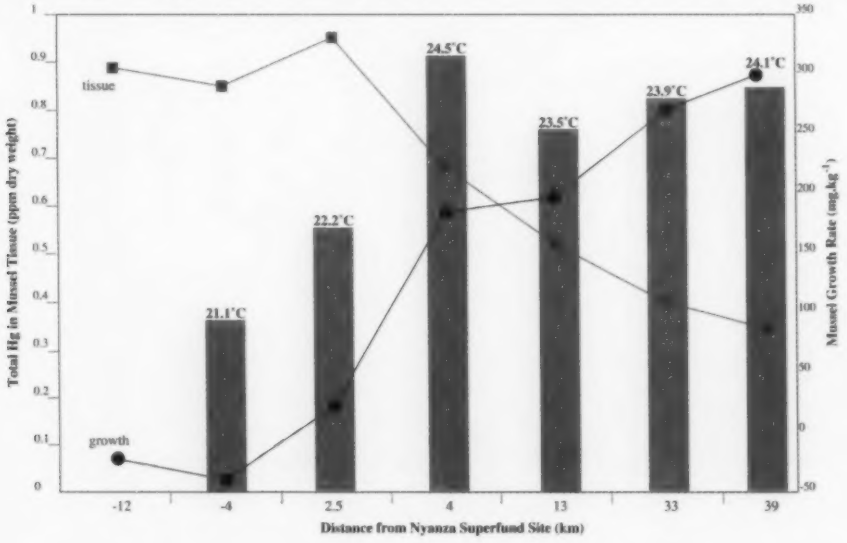

© 2000 NRC Canada

Table 3. Results of regression analyses (r^2 values) for each mussel growth metric versus total Hg, MeHg, and inorganic Hg.

	Tissue total Hg			Tissue MeHg			Tissue inorganic Hg		
Growth metric	Intercept (±SE)	Slope (±SE)	r^2	Intercept (±SE)	Slope (±SE)	r^2	Intercept (±SE)	Slope (±SE)	r^2
Growth rate[a]	881 (46.7)	–1.66 (0.25)	0.9	306 (24.2)	–0.53 (0.13)	0.77	575 (32.2)	–1.13 (0.17)	0.9
Tissue dry weight	1275 (119)	–774 (142)	0.87	437 (51.1)	–254 (60.9)	0.78	838 (88.5)	–520 (106)	0.83
Shell length	948 (59.1)	–220 (36.3)	0.88	325 (30.9)	–68.5 (19.0)	0.72	622 (38.1)	–151 (23.4)	0.89

[a]Whole-animal wet weight.

MeHg concentrations in mussel tissues ranged from 130 to 360 ng·g dry weight^{-1}, with the lowest concentration measured in mussels from station 8 and the highest in mussels from station 1 (reference station). End-of-test MeHg concentrations were significantly higher than initial concentrations at stations 1–5 (Fig. 2).

Analysis of Hg content data revealed slightly different trends than the concentration data. The total Hg content in mussel tissue did not change significantly during the 12-week exposure period (Fig. 3). Except for stations 3 and 4, which increased slightly, total Hg content in mussel tissues was slightly lower at the end of the test. In contrast, MeHg content in mussel tissues increased significantly at all stations, except reference station 2, with the greatest increase at station 4 (Table 2; Fig. 3). The proportion of MeHg within the total Hg content of mussels increased at all stations during the test. MeHg accounted for 30–40% of the total Hg content in mussels at the end of the test compared with an initial composition of 22% MeHg (Table 2).

Total Hg concentrations in tissue were not significantly correlated with total Hg concentrations in sediment at the 95% confidence level ($r = 0.44$). This correlation remained statistically insignificant even after normalizing for total organic C or using the sediment data from Frazier et al. (2000). The correlation did improve ($r = 0.82$) if the reference stations were eliminated.

Mussel growth

Four metrics were used to assess growth: shell length, whole-animal wet weight, tissue weight, and shell weight. Only whole-animal wet weight and shell length were measured for each individual at the start of the test. Therefore, the change (i.e., increase or decrease) could only be determined for these two metrics. Because of the closeness in size (length and weight) distribution among stations at the start of the test, it was assumed that the average tissue weight and shell weight were also similar among stations. Based on this assumption, the end-of-test tissue weights and shell weights were evaluated for statistical differences; any differences observed were assumed to have occurred during the test period.

Mussels at stations 7 and 8 had the greatest increases in tissue weight, shell length, and whole-animal wet weight. In general, mussel growth increased downstream from station 1 to station 8 as shown by increases in whole-animal wet weights, lengths, tissue weights, and shell weights (Fig. 4). Mussels at stations 1 and 2 had negative changes in whole-animal wet weight. Since these mussels had higher than expected Hg concentrations and negative growth, they could not be used for reference, and the planned comparisons could not be made. In general, stations 1, 2, and 3 with little or no growth form a statistical grouping, stations 4 and 5 with intermediate growth, and stations 7 and 8 with the highest growth also form a separate statistical grouping (Duncan's multiple range test).

Comparisons between tissue Hg concentrations and growth

Tissue Hg concentrations decreased away from Nyanza, while mussel growth increased (Fig. 5). Regression analyses were conducted on the three forms of Hg and the three mussel growth metrics (changes in whole-animal wet weight, estimated changes in tissue dry weight, and changes in shell length). The relationship between tissue Hg concentration and growth was strong and consistent for all growth metrics used (Table 3). Based on the r^2 values, for each mussel growth metric, the relationship between total Hg and inorganic Hg and growth was slightly stronger than for MeHg concentration and growth. Correlations for tissue Hg content (on a per animal basis) and mussel growth were not significant.

Temperature

The water temperatures measured during the study were within the natural range for *E. complanata* in the northeastern United States (D.H. Stansbery, Ohio State University, Museum of Biological Diversity, Columbus, Ohio, personal communication) and are not expected to be a significant factor for either bioaccumulation or growth in this species. Temperature ranged from a maximum of 30°C at the start of the study to 13°C at the end. Differences between upstream and downstream stations and between river and impoundment stations were observed.

The mean temperatures were significantly different between most stations, with the exception of stations 4 and 8, stations 5 and 6, stations 5 and 7, and stations 5 and 8 (Fig. 5). Temperature data from station 1 were not included in the temperature analysis due to a malfunction in the temperature recording device. The order of the mean temperatures for stations 2–8 was as follows: station 2 (Wood Street) < station 3 (reservoir 2 inlet) < station 6 (Sherman Street Bridge) < station 5 (Saxonville Impoundment) < station 7 (Fairhaven Bay) < station 8 (Thoreau Street Bridge) < station 4 (reservoir 2).

Station 4 had the lowest average range of temperatures over the weekly periods. Stations 2 and 4 were the only significantly different stations in their range of weekly temperatures.

This temperature pattern and range analysis are consistent with water residence times in a river system. Upstream stations (shorter water residence times) are generally cooler than the downstream stations, and stations in impoundments

© 2000 NRC Canada

(i.e., stations 4, 5, and 7) are generally warmer and have lower variability than faster-flowing river stations.

Discussion

The objectives of this mussel transplant study were to determine how far downstream from the Nyanza site Hg was bioavailable and whether adverse effects were associated with exposure to bioavailable Hg. Results based on evaluations of content data suggest that MeHg was biologically available throughout the study area. Study results are consistent with elevated concentrations of MeHg in the downstream water column (Waldron et al. 2000), in sediments, and in fish tissues (NUS Corporation 1992).

Changes in Hg content, not concentration, were compared to assess Hg uptake. Growth may dilute contaminant concentrations when tissue is added relatively faster than contaminants (Strong and Luoma 1981). This "growth dilution" can obscure uptake patterns resulting in contaminant concentrations that are lower in faster-growing individuals. For example, the MeHg concentration data suggest that mussels at stations 1–5 accumulated MeHg. However, analysis of the content data reveals that the fast-growing mussels at stations 7 and 8 also accumulated MeHg. Concentration data for total Hg suggest accumulation by animals closest to Nyanza and depuration by those downstream. However, the content data indicate that there were no statistically significant changes in total Hg content on a per animal basis. The proportion of the different species of Hg shifted: MeHg increased, while inorganic Hg decreased.

Although inorganic Hg was not directly measured, we assumed that inorganic Hg is equivalent to the difference between total Hg and MeHg. Inorganic Hg content data indicate that mussels at all stations depurated inorganic Hg. Inorganic Hg is depurated more rapidly than MeHg in mussels (Fowler et al. 1978). Mussels closest to the Nyanza site, stations 3 and 4, depurated only 8 and 13% of their inorganic Hg burden (Table 2). Mussels farther downstream depurated 30–40% of their inorganic Hg burden. In other studies, the freshwater *Corbicula* depurated 30–35% of the inorganic Hg (Inza et al. 1998) and the saltwater *Mytilus* depurated 40–65% (Fowler et al. 1978).

Mussels at station 4 (reservoir 2) accumulated the most MeHg content on a per animal basis despite the low concentration of total Hg in sediment measured in this study. Data presented by Frazier et al. (2000) suggest a total Hg concentration in sediments of about 18 mg·kg dry weight^{-1} for reservoir 2 compared with a value of 0.17 mg·kg dry weight^{-1} from our station 4. Our station was located nearshore, at the base of an embankment. Clean soil from the vegetated embankment is likely to have eroded into the local area of our station, reducing the sediment Hg concentration.

Uptake patterns in mussels in the Sudbury River are consistent with the concentrations of aqueous total Hg measured by Waldron et al. (2000). Mussels at stations 3 and 4 in our study took up the most MeHg and depurated the least inorganic Hg, corresponding to high concentrations of total Hg (mean unfiltered Hg: 16 and 7.5 ng·L^{-1}; mean dissolved Hg: 4.9 and 4.8 ng·L^{-1}) measured at sites G and L, respectively, by Waldron et al. (2000). Total Hg and MeHg content was lower in mussels at station 5, corresponding to a decrease in aqueous Hg concentration (mean unfiltered Hg: 3.1 ng·L^{-1}; dissolved mean Hg: 2.2 ng·L^{-1}) measured at site Q by Waldron et al. (2000). Although there are no aqueous Hg data for the Sudbury River near our stations 7 and 8, MeHg uptake by mussels indicate that MeHg was still available as far downstream as the Concord River. The origin of the MeHg accumulated by mussels at these downstream stations is unknown. MeHg could have formed upstream, within the river, or within nearby wetlands (St. Louis et al. 1994; Waldron et al. 2000).

Although both sediment and water are potential sources of Hg to mussels, Tessier et al. (1992) indicate that *E. complanata* actively accumulates Hg from the water and found a significant relationship in laboratory exposures. Based on gut content analysis, Tessier et al. (1984) found that digestive tract particles in *E. complanata* are predominantly in the 10–13 μm size range. These small particles also tend to sequester the highest concentration of contaminants because of their relatively high surface to volume ratio (Boese et al. 1988). Muncaster et al. (1990) noted that the water column was the main source of organic contaminants to *Elliptio* and *Lampsilis* transplanted to Lake St. Clair, Ontario. In our study, Hg in mussels appears to be more closely related to aqueous Hg concentrations than sediment concentrations; however, it is not clear whether the immediate source was dissolved or particulate or both.

Effects from exposure to Hg in the Sudbury River were assessed by comparing changes in growth among stations. Each growth metric (i.e., whole-animal wet weight, change in tissue weight, and change in shell length) strongly correlated with all three forms of Hg evaluated. The highest tissue concentrations of total Hg, inorganic Hg, and MeHg were associated with the lowest mussel growth rates. Tissue residue effects data for Hg are limited but range from 0.25 μg·g wet weight^{-1} in juvenile walleye (*Stizostedion vitreum*) (Friedmann et al. 1996) to 6–20 μg·g wet weight^{-1} in adult fish tissue (Wiener and Spry 1996). Mussel tissue residues (0.13 μg·g wet weight^{-1}) in this study are slightly lower than this range. Mussel growth was not related to location in impounded or free-flowing reaches or to grain size differences.

Water temperature differences measured in the Sudbury River are expected given the nature of the system being tested, and these differences are statistically significant. Average temperatures and mussel growth rates are positively correlated ($r = 0.85$). Lower temperatures at stations 2 and 3 may have affected mussel growth rates at these stations. Temperature may have affected growth directly, or indirectly, such that food and nutrients were less available in areas where temperatures were lower. Temperatures in the four downstream stations varied by only 1°C and do not appear to have affected growth rates. For example, mussels at stations 4 and 8 had statistically similar temperatures but statistically different growth rates.

Station 1 (Whitehall Reservoir) clearly does not represent uncontaminated background conditions, and mussel growth data could not be used as reference data to compare with data from mussels transplanted to stations below Nyanza. The tissue Hg concentrations in mussels from Whitehall Reservoir were among the highest measured in our study. Elevated aqueous concentrations of total Hg and MeHg were measured in two tributary streams of Whitehall Reservoir

© 2000 NRC Canada

during the mussel transplant study (mean total Hg: 9.5 and 3.8 $ng \cdot L^{-1}$; mean total MeHg: 2.8 and 1.0 $ng \cdot L^{-1}$) (J. Colman, U.S. Geological Survey, Northborough, Mass., unpublished data). Resident *Elliptio* in Whitehall Reservoir had higher Hg concentrations than the transplants (S. Mierzykowski, U.S. Fish and Wildlife Service, Maine Field Office, Orono, Maine, unpublished data). Mercury concentrations in Whitehall Reservoir fish measured in a related study were also elevated (T. Haines, U.S. Geological Survey, Biology Resources Division, Orono Field Station, Orono, Maine, unpublished data).

Mussels at reference station 2 did not accumulate MeHg, but the total concentration of Hg increased, perhaps due to loss of tissue (negative growth rates). Mussels transplanted to station 1 also had negative growth rates. Water chemistry was not monitored, but mussel racks in both reference areas were different in appearance than test station racks. Mussel racks at reference station 1 had no algal fouling or plant overgrowth. Plastic label tags on racks at reference station 2 were partly dissolved, and mussel shells were very fragile. Mussels at reference station 2 also had the lowest condition index. The station was located downstream of Cedar Swamp and water chemistry from the swamp may have affected the mussels. Resident *Elliptio* collected from the Cedar Street Bridge area had Hg concentrations similar to those of reference station 2 transplanted mussels (S. Mierzykowski, U.S. Fish and Wildlife Service, Maine Field Office, Orono, Me., unpublished data). In laboratory experiments, mayflies exposed to sediment from these reference areas did not accumulate elevated concentrations of Hg (Naimo et al. 2000), suggesting that the source of Hg to mussels in the reference areas was through the water column and (or) food web transfer.

We are able to conclude that MeHg was bioavailable throughout our study area. *Elliptio complanata* were sensitive to changes in MeHg concentrations, and uptake was greater near the Nyanza site. The effects on mussel growth are correlated with Hg concentrations; however, we cannot conclude that the measured effects are due to Hg exposure. The longitudinal gradient of increasing growth with increasing distance from the Nyanza site may be due to some unmeasured parameter such as food availability.

With the increased use of freshwater bivalves for contaminant biomonitoring, this study highlights the difficulty of finding a source of transplant animals with low initial Hg concentrations. Initial Hg concentrations were high, even though study mussels were collected from a lake removed from direct Hg sources. In another study, the initial Hg concentrations in *Corbicula*, collected from a "clean" river in the southern United States, were twice as high as values in this study (NOAA and EVS Consultants, Inc. 1998). Elevated Hg concentrations in mussels may be a product of regional conditions. Low pH was important in predicting fish tissue Hg concentrations in Massachusetts lakes (Rose et al. 1999) and may be a factor contributing to elevated Hg concentrations in the mussels.

Assessing the exposure and impacts of Hg-contaminated sites on aquatic receptors is particularly challenging due to the increased bioavailability of MeHg in areas affected by low pH. The resulting widespread distribution of Hg-enhanced biota complicates the characterization of background conditions. For monitoring of Hg with transplanted organisms, field-collected source animals may need to be brought into the laboratory and allowed to depurate Hg prior to their use. Locating comparable Hg-free reference stations may require chemical investigations prior to the onset of the study.

Acknowledgments

We thank Susan von Oettingen of the U.S. Fish and Wildlife Service for help in locating a source of test animals and assistance during the initial collection and setup, Tom Gloria and the New England Dive Club for collecting mussels from Lake Massesecum and measuring animals during the setup, Pat Boyd for her expertise in the field, Doug Smith for technical advice on freshwater mussels, David Strayer for guidance regarding mussel population ecology, and the staff of EVS Consultants, Inc. (Berit Bergquist, Dan Hennessy, Rich Sturim, Lorraine Read, and Kimberly Stewart).

References

Bloom, N.S. 1989. Determination of picogram levels of methylmercury by aqueous phase ethylation, followed by cryogenic gas chromatography with cold vapor atomic fluorescence detection. Can. J. Fish. Aquat. Sci. **46**: 1131–1140.

Bloom, N.S. 1992. On the chemical speciation of mercury in edible fish muscle tissue. Can. J. Fish. Aquat. Sci. **49**: 1010–1017.

Bloom, N.S., and Fitzgerald, W.F. 1988. Determination of volatile mercury species at the picogram level by low temperature gas chromatography with cold vapor atomic fluorescence detection. Anal. Chim. Acta, **208**: 151–161.

Boese, B.L., Lee, H., II, and Specht, D.T. 1988. Efficiency of uptake of hexachlorobenzene from water by the tellinid clam *Macoma nasuta*. Aquat. Toxicol. **12**: 345–356.

Curry, C.A. 1977. The freshwater clam *Elliptio complanata*, a practical tool for monitoring water quality. Water Pollut. Res. Can. **13**: 45–52.

Davenport, J., and Chen, X. 1987. A comparison of methods for the assessment of condition in the mussel (*Mytilus edulis* L.). J. Molluscan Stud. **53**: 293–297.

Elder, J.F., and Collins, J.J. 1991. Freshwater molluscs as indicators of bioavailability and toxicity of metals in surface-water systems. Rev. Environ. Contam. Toxicol. **122**: 37–79.

Fowler, S.W., Heyraud, M., and La Rosa, J. 1978. Factors affecting methyl and inorganic mercury dynamics in mussels and shrimp. Mar. Biol. **46**: 267–276.

Frazier, B.E., Wiener, J.G., Rada, R.G., and Engstrom, D.R. 2000. Stratigraphy and historic accumulation of mercury in recent depositional sediments in the Sudbury River, Massachusetts, U.S.A. Can. J. Fish. Aquat. Sci. **57**: 1062–1072.

Friedmann, A.S., Watzin, M.C., Brinck-Johnsen, T., and Leiter, J.C. 1996. Low levels of dietary methylmercury inhibit growth and gonadal development in juvenile walleye (*Stizostedion vitreum*). Aquat. Toxicol. **35**: 265–278.

Goldman Environmental Consultants, Inc. 1994. Water resource study: Sudbury, Assabet, and Concord rivers. Massachusetts Department of Environmental Management, Boston, Mass.

Heit, M., Klusek, C.S., and Miller, K.M. 1980. Trace element, radionuclide, and polynuclear aromatic hydrocarbon concentrations in unionidae mussels from northern Lake George. Environ. Sci. Technol. **14**: 465–468.

Inza, B., Ribeyre, R., and Boudou, A. 1998. Dynamics of cadmium and mercury compounds (inorganic mercury or methylmercury):

© 2000 NRC Canada

uptake and depuration in *Corbicula fluminea*, effects of temperature and pH. Aquat. Toxicol. **43**: 273–285.

JBF Scientific Corporation. 1973. An investigation of mercury problems in Massachusetts. Massachusetts Water Resources Commission, Division of Water Pollution Control, Boston, Mass.

Kauss, P.B., and Hamdy, Y.S. 1991. Polycyclic aromatic hydrocarbons in surficial sediments and caged mussels of the St. Mary's River 1985. Hydrobiologia, **219**: 37–62.

Langdon, R. 1993. Mussel monitoring for toxic contaminants in twelve Lake Champlain tributaries. Vermont Agency of Natural Resources, Department of Environmental Conservation Laboratory, Waterbury, Vt.

McMahon, R.F. 1991. Table 11.5: list of recent investigations involving utilization of bivalves to monitor effect or levels of pollutants in freshwater habitats. *In* Ecology and classification of North American freshwater invertebrates. *Edited by* J.H Thorp and A.P. Covich. Academic Press, Inc., San Diego, Calif.

Metcalfe-Smith, J.L. 1994. Influence of species and sex on metal residues in freshwater mussels (family Unionidae) from the St. Lawrence River, with implications for biomonitoring programs. Environ. Toxicol. Chem. **13**: 1433–1443.

Metcalfe-Smith, J.L., Merriman, J.C., and Batchelor, S.P. 1992. Relationships between concentration of metals in sediment and two species of freshwater mussels in the Ottawa River. Water Pollut. Res. J. Can. **27**: 845–869.

Muncaster, B.W., Hebert, P.D.N., and Lazar, R. 1990. Biological and physical factors affecting the body burden of organic contaminants in freshwater mussels. Arch. Environ. Contam. Toxicol. **19**: 25–34.

Naimo, T.J., Wiener, J.G., Cope, W.G., and Bloom, N.S. 2000. Bioavailability of sediment-associated mercury to *Hexagenia* mayflies in a contaminated floodplain river. Can. J. Fish. Aquat. Sci. **57**: 1092–1102.

NOAA and EVS Consultants, Inc. 1998. Baseline clam monitoring study, Cannelton Industries Site, Sault Ste. Marie, Michigan, summer 1997. NOAA Tech. Memo. NOS ORCA 136. Prepared for U.S. Environmental Protection Agency, Region V, Chicago, Ill.

NUS Corporation. 1992. Final remedial investigation report. Nyanza Operable Unit III — Sudbury River study, Middlesex County, Massachusetts. Vol. I–IV. EPA Work Assignment No. 02-1L15. EPA contract No. 68-W8-0117. U.S. Environmental Protection Agency, Boston, Mass.

Plumb, R.H., Jr. 1981. Procedures for handling and chemical analysis of sediment and water samples. Contract EPA-4805572010. U.S. Environmental Protection Agency/Corps of Engineers Technical Committee on Criteria for Dredged and Fill Material, Washington, D.C.

Puget Sound Estuary Program. 1989. Recommended guidelines for measuring metals in Puget Sound water, sediment, and tissue samples. *In* Recommended protocols for measuring selected environmental variables in Puget Sound. U.S. Environmental Protection Agency, Region 10, Seattle, Wash.

Rose, J., Hutcheson, M.S., West, C.R., Pancorbo, O., Hulme, K., Cooperman, A., DeCesare, G., Isaac, R., and Screpetis, A. 1999. Fish mercury distribution in Massachusetts, USA, lakes. Environ. Toxicol. Chem. **18**: 1370–1379.

Salazar, M.H., and Salazar, S.M. 1995. In-situ bioassays using transplanted mussels. I. Estimating chemical exposure and bioeffects with bioaccumulation and growth. ASTM STP 1218. *In* Third Symposium on Environmental Toxicology and Risk Assessment. *Edited by* J.S. Hughes, G.R. Biddinger, and E. Mones. American Society for Testing and Materials, Philadelphia, Pa.

St. Louis, V.L., Rudd, J.W.M., Kelly, C.A., Beaty, K.G., Bloom, N.S., and Flett, R.J. 1994. Importance of wetlands as sources of methyl mercury to boreal forest ecosystems. Can. J. Fish. Aquat. Sci. **51**: 1065–1076.

Strong, C.R., and Luoma, S.N. 1981. Variations in the correlation of body size with concentrations of Cu and Ag in the bivalve *Macoma balthica*. Can. J. Fish. Aquat. Sci. **38**: 1059–1064.

Tessier, A., Campbell, P.G.C., Auclair, J.C., and Bisson, M. 1984. Relationships between the partitioning of trace metals in sediments and their accumulation in the tissues of the freshwater mollusc *Elliptio complanata* in a mining area. Can. J. Fish. Aquat. Sci. **41**: 1463–1472.

Tessier, L., Vaillancourt, G., and Pazdernik, L.R. 1992. Comparison of mercury bioaccumulation capacity between the short-lived gastropod *Viviparus georgianus* (Lea) and the pelecypod *Elliptio complanata* (Lightfoot) in the freshwater of the St. Lawrence Estuary. Water Pollut. Res. J. Can. **27**: 773–785.

U.S. Fish and Wildlife Service. 1990. Fish surveys, Nyanza Hazardous Waste Site, Sudbury River System, Massachusetts. U.S. Environmental Protection Agency, Waste Management Division, Boston, Mass.

Waldron, M.C., Coleman, J.A., and Breault, R.F. 2000. Distribution, hydrologic transport, and cycling of total mercury and methyl mercury in a contaminated river–reservoir–wetland system (Sudbury River, eastern Massachusetts). Can. J. Fish. Aquat. Sci. **57**: 1080–1091.

Wiener, J.G., and Spry, D.J. 1996. Toxicological significance of mercury in freshwater fish. *In* Environmental contaminants in wildlife: interpreting tissue concentrations. *Edited by* W.N. Beyer, G.H. Heinz, and A.W. Redmon-Norwood. Special Publication of the Society of Environmental Toxicology and Chemistry. Lewis Publishers, Boca Raton, Fla.

Zar, J.H. 1974. Biostatistical analysis. Prentice-Hall, Englewood Cliffs, N.J.

© 2000 NRC Canada

ASSIGNMENT OF COPYRIGHT

Ms. No. _____

To: NATIONAL RESEARCH COUNCIL OF CANADA ("NRC") Research Press

From: _____

_____

_____

_____

(name and address of author signing this form)

This refers to the manuscript entitled: _____

_____

written by myself and the following additional author(s): _____

_____

for publication in: _____

1. I declare that the list of authors fairly conforms to academic conventions about who should be listed. I declare that the manuscript, or its equivalent, has not been submitted for publication elsewhere. If it is accepted for publication by the National Research Council of Canada, I will ensure that it, or its equivalent, is not submitted for publication elsewhere.

2. I declare that I am (check ONE):

☐ (a) the sole owner of the copyright relating to the manuscript,	and →	I **assign** to NRC the entire copyright.
☐ (b) a part owner of the copyright, in conjunction with interests held by co-authors or their employers,	and →	I **assign** to NRC my entire interest in the copyright, and I expect the co-authors to also sign a form like this one.
☐ (c) an agent of my employer with authority to assign the copyright owned by the employer, who is: _____,	and →	I **assign** to NRC, on behalf of my employer, my employer's entire interest in the copyright relating to the manuscript, and I expect the co-authors to also sign a form like this one.
☐ (d) a public servant in Canada (federal, provincial or territorial) or the United Kingdom, so that the copyright is owned by Her Majesty,	and →	I have obtained the approval of my employer, according to the terms of my employment, to grant NRC **non-exclusive permission** to publish the manuscript and administer the copyright.
☐ (e) a public servant of the United States of America, and subject to the law that creates no U.S. copyright for the manuscript,	and →	I **assign** to NRC, on behalf of my employer, my employer's entire interest in any copyright that may exist outside the U.S., and I expect the co-authors to sign a form like this one.

3. I understand that my submission of this document does not guarantee publication, and that publication will not occur until **all authors** have provided a copyright transfer. If the manuscript is not published within 2 years after I sign this, the assignment is revoked.

Signed at _____ on _____

(City and Province/State) (Date)

_____

(Signature)

[Standard NRC form; alterations not acceptable.]

Comments on Copyright Transfer
(with extracts from the *Copyright Act*, Revised Statutes of Canada 1985, chapter C-42, as amended)

The publisher is not permitted to publish the manuscript without permission or an assignment of ownership of copyright. For greatest flexibility, and to be prepared to deal with future uses of the published material, the publisher requires ownership.

The owner may assign the right, but that assignment must be in writing:

13.(4) The owner of the copyright in any work may assign the right, either wholly or partially, and either generally or subject to territorial limitations, and either for the whole term of the copyright or for any other part thereof, and may grant any interest in the right by licence, but no assignment or grant is valid unless it is in writing signed by the owner of the right in respect of which the assignment or grant is made, or by his duly authorized agent.

The owner may be the author, but in many cases, the owner is the author's employer:

13.(3) Where the author of a work was in the employment of some other person under a contract of service or apprenticeship and the work was made in the course of his employment by that person, the person by whom the author was employed shall, in the absence of any agreement to the contrary, be the first owner of the copyright, but where the work is an article or other contribution to a newspaper, magazine or similar periodical, there shall, in the absence of any agreement to the contrary, be deemed to be reserved to the author a right to restrain the publication of the work, otherwise than as part of a newspaper, magazine or similar periodical.

The only exception to taking ownership arises when the manuscript is covered by Crown copyright owned by a Canadian government.

12. Without prejudice to any rights or privileges of the Crown, where any work is, or has been, prepared or published by or under the direction or control of Her Majesty or any government department, the copyright in the work shall, subject to any agreement with the author, belong to Her Majesty and in that case shall continue for the remainder of the calendar year of the first publication of the work and for a period of fifty years following the end of that calendar year.

Governments, and in particular the federal government, do not have a simple mechanism for assigning ownership of this particular type of Crown asset. Therefore, when an author is a public servant so that there is Crown copyright in the manuscript, a simple permission to use is acceptable to the publisher, if it is granted by a person with appropriate authority.

CESSION DU DROIT D'AUTEUR

Document n° _____

Au : CONSEIL NATIONAL DE RECHERCHES DU CANADA («CNRC») - Presses scientifiques

De : _____

_____

_____

_____

(nom et adresse de l'auteur qui signe le présent formulaire)

La présente cession porte sur le document intitulé : _____

_____

rédigé par moi, en collaboration avec l'auteur/les auteurs suivant(s) : _____

_____

aux fins de publication dans : _____

1. Je déclare que la liste des auteurs ci-dessus respecte les pratiques usuelles de rédaction savante quant aux personnes dont le nom doit être cité. Je déclare que le document ou son équivalent n'a pas été soumis à quelque autre organisme aux fins de publication. Si le CNRC accepte de publier le document, je m'assurerai que celui-ci ou son équivalent n'est soumis à aucun autre organisme aux fins de publication sans en obtenir la permission préalable du CNRC.

2. Je déclare être (UN SEUL choix) :

☐	(a) le seul titulaire de droit d'auteur afférent au document,	et →	je **cède** le droit d'auteur intégral au CNRC.
☐	(b) un titulaire partite du droit d'auteur, de concert avec des coauteurs ou leurs employeurs,	et →	je **cède** ma part du droit d'auteur au CNRC et m'attends à ce que les coauteurs signent une entente comparable.
☐	(c) un agent de mon employeur ayant l'autorité de céder le droit d'auteur appartenant à l'employeur, nommément : _____,	et →	je **cède** au CNRC, au nom de mon employeur, la part entière du droit d'auteur afférent au document appartenant à mon employeur, et m'attends à ce que les coauteurs signent une entente comparable.
☐	(d) un fonctionnaire du Canada (fédéral, provincial ou territorial) ou du Royaume-Uni, donc le droit d'auteur appartient à Sa Majesté,	et →	j'ai obtenu de mon employeur, en vertu de mes conditions d'emploi, l'autorisation d'accorder au CNRC la **permission non exclusive** de publier le document et de gérer le droit d'auteur.
☐	(e) un fonctionnaire des États-Unis d'Amérique, donc sujet à la loi qui n'associe aucun droit d'auteur américain au document,	et →	je **cède** au CNRC, au nom de mon employeur, la part entière de quelque droit d'auteur en vigueur ailleurs qu'aux É.-U. appartenant à mon employeur, et m'attends à ce que les coauteurs signent une entente comparable.

3. Je comprends que la soumission du document ne garantit aucunement sa publication et que la publication ne pourra être réalisée tant que **tous les auteurs** n'auront pas signé une cession du droit d'auteur. Si le document n'est pas publié dans les deux années suivant ma signature des présentes, la cession sera automatiquement révoquée.

Signé à _____, le _____

(ville et province/état) (date)

_____

(signature)

[Formulaire normalisé du CNRC; aucune modification permise.]

Commentaires sur la cession du droit d'auteur
(accompagnés d'extraits de la *Loi sur le droit d'auteur*, Lois révisées du Canada 1985, chapitre C-42 modifié)

L'éditeur ne peut publier un document sans la permission ou une cession du droit d'auteur. Pour des raisons de souplesse et en vue de l'utilisation future du document publié, l'éditeur doit devenir titulaire du droit d'auteur.

Le titulaire peut céder le droit, mais cette cession doit être faite par écrit :

13.(4) Le titulaire du droit d'auteur sur une oeuvre peut céder ce droit, en totalité ou en partie, d'une façon générale, ou avec des restrictions territoriales, pour la durée complète ou partielle de la protection; il peut également concéder, par une licence, un intérêt quelconque dans ce droit; mais la cession ou la concession n'est valable que si elle est rédigée par écrit et signée par le titulaire du droit qui en fait l'objet, ou par son agent dûment autorisé.

Le titulaire peut être l'auteur, mais dans plusieurs cas, le titulaire est l'employeur de l'auteur:

13.(3) Lorsque l'auteur est employé par une autre personne en vertu d'un contrat de louage de service ou d'apprentissage, et que l'oeuvre est exécutée dans l'exercice de cet emploi, l'employeur est, à moins de stipulation contraire, le premier titulaire du droit d'auteur; mais lorsque l'oeuvre est un article ou un autre contribution, à un journal, à une revue ou à un périodique du même genre, l'auteur, en l'absence de convention contraire, est réputé posséder le droit d'interdire la publication de cette oeuvre ailleurs que dans un journal, une revue ou un périodique semblable.

La seule exception dans la cession du droit d'auteur est lorsque le document est associé au droit d'auteur de la Couronne, qui appartient au gouvernement du Canada .

12. Sous réserve de tous les droits ou privilèges de la Couronne, le droit d'auteur sur les oeuvres préparées ou publiées par l'entremise, sous la direction ou la surveillance de Sa Majesté ou d'un ministère du gouvernement, appartient, sauf stipulation conclue avec l'auteur, à Sa Majesté et, dans ce cas, il subsiste jusqu'à la fin de la cinquantième année suivant celle de la première publication de l'oeuvre.

Les gouvernements, en particulier le gouvernement fédéral, ne disposent pas d'un mécanisme simple de cession de droit d'auteur pour ce genre de biens de la Couronne. C'est pourquoi lorsqu'un auteur est un fonctionnaire et que, par conséquent, le droit d'auteur appartient à la Couronne, une simple permission d'usage est suffisante pour l'éditeur, pour autant que celle-ci ait été octroyée par une personne jouissant de l'autorité nécessaire pour ce faire.

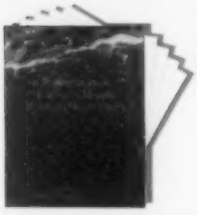

Perspectives on Canadian Marine Fisheries Management

L.S. Parsons and/et W.H. Lear
(*Editors/Directeurs scientifiques*)

446 pages
Hardcover/Édition reliée
November/Novembre1993
ISBN 0-660-15003-4
ISSN 0706-6503
NRC/CNRC 36176
$55.00/55,00 $

This volume, Canadian Bulletin of Fisheries and Aquatic Sciences 226, is a collection of 15 articles describing management approaches in different fisheries arising from the diversity and complexity of Canada's marine fisheries. Visit http://www.nrc.ca/cisti/journals/books/perspe_e.html at the NRC Research Press Web site to view the Table of Contents.

On décrit dans ce document, le Bulletin canadien des sciences halieutiques et aquatiques 226 (un recueil des 15 articles), des approches de gestion de diverses pêches axées sur la diversité et la complexité des pêches maritimes canadiennes. Visitez http://www.nrc.ca/cisti/journals/books/perspe_f.html au site Web des Press scientifiques du CNRC pour consulter la table des matières.

To order copies of this publication/Pour commander des exemplaires de ce livre

- Telephone: (613) 993-0151
- Fax: (613) 952-7656
- Mail orders: Monograph Orders, NRC Research Press, National Research Council Canada, Ottawa, Ontario K1A 0R6, Canada
- Internet e-mail: research.journals@nrc.ca
- World Wide Web: http://www.nrc.ca/cisti/journals/formmono.html

Canadian customers please add 7% GST. Orders from Quebec add a further 6.5% QST to the total price including GST. Make cheque or money order payable to "Receiver General for Canada, credit NRC". Note that for all orders outside Canada, rates are in U.S. Dollars. All sales are final.

- Téléphone : (613) 993-0151
- Télécopieur : (613) 952-7656
- Par la poste : Monographies, Presses scientifiques du CNRC, Conseil national de recherches Canada, Ottawa (Ontario) K1A 0R6, Canada
- Courrier électronique : research.journals@nrc.ca
- World Wide Web : http://www.nrc.ca/cisti/journals/formmofr.html

Les clients canadiens doivent ajouter la TPS de 7 %. Les clients du Québec doivent ajouter 6,5 % de TVQ au montant total, une fois la TPS additionnée. Libellez le chèque ou le mandat à l'ordre du «Receveur général du Canada, au crédit du CNRC». Pour les clients non canadiens, les prix sont en dollars américains. Aucun remboursement.

Please send me ____ copies of/Veuillez me faire parvenir ____ exemplaire(s) de *Perspectives on Canadian Marine Fisheries Management.*

NRC Research Press

Monograph Program

Presses scientifiques du CNRC

Programme de monographies

NRC·CNRC

PLEASE PRINT/LETTRES MOULÉES

☐ Payment enclosed/Paiement inclus ☐ Charge to/Imputer à ☐ Visa ☐ MasterCard

Account number/ N° de compte | | | | | | | | | | | | | | | | | | | | Expiry date/ Date d'expiration_____

Name/Nom

Signature/Signature

Address/Adresse

City/Ville Province/Province

Postal code/Code postal Country/Pays

Telephone/Téléphone Fax/Télécopieur

e-mail/Courrier électronique Date of order/Date de la commande

Guide to the Parasites of Fishes of Canada. Part IV. Trematoda

David I. Gibson

373 pages
Softcover/Édition brochée
March/mars 1996
ISBN 0-660-16403-5
ISSN 0706-6481
NRC/CNRC 40083
$42.95/42,95 $
Canadian Special Publication of Fisheries and Aquatic Sciences/ Publication spéciale canadienne des sciences halieutiques et aquatiques 124

More than 80 keys leading to the identification of more than 220 species of trematode parasites of Canadian fishes and diagnoses of more than 80 family–group taxa and 130 genera are given. Each genus is illustrated. For each species a Canadian host list, locality data, and any relevant remarks are included. Visit http://www.nrc.ca/cisti/journals/40083/133to136.html at the NRC Research Press Web to view a short chapter of this book.

On retrouve plus de 80 clefs qui permettent d'identifier quelque 220 espèces de trématodes parasites des poissons du Canada et la description de plus de 80 taxums de famille/groupe et de 130 genres. Chaque genre y est illustré. À chaque espèce sont associées des données sur l'emplacement et des remarques particulières. Visitez http://www.nrc.ca/cisti/journals/40083/f133to6.html au site Web des Presses scientifiques du CNRC pour afficher un court chapitre du livre.

To order copies of this publication/Pour commander des exemplaires de ce livre

- Telephone: (613) 993-0151
- Fax: (613) 952-7656
- Mail orders: Monograph Orders, NRC Research Press, National Research Council Canada, Ottawa, Ontario K1A 0R6, Canada
- Internet e-mail: research.journals@nrc.ca
- World Wide Web: http://www.nrc.ca/cisti/journals/formmono.html

Canadian customers please add 7% GST. Orders from Quebec add a further 6.5% QST to the total price including GST. Make cheque or money order payable to "Receiver General for Canada, credit NRC". Note that for all orders outside Canada, rates are in U.S. dollars. All sales are final.

- Téléphone : (613) 993-0151
- Télécopieur : (613) 952-7656
- Par la poste : Monographies, Presses scientifiques du CNRC, Conseil national de recherches Canada, Ottawa (Ontario) K1A 0R6, Canada
- Courrier électronique : research.journals@nrc.ca
- World Wide Web : http://www.nrc.ca/cisti/journals/formmofr.html

Les clients canadiens doivent ajouter la TPS de 7 %. Les clients du Québec doivent ajouter 6,5 % de TVQ au montant total, une fois la TPS additionnée. Libellez le chèque ou le mandat à l'ordre du «Receveur général du Canada, au crédit du CNRC». Pour les clients non canadiens, les prix sont en dollars américains. Aucun remboursement.

Please send me ____ copies of/Veuillez me faire parvenir ____ exemplaire(s) de *Guide to the Parasites of Fishes of Canada: Part IV. Trematoda.*

NRC Research Press

Monograph Program

Presses scientifiques du CNRC

Programme de monographies

PLEASE PRINT/LETTRES MOULÉES

☐ Payment enclosed/Paiement inclus ☐ Charge to/Imputer à ☐ Visa ☐ MasterCard

Account no./ Nº de compte | Expiry date/ Date d'expiration

Name/Nom

Signature/Signature

Address/Adresse

City/Ville Province/Province

Postal code/Code postal Country/Pays

Telephone/Téléphone Fax/Télécopieur

e-mail/Courrier électronique Date of order/Date de la commande

NRC·CNRC

Flora of the Yukon Territory

William J. Cody

643 pages
December/décembre 1996
Hardcover/Édition reliée
ISBN 0-660-16406-X
NRC/CNRC 40389
$79.95/79,95 $
Softcover/Édition brochée
ISBN 0-660-15898-1
NRC/CNRC 40390
$49.95/49,95 $

This book treats 1112 species representing 80 families of vascular plants that have been found in or near the Yukon Territory. Descriptions and keys provide information on families, genera, species, subspecies, and varieties. All species are illustrated and dot maps depict known distributions within the Yukon Territory. Visit our Web site at http://www.nrc.ca/cisti/journals/40390/flora.html to view a short chapter of *Flora of the Yukon Territory.*

Ce traité décrit 1112 espèces de plantes vasculaires, représentant 80 familles, qui se retrouvent au Yukon ou aux environs du Territoires. Les descriptions et les clefs présentées offrent de l'information sur les familles, les genres, les espèces, les sous-espèces et les variétés. Toutes les espèces sont illustrées et des cartes de points illustrent la répartition connue au Yukon. Visitez http://www.nrc.ca/cisti/journals/40390/flora_f.html pour afficher un court chapitre du livre.

To order copies of this publication/Pour commander des exemplaires de ce livre

- Telephone: (613) 993-0151
- Fax: (613) 952-7656
- Mail orders: Monograph Orders, NRC Research Press, National Research Council Canada, Ottawa, Ontario K1A 0R6, Canada
- Internet e-mail: research.journals@nrc.ca
- World Wide Web: http://www.nrc.ca/cisti/journals/formmono.html

Canadian customers please add 7% GST. Orders from Quebec add a further 6.5% QST to the total price including GST. Make cheque or money order payable to "Receiver General for Canada, credit NRC". Note that for all orders outside Canada, rates are in U.S. dollars. All sales are final.

- Téléphone : (613) 993-0151
- Télécopieur : (613) 952-7656
- Par la poste : Monographies, Presses scientifiques du CNRC, Conseil national de recherches Canada, Ottawa (Ontario) K1A 0R6, Canada
- Courrier électronique : research.journals@nrc.ca
- World Wide Web : http://www.nrc.ca/cisti/journals/formmofr.html

Les clients canadiens doivent ajouter la TPS de 7 %. Les clients du Québec doivent ajouter 6,5 % de TVQ au montant total, une fois la TPS additionnée. Libellez le chèque ou le mandat à l'ordre du «Receveur général du Canada, au crédit du CNRC». Pour les clients non canadiens, les prix sont en dollars américains. Aucun remboursement.

Please send me copies of/Veuillez me faire parvenir des exemplaires du *Flora of the Yukon Territory*
_____ (hardcover/édition reliée); _____ (softcover/édition brochée).

NRC Research Press

Monograph Program

Presses scientifiques du CNRC

Programme de monographies

PLEASE PRINT/LETTRES MOULÉES

☐ Payment enclosed/Paiement inclus ☐ Charge to/Imputer à ☐ Visa ☐ MasterCard

Account number/ Nº de compte _____ Expiry date/ Date d'expiration _____

Name/Nom

Signature/Signature

Address/Adresse

City/Ville Province/Province

Postal code/Code postal Country/Pays

Telephone/Téléphone Fax/Télécopieur

e-mail/Courrier électronique Date of order/Date de la commande

NRC·CNRC

WWW.CFBS.ORG

43RD ANNUAL MEETING / 43e CONGRÈS ANNUEL

CANADIAN FEDERATION OF BIOLOGICAL SOCIETIES

FÉDÉRATION CANADIENNE DESSOCIÉTÉS DE BIOLOGIE

OTTAWA CONGRESS CENTRE
OTTAWA, ONTARIO
JUNE 22 - 25, 2000

THEME I – APOPTOSIS AND SIGNAL TRANSDUCTION

PLENARY LECTURER
Dr. Gerard Evan, University of California, San Francisco, USA
Oncogene Induced Apoptosis in Cancer: If, How, When and Where?

SYMPOSIA:
Regulation of Apoptosis
Signaling in Apoptosis
Apoptosis and Neurodegenerative Diseases
Apoptosis and Cancer

THEME II – NUTRACEUTICALS AND FUNCTIONAL FOODS

PLENARY LECTURER
Dr. John Milner, Pennsylvania State University, PA
A Food-Based Approach to Disease Risk Reduction: Benefits, Risks and Biomarkers

SYMPOSIA:
The History of Vegetable Oils and their Human Health Effects
Functional Foods and the Evaluation of Health Outcomes
Interfaces Between Science and the Public: Education, Communication and Policies on Functional Foods and Nutraceuticals

GORDIN KAPLAN AWARD

Dr. Michael Smith
University of British Columbia, Vancouver, BC

OTHER

Skeletal Muscle Workshop
Society Award Lectures
Poster Presentations

MINI-SYMPOSIA

To be determined from abstract submissions

CFBS OPEN SCIENCE POLICY FORUM

Abstract's Deadline:
March 15, 2000

For Further Information:
Pour Plus D'information:

Canadian Federation of Biological Societies
215 - 1750 Courtwood Cres., Ottawa, Ontario K2C 2B5
Tel.: (613) 225-8889 Fax.: (613) 225-9621
E-Mail: wantonious@cfbs.org
www.cfbs.org

Gareth L. Lawson and George A. Rose	**1011–1024**	Small-scale spatial and temporal patterns in spawning of Atlantic cod (*Gadus morhua*) in coastal Newfoundland waters
Charles P. Madenjian, Daniel V. O'Connor, and David A. Nortrup	**1025–1032**	A new approach toward evaluation of fish bioenergetics models
Michael R. Penn, Martin T. Auer, Susan M. Doerr, Charles T. Driscoll, Carol M. Brooks, and Steven W. Effler	**1033–1041**	Seasonality in phosphorus release rates from the sediments of a hypereutrophic lake under a matrix of pH and redox conditions
Theodore V. Willis and John J. Magnuson	**1042–1052**	Patterns in fish species composition across the interface between streams and lakes
BIOGEOCHEMISTRY OF MERCURY IN A CONTAMINATED RIVER		BIOGÉOCHIMIE DU MERCURE DANS UN COURS D'EAU CONTAMINÉ
James G. Wiener and Pamela J. Shields	**1053–1061**	Mercury in the Sudbury River (Massachusetts, U.S.A.): pollution history and a synthesis of recent research
Bradley E. Frazier, James G. Wiener, Ronald G. Rada, and Daniel R. Engstrom	**1062–1072**	Stratigraphy and historic accumulation of mercury in recent depositional sediments in the Sudbury River, Massachusetts, U.S.A.
John A. Colman and Robert F. Breault	**1073–1079**	Sampling for mercury at subnanogram per litre concentrations for load estimation in rivers
Marcus C. Waldron, John A. Colman, and Robert F. Breault	**1080–1091**	Distribution, hydrologic transport, and cycling of total mercury and methyl mercury in a contaminated river–reservoir–wetland system (Sudbury River, eastern Massachusetts)
Teresa J. Naimo, James G. Wiener, W. Gregory Cope, and Nicolas S. Bloom	**1092–1102**	Bioavailability of sediment-associated mercury to *Hexagenia* mayflies in a contaminated floodplain river
Nancy Beckvar, Sandra Salazar, Michael Salazar, and Ken Finkelstein	**1103–1112**	An in situ assessment of mercury contamination in the Sudbury River, Massachusetts, using transplanted freshwater mussels (*Elliptio complanata*)

National Research Council Canada
Ottawa, Canada K1A 0R6

Conseil national de recherches Canada
Ottawa, Canada K1A 0R6

Postage paid at Ottawa
Publications mail
Registration No. 1240579

Port payé à Ottawa
Poste-publication
Enregistrement n° 1240579

Canadian Journal of Fisheries and Aquatic Sciences

Volume 57, Number 5, May 2000

Journal canadien des sciences halieutiques et aquatiques

Volume 57, numéro 5, mai 2000

Måns J. Lindell, H. Wilhelm Granéli, and Stefan Bertilsson	**875–885**	Seasonal photoreactivity of dissolved organic matter from lakes with contrasting humic content
David R. Smith, Kenneth P. Burnham, Desmond M. Kahn, Xi He, Cynthia J. Goshorn, Kathryn A. Hattala, and Andrew W. Kahnle	**886–897**	Bias in survival estimates from tag-recovery models where catch-and-release is common, with an example from Atlantic striped bass (*Morone saxatilis*)
W.D. Bowen	**898–905**	Reconstruction of pinniped diets: accounting for complete digestion of otoliths and cephalopod beaks
M.F. Solazzi, T.E. Nickelson, S.L. Johnson, and J.D. Rodgers	**906–914**	Effects of increasing winter rearing habitat on abundance of salmonids in two coastal Oregon streams
Michael A. Banks, Vanessa K. Rashbrook, Marco J. Calavetta, Cheryl A. Dean, and Dennis Hedgecock	**915–927**	Analysis of microsatellite DNA resolves genetic structure and diversity of chinook salmon (*Oncorhynchus tshawytscha*) in California's Central Valley
Colin D. Rennie and Robert G. Millar	**928–938**	Spatial variability of stream bed scour and fill: a comparison of scour depth in chum salmon (*Oncorhynchus keta*) redds and adjacent bed
James A. Hill, Anders Kiessling, and Robert H. Devlin	**939–950**	Coho salmon (*Oncorhynchus kisutch*) transgenic for a growth hormone gene construct exhibit increased rates of muscle hyperplasia and detectable levels of differential gene expression
Matthew G. Mitro and Alexander V. Zale	**951–961**	Predicting fish abundance using single-pass removal sampling
Jon T. Schnute, Al Cass, and Laura J. Richards	**962–979**	A Bayesian decision analysis to set escapement goals for Fraser River sockeye salmon (*Oncorhynchus nerka*)
Lance E. Morgan, Louis W. Botsford, Stephen R. Wing, and Barry D. Smith	**980–992**	Spatial variability in growth and mortality of the red sea urchin, *Strongylocentrotus franciscanus*, in northern California
Clifford E. Kraft and Ladd E. Johnson	**993–1001**	Regional differences in rates and patterns of North American inland lake invasions by zebra mussels (*Dreissena polymorpha*)
John Hampton	**1002–1010**	Natural mortality rates in tropical tunas: size really does matter

Continued on inside back cover / Suite au verso

Canada

Printed in Canada by / Imprimé au Canada par
INTRA MÉDIA INC./datamark systems
Typesetting by / Typographie par
NRC Research Press / Presses scientifiques du CNRC

0706-652X(200005)57:5;1-G